12/11/92

BJR

THE BRITISH
JOURNAL
OF RADIOLOGY

Volume 64 Number 759 March 1991

CUK-H06098-25-P25859

VCH

25

X-ray Diagnosis • Ultrasound • Interventional Radiology
Radiotherapy • Oncology • Hyperthermia
Nuclear Medicine • Nuclear Magnetic Resonance
Radiation Physics • Radiobiology • Radiation Protection

BJR is published by The British Institute of Radiology BIR

You Can Depend On Our Diode Detectors For Patient Dose Verification During Treatment

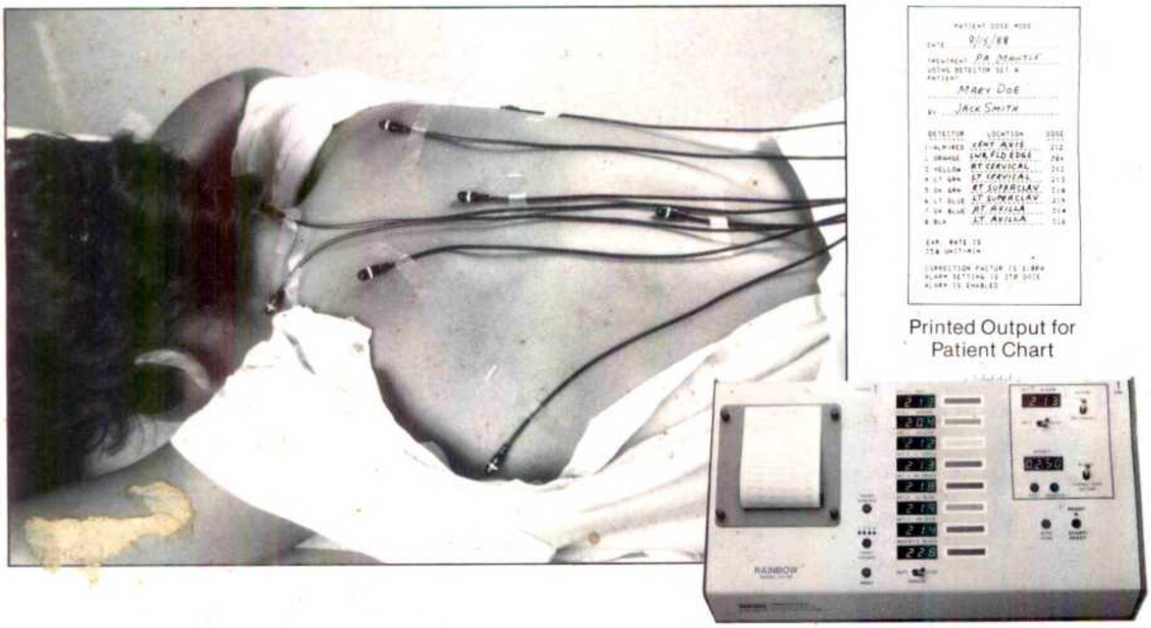

Printed Output for Patient Chart

RAINBOW™

Patient Dose Verification and
QA Beam Analyzer with 8 Displays
for 8 Detectors

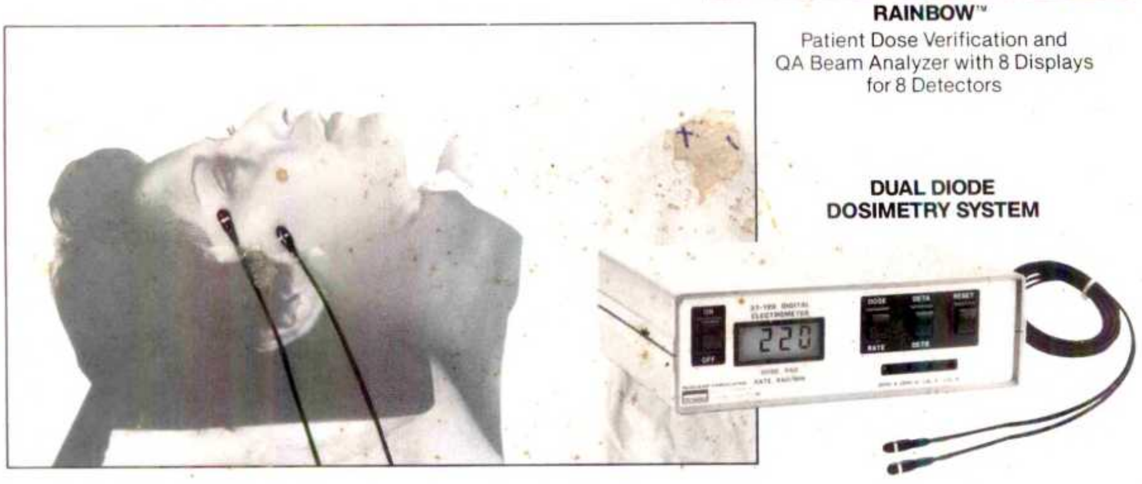

DUAL DIODE DOSIMETRY SYSTEM

- **Instant measurements will help prevent accidental overexposure to patients.**
- **Over 10 years of proven, reliable, dependable performance in the clinical environment.**
- **Detectors for photons and electrons.**
- **Unlimited versatility — use with your electrometer or ours.**

When coupled with a precision electrometer, our Diode Detectors offer the unique combination of high accuracy, ruggedness, small size, immediate readout, and simplicity of operation. The use of noble metal dopings, sophisticated mounting methods and special low noise cable have substantially reduced radiation induced damage, directional sensitivity and induced noise from cable movements, making these detectors perfect for the application of patient dose verification.

For complete details on our Diode Detectors and Diode Dosimetry Systems, request Bulletin 371-14

NUCLEAR ASSOCIATES

VICTOREEN

A Division of VICTOREEN, INC.
100 VOICE ROAD
CARLE PLACE, NY 11514-1593 U.S.A.
(516) 741-6360
FAX (516) 741-5414

*Victoreen, Inc

P25859

BJR THE BRITISH JOURNAL OF RADIOLOGY

Established 1896

The Editorial Committee

Honorary Editors
N. J. McNally, BSc, MSc, PhD
D. G. Shaw, FRCP, FRCR

Deputy Editors
C. K. Bomford, BSc, MPhil, FInstP
D. M. King, MB, BS, FRCR, DMRD

Associate Editors
H. Baddeley, MB, BS, DMRD, FRCR, MRACR
P. R. Blake, MD, MB, BS, BSc, FRCR
J. A. Bullimore, MB, BS, MRCS, LRCP, DMRT, FRCR
R. G. Dale, MSc, PhD, CPhys, FInstP
P. Dawson, BSc, PhD, MB, BS, MRCP, MInstP, FRCR
S. Dische, MD, FRCR
F. A. Duck, PhD, MIEEE
A. H. Freeman, MB, BS, FRCR
R. M. Harrison, BSc, MSc, PhD, FInstP
J. W. Hopewell, BSc, PhD
H. W. C. Loose, DMRD, FRCR
A. M. Peters, BSc, MSc, MB, ChB, MD, MRCPath
D. W. Pilling, MB, ChB, DCH, DMRD, FRCR
J. F. Reidy, MB, BS, FRCP, FRCR
J. R. K. Savage, DSc
R. A. Shields, PhD
D. M. Tait, MB, ChB, MRCP, FRCR
J. Tudor, MB, BS, FRCR
A. R. Valentine, MB, BS, MRCS, LRCP, FRCR, DMRD
G. H. Whitehouse, MB, BS, FRCP, FRCR, DMRD
A. G. Wilson, FRCP, FRCR
E. P. Wraight, MB, BChir, PhD, DMRT

Associate Editors Overseas
S. G. A. Chenery, PhD, FCCPM (North America)
B. J. Cremin, MD, FRCR, FRACR (South Africa)
R. Fox, DPhil (Australia)
M. Takahashi, MD (Japan)
D. M. Taylor, DSc, CChem, FRSC ([illegible]ental Europe)

Managing Editor: T. R. Hogan, BSc, PhD

The British Journal of [illegible] British Institute of R[illegible]land [illegible] W1N 4AT. Telephone 0[illegible] (editorial); Fac[illegible] 071-255 3209. Editorial communications should be addressed to the Honorary Editors in accordance with the Instructions to Authors published in the January issue each year, copies of which may be obtained from the Managing Editor upon request.

Advertisements. Communications should be addressed to the Advertising Manager at the above address. Tel. 071-631 1168.

Subscriptions. The monthly fulfilment is carried out by BJR Subscriptions, PO Box 500, Leicester LE99 0AA, UK. Telephone 0858 410510; Facsimile 0858 434190.

The 1991 annual subscription to *The British Journal of Radiology* is £140 for EEC (incl. UK) readers and £155 for readers in the rest of the world; the 2-year subscription (1991 and 1992) is £275 for EEC (incl. UK) readers and £305 for readers in the rest of the world.

These prices include delivery by sea mail; airmail rates are available on request. Copies of this journal sent to subscribers in Bangladesh, Canada, India, Japan, Pakistan, Sri Lanka and USA are air-speeded for quicker delivery at no extra cost. Subscriptions are on a calendar year basis only.

Back issues prior to the current volume are available from BJR Subscriptions at the address above.

US mailing agents: Mercury Airfreight International Ltd Inc. Second class postage paid at Rahway, NJ, USA. Postmaster: send address corrections to The British Journal of Radiology, c/o Mercury Airfreight International Ltd Inc., 2323 Randolph Avenue, Avenel, NJ 07001, USA.

THE BRITISH INSTITUTE OF RADIOLOGY

BIR

Founded 1897
Incorporated by Royal Charter
Patron: Her Majesty The Queen

The British Institute of Radiology is an association of persons interested in radiology and allied subjects. Meetings are held monthly from October until May. Particulars of membership and other information may be obtained on application to the General Secretary at the Institute, 36 Portland Place, London W1N 4AT. The British Institute of Radiology is a registered charity, no: 215869. Telephone: 071-580 4085 and 071-580 4189 Fax: 071-255 3209.

President
C. A. Joslin, MB, BS, FRCR, DMRT, MIEE, CEng
Honorary Secretaries:
N. W. Garvie, MAMB, BChir, MRCP, DMRD, FRCR, MSc
M. P. Law, BSc, PhD
Honorary Treasurer
D. S. McIntosh, BSc, PhD, MRPharmS, MRSC, MIMC
General Secretary
Mary-Anne Piggott, BSc, MBA, MBIM

Radiology &
Oncology
'91

Brighton Metropole Hotel, 29 April – 1 May 1991

.... the premier radiological
meeting in Europe ....
Join Us!

BIR

Conference Office
British Institute of Radiology
36 Portland Place
London W1N 4AT
Tel 071-580 4085
Fax 071-255 3209

VOL 64 NO 759 MARCH 1991

The British Journal of Radiology

Contents

Review article

Page
"State of the art" transrectal ultrasound imaging in the assessment of prostatic disease 193
R. Clements, G. J. Griffiths and W. B. Peeling

Papers

Acute spinal cord injury: magnetic resonance imaging correlated with myelopathy 201
Y. Yamashita, M. Takahashi, Y. Matsuno, R. Kojima, Y. Sakamoto, T. Oguni, T. Sakae and E. E. Kim

In vivo phosphorus-31 magnetic resonance spectroscopy of normal and pathological breast tissues 210
O. M. Redmond, J. P. Stack, N. G. O'Connor, M. B. Codd and J. T. Ennis

The interchangeability of radioisotope and X-ray based measurements of bone mineral density 217
J. D. Adachi and C. E. Webber

Ultrasound of the pelvis and renal tract combined with a plain film of abdomen in young women with urinary tract infection: can it replace intravenous urography? A prospective study 221
M. M. J. McNicholas, J. F. Griffin and D. F. Cantwell

Unsuspected sphincter damage following childbirth revealed by anal endosonography 225
S. J. D. Burnett, C. Spence-Jones, C. T. M. Speakman, M. A. Kamm, C. N. Hudson and C. I. Bartram

Fracturing and stretching of angioplasty balloon catheters under bending with tension 228
W. D. Jeans, A. Blakeborough and H. W. C. Loose

Final report on the second British Institute of Radiology fractionation study: short *versus* long overall treatment times for radiotherapy of carcinoma of the laryngo-pharynx 232
G. Wiernik, C. J. Alcock, T. D. Bates, J. M. Brindle, J. F. Fowler, W. R. Gajek, S. Goodman, J. L. Haybittle, J. M. Henk, J. W. Hopewell, R. D. Hunter, R. Lindup, D. L. Phillips and M. Rezvani

Application of the linear-quadratic model with incomplete repair to radionuclide directed therapy 242
W. T. Millar

Concomitant pelvic irradiation, 5-fluorouracil and mitomycin C in the treatment of advanced cervical carcinoma 252
G. G. Khoury, A. S. Bulman, C. A. F. Joslin and R. I. Rothwell

Paediatric haemangiomas: the role of radiotherapy 261
S. C. Dutton and P. N. Plowman

Technical note

An iridium-192 applicator for the treatment of stomal recurrence following tracheostomy for subglottic carcinoma 270
R. D. Jones, D. G. Clarkson, R. P. Symonds and S. G. McNee

Case reports

Hepatocellular carcinoma associated with polyarteritis nodosa with symptoms appearing after intra-arterial chemotherapy 272
K. Minakuchi, K. Fujimoto, K. Takada, S. Takashima, K. Nakamura and T. Mitsuhashi

Renal transitional cell carcinoma mimicking medullary sponge kidney 275
M. Choong and G. W. L. Phillips

Metastatic carcinoma to the male breast 277
L. Ramamurthy and R. A. Cooper

Case of the month

There's more to it than meets the eye 279
S. Evans

Correspondence

Choroid plexus cysts and chromosomal defects 281
J. McHugo, G. Constantine and R. Rajah

The prognostic significance of radiologically detected knee joint effusions in the absence of associated fracture 281
P. Lord

Authors' reply 281
T. Maskell and D. Finlay

Proceedings

Proceedings of the British Institute of Radiology
Prediction and measurement of tumour response to treatment, 9 November 1990 282

Book reviews

Nonionizing Radiation Protection, 2nd edn. *M. J. Suess and D. A. Benwell-Morison* (Eds) 287
Advances in Cerebral Spect Imaging. *R. L. Van Heertum and R. S. Tikofsky* (Eds) 287
Guidelines for the Routine Performance Checking of Medical Ultrasound Equipment (IPSM Report 58). *R. E. Richardson* (Ed.) 287
Basic Principles of Radiographic Exposure. *D. C. DeVos* 288
CT and MRI of the Liver and Biliary System. *P. M. Silverman and R. K. Zeman* 288

BIR Bulletin *facing page* 288

© 1991 The British Institute of Radiology. This publication is copyright under the Berne Convention and the Universal Copyright Convention. All rights reserved, apart from any relaxations permitted under national copyright laws, no part of this publication may be reproduced, stored in a retrieval system or transmitted in any form or by any means without the prior permission of the copyright owners. Permission is not, however, required to copy abstracts of papers or of articles on condition that a full reference to the source is shown. Multiple copying of the contents of the publication without permission is always illegal. Published by The British Institute of Radiology, 36 Portland Place, London W1N 4AT. Origination by BPCC Whitefriars Ltd, Tunbridge Wells, and printed and bound in Great Britain by BPCC Wheatons Ltd, Exeter.
ISSN 0007 1285

VOL 64 NO 762 JUNE 1991

The British Journal of Radiology

Contents

Papers

Page

Quickscan: Doppler ultrasound emulation of angiography—its value prior to arteriography in peripheral vascular disease 479
N. M. deSouza, D. H. King, P. Pilgrim, P. Bates, J. F. Reidy and R. G. Gosling

Duplex sonography in splenomegaly 485
L. Jarvis, P. G. Cook, C. M. James, M. Rose, A. G. Prentice and P. A. Dubbins

Focal myositis, a benign inflammatory pseudotumour: CT appearances 489
E. Moskovic, C. Fisher, G. Westbury and C. Parsons

Automated measurement of tumour extent in patients with colorectal liver metastases from X-ray computed tomography 494
S. Perring, T. M. Hunt, J. S. Fleming, R. M. Blaquiere and I. Taylor

Quantitative magnetic resonance imaging in cervical carcinoma: a report on 30 cases 498
R. Santoni, M. Bucciolini, C. Chiostrini, L. Cionini and R. Renzi

Fetal blood sampling from the intrahepatic vein for rapid karyotyping in the second and third trimesters 505
P. Nicolaidis, U. Nicolini, N. M. Fisk, Y. Tannirandorn, H. Nasrat and C. H. Rodeck

Assessment of the psychological impact of a breast screening programme 510
A. R. Bull and M. J. Campbell

Stage distribution of breast cancer: a basis for the evaluation of breast screening programmes 516
A. Bull, L. Mountney and H. Sanderson

The effect on pulmonary function of tangential field technique in radiotherapy for carcinoma of the breast 520
M. B. Lund, K. I. Myhre, H. Melsom and B. Johansen

The reduction in radiation dose for intra-oral radiographs by the use of thin K-edge filters 524
D. S. MacDonald-Jankowski and C. P. Lawinski

Quantitative assessment of a new dental imaging system 529
A. Walker, K. Horner, J. Czajka, A. C. Shearer and N. H. F. Wilson

Ovarian ablation failures by radiation: a comparison of two dose schedules 537
S. F. Leung, S. Y. Tsao, P. M. L. Teo, P. H. K. Choi and W. C. T. Shiu

Estimation of doses to patients from "complex" conventional X-ray examinations 539
A. Calzado, E. Vañó, P. Morán, C. Castellote, S. Ruiz and L. González

Technical note

Assessment of a radiotherapy beam analyser 547
J. A. Mills and P. Martin-Smith

Case reports

Positioning for plain spinal radiography producing paraplegia in a patient with ankylosing spondylitis 549
S. S. Upadhyay, E. K. W. Ho and L. C. S. Hsu

Atypical skeletal tuberculosis mimicking neoplasm 551
I. F. Abdelwahab, S. Kenan, G. Hermann, M. Lewis, M. Klein and J. G. Rabinowitz

Demonstration of intramedullary tuberculomas by magnetic resonance imaging: a report of two cases 555
A. Jena, A. K. Banerji, R. P. Tripathi, P. K. Gulati, R. K. Jain, S. Khushu and M. L. Sapra

Oesophageal atresia and other disorders with a similar antenatal presentation 557
A. C. Havard and L. M. MacDonald

Case of the month

A dense problem 559
D. O'Keeffe and J. E. Adams

Correspondence

Irregular-shaped fields in electron radiotherapy 561
P. B. Smith

Authors' reply—Performance of a commercially available field flatness device 561
J. H. Plane

Authors' reply—Choroid plexus cysts and chromosomal defects 562
J. G. Thorpe-Beeston and K. H. Nicolaides

cGy vs Gy 562
R. Abadir

Energy imparted to the patient during fluoroscopy using magnified fields of view 563
C. J. Kotre, N. W. Marshall and K. Faulkner

Haematopoiesis in the liver: the role of ^{99}Tc^{m} 564
M. Abboud and S. K. Morcos

Authors' reply 564
M. Bradley and C. Metreweli

Book reviews

Hyperthermic Oncology. Vol. 1. Summary Papers. *T. Sugahara and M. Saito* (Eds) 565
Radiation Exposure and Occupational Risks. *E. Scherer, C. Streffer and K. Trott* (Eds) 565
Year Book of Diagnostic Radiology 1990. *D. G. Bragg et al.* (Eds) 565
Nuclear Medicine Annual 1989. *L. M. Freeman and H. S. Weissmann* (Eds) 566
Ultrasound in Neurosurgery. *J. M. Rubin and W. F. Chandler* 566

BIR Bulletin *facing page* 566

© 1991: The British Institute of Radiology. This publication is copyright under the Berne Convention and the Universal Copyright Convention. All rights reserved, apart from any relaxations permitted under national copyright laws, no part of this publication may be reproduced, stored in a retrieval system or transmitted in any form or by any means without the prior permission of the copyright owners. Permission is not, however, required to copy abstracts of papers or of articles on condition that a full reference to the source is shown. Multiple copying of the contents of the publication without permission is always illegal. Published by The British Institute of Radiology, 36 Portland Place, London W1N 4AT. Origination by BPCC Whitefriars Ltd, Tunbridge Wells, and printed and bound in Great Britain by BPCC Wheatons Ltd, Exeter.
ISSN 0007 1285

VOL 64 NO 763 JULY 1991

The British Journal of Radiology

Contents

Editorial

Page

The guidance notes revisited: advice to patients leaving hospital after diagnostic nuclear medicine 567
R. A. Shields

Papers

Lymphoproliferative disorders of the thyroid gland: radiological appearances 569
K. Kasagi, H. Hatabu, Y. Tokuda, H. Yamabe, A. Hidaka, K. Yamamoto, Y. Iida, T. Misaki, T. Mori, K. Endo and J. Konishi

Fibrous dysplasia of the skull: disease activity in relation to age 576
M. L. Davies and P. Macpherson

The extrapleural fat in empyema: CT appearance 580
J. E. Takasugi, J. D. Godwin and S. A. Teefey

The ocular effects of hyoscine-*n*-butylbromide ("Buscopan") in radiological practice 584
G. R. J. Sissons, A. McQueenie and M. Mantle

A comparison between iotrolan, a non-ionic dimer, and a hyperosmolar contrast medium, Urografin, in hysterosalpingography 587
C. Brokensha and G. Whitehouse

Real-time digital contrast enhancement and magnification in the assessment of acute elbow injuries 591
P. Holland, A. M. Davies, E. Morris, J. Fowler, R. Wellings and P. N. M. Tyrrell

Clinical application of an electronic imaging device for assisting patient set-up in radiotherapy 596
J. P. Wade and D. Nicholas

An innovative method for neuraxis radiotherapy using partial transmission block technique 603
P. N. Plowman and D. Doughty

Dose to red bone marrow from natural radon and thoron exposure 608
R. B. Richardson, J. P. Eatough and D. L. Henshaw

Case reports

Anaphylactoid reaction associated with the use of ^{99}Tc^{m} hexamethyl propylene amine oxime as a leukocyte labelling agent 625
M. H. Giaffer, W. B. Tindale, S. Senior and C. D. Holdsworth

Radiology of secondary amyloidosis of the stomach in a patient with rheumatoid arthritis 626
S. Kawamura, A. Imai, M. Kawamura, M. Kataoka, H. Itoh, A. Komatsu and K. Hamamoto

Sling left pulmonary artery with congenital airway stenosis: non-invasive investigation and conservative management? 629
G. M. A. Hendry, A. T. Edmunds, T. G. Marshall and N. Chalmers

Laurence–Moon–Biedl syndrome: renal ultrasound appearances in the neonate 631
S. J. Garber and R. de Bruyn

Intracranial chondrosarcoma in a patient with Ollier's disease 633
A. G. Clifton, B. E. Kendall, H. A. Crockard and T. Hughes

Case of the month

A clinical red herring 637
C. R. Murch and A. J. Newman Taylor

Correspondence

A new phantom for mammography 639
B. M. Moores

Author's reply 639
J. Law

Scoring of image quality phantom films in mammography 640
A. Robinson and A. C. Underwood

Author's reply 641
J. Law

Body aprons in radiation protection 641
L. J. Ramsey

The role of the single photon emission computed tomography (SPECT) in detection of ossific mediastinal and pulmonary metastases 642
P. R. Goddard and E. Rhys Davies

Proceedings

Proceedings of the British Medical Ultrasound Society 22nd Annual Meeting 643

Book reviews

Differential Diagnosis in Abdominal Ultrasound. *R. A. L. Bisset and A. N. Khan* 671
Diagnostic Ultrasound of Fetal Anomalies. *D. A. Nyberg, B. S. Mahony and D. H. Pretorius* 671
Doppler Echocardiography. An Illustrated Clinical Guide. *P. Wilde* 671
Video Atlas of 2-Dimensional Colour Flow Doppler Echocardiography. *G. M. Gura* 671
Arthrosonography. *H. Sattler and U. Harland* 672
Monoclonal Antibodies in Immunoscintigraphy. *J.-F. Chatal* (Ed.) 672

BIR Bulletin *facing page* 672

© 1991: The British Institute of Radiology. This publication is copyright under the Berne Convention and the Universal Copyright Convention. All rights reserved, apart from any relaxations permitted under national copyright laws, no part of this publication may be reproduced, stored in a retrieval system or transmitted in any form or by any means without the prior permission of the copyright owners. Permission is not, however, required to copy abstracts of papers or of articles on condition that a full reference to the source is shown. Multiple copying of the contents of the publication without permission is always illegal. Published by The British Institute of Radiology, 36 Portland Place, London W1N 4AT. Origination by BPCC Whitefriars Ltd, Tunbridge Wells, and printed and bound in Great Britain by BPCC Wheatons Ltd, Exeter.
ISSN 0007 1285

1991, *The British Journal of Radiology*, *64*, 193–200

VOLUME 64 NUMBER 759 MARCH 1991

The British Journal of Radiology

Review article

"State of the art" transrectal ultrasound imaging in the assessment of prostatic disease

By R. Clements, MA, FRCS, FRCR, G. J. Griffiths, MD, FRCR and W. B. Peeling, MA, FRCS

Departments of Radiology and Urology, Royal Gwent Hospital and St Woolos Hospital, Newport, Gwent, UK

(*Received September 1990*)

Keywords: Prostatic disease, Transrectal ultrasound

Three major developments have occurred in recent years which have increased our understanding of prostatic disease: a major reassessment of the anatomy of the prostate, the development of the serum assay for prostate-specific antigen, and developments in prostatic imaging. The prostate gland has traditionally been regarded as an organ with a relatively simple anatomical structure, based on a system of lobes, as proposed by Lowsley (1912). Lowsley's concept was, however, based on observations of fetal prostate glands and this system cannot now be accepted. A zonal system of anatomy of the prostate was initially proposed by McNeil in 1969 and was fully described in 1981. This concept has been supported by work by Blacklock and Boushill (1977). In McNeil's system the prostate is considered as three glandular zones, transition, central and peripheral, and one non-glandular region, the anterior fibromuscular stroma. The urethra and ejaculatory ducts pass through these zones (Fig. 1). It is important to appreciate this concept of prostatic anatomy as these zones can be identified by transrectal ultrasound with state of the art ultrasound transducers and magnetic resonance (MR) imaging. In the young adult prostate, the transition zone constitutes about 5% of prostatic glandular tissue and is located on both sides of the prostatic urethra; it is in this zone that benign hyperplasia develops. The transition zone is separated from the central and peripheral zones of the prostate by the surgical capsule. The central zone is relatively resistant to disease processes and constitutes about 25% of prostatic glandular tissue in the young adult. It is situated around the base of the prostate and the ejaculatory ducts pass through central zone tissue to reach the verumontanum. The peripheral zone constitutes 70% of prostatic glandular tissues and lies on the posterior and lateral aspects of the gland. Its ducts drain into the urethra distal to the verumontanum.

Prostate-specific antigen (PSA) is a glyco-protein found only in the cytoplasm of prostatic epithelial cells, and its measurement represents a significant improvement over prostatic acid phosphatase as a serum marker for prostate cancer. Two assays are currently commercially available, one produced by Hybritech Inc., a two-site immunoradiometric test with monoclonal antibodies, and a second produced by Yang Laboratories, uses a conventional radio-immuno-assay technique with a polyclonal serum. There is no clinical superiority of one over the other, but the Yang method consistently results in higher values and it is important that clinical laboratories should state the name of the assay along with their results. Prostate-specific antigen measurements have a number of applications in the management of patients with prostate cancer and can be used as an aid to the staging of established disease, for monitoring response to treatment, and potentially for screening and the early detection of prostate cancer. Serum levels may also be slightly elevated in benign prostatic hyperplasia and it is necessary to allow for the presence of benign hyperplasia in the interpretation of the assay result. This will be discussed subsequently in more detail.

The third recent development is the use of transrectal ultrasound (TRUS). This is a simple, safe and minimally invasive method of imaging the prostate. Early scans were obtained with a chair-mounted 3.5 MHz probe, but contemporary equipment uses a hand-held transducer with a frequency ideally between 6 and 7 MHz. A variety of different probes are available from different manufacturers with sector, linear or annular array transducers and these may be arranged in a biplanar or multiplanar arrangement; some modern probes permit

---

Address for correspondence: Dr R. Clements, Main X-Ray Department, Royal Gwent Hospital, Gwent NP9 2UB, UK.

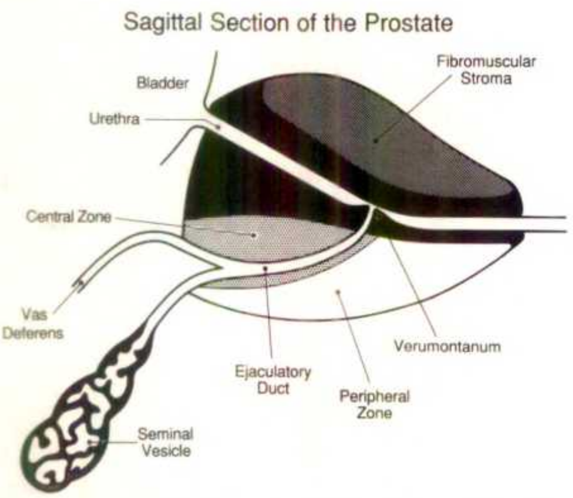

Figure 1. Anatomical diagram of a sagittal section of the prostate and seminal vesicles.

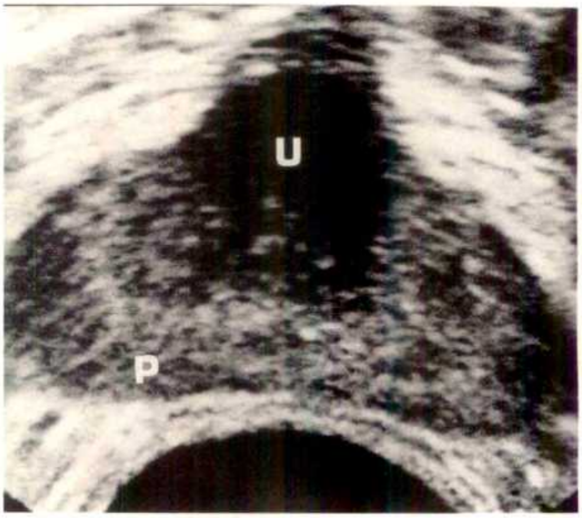

Figure 3. Axial 7 MHz scan showing urethra and surrounding muscle (U), and peripheral zone (P).

the additional possibility of Doppler imaging. A prostate scan may be easily performed with the patient lying in the left lateral decubitus position. The transducer is inserted into the rectum and a water-filled condom around the tip of the probe acts as an acoustic window. Axial or sagittal images of the prostate may be obtained. The axial projection is necessary for assessing the symmetry of the gland and for computing the volume of the gland. Scanning in the sagittal plane is much better for assessing the base and the apex of the gland and for performing prostatic biopsy under ultrasound guidance. It is necessary to obtain views in both planes for a comprehensive examination of the gland. Transrectal ultrasound with a contemporary probe has the ability to demonstrate the three zones of the prostate, the ejaculatory ducts, the seminal vesicles and the urethra (Figs 2–4). The volume of the gland can be accurately measured and the texture of the gland can be assessed for the presence of benign hyperplasia (Figs 5 and 6) or cancer (Figs 7 and 8).

It is the authors' belief that the three developments outlined will be important in transforming our approach to the management of prostatic disease within the next decade and in particular our management of prostatic cancer. The parallel developments of our understanding of prostatic anatomy and the technological advances in TRUS now permit excellent imaging of

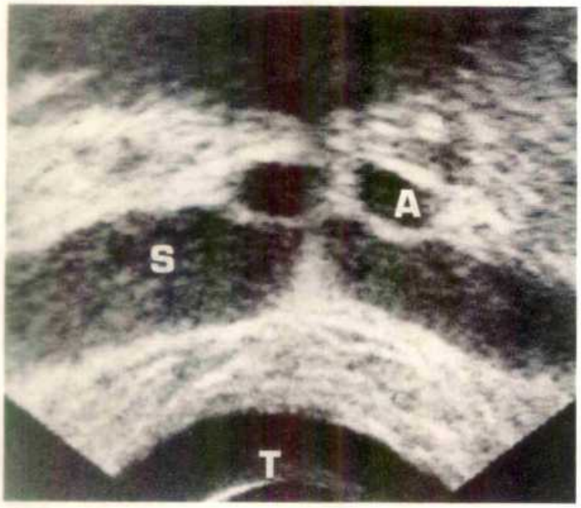

Figure 2. Axial 7 MHz scan at bladder base, demonstrating seminal vesicles (S) and ampullae of vas deferens (A). The transducer (T) is within the rectum.

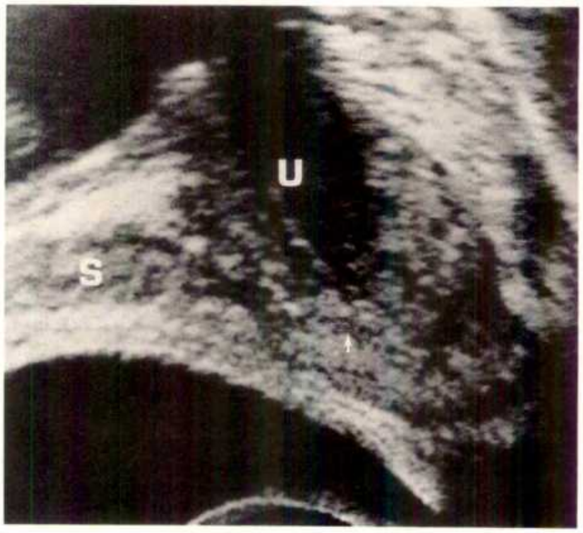

Figure 4. Sagittal 7 MHz scan demonstrating seminal vesicle (S), urethra (U), and ejaculatory duct (arrow).

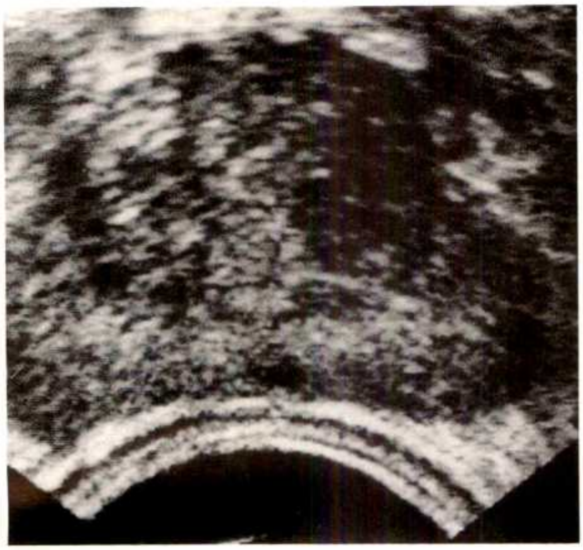

Figure 5. Axial 7 MHz scan. A moderate size adenoma of benign hyperplasia is present in the transition zone.

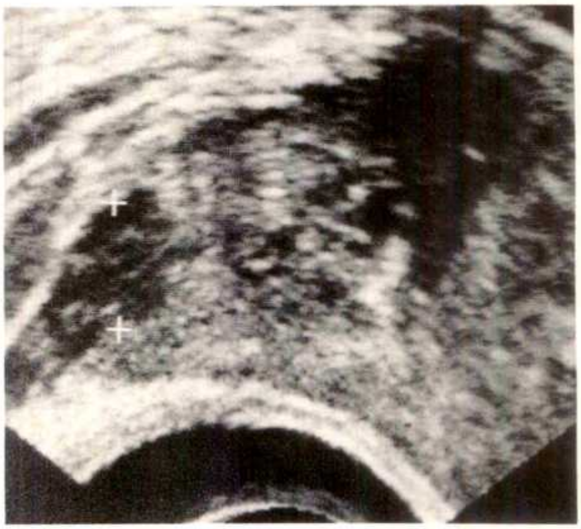

Figure 7. Axial 7 MHz scan with a 0.9 cm hypoechoic cancer in the right peripheral zone.

the internal structure of the prostate and it is now possible to demonstrate the location and routes of spread of cancer within the gland. It is thus possible to devise a logical approach to treatment instead of the relatively haphazard approach that has been adopted previously where the internal structure of the gland could not be identified and histological tissue was often obtained by transurethral resection of the periurethral part of the prostate, or by digitally guided biopsy.

Cancer of the prostate is a major source of mortality and morbidity and in most developed countries is the second most common malignancy after lung cancer in men (Silverberg & Lubera, 1983). The incidence of the disease may be increasing with 8879 new cases registered in England and Wales in 1982 (Office of Population Censuses and Surveys, 1985) and 9524 cases in 1984 (Office of Population Censuses and Surveys, 1988). This may in part be a reflection of increased detection of the disease, a view strengthened by evidence from the United States where prostatic cancer has recently overtaken lung cancer as the tumour with the highest incidence in American men.

Transrectal ultrasound provides the only currently available imaging technique for identifying early pros-

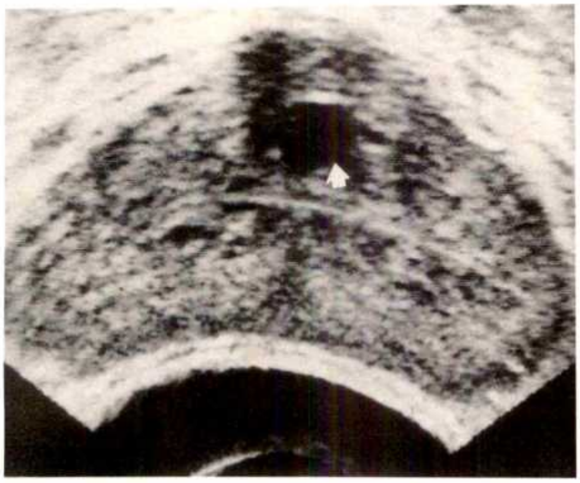

Figure 6. Axial 7 MHz scan with evidence of benign prostatic hyperplasia. An area of cystic change (arrow) is present within the adenoma.

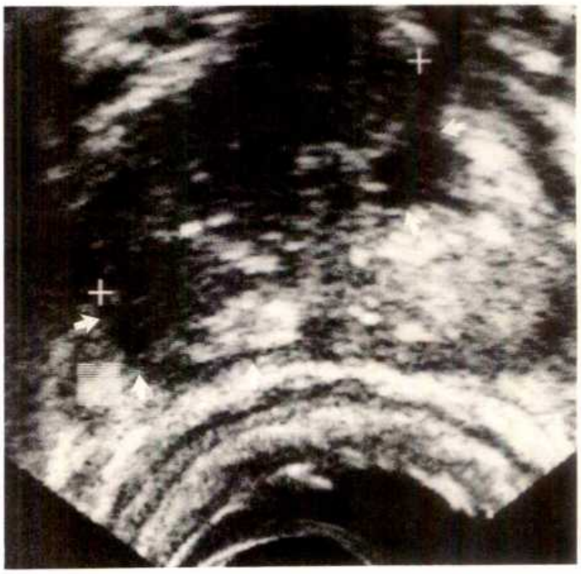

Figure 8. Axial 7 MHz scan. An extensive cancer is present involving the right lobe of the prostate (arrows).

tatic cancer. Various studies have been performed in South Wales in the past decade to evaluate the use of TRUS in the management of prostatic disease, and the ultrasound appearances of prostatic cancer have been controversial. Early reports suggested that cancer could be hyperechoic (Rifkin et al, 1983). Initial reports from South Wales suggested that cancer could be hyperechoic or hypoechoic (Peeling et al, 1979) but this assumption was questioned when an ultrasound-guided biopsy service commenced in 1983. Ultrasound-guided biopsy enabled correlation of histology with the ultrasound image for the first time. This correlation had not been possible previously when the histological assessment was based on material obtained at transurethral prostatectomy and the precise site of the cancer within the prostate was not known.

A retrospective analysis of the ultrasound appearances of the prostate and periprostatic tissues in 221 patients with a histologically confirmed diagnosis of prostatic cancer was undertaken in 1984 (Griffiths et al, 1987). The results of this study indicated that an ill defined hypoechoic area was the commonest appearance of prostatic cancer, and this was seen in 96% of the 221 patients. The cancers were staged into confined (T_0, T_1, T_2) and unconfined T_3 cancers. A breach of the capsule was seen in 55% of cases. In the unconfined group, all cancers were hypoechoic in comparison with 92% of the confined group. In the confined group, the areas of abnormal echogenicity were present in more than one prostatic quadrant in 76%; most commonly two quadrants were affected. In 70% of cases of extensive but confined cancer there was loss of demarcation between the inner and outer parts of the prostate, and in 3% of proven prostatic cancers no definite abnormality was observed. The seminal vesicles showed definite evidence of infiltration in 10% of cases. The scans analysed in this study were performed between 1982 and 1984 using 3.5 MHz and 4 MHz transducers. Prostate scanning is now undertaken using higher frequency transducers, *e.g.* 6–7 MHz, and it is probable that some tumours previously considered isoechoic would be visible with a contemporary probe. The study above demonstrated that the vast majority of prostatic cancers are hypoechoic. A similar view was reported by Lee et al (1985) at the same time, based on the studies of radical prostatectomy specimens. All of the histologically proven cancers in their study were hypoechoic, although eight hypoechoic lesions in the peripheral zone were benign on biopsy. It is now generally accepted that with 7 MHz probes, the majority of prostatic cancers are hypoechoic (Figs 7–9). Unfortunately, although the majority of cancers are hypoechoic, not all hypoechoic lesions are malignant. Ultrasound-guided biopsy of the prostate has demonstrated that the following lesions may appear as hypoechoic areas within the gland: adenocarcinoma, atypical glandular hyperplasia, prostatic atrophy, granulomatous prostatitis, ductal dilatation, and muscle around the ejaculatory ducts. The definitive analysis of a hypoechoic area can only be obtained by biopsy, and this now simple procedure can be performed under antibiotic cover by the transrectal route on an outpatient basis at the time of scanning using a biopty gun without local anaesthesia.

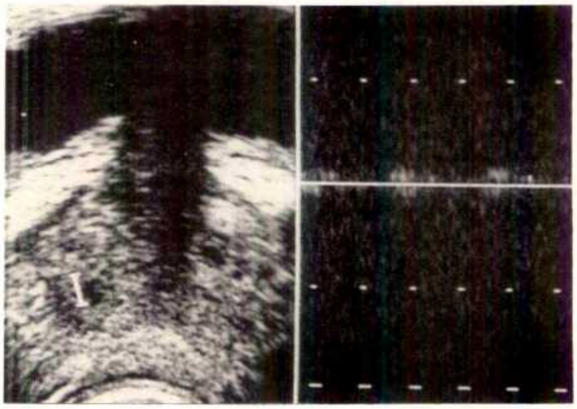

Figure 9. Axial 7 MHz scan demonstrating a Doppler signal from the hypoechoic area in the prostate.

The transrectal biopsy route represents a marked advance over the previously used transperineal route for ultrasound-guided biopsy, and the technique is well described by Torp-Pedersen and Lee (1989). About 100 biopsies have now been performed by this route in our unit without complication, but some authorities have now performed many hundreds of biopsies by this route without any significant complications. We previously performed a series of ultrasound-guided biopsies of the prostate by the transperineal route and these have recently been reviewed (Clements et al, 1990). One hundred and fifty-seven consecutive transperineal biopsies of the prostate were performed under ultrasound guidance, and the clinical and ultrasound features of 143 patients were reviewed. Initially, 28 biopsies were performed using general anaesthetic at the time of cystoscopy but subsequently 115 biopsies were performed under local anaesthetic as an outpatient procedure with minimal complications. The transperineal technique was, however, cumbersome and time consuming, and the development of ultrasound-guided prostatic biopsy by the transrectal route has been a great advance and should now be regarded as the standard approach for performing ultrasound-guided prostate biopsy.

A hypoechoic area within the prostate may be cancer, but histological confirmation of the diagnosis by biopsy is needed. Some clues about the nature of a hypoechoic lesion may be obtained from the site of the lesion, for example, most cancers originate within the peripheral zone. It has been realized within the last 3 years, however, that cancer of the prostate may be multifocal and that the transition zone may be a site for cancer in up to 30% of patients. This basic pathological observation had not previously been appreciated and it is only through the high-definition images produced by modern transducers and detailed ultrasound-guided biopsies that this has become apparent. It is the transition zone of the prostate which is resected at transurethral prostatectomy and it now appears that the majority of T_0 cancers are tumours developing within the transition zone and not impalpable peripheral zone tumours invading the transition zone as had previously been thought. One potential field of future research is to explore the use of pulsed wave Doppler ultrasound for assessing hypoechoic areas of the prostate. It is postulated that it may be possible to differentiate areas of prostatitis, cancer and atrophy within the prostate using Doppler ultrasound. It is possible with some modern transducers to undertake such an analysis (Fig. 9), but such work is currently in its infancy, and no results of a detailed analysis of this possibility are yet available.

Past studies have indicated that digital examination is not accurate for T-category staging of prostate cancer (Byar et al, 1972). Usually the cancer is understaged by digital examination, and most of the errors occur by not detecting antero-lateral breaches of the capsule (Brooman et al, 1981). Transrectal ultrasound can improve the accuracy of staging prostatic carcinoma by detecting capsular breaches, and assessing apical or seminal vesicle involvement. It is these factors which upstage a cancer from a confined T_1 or T_2 tumour to the T_3 stage. A cadaver study (Jones et al, 1989) has demonstrated that TRUS is an accurate method of staging prostatic cancer, the 13 unconfined cancers all showed penetration of the true capsule and infiltration into periprostatic fat. The main limitation of TRUS in T-category staging is an inability to detect microscopical invasion of the capsule. As regards seminal vesicle invasion, Scardino et al (1989) found that any cancer of the base of the prostate measuring over 2 cm in diameter is associated with seminal vesicle invasion. The current criteria advocated by Lee et al (1989) for seminal vesicle or ejaculatory duct involvement by cancer are (a) a "halo" sign around the ejaculatory duct produced by surrounding tumour, (b) obliteration or displacement of the ejaculatory duct by cancer, (c) cancer spreading directly into a seminal vesicle, and (d) an extra prostatic mass at the entrance of the seminal vesicle obliterating the seminal vesicle–prostate angle.

Magnetic resonance imaging has been claimed to be superior to TRUS in staging prostatic cancer. In a study of 27 patients, TRUS was better than MR imaging for the detection of intraglandular cancer and capsular disruption (Friedman et al, 1988). Magnetic resonance imaging was however considered superior in this study for assessing seminal vesicle invasion. The use of an endorectal surface coil with MR imaging (Schnall et al, 1989) may provide further advantages. More studies are necessary to evaluate the relative importance of TRUS and MR imaging in the staging of prostatic cancer.

The measurement of serum PSA provides important further information in the assessment of the prostate for malignancy and is a useful test in conjunction with TRUS in the assessment of prostatic disease. Establishment of a normal range for PSA has been a problem because without careful histological examination of the entire prostate, the absence of carcinoma, benign hyperplasia or other pathology cannot be excluded. Given the high incidence of asymptomatic carcinoma as well as benign hyperplasia, the clinical absence of disease does not preclude their existence. For the Hybritech assay, Chan et al (1987) describe the reference ranges between 0 and 4 ng/ml. Ercole et al (1987) reported PSA levels less than 4 ng/ml in 97% of normal men over 40 years of age. Any procedure that causes significant prostatic tissue injury such as urethral instrumentation, prostatic surgery or biopsy, or prostate massage may, however, result in elevation of PSA. Both benign hyperplasia and carcinoma may cause elevation of the PSA, although the elevation caused by benign hyperplasia is usually slight. Large rises in the PSA levels indicate prostatic malignancy and cause few problems, but there may be difficulty with interpreting smaller elevations, when there is co-existing benign hyperplasia. Attempts have been made to quantify the expected element of PSA elevation caused by benign hyperplasia by relating it to the volume of the gland measured ultrasonically. This should then give an indication of whether the elevation in PSA is due to associated malignancy. In a preliminary study, we reviewed the PSA levels (Hybritech) and ultrasound-determined prostatic volumes of 50 patients with histologically proven hyperplasia and 40 patients with proven cancer. There is correlation between the log PSA and prostatic volume in the benign group. Regression analyses demonstrate that volume has a considerable impact on interpretation of the PSA, and volume corrections are likely to be useful for PSA levels above 10 mg/ml. From the data in this series of patients it appears that PSA corrected for volume will be highly specific (approximately 98%) but not highly sensitive (approximately 90%). This series, however, only related the PSA to overall gland volume, and it is more accurate to relate it to the ultrasound-determined volume of the transition zone, *i.e.* the volume of the adenoma of benign hyperplasia. This has been attempted in our unit using the 4 MHz probe, but it proved difficult to obtain reliable and objective measurements of the adenoma volume as the outline of the surgical capsule was seen with variable clarity. The measured volumes were subjective and difficult to repeat reliably. This problem is largely overcome using the higher frequency transducers as the differentiation of the prostatic zones is more clearly seen. A programme to measure the volume of the adenoma related to PSA measurements is in progress in our unit. Similar work reported by Stamey (1989) suggests that a ratio of 0.35 ng PSA per millilitre of benign transition zone tissue may be appropriate for evaluating the pre-operative PSA and assessing the likelihood of co-existing non-palpable cancers. The interpretation of the slightly elevated PSA is thus not yet straightforward but shows potential in conjunction with prostatic ultrasound in detecting non-palpable cancer.

Palpable prostatic cancer may be diagnosed by digital examination or transrectal ultrasound; unfortunately, however, not all prostatic nodules are malignant. Jewett (1956) reported a series of 211 palpable prostatic nodules of which 103 were malignant and 108 were benign. A wide variety of different prostatic conditions such as benign hyperplasia, calculi, prostatitis, tuberculosis and prostatic infarcts may be felt digitally as a prostatic nodule and confused clinically with a confined prostatic cancer. Clements et al (1988) reviewed the digital examinations and ultrasound scans of 193 patients with prostatic nodules to compare the accuracy of rectal examination and TRUS in the assessment of prostatic nodules. Eighty-eight patients were proven to have a cancer and TRUS suggested the diagnosis in 83 of the 88. In 39 of the 83, ultrasound revealed an advanced unconfined cancer rather than the confined cancers suggested clinically. A prostatic cancer was diagnosed digitally in 83 patients yet in only 55 of the 83 (66%) was cancer proven histologically. It was felt that one cause of an incorrect digital examination might be misinterpretation of prostatic calcification for cancer, and this study also assessed ultrasonically the presence of calcification within the nodular prostate to see whether this might be a cause of a false positive examination. Calcification was present in 33 of the 55 patients (60%) with proven cancer, and in 17 (60.7%) of the remaining 28 patients with a false positive digital examination. It is thus unlikely that prostatic calcification is a cause of a false positive examination of the prostatic nodule.

As it does not involve ionizing radiation, TRUS is an ideal imaging technique for the follow-up of patients being treated for prostatic cancer, permitting sequential objective assessments of the gland texture and capsular integrity, with accurate measurements of prostatic volume. In combination with PSA measurements and digital rectal examination (DRE), it may be useful for detecting early prostate cancer, and screening programmes based on TRUS, PSA, and DRE are now in progress in a number of centres. In combination with PSA measurements we have found TRUS to be a valuable assessment tool which can be used in clinical trials of different treatment regimens for prostatic cancer (Clements et al, 1989). Following treatment by orchidectomy or radiotherapy, it is our experience that the gland becomes smaller and assumes a more circular shape. A variable series of changes in the ultrasound appearances may be seen during treatment. In some patients this area of abnormal echogenicity may persist whilst in others it disappears and the gland becomes isoechoic. The integrity of the capsule may become apparently restored in a patient with a previous unconfined cancer that exhibited a capsular breech. It may, however, be extremely difficult to demonstrate ultrasonically whether there is active cancer still present and biopsy may be necessary to assess this. In trials of patients treated in phase II, and phase III studies of the effects of the depot formulation of the luteinizing hormone releasing hormone analogue goserelin, serial measurements of prostatic volume were obtained in 53 of the 97 patients with metastatic cancer in the trials. A decrease in prostatic volume was seen in 50 of the 53 patients at 3 months. The 53 patients in whom serial volume measurements were obtained may be subdivided into 17 with stable disease and 36 with progressive disease. Following treatment there was a consistent mean reduction in the volume of the prostate in association with supression of plasma testosterone levels to castrate ranges and a fall in the level of plasma prostatic acid phosphatase. The maximum decrease in volume occurred during the first 3 months of treatment. The rate of change in prostatic volume was similar in those patients with progressive disease and those with stable disease, and in the experience of the authors, in contrast to that of Carpentier and Schroeder (1984), the amount of volume change at 3 months has not been a useful guide to subsequent prognosis.

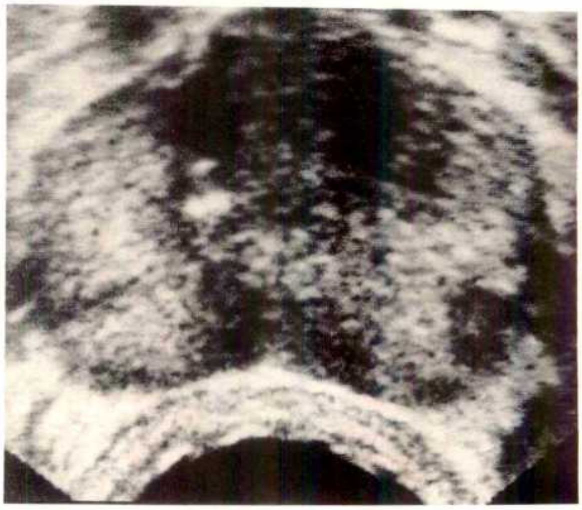

Figure 10. Axial 7 MHz scan in a patient with prostatitis: hypoechoic areas are present in the peripheral zone.

Most interest in TRUS has centred on its value in the detection of prostatic cancer, but it has roles in the assessment of benign diseases of the prostate also. It may be useful in patients with suspected prostatitis in providing supporting evidence of a diagnosis of chronic prostatitis and separating this from prostatodynia (Fig. 10) (Griffiths et al, 1984, 1990). Ejaculatory duct cysts and seminal vesicle cysts may be demonstrated by TRUS and may be aspired under ultrasound guidance if symptomatic. We have recently undertaken a retrospective review of 52 consecutive patients presenting with haemospermia (Etherington et al, 1990). Scan abnormalities were detected in 43 patients (83%). The patients included 24 with benign prostatic hyperplasia, three with seminal vesicle cysts, four with seminal vesicle calculi, two with marked asymmetry of the seminal vesicles and two patients with prostatitis. Prostatic calcification was noted in 32 patients and in eight patients this was in the region of the verumontanum or the ejaculatory ducts. Many clinicians feel that extensive and invasive investigations are unwarranted in the assessment of haemospermia, but the possibility of underlying malignancy is a major cause of anxiety in men with this symptom and the diagnosis of a specific abnormality by TRUS can reassure both the patient and the clinician that the cause of the symptom has been found. It may be recommended as the initial and possibly the only imaging investigation needed in patients presenting solely with haemospermia. It may also be used in the assessment of male patients with infertility: congenital absence of the seminal vesicles, or ejaculatory duct obstruction might be demonstrated in patients with azoospermia.

Much remains unknown about the prostate. Urologists have traditionally concentrated on transurethral resection to establish a diagnosis in patients with outflow obstruction, and digitally guided biopsy for the palpably abnormal gland. Treatment of prostatic cancer has varied between radical prostatectomy, various forms of radiotherapy, hormonal manipulation and deferred treatment. At least 80% of patients with prostatic cancer present with advanced and therefore incurable T_3 tumours. This situation is now changing in America, where the developments in anatomy, PSA and TRUS are leading towards earlier detection of cancer, and more accurate local staging, and newer techniques of radical surgery with nerve sparing are preventing the development of post-operative impotence following radical prostatectomy. Cancer of the prostate is not the innocent disease it is often thought to be and the 10 year survival of patients presenting with incidental impalpable T_0 tumours discovered at transurethral resection for outflow obstruction is lower than previously thought. We believe that the next decade will witness a major reappraisal of the current investigation and management of prostatic disease, and that radiologists and urologists in training should seize the opportunity to become proficient in the use of prostatic ultrasound.

Acknowledgments

The authors wish to thank the Medical Illustration Department of the Royal Gwent Hospital for providing the illustrations and Mrs B. Pritchard for typing the manuscript and expert secretarial help.

References

Blacklock, N. J. & Boushill, K., 1977. The zonal anatomy of the prostate in man and in the rhesus monkey (*Macaca mulatta*). *Urology Research, 5,* 163–167.

Brooman, P. J. C., Peeling, W. B., Griffiths, G. J., Roberts, E. E. & Evans, K. T., 1981. A comparison between digital examination and per rectal ultrasound in the evaluation of the prostate. *British Journal of Urology, 53,* 617–620.

Byar, D. R., Mostofi, F. K. & the Veterans Administration Co-operative Urological Research Group (VACURG), 1972. Carcinoma of the prostate: prognostic evaluation of certain pathological features in 208 radical prostatectomies examined by step sections techniques. *Cancer, 30,* 5–13.

Carpentier, P. J. & Schroeder, F. H., 1984. Transrectal ultrasonography in the follow up of prostatic carcinoma patients: a new prognostic parameter. *Journal of Urology, 131,* 903–905.

Chan, D. W., Bruzek, D. J., Oesterling, J. E., Rock, R. C. & Walsh, P. C., 1987. Prostatic specific antigen as a marker for prostate cancer: a monoclonal and a polyclonal immunoassay compared. *Clinical Chemistry, 33,* 1916–1920.

Clements, R., Griffiths, G. J., Peeling, W. B., Roberts, E. E. & Evans, K. T., 1988. How accurate is the index finger? A comparison of digital and ultrasound examination of the prostatic nodule. *Clinical Radiology, 39,* 87–89.

Clements, R., Griffiths, G. J., Peeling, W. B. & Edwards, A. M., 1989. Transrectal ultrasound in monitoring response to treatment of prostatic disease. *Urological Clinics of North America, 16,* 735–740.

Clements, R., Griffiths, G. J., Peeling, W. B. & Ryan, P. G., 1990. Experience with ultrasound guided transperineal prostatic needle biopsy 1985 to 1988. *British Journal of Urology, 65,* 362–367.

Ercole, C. J., Lange, P. H., Moatkisen, M., Chiou, R. K., Reddy, P. K. & Vessella, R. C., 1987. Prostate specific antigen and prostatic acid phosphatase in the monitoring and staging of patients with prostatic cancer. *Journal of Urology, 138,* 1181–1184.

Etherington, R., Clements, R., Griffiths, G. J. & Peeling, W. B., 1990. Transrectal ultrasound in the investigation of haemospermia. *Clinical Radiology, 41,* 175–177.

Friedman, A. C., Seidman, E. J., Radecki, P. D., Lev Toaff, A. & Caroline, D. F., 1988. Relative merits of MRI, transrectal endosonography and C. T. in the diagnosis and staging of carcinoma of the prostate. *Urology, 31,* 530–537.

Griffiths, G. J., Crooks, A. J., Roberts, E. E., Evans, K. T., Buck, A. C., Thomas, P. J. & Peeling, W. B., 1984. Ultrasonic appearances associated with prostatic inflammation: a preliminary study. *Clinical Radiology, 35,* 343–345.

Griffiths, G. J., Clements, R., Jones, D. R., Roberts, E. E., Peeling, W. B. & Evans, K. T., 1987. The ultrasonic appearances of prostatic cancer with histological correlation. *Clinical Radiology, 38,* 219–227.

Griffiths, G. J., Clements, R. & Peeling, W. B., 1990. Prostatic inflammatory disease and calculi. In *Prostatic Ultrasonography,* ed. by M. Resnick (B. C. Decker Inc., Philadelphia), Chapter 13, pp. 123–152.

Jewett, H. J., 1956. Significance of the palpable prostatic nodule. *Journal of the American Medical Association, 160,* 838–839.

Jones, D. R., Griffiths, G. J., Parkinson, M. C., Evans, K. T., Roberts, E. E., Davies, R. L., Harrison, T. J. & Peeling, W. B., 1989. Comparative histopathology, microradiography and per rectal ultrasonography of the prostate gland using cadaver specimens. *British Journal of Urology, 63,* 508–511.

Lee, F., Gray, J. M., McLeary, R. D., Meadows, T. R., Kumasaka, G. H., Borlaza, G. S., Straub, W. H., Soloman, M. H., McHugh, T. A. & Wolf, R. A., 1985. Transrectal ultrasound in the diagnosis of prostate cancer: location, echogenicity, histopathology, and staging. *Prostate, 7,* 117–129.

Lee, F., Littrup, P. J., Torp-Pedersen., S. T., Mettlin, C., McHugh, T. A., Gray, J. M., Kumasaka, G. H. & McLeary, R. D., 1988. Prostate cancer: comparison of transrectal ultrasonography and digital rectal examination for screening. *Radiology, 168,* 389–394.

Lee, F., Torp-Pedersen, S. T., Siders, D. B., Littrup, P. J. & McLeary, R. D., 1989. Transrectal ultrasound in the diagnosis and staging of prostatic carcinoma. *Radiology, 170,* 609–615.

Lowsley, O. S., 1912. The development of the human prostate gland with reference to the development of other structures of the neck of the urinary bladder. *American Journal of Anatomy, 13,* 299–349.

McNeil, J. E., 1969. Origin and development of cancer in the prostate. *Cancer, 23,* 24–34.

McNeil, J. E., 1981. The zonal anatomy of the prostate. *Prostate, 2,* 35–49.

Office of Population Censuses and Surveys, 1985. Cases of diagnosed cancer registered in England and Wales in 1982. *Series MBI No. 14* (HMSO, London).

Office of Population Censuses and Surveys, 1988. Cases of diagnosed cancer registered in England and Wales in 1984. *Series MBI No. 16* (HMSO, London).

Peeling, W. B., Griffiths, G. J., Evans, K. T. & Roberts, E. E., 1979. Diagnosis and staging of prostatic cancer by transrectal ultrasonography; a preliminary study. *British Journal of Urology, 51,* 565–569.

Rifkin, M. D., Kertz, A. B., Choi, H. Y. & Goldberg, B. B., 1983. Endoscopic ultrasonic evaluation of the prostate using a transrectal probe: prospective evaluation and acoustic characterization. *Radiology, 149,* 265–271.

Scardino, P. T., Shinohara, K., Wheeler, T. M. & Carter, S. C., 1989. Staging of prostate cancer. *Urological Clinics of North America, 16,* 713–734.

Schnall, M. D., Lenkinski, R. E., Pollock, H. M., Imai, Y. & Kressel, H. Y., 1989. Prostate: MR imaging with an endorectal surface coil. *Radiology, 172,* 570–574.

Silverberg, E. & Lubera, J. A., 1983. A review of American Cancer Society estimates of cancer cases and death. *A Cancer Journal for Clinicians, 33,* 2–8.

Stamey, T., 1989. Prostate specific antigen. In *Proceedings of the Fourth International Symposium on Transrectal Ultrasound in the Diagnosis and Management of Prostate Cancer, Chicago, 1989* pp. 24–28.

Torp-Pedersen, S. T., & Lee, F., 1989. Transrectal biopsy of the prostate guided by transrectal ultrasound. *Urological Clinics of North America, 16,* 703–712.

1991, *The British Journal of Radiology*, *64*, 201–209

Acute spinal cord injury: magnetic resonance imaging correlated with myelopathy

By Yasuyuki Yamashita, MD, Mutsumasa Takahashi, MD, Yasuharu Matsuno, MD, Ryutaro Kojima, MD, Yuji Sakamoto, MD, Tasturo Oguni, MD, *Terumi Sakae, MD and †E. Edmund Kim, MD

Department of Radiology, Kumamoto University, School of Medicine, 1-1-1, Honjo, Kumamoto 860, *Orthopaedic Department, Kumamoto Orthopaedic Hospital, 1-15-7 Kuhonji, Kumamoto 862, Japan and †Department of Diagnostic Radiology, University of Texas MD Anderson Cancer Center, 1515 Holcombe, Houston, Texas 77030, USA

(*Received June 1990 and in revised form August 1990*)

Keywords: Spinal cord, Wounds and injuries, MR studies, Spine, Myelopathy.

Abstract. Thirty-one patients (29 males and two females, 13–87 years of age (mean, 46.7 years)) with acute spinal cord injury were studied by MR (magnetic resonance) imaging and the results were correlated with neurological findings. Magnetic resonance images were obtained with a 0.5 T superconductive MR scanner (Phillips Gyroscan S5). Initial imaging was performed within 24 hours after trauma in 13 patients, 1–7 days in 13 patients and 7–14 days in five patients. Twenty-six patients underwent follow-up examinations with MR imaging. Cord abnormalities including cord compression (23 patients), cord swelling (seven patients), and abnormal signal intensities on either T_1 or T_2-weighted images (26 patients) were observed on initial examination. Multivariate analysis showed that cord compression and abnormal intensities on T_1-weighted images were important prognostic indicators. Hyperintensity on T_2-weighted images was non-specific but correlated well with clinical recovery. Magnetic resonance imaging is useful in predicting the prognosis and for planning treatment following spinal cord injuries.

Spinal cord injury is a very serious problem with much research directed to diagnosis, pathology, therapy and prognosis. The imaging techniques traditionally used include computed tomography and myelography along with conventional radiography (Brant-Zawadzki et al, 1981; Post & Green, 1983), but these, however, cannot directly demonstrate changes in the spinal cord. Magnetic resonance (MR) imaging has been able to demonstrate a variety of spinal cord abnormalities including haemorrhage, oedema, cysts and myelomalacia in the traumatized cords in patients (McArdle et al, 1986a; Kadoya et al, 1987; Kulkarni et al, 1987; Tarr et al, 1987; Beers et al, 1988; Goldberg et al, 1988; Mirvis et al, 1988; Quencer, 1988) and experimental animals (Hackney et al, 1986; Chakeres et al, 1987).

In this report, we analyse 31 cases of acute spinal cord injury and evaluate MR findings for predicting prognosis.

Materials and methods

Thirty-one patients (29 males and two females, 13–87 years of age (mean, 46.7 years)) with acute spinal cord injury were studied by MR imaging between June 1987 and June 1989 at the Kumamoto University and its affiliated hospitals. In 13 patients, MR imaging was performed within 24 hours after injury. Thirteen patients underwent MR imaging within 7 days, and five patients between 7 and 14 days after injury. After admission to the hospital, plain radiography was performed followed by MR imaging before a reduction procedure. Magnetic resonance imaging before and after cervical traction was obtained in six patients to evaluate the changes in the spinal cord.

Traction for dislocated vertebrae was performed in 11 patients, and surgical decompression in 13 patients. Eighteen patients were treated conservatively. One patient died 5 days after injury. Follow-up MR imaging was performed in 26 patients who showed cord abnormalities on the initial examination.

The neurological function of the spinal cord at the time of MR imaging and the clinical outcome was classified according to Frankel's classification (Frankel et al, 1969): A, complete injury (no neurological function beyond the level of the cord injury); B, preserved sensation only; C, preserved non-functional motor power; D, preserved functional motor power; and E, complete recovery or no neurological deficit. Patients who showed transient loss of neurological function (considered as spinal cord contusion) or no neurological deficit were not included in this study. At admission, 16 patients were classed as Frankel A, one B, 10 C and four D. In patients with incomplete injury (Frankel C, D), transverse myelopathy and central cord syndrome were each observed in nine patients.

Patients were followed up clinically from 6 to 20 months after injury. Twelve patients showed no neurological improvement from complete injury (poor prognosis). Seven patients showed some improvement but with a remaining neurological deficit (fair prognosis).

Address reprint requests to Yasuyuki Yamashita, MD, Department of Radiology, Kumamoto University School of Medicine, 1-1-1 Honjo, Kumamoto 860, Japan.

Table I. Multivariate regression analysis of prognostic factors

Variates (factors)	Coefficient	t*	p
Cord compression	0.736	2.165	0.040
Cord swelling	0.301	0.631	0.534
T_1	0.487	1.096	0.283
T_2	0.025	0.062	0.951

Proportion (R) 0.277, $F = 2.491$.
Scores for variates: 0 if no, 1 if yes.
Prognosis: 1 if good, 2 if fair, 3 if poor.
*t = coefficient/standard error.
T_1: T_1-weighted SE image; T_2: T_2-weighted SE image.

Twelve patients recovered fully or almost so, from complete or incomplete injury (good prognosis).

Magnetic resonance imaging was performed with a 0.5 T superconductive MR scanner (Philips Gyroscan S5) with a surface coil. Spin-echo (SE) images were obtained with a 400–450/30/4 time to repeat (TR)/time to echo (TE)/excitations) sequence for T_1-weighted images, a 1600–1800/50/2 (TR/TE/excitations) sequence for proton density images and a 1600–1800/100/2 (TR/TE/excitations) sequence for T_2-weighted images. The slice thickness was 5 mm with a gap of 2 mm. Patients in poor condition were examined with reduced averagings. Images were acquired using a surface coil (field of view (FOV) $6 \times 15\ \text{cm}^2$) on a 256×256 matrix. Gd-DTPA (0.1 mmol/kg) was used in three selected cases.

To assess the relationship of MR imaging with prognosis of myelopathy, multivariate regression analysis was performed using initial MR spinal cord findings as variables (Pearson, 1901). Scores were given in each category (see Table I) and standard partial regression coefficients, t-value and partial correlation coefficients were calculated. In this analysis, the prognostic significance of each factor is assessed separately while considering the prognostic significance of the other factors simultaneously.

Results: MR findings of acute spinal cord injuries

Skeletal and ligamentous abnormalities

Fractures of the vertebral body were observed in nine patients and subluxations in 16 patients. Ligamentous tears associated with subluxations were observed in eight patients. Haematomas around the ligaments or discs were observed in 13 patients and haematomas of the soft tissue in 15. These changes were frequently observed in patients with severe spinal cord dysfunction

Table II. Spine and ligament abnormality in spinal cord injury

Initial spinal cord function*	Number of patients	Spine		Ligament tear	Haematoma of ligament and/or disc
		Fracture	Subluxation		
A/B	18	6	10	7	11
C	10	3	5	0	2
D	3	0	1	1	0

*According to Frankel's classification: A, complete injury; B, preserved sensation only; C, preserved non-functional motor power; D, preserved functional motor power; E, complete recovery or no neurological deficit.

Table III. Cord abnormality in initial study and prognosis

Initial spinal cord function*	Recovery	Number of patients	Cord compression	Cord swelling	Abnormal intensity	
					T_1	T_2
A/B (18 patients)	Poor	12	10	5	6	11
	Fair	5	5	0	0	4
	Good	1	1	0	0	0
C (10 patients)	Poor	0	—	—	—	—
	Fair	2	1	0	0	2
	Good	8	5	1	1	6
D (3 patients)	Poor	0	—	—	—	—
	Fair	0	—	—	—	—
	Good	3	1	1	1	3

*According to Frankel's classification.
T_1: T_1-weighted SE image; T_2: T_2-weighted SE image.

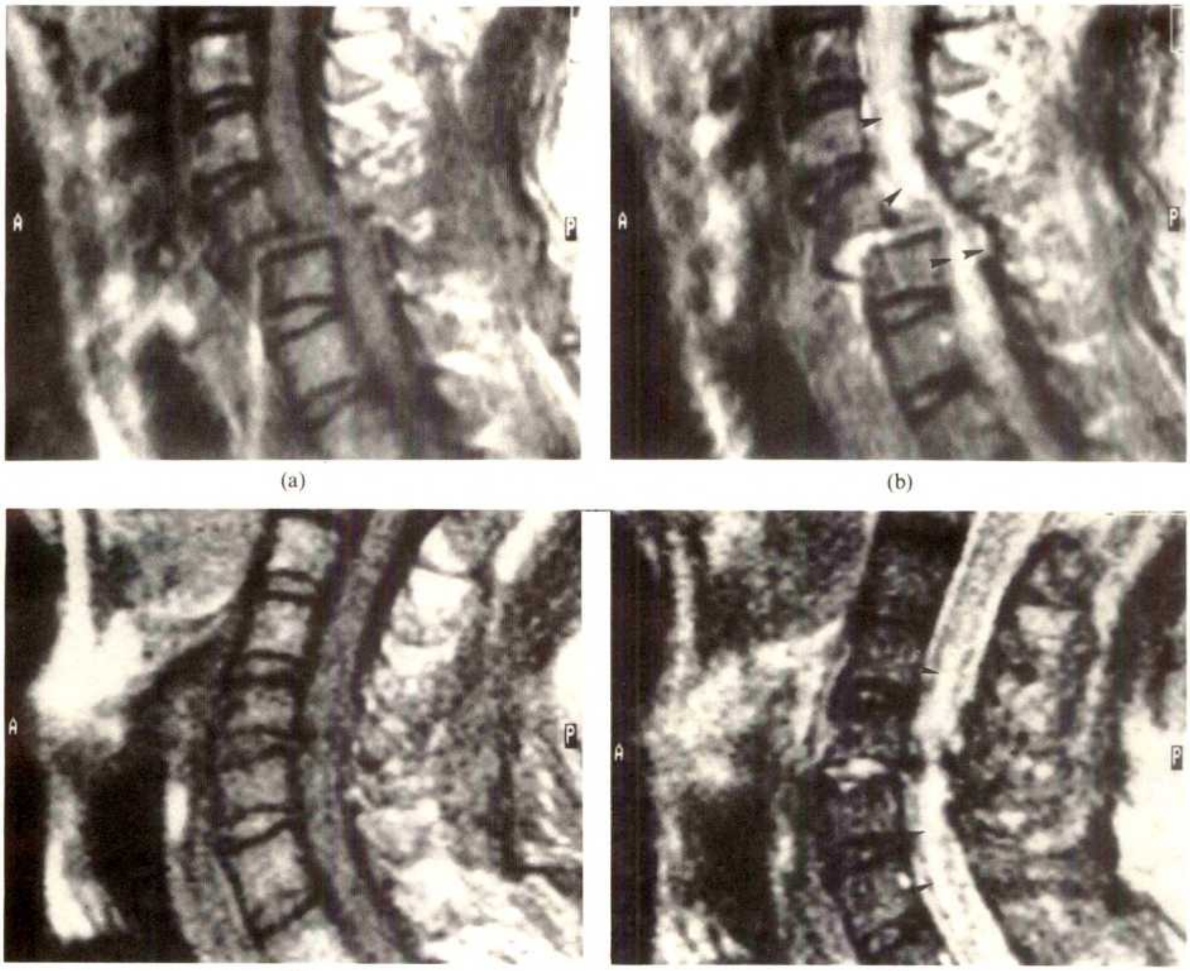

(a) (b) (c) (d)

Figure 1. Magnetic resonance imaging of a 26-year-old man obtained 40 hours after fall. He showed complete tetraplegia at the time of admission and died 5 days after injury because of respiratory failure. (a) Sagittal SE 400/30 image before cervical reduction surgery shows marked spinal cord compression by C6 and herniated disc of C5-6. (b) Sagittal SE 1600/100 image shows hyperintensity of the cord (arrowheads) with hyperintensity lesion of the anterior longitudinal ligament and C5-6 disc, and posterior longitudinal ligament. Hyperintensity of the cervical soft tissue is also observed. (c) Sagittal SE 400/30 image immediately after cervical traction reveals cord swelling. Cord is still compressed at C5-6. (d) Sagittal SE 1600/100 image shows marked longitudinal hyperintensity in the grey matter of the cord (arrowheads).

(Table II). In 12 patients, no skeletal or ligamentous injuries were observed in spite of the cord injuries. Ossification of the posterior longitudinal ligament was observed in seven of these patients.

Spinal cord abnormalities

The spinal cord abnormalities demonstrated by MR imaging were cord compression, swelling and abnormal signal intensities within the spinal cord (Table III). Spinal cord compression was observed in 23 patients (severe in 11 patients and slight in 12). The causes of spinal cord compression included subluxation of the vertebral body in 11 (Figs 1–3), ossification of the posterior longitudinal ligament in seven (Fig. 4), osteophyte or herniated disc (Fig. 5) in five each.

Slight cord swelling was observed in seven patients on the initial study (Figs 1 and 5), including four patients who developed marked swelling after cervical traction (Fig. 6). Two patients did not show cord swelling after cervical traction in spite of severe cord compression (Fig. 2).

Abnormal signal intensities from the spinal cord were observed in 26 patients (six patients with hyperintensity (Fig. 3), four patients with hypointensity on T_1-weighted images (Fig. 5), and 26 patients with hyperintensity on T_2-weighted images). Twenty patients showed abnormal signal intensities with cord compression, while six patients showed abnormal cord signal

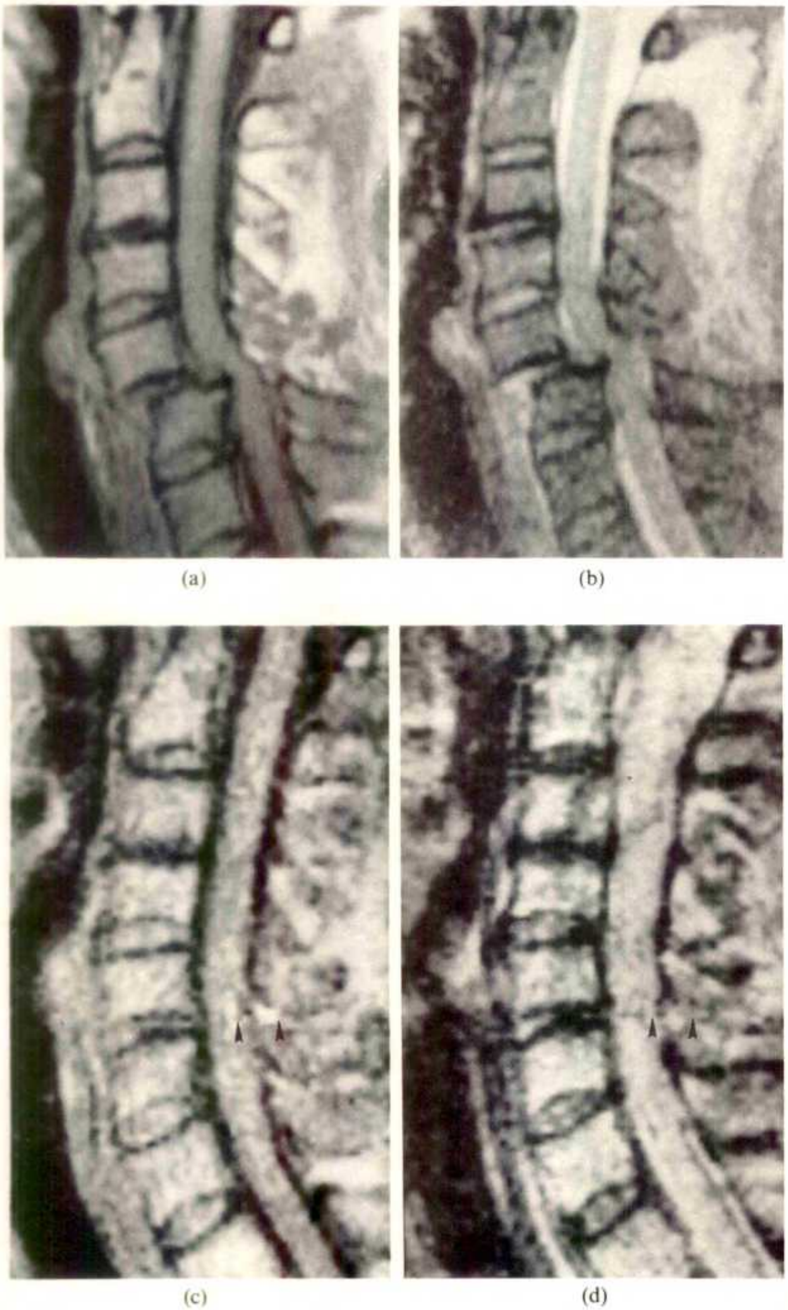
(a) (b)
(c) (d)

Figure 2. Magnetic resonance imaging of a 60-year-old man obtained 8 hours after injury. He showed complete paraplegia at the time of admission but recovered after treatment (Frankel A–C). (a) Sagittal SE 400/30 image shows subluxation of C5, disruption of the anterior longitudinal ligament. The spinal cord is severely compressed but the signal intensity is normal. (b) Sagittal SE 1600/100 image shows hyperintensity along the anterior longitudinal ligament, C4-5 disc and posterior longitudinal ligament. Hyperintensity of the cervical soft tissue is also observed. The cord shows no abnormal signal intensity. Magnetic resonance imaging immediately after cervical traction (one averaging) reveals no cord swelling with no abnormal signal intensity on (c) SE 400/30 and (d) 1600/100 images. Artifact due to traction device is seen (arrowheads).

intensities without demonstration of cord compression (Fig. 4).

The central cord syndrome was frequently observed in patients without subluxation or fracture. Ossification of the posterior longitudinal ligament was present in four out of nine patients. Eight of the nine patients with central cord syndrome showed spotty hyperintensity on T_2 weighted images (Fig. 4).

Relationship of MR findings and functional prognosis

Patients who showed poor recovery tended to have severe cord compression, cord swelling and abnormal intensity on T_1 and T_2-weighted images (Table III). These four MR findings were analysed for prognostic significance. The results showed that the degree of cord compression was the most important prognostic indicator, followed by abnormal intensity on T_1-weighted

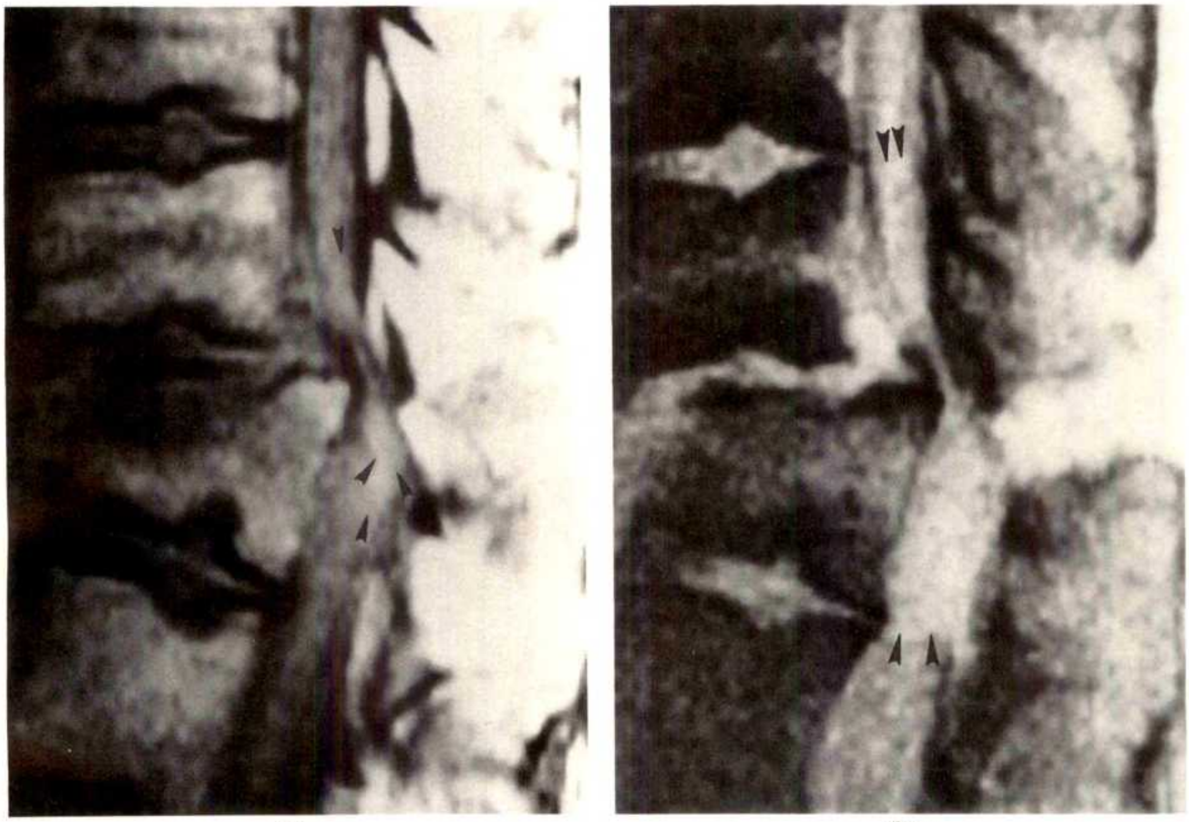
(a) (b)

Figure 3. Magnetic resonance imaging of a 27-year-old man obtained 5 hours after injury. He showed complete paraplegia at the time of admission and did not show any neurological improvement (Frankel A–A). (a) Sagittal SE 400/30 image shows subluxation of T11. The spinal cord is severely compressed and showed slight hyperintensity (arrowheads). (b) Sagittal SE 1600/100 image shows hyperintensity along the disc and posterior longitudinal ligament and posterior compartment. The cord shows hyperintensity within the cephalic and caudal portion of the cord, more extensively than SE 400/30 image (arrowheads).

images (Table I). Cord swelling and hyperintensity on T_2-weighted images were frequently observed in patients with poor progress, but multivariate analysis showed these findings were non-specific.

Follow-up MR studies

Two patients developed extensive irregular intensity both on T_1 and T_2-weighted images after cervical traction (Figs 1 and 4).

Hyperintensity on T_2 weighted images in eight patients persisted during the chronic stage (Fig. 6), decreased in eight patients, disappeared in two patients and progressed in one patient. Patients whose hyperintensity progressed or persisted tended to have poor prognosis, while patients whose hyperintensity decreased or disappeared tended to have good prognosis (Table IV).

Most of the patients who showed abnormal intensity on T_1-weighted images did not show reversal of signal intensity. Two patients with isointensity and three patients with hyperintensity on T_1-weighted images during the acute stage developed hypointensity during the chronic stages, and hypointensity during the acute stage progressed during the chronic stage in two patients. Two patients cannot be evaluated for spinal cord changes because of artifacts due to surgery.

Table IV. Correlation of cord intensity changes on follow-up MR imagings and prognosis*

	T_1			T_2			
	NC	C	N	NC	De	Di	N
Poor (12 patients)	1	5	6	7	2	0	3
Fair (5 patients)	0	1	4	2	2	0	1
Good (9 patients)	1	0	8	1	3	2	3

*Twenty-six cases who received follow-up examination.
T_1: T_1-weighted SE image; T_2: T_2-weighted SE image; NC: no change or progression of abnormal intensity on either T_1 or T_2; C: hyperintensity changed into hypointensity on T_1; De: hyperintensity decreased on T_2; Di: hyperintensity disappeared on T_2; N: normal intensity from initial examination.

P25859

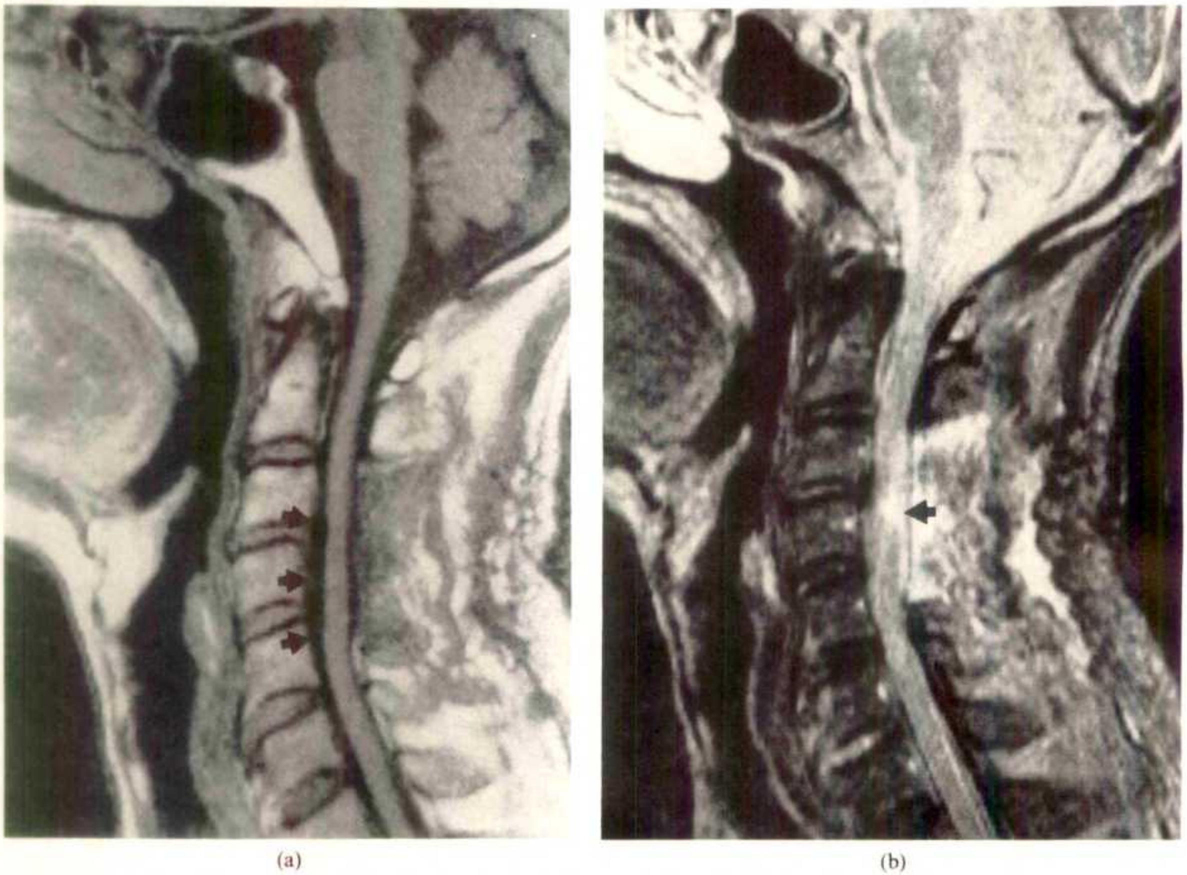

Figure 4. Magnetic resonance imaging of a 52-year-old man obtained 5 hours after injury. He showed incomplete paraplegia more severe in the upper extremities at the time of admission (considered as central cord syndrome) but recovered after conservative treatment (Frankel C–D). (a) Sagittal SE 400/30 image shows no fracture or subluxation of vertebral bodies. The spinal cord is compressed by ossification of the posterior longitudinal ligament (arrows). (b) SE 1600/100 image, the cord shows spotty hyperintensity (arrow). Hyperintensity of the soft tissue of the neck is observed.

Discussion

Magnetic resonance imaging in spinal cord injury has been shown to be useful in evaluating spinal cord changes as well as disc, ligament and osseous abnormalities (McArdle et al, 1986a; Kadoya et al, 1987; Goldberg et al, 1988; Mirvis et al, 1988). However, MR imaging of acute spinal cord injuries has not been fully evaluated because of the difficulty in imaging critically ill patients in the presence of ferromagnetic stabilization devices and life support systems. A cervical halo will often prevent use of a surface coil. In this series, we performed MR imaging before these devices were attached to the patients. Recently, a pulley device attached to a water bag that allows constant traction within an MR magnet in ventilator-dependent patients has been developed (McArdle et al, 1986b; Quencer, 1988).

Changes in acute spinal cord injury have been well demonstrated in experimental animals and human patients (Davison, 1943; Assenmacher & Ducker, 1971; Ducker et al, 1971; Wagner et al, 1971; Dohrmann, 1972; Osterholm, 1974; Ducker, 1976; Foo et al, 1981). Depending on the degree of trauma, the spinal cord may appear grossly normal or show various degrees of contusion, swelling and transection. Parenchymal changes of the spinal cord after injury are related to various factors including blood flow, tissue fluid and osmotic changes, haemorrhage, and enzymatic and biochemical activities. Necrosis with variable haemorrhage is visible by 2 hours and extends considerably by 4 hours. At an early stage, infarction also develops, especially at the grey–white matter junction (Zuelch, 1954; Turnbull et al, 1966). Following the acute stage of 5–7 days, edema, and metabolic and vascular changes in the traumatized cord decrease, and some neurological recovery is expected as a result (Quencer, 1988).

Pathological changes occurring from the trauma within the spinal cord are demonstrated as abnormal intensity and swelling on MR imaging. At low-field MR scan, the T_1 relaxation time of haemorrhage is similar to

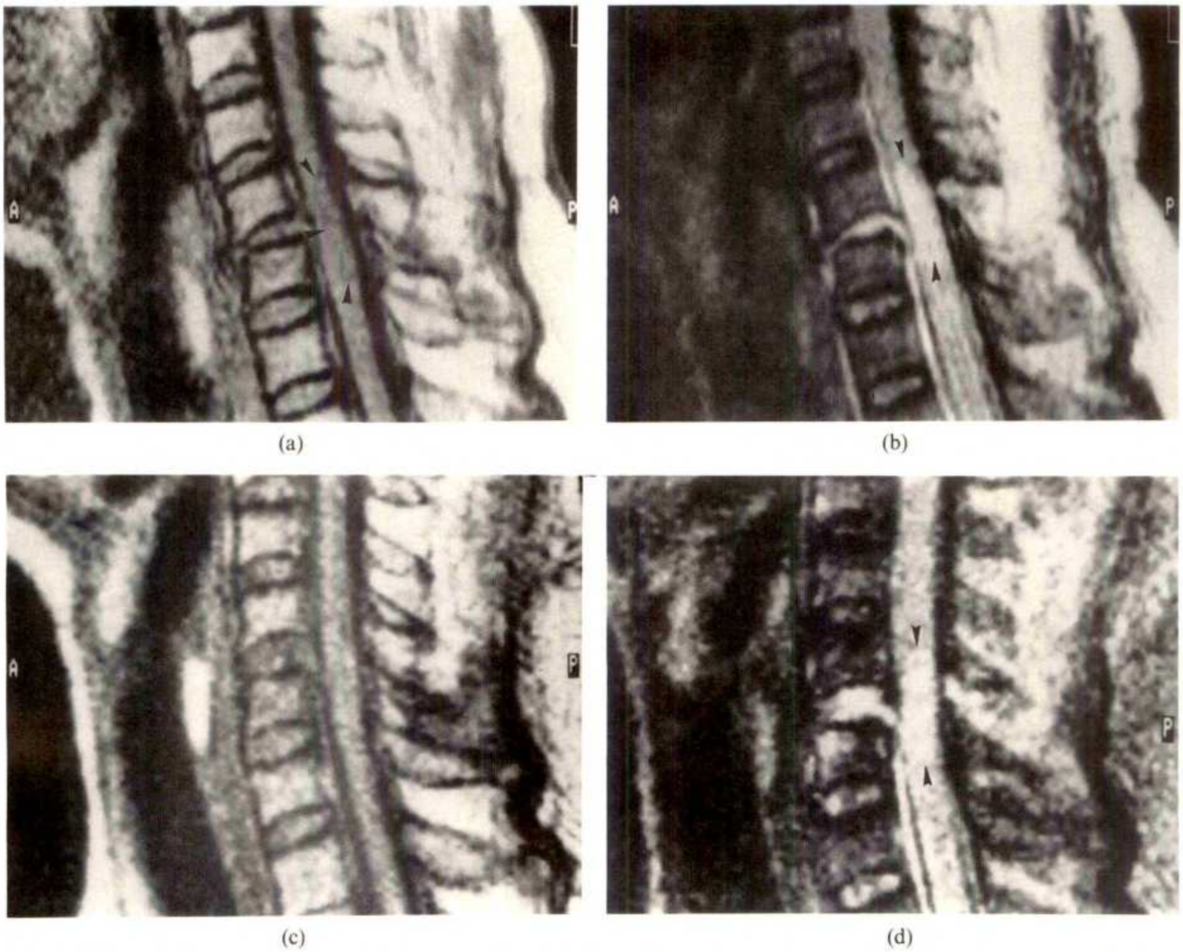

Figure 5. Magnetic resonance imaging of a 63-year-old man obtained 12 hours after injury. He showed complete tetraplegia at the time of admission and did not show any signs of recovery (Frankel A–A). (a) Sagittal SE 400/30 image after cervical reduction shows slight hypointensity of the cord with cord swelling (arrowheads). (b) Sagittal SE 1600/100 image shows hyperintensity of the cord (arrowheads) with hyperintensity of the anterior longitudinal ligament, C5-6 disc and posterior longitudinal ligament. (c) Magnetic resonance imaging 6 days after trauma (one averaging) reveals no cord swelling with normal intensity on SE 400/30. (d) Sagittal SE 1600/100 image shows hyperintensity of the cord (arrowheads) and disc. This hyperintensity did not disappear on MR imaging performed 30 days after trauma.

that of grey matter, whereas the T_2 relaxation time is significantly longer (Delapaz et al, 1984; Chiro, 1986; Beers et al, 1988). Therefore, the acute haematoma is isointense on T_1-weighted images and hyperintense on T_2-weighted images (Kadoya et al, 1987). These findings are similar to those of oedema. In contrast, at high-field MR scan, spinal cord haemorrhage is seen as an area of slight hypointensity on T_2-weighted images similar to haemorrhages in the brain in their very earliest stages (Hackney et al, 1986; Tarr et al, 1987; Quencer, 1988).

Kulkarni et al (1987) compared the signal intensity with neurological improvement using a 1.5 T MR system. They concluded that patients with low intensity on T_2-weighted images (considered to represent haematomyelia) had a poor prognosis. The frequency of haematomyelia, however, is rare in a large autopsy series in patients with acute spinal cord injuries (Blackwood, 1963; de la Torre, 1981). Therefore, it is unlikely that most of the patients with irreversible cord injury have haematomyelia.

Many factors affect prognosis. Based on MR imaging findings in the acute stage, we can predict the prognosis to some extent. The degree of cord compression appears to be the most important factor. However, some patients with severe cord compression who showed normal intensity on T_1 and T_2-weighted images had a good prognosis. Most patients who showed abnormal intensity on T_1-weighted images did not later recover. Hyperintensity itself on T_2-weighted images seems nonspecific. Most patients who had myelopathy showed

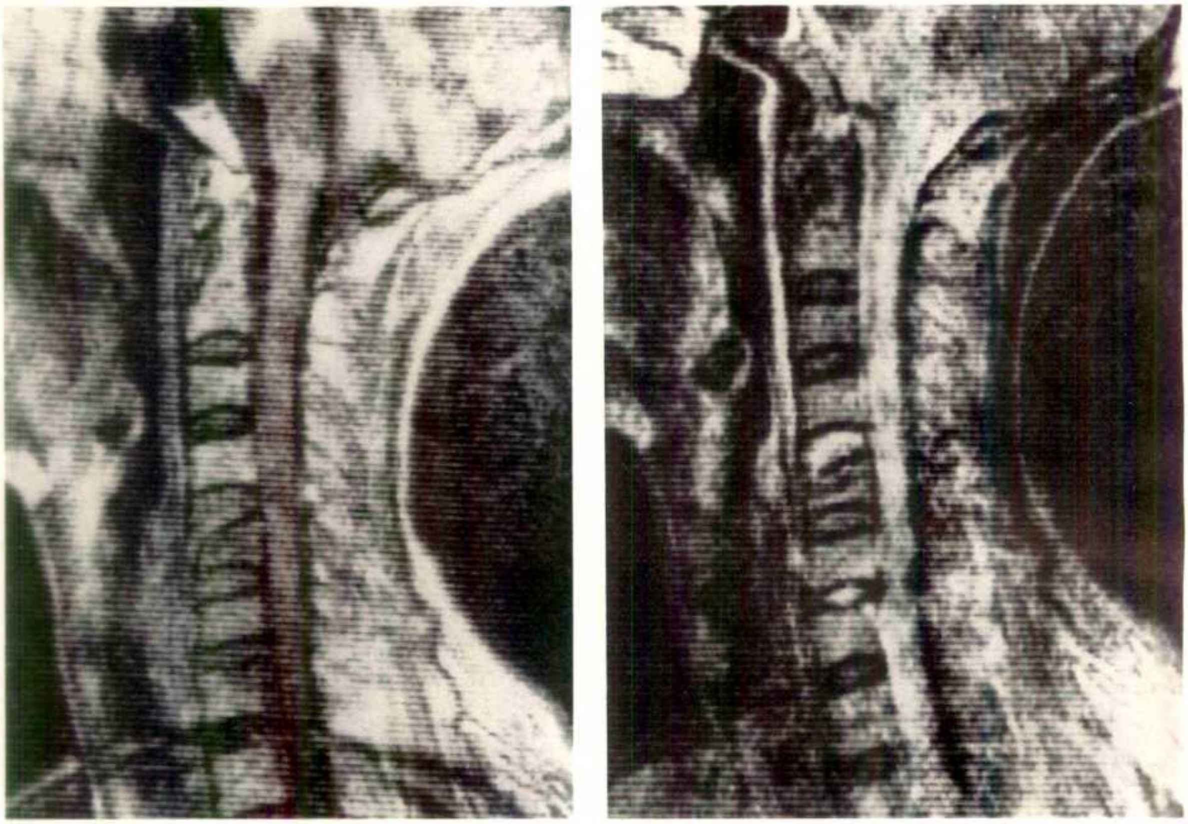

Figure 6. Magnetic resonance imaging of a 66-year-old man obtained 4 hours after a traffic accident. He showed complete paraplegia with no recovery (Frankel A–A). Magnetic resonance imaging 4 days after cervical traction reveals marked swelling of the spinal cord with irregular intensity both on sagittal SE 400/30 (a) and 1800/100 (b) images.

hyperintensity on T_2-weighted images regardless of outcome. However, a follow-up MR study showed good correlation between the changes in spinal cord signal intensity on T_2-weighted images and neurological recovery. The intensity on T_2-weighted images is considered to be a useful sign for clinical follow-up. Hyperintensity decreased or disappeared in patients with good recovery, while hyperintensity was unchanged in patients with a subsequent poor prognosis.

Patients who developed the central cord syndrome showed a spotty hyperintensity in the acute or chronic stages, probably representing persistent oedema, gliosis or a small haematomyelia in the central grey matter as a result of a lesser degree of trauma (Blackwood, 1963; Fox et al, 1988). This syndrome was frequently observed in patients without fracture and subluxation. Most of the patients had spinal canal stenosis (ossification of posterior longitudinal ligament, etc.) when minor trauma can cause spinal cord damage.

Magnetic resonance examination of acute injury in patients with incomplete injuries is considered to be particularly important (de la Paz et al, 1984). Traumatic disc herniation in association with a fracture, dislocation and a hematoma compressing the spinal cord requires immediate surgery. Some degree of neurological improvement can be expected in patients without severe cord compression or abnormal signal intensity on T_1 weighted images.

References

ASSENMACHER, D. R. & DUCKER, T. B., 1971. Experimental traumatic paraplegia: the vascular and pathological changes seen in reversible and irreversible spinal-cord lesions. *Journal of Bone and Joint Surgery, American Volume, 53*, 671–680.

BEERS, G. J., RAQUE, G. H., WAGNER, G. G., SHIELDS, C. B., NICHOLS, G. R. II., JOHNSON, J. R. & MEYER, J. E., 1988. MR imaging in acute cervical spine trauma. *Journal of Comptuter Assisted Tomography, 12*, 755–761.

BLACKWOOD, W., 1963. Vascular disease of the central nervous system. In *Greenfield's Neuropathology*, ed. by M. Blackwood, W. H. McMenemy, A. Meyer, R. M. Norman & D. S. Russel (Williams & Wilkins, Baltimore).

BRANT-ZAWADZKI, M., MILLER, E. M. & FEDERLE, M. P., 1981. CT in the evaluation of spinal trauma. *American Journal of Roentgenology, 136*, 369–375.

CHAKERES, D. W., FLICKINGER, F., BRESNAHAN, J. C., BEATTIE, M. S., WEISS, K. L., MILLER, C. & STOKES, B. T., 1987. MR imaging of acute spinal cord trauma. *AJNR, 8*, 5–10.

Chiro, G. D., Brooks, R. A. & Girton, M. E., 1986. Sequential MR studies of intracerebral hematomas in monkey. *American Journal of Neuroradiology, 7*, 193–199.

Davison, C., 1943. Pathology of the spinal cord as a result of trauma. *Research Publications, Association for Research in Nervous and Mental Diseases, 24*, 151–187.

Dohrmann, G. J., 1972. Experimental spinal cord trauma: a historical review. *Archives of Neurology (Chicago), 27*, 468–473.

Ducker, T. B., 1976. Experimental injury of the spinal cord. In *Handbook of Clinical Neurology. Vol. 25, Injuries of the Spine and Spinal Cord*, ed. by P. J. Vinkun (North Holland, Amsterdam) pp. 9-26.

Ducker, T. B., Kindt, G. W. & Kempe, L. C., 1971. Pathological findings in acute experimental spinal cord trauma. *Journal of Neurosurgery, 35*, 700–708.

Foo, D., Bignami, A. & Rossier, A. B., 1981. Posttraumatic anterior spinal cord syndrome: pathological studies of two patients. *Surgical Neurology, 17*, 370.

Fox, J. L., Wener, L., Drennan, D. C., Manz, H. J., Won, D. J. & Al-Mefty, O., 1988. Central spinal cord injury: magnetic resonance imaging confirmation and operative consideration. *Neurosurgery, 22*, 340–347.

Frankel, H. L., Hancock, D. O., Hyslop, G., Melzak, J., Michaesis, L. S., Ungar, G. H., Vernon, J. D. S. & Wilsh, J. J., 1969. The value of postural reduction in initial management of closed injuries of the spine with paraplegia and tetraplegia. *Paraplegia, 7*, 179–192.

Goldberg, A. L., Rothfus, W. E., Deeb, Z. L., Daffner, R. H., Lupetin, A. R., Wilberger, J. E. & Prostko, E. R., 1988. The impact of magnetic resonance on the diagnostic evaluation of acute cervicothoracic spinal trauma. *Skeletal Radiology, 17*, 89–95.

Hackney, D. B., Asato, R., Joseph, P. M., Carvlin, M. J., McGrath, J. T., Grossman, R. I., Kassab, E. A. & de Simone, D., 1986. Hemorrhage and edema in acute spinal cord compression: demonstration by MR imaging. *Radiology, 161*, 387–390.

Kadoya, S., Nakamura, T., Kobayashi, S. & Yamamoto, Y., 1987. Magnetic resonance imaging of acute spinal cord injury. *Neuroradiology 29*, 252–255.

Kulkarni, M. V., McCardle, C. B., Kopanicky, D., Miner, M., Cotler, H. B., Lee, K. F. & Harris, J. H., 1987. Acute spinal cord injury: MR imaging at 1.5 T. *Radiology, 164*, 837–843.

McArdle, C. B., Crofford, M. J., Mirafakhraee, M., Amparo, E. G. & Calhoun, J. S., 1986a. Surface coil MR of spinal trauma: preliminary experience. *AJNR, 7*, 885–893.

McArdle, C. B., Wright, J. W., Prevost, W. J., Dornfest, D. J. & Amparo, E. G., 1986b. MR imaging of the acutely injured patient with cervical traction. *Radiology, 159*, 273–274.

Mirvis, S. E., Geisler, F. H., Jelinek, J. J., Joslyn, J. N. & Gellad, F., 1988. Acute cervical spine trauma: evaluation with 1.5-T MR imaging. *Radiology, 166*, 807–816.

Osterholm, J. L., 1974. The pathophysiological response to spinal cord injury: the current status of related research. *Journal of Neurosurgery, 40*, 3–33.

de la Paz, R. L., New, P. F. J., Buonanno, F. S., Kistler, J. P., Oot, R. F., Rosen, B. R., Taveras, J. M. & Brady, T. J., 1984. MR imaging of intracranial hemorrhage. *Journal of Computer Assisted Tomography, 8*, 599–607.

Pearson, K., 1901. On lines and planes of closest fit to systems of points in space. *Philosophical Magazines and Journal of Science, 2*, 559–572.

Post, M. J. & Green, B. A., 1983. Use of computed tomography in spinal trauma. *Radiologic Clinics of North America, 21*, 327–375.

Quencer, R. M., 1988. The injured spinal cord: evaluation with magnetic resonance and intraoperative sonography. *Radiologic Clinics of North America, 26*, 1025–1045.

Tarr, R. W., Drolshager, L. F., Kerner, T. C., Allen, J. H., Partain, C. L. & James, A. E., Jr., 1987. MR imaging of recent spinal trauma. *Journal of Computer Assisted Tomography, 11*, 412–417.

de la Torre, J. C., 1981. Spinal cord injury: review of basic and applied research. *Spine, 6*, 315–335.

Turnbull, I. M., Brieg, A. & Hassler, O., 1966. Blood supply of cervical spinal cord in man: a microangiographic study. *Journal of Neurosurgery, 24*, 951–965.

Wagner, F. C., Dorman, G. J. & Bucy, P. C., 1971. Histopathology of transitory traumatic paraplegia in the monkey. *Journal of Neurosurgery, 35*, 272–276.

Zuelch, K. J., 1954. Mangeldurchblutung an der Grenzzone zweiter Gefaessgebiete als Ursache bisher ungeklaerter Rueckenmarksschaedigungen. *Surgical Neurology, 172*, 81–101.

1991, *The British Journal of Radiology*, *64*, 210–216

In vivo phosphorus-31 magnetic resonance spectroscopy of normal and pathological breast tissues

By O. M. Redmond, PhD, J. P. Stack, MRCPI, FFR(RCSI), N. G. O'Connor, SRN, M. B. Codd, MB, MPH and J. T. Ennis, MD, FRCPI, FRCR

Institute of Radiological Sciences, 52 Eccles Street, Dublin 7, Ireland

(*Received November 1989 and in revised form August 1990*)

Keywords: Phosphorus-31 MRS, Breast, Malignant, Benign, Tissue characterization

Abstract. *In vivo* phosphorus-31 magnetic resonance spectroscopy, at 1.5 T, in addition to magnetic resonance imaging and mammography, was performed on the breast tissue of 59 subjects, using a 40 mm or 80 mm surface coil for spectral localization. The patients were divided into three groups: Group 1, 46 control subjects; Group 2, nine patients with breast carcinoma; Group 3, four patients with benign breast disease. The relationship of age, menopausal status, breast size and pattern, use of contraceptive pill and history of breast disease to spectral characteristics of breast tissue was examined for the control group. In multivariate analysis, only menopausal status and age were found to be significantly related to tissue biochemistry. Pre-menopausal women had reduced phosphocreatine (PCr) (%) ($p = 0.02$), and increased phosphomonoesters (PMEs) and β-nucleotide triphosphate (β-NTP) (%) ($p = 0.05$), while the fat-to-water ratio was higher in older women ($p = 0.02$). No significant differences were identified between the control subjects and the patients with benign breast disease. When spectra from patients with breast carcinoma were compared with an age-matched volunteer group, α- and γ-NTP (%) were found to be higher in the cancer tissue ($p < 0.01$ and $p = 0.01$, respectively), while PCr (%) was reduced ($p < 0.01$). The ratio β-NTP:PCr was higher in the carcinoma group of patients ($p < 0.05$). *In vivo* phosphorus-31 magnetic resonance spectroscopy is a non-invasive examination which may prove useful in the early differentiation of malignant breast disease from normal and benign conditions.

It is estimated that one in 14 women in western society can expect to develop breast carcinoma in their lives, but there is, as yet, no single biochemical test to identify women "at risk". The main risk factors associated with breast carcinoma include menstrual, reproductive and family histories (Kelsey, 1979; Ottman et al, 1983). Strong and/or prolonged oestrogen stimulus has also been associated with increased risk, although the mechanism of action is poorly understood (Vihko & Apter, 1986). This suggests that there may be an, as yet, unidentified high risk endocrine or biochemical profile.

Phosphorus-31 magnetic resonance spectroscopy (MRS) is a non-invasive technique that has been used for many years to study metabolism *in vitro* and experimental animals *in vivo* (Moon & Richards, 1973; Cozzane & Jardetzky, 1976; Ackerman et al, 1980; Evanochko et al, 1982; Ng et al, 1982; Evanochko et al, 1983, 1984; Hollander, 1986; Irving et al, 1986; Mountford et al, 1986; Sijens et al, 1987). The phosphorus-containing biomolecules, which contribute to the spectrum, include the low energy phosphomonoesters (PMEs) and phosphodiesters (PDEs), thought to be important precursors in cell membrane formation and products of phospholipid catabolism respectively (Cozzane & Jardetzky, 1976). The relative concentration of the inorganic phosphate (Pi) peak and the high energy phosphates, phosphocreatine (PCr) and nucleotide triphosphates (NTP), provide valuable information with respect to tissue energetics, while the position of Pi is an indicator of intracellular tissue pH. (This is calculated by measuring the chemical shift of Pi, which varies within the physiological pH range to a peak of fixed position within this range, such as PCr or β-NTP.)

Whole-body MR imagers, operating at 1.5 T or greater, have recently become available, enabling *in vivo* MRS of human tissues to be performed. Owing to the superficial nature of breast tissue, surface coils were used in this study to obtain phosphorus-31 spectra. This is a simple and quick method of spectral localization; however, the risk of contamination from adjacent muscle tissue is high.

To date, phosphorus-31 MRS of human breast tissue has been attempted by a small number of groups (Cohen et al, 1986; Degani et al, 1986; Oberhaensli et al, 1986; Sijens et al, 1987; Merchant et al, 1988; Redmond et al, 1988; Sijens et al, 1988). Using perchloric acid extracts, Merchant et al (1988) demonstrated that malignant, benign and non-involved breast tissue could be differentiated *in vitro* on the basis of phosphorus-31 MR spectra. *In vivo* results have varied considerably, which is not surprising since patient numbers tended to be very small. A number of groups (Degani et al, 1986; Oberhaensli et al, 1986; Merchant et al, 1988; Redmond et al, 1988) have obtained phosphorus-31 spectra of breast carcinoma *in situ* and found an increase in the concentration of PME in breast carcinomas and a decrease in the fat-to-water ratio (FWR). To our knowledge, there has been no extensive study to investigate the variation in phosphorus-31 metabolites in normal breast tissue.

We performed *in vivo* phosphorus-31 MRS on 46 normal volunteers and examined the relative concentra-

---

Address correspondence to: Dr O. M. Redmond, Institute of Radiological Sciences, 52 Eccles Street, Dublin 7, Ireland.

tions of phosphorus-31 metabolites in relation to the following factors: age, stage of menstrual cycle, breast size and pattern, use of contraceptive pill and history of breast disease. We also attempted to characterize benign and malignant breast lesions on the basis of their *in vivo* phosphorus-31 MR spectra.

Patients and methods

Phosphorus-31 MRS and magnetic resonance imaging (MRI) were performed on a total of 59 women who were divided into three groups. Group 1 consisted of 46 volunteers (mean, 45 years; range, 20–68 years). The volunteers were asked to complete a questionnaire which gave information with respect to menopausal status, use of contraceptive pill, family history of breast disease and history of breast feeding. Group 2 ($n = 9$) had biopsy proven breast carcinoma (mean, 58 years; range, 49–74 years). One patient (patient 13) had bilateral breast carcinoma. Spectra from both breasts were very similar and only one set of peak areas (from the left breast) was included for data analysis (see Table I). All of these patients had MRI and MRS examinations prior to surgery and/or chemotherapy. Group 3 consisted of four patients with biopsy proven benign breast disease (mean, 52 years; range, 48–57 years), all of whom had MRI and MRS performed.

Magnetic resonance imaging and MRS were carried out with a whole-body 1.5 T superconducting magnet (Siemens Magnetom). Both breasts were imaged with the patient in a supine position, the body coil acting as the transmitter and receiver. A multislice T_1-weighted sequence (repetition time (TR) = 0.5 s, echo time (TE) = 17 ms) was used as a localization technique for spectroscopy as the phosphorus-31 surface coil was in position during the sequence. In addition, this sequence gave useful information with respect to breast size and pattern, and location and size of any lesions. From these MR images, the breast pattern was deemed to be (1) largely glandular (less than 30% fat), (2) mixed glandular and fatty (30–70% fat), or (3) fatty (greater than 70% fat). Breast size was determined from the maximum distance from the skin of the breast to the chest wall. While supine positioning of the patient increased the likelihood of muscle contamination, we attempted to minimize this by using the 40 mm diameter surface coil when the distance from the skin to the chest wall was less than or equal to 5 cm. When this distance was greater than 5 cm, the 80 mm coil was used. The transmitter voltage was selected (from calibration graphs constructed from phantom studies) depending on coil size and the distance from the skin to the chest wall, in order to obtain the maximum signal from the breast tissue with minimal contamination from muscle. Hydrogen-1 images were acquired with the phosphorus-31 surface coil acting as receiver. Although the volumes sampled at hydrogen and phosphorus frequencies do not correlate precisely, owing to differences in coil sensitivity at the different frequencies, this procedure is useful to ensure accurate positioning of the surface coil and to give a rough estimate of the sampled volume of the resulting spectral data.

Initially, equal numbers of spectra were obtained from the right and left breasts. It soon became apparent, however, that spectra from the left breast had inferior resolution due to cardiac motion. Consequently, spectra were preferentially obtained from the right breast. Shimming of the magnetic field B_0 to the sensitive volume of the surface coil was done at hydrogen frequency (63 MHz) until the resolution (full width at half maximum (FWHM)) of the proton peak from tissue water was less than 0.5 ppm. This was not always possible, however, owing to respiratory and cardiac movement and in a small number of cases ($n = 3$) the resolution (FWHM) was as poor as 1.0 ppm.

Table I. Characteristics of patient group

Patient	Age (years)	Histology	Remarks
1	51	Infiltrating intraductal carcinoma	2 × 1 cm^3 masses
2	53	Infiltrating, poorly differentiated ductal carcinoma	5 cm diameter, metastatic disease in 3 axillary nodes
3	56	Infiltrating, poorly differentiated ductal carcinoma	5 cm diameter, metastatic disease in 7 axillary nodes
4	49	Infiltrating, high-grade poorly differentiated carcinoma	13 cm diameter
5	74	Infiltrating ductal carcinoma	2 cm diameter
6	56	Diffusely infiltrative, poorly differentiated lobular carcinoma	8 cm diameter, metastatic disease in 7 axillary nodes
7	65	Infiltrating intraductal and intralobular carcinoma	3 cm diameter
8	65	Ductal adenocarcinoma	3 cm diameter
9	52	Fibrocystic disease/focal epitheliosis	Multiple small cysts ($\leqslant$ 1 cm)
10	57	Benign dysplastic breast disease	
11	48	Fibrocystic disease	
12	53	Fibrocystic disease	Diameter of cyst, 3 cm aspirated
13	58	Bilateral infiltrating ductal carcinoma	Left breast 10 cm diameter, right breast 8 cm diameter

Phosphomonoester, Pi and PDE peaks were poorly resolved in the corresponding phosphorus-31 spectra and they were not included in subsequent analyses. The FWR was calculated from the relative areas of the fat and water peaks in the hydrogen spectra. One hundred and twenty-eight pulse excitations were used for the phosphorus-31 spectra with $TR = 6$ s, delay time $De = 500\ \mu s$, and dwell time $Dw = 400\ \mu s$ for 512 data points (12.48 min).

Multiplication of the free induction decay (FID) by a decaying exponential was introduced in cases of poor signal-to-noise ratio. This results in a signal with enhanced signal-to-noise ratio, but also with increased linewidth. Following Fourier transformation of the FID data, from the time to the frequency domain, the spectra were phase corrected and baseline subtracted as required. The subtracted baseline consisted of polynomial sections, computer constructed, from up to 64 fitting points specified by the user. Peak areas were calculated by plotting the spectra on graph paper and extending the peak sides to the baseline. Where lines from different peaks overlapped, the angle of the uppermost vertex of the resulting triangle was bisected. The number of squares per peak was then counted and the peak areas were expressed as a percentage of the total spectral phosphorus-31 metabolites. Peak ratios were also calculated in an attempt to minimize noise differences between spectra. The pH was read off a standard curve of pH *versus* |PCr–Pi| chemical shift.

Lateral views of both breasts were acquired with xeromammography in volunteers over 40 years old (or over 35 years old if in a high risk group). Both lateral and antero-posterior views were acquired in Groups 2 and 3 (*i.e.* in the patients with pathological lesions). Of the nine patients with breast carcinoma, four had immediate surgery, two had surgery following chemotherapy, and three had chemotherapy with no surgery.

Patient details and phosphorus-31 MR spectral characteristics were entered into pre-coded data sheets to facilitate computer analysis. Statistical analysis was carried out, using SAS (statistical analysis system), on an IBM mainframe computer. Univariate analyses consisted of Student's t-tests or χ^2 tests as appropriate. The data were also subjected to multivariate analysis using multiple regression. The relationships of PME, Pi, PDE, PCr, γ-NTP, α-NTP and β-NTP peak areas (as percentages) as well as the FWR and chemical shift of |PCr–Pi|, to age, family history, use of contraceptive pill, breast feeding, pre- or post-menopause, breast size and pattern, were examined.

Results

Table II shows the results of the questionnaire obtained from the volunteer group. Twenty-eight of the women examined were pre-menopausal while 17 were post-menopausal. The mean age was 45.1 ± 10.8 years, 21 volunteers being less than or equal to 45 years old and the remaining 25 being over 45 years old. Fifteen women had a maximum distance of less than 5 cm from the skin to the chest wall, as seen at MRI with the patient in a supine position, while this was greater than or equal to 5 cm in the remaining 31 patients.

Table II. Details of volunteer group

		Number	Percentage
Age (years)	≤45	21	46
	>45	25	54
Family history of breast cancer	Yes	8	17
	No	38	83
Use of contraceptive pill	Yes	2	4
	No	44	96
Breastfed at least 1 child	Yes	16	35
	No	30	65
Menopause	Pre	28	62
	Post	17	38
Maximum antero-posterior breast size (from MRI)	<5 cm	15	33
	≥5 cm	31	67
Breast pattern % fat (from MRI)	<30%	13	28
	30–70%	19	41
	>70%	14	31

Magnetic resonance spectroscopy was performed on the right breast of 40 volunteers and on the left breast of six. Examination of the right breast provided optimal spectral resolution. The spectral resolution was considered good in 15 volunteers (FWHM less than or equal to 0.5 ppm), fair in 23 (FWHM of 0.5–0.7 ppm), and poor in eight (FWHM greater than 0.7 ppm). Phosphomonoester, Pi and PDE peaks were the most dificult to resolve. An increased number of acquisitions (with a considerable increase in MRS examination time!) should increase the spectral resolution and signal-to-noise ratio (SNR) of normal breast tissue spectra. Some degree of spectral contamination, evident from

Table III. Mean phosphorus-31 metabolite peak areas (±1 SD) expressed as the percentage of total phosphorus-31 spectral area in the volunteer group (Group 1), patients with breast carcinoma (Group 2) and patients with benign breast disease (Group 3)

	Group 1 ($n = 46$)	Group 2 ($n = 9$)	Group 3 ($n = 4$)
	Mean (SD)	Mean (SD)	Mean (SD)
Age	45.1 (10.8)	58.3 (8.1)	52.6 (3.6)
PME	[a]10.3 (4.6)	9.9 (4.6)	10.3 (4.0)
Pi	[a]13.7 (3.2)	10.8 (2.6)	11.6 (3.0)
PDE	[a]12.7 (3.8)	18.3 (8.4)	10.6 (6.0)
PCr	30.3 (6.3)	24.3 (12.3)	32.4 (6.6)
γ-NTP	10.3 (1.5)	13.2 (2.0)	10.9 (1.9)
α-NTP	12.4 (2.0)	14.8 (2.8)	13.5 (1.6)
β-NTP	10.1 (1.6)	9.8 (1.3)	10.9 (2.0)
pH	7.08 (0.12)	7.23 (0.13)	7.01 (0.23)
F:W	1.03 (0.74)	0.98 (0.7)	1.07 (1.00)

[a] PME, Pi and PDE peak areas from three volunteer subjects were not included owing to poor spectral resolution; $n = 43$ for these three values.

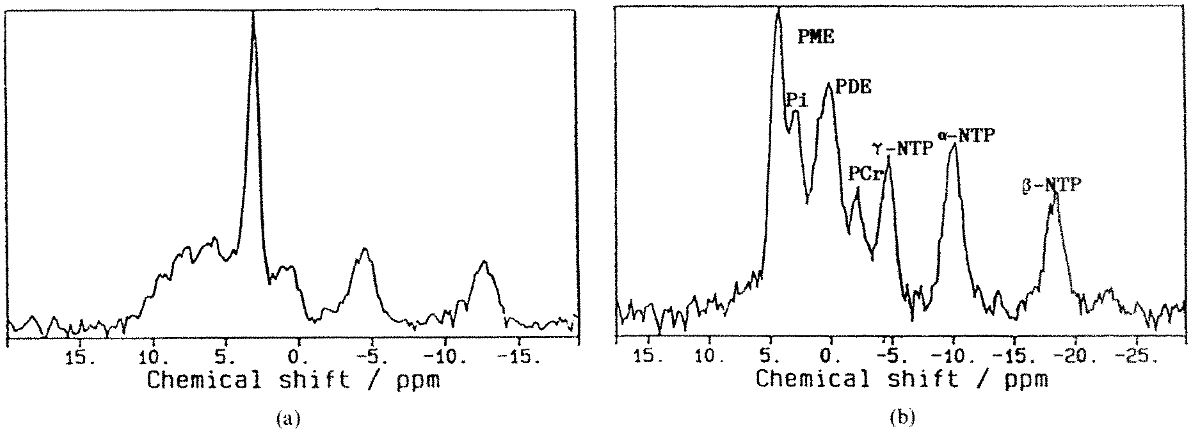

(a) (b)

Figure 1. Phosphorus-31 MR spectra of (a) normal breast tissue and (b) breast carcinoma prior to therapy.

the prominent PCr peaks, was evident in most volunteer spectra. Table III shows the mean (±SD) phosphorus-31 metabolic peak areas in the volunteer and two patient groups.

Figure 1 shows a phosphorus-31 spectrum of normal breast tissue compared with a spectrum obtained from a breast carcinoma. Phosphodiesters are elevated and PCr is reduced in the breast carcinoma spectrum.

When patient data and spectral characteristics were subjected to univariate analysis, a number of significant relationships were observed (see Table IV). Phosphomonoester (%) and PCr (%) were significantly associated with both menopausal status and age; β-NTP was significantly associated with both menopausal status and breast pattern, while the FWR was associated with menopausal status, age, breast pattern and size. No association was observed between any spectral characteristics and variables such as history of breast

Table IV. Univariate and multivariate analyses of PME (%), β-NTP (%), PCr (%) and F:W ratio (±1 SD) *versus* menopausal status, age, breast pattern and breast size in the volunteer group

	PME (%) Mean (SD)	β-NTP (%) Mean (SD)	PCr (%) Mean (SD)	F:W Mean (SD)
Menopausal status				
Pre-menopausal	11.6 (4.8)	10.4 (1.5)	28.2 (4.7)	0.74 (0.5)
Post-menopausal	8.3 (3.7)	9.3 (1.4)	33.5 (7.5)	1.45 (0.9)
Significance level				
Univariate	$p = 0.02$	$p = 0.04$	$p = 0.02$	$p = 0.005$
Multivariate	NS ($p = 0.06$)	$p = 0.05$	$p = 0.02$	NS
Age				
≤ 45 years	11.8 (4.8)	10.3 (1.5)	28.2 (4.8)	0.69 (0.4)
> 45 years	9.0 (4.1)	9.9 (1.7)	32.3 (7.0)	1.28 (0.8)
Significance level				
Univariate	$p = 0.05$	NS	$p = 0.04$	$p = 0.005$
Multivariate	NS	NS	NS	$p = 0.02$
Breast pattern				
< 30% fat	11.8 (5.7)	10.7 (1.6)	28.5 (4.9)	0.83 (0.7)
> 70% fat	8.4 (3.6)	9.2 (1.5)	33.4 (8.0)	1.61 (0.8)
Significance level				
Univariate	NS	$p = 0.03$	NS	$p = 0.02$
Multivariate	NS	NS	NS	NS
Breast size				
[a]Diameter ≥ 5 cm	10.3 (4.1)	10.6 (1.7)	29.9 (5.3)	1.19 (0.7)
[a]Diameter < 5 cm	10.3 (4.9)	9.8 (1.5)	30.4 (6.9)	0.70 (0.7)
Significance level				
Univariate	NS	NS	NS	$p = 0.04$
Multivariate	NS	NS	NS	NS

[a]Diameter is the maximum antero-posterior diameter.

feeding, use of contraceptive pill and family history of breast cancer.

Multivariate analysis of this data showed phosphorus metabolism of breast tissue to be most strongly associated with menopausal status of the volunteer. The high energy phosphates (β-NTP and PCr) were both significantly related to menopausal status. When age and menopausal status were considered together in relation to PME (%), using a multivariate model, "age" was not found to be statistically significant, while "menopausal status" only tended towards significance ($p = 0.06$). This suggests that "age" may be a confounding factor for "menopausal status" in relation to PME (%). The statistical significance of PME (%) with respect to menopausal status should improve with increased numbers. Multivariate analysis of the FWR with age, menopausal status, breast pattern and size showed "age" to be the most significant factor ($p = 0.02$).

The nine patients with breast carcinoma were compared with an age-matched group of volunteers ($n = 12$). Stronger signal and improved spectral resolution were readily obtained from malignant breast tissue compared with normal breast tissue, despite similar acquisition parameters. The mean peak areas (%) for each of the phosphorus-31 metabolites is shown in Table V. Mean Pi and PCr (%) and FWR were all reduced in the carcinoma group, while PDE, α-NTP and γ-NTP (%) were increased. When subjected to statistical analysis, however (Student's t-test), only the differences in percentage of γ-NTP ($p = 0.01$), α-NTP ($p < 0.01$), and PCr ($p < 0.01$) were statistically significant.

When ratios of phosphorus-31 metabolites were calculated, Pi:PDE was lower in the carcinoma group of patients ($p = 0.10$) while β-NTP:PCr was higher ($p < 0.05$). Mean PDE:PCr values were also considerably higher in the breast carcinoma tissues although the differences were not statistically significant. The mean pH value for the carcinoma group was pH 7.23±0.13. This is higher than that observed in the volunteer group (pH 7.08±0.12) although the difference is not statistically significant.

Table V. Phosphorus-31 metabolite peak areas (%) (±1SD) in patients with breast carcinoma *versus* an age-matched control group

	Volunteers ($n = 12$)	Breast carcinoma ($n = 9$)	Significance level
	Mean (SD)	Mean (SD)	Mean
PME	8.30 (4.0)	9.9 (4.6)	NS
Pi	13.1 (3.3)	10.8 (2.6)	NS
PDE	12.9 (1.1)	18.3 (8.4)	NS
PCr	32.9 (80)	24.3 (12.3)	$p < 0.01$
γ-NTP	10.8 (1.6)	13.2 (2.0)	$p = 0.01$
α-NTP	12.4 (2.3)	14.8 (2.8)	$p < 0.01$
β-NTP	9.4 (1.5)	9.8 (1.3)	NS
pH	7.08 (0.12)	7.23 (0.13)	NS
F:W	1.64 (0.8)	0.98 (0.7)	NS
Pi:PDE	1.10 (0.4)	0.67 (0.3)	$p = 0.10$
PDE:PCr	0.44 (0.3)	1.13 (0.9)	NS
β-NTP:PCr	0.30 (0.1)	0.52 (0.3)	$p < 0.05$

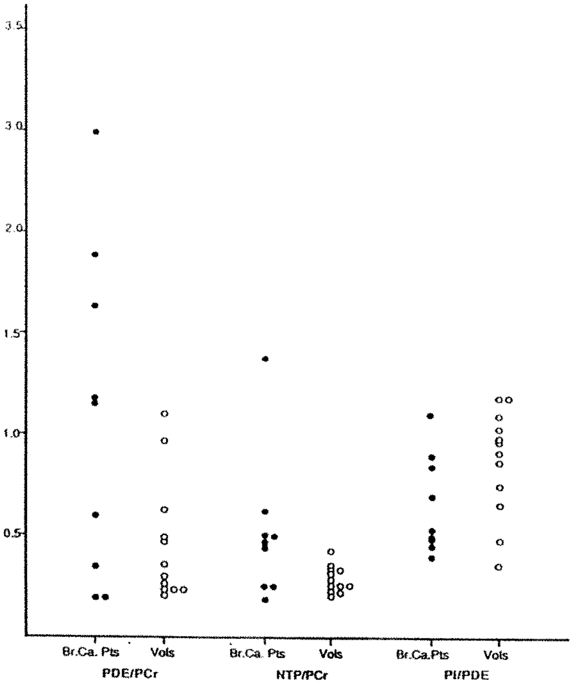

Figure 2. Pi:PDE, PDE:PCr and β-NTP:PCr ratios in breast carcinoma (●) *versus* normal breast tissue (○) from an age-matched group of 12 volunteers.

Figure 2 is a graph of Pi:PDE, PDE:PCr and β-NTP:PCr ratios in breast carcinoma compared with normal breast tissue from an age-matched volunteer group.

Mean phosphorus-31 metabolite peak areas for patients with benign breast disease are given in Table VI. These results suggest an increase in PME levels and a reduction in Pi and PDE values and in

Table VI. Phosphorus-31 metabolite peak areas (%) (±1 SD) for patients with benign breast disease *versus* control group

	Volunteers ($n = 12$)	Benign breast disease ($n = 4$)
	Mean (SD)	Mean (SD)
PME	8.3 (4.0)	10.3 (4.0)
Pi	13.1 (3.3)	11.6 (3.0)
PDE	12.9 (1.1)	10.6 (6.0)
PCr	32.9 (8.0)	32.4 (6.6)
γ-NTP	10.8 (1.6)	10.9 (1.9)
α-NTP	12.4 (2.3)	13.5 (1.6)
β-NTP	9.4 (1.5)	10.9 (2.0)
pH	7.08 (0.12)	7.01 (0.2)
F:W	1.64 (0.8)	1.07 (1.0)

FWRs in the patient group, although the patient numbers are too small to allow reliable statistical analysis.

Discussion

This study demonstrates that differences in tissue biochemistry can be detected in breasts of normal volunteers ($n = 46$) depending on menopausal status and age. High energy NTPs, such as adenosine triphosphate (ATP), were elevated in pre-menopausal women compared with post-menopausal women. Peak areas of PMEs, which include contributions from phosphorylcholine, phosphorylethanolamine, glucose and fructose phosphates, as well as other sugars, were also elevated in the pre-menopausal group.

Phosphorus-31 MRS identified a doubling of the mean FWR in the breast tissue of volunteers over 45 years old, compared with those less than 45 years old. This is in agreement with autopsy studies and corresponds with fatty replacement of parenchyma in breast tissue with time. The increased fat content of older breast tissue may have a role in local oestrogen production which may be especially important in the case of post-menopausal women (Miller, 1986), as the supply of preformed active hormone reaching the breast declines after the menopause.

Phosphocreatine (%) was reduced in the breast tissue of pre-menopausal women while NTP (%) was increased. This is contrary to the finding of Sijens et al (1988) who, in a small study of four normal controls (range 25–40 years), showed elevated PCr relative to five patients with malignant breast tumours. Their conclusion that "PCr is high in young women" may, in fact, relate more to reduced PCr in carcinomatous breast tissue as opposed to elevated PCr in young control subjects. Older, post-menopausal control subjects were not investigated.

The pill has been suspected of being a cancer induction agent, particularly in women on long-term medication. Only two women in the group of volunteers had used the contraceptive pill and these showed no significant differences from the rest of the group, although the patient number is obviously too small to draw any conclusions. History of breast feeding or family history of breast carcinoma could not be shown to correlate with any specific spectral characteristics. A wide range of pH values was obtained in this group (pH 6.9–7.4), which did not appear to correlate with any of the variables investigated. Improved localization techniques, however, with the elimination of possible contamination by underlying muscle tissue is required to confirm these findings.

We were unable to differentiate benign breast disease from normal breast tissue on the basis of *in vivo* phosphorus-31 spectra. This may have been because of the low numbers investigated in this group ($n = 4$), making statistical analysis with the other two groups both difficult and unreliable. It may also be due to partial voluming effect with contamination of benign breast tissue spectra with signal from surrounding normal breast tissue. This is also a problem with the malignant tumours studied. Some of these were smaller than the 4 cm surface coil used, and spectral contamination from surrounding normal breast tissue could reduce the differences observed between the malignant and control groups. Degani et al (1986) differentiated benign breast lesions ($n = 5$) from breast carcinoma ($n = 9$) *in vitro*, on the basis of reduced PME and NTP in the benign group relative to the carcinoma group. Neither group, however, was compared with normal breast tissue. Another group (Merchant et al, 1988) again performing *in vitro* phosphorus-31 MRS of human breast tissue extracts, examined the same three tissue groups as ourselves (malignant, benign and normal breast parenchymal specimens). They found that PME metabolism was altered in all neoplastic tissues relative to non-involved tissues, that PCr was elevated in benign disease, and that benign breast disease showed an increase in an uncharacterized phosphate, resonating at 3.66δ, relative to the shift position of phosphoric acid. We did not observe any of these changes.

Even if the number of patients in this group were increased in our study, it is still unlikely that *in vivo* phosphorus-31 MRS would have the potential to differentiate "normal" breast tissue from "benign breast disease", as the term "benign breast disease" is used to encompass a wide range of pathologies including mammary cysts, adenosis, fibroadenomas, apocrine changes and epithelial hyperplasia (Love et al, 1982). Even in the work of Merchant et al (1988) referred to above, the benign specimens ($n = 8$) included a very wide range of benign breast disease, *i.e.* fibrocystic disease, fibroadenoma, benign cystic changes and focal fibrosis. In a recent American study, in which 360 women with no history of breast problems were autopsied, 58% were shown to have "benign breast disease".

In the group of patients with breast carcinoma ($n = 9$), PCr values (%) were lower than in either the control group or the patient group with benign breast disease ($p < 0.01$). This is in agreement with the work of many other groups (Evanochko et al, 1984; Oberhaensli et al, 1986; Merchant et al, 1988; Sijens et al, 1988). Mean PDE (%) was increased in the breast carcinoma group, although the range of values in each group was quite high. A similar increase in breast carcinoma PDE (%) was identified by Sijens et al (1988) and probably represents a rapid turnover in phospholipids with a simultaneous formation of new cells. Reduced Pi:PDE ($p = 0.10$) and increased PDE:PCr ratios were observed in the group of patients with breast carcinoma, possibly owing to increased PDE (%). The statistical significance of these findings should improve with increased patient numbers. Expressing phosphorus-31 metabolite peak areas as ratios minimizes the effect of different levels of spectral noise, and therefore enables a more accurate comparison between spectra. Greater numbers are required to determine if elevated PDE (%) is a useful indicator of malignant breast disease.

γ-NTP (%) was found to be elevated in breast carcinoma tissue relative to the other two groups ($p = 0.01$)

as was α-NTP (%) ($p < 0.01$). This suggests that levels of nucleotide diphosphates, most probably ADP, which contribute to the phosphorus-31 spectra in the same region as the γ-NTP and α-NTP peaks, are elevated in breast carcinoma tissue.

Mean pH values for the carcinoma group were higher than those observed in either the volunteer group or the benign group, although this difference was not statistically significant. This would agree, however, with other work demonstrating the alkaline nature of breast carcinomas (Oberhaensli et al, 1986). It suggests that these carcinomas are well vascularized and/or oxygenated and, while a small number of dispersed hypoxic cells could easily escape detection by *in vivo* MRS, that they were not the predominant population in the tumours studied. (The presence of even a small number of hypoxic cells, however, could be highly significant in determining the success or failure of treatment, particularly with radiotherapy.)

Conclusion

This study has shown that is is possible, using phosphorus-31 MRS, to detect differences in breast tissue biochemistry in a group of control subjects on the basis of age and menopausal status. Likewise, this non-invasive *in vivo* technique identified abnormalities in phosphorus metabolism in carcinomatous breast tissue. Magnetic resonance spectroscopy may, therefore, improve the differentiation of benign but symptomatic tumours, such as fibroadenomas, from malignant disease.

Magnetic resonance spectroscopy also has potential in monitoring response to therapy. Of the nine patients with malignant breast disease evaluated in this study, five had follow-up MRS examinations post-chemotherapy (mean 14 per patient). Spectral changes were monitored and are currently being evaluated with respect to patient response.

Acknowledgments

We would like to thank the Irish Health Research Board for partial funding of this project.

References

Ackerman, J., Grove, T., Wong, G., Gadian, D. & Radda, G.K. 1980. Mapping of metabolites in whole animals by ^{31}P NMR using surface coils. *Nature, 283,* 167–170.

Cohen, J. S., Lyon, R. C., Chen, C., Faustino, P. J., Batist, G., Shoemaker, M., Rubalcaba, E. & Cowan, K. H., 1986. Differences in phosphate metabolite levels in drug-sensitive and -resistant human breast cancer cell lines determined by P-31 magnetic resonance spectroscopy. *Cancer Research, 46,* 4087–4090.

Cozzane, P. J. & Jardetzky, O., 1976. Phosphorus-31 Fourier transform nuclear magnetic resonance study of mononucleotides and dinucleotides: 1. Chemical shifts. *Biochemistry, 15,* 4853–4859.

Degani, H., Horowitz, A. & Itzchak, Y., 1986. Breast tumours: evaluation with P-31 MR spectroscopy. *Radiology, 161,* 53–56.

Evanochko, W. T., Ng, T. C., Glickson, J. D., Durrant, J. R. & Corbett, T. H., 1982. Human tumours as examined by in vivo ^{31}P-NMR in athymic mice. *Biochemical and Biophysical Research Communications, 109,* 1346–1352.

Evanochko, W. T., Ng, T. C., Lilly, M. B., Lawson, A. J., Corbett, T. H., Durrant, J. R., & Glickson, J. D., 1983. In vivo ^{31}P study of the metabolism of murine mammary 16/C adenocarcinoma and its response to chemotherapy, x-radiation and hyperthermia. *Proceedings of the National Academy of Sciences of the United States of America, 80,* 334–338.

Evanochko, W. T., Ng, T. C. & Glickson, J. D., 1984. Applications of in vivo NMR spectroscopy to cancer. *Magnetic Resonance in Medicine, 1,* 508–534.

Hollander, J., 1986. In vivo tissue analysis by NMR spectroscopy. *Diagnostic Imaging Clinical Medicine, 55,* 9–19.

Irving, M. G., Simpson, S. J., Field, J. & Doddrell, D. M., 1985. Use of high resolution ^{31}P-labelled topical magnetic resonance spectroscopy to monitor in vivo tumour metabolism in rats. *Cancer Research, 45,* 481–486.

Kelsey, J. L., 1979. A review of the epidemiology of human breast cancer. *Epidemiologic Reviews, 1,* 74–109.

Love, S. M., Gellman, R. S. & Silen, W., 1982. Fibrocystic "disease" of the breast—a non-disease? *New England Journal of Medicine, 307,* 1010–1014.

Merchant, T. E., Gierke, L. W., Meneses, P. & Glonek, T., 1988. ^{31}P magnetic resonance spectroscopic profiles of neoplastic human breast tissues. *Cancer Research, 48,* 5112–5118.

Miller, W. R., 1986. Steroid metabolism in breast cancer. *Reviews on Endocrine-Related Cancer, 23,* 23–30.

Moon, R. B. & Richards, J. H., 1973. Determination of intracellular pH by ^{31}P magnetic resonance. *Journal of Biological Chemistry, 248,* 7276–7278.

Mountford, C., May, G., Williams, P., Tattersall, M., Russell, P., Saunders, J., Holmes, K., Fox, R., Barr, J. & Smith, I., 1986. Classification of human tumours by high-resolution magnetic resonance spectroscopy. *Lancet, 1,* 641–653.

Ng, T. C., Evanochko, W. T., Hiramoto, R. N., Ghanta, V. K., Lilly, M. B., Lawson, A. J., Corbett, T. H., Durrant, J. R. & Glickson, J. D., 1982. ^{31}P-NMR spectroscopy of in vivo tumours. *Journal of Magnetic Resonance, 49,* 271–296.

Oberhaensli, R. D., Hilton-Jones, D., Bore, P. J., Hands, L. J., Rampling, R. P. & Radda, G. K., 1986. Biochemical investigation of human tumours in vivo with phosphorus-31 magnetic resonance spectroscopy. *Lancet, 11,* 8–11.

Ottman, R., Pike, M. C., King, M. & Henderson, B. E., 1983. Practical guide for estimating risk for familial breast cancer. *Lancet, 2,* 556–558.

Redmond, O., Stack, J. P., Scully, M., Dervan, P., Carney, D. & Ennis, J. T., 1988. Tissue characterisation and spectral analysis of malignant tumours following chemotherapy. *Tumor Diagnostik und Therapie, 9,* 167–168.

Sijens, P. E., Wijrdeman, H. K., Vermeulen, J. W. A H. & Luyten, P. R., 1987. NMR spectroscopy of human breast tumours before and after radiotherapy using a 1.5 T MRI system. In *Proceedings of the Society for Magnetic Resonance in Medicine, Sixth Annual Meeting and Exhibition, New York, Vol. 2,* p. 979.

Sijens, P. E., Wijrdeman, H. K., Moerland, M. A., Bakker, C. J. G., Vermeulen, J. W. A. H. & Luyten, P.R., 1988. Human breast cancer in vivo: H-1 and P-31 MR spectroscopy at 1.5 T. *Radiology, 169,* 615–620.

Vihko, R. & Apter, D., 1986. Hormonal profile and predisposition to breast cancer. *Reviews on Endocrine-Related Cancer, 23,* 11–15.

1991, *The British Journal of Radiology*, *64*, 217–220

The interchangeability of radioisotope and X-ray based measurements of bone mineral density

By J. D. Adachi and C. E. Webber

Departments of Medicine and Radiology, Faculty of Health Sciences, McMaster University, Hamilton, Ontario, Canada

(Received June 1990 and in revised form August 1990)

Keywords: Dual photon absorptiometry, Radioisotope source, X-ray sources, Spine and hip, Intercomparison

Abstract. Lumbar spine and femoral neck bone mineral density (BMD) were measured with a Novo radioisotope based dual photon densitometer and with a Lunar X-ray densitometer in 94 subjects attending a Metabolic Bone Disease Clinic. There was a strong correlation between results obtained from each machine for the same skeletal site. The correlation coefficients for the spine and femoral neck were 0.97 and 0.88, respectively. The differences between results from each machine were normally distributed with a mean bias of 37.5% for the spine and 27.8% for the femur, which arise principally from differences in machine calibration. In each case the BMD was greater when measured by X-ray absorptiometry. The range for the bias was approximately 25–50% for the spine and 10–45% for the femoral neck. The results from these two machines are not interchangeable. When subjects who are participating in long term studies using a radioisotope densitometer are transferred to an X-ray densitometer, an individual conversion factor must be measured at each site for each subject.

Dual photon absorptiometry is a widely used technique for the measurement of bone mass. The original clinical machines used a radioactive isotope as the source of dual energy photons. Recent technological developments have replaced the radioisotope source with an X-ray tube which produces a dual photon beam by kVp switching or by rare-earth filtration. The X-ray based machines have considerable advantages with improved precision, reduced radiation dose, decreased measurement time, better spatial resolution and increased diagnostic sensitivity with the potential of lateral lumbar spine measurements. It is necessary to know whether the results obtained for one subject on an X-ray based machine can be compared reliably with previous results obtained for the same subject on a radioisotope based machine. The purpose of this work was to compare lumbar spine and femoral neck bone mineral density (BMD) measurements on such machines in a population at risk of osteoporosis.

Materials and methods

Radioisotope dual photon absorptiometry was performed using a Novo BMC-LAB 22a with a gadolinium 153 source. This machine is calibrated to yield an area BMD for the L2 to L4 lumbar vertebrae in units of grams of hydroxyapatite per square centimetre. For measurements in the proximal femur, the Novo machine provides the area density in the same units for the femoral neck.

X-ray dual photon absorptiometry was performed using a Lunar DPX. Area densities in units of grams of bone mineral per square centimetre for L2 to L4 and for the femoral neck were used for comparison with the radioisotope machine.

Volunteers were solicited from patients attending an outpatient Metabolic Bone Disease Clinic during the period February to March 1989. A total of 94 consecutive subjects (59 women and 35 men) were enrolled. The ages of the women ranged from 21 to 85 years with a mean and standard deviation of 61.7 ± 13.0. The body mass index for women ranged from 15.9 to 35.6 kg/m^2 with a mean and standard deviation of 26.0 ± 4.8. The ages of the men ranged from 23 to 81 years with a mean and standard deviation of 60.4 ± 13.6 years. The body mass index for males ranged from 19.3 to 42.0 kg/m^2 with a mean and standard deviation of 25.6 ± 4.5. Lumbar spine and proximal femur scans were attempted in each subject on the same day using both machines.

Lumbar spine BMD measurements on each machine were available for 87 subjects (55 women and 32 men). In six of the seven remaining patients it was not possible to perform the scan on the radioisotope machine because of obesity. For the seventh patient it was not possible to perform the scan on either machine because of obesity. In these seven patients the body mass index averaged 32.0.

Femoral neck BMD was measured on each machine in 86 subjects (55 women and 31 men). In 72 subjects the right hip was measured while in 14 the left hip was measured. Of the remaining eight patients, femoral neck scans were not performed on the radiosotope based absorptiometer in four, while in three patients different hips were measured on each machine. For one patient, femoral scans were not performed on either machine. The results obtained from each machine were compared by regression analysis for both the lumbar spine and the

---

Address correspondence to C. Webber, Department of Nuclear Medicine, Chedoke-McMaster Hospitals, 1200 Main Street West, Hamilton, Ontario, Canada, L8N 3Z5.

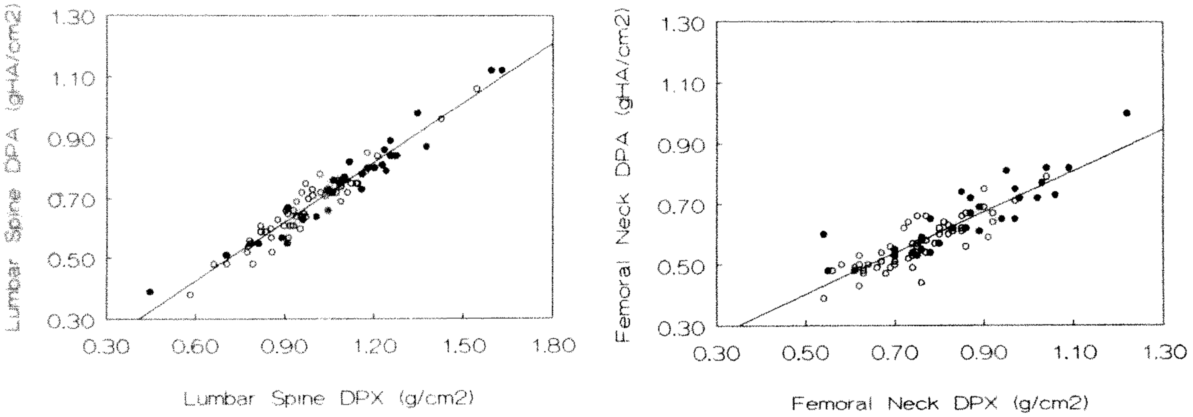

(a) (b)

Figure 1. Comparison of (a) lumbar spine and (b) femoral neck BMD measurements in men (●) and women (○) using radioisotope (DPA) and X-ray (DPX) based densitometers.

femoral neck. The bias between machines was established for each site from the distribution of differences between each machine. The 95% confidence limits for the range of differences were calculated using the *t* distribution.

Results

The comparison between BMD measurements using the two absorptiometers is shown in Fig. 1 for both the lumbar spine and femoral neck. There was no statistically significant difference between either the slopes or the intercepts of regression lines fitted separately to the data for males and females. For the lumbar spine the regression equation for the whole group ($n = 87$) is

$$\text{DPA} = 0.033 + 0.653\ \text{DPX}$$

where DPA and DPX are respectively the BMD values measured by γ-ray and X-ray absorptiometry. The correlation coefficient for the lumbar spine is 0.97. For the femoral neck, the regression equation for the whole group ($n = 86$) is

$$\text{DPA} = 0.063 + 0.678\ \text{DPX}$$

and the correlation coefficient is 0.88.

The difference between the DPX and DPA lumbar spine measurements for each subject is shown in Fig. 2 as a function of the mean BMD. For the whole group the regression equation is

$$\text{DPX} - \text{DPA} = -0.018 + 0.395\ \text{BMD}$$

and the correlation coefficient is 0.85. The standard error of an estimated difference is 0.043 g/cm^2. Also shown in Fig. 2 are the equivalent data for the difference between the femoral neck measurements. For the whole group the regression equation is

$$\text{DPX} - \text{DPA} = 0 + 0.275\ \text{BMD}$$

and the correlation coefficient is 0.49. The standard error of an estimated difference is 0.058 g/cm^2.

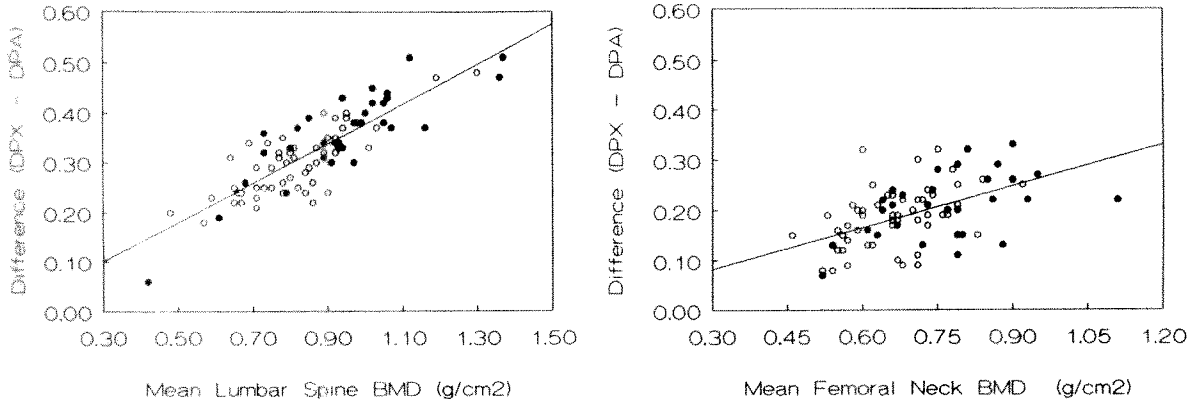

(a) (b)

Figure 2. Absolute differences between machines for (a) lumbar spine and (b) femoral neck BMD measurements in men (●) and women (○).

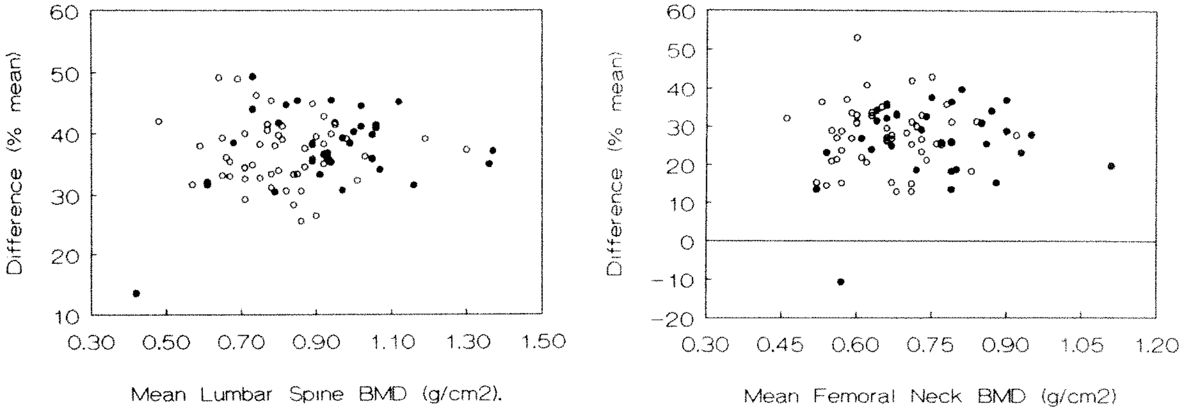

(a)

(b)

Figure 3. Percentage differences between machines for (a) lumbar spine and (b) femoral neck BMD measurements in men (●) and women (○).

When the differences between results for the two machines are expressed as a percentage of the mean BMD, the data shown in Fig. 3 are obtained. The percentage differences for both sites were normally distributed. For each site there is a single outlier. For the spine the outlier corresponds to a male subject aged 63 who weighed 55 kg. His mean lumbar BMD was 0.42 g/cm^2 and his mean femoral neck BMD was 0.55 g/cm^2. The outlier for the femoral neck data is again a male aged 74 who weighed 58 kg. His mean lumbar spine BMD was 0.61 g/cm^2 and his mean femoral neck BMD was 0.57 g/cm^2. Excluding these two subjects, the mean difference between lumbar spine measurements was 37.5%. The standard deviation of the difference was 5.1%. For these patients, 95% of the differences between the two measurements of lumbar spine BMD were between 27.4 and 47.6% and the X-ray measurement was always greater than the γ-ray measurement. For the femoral neck, the mean difference was 27.8 ± 7.7%, and 95% of the differences between the two measurements of femoral neck BMD were between 12.5 and 43.2% with the X-ray measurement being greater in all but one case.

Confidence limits for the mean difference and for the upper and lower limits of the range of differences can be derived. These values will apply to the entire population from which our sample was drawn. For the lumbar spine the 95% confidence interval for the bias between machines is 36.4–38.6%. The confidence interval for the lower limit is 25.4–29.2% and for the upper limit, the interval is 45.8–49.6%. These narrow intervals reflect the large number of subjects in our sample. For the femoral neck, the 95% confidence interval for the bias is 26.4–29.2%. The interval for the lower limit is 9.5–15.3% and that for the upper limit is 40.3–46.1%.

The difference between the lumbar spine measurements in each patient was not correlated with the difference between the femoral neck measurements in the same patient ($r = 0.21$).

Discussion

Bias between BMD measurements made on a pair of dual photon densitometers will arise when one machine is calibrated in terms of hydroxyapatite mass and the other in terms of bone mineral mass. Differences comparable with those reported here have been documented previously in such machines using gadolinium 153 sources (Webber, 1989). Bias is also observed between machines that are both calibrated in terms of mineral mass. Pacifici et al (1988) found for 52 women that lumbar spine BMD measured with a Lunar radioisotope machine averaged 6.8% greater than that measured on a Hologic X-ray machine. Wahner et al (1988) showed that for 15 subjects measured on another pair of Lunar and Hologic machines, the radioisotope result was between 2 and 20% greater than the X-ray measurement. For a third pair of Lunar and Hologic machines, Strause et al (1989) established a bias in lumbar spine BMD of between 25 and 30% in 115 normal post-menopause women. When a radioisotope and an X-ray machine from the same manufacturer were compared in 41 subjects, lumbar spine BMD was only about 3% greater using γ-radiation (Mazess & Barden, 1988). McClung and Roberts (1989) measured lumbar spine and femoral neck BMD in 93 subjects on each of three machines: an X-ray and a γ-ray densitometer from Lunar and a Hologic X-ray machine. They concluded that the biases between the three machines limited the direct comparison of data between any pair of machines except perhaps when the lumbar spine is measured on two X-ray machines. Finally Blake et al (1989) compared spine and femoral neck BMD measurements in 20 women on a Novo radioiostope machine and a Hologic X-ray machine and showed that, on average, the gadolinium 153 results were less for the spine but equal for the femoral neck. There was considerable variation between subjects in the observed bias.

The results of the lumbar spine BMD measurements on our two machines were strongly correlated. The strength of the correlation for the femoral neck was not as good. The extent of these correlations should not be surprising since, in both machines, the transmission of low energy photons through the same object is measured. Reported correlations between pairs of machines have varied from 0.94 to 0.99 for the lumbar spine (Mazess & Barden, 1988, Pacifici et al, 1988; Wahner et al, 1988; Strause et al, 1989). McClung and Roberts (1989) in their intercomparison of three machines also showed that correlations for the femoral neck were generally poorer than those for the lumbar spine. Correlation coefficients which approach unity convey the impression that the value measured for BMD on one machine will allow the reliable prediction of the BMD which would be measured on another machine. Such an approach has been suggested (Pacifici et al, 1988; Wahner et al, 1988; Slosman et al, 1989). However, to assess agreement between two instruments the important parameter is the range of observed differences and not the correlation (Bland & Altman, 1986). Our work has shown that in a population at risk of osteoporosis, differences between a Lunar X-ray machine and a Novo γ-ray machine may range from 25 to 50% for the lumbar spine and 10 to 45% for the femoral neck. If measurements were repeated on a single subject on the same day using either one of these machines, the range of differences would be much smaller. For gadolinium 153 machines, the standard deviation of values is typically about 2–4% (LeBlanc et al, 1986; Nilas et al, 1988). For X-ray machines, the reproducibility is improved by a factor of about 2 (Mazess & Barden, 1988; Pacifici et at, 1988; Wahner et al, 1988). For the femoral neck, reproducibility is not as good as for the lumbar spine and, in addition, the improvement with an X-ray source is not as significant as for the spine (Slosman et al, 1989).

When the same subject is measured at the same site on different machines, a large bias can be introduced but, more importantly, the range of that bias is wide. This implies that there are subject dependent factors which influence the difference between the two absorptiometers. The lack of correlation between the lumbar spine and femoral neck differences suggests that the subject dependent factors are also site specific. The broad range of differences means that machines cannot be used interchangeably for sequential measurements on a single subject and for longitudinal studies an individual conversion factor must be measured at each measurement site for each subject.

References

Blake, G., Rodin A. & Fogelman, I, 1989. A comparative study of dual photon absorptiometry and dual energy X-ray absorptiometry. *Journal of Bone and Mineral Research, 4*, Suppl. 1, S398.

Bland, J. M. & Altman, D. G., 1986. Statistical methods for assessing agreement between two methods of clinical measurement. *Lancet, 1*, 307–310.

LeBlanc, A. D., Evans, H. J., Marsh, C., Schneider, V., Johnson, P. C. & Jhingran, S. G., 1986. Precision of dual photon absorptiometry measurements. *Journal of Nuclear Medicine, 27*, 1362–1365.

Mazess, R. B. & Barden, H. S., 1988. Measurement of bone by dual photon absorptiometry (DPA) and dual energy X-ray absorptiometry (DEXA). *Annales Chirurgiae et Gynaecologiae, 77*, 197–203.

McClung, M. & Roberts, L., 1989. Correlation of bone density measurements by 153-Gd and X-ray dual photon absorptiometry. *Journal of Bone and Mineral Research, 4*, Suppl. 1, S368.

Nilas, L., Hassager, C. & Christiansen, C., 1988. Long term precision of dual photon absorptiometry in the lumbar spine in clinical settings. *Bone and Mineral, 3*, 305–315.

Pacifici, R., Rupich, R., Vered, I., Fischer, D. C., Griffin, M., Susman, N. & Avioli, L. V., 1988. Dual energy radiography (DER): a preliminary comparative study. *Calcified Tissue International, 43*, 189–191.

Slosman, D. O., Rizzoli, R., Donath, A. & Bonjour, J. P., 1989. Quantitative digital radiography and conventional dual photon bone densitometry: study of precision at the levels of spine, femoral neck and shaft. *Journal of Bone and Mineral Research, 4*, Suppl., S394.

Strause, L., Bracker, M., Saltman, P., Sartoris, D. & Kerr, E., 1989. A comparison of quantitative dual energy radiographic absorptiometry and dual photon absorptiometry of the lumbar spine in postmenopausal women. *Calcified Tissue International, 45*, 288–291.

Wahner, H. W., Dunn, W. L., Brown, M. L., Morin, R. L. & Riggs, B. L., 1988. Comparison of dual-energy X-ray absorptiometry and dual photon absorptiometry for bone mineral measurements of the lumbar spine. *Mayo Clinic Proceedings, 63*, 1075–1084.

Webber, C. E., 1989. Some factors which influence the evaluation of a dual photon measurement of lumbar spine bone mineral mass. *Journal of the Canadian Association of Radiologists, 40*, 87–91.

1991, *The British Journal of Radiology*, *64*, 221–224

Ultrasound of the pelvis and renal tract combined with a plain film of abdomen in young women with urinary tract infection: can it replace intravenous urography?

A prospective study

By M. M. J. McNicholas, MRCPI, FFR.RCSI, J. F. Griffin, FFR.RCSI and D. F. Cantwell, MD, FRCPI, FRCR, FFR.RCSI

Department of Diagnostic Radiology, St Vincent's Hospital, Dublin 4, Ireland

(*Received August 1990 and in revised form October 1990*)

Keywords: Sonography, Urography, Urinary tract infection, Women

Abstract. Urinary tract infection (UTI) is common in women and intravenous urography (IVU) is a frequently requested radiological investigation for recurrent UTI. The aim of this study was to assess whether pelvic and renal ultrasound combined with a plain film of the abdomen (KUB) could replace IVU as the initial radiological investigation in young women with recurrent UTI. Ninety-four young women with recurrent UTI who were referred for IVU were studied. Ultrasound of the pelvis and renal tract was performed, and information obtained from ultrasound and KUB was compared with that obtained from the IVU examination. Patient management was altered as a result of radiological investigation in eight cases. A case of staghorn calculus and a case of pelviureteric junction obstruction were diagnosed by both IVU and ultrasound with KUB. An intrarenal abscess was diagnosed by ultrasound in a patient with a normal IVU. In addition ultrasound demonstrated significant findings in the pelvis, including ovarian and uterine abnormalities and an ectopic and an intrauterine pregnancy. In all cases the patient had symptoms referable to the urinary tract and a history of documented UTI. The KUB did not yield any unsuspected finding not diagnosed by ultrasound, but did serve to delineate more clearly the extent of calculus disease in two patients. We suggest that ultrasound of the pelvis and renal tract combined with a KUB should be the radiological investigation of choice in young women with UTI.

Several studies have shown that the diagnostic yield of intravenous urography (IVU) in young women with uncomplicated urinary tract infection (UTI) is very low and that IVU findings alter patient management in only 1–2% (Fowler & Pulaski, 1981; Lieberman & Macchia, 1982; de Lange & Jones, 1983). Furthermore, it is shown to have a poor cost benefit ratio (Fair et al, 1979; Fairchild et at, 1982; Newhouse et al, 1982) and it is suggested that this examination should only be performed on patients who have other "risk factors" such as haematuria, calculus disease or biochemical evidence of impaired renal function (Fairchild et al, 1982; Lieberman & Macchia, 1982; de Lange & Jones, 1983). Ultrasound has been shown to be an effective alternative to IVU in many renal tract diseases (Lewis-Jones et al, 1989). Ultrasound of the bladder and renal tract combined with a plain film of the abdomen (KUB) is now well established as the initial investigation in the assessment of children with UTI (Gordon, 1990). A recent study has compared ultrasound of the kidneys and a KUB with IVU in patients with UTI of both sexes and of all ages but the bladder was not filled specifically for the ultrasound examination (Spencer et al, 1990). The authors showed ultrasound to be as accurate as IVU in the diagnosis of pathology in their study group.

Young women constitute a special subgroup of patients with UTI. Urinary infection is relatively common in women (Stamey, 1980) and in our experience young women with UTI account for up to 10% of all IVU referrals. Young women of childbearing age are also a group in whom particular care should be taken to avoid unnecessary irradiation to the abdomen. It is therefore surprising that the value of ultrasound of the pelvis and abdomen has not been formally evaluated in these patients.

We performed a prospective study of young women with recurrent UTI. The aim of the study was to compare the value of ultrasound and a KUB with IVU.

Patients and methods

Ninety-four consecutive pre-menopausal women who were referred for IVU with a diagnosis of recurrent UTI were studied. The patients ranged in age from 13 to 45 years with a mean of 26.8 years. Two thirds were referred by a hospital doctor and the remainder were referred by their family doctor. Twenty-four patients (26%) had undergone a previous IVU examination and three had two or more previous IVU examinations. The mean duration since the last menstrual period was 15 days.

Address correspondence to Dr Michelle McNicholas, St Vincent's Hospital, Dublin 4, Ireland.

All patients were symptomatic at the time of referral. The patients were questioned about previous infection and in the case of hospital-referred patients the case notes were studied. All patients had one or more laboratory proven urinary tract infections. Only patients with uncomplicated UTI were studied. Patients with other problems such as diabetes, frank haematuria or evidence of impaired renal function were excluded from the study.

In performing the IVU, a plain film was taken including the renal areas and bladder. Sodium iothalamate (50 ml) was injected intravenously unless there was a history of allergy, in which case low osmolar contrast was used. An immediate film was taken and compression applied. Films were exposed at 5 and 10 minutes and a full length film after release of compression was obtained at 20 minutes. Nephrotomography was performed at the discretion of the supervising radiologist.

Following IVU examination the patient was instructed to fill her bladder. Ultrasound of the pelvis and renal tract was performed using an ATL Ultramark 4 machine with 3 MHz and 5 MHz transducers. Ultrasound was reported with the KUB but without access to the remainder of the IVU examination. All IVU examinations were reported by one author (D.F.C.), and the results were compared.

Results

Patients in whom imaging altered clinical management

Eight patients had diagnoses which altered their management (Table I). Three patients had pathological findings related to the renal tract and five had significant findings in the pelvis. Of those with renal findings, all three were diagnosed by ultrasound plus KUB while two were diagnosed by IVU. The pelvic findings were diagnosed by ultrasound alone. Six significant diagnoses were made exclusively by ultrasound. An ectopic pregnancy was diagnosed in a 25-year-old patient with lower abdominal pain, dysuria and a current laboratory proven urinary infection. Another 25-year-old woman with frequency and dysuria had an 8-week pregnancy diagnosed by ultrasound. Her last menstrual period was given as 24 days and she had denied the possibility of pregnancy. Two ovarian lesions were detected. One was a mixed solid and cystic lesion in a 14-year-old girl who at surgery had haemorrhage into a multilocular cyst. A 26-year-old patient with frequency, lower abdominal pain and a current UTI had a 7 cm ovarian cyst detected. This was resected because of its size and failure to regress on follow-up scans. A 38-year-old patient who complained of frequency, urgency and stress incontinence had multiple large uterine fibroids and underwent hysterectomy. Only one significant renal finding was diagnosed exclusively by ultrasound. This patient was a 13-year-old girl with dysuria, frequency and loin pain. Ultrasound showed a 1.5 cm intrarenal mass. Computed tomography showed an enhancing lesion with a fluid level consistent with an abscess. Follow-up ultrasound showed resolution with aggressive antibiotic therapy. Intravenous urogram had shown no abnormality.

Imaging diagnoses which did not alter treatment

Eleven other abnormalities were demonstrated which did not alter patient management (Table II). Seven renal abnormalities were demonstrated by both modalities. Four of these were not considered to be significant (duplex system, absent kidney and post partum dilatation). Three diagnoses, though relevant, did not actually alter clinical management (scarring and intrarenal calculus). Similarly, the findings made by pelvic ultrasound in this group, though considered pathological, did not alter patient management.

Table I. Imaging diagnoses which altered patient management

Patient, age	Days since last menstrual period	Symptoms	Diagnosis	Diagnosed by
Renal pathology				
AK, 13	10	Loin pain, frequency, dysuria	Intrarenal abscess	Ultrasound
EW, 24	21	Loin pain, dysuria	Staghorn calculus	Ultrasound and IVU
MG, 29	18	Loin pain	Severe pelviureteric junction obstruction	Ultrasound and IVU
Incidental pelvic findings				
CR, 38	9	Lower abdominal pain, urgency, incontinence	Large uterine fibroids	Ultrasound
DF, 25	2	Frequency, lower abdominal pain	7 cm ovarian mass	Ultrasound
JC, 14	31	Lower abdominal pain, dysuria	5 cm ovarian mass	Ultrasound
BT, 25	10	Lower abdominal pain, dysuria, frequency	Ectopic pregnancy	Ultrasound
SM, 25	24	Frequency, dysuria	8-week intrauterine pregnancy	Ultrasound

Table II. Imaging diagnoses which did not alter patient management

Diagnosis	Patients	Diagnosed by
Renal findings		
Renal scarring	1	Ultrasound and IVU
Scarring and intrarenal calculus	1	Ultrasound and IVU
Absent kidney	1	Ultrasound and IVU
Post partum ureteric dilatation	2	Ultrasound and IVU
Duplex ureter	2	Ultrasound and IVU
Incidental pelvic findings		
Uterine fibroids	2	Ultrasound
Ovarian cyst < 5 cm	2	Ultrasound

Value of the KUB

The KUB did not yield any information which was not available from the ultrasound examination. However, in the two patients with calculus disease it was helpful in delineating the extent of this.

Discussion

Two important points have emerged from this study. The first is that ultrasound of the renal tract plus a KUB is comparable with IVU in the diagnosis of renal pathology in young women with UTI. The second is the high yield of pelvic ultrasound in diagnosing unsuspected conditions in the pelvis including pregnancy.

The intravenous urogram yields information on renal size and contour, collecting systems and bladder. Ultrasound also gives information on renal size, shape and internal architecture. Nephrocalcinosis may be diagnosed as may renal calculi (Hill et al, 1985), and the addition of a KUB will ensure that small calculi are not missed. Ultrasound will detect even minimal dilatation of the collecting systems. The bladder is readily assessed when full and abnormalities such as calculi or diverticula can be diagnosed. Bladder emptying can also be measured.

Ultrasound is the examination of choice to demonstrate the pelvic organs and will diagnose conditions such as ovarian cysts, uterine fibroids, pelvic inflammatory disease, endometriosis or unsuspected pregnancy—findings which will not be diagnosed by IVU but which may coexist with UTI, especially in this group of patients.

To justify any examination, the risks and costs incurred should be balanced against the yield of diagnostic information of benefit to the patient. IVU is an expensive investigation, especially when low osmolar contrast is used (Dawson et al, 1983). It is invasive, has significant side effects (Owens & Ennis, 1980) and an associated mortality (Hartman et al, 1982). It involves a considerable dose of irradiation to the gonads (Ewen et al, 1972). Our study group is one where irradiation to the gonads should be avoided and the possibility of unsuspected pregnancy borne in mind at all times. The incidence of important renal abnormalities in this study was low (2%) and comparable with many previous studies (Fowler & Pulaski, 1981; Lieberman & Macchia, 1982; Newhouse et al, 1982; de Lange & Jones, 1983). This implies a poor cost-benefit ratio for IVU in this group of patients.

Ultrasound, in contrast to IVU, has no known risks in diagnostic usage. It is non-invasive, inexpensive and acceptable to the patient. It imparts no radiation and if unsuspected pregnancy is diagnosed, further radiological investigation (including KUB) can be avoided. In experienced hands it is a relatively quick examination once the bladder is full. The yield in terms of altered patient management in this study was 8.5%. We feel that this is cost effective and justifies ultrasound as a diagnostic test in our study group.

Based on the findings of this study we suggest that the IVU be abandoned as the initial radiological investigation in young women with uncomplicated UTI. We further recommend that ultrasound of the pelvis and renal tract followed by a plain film of the abdomen should be the investigation of choice in this group of patients.

Acknowledgments

The authors would like to thank the radiography staff at St Vincent's Hospital for their enthusiastic cooperation during the study period. In particular, Ms Joan Miller, Senior Ultrasonographer, was of invaluable assistance.

References

Dawson, P., Grainger, R. G. & Pitfield, J., 1983. The new low-osmolar contrast media: a simple guide. *Clinical Radiology*, *34*, 221–226.

Ewen, K., Schmitt, G. & Kaufman, H., 1972. Gonadenexpositionen bei drei Roentgendiagnostischen Standarduntersuchungen. *Roentgen Fortschritte*, *116*, 808–817.

Fair, W. R., McClennan, B. L. & Jost, R. G., 1979. Are excretory urograms necessary in evaluating women with urinary tract infection? *Journal of Urology*, *121*, 313–315.

Fairchild, T. N., Shuman, W. & Berger, R. E., 1982. Radiographic studies for women with recurrent urinary tract infections. *Journal of Urology*, *128*, 344–345.

Fowler, J. E. & Pulaski, E. T., 1981. Excretory urography, cystography and cystoscopy in the evaluation of women with urinary tract infection. *New England Journal of Medicine*, *304*, 462–465.

Gordon, I., 1990. Urinary tract infection in paediatrics: the role of diagnostic imaging (review article). *British Journal of Radiology*, *63*, 507–511.

Hartman, G. W., Hattery, R. R., Witten, D. M. & Williamson, B., 1982. Mortality during excretory urography: Mayo Clinic experience. *American Journal of Roentgenology*, *139*, 919–922.

Hill, M. C., Rich, J. I., Mardiat, J. G. & Finder, C. A., 1985. Sonography vs excretory urography in acute flank pain. *American Journal of Roentgenology*, *144*, 1235–1238.

de Lange, E. E. & Jones, B., 1983. Unnecessary intravenous urography in young women with recurrent urinary tract infections. *Clinical Radiology*, *34*, 551–553.

Lewis-Jones, H. G., Lamb, G. H. R. & Hughes, P. L., 1989. Can ultrasound replace the intravenous urogram in preliminary investigation of renal tract disease? *British Journal of Radiology*, *62*, 977–980.

Lieberman, E. & Macchia, R. J., 1982. Excretory urography in women with urinary tract infection. *Journal of Urology*, *127*, 263–264.

Newhouse, J. H., Rhea, J. T., Murphy, R. X. & Pfister, R. C., 1982. Yield of screening urography in young women with urinary tract infection. *Urologic Radiology*, *4*, 187–190.

Owens, A. & Ennis, M., 1980. Arrythmias occurring during intravenous urography. *Clinical Radiology*, *31*, 291–295.

Spencer, J., Lindsell, D. & Mastorakou, I., 1990. Ultrasonography compared with intravenous urography in investigation of urinary tract infection in adults. *British Medical Journal*, *301*, 221–224.

Stamey, T. A., 1980. Urinary tract infections in women. *Pathogenesis and Treatment of Urinary Tract Infection* (Williams and Wilkins, Baltimore, MD) pp. 122–210.

1991, *The British Journal of Radiology*, *64*, 225–227

Unsuspected sphincter damage following childbirth revealed by anal endosonography

By Sarah J. D. Burnett, MRCP, Clive Spence-Jones, FRCS, MRCOG, Christopher T. M. Speakman, FRCSEd, Michael A. Kamm, MRCP, FRACP, Christopher N. Hudson, FRCOG and *Clive I. Bartram, FRCR, FRCP

Departments of Radiology and Physiology, St Mark's Hospital, City Road, London EC1V 2PS, UK

(Received August 1990 and in revised form September 1990)

Keywords: Anal sphincters, Delivery, Ultrasonography

Abstract. Anal endosonography was performed in 62 consecutive patients with incontinence of flatus or faeces following obstetric trauma, and in 18 parous controls. Of the incontinent group, 90% had defects in the external sphincter, 65% in the internal sphincter and 44% disruption of the perineal body, compared with none of the controls. This triad of lesions is pathognomonic of obstetric trauma. Anal endosonography revealed a higher prevalence of sphincter damage than expected from anorectal physiology tests, and therefore has a role in screening patients following complicated or difficult deliveries.

The prevalence of faecal incontinence after childbirth is unknown, but referrals to coloproctology centres are not uncommon. The magnitude of the problem may be underestimated, as many patients are reluctant to admit to incontinence (Leigh & Turnberg, 1984). However, in a prospective study of 122 women, two developed frank incontinence soon after delivery (Snooks et al, 1986).

Anorectal physiology studies have identified two major causes of incontinence: pudendal neuropathy, causing late incontinence, and traumatic rupture of the external anal sphincter, causing early incontinence.

The pudendal nerve supplies the external anal sphincter. A neuropathy has been implicated as the main cause of idiopathic incontinence, and is indicated by a prolonged pudendal nerve terminal motor latency (greater than 2.2 ms). This is a test of nerve conduction. Using a special finger glove, one electrode is placed close to the pudendal nerve as it courses over the ischial spine, in order to stimulate it, and the time taken for the electrical impulse to contract the external sphincter is measured (Kiff & Swash, 1984). Stretching of these nerves during childbirth is thought to lead to progressive denervation of the striated anal sphincter muscles, with incontinence resulting many years later. Even soon after childbirth, the effect of pelvic floor stretching on nerve function can be observed. A pudendal neuropathy has been found in 42% of all vaginal deliveries at 48–72 hours, with 14% still affected at 2 months (Snooks et al, 1984).

Alternatively, the sphincter mechanism may be exposed to direct trauma, and rupture of the external anal sphincter (Green & Soohoo, 1989) is identified by a combination of digital assessment of the external sphincter, and mapping with a concentric electromyography needle (Browning et al, 1988). This is painful, and multiple needle insertions are required for detailed mapping of the external anal sphincter.

Some information may be inferred from anal manometry, where a small pressure probe within the anal canal is used to measure the resting and squeeze pressures (Read & Bannister, 1985). The internal sphincter is responsible for about 85% of the resting pressure (Duthie & Watts, 1965), so that a low resting pressure suggests damage to the internal sphincter. The squeeze pressure depends on good contraction of the external sphincter and puborectalis muscles, and may be reduced if this part of the sphincter is damaged.

Before anal endosonography, the morphology of the anal sphincters could not be imaged in detail; this technique is unique in being able to image both the internal and external sphincters, and has provided the first opportunity to assess directly the damage to the sphincter complex after childbirth.

Materials and methods

Anal endosonography was performed on 62 women (aged 22–63, mean 39 years) of differing parity, referred to the Department of Anorectal Physiology with incontinence of flatus and/or faeces, where the only identifiable predisposing factor was obstetric trauma during vaginal delivery. Patients with previous anal surgery, inflammatory bowel disease, diabetes or neurological disease were excluded. Unfortunately, a precise obstetric history was not available, and although the majority of women could remember forceps being applied, many

---

*Author for correspondence.

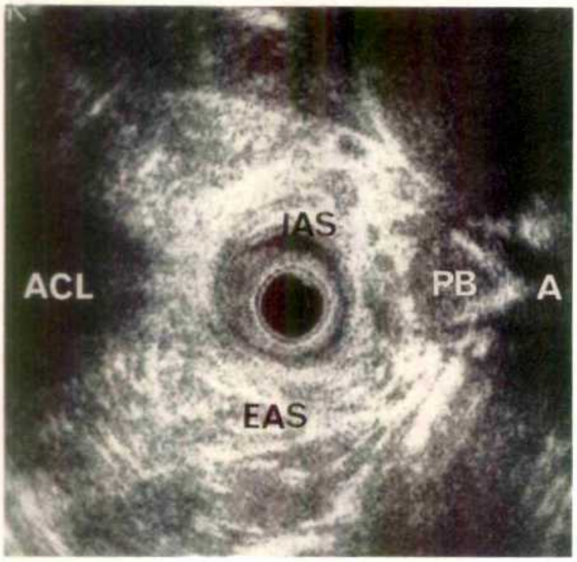

Figure 1. Normal anatomy in mid-level anal canal. The probe is rotated so that anterior is on the right (A), corresponding to the patient's left lateral position. The perineal body (PB) is seen anterior as an ovoid body of moderate echogenicity. The anococcygeal ligament (ACL) creates a hypoechoic triangular wedge posteriorly. The internal anal sphincter (IAS) is a well defined hypoechoic inner ring. The external anal sphincter (EAS) shows the typical linear pattern of striated muscle.

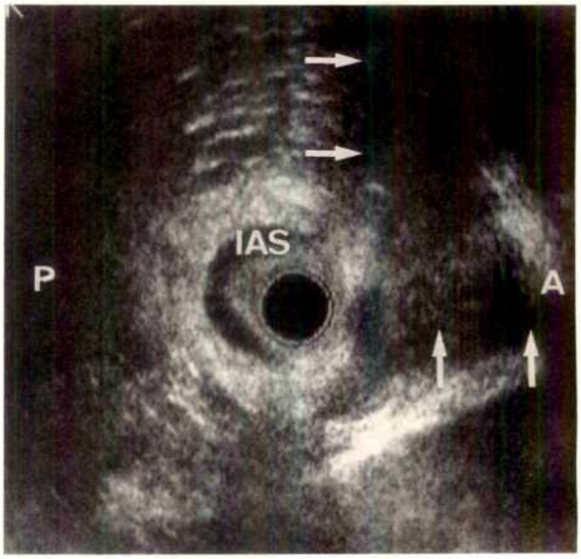

Figure 2. The typical triad of defects following obstetric trauma. There is a wedge-shaped defect in the external anal sphincter in the right anterolateral quadrant (arrows), with loss of definition of the perineal body, and an anterior defect in the internal anal sphincter.

were unable to say if they had an episiotomy performed or if they had been allowed to tear.

A control group of 18 parous women (aged 25–75, mean 50 years) without anorectal dysfunction or surgery were also studied, having given written informed consent. These patients were attending the colonoscopy department for the investigation of rectal bleeding.

All subjects underwent anal endosonography using a Brüel and Kjaer 7 MHz scanner with a rotating endoprobe of focal length 3 cm. This was fitted with a hard sonolucent plastic cone of 1.7 cm external diameter and filled with degassed water for acoustic coupling. Radial images throughout the anal canal were obtained, with the patient in the left lateral position. The image on the screen has "12 o'clock" on the left and therefore directly mirrors the position of the patient. The technique is rapid and well tolerated (Law & Bartram, 1989), and the normal appearance in a female is shown in Fig. 1.

An external anal sphincter defect was defined as a wedge-shaped loss of normal striated muscle appearance, which could be either hyperechoic, hypoechoic or of mixed echogenicity relative to normal muscle. These sonographic appearances have been confirmed as muscle defects during simultaneous anal endosonography and electromyography (Burnett et al, 1990). An internal sphincter defect presented as a gap in the continuity of the hypoechoic ring of smooth muscle. Defects were measured in hours, as from a clock face with 12 o'clock anteriorly. The normal female perineal body is seen as a complex ovoid structure situated anteriorly. Perineal body disruption was defined as loss of definition of the normal perineal structures with an overall amorphous featureless appearance.

Forty-nine of the 62 incontinent patients had anal manometry and pudendal nerve terminal motor latencies performed using standard methods.

Results

Anal endosonography revealed that 56 out of 62 (90%) incontinent patients had an external anal sphincter defect, each situated in the right anterolateral quadrant with a mean size of 3.6 hours. Forty out of 62 (65%) had an internal sphincter defect, also all in the right anterolateral quadrant, of mean size 4.2 hours. Thirty-seven (60%) had lesions in both sphincters. Twenty-five out of 57 (44%) patients in whom the perineal body was studied had disruption of the perineal body (Fig. 2).

Of the 49 patients who underwent anorectal physiology studies, external sphincter defects were found in 45, but only 19 (42%) had a squeeze pressure below the lower limit of the normal, and of the 34 patients with internal sphincter defects, only 11 (32%) had a resting pressure below the lower limit of normal. There was no significant difference in either the resting or squeeze pressures for patients with or without pudendal neuropathies.

A pudendal neuropathy was present in 28 out of 49 (57%). In 19 patients (68%) the neuropathy was associated with lesions of both sphincters, in six (21%) with damage to the external sphincter only, and in one (4%) with damage to the internal sphincter only. Two patients (7%) with normal morphology had pudendal neuropathies but both of these women were studied within 3 months of delivery. Conversely, of 21 women without a pudendal neuropathy, none had normal morphology.

None of the control group had a defect in either the internal or external anal sphincters, and all had normal perineal bodies. Anorectal physiology was not performed on the control group.

Discussion

With the advent of anal endosonography, it has become possible to image defects in both the external and internal sphincters, providing another dimension to the investigative options for the clinician. It is used to provide anatomical information, complementary to the functional data provided by anorectal physiology.

Ultrasound has shown a high prevalence of internal sphincter damage in obstetric trauma, hitherto unrecognized. Although it has previously been believed that a normal anal resting pressure indicated "no abnormality of internal sphincter function" (Snooks et al, 1984), in our subjects 68% of those women with an internal sphincter lesion had a normal resting pressure.

Only anal endosonography can reveal that internal sphincter lesions are frequently associated with a complex of a right anterolateral external sphincter defect and disruption of the perineal body. The common association of these findings indicates a common aetiology and may well reflect the practice of right posteromedial episiotomy in this country. Although prolonged or traumatic deliveries are more likely to result in both sphincter damage and pudendal neuropathy, determining the exact cause requires a further prospective study.

An experienced clinician is able to make some assumptions about defects in the external anal sphincter by digital examination, and may use electromyographic mapping in cases where scarring causes difficulty in determining defects in the muscle ring of the external sphincter (Browning et al, 1988). Anorectal physiology is time consuming and may be unpleasant for the patient, and its value in predicting outcome after postanal repair is disputed (Womack et al, 1988; Scott et al, 1990). Although the presence of a pudendal neuropathy is clearly significant in the pathogenesis of incontinence, it was present in only 57% of our patients whereas over 95% had some morphological damage. Intact sphincter musculature is important to maintain continence (Browning et al, 1988; Duthie & Watts, 1965).

Endosonography is a developing branch of ultrasound with applications in many different fields. Incontinence immediately following childbirth is a dramatic symptom, and suggests that the patient has ruptured part of the external sphincter. Although this may be obvious clinically, anal endosonography will confirm how much of the external sphincter has been damaged and if the internal sphincter is also involved, which is more difficult to appreciate clinically. Its role in evaluating asymptomatic patients after a difficult or complicated delivery is as yet unclear. This study suggests that many of these patients will have suffered sphincter damage and that this is a contributory factor in cases with delayed onset of incontinence. It is possible that early sphincter repair might prevent this, but at present the only firm indication for the examination must be that the patient has become incontinent.

References

Browning, G. P., Motson, R. W. & Henry, M. M., 1988. Combined sphincter repair and postanal repair for the treatment of complicated injuries to the anal sphincters. *Annals of the Royal College of Surgeons of England, 70,* 324–328.

Burnett, S. J. D., Speakman, C. T. M., Kamm, M. A. & Bartram, C. I., 1990. Confirmation of endosonographic detection of external anal sphincter defects by simultaneous electromyographic mapping. *British Journal of Surgery,* in press.

Duthie, H. L. & Watts, J. M., 1965. Contribution of the external sphincter to the pressure zone in the anal canal. *Gut, 6,* 64–68.

Green, J. R. & Soohoo, S. L., 1989. Factors associated with rectal injury in spontaneous deliveries. *Obstetrics and Gynecology, 73,* 732–738.

Kiff, E. & Swash, M., 1984. Slowed conduction in the pudendal nerves in idiopathic (neurogenic) faecal incontinence. *British Journal of Surgery, 71,* 614–616.

Law, P. J. & Bartram, C. I., 1989. Anal endosonography: technique and normal anatomy. *Gastrointestinal Radiology, 14,* 349–353.

Leigh, R. J. & Turnberg, L. A., 1982. Faecal incontinence: the unvoiced symptom. *Lancet, 1,* 1349–1351.

Read, N. W. & Bannister, J. J., 1985. Anorectal manometry. In *Coloproctology and the Pelvic Floor,* ed. by M. M. Henry and M. Swash (Butterworths, London), chapter 4, pp. 66–69.

Scott, A. D. N., Henry, M. M. & Phillips, R. K. S., 1990. Clinical assessment and anorectal manometry before postanal repair: failure to predict outcome. *British Journal of Surgery, 77,* 628–629.

Snooks, S. J., Setchell, M., Swash, M. & Henry, M. M., 1984. Injury to innervation of pelvic floor musculature in childbirth. *Lancet, 2,* 546–550.

Snooks, S. J., Swash, M., Henry, M. M. & Setchell, M., 1986. Risk factors in childbirth causing damage to the pelvic floor innervation. *International Journal of Colorectal Disorders, 1,* 20–24.

Womack, N. R., Morrison, J. F. B. & Williams, N. S., 1988. Prospective study of the effects of postanal repair in neurogenic faecal incontinence. *British Journal of Surgery, 75,* 48–52.

1991, *The British Journal of Radiology 64*, 228–231

Fracturing and stretching of angioplasty balloon catheters under bending with tension

By W. D. Jeans, FRCR, A. Blakeborough, PhD and *H. W. C. Loose, FRCR

Departments of Radiodiagnosis and Civil Engineering, University of Bristol, Bristol, UK and *Freeman Hospital, Newcastle upon Tyne, UK

(Received January 1990 and in revised form September 1990)

Keywords: Angioplasty, Catheterization, Balloon catheters

Abstract. Eight catheters from five manufacturers have been subjected to tests which combined bending and tension. Three failure mechanisms have been identified. These included separation of the balloon from its proximal attachment to the shaft, fracture of the shaft at its junction with the balloon, and undue ductility of the shaft. It is concluded that good catheter design should ensure that there is no sudden change in stiffness along the length of the catheter, and that the optimum relationship of ductility to stiffness has not yet been defined for catheters. Recommendations relating to these characteristics could be included in the British Standards relating to angioplasty balloon catheters.

Mechanical problems with angioplasty balloon catheters that cause difficulties for the angiographer are relatively rare, and until recently those reported were related to failure of the balloon to deflate (Schneider et al, 1985), rupture of the balloon (Yune & Klatte, 1980) or rupture of arteries (Simonetti et al, 1983; Murphy et al, 1987; Henson et al, 1988).

Recently, a hazard notice was issued by the Department of Health following the separation of the balloon and distal end of a catheter from its shaft on withdrawal from a renal artery (Department of Health, 1988). Avulsion of an Olbert type balloon in a patient with scar tissue in the groin has been reported (Law & Dacie, 1989). This report provoked two letters reporting similar incidents with the same type of catheter, in one of which the balloon failed to deflate (Raphael & Pardy, 1989; Timmis, 1989). We have previously reported on the behaviour of balloons in angioplasty catheters (Henson et al, 1988; Jeans et al, 1989) and, in view of these newly reported problems, have now carried out tests on a series of catheters to assess the mechanical effects of pulling with varying loads on balloon catheters held at an acute angle.

Method

An apparatus was constructed to hold a balloon catheter so that an increasing load could be attached to one end, whilst the balloon end was held still. A metal tube of 1.5 cm internal diameter was welded to a plate attached to a metal framework by a bolt. A thickwalled Portex plastic tube with an internal diameter of either 5.7 mm or 3 mm was fixed within the metal tube, with one end projecting 2 cm from it. The balloon was placed without a guidewire within the thickwalled plastic tube, which was set at 135° to the line of the catheter shaft, to simulate the maximum angulation to the aorta seen in renal arteries and that between the two common iliac arteries.

The catheter shaft was led upwards to a pulley placed directly above the end of the thickwalled plastic tube, and then at 90° to a second pulley and downwards so that its end could be attached to a metal weight carrier, weighing 480 g (Fig. 1). The 2 cm free end of the thickwalled plastic tube provided a slight curve between the balloon segment and the shaft of the catheter.

The balloon and distal 25 cm of the catheter being

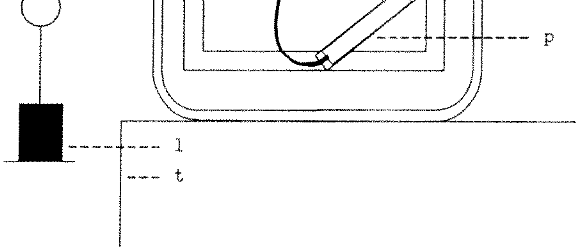

Figure 1. Diagram of experimental set-up showing balloon within thickwalled plastic tube held at 135° to the shaft of the catheter. w = waterbath; p = thickwalled plastic tube containing inflated balloon; l = load carrier; t = table.

Professor W. D. Jeans, College of Medicine, Sultan Qaboos University, PO Box 32485, Al-Khod, MUSCAT, Sultanate of Oman.

Table I. Balloon catheters tested, with loadings achieved and results (MRP is maximum recommended pressure)

Test number	Make	Balloon			Catheter length and type	Expiry date	Identification number	Maximum load achieved (kg)	Results and comments
		Length (mm)	Diameter (mm)	MRP (atm)					
1	Eschmann	50	6	17	90 cm	n.a.	D8158	5.78	Shaft—slight stretching. Balloon—outer sheath of balloon pulled away at proximal end.
2	Meditech	40	7	17	75 cm Blue Max	9/91	119448	2.98	Shaft—slight stretching. Balloon—pulled away from proximal fixation, and everted.
3	Meadox (Olbert)	40	7	12 bar	90 cm (6F)	5/91	3779, batch 799462	2.88	Shaft—considerable stretching, so no further loading possible. No break occurred.
4	Bard (USCI)	40	7	10	80 cm PE PLUSII	n.a.	972360	6.98	Shaft—slight stretching. Balloon—pulled out intact. No break occurred.
5	Bard (USCI)	40	5	10	80 cm PE PLUSII	n.a.	979720	6.68	Shaft—torn on one side, but kept in continuity by outer layer. Balloon—pulled out intact.
6	Cook	40	6	15	80 cm Omega NV	12/92	132886.01	2.98	Shaft—slight stretching. Balloon—pulled out intact. No break occurred.
7	Cook	40	6	15	80 cm Omega NV	5/92	108903.01	4.98	Shaft—slight stretching. Balloon—pressure leak at junction of shaft and balloon.
8	Cook	100	4	10	80 cm Omega C TM	10/89	031736.01	0.98	Shaft—clean break at junction of catheter and proximal balloon end. Balloon—pressure leak when angled at 135° initially.

tested were immersed in a water bath at 38°C, and the balloon was blown up within the plastic tube to 8 atm pressure, after being positioned so that the junction of its proximal end with the shaft was at the edge of the thickwalled plastic tube. 110 g weights were then loaded onto the carrier until either the catheter or the balloon failed, or the balloon pulled out of the thickwalled plastic tube.

Results

Seven catheters of 7F and one of 6F diameter from five manufacturers were taken from angiography room stocks and tested before their stated expiry date (where this was given). The results are shown in Table I.

In three catheters no break occurred, and the experiment was terminated. In Tests 4 and 6 the balloon pulled out of the thickwalled plastic tube, one with a

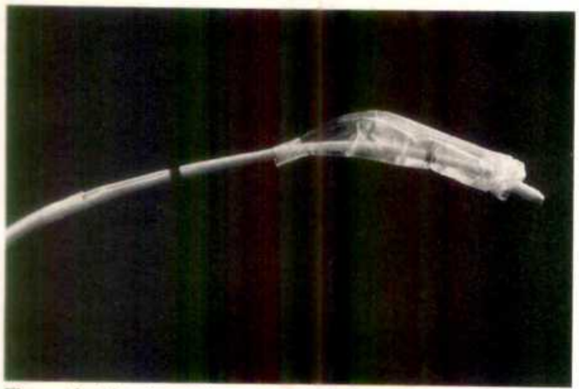

Figure 2. Number 2 in test series. Separation of proximal attachment of balloon from shaft, with eversion of balloon, at loading of 2.88 kg.

load of 6.98 kg and the other with 2.98 kg. In Test 3 the catheter (similar to the type used by Law and Dacie) stretched so far that it could not be given a loading greater than 2.88 kg, when the loaded carrier reached the floor.

In two catheters (Tests 5 and 7) no complete break occurred, but in one the shaft tore on one side and was held together by its outer plastic layer, and in the other there was a pressure leak at the junction of the balloon and shaft.

Breaks occurred in three catheters. In Test 1 the outer sheath of the balloon pulled away from its lining sheath proximally; in Test 2 the balloon pulled away from its proximal fixation and everted (Fig. 2); in Test 8 (the type subject to the hazard notice) there was a clean break at the junction of the balloon and shaft, at a loading of 0.98 kg (Fig. 3).

Discussion

The fracture of the catheters is an interesting case of poor design. To understand the mechanism of failure some technical engineering terms need to be outlined. Stiffness has to do with the relative deformability of a material under load, and the greater the load required to produce a given deformation, the stiffer a material is said to be. Bending stiffness is the manifestation of this property when the deformation is the change in the curvature of an object. For example, the force required to bend a wire round a pulley is a measure of the bending stiffness of the wire. Ductility is the property of a material that enables it to be drawn out to a considerable extent before rupture and at the same time to sustain an appreciable load. A non-ductile material is said to be brittle, in that it fractures with little or no elongation (Davis et al, 1982).

Catheters have to have a smooth surface to allow easy insertion and extraction. For catheter 8, which fractured completely, the surface was made smooth by grinding the shaft to produce a narrow segment with a shoulder to which the balloon was attached. This particular design produced a very stiff balloon connected to a flexible shaft. Bending of this with the shaft in tension produces a sharp kink at the junction of the balloon and the shaft where all the deformation is concentrated. The catheter material there did not possess enough ductility to sustain the load and the catheter failed in tension from the tensile bending stresses caused by the kink. The load required to fracture this catheter was about one third of that required to cause failure in the next weakest catheter.

It is good engineering practice to ensure that a structure has no sudden changes in bending stiffness along its length, since bending stresses at the point of change are likely to result in failure, and it appears that this practice should apply to catheters also. The other two Cook catheters of later manufacture did not fracture, but one developed a pressure leak from the proximal junction when angled.

The Olbert catheter shaft has the property of being very ductile and is therefore unlikely to fail under bending stresses. The sample tested began to stretch extensively at a much lower load than that applied to other catheters. This has the possible advantage that no

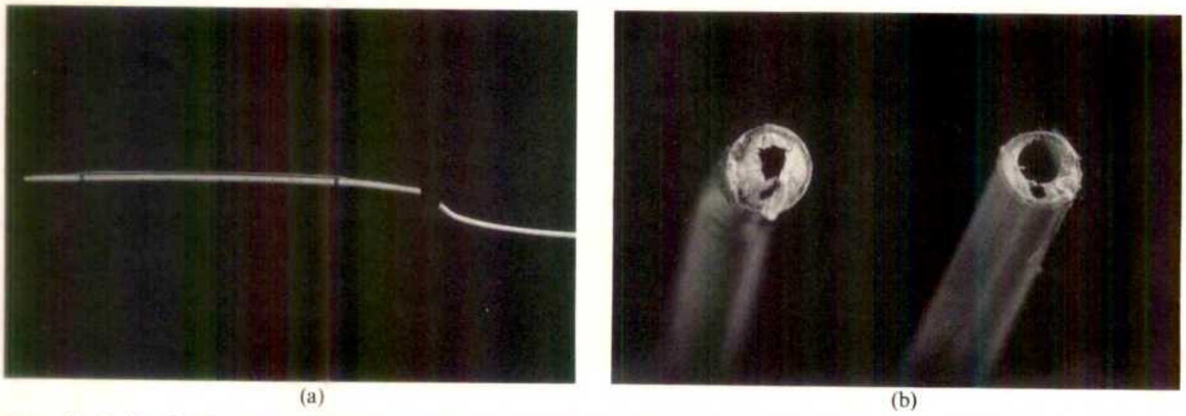

(a) (b)

Figure 3. (a) Number 8 in test series: site of break at a loading of 0.98 kg. (b) View of adjacent ends of catheter showing clean fracture.

great force can be applied in withdrawing the catheter, which may protect the patient's arteries, but has the disadvantage that if difficulties occur during withdrawal pulling causes the catheter to elongate and ultimately to rupture so that surgical removal may be needed. This particular catheter shows more ductility than we think is desirable. Polyurethane catheters used in the central venous system have been shown to have less variation in their elastic characteristics than those made of Polyvinyl or silicone, with silicone catheters offering less resistance to bending (Cervera et al, 1989). It is apparent that the optimum balance between ductility and stiffness remains to be established. Pulling at an angle is more liable to cause fracturing, and this reinforces the need when the catheter shaft is angled (as may occur in the renal artery or when dilating an iliac artery following a retrograde femoral puncture on the opposite side) to follow the standard practice of ensuring that the balloon is completely deflated before removal. The catheter should be withdrawn over a guidewire, and the movement of the balloon markers monitored fluoroscopically. If the area of insertion is scarred or an arterial graft is present insertion should be through an introducer (Law & Dacie, 1989), or a catheter with less ductility than the Olbert should be used.

These results also suggest that standards for the ductility and stiffness of angioplasty catheters should be added to the proposed British Standards recommendations.

References

CERVERA, M., DOLZ, M., HERRAEZ, J. V. & BELDA, R., 1989. Evaluation of the elastic behaviour of central venous PVC, polyurethane and silicone catheters. *Physics in Medicine and Biology*, *34*, 177–183.

DEPARTMENT OF HEALTH, 1988. Hazard notice, HC (Hazard) (88) 26.

DAVIS, H. E., TROXELL, G. E. & HAUCK, G. F. W., 1982. *The Testing of Engineering Materials*, 4th edn (McGraw-Hill, New York).

HENSON, J. H. L., JEANS, W. D., NEWHAM, J., PAICE, C. & BLAKEBOROUGH, A., 1988. Assessment of angioplasty balloon catheters: preliminary studies. *British Journal of Radiology*, *61*, 1026–1031.

JEANS, W. D., HENSON, J. H. L., HOLLOWAY, T. M. A., FORMAN, A. G. G. & BLAKEBOROUGH, A., 1989. Assessment of angioplasty balloon catheters: further studies. *British Journal of Radiology*, *62*, 121–126.

LAW, P. & DACIE, J. E., 1989. Avulsed Olbert balloon—an avoidable complication of percutaneous transluminal angioplasty. *Clinical Radiology*, *40*, 88–90.

MURPHY, T. P., CRONAN, J. J., PAOLELLA, L. P., DORFMAN, G. S. & FRANCIS, W. W., 1987. Arterial rupture without balloon rupture during percutaneous transluminal angioplasty. *Journal of Vascular Surgery*, *6*, 528–530.

RAPHAEL, M. J. & PARDY, B. J., 1989. Avulsed Olbert balloon. *Clinical Radiology*, *40*, 542–543.

SCHNEIDER, J. R., JOHNSRUDE, I. S., LUND, G., RYSAVY, J., ANDERSON, R. W. & AMPLATZ, K., 1985. Percutaneous catheter balloons: failure to deflate. *Radiology*, *155*, 832.

SIMONETTI, G., ROSSI, P., PASSARIELLO, R., FARAGLIA, V., SPARTERA, C., PISTOLESE, R. & FIORANI, P., 1983. Iliac artery rupture: a complication of transluminal angioplasty. *American Journal of Roentgenology*, *140*, 989–990.

TIMMIS, B., 1989. Avulsed Olbert balloon. *Clinical Radiology*, *40*, 543.

YUNE, H. Y. & KLATTE, E. C., 1980. Circumferential tear of percutaneous transluminal angioplasty catheter balloon. *American Journal of Roentgenology*, *135*, 395–396.

1991, *The British Journal of Radiology*, *64*, 232–241

Final report on the second British Institute of Radiology fractionation study: short *versus* long overall treatment times for radiotherapy of carcinoma of the laryngo-pharynx*

By [1]G. Wiernik, MD, FRCR (Chairman), [2]C. J. Alcock, MRCP, FRCR, [3]T. D. Bates, MCRA, FRCR, [4]J. M. Brindle, DMRT, FRCR, [5]J. F. Fowler, DSc, PhD (Joint Honorary Secretary), [6]W. R. Gajek, MD, FRCR, [7]S. Goodman, MA, FRCR, [8]J. L. Haybittle, MA, PhD (Consultant Statistician), [9]J. M. Henk, MA, FRCR, [1]J. W. Hopewell, BSc, PhD (Joint Honorary Secretary), [10]R. D. Hunter, MRCP, FRCR, [11]R. Lindup, DRCOG, FRCR, [12]D. L. Phillips FRCOG, FRCR and [1]M. Rezvani, MSc, PhD (Data Manager/Statistician)

The British Institute of Radiology, 36 Portland Place, London W1N 4AT

(*Received June 1990 and in revised form November 1990*)

Keywords: Fractionation, Radiotherapy, Cancer, Laryngo-pharynx

Abstract. The second British Institute of Radiology trial of dose fractionation in radiotherapy compared two groups of prospectively randomized patients with squamous carcinoma of the laryngo-pharynx; one group was treated in a short (≤4 weeks) and the other in a long (>4 weeks) overall time. Treatment in any one centre could be given, with no planned gap in the course of treatment, either as a conventional, daily (5 fractions per week regime) or as 3 fractions per week. A total of 611 patients were allocated to treatment, of whom nine have had to be excluded from the analysis for a lack of information. Patients were admitted to the trial from January 1976 to December 1985 and were followed up for a maximum of 10 years and a minimum of 3 years. A reduction in total dose was made for use in the short compared with the long treatment regime. This reduction in total dose varied between 18% and 22% depending on whether 5 fractions or 3 fractions per week regimes were used. Overall, no statistically significant differences have been found between the two arms of the trial. The patients treated with 5 fractions per week in a short overall treatment time showed fewer late normal tissue effects. An analysis based on stratification by age, stage and anatomical site gave a relative risk (short/long overall treatment time) for deaths of 1.23 with a 95% confidence interval from 0.96 to 1.59. Analyses stratified for stage and site gave relative risks with 95% confidence intervals of 1.10 (0.84–1.44) for local recurrences/tumour persistence, and 1.01 (0.70–1.45) for laryngectomies.

The British Institute of Radiology (BIR) Fractionation Working Party has now successfully completed two prospective, randomized, multicentre clinical trials of radiotherapy in the treatment of carcinoma of the laryngo-pharynx. The final report on the first BIR trial which compared 3 fractions per week (3F/wk) *versus* 5 fractions per week (5F/wk) treatments (BIR Working Party, 1990) showed no statistically significant differences between the two arms of that trial in any of the main group analyses. A number of different analyses that are based on the data from the first trial and are pertinent to this second BIR trial have also been published (Alcock et al, 1990; Barrett et al, 1990; Rezvani et al, 1989, 1990; Haybittle et al, 1990; Wiernik et al, 1990). In the early 1940s a number of radiotherapy centres in the United Kingdom had to change their

---

Patients were entered into the trial from the following centres: Bristol (J. Bullimore, S. Goodman); Liverpool (J. E. Dalby); London: Charing Cross (N. Howard, B. M. Southcott); Middlesex Hospital (R. J. Berry, N. M. Bleehen); Royal Marsden Hospital (J. M. Henk); St Thomas' Hospital (T. D. Bates, A. R. Timothy); University College Hospital (J. S. Tobias); Manchester (R. D. Hunter, R. S. Pointon on behalf of all Consultants); Oxford (C. J. Alcock, K. R. Durrant, A. H. Laing, C. H. Paine, G. Wiernik); Plymouth (J. M. Brindle); Southend (D. L. Phillips); Stoke on Trent (R. Lindup); Swansea (W. R. Gajek, D. K. Sambrook).

*Reprints are available from The British Institute of Radiology, Publications Office, 36 Portland Place, London W1N 4AT at £3 per copy or $ equivalent (remittance with order please).

Postal addresses: [1]Research Institute, Churchill Hospital, Headington, Oxford OX3 7LJ; [2]Department of Radiotherapy & Oncology, Churchill Hospital, Headington, Oxford OX3 7LJ; [3]Department of Radiotherapy & Oncology, St Thomas' Hospital, London SE1 7EH; [4]Radiotherapy Department, Plymouth General Hospital, Freedom Fields, Plymouth PL4 7JJ; [5]Department of Human Oncology, K4/336 Clinical Science Centre, 600 Highland Avenue, Madison, WI 53792 USA; [6]Department of Radiotherapy & Oncology, Singleton Hospital, Sketty, Swansea SA2 8QA; [7]Radiotherapy Centre, Horfield Road, Bristol BS2 8ED; [8]MRC Cancer Trials Office, 7 Green Street, Cambridge CB2 3JU; [9]Department of Radiotherapy & Oncology, The Royal Marsden Hospital, Downs Road, Sutton, Surrey SM2 5PT; [10]Radiotherapy Department, Christie Hospital & Holt Radium Institute, Withington, Manchester M20 9BX; [11]Department of Radiotherapy & Oncology, North Staffordshire Royal Infirmary, Hartshill, Stoke-on-Trent, Staffordshire ST4 7LN; [12]Radiotherapy Department, Southend General Hospital, Prittlewell Chase, Westcliff-on-Sea, Southend, Essex SS0 0RY.

radiation treatment regimes from an overall time of 6 weeks to 3 weeks for logistic and economic reasons. The BIR Fractionation Working Party considered that no scientific justification for such a change had been reported in the literature and, indeed, that it remained an open question as to whether the long or the short overall treatment time gave rise to relatively better or worse tumour and/or normal tissue effects. It was therefore decided to test these questions in a formal clinical trial. An interim report based on results from the second BIR trial (BIR Working Party, 1989) showed no statistically significant differences between the two arms of the trial at that time. It had been planned to continue the follow-up of all patients entered into this second trial until the completion of 10 years from the start of their radiation treatment, or to earlier death, but the analyses performed on the data of the first trial (Haybittle et al, 1990) showed that, after 3 years' follow-up, the number of patients developing recurrence or late normal tissue damage was small and contributed little to the power of the comparison between the two arms of the trial. We have therefore prepared this final report of the second trial when all patients included in the analyses have completed at least 3 years of follow-up since the start of their radiation treatment.

Materials and methods

Full details concerning the running of this trial were given in the interim report (BIR Working Party, 1989) and there have been no material changes in these since then except that it has been possible to obtain missing data for a further 27 patients who were omitted from the analyses for the interim report, so that the number of cases analysed for this final report has risen to 602. Of the 611 patients who were randomized, nine have had to be excluded (five in the short and four in the long overall treatment time arms) because it proved impossible to obtain adequate diagnostic and treatment information on them. This left 295 in the short overall treatment time (≤4 weeks, range 3–4 weeks) and 307 in the long overall time (>4 weeks, range 5–8 weeks) groups.

Throughout this report the latest TNM Classification (UICC, 1987) has been adopted for patients who have been grouped according to either their T status (extent of primary tumour) or S status (stage grouping). For their N status (regional lymph node metastasis) the previous TNM classification (UICC, 1978) has had to be adopted for the same principles as set out in the final report on the first BIR fractionation trial (BIR Working Party, 1990). The trial protocol excluded all patients in the M1 category (positive distant metastases).

A review of the histological sections from the original biopsies has been carried out by Dr Peter Millard. These had been submitted by the referring centre for 498 patients (81.5%) out of the 611 patients that were randomized into this study. On review of this material Dr Millard confirmed the diagnosis of squamous cell carcinoma in 445 patients (89.4%). In 46 patients (9.2%) the particular histological slide provided for review did not display tissue on which a firm diagnosis of squamous cell carcinoma could be made, but it has to be remembered that the slides submitted to the BIR were likely to be cuts further into the block than the section on which the original histopathologist based his diagnosis. The biopsy from a laryngo-pharynx carcinoma is often very small and thus the above figures would appear to be well within the expected range. In seven patients (1.4%) the material on the histological section that was submitted was inadequate for assessment. Analyses relating parameters such as degree of differentiation with survival are being evaluated and will be submitted for publication elsewhere (Wiernik et al, 1991).

Results

Distribution of patients

The updated data for the distribution of patients in the trial are given in Table I. They show an almost equal allocation of patients into the groups that related closely to the major prognostic factors such as the TNM classification and the anatomical site. There were minor differences in the N3 and S4 categories but as the total number of patients involved in these groups was small,

Table I. Number of patients distributed by randomization into short (S) and long (L) overall treatment time groups. They are categorized according to the TNM classification and anatomical site

TNM Classification	T1		T2		T3		T4		N0		N1		N2		N3		S1		S2		S3		S4	
Overall treatment times	S	L	S	L	S	L	S	L	S	L	S	L	S	L	S	L	S	L	S	L	S	L	S	L
Anatomical site																								
Larynx	116	127	64	58	67	61	—	—	245	240	2	3	—	2	—	1	116	126	63	56	68	61	—	3
Pharynx	2	4	5	2	—	—	—	—	4	5	2	—	1	—	—	1	1	4	3	1	2	—	1	1
Dual tumours	—	2	5	12	31	35	5	6	33	37	2	7	3	2	3	9	—	1	5	7	29	32	7	15
Total number of patients	118	133	74	72	98	96	5	6	282	282	6	10	4	4	3	11	117	131	71	64	99	93	8	19

this is not considered to be of importance when considering the overall results of this trial.

The data related to the age of patients that are quoted in this report are based on only 583 patients as the information on the date of birth of 19 patients was not available. Eleven of these were randomized to the short and eight to the long overall time regimes, 17 were male and two were female. The mean age for the 284 patients in the short overall time group was 62.9 years (range 31–88 years) and for the 299 patients in the long overall time group it was also 62.9 years (range 38–84 years). When patients were sub-divided by sex, the 517 male patients had a mean age of 62.9 years (range 31–88 years) and the 66 female patients had a mean age of 63.2 years (range 32–79 years).

Tumour responses

Observed survival rates. There have been no material changes in the data since the previous interim report (BIR Working Party, 1989). However, a more comprehensive set of data than those given previously is shown in Table II. There were no statistically significant differences between the survival rates in the two arms of the trial when the groups were compared as a whole or in sub-groups by TNM stage, nodal status or anatomical site. The survival curves are compared in Fig. 1a, which also includes a curve representing the survival of all patients in the previous trial (3F/wk *versus* 5F/wk). The statistical comparisons have been performed by the method described by Mantel (1966) for the periods 0–5 years and 0–10 years, the χ^2 and p values in Fig. 1 and Table II referring to comparisons over these two periods. The observed survival rates have not been corrected for the age of the patients or for mortality of patients from causes other than cancer of the laryngo-pharynx.

In analysing the results of the previous trial, age, stage and anatomical site were found to be important independent prognostic factors for survival. A comparison between the two arms of the present trial, stratified for these three factors, is shown in Table III. The difference between long and short overall times is not significant at the 5% level ($\chi^2 = 2.64$; $p = 0.10$) and corresponds to a relative risk (short/long) of 1.23 with a 95% confidence interval from 0.96 to 1.59.

Tumour-free rates. A comparison of the tumour-free rates is shown in Table IV and Fig. 1b. The tumour-free rate, at a given time, is the probability of having had neither persistent nor recurrent tumour at the primary site up to that time. A total of 213 patients had persistent or recurrent tumour at the primary site, of whom 105 were treated in the short and 108 in the long overall time groups. There are no statistically significant differences between the two arms of the trial either as a whole or when sub-divided by TNM stage or anatomical site. In the N1N2N3 sub-group there is a difference in favour of long overall time which can hardly be considered significant, bearing in mind that the nominal p-value can be misleadingly low in a sub-group analysis. This is a very small group of 38 patients and represents only 6% of all patients in the trial. In the previous fractionation trial (3F/wk *versus* 5F/wk) stage and anatomical site were found to be important independent prognostic factors for recurrence and laryngectomy. A comparison between the two arms of the present trial, stratified for these two prognostic factors, is given in Table V. The

Table II. Percentage observed survival rates (±SE) with main and sub-group analyses for short (S) and long (L) overall treatment times at 5 and 10 years after the start of treatment

TNM classification	Treatment group	Number of patients	Follow-up period (years)					
			5			10		
			% alive ± SE	χ^2	p	% alive ± SE	χ^2	p
All patients main-group	S L	295 307	57 ± 3 62 ± 3	1.59	0.21	42 ± 5 46 ± 4	0.91	0.34
S1 sub-group	S L	117 131	76 ± 4 74 ± 4	0.15	0.70	68 ± 6 56 ± 7	0.46	0.50
S2S3S4 sub-group	S L	178 176	45 ± 4 54 ± 4	2.54	0.11	30 ± 6 39 ± 5	2.13	0.14
N0 sub-group	S L	282 282	58 ± 3 65 ± 3	2.49	0.11	47 ± 5 49 ± 4	1.59	0.21
N1N2N3 sub-group	S L	13 25	23 ± 12 30 ± 9	0.45	0.50	5 ± 7 11 ± 8	0.31	0.58
Larynx sub-group	S L	247 246	61 ± 3 68 ± 3	1.80	0.18	48 ± 5 52 ± 5	1.46	0.23
Pharynx and dual tumours sub-group	S L	48 61	34 ± 7 40 ± 6	0.78	0.38	22 ± 9 23 ± 7	0.22	0.64

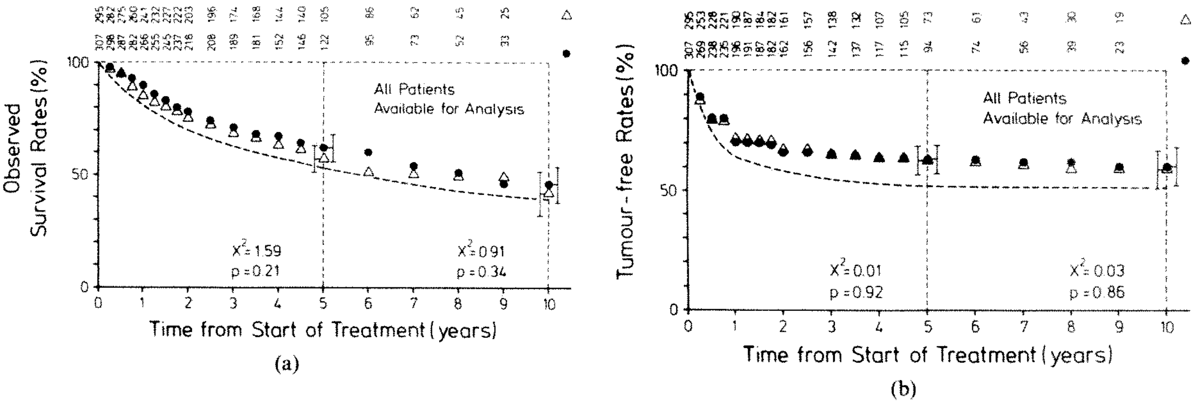

(a) (b)

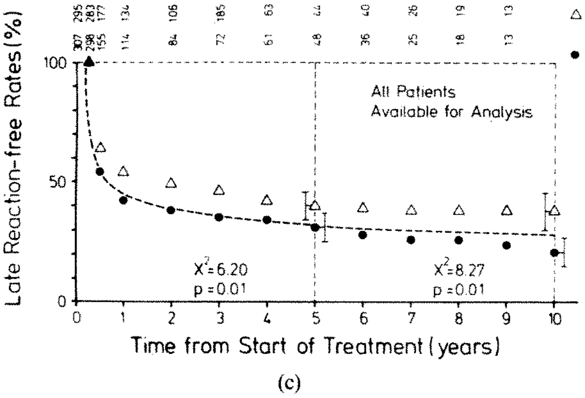

(c)

Figure 1. (a) Percentage observed survival, (b) tumour-free rates and (c) late reaction-free rates plotted against the time in years from the start of radiation treatment. Treatment was given in a short overall time (△) or a long overall time (●). Data for all patients in the first BIR fractionation trial are given for comparison (----).

Table III. Stratified analysis of the number of deaths, by age, TNM stage and anatomical site

Patient age (years)	Site	TNM stage	Overall treatment time					
			Short			Long		
			Number of patients	Observed deaths	Expected deaths	Number of patients	Observed deaths	Expected deaths
⩽ 65	Larynx	S1	75	14	15.19	73	15	13.81
		S2S3S4	78	38	31.91	71	26	32.09
	Pharynx and dual tumours	S1	0	0	0	2	2	2
		S2S3S4	31	20	18.18	35	20	21.82
> 65	Larynx	S1	40	12	10.53	51	14	15.47
		S2S3S4	47	29	27.11	44	25	26.89
	Pharynx and dual tumours	S1	0	0	0	3	3	3
		S2S3S4	10	13	7.47	20	15	17.53
		Total	284	123	110.39	299	120	132.61

Statistical comparison: log rank $\chi^2 = 2.64$, $p = 0.10$. This table is based on only 583 patients as the age of 19 patients was not known.

Table IV. Percentage tumour-free rates (±SE) with main and sub-group analyses for short (S) and long (L) overall treatment time groups

TNM classification	Treatment group	Number of patients	Follow-up period (years) 5			10		
			% ±SE	χ^2	p	% ±SE	χ^2	p
All patients	S	295	63± 3	0.01	0.92	59±4	0.03	0.86
main-group	L	307	63± 3			60±4		
S1	S	117	76± 4	0.25	0.62	70±6	0.11	0.74
sub-group	L	131	74± 4			72±5		
S2S3S4	S	178	54± 4	0.04	0.84	52±4	0.05	0.82
sub-group	L	176	55± 4			52±5		
N0	S	282	65± 3	0.01	0.92	62±4	0.01	0.92
sub-group	L	282	65± 3			62±4		
N1N2N3	S	13	15±10	4.38	0.04	8±7	—	—
sub-group	L	25	43±11			[a]—		
Larynx	S	247	66± 3	0.12	0.73	64±4	0.09	0.76
sub-group	L	246	67± 3			62±4		
Pharynx and dual tumours	S	48	40± 8	1.50	0.22	34±9	1.91	0.17
sub-group	L	61	53± 7			53±7		

[a] In this sub-group there were no patients at risk in the long overall treatment time group beyond 9 years.

difference between the two arms is not statistically significant ($\chi^2 = 0.49$; $p = 0.48$) and corresponds to a relative risk (short/long) of 1.10 with a 95% confidence interval from 0.84 to 1.44.

When the tumour-free curves for the present trial are compared with that for the previous trial (also plotted in Fig. 1b), it can be seen that the low probability of recurrence after 3 years has been confirmed. The fact that the patients in the present trial have done better than those in the previous trial may, in part, be related to the latter including a lower percentage both of N0 patients (86% compared with 94%) and of patients with larynx tumours (73% compared with 82%) (Table VI).

Laryngectomy-free rates. The laryngectomy-free rates at 5 and 10 years are shown in Table VII. There were no statistically significant differences between the two arms of the trial either overall or when sub-divided by TNM stage, nodal status or anatomical site. The total number of laryngectomies that had been reported up to December 1988, when the follow-up of the patients for the purposes of the trial was terminated, was 115, *i.e.* 56 and 59 in the short and long overall treatment time groups, respectively. Of these, all except four in the short and one in the long overall time groups were performed for recurrent tumour, though it has not been possible to obtain confirmation of this from histopatho-

Table V. Stratified analysis of the number of patients with persistent or recurrent tumours by TNM stage and anatomical site

		Overall treatment time Short			Long		
Anatomical site	TNM stage	Number of patients	Observed	Expected	Number of patients	Observed	Expected
Larynx	S1	116	25	26.18	126	29	27.82
	S2S3S4	131	52	50.12	120	52	53.88
Pharynx and	S1	1	1	0.50	5	2	2.50
dual tumours	S2S3S4	47	27	23.12	56	25	28.88
Total		295	105	99.92	307	108	113.08

Statistical comparison: log rank $\chi^2 = 0.49$, $p = 0.48$. No significant difference.

Table VI. Percentage distribution of total number of patients analysed in the first (1) and second (2) BIR fractionation trials grouped according to the TNM classification

TNM classification	T1		T2T3T4		N0		N1N2N3		S1		S2S3S4		Totals	
BIR fractionation trial	1	2	1	2	1	2	1	2	1	2	1	2	1	2
Anatomical site														
Larynx	45	40	28	42	70	81	3	1	44	40	29	42	73	82
Pharynx	5	1	2	1	4	1	3	1	2	1	5	1	7	2
Dual tumours	1	0	19	16	12	12	8	4	1	0	19	16	20	16

logical reports on the excised larynx in two patients treated in the short and six patients treated in the long overall time groups. A comparison, stratified for stage and anatomical site, is shown in Table VIII. There was no significant difference between the two arms of the trial ($\chi^2 = 0.001$; $p = 0.99$). The relative risk (short/long) was 0.99 with a 95% confidence interval from 0.69 to 1.43).

Normal tissue reactions

Acute reactions. Because the First Interim Progress Report (BIR Working Party, 1989) was prepared when all patients had already developed their maximum acute radiation reaction, there has been no material change from the data for acute reactions published in that report. The few patients for whom data have now been obtained have not altered the previous findings; 93% of patients treated with a short and 94% of patients treated with a long overall time regime showed some kind of early reaction.

Late reactions. The late reaction-free rates in the two arms of the trial are compared in Fig. 1c. The time to the first recording of any type of late reaction has been used for this analysis. There is a statistically significant difference between the two arms of the trial ($\chi^2 = 6.20$, $p = 0.01$ for 0–5 years and $\chi^2 = 8.27$, $p < 0.01$ for 0–10 years), the patients in the short overall time group showing fewer late reactions. When the late reaction-free curve derived from the data of the first BIR fractionation trial (BIR Working Party, 1990), also shown in Fig. 1c, is compared with the curves resulting from the data of the second trial then it can be seen that it corresponds more closely with the curve resulting from the long than from the short overall treatment time group. The probability of presentation of any kind of late reaction by a patient alive at a given time is

Table VII. Percentage laryngectomy-free rates (±SE) with main and sub-group analyses for short (S) and long (L) overall treatment time groups

TNM classification	Treatment group	Number of patients	Follow-up period (years)					
			5			10		
			% ±SE	χ^2	p	% ±SE	χ^2	p
All patients main-group	S L	295 307	77± 3 79± 3	0.09	0.76	77+ 3 75± 4	0.02	0.89
S1 sub-group	S L	117 131	85± 4 88± 3	0.27	0.60	85± 4 86± 4	0.12	0.73
S2S3S4 sub-group	S L	178 176	71± 4 71± 4	0.01	0.92	71± 4 67± 5	0.03	0.86
N0 sub-group	S L	282 282	78± 3 78± 3	0.01	0.92	78± 3 75± 4	0.05	0.82
N1N2N3 sub-group	S L	13 25	52±18 83± 9	3.68	0.06	52±18 —[a]	—	—
Larynx sub-group	S L	247 246	79± 3 78± 3	0.15	0.70	79± 3 75± 4	0.32	0.57
Pharynx and dual tumours sub-group	S L	48 61	63± 8 79± 7	2.71	0.10	63± 8 79± 7	2.71	0.10

[a] In this sub-group there were no patients at risk in the long overall treatment time group beyond 9 years.

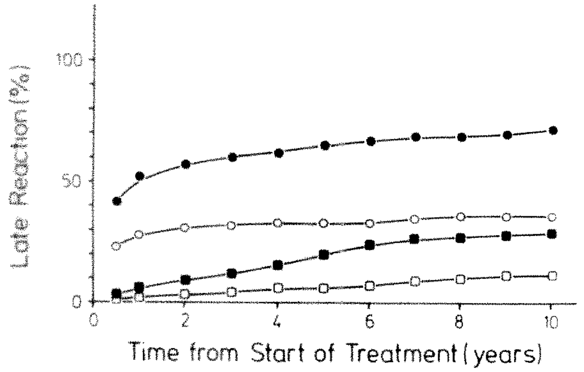

Figure 2. Percentage of various late normal tissue reactions *versus* time from the start of radiation treatment. These include telangiectasia of skin (□), telangiectasia of mucous membrane (■), oedema of mucous membrane (○) and any kind of late reaction (●).

shown in Fig. 2 together with curves for the common types of late reactions observed. In the first trial, where all patients were followed up for 10 years, 8% of those patients presenting with late reactions did so after 3 years. The percentage for the present trial is also 8%, although follow-up of all patients to 10 years would be expected to increase this figure slightly.

Discussion

When the percentage distribution of patients entered into the first and second BIR fractionation trials are compared on the basis of the TNM classification of tumours (Table VI), then it can be seen that there were more patients with primary larynx tumours (82%) in the second than in the first BIR fractionation trial (73%). Also, in the second trial, there were more patients with moderately advanced tumours in the larynx group, T2 and T3 categories, there being 42% as compared with 28% in the first fractionation trial (BIR Working Party, 1990). Patients who had even more advanced laryngeal tumours that involved pharyngeal structures have been included in the dual tumours category in this report (Wiernik et al, 1990). No material difference was found between the allocation of patients to either arm in the dual tumours category in both the trials (Table VI). Attention is drawn to the fact that there were no patients allocated to the T4 larynx category in either of the two BIR fractionation trials as all patients who had laryngeal tumours that involved pharyngeal structures were allocated to the dual tumours and not the larynx category (UICC, 1987). There were also fewer early primary pharyngeal tumours in the second trial but as this category involved so few patients this difference is too small to influence the analyses of the complete data from the second trial.

When the survival of patients with different T category larynx tumours, with no enlarged nodes at presentation, are compared (Fig. 3) then it can be seen that for the T1N0 group the data can be expressed adequately by a mono-exponential curve. For the T2N0 data from this second BIR trial, it is not possible to fit a biexponential curve, as was the case for the T2N0 group in the first BIR trial (Wiernik et al, 1990); the best fit was obtained from a mono-exponential with a constant term which significantly improved the fit compared with a simple mono-exponential curve ($p<0.01$). For the T3N0 data, however, it is possible to fit a biexponential curve for both the first and second BIR trials, the data differing from a mono-component fit at $p<0.0001$ in both the first trial and in the second trial. There was no statistically significant difference for the T3N0 data between a mono-exponential with a constant term and a biexponential fit and, therefore, the former type of analysis, being simpler, is to be preferred. Statistical comparison between the survival curves for the T1, T2 and T3 groups shows them to be significantly different ($p<0.001$).

The data for tumour-free rates have not altered materially since the publication of the First Interim Report (BIR Working Party, 1989). The actuarially calculated persistent and recurrent tumour rate at 10

Table VIII. Stratified analysis of the number of patients who had a laryngectomy by TNM stage and anatomical site

		Overall treatment time					
		Short			Long		
Anatomical site	TNM stage	Number of patients	Observed	Expected	Number of patients	Observed	Expected
Larynx	S1	116	14	13.30	126	14	14.70
	S2S3S4	131	29	33.30	120	35	30.70
Pharynx and dual tumours	S1	1	0	0	5	0	0
	S2S3S4	47	13	9.59	56	10	13.41
Total		295	56	56.19	307	59	58.81

Statistical comparison: log rank $\chi^2 = 0.001$, $p = 0.99$. No significant difference.

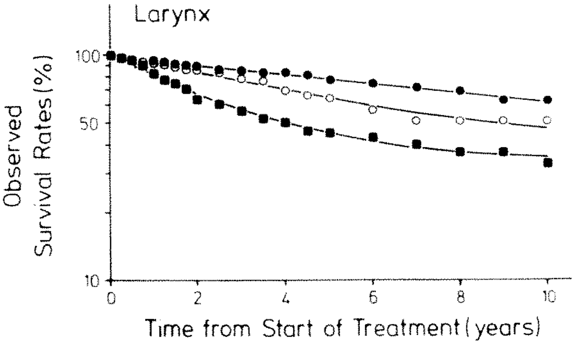

Figure 3. Percentage observed survival rates *versus* time from the start of radiation treatment of larynx tumours. No correction was made for the age of the patients or for patient mortality not related to cancer. T1N0 category (●), T2N0 category (○) and T3N0 category (■).

years of 41% in this trial was not materially lower than the 47% rate found in the first BIR fractionation trial (BIR Working Party, 1990).

Now that the final assessment has been made, it is appropriate to look critically at the balance of site sub-groups, for instance, in the two arms of the trial, so as to adjust for any slight imbalances by correction of the raw data by stratification with respect to factors having a major prognostic influence. Because the age of the patient, the anatomical site and the stage of the tumour were shown to be important prognostic factors in determining the survival of the patients entered into the first BIR fractionation trial (BIR Working Party, 1990), it was considered necessary to examine these factors in relation to the data from this second trial. The results of this analysis are shown in Table III, from which it can be seen that comparison of the data related to those patients treated in a short overall time with that of those treated in a long overall time showed no statistically significant difference ($\chi^2 = 2.64$, $p = 0.10$).

Salvage laryngectomy is a method of treatment that can only be offered to a limited number of patients who have persistent tumour or who develop a recurrence at the primary site. Laryngectomy is, therefore, not necessarily a form of treatment that is equally applicable to patients in both arms of the trial. The fact that 47% of patients with persistent or recurrent tumours had a laryngectomy in the first trial, compared with 52% in the second trial, may reflect the changes in the proportion of patients with larynx and pharynx tumours or advances in surgical feasibility, through intensive care units and in anaesthesia, over the decade that separated the two trials, although the difference is not significant. Further details related to laryngectomy and laryngectomy-free survival are reported elsewhere (Alcock et al, 1991).

Although there were a moderately large number of patients admitted into this trial there were very small numbers available for assessment at 10 years in some of the sub-groups analysed, as shown in Tables II, IV and VII. Thus these data must be construed with great caution.

At the time of preparation of the First Interim Progress Report (BIR Working Party, 1989) it was still considered necessary to collect the data for late radiation reactions between the third and tenth year from the start of the radiation treatment for all patients that survived that long. Since then further analysis of the data collected for the first BIR fractionation trial has shown that 80% of patients showing some form of late radiation reaction did so by the end of the first year, this rising to 92% by the end of the third year, after the start of radiation treatment (Rezvani et al, 1989). The pattern in the second trial has been found to be similar. The probabilities, estimated by a life-table method, of presentation of various late normal tissue reactions that have occurred in the patients treated in the second BIR fractionation trial are shown in Fig. 2.

In the results section of this report it has been shown that there was a statistically significant difference in the late radiation reactions between the short, which had the lower incidence, and the long overall treatment time groups. It must be remembered that it is the acute normal tissue reactions that are dose-limiting with these particular fractionation regimes and this quality of radiation. Hence, the level of dose reduction that was recommended for any short overall treatment time group, which in itself was based on the standard long overall treatment time schedule that was in use at that centre, was calculated so as to give rise to a similar level of acute radiation reaction in the normal tissues in both treatment groups. The actual dose reduction in any one centre varied between 18% and 22%, the precise figure being dependent on all the fractionation factors applicable in that centre such as total number of fractions, interval between individual fractions and overall treatment time. This led to the patients in the short overall time group receiving a lower total radiation dose in a smaller number of fractions, but mostly with a larger dose per fraction. Both total dose and dose per fraction are closely related to late radiation damage but the former may have had a relatively greater effect under the particular circumstances of this trial.

When examining the fraction schedules used in the second BIR trial, by those centres contributing more than 10 patients into each arm of the trial, then some overlap becomes evident (BIR Working Party, 1989). In the "short" 5F/wk and the "long" 3F/wk sub-groups a similar range of dose/fraction was used with an average value in each instance of ~3.1 Gy. However, in the case of the "long" 3F/wk regime approximately three additional fractions were delivered which resulted in a higher total dose when compared with the "short" 5F/wk regime. This may account for the higher late reaction-free rates in patients in the latter group at both 5 and 10 years (Table IX). The incidence of late reactions is not believed to be influenced by the length of the treatment time (Fowler, 1989). The similarity in the acute changes seen in the same two groups suggests that the additional three dose fractions in the long 3F/wk group compen-

Table IX. Comparison of short (S) *versus* long (L) overall treatment time groups in patients treated with either 3F/wk or 5F/wk fractionation regimes

End-points	F/wk	Treatment group	Number of patients	Follow-up period (years)					
				5			10		
				% ±SE	χ^2	p	% ±SE	χ^2	p
Observed survival rates	3	S	110	63±5	0.92	0.34	49±6	1.11	0.29
		L	117	70±5			60±6		
	5	S	185	53±4	0.78	0.38	39±7	0.02	0.89
		L	190	58±4			37±5		
Tumour-free rates	3	S	110	56±5	1.72	0.19	51±6	2.49	0.11
		L	117	67±5			67±5		
	5	S	185	67±4	0.90	0.34	64±5	1.09	0.30
		L	190	61±4			55±4		
Laryngectomy-free rates	3	S	110	76±5	0.38	0.54	76±5	0.38	0.54
		L	117	80±4			80±4		
	5	S	185	78±3	0.01	0.92	78±6	0.11	0.74
		L	190	78±3			71±6		
Late reaction-free rates	3	S	110	26±4	0.58	0.45	20±5	0.71	0.40
		L	117	25±5			20±5		
	5	S	185	49±4	7.02	0.008[a]	49±4	9.53	0.002[a]
		L	190	35±4			22±6		

[a] In evaluating the significance of these results it should be remembered that the above analyses are based on sub-groups and that more realistic p-values could be higher.

sate for the effects of proliferation in the target cell population over the extended period of treatment. This would be in keeping with the previously published concept of the importance of treatment time for acute reactions in normal tissues (Denekamp, 1973) but conflicts with recent results from studies in human skin (Turesson & Thames, 1989). These human studies suggest no significant time factor for acute reactions for treatments given in up to 6 weeks. It should also be remembered that the incidence of any type of acute reaction was very high for all sub-groups in the BIR study, *i.e.* >90%. This may mitigate against the value of the acute reaction data as a sensitive indicator of any change in biologically effective dose. These factors may provide a partial explanation for the higher incidence of patients surviving free of any kind of late reaction in the "short" as compared with the "long" 5F/wk sub-group (Table IX). The effect of the associated change in late reactions with dose/fraction from ~3.1 Gy to ~2.06 Gy per fraction would, on the basis of other clinical and radiobiological data, have been expected to be the reverse of the current findings for the same level of acute normal tissue damage (Turesson & Notter, 1984).

In the light of the first BIR fractionation trial (BIR Working Party, 1990) it appeared appropriate to examine separately the effect of short versus long overall treatment time regimes in those patients treated with 3 fractions per week and those treated with 5 fractions per week. Analyses were performed based on all patients randomized into the trial, using observed survival, tumour-free and laryngectomy-free rates as end-points (Table IX). Sub-group analyses similar to those shown in Table II were also undertaken. No statistically significant differences were found in any of these analyses.

Conclusions

Several conclusions may be drawn from the data collected in the BIR fractionation trial comparing a short with a long overall treatment time. First, no statistically significant benefit was demonstrated for patients from treatment regimes given in long compared with short overall treatment times with respect to survival, tumour-free or laryngectomy-free rates. Secondly, the acute radiation reactions in the normal tissues were, as planned, similar in the two treatment regimes when an appropriate dose reduction had been made in modifying a standard long treatment protocol to one employing a shorter overall treatment time. Thirdly, when all patients available for analysis in this trial were assessed, fewer late normal tissue reactions were noted in patients treated with a 5F/wk short regime than with any of the other regimes though all groups had had similar acute reactions; the possible reasons for these findings are discussed. The current analyses have confirmed the minimal contribution to the survival and tumour-free results that is made by the collection of data between the third and tenth year in the radiation treatment of laryngo-pharyngeal cancer. Considerable time and expenditure could be saved in similar future trials, without detriment to the results by curtailment of the follow-up period.

Acknowledgments

The authors wish to express their thanks to the Council of the British Institute of Radiology for their help, the Medical Research Council for continued special project grant support throughout the prolonged period of the trial, the Churchill Hospital Research Institute Fund for the provision of computer facilities and the Radiological Research Trust of the British Institute of Radiology and the Royal College of Radiologists for a grant that helped to retain the services of the Data Manager. They also wish to thank the University of Oxford for access to their computer facilities. They wish to thank Dr Peter Millard of the John Radcliffe Hospital, Oxford for reviewing the histopathological sections that were submitted to the BIR for the majority of patients entered into the trial and Mrs Margaret Staff for assistance with data collection. Finally, we wish to thank most sincerely the very many colleagues who have contributed to this work from departments of radiotherapy and oncology, otolaryngology and pathology in the multiple centres that co-operated to allow these clinical trials to be conducted successfully.

References

ALCOCK, C. J., FOWLER, J. F., HAYBITTLE, J. L., HOPEWELL, J. W., REZVANI, M. & WIERNIK, G., 1991. Salvage surgery following irradiation with different fractionation regimes in the treatment of carcinoma of the laryngo-pharynx: experience gained from a British Institute of Radiology study. *Journal of Laryngology and Otology*, in press.

BARRETT, J. H., DAVY, T. J., DIXON-BROWN, A., GOODMAN, D., LAWSON, R. C., ORMSBY, P. L., SAUNDERS, J. E., WILLIAMS, P. C., FOWLER, J. F. & WIERNIK, G., 1990. Dosimetric intercomparison in the British Institute of Radiology fractionation study of 3F/week *versus* 5F/week in radiotherapy of laryngo-pharynx cancer. *British Journal of Radiology*, *63*, 125–127.

BIR WORKING PARTY, 1989. First Interim Progress Report on the second British Institute of Radiology Fractionation study: Short *versus* long overall treatment times for radiotherapy of carcinoma of the laryngo-pharynx. *British Journal of Radiology*, *62*, 450–456.

——1990. Final Report of the general clinical results of the British Institute of Radiology fractionation study of 3F/week *versus* 5F/week in radiotherapy of the laryngo-pharynx. *British Journal of Radiology*, *63*, 169–180.

DENEKAMP, J., 1973. Changes in the rate of repopulation during multifraction irradiation of mouse skin. *British Journal of Radiology*, *46*, 381–387.

FOWLER, J. F., 1989. The linear-quadratic formula and progress in fractionated radiotherapy. *British Journal of Radiology*, *62*, 679–694.

HAYBITTLE, J. L., ALCOCK, C. J., FOWLER, J. F., HOPEWELL, J. W., REZVANI, M. & WIERNIK, G., 1990. Recruitment, follow-up and analysis times in clinical trials of cancer treatment: a case study. *British Journal of Cancer*, *62*, 687–691.

MANTEL, N., 1966. Evaluation of survival data and two new rank order statistics arising in its consideration. *Cancer Chemotherapy Reports*, 5, 163–170.

REZVANI, M., ALCOCK, C. J., FOWLER, J. F., HAYBITTLE, J. L., HOPEWELL, J. W. & WIERNIK, G., 1989. A comparison of the normal tissue reactions in patients treated with either 3F/week or 5F/week in the BIR trial of radiotherapy for carcinoma of the laryngo-pharynx. *International Journal of Radiation Biology*, *56*, 717–720.

——1991. Results of the BIR study of 3F/week *versus* 5F/week in the treatment of carcinoma of the laryngo-pharynx by radiotherapy: Normal tissue reactions. *International Journal of Radiation Oncology, Biology, Physics* (submitted for publication).

TURESSON, I. & NOTTER, G., 1984. The influence of fraction size in radiotherapy on the late normal tissue reaction. I. Comparison of the effects of daily and once-a-week fractionation on human skin. *International Journal of Radiation Oncology, Biology, Physics*, *10*, 593–598.

TURESSON, I. & THAMES, H. D., 1989. Repair capacity and kinetics of human skin during fractionated radiotherapy: erythema, desquamation and telangiectasia after 3 and 5 years follow up. *Radiotherapy and Oncology*, *15*, 169–188.

UICC, 1978. *TNM Classification of Malignant Tumours*, 3rd edn (International Union Against Cancer, Geneva).

——1987. *TNM Classification of Malignant Tumours*, 4th edn (International Union Against Cancer, Springer-Verlag, London).

WIERNIK, G., ALCOCK, C. J., FOWLER, J. F., HAYBITTLE, J. L., HOPEWELL, J. W. & REZVANI, M., 1990. The predictive value of tumour classification compared with the results of the British Institute of Radiology fractionation trial in the treatment of carcinoma of the laryngo-pharynx. *The Laryngoscope*, *100*, 863–872.

WIERNIK, G., MILLARD, P. R. & HAYBITTLE, J. L., 1991. The predictive value of histological classification into degrees of differentiation of squamous cell carcinoma of the laryngopharynx compared with the survival of patients. *Clinical Oncology* (in preparation).

1991, *The British Journal of Radiology*, *64*, 242–251

Application of the linear-quadratic model with incomplete repair to radionuclide directed therapy

By William T. Millar, BSc, PhD

Department of Clinical Physics and Bioengineering, 11 West Graham Street, Glasgow and Department of Radiation Oncology, University of Glasgow, Beatson Oncology Centre, Western Infirmary, Glasgow, UK

(Received January 1990 and in revised form August 1990)

Keywords: Radionuclide directed therapy, Linear-quadratic model

Abstract. The linear-quadratic (LQ) model for fractionated external beam therapy has been modified by previous authors to include the effects due to an exponentially decaying dose rate. However, the LQ model has now been extended to include a general time varying dose rate profile, and the equations can be readily evaluated if an exponential radiation damage repair process is assumed. These equations are applicable to radionuclide directed therapy, including brachytherapy. Kinetic uptake data obtained during radionuclide directed therapy may therefore be used to determine the radiobiological dosimetry of the target and non-target tissues. Also, preliminary tracer studies may be used to pre-plan the radionuclide directed therapy, provided that tracer and therapeutic amounts of the radionuclide carrier are identically processed by the tissues. It is also shown that continuous radionuclide therapy will induce less damage in late-responding tissues than 2 Gy/fraction external beam therapy if the ratio of the maximum dose rate and the sublethal damage repair half-life in the tissue is less than 1.0 Gy. Similar inequalities may be derived for β-particle radionuclide directed therapy. For example, it can be shown that radionuclide directed therapy will induce less damage to slowly repopulating tissue than 2 Gy/fraction external beam therapy for the same total dose if the maximum percentage initial uptake in tissue is less than 0.046%/g or 0.23%/g for an injected activity of 50 mCi of ^{90}Y or ^{131}I, respectively.

Radionuclide directed therapy has the potential for delivering sterilizing doses of radiation to targeted tissues, *e.g.* radioimmunotherapy with ^{131}I, ^{90}Y labelled antibodies and ^{131}I labelled methyl iodobenzylguanidine (Beierwaltes, 1987; Epenetos et al, 1987; Order et al, 1987; Darte et al, 1988; DeNardo et al, 1988; Lashford, 1988; Lashford et al, 1988; Sharkey et al, 1988). Nevertheless, non-targeted tissues may receive high doses and it has been shown that hepatic uptake of radiolabelled antibodies can be significant (Lashford et al, 1987). Bone uptake of ^{90}Y may increase the dose to the marrow (Stewart et al, 1988), whilst radiolabelled carriers may show uptake or long residence times in the kidney with consequently high renal and bladder doses. The dose to sensitive non-target tissues will therefore limit the amount of radionuclide which can be administered.

The linear-quadratic (LQ) model has been relatively successful in the attempt to relate tissue damage during fractionated radiotherapy to the total administered dose and the dose per fraction (Barendsen, 1982; Withers et al, 1983; Withers, 1986; Fowler, 1987). Each fraction is delivered in a short duration of time and the time between fractions is sufficiently long to permit sublethal radiation induced damage to be repaired. The LQ equation has been extended to include continuous irradiation (Dale, 1985; Thames, 1985), and the equations describing the effect due to an exponentially decaying source have been derived (Dale, 1985).

It is important to be able to assess the damage induced in target and non-target tissues by a general time varying dose rate profile due to internally administered radionuclides. This will enable the merits of various protocols to be determined and compared with standard treatment schedules including, for example, fractionated external beam radiotherapy. Since the LQ model is not linear, the induced damage is a non-linear function of the time varying dose rate and cannot simply be calculated by scaling up from the integrated dose estimate from the tracer studies.

This paper is therefore an attempt to derive the equations for continuous irradiation for any general time varying dose rate which would be applicable to both radionuclide directed therapy and brachytherapy of non-proliferating tissues. It is also shown that tracer studies may be used to pre-plan radionuclide directed therapy, provided that the radionuclide tracer studies adequately reflect the kinetics of therapy levels of radionuclide. Since the majority of radionuclide directed therapy protocols are delivered over a short period of time, tissue repopulation is not a significant problem. Although this is not necessarily the case for brachytherapy or external beam therapy, tissue repopulation is not addressed in this paper. Nevertheless, the equations presented here may be used to assess tissue repopulation effects by incorporating the linear time factor proposed by Travis and Tucker (1987).

Only beta and gamma emitting radionuclide therapy will be considered.

Methods and results

The standard LQ equation and associated terminology are briefly outlined in Appendix 1 and the equations for time varying dose rates are derived in Appendix 2. Using eqn (2.14) and the definitions of ERD and RE in Appendix 1, the equations for the surviving fraction of a population of clonogenic cells exposed to a continuous general time varying radiation dose rate can be shown to be

$$\log\{S(T)\} = \exp\{-\mathrm{ERD}(T)\} \quad (1)$$

$$\mathrm{ERD}(T) = D_{\mathrm{T}}(T)\mathrm{RE}(T) \quad (2)$$

$$\mathrm{RE}(T) = 1 + \frac{2}{D_{\mathrm{T}}(T)(\alpha/\beta)} \times \int_0^T \mathrm{d}t\,\dot{D}(t) \int_0^t \dot{D}(w)\exp\{-\mu(t-w)\}\,\mathrm{d}w \quad (3)$$

ERD(T) is the extrapolated response dose (damage effect for a particular value of α/β): $\mathrm{ERD}(T) = -(1/\alpha)\log\{S(T)\}$ (Gy); $S(T)$ is the surviving fraction of cells at time T; RE(T) is the relative effectiveness per unit dose at time T; $D_{\mathrm{T}}(T)$ is the total administered radiation dose at time T (Gy); T is the duration of continuous irradiation; $\dot{D}(t)$ is the dose rate at time t (Gy per unit time); μ is the tissue repair constant for exponential repair (reciprocal of time), $\mu = \log(2.0)$/tissue repair half-life; α/β is the ratio of α to β for fractionated radiotherapy using the standard LQ model, eqn (1.6) (Gy).

Although these equations appear more complex than the standard LQ equation, the computations are readily carried out on a computer. If the activity–time profiles (*i.e.* dose rate–time profiles) of internally administered radionuclides can be determined (for example by imaging using a gamma camera), the integrations may be computed using Simpson's rule or gaussian quadrature. However, since these algorithms require the evaluation of the dose rate at times for which measurements are not available, interpolation can be easily carried out using cubic spline representations of known dose rate–time profile data. In brachytherapy applications, the time dependence of the dose rate can be readily determined.

Application to radionuclide directed therapy and brachytherapy

During radionuclide directed therapy, the dose rate–time profile to any volume (*e.g.* organ) may be factorized:

$$\dot{D}(t) = \dot{D}_{\max} f(t) \quad (4)$$

where $\dot{D}_{\max}$ is the maximum dose rate observed and $f(t)$ is the profile function of time such that the maximum value of $f(t) = 1.0$, *i.e.* $\max\{f(t)\colon 0 \leqslant t \leqslant T\} = 1.0$.

The function $f(t)$ incorporates the combined effects of radionuclide decay, tissue uptake and clearance of the radionuclide carrier. If the tissue kinetics of the radionuclide can be determined during therapy, for example by using gamma camera imaging, then $f(t)$ can be determined by taking radionuclide decay into account. Alternatively, f(t) may be inferred from previous tracer studies provided that both the tracer and therapeutic amounts of the radionuclide carrier are processed identically by the tissues.

The dose rate–time profile for brachytherapy may be similarly defined. In this instance, $f(t)$ simply reflects radionuclide decay, *i.e.* $f(t) = \exp(-\lambda t)$, where λ is the radionuclide decay constant.

Inserting eqn (4) into eqn (3) gives

$$\mathrm{RE}(T) = 1 + \frac{2\dot{D}^2_{\max}}{D_{\mathrm{T}}(T)(\alpha/\beta)} \times \int_0^T \mathrm{d}t\,f(t) \int_0^t f(w)\exp\{-\mu(t-w)\} \quad (5)$$

$$= 1 + \frac{2\dot{D}^2_{\max}}{D_{\mathrm{T}}(T)(\alpha/\beta)}\,\psi_2(T) \quad (6)$$

where

$$\psi_2(T) = \int_0^T \mathrm{d}t\,f(t) \int_0^t f(w)\exp\{-\mu(t-w)\}\,\mathrm{d}w \quad (7)$$

and is independent of the radionuclide activity (*i.e.* dose rate). The parameter $\psi_2(T)$ can be calculated from the profile function $f(t)$ for the volume of interest, and the expected ERD and RE determined for any therapy dose for a given α/β ratio. Conversely, for both radionuclide directed therapy and brachytherapy, the $\dot{D}_{\max}$ (and therefore the activity) required for a particular ERD can be calculated using eqn (3.4) in Appendix 3. Equation (3.4) may therefore be used to determine the dosimetry requirements for equivalence between different irradiation protocols for a given tissue (*i.e.* same surviving fraction for the same values of α, α/β).

Comparison of continuous radiation therapy and fractionated external beam radiotherapy at 2 Gy/fraction

The effect of the radiation dose on tissue is highly dependent on the dose rate. Consequently, the effects due to radionuclide therapy (including brachytherapy) and external beam therapy may be significantly different. Using eqns (1.4) and (4.6), it can be seen that the relative effectiveness per unit dose (RE) due to radionuclide therapy will always be less than the RE due to external beam therapy at 2 Gy/fraction if $\dot{D}_{\max}/\mu < 1$ Gy. If $\dot{D}_{\max}/\mu > 1$ Gy, then the relative RE values will depend on the function $f(t)$. However, equivalence with external beam therapy at 2 Gy/fraction will occur if $\dot{D}_{\max}/\mu = 1.0$ Gy for constant dose rate radionuclide therapy where the irradiation time is much greater than the repair half-life (Appendix 5, eqn 5.14). Also, the constant dose rate radionuclide therapy will be more damaging if $D_{\max}/\mu > 1.0$ Gy. Since repopulation has not been considered, it is evident that these conclusions will only be valid if the repopulation level is small during the total irradiation time for the fractionated radiotherapy.

Thus for the same administered radiation dose, regardless of the α/β ratio, radionuclide directed therapy and brachytherapy will induce less damage to a slowly repopulating tissue (including tumour) than 2 Gy/fraction external beam therapy if $\dot{D}_{\max}/\mu < 1$ Gy.

Radionuclide directed therapy

Some of the implications of these equations are discussed below. The terms % initial activity/g and % activity/g will be used rather than the more common

% initial dose/g and % dose/g to minimize any confusion between activity and dose. The % activity/g is decay corrected, whilst the % initial activity/g refers to the actual activity (decaying)/g in the tissue expressed as a percentage of the initial activity injected.

Effect of the biological effective radionuclide half-life in radionuclide directed therapy. Suppose two internally administered radionuclides 1 and 2 are each rapidly taken up by the same organ, deliver the same dose but have different biologically effective radionuclide decay rates λ_{e1} and λ_{e2} respectively. Under these circumstances, it can be shown that (Appendix 5, eqn 5.8)

$$\mathrm{RE}(1) = \mathrm{RE}(2) + (\lambda_{e1} - \lambda_{e2})\delta \tag{8}$$

where $\delta = D_T/\{\mu(\alpha/\beta)\}$ and D_T is the total dose. In order to maintain the same total dose, the initial dose rates for each radionuclide will be different. If $\lambda_{e2} < \lambda_{e1}$, then $\mathrm{RE}(1) > \mathrm{RE}(2)$.

If we now assume that the biologically effective radionuclide decay rate in the tissue λ_e is due to a combination of both radionuclide decay λ and biological clearance with clearance rate λ_b, then $\lambda_{e1} = \lambda_1 + \lambda_b$ and $\lambda_{e2} = \lambda_2 + \lambda_b$. It can therefore be seen that for two radionuclides with the same biological clearance rate and delivering the same total dose, $\lambda_{e1} - \lambda_{e2} = \lambda_1 - \lambda_2$, and so

$$\mathrm{RE}(1) = \mathrm{RE}(2) + (\lambda_1 - \lambda_2)\delta \tag{9}$$

i.e. the difference between RE(1) and RE(2) depends on the two radionuclide decay rates. For example, if ^{90}Y (half-life, 64 h, *i.e.* decay constant $\lambda_1 = 0.01083\ \mathrm{h}^{-1}$) and ^{131}I (half-life, 193 h, *i.e.* decay constant $\lambda_2 = 0.00359\ \mathrm{h}^{-1}$) labelled carriers exhibiting the same biological clearance are compared, then

$$\mathrm{RE}(^{90}\mathrm{Y}) = \mathrm{RE}(^{131}\mathrm{I}) + 0.007248\delta \tag{10}$$

for the same total dose.

Although these results are only valid for an exponential clearance of radionuclide from the tissue delivering the same total dose, an approximation to this situation is relatively common. The preferred choice of radionuclide may be ascertained by using simple equations such as these in conjunction with the other dosimetric requirements, for example, β-particle range.

Comparison with fractionated external beam radiotherapy. It is important to be able to assess the "effective damage" which is induced using different radionuclides and to be able to compare the results with established protocols. Imaging of radionuclide–carrier distributions and kinetics give useful information and permit the time course of the % initial activity/g uptake in a tissue to be determined. This is a measure of the dose which can be delivered to the tissue. It can be shown that the maximum dose rate $\dot{D}_{\max}$ in a tissue can be simply related to the maximum value of the % initial activity/g for internally administered radionuclides (Appendix 6, eqn 6.4).

The majority of radionuclide directed therapy protocols utilize β-particle emitting radionuclides, *e.g.* ^{131}I, ^{90}Y. Suppose that the radionuclide is taken up by a volume of tissue. If the dimensions of the irradiated volume are of the order of or greater than the β-particle range, virtually all of the emitted energy is absorbed within the volume. Hence, the absorbed dose fraction $\Phi \approx 1$. This approximation will only be valid if the radiation dose to the tissue is due primarily to local uptake in the volume. However, there will always be a dose due to irradiation from non-local tissues when using γ emitters such as ^{131}I. Nevertheless, the γ dose will usually be small relative to the local β-particle dose. The 90 percentile distance for β-particle emissions for ^{131}I and ^{90}Y are approximately 0.082 cm and 0.52 cm respectively (Berger, 1971). Therefore, using eqns (6.6) and (6.7)

$$\dot{D}_{\max}\,(\mathrm{Gy/h}) = 0.2A_{\mathrm{inj}}(\mathrm{mCi})(\%\ \text{initial activity/g})_{\max} \quad \text{for } ^{90}\mathrm{Y}$$

$$\dot{D}_{\max}\,(\mathrm{Gy/h}) = 0.04A_{\mathrm{inj}}(\mathrm{mCi})(\%\ \text{initial activity/g})_{\max} \quad \text{for } ^{131}\mathrm{I}$$

Applying eqn (4.6), it can be seen that the induced radiation damage to a slowly repopulating tissue will always be less than for 2 Gy/fraction external beam therapy for the same total dose if $\dot{D}_{\max}/\mu \leqslant 1$ Gy, *i.e.*

$$(\%\ \text{initial activity/g})_{\max} < 5\mu(\mathrm{h}^{-1})/A_{\mathrm{inj}}(\mathrm{mCi}) \quad \text{for } ^{90}\mathrm{Y} \tag{11}$$

$$(\%\ \text{initial activity/g})_{\max} < 25\mu(\mathrm{h}^{-1})/A_{\mathrm{inj}}(\mathrm{mCi}) \quad \text{for } ^{131}\mathrm{I} \tag{12}$$

Most of the radionuclide activity in radionuclide directed therapy is taken up by non-targeted tissue. It is the resultant dose to these normal tissues which limits the amount of activity which can be used. Suppose, for example, that 50 mCi of radionuclide activity is injected. If it is assumed that $\mu = 0.46\ \mathrm{h}^{-1}$ for a particular non-targeted late-responding tissue, then the upper limits for the (% initial activity/g)$_{\max}$ are 0.046%/g and 0.23%/g for ^{90}Y and ^{131}I respectively. Consequently, radionuclide therapy will always be less damaging to that tissue than 2 Gy/fraction external beam therapy provided these upper limits are not exceeded. The maximum limits for any slowly repopulating tissue may be calculated if the repair rate μ is known. However, the repair rate for many tumours is greater than $0.46\ \mathrm{h}^{-1}$ (Steel, 1987). Hence, the upper limits calculated above for a 50 mCi radionuclide injection are an underestimate for such tissues.

Applications

Several applications of the continuous irradiation equations are discussed in the following examples. Following Dale (1985), it will be assumed that $\mu = 0.46\ \mathrm{h}^{-1}$ unless otherwise indicated. For many tumours, $\alpha/\beta > 10.0$ Gy. However, for large values of α/β, the quadratic effect in the LQ model diminishes and so the RE tends to 1.0 per unit dose for continuous irradiation at low dose rates. In the following examples it will be assumed that $\alpha/\beta = 10$ Gy for tumour tissue. The range of repair half-lives, α, β and α/β for several tissues is well documented (Thames & Hendry, 1987).

Application 1. ^{131}I labelled monoclonal antibody UJ13A radionuclide therapy has been used for the treat-

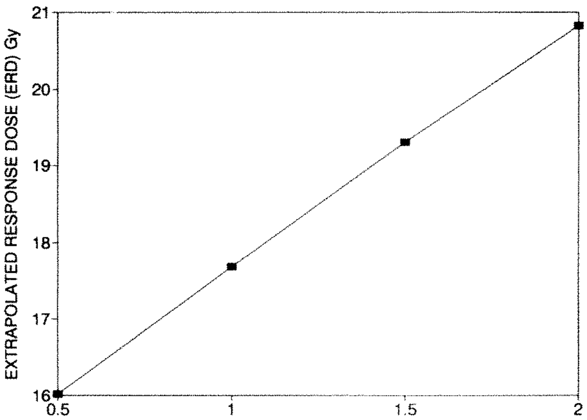

Figure 1. The influence of the assumed sublethal damage repair half-life for the liver on the implied ERD. The radionuclide kinetics are detailed in application 1 in the main text.

ment of disseminated neuroblastoma in children (Lashford et al, 1987). Although significant hepatic uptake was observed, this is a relatively common phenomenon in radioimmunotherapy. Consequently, the liver is likely to be one of the major dose limiting organs in this type of therapy. The radiobiological implications are therefore important in the design and implementation of radioimmunotherapy protocols.

Using the data presented for patient 2 (Lashford et al, 1987) and assuming an average half-life of 23.0 h in the liver (Kemshead et al, 1986), the maximum dose rate is 0.431 Gy/h for an injected activity of 55 mCi. Applying eqns (2) and (3) and using an α/β ratio of 2.5 Gy for the liver (Fisher & Hendry, 1988; Withers, 1988), the total dose, ERD and RE are 14.3 Gy, 19.3 Gy and 1.35 per unit dose, respectively. The influence of the assumed repair half-life on these results can be seen in Fig. 1.

Conversely, suppose it is desired to give the equivalent of a sub-tolerance dose of 24 Gy to the liver (delivered by external 2 Gy/fraction therapy where ERD = 43.2 Gy, RE = 1.8 per unit dose). The required activity to obtain the same ERD using radionuclide therapy would be 101 mCi with an RE of 1.64 per unit dose and a total dose of 26.3 Gy (using eqn (3.4) to obtain $\dot{D}_{\max}$ and therefore the required activity). The larger RE factor reflects the increased dose rate. Therefore, 24 Gy delivered to the liver by external beam therapy at 2 Gy/fraction is equivalent to 26.3 Gy using the radionuclide therapy protocol.

Application 2. The infusion of ^{131}I labelled lipiodol or ethiodol via the hepatic artery has been used for the treatment of hepatoma (Madsen et al, 1988; Nakajo

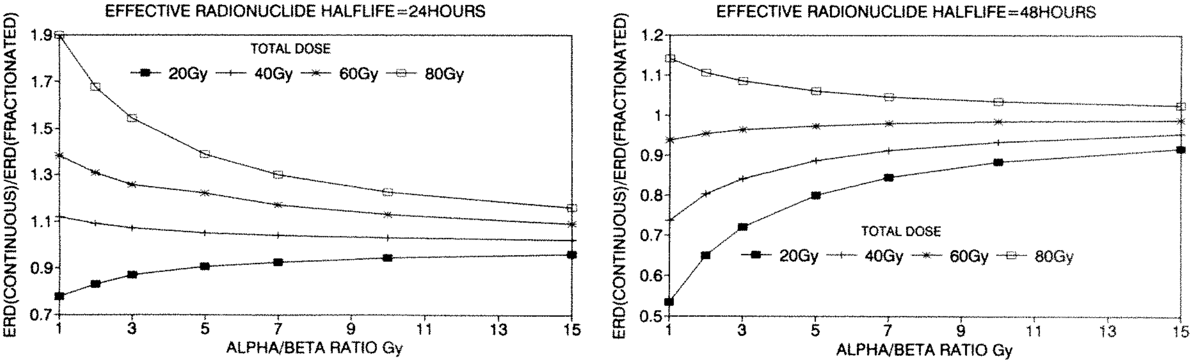

(a) (b)

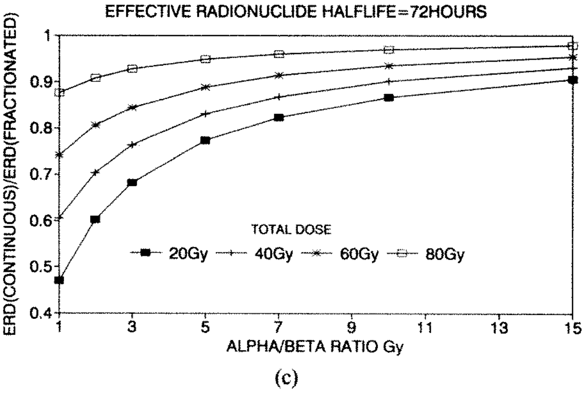

(c)

Figure 2. The damage induced by continuous radionuclide therapy relative to 2 Gy/fraction external beam therapy for the same total dose is expressed as the ratio RE(radionuclide)/RE(2 Gy/fraction). The variation with α/β is shown for several biologically effective radionuclide half-lives, and the total dose is calculated for an infinite time exposure. The maximum dose rate will increase as the biologically effective radionuclide half-life decreases, for the same total dose. Effective half-lives are (a) 24 h, (b) 48 h, (c) 72 h.

et al, 1988). In this application, the clearance of the radionuclide from both the tumour and normal tissue was a biexponential function of time. Using the raw data presented by Nakajo et al (1988) for patient 3, and eqns (2) and (3), the following results are obtained. The injection of 34.5 mCi gives a total dose to the liver of 13.9 Gy with an RE of 1.10 per unit dose and an ERD of 15.2 Gy; and for the tumour (assuming an α/β ratio of 10) the values are 116 Gy, 1.15 per unit dose and 133 Gy, respectively. The initial dose rates to the liver and tumour are 0.118 Gy/h and 0.688 Gy/h, respectively. For a 64.1 mCi injection, the total dose, RE and ERD to the liver are 25.7 Gy, 1.19 per unit dose and 30.5 Gy, while for the tumour the results are 214 Gy, 1.27 per unit dose and 270 Gy. The initial dose rates to the liver and tumour are 0.22 Gy/h and 1.27 Gy/h, respectively. The effective biological half-life for liver and tumour ranged between 3 and 6 days.

Suppose that the liver dose had been delivered by external beam therapy as an integral number of fractions of 2 Gy/fraction (plus one extra fraction slightly less than 2 Gy to make up the total dose). Using eqn (1.6), it was calculated that the RE (external beam) ≈ 1.8 per unit dose. Since this is significantly greater than the RE due to the radionuclide therapy, external beam therapy would have been much more damaging to the liver for the same physical dose.

It was assumed that the sublethal damage repair half-life for the tumour was the same as the liver in the calculation of the tumour ERD during radionuclide therapy. However, it has been shown that the repair half-life is often much less than 1.5 h for many tumours (Steel, 1987). It can be seen from eqn (4.6) that the maximum limit for the RE (radionuclide) decreases as the repair rate increases. Consequently, radionuclide therapy may result in a low RE dose to the tumours with high α/β ratios and rapid repair rates, *i.e.* RE ≈ 1.0 per unit dose. Under these circumstances, the ERD will approximate to the physical dose D_T.

Application 3. Consider a radionuclide therapy protocol (radionuclide directed therapy or brachytherapy) where the delivered dose rate is an exponentially decreasing function of time. The ratio of the ERD (radionuclide) to the ERD (external beam) for 2 Gy/fraction is shown in Fig. 2 as a function of the α/β ratio for the same total delivered dose. The ERD (radionuclide) was computed using eqn (2) while the ERD (external beam) was calculated using eqn (1.3) (Appendix 1). The influence of the biologically effective radionuclide decay half-life can also be seen in Fig. 2. As the α/β ratio increases, the difference between the two protocols is greatly reduced.

The family of curves relating the ERD ratios are highly dependent on the initial dose rate (which reflects the total dose). Therefore, radionuclide therapy will induce greater damage than 2 Gy/fraction external beam therapy only at very high initial dose rates (*e.g.* rapid radionuclide clearance for a given total dose using radionuclide directed therapy). This effect will be relatively greater for low α/β ratios.

Discussion

The use of the LQ model in conventional fractionated radiotherapy has proven to be relatively successful in the assessment of induced tissue damage. The expected effects due to various protocols can therefore be calculated and compared. It is possible that the extension of these equations to continuous time varying dose rates will be equally valid. The equations in Appendices 2 and 3 permit the ERD and RE values to be calculated for a known time varying dose rate. Alternatively, the required dose rate and total dose may be calculated for a particular ERD. Also, inequalities such as those presented in eqns (11) and (12) may be used to estimate the maximum possible amount of damage induced by radionuclide directed therapy relative to 2 Gy/fraction external beam therapy, for the same total dose. Consequently, various protocols may be assessed prior to therapy if the kinetics of proposed radionuclide carriers for radionuclide directed therapy are known *a priori*.

It would appear that the damage effect to slowly repopulating tumour tissue will be less than for 2 Gy/fraction external beam therapy with the degree of targeting currently achievable using radioimmunotherapy (*i.e.* $\dot{D}_{\max}/\mu < 1$ Gy). This is particularly true for tumours with rapid repair rates due to the resultant decrease in $\dot{D}_{\max}/\mu$. The uncertainty in tumour parameters precludes an accurate estimate of ERD. However, $\alpha/\beta \geqslant 10$ Gy for many tumours and so RE (2 Gy/fraction) $\leqslant 1.2$ per unit dose. Since RE for any radiation therapy is greater than 1.0 per unit dose, the difference between 2 Gy/fraction external beam therapy and radionuclide therapy will be comparatively small for the same dose. The ERD due to low dose rate radionuclide therapy and the physical dose will be very similar for tumours with high α/β ratios and rapid sublethal damage repair rates.

However, the reduction in the RE (radionuclide) relative to RE (2 Gy/fraction) will generally be more significant for late responding tissues such as liver and kidney with α/β ratios of approximately 2.5 Gy (Fisher & Hendry, 1988) and 0.5–4.0 Gy (Hopewell & Wiernik, 1977; Williams & Denekamp, 1984), respectively. This is exemplified by the data in Fig. 2 for an effective radionuclide half-life greater than 24 h. Hence, low dose rate radionuclide therapy may be used to deliver a reduced ERD to late reacting tissues relative to 2 Gy/fraction external beam therapy, for the same physical dose. Alternatively, a larger radionuclide dose may be delivered to achieve the same ERD due to 2 Gy/fraction external beam therapy. The LQ equations may therefore be used to assess various irradiation protocols in terms of their normal tissue damage, provided the dose rate–time profile function and the α/β ratio are known. For example, the amount of activity to stay within normal tissue tolerance may be determined. Similar conclusions have been reached by Dutreix (1989).

The above implications may be illustrated using the results from Application 1 in the previous section. It was shown that the dose to the liver due to a 55 mCi injection of ^{131}I labelled antibody is 14.3 Gy with an RE of 1.35 per unit dose. If it were desired to administer a radionuclide therapy which gave the equivalent of a sub-tolerance dose of 24 Gy to the liver delivered by 2 Gy/fraction external beam therapy, then the implied ERD is 43.2 Gy. Using this value in eqn (3.4) to obtain $\dot{D}_{\max}$, it is found that the equivalent ERD would be obtained for 101 mCi ^{131}I labelled antibody. This would result in an 83.6% increase in the administered activity. However, the percentage increase in the ERD to the liver was 123% (due to the increase in the RE) and would be at least 83.6% for the tumour. Although the ERD to the liver is below tolerance, it is likely that the administration of such high activities of ^{131}I labelled antibody would result in bone marrow suppression. Nevertheless, it has been suggested that this problem could be circumvented by bone marrow rescue (Lashford et al, 1987; O'Donoghue & Wheldon, 1988).

The effect of repopulation may also play an important role in determining the effect of various irradiation protocols. Although repopulation may not have a major effect in the radiobiological dosimetry of radioimmunotherapy owing to the short treatment times, this may not be true for brachytherapy or external beam therapy. Therefore, the equations derived here and by Dale (1985) will only be applicable to situations where repopulation is not significant. However, the effects of repopulation can be intuitively taken into account by adding a linear time factor onto the equations for the extrapolated response dose (Travis & Tucker, 1987; Dale, 1988; Yaes, 1988; Fowler, 1989).

Although systemic radionuclide directed therapy has the potential for delivering high radiation doses to targeted tissues, regional radionuclide therapy is likely to prove more highly effective, *e.g.* intrathecal and intraperitoneal therapy, and isolated limb perfusion. It is probable that high target-to-non-target ratios of radionuclide uptake could be obtained by using a preinfusion of streptavidin labelled antibody (Hnatowich et al, 1987). Radiolabelled (^{67}Cu, ^{199}Au, ^{131}I, ^{211}At) biotin could then be infused after a suitable period of time to allow for maximum binding and clearance of non-bound antibody. Since biotin is a relatively small molecule, rapid binding to the remaining streptavidin should occur. A similar concept would be to use boron labelled antibody which could be locally activated by an external beam of neutrons (boron neutron capture therapy) at a later time to deliver localized α-particle therapy (Barth et al, 1982). Such procedures could therefore reduce the dose received by dose limiting organs and non-target tissue whilst enhancing the target dose.

Appendix 1

If a tissue is exposed to a radiation dose of magnitude D, then the standard LQ equation is of the form:

$$\log(S) = -\alpha D - \beta D^2 \tag{1.1}$$

where S is the surviving fraction of cells in the tissue, and α, β are tissue specific constants.

If a total dose D_T is given by N separate fractions of equal magnitude d_N with sufficient time between fractions to permit the repair of sub-lethal damage, then

$$\begin{aligned}\log(S) &= N(-\alpha d_N - \beta d_N^2)\\ &= -\alpha D_T\left\{1 + \frac{d_N}{(\alpha/\beta)}\right\}\end{aligned} \tag{1.2}$$

and

$$-\frac{1}{\alpha}\log(S) = D_T\left\{1 + \frac{d_N}{(\alpha/\beta)}\right\} \tag{1.3}$$

The damage effect for a particular tissue can be defined as $-(1/\alpha)\log(S)$ (Barendsen, 1982). This quantity can be equated with the dose required to produce that effect had it been given as a large number of fractions such that $\lim(N \to \infty)\Sigma d_N = D_T$ and is known as the ERD (extrapolated response dose). The relative effectiveness per unit dose (RE) is defined as

$$\mathrm{RE} = \left\{1 + \frac{d_N}{(\alpha/\beta)}\right\} \tag{1.4}$$

and so

$$\mathrm{ERD} = D_T \mathrm{RE} \tag{1.5}$$

The ERD is linearly additive (Dale, 1986) and so a series of n different protocols ($i = 1, \ldots, n$) may be superimposed to obtain the total ERD

$$\begin{aligned}\mathrm{ERD} &= \sum_{i=1}^{n} \mathrm{ERD}_i\\ &= \sum_{i=1}^{n} D_{Ti}\left\{1 + \frac{d_{Ni}}{(\alpha/\beta)}\right\}\end{aligned} \tag{1.6}$$

where D_{Ti} is the total dose and d_{Ni} is the dose/fraction for the ith protocol.

Although these equations are applicable to standard radiotherapy protocols, the formalism is not applicable to radionuclide directed therapy where the dose rate is a continuously variable function of time during therapy.

Appendix 2

The LQ equation may be derived and extended using a simple deterministic approach and making several basic assumptions. Consider a population $N(t)$ of clonogenic cells at time t which have been irradiated. If one considers the damage accumulation model (Payne & Garrett, 1975; Roesch, 1978), then the following holds.

(1) There is a cell loss component directly proportional to the number of cells $N(t)$ and the dose rate $\dot{D}(t)$ (*i.e.* this component refers to the probability of inducing a lesion resulting in direct sterilization)

$$\frac{1}{N(t)}\frac{\mathrm{d}N(t)}{\mathrm{d}t} = -\alpha\dot{D}(t) \tag{2.1}$$

where α is a tissue specific constant.

(2) At any time t there is a secondary component of lethal damage. This is related both to the past history $H(t)$ of accumulated damage already incurred (which has not resulted in cell sterilization), *i.e.* sublethal damage,

and subsequent interaction with the current dose rate $\dot{D}(t)$. This component of the induced lethal damage may be written

$$\frac{1}{N(t)}\frac{\mathrm{d}N(t)}{\mathrm{d}t} \propto -\dot{D}(t)H(t) \tag{2.2}$$

If there is no coupling between the separate historical events, *i.e.* the function $H(t)$ can be represented as a linearly additive superposition of damage, then

$$H(t) = \int_0^t H_{\mathrm{d}}(t, w)\,\mathrm{d}w \tag{2.3}$$

where $H_{\mathrm{d}}(t, w)$ is the function describing the relation between damage incurred at time w which still persists at time t, *i.e.* some of the damage may have been repaired. If the damage incurred at time w is proportional to the dose rate pertaining at that time, *i.e.* $\dot{D}(w)$, and the damage repairs with a repair function $R(t-w)$, where $t-w$ is the time between the initiation of damage at time w and some later time t, and $R(0) = 1.0$, then

$$H_{\mathrm{d}}(t, w) \propto \dot{D}(w)R(t-w) \tag{2.4}$$

Therefore

$$H(t) = \beta' \int_0^t \dot{D}(w)R(t-w)\,\mathrm{d}w \tag{2.5}$$

where β' is a tissue specific constant, and

$$\frac{1}{N(t)}\frac{\mathrm{d}N(t)}{\mathrm{d}t} = -\beta'\dot{D}(t)\int_0^t \dot{D}(w)R(t-w)\,\mathrm{d}w \tag{2.6}$$

Combining eqns (2.1) and (2.6) gives

$$\frac{1}{N(t)}\frac{\mathrm{d}N(t)}{\mathrm{d}t} = -\alpha\dot{D}(t) - \beta'\dot{D}(t)\int_0^t \dot{D}(w)R(t-w)\,\mathrm{d}w \tag{2.7}$$

Integration gives the surviving fraction $S(T)$ at time T:

$$S(T) = \exp\left\{-\alpha\int_0^T \dot{D}(t) - \beta'\int_0^T \mathrm{d}t\,\dot{D}(t) \times \int_0^t \dot{D}(w)R(t-w)\,\mathrm{d}w\right\} \tag{2.8}$$

$$\log\{S(T)\} = -\alpha D_{\mathrm{T}}(T) - \beta'\int_0^T \mathrm{d}t\,\dot{D}(t)\int_0^t \dot{D}(w)R(t-w)\,\mathrm{d}w \tag{2.9}$$

where $D_{\mathrm{T}}(T)$ is the total dose at time T.

If we consider $\dot{D}(t) = \text{constant} = \dot{D}$, and $R(t-w) = 1.0$, *i.e.* no repair, then

$$\begin{aligned}\log\{S(T)\} &= -\alpha D_{\mathrm{T}}(T) - \beta'\dot{D}^2\int_0^T \mathrm{d}t\int_0^t \mathrm{d}w\\ &= -\alpha D_{\mathrm{T}}(T) - 0.5\beta'\dot{D}^2T^2\\ &= -\alpha D_{\mathrm{T}}(T) - 0.5\beta' D_{\mathrm{T}}(T)^2\end{aligned} \tag{2.10}$$

This represents a dose $D_{\mathrm{T}}(T)$ given in a very short time (*i.e.* short compared with the repair half-life) and is therefore equivalent to the standard LQ equation for a single fraction. Since it is assumed that β and β' are tissue specific constants and independent of $\dot{D}(t)$ and $D_{\mathrm{T}}(T)$, comparison with the standard LQ equation shows that

$$\beta' = 2\beta$$

and so

$$\log\{S(T)\} = -\alpha D_{\mathrm{T}}(T) - 2\beta\int_0^T \mathrm{d}t\,\dot{D}(t)\int_0^t \dot{D}(w)R(t-w)\,\mathrm{d}w \tag{2.11}$$

If the tissue is undergoing exponential repair of sublethal damage, then $R(u) = \exp(-\mu u)$ where μ is a repair constant and u is the time interval after the induction of the damage, and so

$$\log\{S(T)\} = -\alpha D_{\mathrm{T}}(T) - 2\beta\int_0^T \mathrm{d}t\,\dot{D}(t)\int_0^t \dot{D}(w)\exp\{-\mu(t-w)\}\,\mathrm{d}w \tag{2.12}$$

and

$$-\frac{1}{\alpha}\log\{S(T)\} = D_{\mathrm{T}}(T) + 2(\beta/\alpha) \times \int_0^T \mathrm{d}t\,\dot{D}(t)\int_0^t \dot{D}(w)\exp\{-\mu(t-w)\}\,\mathrm{d}w \tag{2.13}$$

$$= D_{\mathrm{T}}(T)\left[1 + \frac{2}{(\alpha/\beta)D_{\mathrm{T}}(T)} \times \int_0^T \mathrm{d}t\,\dot{D}(t)\int_0^t \dot{D}(w) \times \exp\{-\mu(t-w)\}\,\mathrm{d}w\right] \tag{2.14}$$

Appendix 3

The required maximum dose rate for a given ERD can be calculated as follows. From eqns (2), (3) and (4)

$$\begin{aligned}\mathrm{ERD}(T) &= \dot{D}_{\max}\int_0^T f(t)\,\mathrm{d}t + \frac{2\dot{D}^2_{\max}}{(\alpha/\beta)} \times \int_0^T \mathrm{d}t\,f(t)\int_0^t f(w)\exp\{-\mu(t-w)\}\,\mathrm{d}w\\ &= \dot{D}_{\max}\psi_1(T) + \frac{2\dot{D}^2_{\max}}{(\alpha/\beta)}\psi_2(T)\end{aligned} \tag{3.1}$$

where

$$\psi_1(T) = \int_0^T f(t)\,\mathrm{d}t \tag{3.2}$$

$$\psi_2(T) = \int_0^T \mathrm{d}t\,f(t)\int_0^t f(w)\exp\{-\mu(t-w)\}\,\mathrm{d}w \tag{3.3}$$

Solving the quadratic eqn (3.1) for $\dot{D}_{\max}$ gives

$$\dot{D}_{\max} = -\frac{(\alpha/\beta)}{4}\frac{\psi_1(T)}{\psi_2(T)} \pm \left\{\frac{(\alpha/\beta)^2}{16}\frac{\psi_1^2(T)}{\psi_2^2(T)} + \frac{(\alpha/\beta)}{2}\frac{\mathrm{ERD}(T)}{\psi_2(T)}\right\}^{0.5}$$

Since $\dot{D}_{\max} > 0$,

$$\dot{D}_{\max} = -\frac{(\alpha/\beta)}{4}\frac{\psi_1(T)}{\psi_2(T)} + \left\{\frac{(\alpha/\beta)^2}{16}\frac{\psi_1^2(T)}{\psi_2^2(T)} + \frac{(\alpha/\beta)}{2}\frac{\mathrm{ERD}(T)}{\psi_2(T)}\right\}^{0.5} \quad (3.4)$$

Appendix 4

The maximum value of RE for any time varying dose rate profile can be calculated as follows. From Appendix 2, eqn (2.14)

$$\mathrm{RE}(T) = 1 + \frac{2}{(\alpha/\beta)D_{\mathrm{T}}(T)} \times \int_0^T \mathrm{d}t\,\dot{D}(t)\int_0^t \dot{D}(w)\exp\{-\mu(t-w)\}\,\mathrm{d}w \quad (4.1)$$

$$= 1 + \frac{2}{(\alpha/\beta)}\zeta(T) \quad (4.2)$$

where

$$\zeta(T) = \frac{1}{D_{\mathrm{T}}(T)}\int_0^T \mathrm{d}t\,\dot{D}(t)\int_0^t \dot{D}(w)\exp\{-\mu(t-w)\}\,\mathrm{d}w \quad (4.3)$$

If $\dot{D}(t) = \dot{D}_{\max} f(t)$, where $\dot{D}_{\max}$ is the maximum dose rate observed, *i.e.* $f(t) \leqslant 1.0$, then

$$D_{\mathrm{T}}(T) = \int_0^T \dot{D}(t)\,\mathrm{d}t = \dot{D}_{\max}\int_0^T f(t)\,\mathrm{d}t \quad (4.4)$$

Therefore

$$\zeta(T) \leqslant \frac{\dot{D}_{\max}}{D_{\mathrm{T}}(T)}\int_0^T \mathrm{d}t\,\dot{D}(t)\int_0^t f(w)\exp\{-\mu(t-w)\}\,\mathrm{d}w$$

$$\leqslant \frac{\dot{D}_{\max}}{D_{\mathrm{T}}(T)}\int_0^T \mathrm{d}t\,\dot{D}(t)\int_0^t \exp\{-\mu(t-w)\}\,\mathrm{d}w$$

$$\leqslant \frac{\dot{D}_{\max}}{\mu D_{\mathrm{T}}(T)}\{1-\exp(-\mu T)\}\int_0^T \dot{D}(t)\,\mathrm{d}t$$

$$\leqslant \frac{\dot{D}_{\max}}{\mu}\{1-\exp(-\mu T)\} \quad (4.5)$$

Therefore, $\zeta(T) \leqslant \dot{D}_{\max}/\mu$, and

$$\mathrm{RE}(T) \leqslant 1 + \frac{2}{(\alpha/\beta)}\frac{\dot{D}_{\max}}{\mu} \quad (4.6)$$

Appendix 5

If $\dot{D}(t)$ is assumed to be purely an exponentially decreasing function of time with biologically effective half-life τ_{e} (biologically effective decay constant $\lambda_{\mathrm{e}} = 0.693/\tau_{\mathrm{e}}$), then

$$\mathrm{RE}(T) - 1 = \frac{2}{(\alpha/\beta)D_{\mathrm{T}}(T)} \times \int_0^T \mathrm{d}t\,\dot{D}(t)\int_0^t \dot{D}(w)\exp\{-\mu(t-w)\}\,\mathrm{d}w \quad (5.1)$$

$$= \frac{2\dot{D}_{\max}^2}{(\alpha/\beta)D_{\mathrm{T}}(T)} \times \int_0^T \exp\{-(\lambda_{\mathrm{e}}+\mu)t\}\,\mathrm{d}t\int_0^t \exp\{(\mu-\lambda_{\mathrm{e}})w\}\,\mathrm{d}w \quad (5.2)$$

$$= \frac{2\dot{D}_{\max}^2}{(\alpha/\beta)D_{\mathrm{T}}(T)(\mu-\lambda_{\mathrm{e}})} \times \left\{\frac{1-\exp(-2\lambda_{\mathrm{e}}T)}{2\lambda_{\mathrm{e}}} - \frac{1-\exp\{-(\mu+\lambda_{\mathrm{e}})T\}}{\mu+\lambda_{\mathrm{e}}}\right\} \quad (5.3)$$

Equation (5.3) defines the RE for an irradiation of duration T and is applicable to both brachytherapy and internally administered radionuclide directed therapy.

Specific applications

Decaying radionuclide: long time exposure. If the tissue is exposed to a radionuclide dose with a biologically effective decay rate λ_{e}, then the RE at some time T much greater than the biologically effective decay half-life can be found by taking the limit as $\lambda_{\mathrm{e}}T \to \infty$ in eqn (5.3)

$$\mathrm{RE} = 1 + \frac{\dot{D}_{\max}^2}{(\alpha/\beta)D_{\mathrm{T}}(T)(\mu+\lambda_{\mathrm{e}})\lambda_{\mathrm{e}}} \quad (5.4)$$

where D_{T} is the total dose. This equation is identical to that derived by Dale (1985).

Since D_{T} is the total dose as $T \to \infty$, $D_{\mathrm{T}} = \dot{D}_{\max}/\lambda_{\mathrm{e}}$, so

$$\mathrm{RE} - 1 = \frac{\lambda_{\mathrm{e}}D_{\mathrm{T}}}{(\alpha/\beta)(\mu+\lambda_{\mathrm{e}})} \quad (5.5)$$

If the biologically effective radionuclide decay half-life is much greater than the radiation damage repair half-life, then $\lambda_{\mathrm{e}} \ll \mu$ and so

$$\mathrm{RE} = 1 + \frac{\lambda_{\mathrm{e}}D_{\mathrm{T}}}{(\alpha/\beta)\mu} \quad (5.6)$$

For any two radionuclides delivering the same dose D_{T}, but with different biologically effective decay rates $\lambda_{\mathrm{e}1}$ and $\lambda_{\mathrm{e}2}$ from the organ, then

$$\mathrm{RE}(1) - \mathrm{RE}(2) = \frac{D_{\mathrm{T}}(\lambda_{\mathrm{e}1}-\lambda_{\mathrm{e}2})}{(\alpha/\beta)\mu} \quad (5.7)$$

RE(2) can be written as $\mathrm{RE}(2) = 1 + \delta\lambda_{\mathrm{e}2}$, where $\delta = D_{\mathrm{T}}/\mu(\alpha/\beta)$ and so

$$\mathrm{RE}(1) = \mathrm{RE}(2) + (\lambda_{\mathrm{e}1}-\lambda_{\mathrm{e}2})\delta \quad (5.8)$$

or

$$\mathrm{RE}(1) = \mathrm{RE}(2) + 0.693\,\frac{(\tau_{e2} - \tau_{e1})}{\tau_{e1}\tau_{e2}}\,\delta \qquad (5.9)$$

where τ_e is the biologically effective radionuclide decay half-life. If $\tau_{e2} > \tau_{e1}$, then $\mathrm{RE}(1) > \mathrm{RE}(2)$.

Constant dose rate. If the tissue is exposed to a constant dose rate $\dot{D}_c$, *i.e.* $\lambda_e \to 0$, then eqn (5.2) reduces to

$$\mathrm{RE}(T) - 1 = \frac{2\dot{D}_c^2}{(\alpha/\beta)D_T(T)} \times \int_0^T \exp(-\mu t)\,\mathrm{d}t \int_0^t \exp(\mu w)\,\mathrm{d}w \qquad (5.10)$$

$$= \frac{2\dot{D}_c^2}{\mu(\alpha/\beta)D_T(T)} \int_0^T \{1 - \exp(-\mu t)\}\,\mathrm{d}t \qquad (5.11)$$

$$= \frac{2\dot{D}_c^2}{\mu(\alpha/\beta)D_T(T)} \left[T - \frac{1}{\mu}\{1 - \exp(-\mu T)\} \right] \qquad (5.12)$$

$$= \frac{2\dot{D}_c}{\mu(\alpha/\beta)} \left[1 - \frac{1}{\mu T}\{1 - \exp(-\mu T)\} \right] \qquad (5.13)$$

since the total dose $D_T(T) = \dot{D}_c T$, where T is the radiation exposure time. Equation (5.14) has also been derived by Dale (1985). If the exposure time is much greater than the repair half-life, *i.e.* $\mu T \to \infty$, eqn (5.13) reduces to

$$\mathrm{RE}(T) = 1 + \frac{2\dot{D}_c}{\mu(\alpha/\beta)} \qquad (5.14)$$

Appendix 6

The relationship between the dose rate and the % initial uptake can be determined if the absorbed dose fraction is known. Let

$P(t)$ be the % initial activity/g in the tissue at time t, *i.e.* the actual activity per gram at time t (decaying) expressed as a percentage of the administered activity,

$A(t)$ be the activity in the tissue at time t, and

$\dot{D}(t)$ the dose rate in the tissue at time t,

$\dot{D}_{\max}$ be the maximum dose rate, and

A_{inj} be the injected activity (μCi until otherwise indicated).

m is the mass of the tissue (g), and

Δ is the equilibrium dose constant (g cGy)/(μCi h).

Then

$$P(t) = 100\,\frac{A(t)}{m}\,\frac{1}{A_{\mathrm{inj}}} \qquad (6.1)$$

Also using the MIRD formalism (Berger, 1971)

$$\dot{D}(t) = \frac{A(t)}{m}\,\Phi\Delta\ \mathrm{cGy/h} \qquad (6.2)$$

$$= 0.1\Delta A_{\mathrm{inj}}(\mathrm{mCi})P(t)\Phi\ \mathrm{Gy/h} \qquad (6.3)$$

where $0 \leqslant \Phi \leqslant 1.0$ is dependent on the radionuclide distribution (which may vary with time) within the volume, and the point dose distribution function for the radionuclide. Therefore

$$\dot{D}_{\max} = 0.1\Delta A_{\mathrm{inj}}(\mathrm{mCi})P_{\max}\Phi\ \mathrm{Gy/h} \qquad (6.4)$$

where $P_{\max}$ is the maximum % initial activity/g occurring within the tissue.

β-particle radionuclide therapy

For β-particle radionuclide therapy, $\Phi \approx 1.0$ for irradiated volumes with dimensions of the order of or greater than the β-particle range. Therefore

$$\dot{D}_{\max} = 0.1\Delta A_{\mathrm{inj}}(\mathrm{mCi})P_{\max}\ \mathrm{Gy/h} \qquad (6.5)$$

For ^{90}Y, $\Delta = 2.0$ (g cGy)/(μCi h) approximately, and for ^{131}I, $\Delta = 0.4$ (g cGy)/(μCi h) approximately, where only the β-particle dose is considered for ^{131}I. Therefore

$$\dot{D}_{\max} = 0.2A_{\mathrm{inj}}(\mathrm{mCi})(\%\ \text{initial activity/g})_{\max}\ \mathrm{Gy/h} \quad \text{for } ^{90}\mathrm{Y} \qquad (6.6)$$

and

$$\dot{D}_{\max} = 0.04A_{\mathrm{inj}}(\mathrm{mCi})(\%\ \text{initial activity/g})_{\max}\ \mathrm{Gy/h} \quad \text{for } ^{131}\mathrm{I} \qquad (6.7)$$

Acknowledgments

I would like to thank Professor A. Barrett, Beatson Oncology Centre, for her interest and help in this project.

References

BARENDSEN, G. W., 1982. Dose fractionation, dose rate and isoeffect relationships for normal tissue responses. *International Journal of Radiation Oncology, Biology, Physics, 8,* 1981–1997.

BARTH, R. F., JOHNSON, C. W., WEI, W. Z., CAREY, W. H., SOLOWAY, A. H. & MCGUIRE, J., 1982. Neutron capture therapy using boronated monoclonal antibodies against tumour associated antigens. *Cancer Detection and Prevention, 5,* 315.

BERGER, M. J., 1971. Distribution of absorbed dose around point sources of electrons in water and other media. MIRD pamphlet No. 7, *Journal of Nuclear Medicine, 5,* 5.

BEIERWALTES, W. H., 1987. Treatment of neuroblastoma with ^{131}I-MIGB: dosimetric problems and perspectives. *Medical and Pediatric Oncology, 15,* 188–191.

DALE, R. G., 1985. The application of the linear quadratic dose-effect equation to fractionated and protracted radiotherapy. *British Journal of Radiology, 58,* 515–528.

DALE, R. G., 1986. A graphical method to simplify the application of the linear quadratic dose-effect equation to fractionated radiotherapy. *British Journal of Radiology, 59,* 1111–1115.

DALE, R. G., 1988. Time-dependent tumour repopulation factors in linear quadratic models—implications for treatment strategies. *Radiotherapy and Oncology, 15,* 371–382.

DARTE, L. & TENNVALL, J., 1988. Enhanced therapeutic tumour dose of ^{131}I-MIBG by accelerated diuresis. *European Journal of Nuclear Medicine, 14,* 512–514.

DENARDO, S. J., DENARDO, G. L., O'GRADY, L. F., LEVY, N. B., MILLS, S. L., MACEY, D. J., MCGAHAN, J. P., MILLER, C. H. & EPSTEIN, A. L., 1988. Pilot studies of radioimmunotherapy of B cell lymphoma and leukemia using 131-I Lym-1 monoclonal antibody. *Antibody, Immunoconjugates and Radiopharmaceuticals, 1,* 1, 17–33.

Dutreix, J., 1989. Expression of the dose rate effect in clinical curietherapy. *Radiotherapy and Oncology, 15,* 25–37.

Epenetos, A. A., Munro, A. J., Stewart, S., Rampling, R., Lambert, H. E., McKenzie, C. G., Soutter, P., Rahemtulla, A., Hooker, G., Sivolapenko, G. B., Snook, D., Courtenay-Luck, N., Dhokia, B., Krausz, T., Taylor-Papadimitriou, J., Durbin, H. & Bodmer, W. F., 1987. Antibody-guided irradiation of advanced ovarian cancer with intraperitoneally administered radiolabelled monoclonal antibodies. *Journal of Clinical Oncology, 5,* 12, 1890–1899.

Fisher, D. R. & Hendry, J. H., 1988. Dose fractionation and hepatocyte clonogens: $\alpha/\beta = 1-2$ Gy, and β decreases with increasing delay before assay. *Radiation Research, 113,* 51–57.

Fowler, J. F., 1987. Short and long fractionated schedules in radiotherapy and a proposed improvement. *British Journal of Radiology, 60,* 777–779.

Fowler, J. F., 1989. The linear-quadratic formula and progress in fractionated radiotherapy. *British Journal of Radiology, 62,* 679–694.

Hnatowich, D. J., Virzi, F. & Rusckowski, M., 1987. Investigations of avidin and biotin for imaging applications. *Journal of Nuclear Medicine, 28,* 1294–1302.

Hopewell, J. W. & Wiernik, G., 1977. Tolerance of pig kidney to fractionated X-irradiation. *Radiobiological Research and Radiotherapy,* Vol. 1 (IAEA, Vienna), pp. 65–73.

Kemshead, J. T., Jones, D. H., Lashford, L. S., Pritchard, J., Gordon, I., Breatnach, F. & Coakham, H. B., 1986. 131-I coupled to monoclonal antibodies as therapeutic agents for neuroectodermally derived tumours: fact or fiction. *Cancer Drug Delivery, 3,* 1, 25–43.

Lashford, L. S., 1988. The biodistribution and pharmacokinetics of meta-iodobenzylguanidine in childhood neuroblastoma. *European Journal of Nuclear Medicine, 13,* 574–577.

Lashford, L. S., Davies, A. G., Richardson, R. B., Bourne, S. P., Bullimore, J. A., Eckert, H., Kemshead, J. T. & Coakham, H. B., 1988. A pilot study of ^{131}I monoclonal antibodies in the therapy of leptomeningeal tumours. *Cancer, 61,* 857–868.

Lashford, L. S., Jones, D., Pritchard, J., Gordon, I., Breatnach, F. & Kemshead, J. T., 1987. Therapeutic application of radiolabelled monoclonal antibody UJ13A in children with disseminated neuroblastoma. *NCI Monograph No. 3,* 53–57.

Madsen, M. T., Park, C. H. & Thakur, M. L., 1988. Dosimetry of iodine-131 ethiodol in the treatment of hepatoma. *Journal of Nuclear Medicine, 29,* 1038–1044.

Nakajo, M., Kobayashi, H., Shimabukuro, K., Shirono, K., Sakata, H., Taguchi, M., Uchiyama, N., Sonoda, T. & Shinohara, S., 1988. Biodistribution and in vivo kinetics of iodine-131 lipiodol infused via the hepatic artery of patients with hepatic cancer. *Journal of Nuclear Medicine, 29,* 1066–1077.

O'Donoghue, J. A. & Wheldon, T. E., 1988. Predictable allowable doses to normal organs for biologically targeted radiotherapy. *British Journal of Radiology, 61,* 264–266.

Order, S. E., Klein, J. L. & Leichner, P. K., 1987. Hepatoma: model for radiolabelled antibody in cancer treatment. *NCI Monograph No. 3,* 37–41.

Payne, M. G. & Garrett, W. R., 1975. Applications of microdosimetry to models of cell survival. *Radiation Research, 63,* 201–210.

Roesch, W. C., 1978. Models of the radiation sensitivity of mammalian cells. *Third Symposium on Neutron Dosimetry in Biology and Medicine* (Commission of the European Communities, Luxembourg), pp. 1–27.

Sharkey, R. M., Kaltovich, F. A., Shih, L. B., Fand, I., Govelitz, G. & Goldenberg, D. M., 1988. Radioimmunotherapy of human colonic cancer xenografts with ^{90}Y-labelled monoclonal antibodies to carcinoembryonic antigen. *Cancer Research, 48,* 3270–3275.

Steel, G. G., 1987. Recovery kinetics deduced from continuous low dose-rate experiments. *Radiotherapy and Oncology, 14,* 337–343.

Stewart, J. S., Hird, V., Snook, D., Sullivan, M., Myers, M. J. & Epenetos, A. A., 1988. Intraperitoneal ^{131}I- and ^{90}Y-labelled monoclonal antibodies for ovarian cancer: pharmacokinetics and normal tissue dosimetry. *International Journal of Cancer, 3,* 71–76.

Thames, H. D., 1985. An "incomplete repair" model for survival after fractionated and continuous irradiations. *International Journal of Radiation Oncology, Biology, Physics, 47,* 319–339.

Thames, H. D. & Hendry, J. H., 1987. *Fractionation in Radiotherapy* (Taylor and Francis, London).

Travis, E. L. & Tucker, S. L., 1987. Isoeffect models and fractionated radiotherapy. *International Journal of Radiation Oncology, Biology, Physics, 13,* 283–287.

Williams, M. V. & Denekamp, J., 1984. Radiation induced renal damage in mice: influence of fraction size. *International Journal of Radiation Oncology, Biology, Physics, 10,* 885.

Withers, H. D., 1986. Predicting late normal responses. *International Journal of Radiation Oncology, Biology, Physics, 12,* 4, 693–698.

Withers, H. D., 1988. In *Principles and Practice of Radiation Oncology,* ed. by C. A. Perez & L. W. Brady (J. B. Lippincott, Philadelphia, PA).

Withers, H. R., Thames, H. D. & Peters, L. J., 1983. A new isoeffect curve for change in dose per fraction. *Radiotherapy and Oncology, 1,* 187–191.

Yaes, R. J., 1988. Some implications of the linear quadratic model for tumor control probability. *International Journal of Radiation Oncology, Biology, Physics, 14,* 147–157.

1991, *The British Journal of Radiology*, 64, 252–260

Concomitant pelvic irradiation, 5-fluorouracil and mitomycin C in the treatment of advanced cervical carcinoma

By *G. G. Khoury, MB BS, MRCP, FRCR, A. S. Bulman, MS, FRCS, FRCR, C. A. F. Joslin, MB BS, FRCR, DMRT and R. I. Rothwell, MB BS, FRCS, FRCR

University Department of Radiotherapy and Regional Radiotherapy Centre, Cookridge Hospital, Leeds LS16 6QB, UK

(*Received July 1990 and in revised form September 1990*)

Keywords: Uterine cervix cancer, Concomitant chemotherapy and radiotherapy, 5-Fluorouracil, Mitomycin C

Abstract. This was a Phase II study of 24 late (FIGO) Stage IIb and 39 Stage III patients. External beam radiotherapy was given daily, five days a week, using 15 × 15 cm parallel opposed pelvic fields. The first 20 patients had 45.00 Gy mid-plane dose in 20 fractions, Days 1–28, the last 43 patients had 50.40 Gy in 28 fractions, Days 1–43. This was followed by an intracavitary boost of 17.00 Gy to Point A in two fractions over seven days. The first seven patients had concomitant 5-fluorouracil (5FU) 1 g/m^2/day (maximum 1.5 g/day) Days 2–5, 30–33 and 57–60, with mitomycin C 10 mg/m^2 (maximum 15 mg) Days 2 and 57. Two patients had WHO Grade 4 cytopenia, and only two were able to have full dose intensity. The 5FU dose was reduced to 0.8 g/m^2/day, for Days 2–5 and 30–33; mitomycin C was given on Day 2 only. Treatment morbidity with the reduced chemotherapy intensity was comparable with that of radiotherapy alone. Median follow-up was 16 months (range 6–44). Median survival was 35 months. The results were compared with historical controls treated using the same radiation method alone. Two-year survival for late Stage IIb patients was 67% with the combination and 72% with radiotherapy alone; for Stage III, 67% and 49% respectively. Two-year pelvic control for late Stage IIb was 87% (combination) and 84% (radiotherapy alone) and for Stage III, 61% and 55% respectively. In contrast to reports from other centres, these results do not show an overall significant improvement on radiotherapy alone. A Phase III study may not be practicable.

The prognosis of advanced carcinoma of the cervix is poor and has shown little improvement in the last 20 years (Jolles, 1980). The incidence of failure to control pelvic disease following radical irradiation alone for Stage IIIb disease is about 45% (Joslin, 1990).

This is associated with poor survival and related to a high incidence of metastatic disease—26% of patients treated for Stage III cancer of the cervix subsequently developed metastases either alone or in combination with pelvic failure (Joslin, 1990). Radiotherapy under hyperbaric oxygen has been shown to improve local disease control with an increase in morbidity also; the technique is too laborious for routine use (Watson et al, 1978). The giving of a radio-sensitizer (misonidazole) during irradiation has also been reported as offering no worthwhile benefit (Dische, 1985), probably because it was too toxic to give an effective dose.

Certain cytotoxic drugs active against cervical cancer have been identified as providing some benefits to patients with recurrent or metastatic disease although responses are usually incomplete and short lived (Meanwell et al, 1986; Sabir et al, 1989). One of the claimed advantages of giving cytotoxic drugs prior to radical irradiation is a reduction in tumour bulk, with improved local disease control following radiotherapy (Symonds et al, 1987). Others report this approach is practicable without any significant increase in morbidity (Friedlander et al, 1984; Blake et al, 1986). It is also claimed that patients who initially respond to cytotoxic chemotherapy have a higher probability of achieving complete response following irradiation as opposed to poor responders to chemotherapy who then tend not to respond to irradiation and have a bad prognosis (Symonds et al, 1987). One reported randomized study of neo-adjuvant cytotoxic chemotherapy and radiotherapy versus radiotherapy alone in advanced cervical cancer used a combination of methotrexate, chlorambucil, vincristine and cisplatin (Chauvergne et al, 1988). While the initial response rate to chemotherapy was 35%, following completion of treatment the overall response rate was the same for both arms of the trial. The three year survival of 58% was the same in both groups of patients and the number of local and metastatic failures also the same. Thirteen patients also receiving chemotherapy were reported as having WHO Grade 3–4 morbidity; two of them died owing to myelosuppression.

While the interaction of cytotoxic drugs and irradiation given simultaneously is not fully understood at the cellular level, there are some experimental and clinical data available. Byfield et al (1982) reported on the

---

Address for correspondence: Professor C. A. F. Joslin, University of Leeds Department of Radiotherapy, Cookridge Hospital, Leeds LS16 6QB, UK.

*Current address: Department of Radiotherapy, St Mary's Hospital, Portsmouth PO3 6AD, UK.

effects of combining 5-fluorouracil (5FU) and irradiation on cell killing in tissue culture. Enhanced cell killing was seen when HeLa cells were continuously exposed to 5FU for periods of 48 hours or more following X-ray exposure: when the cells were exposed to 5FU prior to radiotherapy (the 5FU was absent during irradiation) there was no enhancement. Since the plasma half-life of 5FU is only 11 minutes (MacMillan et al, 1978) continuous infusion is required to maintain a consistent plasma level in patients. Although there is no evidence that mitomycin C alone enhances the effect of radiation (Rockwell & Kennedy, 1979), when used concurrently with 5FU the combination has been reported as giving promising early results in Phase II studies for treating carcinoma of the anus and oesophagus (Cummings et al, 1982; Nigro et al, 1983; Keane et al, 1985; Sischy, 1985) and a Phase III multicentre study of concomitant therapy in carcinoma of the anus is currently underway in the UK (UKCCCR Anal Cancer Study, 1988). 5FU and mitomycin C have also been combined with irradiation in treating patients with advanced carcinoma (Thomas et al, 1984; John et al, 1987; Evans et al, 1988; Ludgate et al, 1988) and recurrent (Thomas et al, 1987) carcinoma of the cervix.

Phase II studies of irradiation with concomitant cisplatin (Choo et al, 1986; George et al, 1986; O'Reilly et al, 1986) and hydroxyurea (Stehman et al, 1986) have been reported and also one Phase III study of hydroxyurea compared with radiation alone (Piver et al, 1983). None of these have shown survival or local control rates clearly superior to those obtained in similar staged patients in other institutions employing radiotherapy alone.

We decided that we should carry out a Phase II study using a combination of 5FU and mitomycin C concomitantly with irradiation in an attempt to determine whether we could improve local disease control rates and mortality without increasing morbidity.

Materials and methods

Entry into the study was limited to patients aged 75 years or less, presenting with advanced carcinoma of the cervix FIGO Stages IIB (late) to IIIB. All patients underwent full clinical examination, full blood count, serum estimations of urea, electrolyte and liver function, chest radiograph and intravenous urogram followed by FIGO staging and biopsy under anaesthetic. Our classification of a late Stage IIB tumour was where parametrial extension was half way or more towards the pelvic side wall on one or both sides. Patients were excluded if their general condition was poor (WHO performance status 3 or more), or they manifested other adverse factors, *e.g.* uraemia, unsuitability for a general anaesthetic, large bowel inflammatory disease and previous pelvic surgery.

Treatment

A summary of the treatment regimes is given in Figs 1(a) and 1(b).

Radiotherapy. External beam irradiation was commenced within one or two days following examination under anaesthesia (EUA). Parallel opposed pelvic fields were used. The lower edge of the field was 1 cm above the lower border of the obturator foramen, or at least 1 cm below the lowest vaginal extension of disease. The upper edge was at the junction of the 4th and 5th lumbar vertebrae. The lateral borders were at least 1 cm beyond the bony landmarks of the true pelvis (the usual field size was 15 cm × 15 cm at the skin surface) with leading off of the corners of the fields. Treatment was delivered using photons from 6 or 8 MV linear accelerators, treating daily for 5 days each week. The first 20 patients received a mid-plane dose of 45 Gy in 25 fractions each of 1.8 Gy (time, dose and fractionation (TDF), 70). Experience with these 20 patients showed that local reactions were not significantly increased by the concomitant chemotherapy and the radiation dose was subsequently increased, keeping the fraction size at 1.8 Gy, to the TDF equivalent of our previous standard radical treatment. The last 43 patients received 50.4 Gy in 28 fractions each of 1.8 Gy (TDF, 79). Seven to 10 days following completion of the external beam irradiation, all patients had an EUA and, provided there was good tumour regression, then received intracavitary high-dose-rate irradiation, using cobalt 60, to deliver 8.5 Gy to the Manchester Point A, this was repeated 1 week later. In those patients with a poor tumour response or in whom intracavitary irradiation was not practicable, a booster dose of 15 Gy in seven fractions over 9 days was given, restricted to the central pelvis using parallel opposed fields of $12 \times 10\ \text{cm}^2$.

The same radiation method was in use in the 8 year period up to 1984, although using a fraction size of 2.25 Gy, and stage matched patients from this period were used as historical controls. The radiation dose for these patients was 45 Gy mid plane in 20 fractions over 28 days (TDF, 79). Depending on tumour response a boost was given 2 weeks later either by high-dose-rate intracavitary irradiation to deliver 8.5 Gy on each of two occasions spaced 1 week apart or, in patients with a poor response, by a dose of 15 Gy in 7 fractions using external beam irradiation.

Cytotoxic therapy. Mitomycin C 10 mg/m^2 (maximum 15 mg) was given as an intravenous bolus on Day 2. On the same day 5FU infusion was commenced. The first seven patients received a dose of 1 g/m^2/24 hours for 4 days (maximum 1.5 g/24 hours). In subsequent patients the dose was reduced to 0.8 g/m^2/24 hours (maximum 1.2 g/24 hours) for 4 days. The 4-day 5FU infusion was repeated at the same dosage starting on Day 30. Two of the first seven patients were given mitomycin C and a third 4-day infusion of 5FU starting on Day 58, the intention to give this third cycle of treatment was dropped after treating Patient 7. Chemotherapy dose intensity was reduced after Patient 7 because of clinically significant cytopenia.

Toxicity

Toxicity was graded using WHO criteria for blood count, nausea and/or vomiting, diarrhoea and

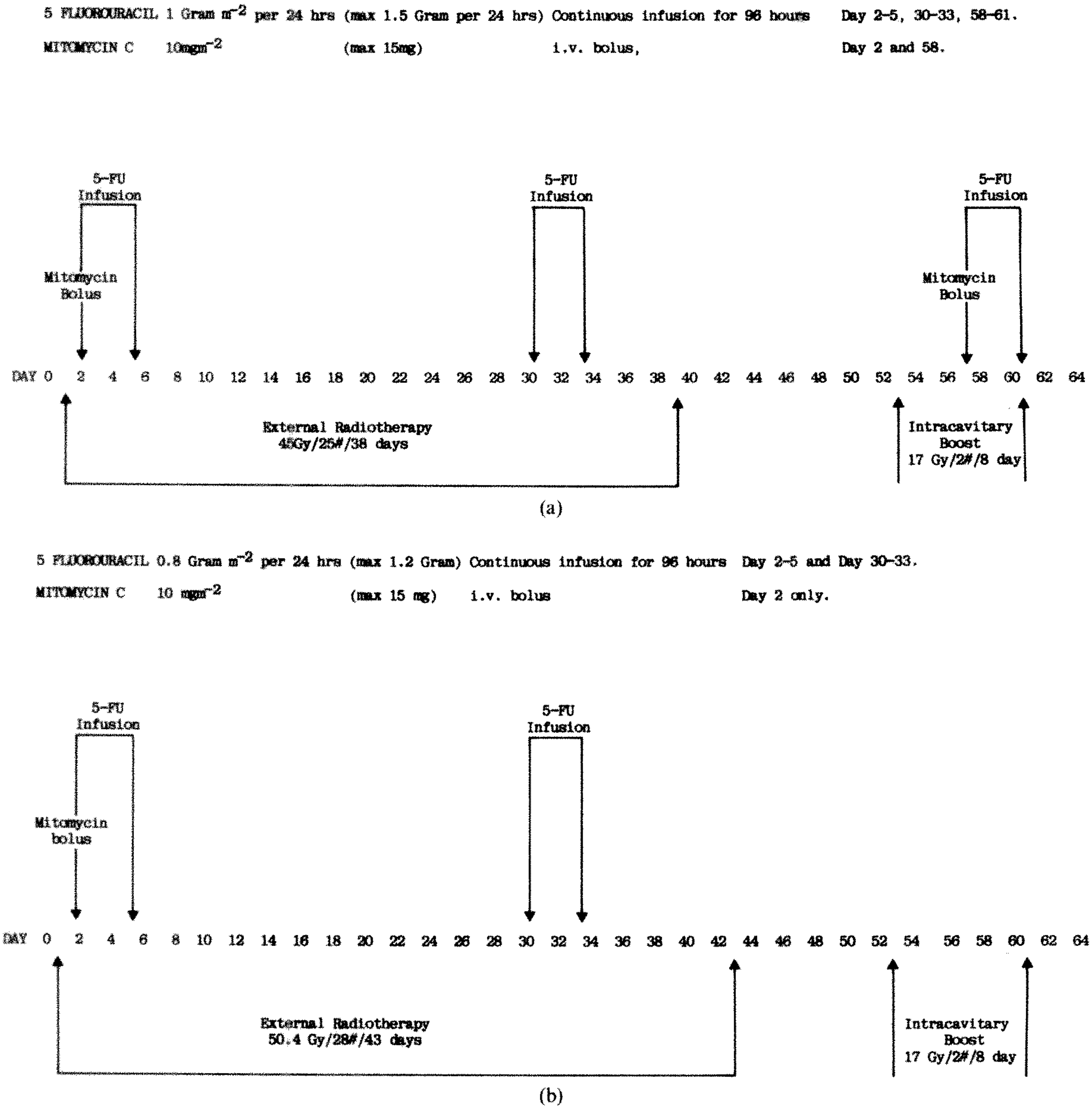
5 FLUOROURACIL 1 Gram m-2 per 24 hrs (max 1.5 Gram per 24 hrs) Continuous infusion for 96 hours Day 2-5, 30-33, 58-61.
MITOMYCIN C 10mgm-2 (max 15mg) i.v. bolus, Day 2 and 58.
5-FU Infusion
5-FU Infusion
5-FU Infusion
Mitomycin Bolus
Mitomycin Bolus
DAY 0 2 4 6 8 10 12 14 16 18 20 22 24 26 28 30 32 34 36 38 40 42 44 46 48 50 52 54 56 58 60 62 64
External Radiotherapy 45Gy/25#/38 days
Intracavitary Boost 17 Gy/2#/8 day
(a)
5 FLUOROURACIL 0.8 Gram m-2 per 24 hrs (max 1.2 Gram) Continuous infusion for 96 hours Day 2-5 and Day 30-33.
MITOMYCIN C 10 mgm-2 (max 15 mg) i.v. bolus Day 2 only.
5-FU Infusion
5-FU Infusion
Mitomycin bolus
DAY 0 2 4 6 8 10 12 14 16 18 20 22 24 26 28 30 32 34 36 38 40 42 44 46 48 50 52 54 56 58 60 62 64
External Radiotherapy 50.4 Gy/28#/43 days
Intracavitary Boost 17 Gy/2#/8 day
(b)

Figure 1. Concomitant chemotherapy and radiotherapy: (a) initial regime A (used in first seven patients); (b) current regime B.

mucositis. Symptoms severe enough to require a break in radiotherapy were graded 2. Abdominal colic was graded using categories as for diarrhoea.

End-points

Patients entered the study on the day of EUA and were further assessed 1 month after completing treatment following which they were seen every 3 months if asymptomatic or more frequently as required. Follow-up investigations were not performed on a routine basis but as indicated by symptoms. The time to local recurrence or development of metastases was taken from the time of substantive diagnosis. Local recurrence was defined as recurrence occurring within the field of irradiation. The Kaplan–Meier method was employed to plot life table graphs.

Results

Since June 1986, 63 patients have been entered into the study. Patients have each been followed up for a minimum of 6 months and are evaluable for response to treatment and early toxicity. Patients were staged as shown in Table I, with histology as shown in Table II. They ranged in age from 24 to 73 years.

Table I. FIGO stage distribution

Stage	Number of patients
Late IIB	24
IIIA	1
IIIB	38
Total number of patients	63

Table III. Number of patients showing acute toxicity (WHO grading system)

	WHO grade				
	0	1	2	3	4
Haemoglobin	26	24	11	2	0
WBC	22	18	18	4	1
Platelets	52	6	2	0	3
Nausea and/or vomiting	51	10	1	1	0
Diarrhoea	25	33	2	2	1
Abdominal pain	48	10	4	1	0

Ten patients did not receive a second infusion of 5FU, in five the primary reason was cytopenia (regime A two patients, regime B three patients), in two diarrhoea or abdominal pain, and in single cases chest infection, pyometrium and family illness prevented further chemotherapy being given. Five of these 10 patients are now dead. Life table analysis comparing these patients with those who received the full chemotherapy dose intensity showed no difference.

Because of poor tumour regression, two patients, one with late Stage IIB and one with bilateral Stage IIIB disease, received booster treatment by external irradiation to the inner pelvis. One Stage IIIB patient with procidentia was unsuitable for intracavitary treatment and after completing external beam irradiation was treated by surgery, but unfortunately died in the postoperative period. In the historical control group, 20% of patients had external beam rather than intracavitary boost because of poor initial tumour regression.

Acute effects

The overall haematological toxicity is shown in Table III. Two of the initial seven patients experienced Grade 4 haematological toxicity. In the first, nadir counts of white blood corpuscles (WBC) 0.5×10^9/l on Day 12, platelets 25×10^9/l on Day 19 and haemoglobin 8.1 g/dl were associated with Grade 4 haemorrhagic diarrhoea and Grade 2 oral mucositis. This patient required a blood transfusion, intravenous fluids and antibiotics but made a full recovery. In the second patient, a platelet count of 25×10^9/l, WBC 3.2×10^9/l and haemoglobin 8.6 g/dl were seen on Day 15 without bleeding or sepsis, although associated with Grade 2 vomiting and Grade 2 mucositis. Following a dose reduction of 5FU from 1.0 g/m^2 to 0.8 g/m^2, one further case of thrombocytopenia occurred (platelets 13×10^9/l on Day 19, WBC 1.8×10^9/l and haemoglobin 7.7 g/dl) again without overt sepsis or bleeding but associated with Grade 2 oral mucositis and diarrhoea. All of these patients had normal pre-treatment cell counts, renal and hepatic biochemical function. One patient who was treated by regime B suffered severe Grade 3 diarrhoea with Grade 2 abdominal colic and moist desquamation of the groin skin folds without cytopenia. All of the above four patients died from recurrent disease, but did not develop any significant late effects at a mean follow-up time of 18 months (range 13–26 months). One further patient who suffered vomiting, diarrhoea and abdominal pain of Grade 3 severity had a previous history of undiagnosed abdominal symptoms and required opiate analgesia during radiotherapy. This patient is now disease free and continues with the same symptoms as prior to treatment.

Table II. Histological distribution

	Dead	Alive	Total
Squamous carcinoma			
Well differentiated	2	5	7
Moderately differentiated	7	18	25
Poorly differentiated	10	12	22
Not classified	0	3	3
Adenosquamous	1	2	3
Adenocarcinoma	0	3	3
Total	20	43	63

For 248 historical control patients and the 63 study patients, the overall incidence of moist skin reactions was 6% and 7%, abdominal pain 18% and 24%, and diarrhoea 48% and 60% respectively.

Late effects

Of the 20 patients who died, two developed persistent urinary frequency which initially was thought to be treatment related but both subsequently developed central pelvic recurrence. A third patient developed a vesico-vaginal fistula, again in association with persistent carcinoma. One patient developed small bowel obstruction at 24 months which required surgical resection. While the patient's initial recovery was satisfactory she died on the 12th post-operative day following perforation of the small bowel proximal to the anastomosis.

Of the 38 patients still alive with no clinical evidence of local recurrence, three have developed small bowel symptoms, one had a resection for acute obstruction, barium studies in one patient showed small bowel thickening and was treated with steroids, one patient refused any specific treatment and remains reasonably well.

Stenosis of the upper vagina has been common in those patients not sexually active, one has complained

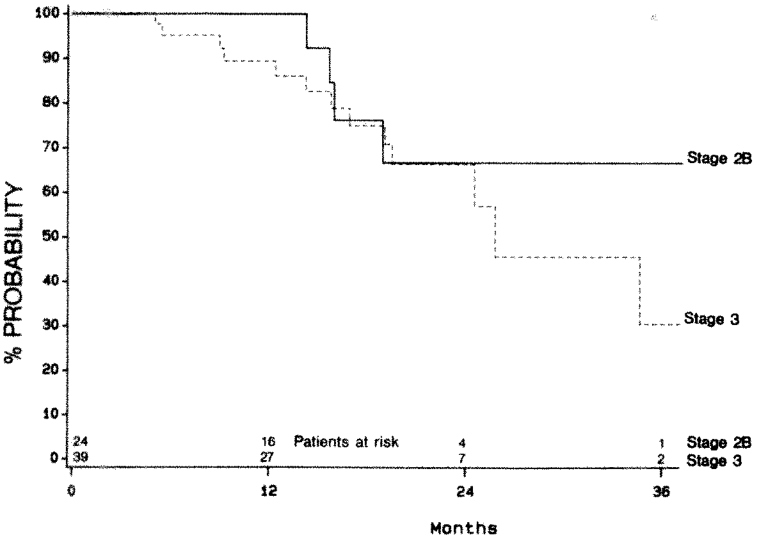

Figure 2. Survival by stage.

of persistent dyspareunia, and one of postcoital bleeding related to telangiectasia of the vaginal vault epithelium.

Control of disease

The initial tumour response to external beam radiotherapy with chemotherapy was more rapid than expected. In the historical control group, 20% of patients were unsuitable for an intracavitary boost because of a poor tumour response, whereas in the study group only 5% were unsuitable. An analysis of survival, local pelvic recurrence and disease-free survival has been carried out, stratified according to the stage of disease.

The median follow-up time for the 63 evaluable patients was 16 months (range 6–44 months). Survival by stage is shown in Fig. 2, disease-free survival by stage in Fig. 3, and local pelvic disease control by stage in Fig. 4. Figure 2 shows a non-significant trend for improved survival for late Stage IIB compared with Stage III up to 12 months. No significant difference between Stages IIB and III has been demonstrated for local recurrence or disease-free survival.

One- and 2-year survival and local control rates for both the study group and historical control groups of patients are shown in Table IV. The results for Stage IIB patients are similar, whereas the results for

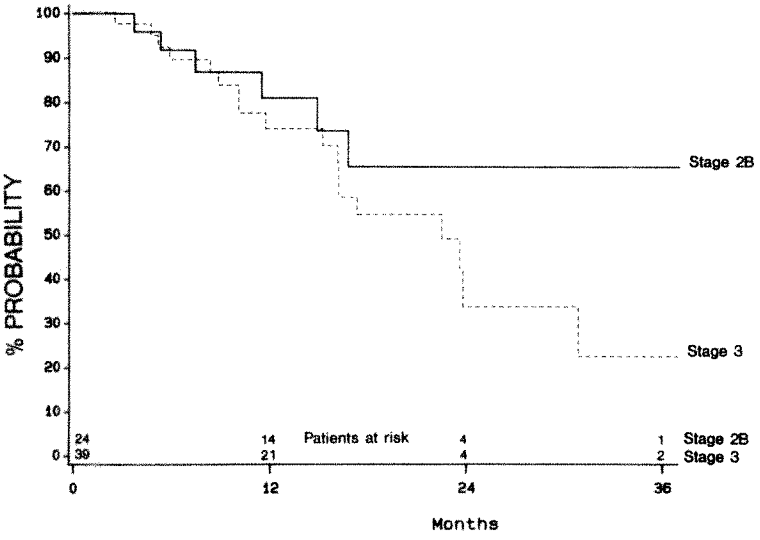

Figure 3. Disease-free survival by stage.

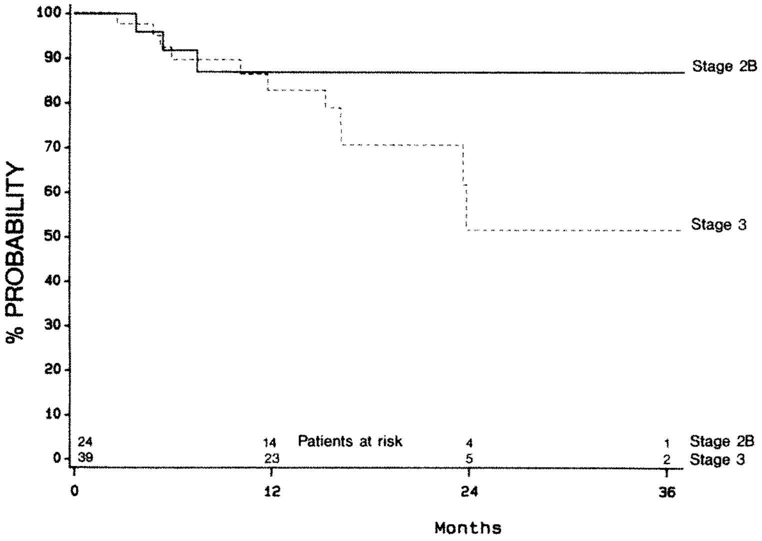

Figure 4. Pelvic control by stage.

Stage III patients show that the study group has a 2-year survival of 67% compared with 49% (comparison of binomial proportions statistic 2.045, $p = 0.05$) for the historical controls; local pelvic disease control was 61% compared with 55% respectively; this difference was not significant.

Current clinical status of patients

Of the 24 stage IIB patients, 15 are alive and clinically disease free, two are alive with clinical suspicion of local recurrence, three have died following local recurrence alone, three have died of metastatic disease with local control and one died post-operatively following surgery for radiation-induced small bowel obstruction.

Of the 39 Stage III patients, 26 are alive, 20 are disease free, two are alive with pelvic recurrence and liver metastases, one patient is alive with local recurrence alone and three patients are alive with metastatic disease alone. Of the dead patients, four died from local disease only, three from metastases only, three from both local recurrence and metastases. Three patients died of unrelated causes, one of myocardial infarct, one of proven lung cancer and one following surgery for a procidentia.

Local disease control at the time of death

At the time of death, local disease control for Stage III patients in the study group and historical controls respectively, was 6/13 (46%) and 26/115 (23%) (comparison of binomial proportions statistic 1.86, $p = 0.06$). For late stage IIB patients in the study group, local control at death was 4/7 (57%); no historical comparative data for this subgroup were available.

Discussion

In terms of morbidity we have not found a clinically significant increase in acute gut or bladder toxicity over that expected from the same dose of radiotherapy alone. The single case of Grade 4 thrombocytopenia seen with regime B indicates that concomitant treatment with

Table IV. Comparison of percentage survival and local recurrence with historical data

Stage		Survival (%)		Local control (%)	
		Concomitant radiotherapy and chemotherapy	Historical controls, radiotherapy alone	Concomitant radiotherapy and chemotherapy	Historical controls, radiotherapy alone
Late IIB	1 year	100	86	87	86
	2 years	67	72	87	84
III	1 year	89	67	82	61
	2 years	67[a]	49[a]	61	55

Numbers of late Stage IIB patients treated were 24 (radiotherapy and chemotherapy) and 135 (radiotherapy alone); numbers of Stage III patients treated were 39 (radiotherapy and chemotherapy) and 185 (radiotherapy alone).

[a] Comparison of binomial statistic 2.045, $p = 0.05$; the other differences are not significant at the 5% level.

Table V. Comparison of results from different centres of treating advanced carcinoma of the cervix with concomitant radiotherapy, 5FU and mitomycin C

Study	Number of patients			Months follow-up		Alive and disease free	
	Stage II	Stage III	Stage IV	Median	Range	Number	Percentage
Thomas et al, 1984	7	14	3	6	4–24	16	59
John et al, 1987	4	5	1	20	6–37	8	80
Evans et al, 1988	2	8	0	17	7–38	7	70
Ludgate et al, 1988	19	17	2	20	5–36	26	68
Current study	24	39	0	16	6–44	35	56
Thomas et al, 1987	17 recurrent			34	4–58	8	47

5FU and mitomycin C is potentially more toxic than radiotherapy alone, although there have been no acute cytopenic treatment-related deaths in the 145 patients treated with similar drugs reported from other centres whose responses are summarized in Table V. A general increase in acute skin reactions in the study group of patients was not considered clinically significant. It is too soon to determine whether the addition of chemotherapy during the standard course of radiotherapy increases the incidence of late morbidity, but thus far no increase has been seen.

Reports from other centres have suggested that the results obtained with concomitant 5FU and mitomycin C with radiotherapy for patients with advanced carcinoma of the cervix are superior to those using radiotherapy alone. In terms of the proportion of patients who remain alive and disease free, the four reports of primary concomitant treatment summarized in Table V all show results which are better than those expected; results which we have not been able to confirm for advanced Stage IIB but which we agree with for Stage III. There are, however, certain differences in technique in this study compared with the others. For example, in both reports from Princess Margaret Hospital, Toronto (Thomas et al, 1984, 1987), most patients were treated with a gap of 2½ weeks during the course of external beam irradiation, a split course was also employed by Evans et al (1988). The split course was used to allow chemotherapy to be given at dose levels which we initially employed, 5FU 1 g/m^2/day for 96 hours, although the effective dose of radiation was reduced and repopulation of the tumour as well as of normal tissues may have taken place as a result. Whilst continuous daily fractionation was employed in two other reports (John et al, 1987; Ludgate et al, 1988), the prescribed radiation dose was also reduced from that normally given. A further difference in the chemotherapy used by John et al (1987) was to use cisplatin at 75 mg/m^2 with 5FU in the second cycle of concomitant treatment. We found unacceptable toxicity in our first seven patients when 5FU 1 g/m^2/day for 96 hours and mitomycin C 10 mg/m^2 were added to the standard radiation dosage. Rather than compromise the effective dose of radiation, we opted to reduce the chemotherapy intensity.

At first consideration our results suggest that disease control has been improved to a statistically significant extent as seen in the 2-year survival data for Stage III patients which improves from 49% for radiotherapy alone to 67% with concomitant 5FU and mitomycin C. Also encouraging has been the finding of a significant increase in local pelvic control seen in Stage III patients at the time of death from 23% with radiotherapy alone to 46% with concomitant treatment and the non-significant trend for improved local control in the study patients compared with the control patients (Table IV). Any improvement in local control may be due to the greater proportion (95%) of study patients able to receive an intracavitary insertion compared with historical controls (80%). A number of factors to be set against these positive findings include the fact that no overall increase in survival is apparent and the finding retrospectively of a benefit in one subgroup reduces the credibility of the 5% significance test. Also, our results indicate that Stage III patients benefit whereas Stage IIB patients do not, which is the converse of the result of Ludgate et al (1988). It is not known whether concomitant chemotherapy is acting by local synergism or by direct cytotoxic effect on distant micro metastases. The higher proportion of patients able to receive an intracavitary boost in the study group and the improved local control at the time of death argue more in favour of some increased local effect. However, the statistically significant difference seen in local control at death is particularly suspect in view of the short follow-up, since five of our patients (two Stage IIB, three Stage III) are alive with local recurrence and will undoubtedly die with residual disease. It is possible that the significant differences found are statistical artefacts due to the small numbers of patients and error due to using historical rather than randomized control patients.

Our results indicate that, despite the excellent early tumour regression seen during treatment, the benefit of concomitant chemotherapy in terms of reduced mortality and increased pelvic control rates may not be as great as that suggested by other reports. Estimates of potential benefit in Phase II studies such as these are important in planning the feasibility of a Phase III study, which will be necessary if we are to determine the true contribution made by the addition of concomitant chemotherapy. An optimistic view of our results suggests that the improved survival rates for Stage III patients may lie between 10% and 20%. A 90% chance of detecting such a difference at the 5% significance level would require 1000 patients for a 10% difference, and 280 patients for a 20% difference. 3963 cases of carcinoma of the cervix were registered in the whole of the UK in 1980 and, assuming that 27% were Stage III, approximately 1070 Stage III patients would be expected to present annually. It is of course arguable how many could be entered into a study, but recruitment of sufficient patients is likely to require a multicentre approach.

Currently we continue to use concomitant radiotherapy, 5FU and mitomycin C for advanced stage patients with cervical carcinoma because more patients exhibit regression of the primary tumour at the time of intracavitary irradiation. More patients therefore complete the treatment as originally prescribed rather than having to receive a boost with additional external beam therapy.

Acknowledgments

We wish to thank all those gynaecologists and consultants who supported this study by referring patients, especially Dr Ash, Dr Cartwright, Dr Jones and Dr Stone of Cookridge Hospital. We also acknowledge with thanks Dr D. Joanes of the Department of Mathematics who provided expert statistical advice and produced Figs 2–4, and Mrs K. Breton for typing the manuscript.

References

Blake, P. R., Branson, A. N. & Lambert, H. E., 1986. Combined radiotherapy and chemotherapy for advanced carcinoma of the cervix. *Clinical Radiology, 37,* 465–469.

Byfield, J. E., Calabro-Jones, P., Klisak, I. & Kulhanian, F., 1982. Pharmacologic requirements for obtaining sensitization of human tumour cells *in vitro* to combined 5-fluorouracil or ftorafur and x-rays. *International Journal of Radiation Oncology, Biology and Physics, 8,* 1923–1933.

Chauvergne, J., Rohart, J., Heron, J. F., Fargeot, P., Berlie, J., David, P. & George, M., 1988. Randomised phase III trial of neoadjuvant chemotherapy versus radiotherapy in stage IIB and III carcinoma of the cervix: co-operative study of the French oncology centres. *Proceedings of the American Society of Clinical Oncology, 7,* 136.

Choo, Y. C., Choy, T. K., Wong, L. C. & Ma, H. K., 1986. Potentiation of radiotherapy by cis-dichlorodiammine platinum in advanced cervical carcinoma. *Gynecologic Oncology, 23,* 94–100.

Cummings, B. J., Rider, W. D., Harwood, A. R., Keane, T. J., Thomas, G. M., Erlichman, C. & Fine, S., 1982. Combined radical radiation therapy and chemotherapy for primary squamous cell carcinoma of the anal canal. *Cancer Treatment Reports, 66,* 489–492.

Dische, S., 1985. Radiotherapy of cervical cancer. *Clinics in Obstetrics and Gynecology, 12,* 203–227.

Evans, L. S., Kersh, C. R., Constable, W. C. & Taylor, P. T., 1988. Concomitant 5-fluorouracil, mitomycin C and radiotherapy for advanced gynaecologic malignancies. *International Journal of Radiation Oncology, Biology and Physics, 15,* 901–906.

Friedlander, M. L., Atkinson, K., Coppleson, J. V. M., Elliott, P., Green, D., Houghton, R., Solomon, H. J., Russell, P. & Tattersall, M. H. N., 1984. The integration of chemotherapy into the management of locally advanced cervical cancer: a pilot study. *Gynecologic Oncology, 19,* 1–7.

George, M., Haie, C., Pejovic, M. H., Horiot, J. C., Fenton, J., Lefloch, O. & Heron, J. F., 1986. Combination of radiotherapy and chemotherapy in the primary treatment of advanced uterine cervix carcinoma: three year results. *Proceedings of the American Association of Clinical Oncology, 5,* 440.

John, M., Cooke, J. K., Flam, M., Padmanabhan A. & Mowry, P. A., 1987. Preliminary results of concomitant radiotherapy and chemotherapy in advanced cervical carcinoma. *Gynecologic Oncology, 28,* 101–110.

Jolles, B., 1980. Long term results of treatment of carcinoma of the cervix. *British Journal of Obstetrics and Gynaecology, 87,* 315–321.

Joslin, C. A. F., 1990. Radiotherapy of the cervix, uterine corpus and ovary. In *Clinical Gynaecological Oncology,* ed. by Shepherd and Monaghan (Blackwell Scientific, Oxford).

Keane, T. J., Harwood, A. R., Elhakim, T., Rider, W. D., Cummings, B. J., Ginsberg, R. J. & Cooper, J. C., 1985. Radical radiation therapy with 5 fluorouracil infusion and mitomycin C for oesophageal squamous carcinoma. *Radiotherapy and Oncology, 4,* 205–210.

Ludgate, S. M., Crandon, A. J., Hudson, C. N., Walker, Q. & Langlands, A. O., 1988. Synchronous 5-fluorouracil, mitomycin C, and radiation therapy in the treatment of locally advanced carcinoma of the cervix. *International Journal of Radiation Oncology, Biology and Physics, 15,* 893–899.

MacMillan, W. E., Wolberg, W. H. & Welling, P. G., 1978. Pharmacokinetics of fluorouracil in humans. *Cancer Research, 38,* 3479–3482.

Meanwell, C. A., Mould, J. J., Blackledge, G., Lawton, F. G., Stuart, N. S. A., Kavanagh, J., Latief, T. N., Spooner, D. & Chetiyawardana, A. D., 1986. Phase II study of ifosphamide in cervical cancer. *Cancer Treatment Reports, 70,* 727–730.

Nigro, N. D., Seydel, H. G., Considine, B., Vaitkevicius, V. K., Leichman, L. & Kinzie, J. J., 1983. Combined preoperative radiation and chemotherapy for squamous cell carcinoma of the anal canal. *Cancer, 51,* 1826–1829.

O'Reilly, S. E., Swenerton, K. D., Manji, M., Acker, B., Benedet, J. L. & Elit, L., 1986. Concomitant cisplatin and radiotherapy in advanced cervical squamous cell carcinoma. *Proceedings of the American Association of Clinical Oncology, 5,* 115.

Piver, M. S., Barlow, J. J., Vongtama, V. & Blumenson, L., 1983. Hydroxyurea: a radiation potentiator in carcinoma of the uterine cervix. A randomised double blind study. *American Journal of Obstetrics and Gynecology, 147,* 803–808.

Rockwell, S. & Kennedy, K. A., 1979. Combination therapy with radiation and mitomycin C: preliminary results with EMT 6 tumour cells *in vitro* and *in vivo*. *International Journal of Radiation Oncology, Biology and Physics, 5,* 1673–1676.

Sabir, A. A., Khoury, G. G., Joslin, C. A. F. & Head, C., 1989. Treatment of recurrent and metastatic carcinoma of cervix with chemotherapy: a comparison of low dose methotrexate with adriamycin and methotrexate. *Clinical Oncology, 1,* 70–74.

SISCHY, B., 1985. The use of radiation therapy combined with chemotherapy in the management of squamous cell carcinoma of the anus and marginally resectable adenocarcinoma of the rectum. *International Journal of Radiation Oncology, Biology and Physics, 11,* 1587–1593.

STEHMAN, F., JOBSON, V., BUNDY, B., FOWLER, W. & WHITNEY, C., 1986. A randomised trial of hydroxyurea versus misonidazole adjunct to radiation therapy in stages IIB, III, IVA carcinoma of cervix. A gynecologic oncology group study. *Proceedings of the American Society of Clinical Oncology, 5,* 121.

SYMONDS, R. P., HABESHAW, T., WATSON, E. R. & KAYE, S. B., 1987. Combination chemotherapy prior to radical radiotherapy for stage III and IV carcinoma of the cervix. *Clinical Radiology, 38,* 273–274.

THOMAS, G., DEMBO, A., BEALE, F., BEAN, H., BUSH, R., HERMAN, J., PRINGLE, J., RAWLINGS, G., STURGEON, J., FINE, S. & BLACK, B., 1984. Concurrent radiation, mitomycin C and 5 fluorouracil in poor prognosis carcinoma of the cervix. Preliminary results of a phase I–II study. *International Journal of Radiation Oncology, Biology and Physics, 10,* 1785–1790.

THOMAS, G. M., DEMBO, A. J., BLACK, B., BEAN, H. A., BEALE, F. A., PRINGLE, J. R., RAWLINGS, G. & DEPETRILLO, D., 1987. Concurrent radiation and chemotherapy for carcinoma of the cervix recurrent after radical surgery. *Gynecologic Oncology, 27,* 254–260.

UKCCR ANAL CANCER TRIAL, 1988. CRC Clinical Trials Centre (Rayne Institute, London).

WATSON, E. R., HALNAN, K. E., DISCHE, S., SAUNDERS, M. I., CADE, I. S., MCEWAN, J. B., WIERNICK, G., PERRINS, D. J. D. & SUTHERLAND, I., 1978. Hyperbaric oxygen and radiotherpy. A Medical Research Council trial in carcinoma of the cervix. *British Journal of Radiology, 51,* 879–887.

1991, *The British Journal of Radiology*, *64*, 261–269

Paediatric haemangiomas: the role of radiotherapy

By S. C. Dutton and P. N. Plowman, MD, FRCR

Department of Radiotherapy, St Bartholomew's Hospital, West Smithfield, London EC1 and Department of Oncology, The Hospital for Sick Children, Great Ormond Street, London WC1N 3JH

(*Received June 1990 and in revised form August 1990*)

Keywords: Haemangiomas, Paediatrics, Radiotherapy

Abstract. Radiotherapy currently maintains an occasional place in the therapy of complicated haemangiomas of childhood. Eight such childhood benign lesions have been so treated at St Bartholomew's Hospital in the last 10 years. The case histories are presented before being discussed in the context of other therapies available (no treatment, steroids, embolism and surgery), radiation technique used and radiation dose prescription advised.

Although, historically, radiotherapy was successfully employed to treat haemangiomas in childhood, this practice has largely disappeared with the recognition of late risks associated with irradiating these benign lesions, and the spontaneous involution of some with time. However, in certain situations, radiotherapy is indicated.

There are several types of angiomas seen in infancy and childhood. The "neonatal stain" on the head and neck fades spontaneously, whilst the "salmon patch" remains unchanged. The "port wine stain" is a sharply defined area of intense intradermal erythema that persists throughout life. "Spider" angiomas may arise at any age, and childhood lesions may spontaneously resolve. The "strawberry" (capillary) haemangioma presents at birth or soon afterwards, most commonly located on the head and neck. Initially, strawberry naevi may grow rapidly. Historically, it was this fast enlargement and quick response to low dose radiotherapy that led to the once widespread use of radiation in their treatment. However, after the age of 9 months, most lesions spontaneously involute. Lister reported that 50% of untreated strawberry naevi completely resolve by 5 years (Lister, 1938). Occasionally, strawberry naevi grow to enormous size, ulcerate, and even when they involute, lead to late scarring. "Cavernous" haemangiomas are subcutaneous lesions with less easily distinguishable margins on the skin. They are present at birth or appear in the first 6 months of life, and may occur anywhere in the body (vertebrae, liver, pericardium, orbit, and subglottis all described). Cavernous haemangiomas may also be complicated by thrombocytopenia and consumption coagulopathy due to sequestration within the lesion (Kasabach–Merritt syndrome). The natural history of cavernous haemangiomas is similar to that of strawberry naevi with a growth phase, plateau phase, and subsequent involution phase. During the growth phase, the haemangioma may reach gigantic size with major clinical repercussions. The involution phase may be incomplete, and then the haemangioma may enlarge pro rata with the child's growth (Lister, 1938).

Although similar clinically (Dargeon, 1960), haemangiomas can be differentiated histologically from haemangioendotheliomas. Haemangiomas are composed of large vascular structures lined by flat epithelial cells, and haemangioendotheliomas have vascular spaces lined by one or more layers of thick endothelial cells. Both histological types may occur in the same individual or even in the same tissue specimen (Dehner & Ishak, 1971).

Lymphangiomas are distinguishable from haemangiomas both in their histology and natural history. Rarely, one lesion contains both elements. Lymphangiomas may be cystic or diffuse, enlarge very slowly throughout childhood, very rarely spontaneously regress, and have a tendency to recurrent cellulitis (Edgerton, 1976).

In the last 10 years, eight children with haemangiomas/lymphangiomas have been treated at this hospital by radiotherapy. The cases are described, and then the historical treatment of these lesions is reviewed before we conclude on the place of radiotherapy in the management of haemangiomas in the 1990s.

Case reports

Case 1

This previously well baby girl presented acutely, aged 4 months, with stridor. Direct laryngoscopy revealed a pink subglottic swelling consistent with haemangioma. A computed tomographic (CT) scan demonstrated a large vascular tumour extending from the level of the hyoid down to the carina, compressing the length of the trachea on the left. An arteriogram demonstrated a vascular mass fed by branches of the left subclavian and

---

Address for reprint requests: Dr P. N. Plowman, Radiotherapy Department, St Bartholomew's Hospital, London EC1A 7BE.

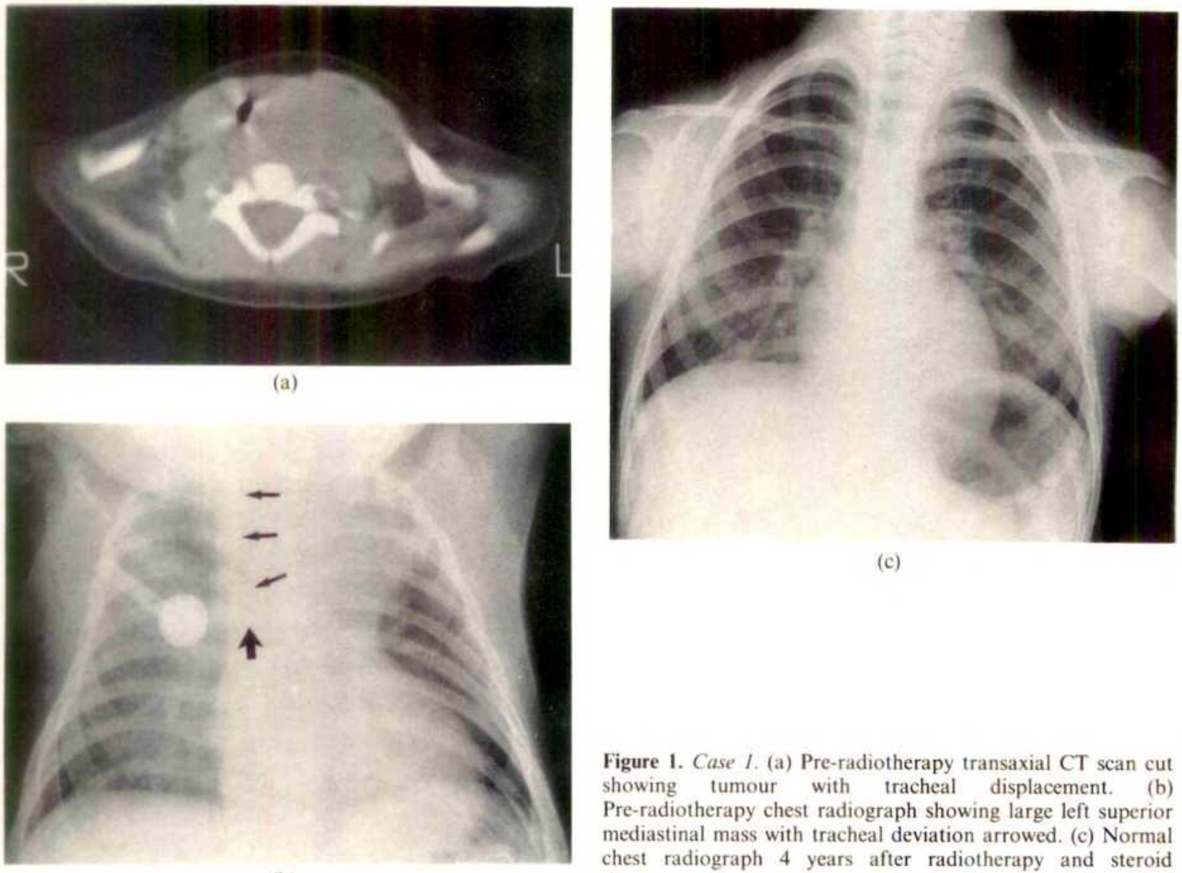
(a)

(b)

(c)

Figure 1. *Case 1.* (a) Pre-radiotherapy transaxial CT scan cut showing tumour with tracheal displacement. (b) Pre-radiotherapy chest radiograph showing large left superior mediastinal mass with tracheal deviation arrowed. (c) Normal chest radiograph 4 years after radiotherapy and steroid therapy.

left vertebral arteries. In view of acutely worsening stridor, embolization of the haemangioma using dura "soup" was performed uneventfully. Subsequent CT scans 6 days later failed to show any resolution of the mass, and the lesion was then biopsied under general anaesthesia. Histology confirmed benign haemangioendothelioma. Because of continued respiratory difficulty, radiotherapy was given. Telecobalt radiotherapy under general anaesthesia was applied to a 9.2 cm × 6.5 cm field over the left anterior chest to a total dose of 1065 cGy in 6 fractions over 7 days. A 3-week course of oral dexamethasone (2 mg/day) was started on the first day of radiotherapy as prophylaxis for laryngeal edema. One week after completion of radiotherapy she was clinically improved and extubated uneventfully. Repeat CT scan demonstrated a marked decrease in size of the lesion and less tracheal compression. One week later she was discharged home. Of note, platelet count was normal throughout her admission. She was followed with serial chest radiographs which showed the mass steadily decreasing in size, becoming undetectable 8 months after radiotherapy (Fig. 1). She remains well with a normal chest radiograph and thyroid function tests 4 years after treatment.

Case 2

This previously well baby boy was noted to have an erythematous lesion on his left ankle at 4 months of age. The lesion grew slowly for 2 months, then suddenly increased in size. Biopsy demonstrated benign haemangioendothelioma. Two months later, the haemangioma was partially excised. Several weeks postoperatively, the haemangiomas progressed to "overrun" the lower leg from the toes circumferentially to the knee. The whole lower leg became taut and uncomfortable. Amputation was considered but radiotherapy recommended initially. Before treatment, the foot was noted to be 1 cm longer, the lower leg 2 cm longer, and the lower leg girth 8 cm larger on the involved left side. Radiography revealed erosive lesions of the left talus and calcaneus with associated soft tissue enlargement. Full blood count revealed a haemoglobin of 10.0 g/dl and platelets of 27×10^9/l consistent with Kasabach–Merritt syndrome; however, there was no evidence of bruising or bleeding. A course of telecobalt radiotherapy was delivered using parallel opposed portals. A total dose of 1840 cGy in 11 fractions over 14 days was given. After 6 fractions, there was a decrease in erythema and discomfort of the leg. A 7-day course of

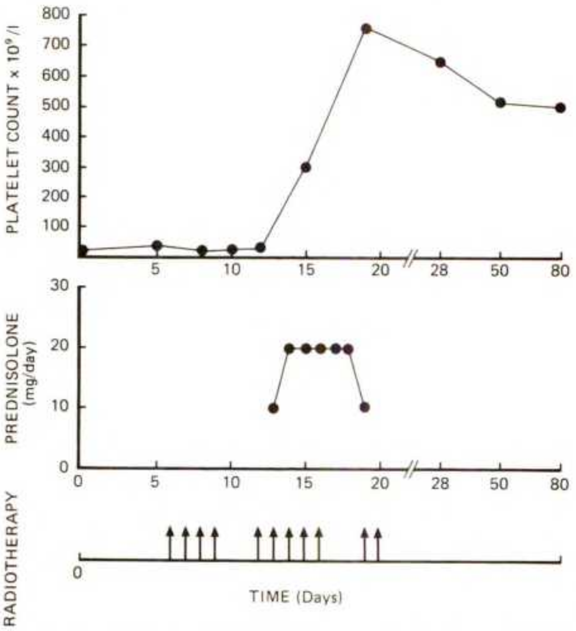

Figure 2. *Case 2.* Plot of platelet count in relation to radiotherapy and prednisolone therapy.

prednisolone (20 mg/day) was started at this time because of persistent thrombocytopenia. Two days later, there was marked clinical improvement, and an increase in platelet count to 305×10^9/l. The platelet count remained normal after cessation of all therapy (Fig. 2). One month after completion of radiotherapy, radiographs showed increased density of the small bones of the left foot. Three months later, there was no evidence of persistent haemangioma. At 5½ years of age, he is completely well with a left lower leg 2.5 cm shorter than the right (Fig. 3).

Case 3

This baby girl was well until 3 weeks of age when a discoloured swelling in the right axilla was noted which "suddenly" increased in size. On admission to hospital, the haemoglobin was 7.5 g/dl, platelets 24×10^9/l and fibrinogen 0.6 g/l, consistent with Kasabach–Merritt syndrome. She deteriorated in hospital with respiratory distress and a more abnormal blood clotting picture (fibrinogen 0.32 g/l, PT 20/12, and PTT 67/37). A chest radiograph demonstrated a large soft tissue mass over the right chest and shoulder, an extensive right pleural effusion, and mediastinal shift to the left. Prednisolone 15–25 mg/day was administered, and she improved

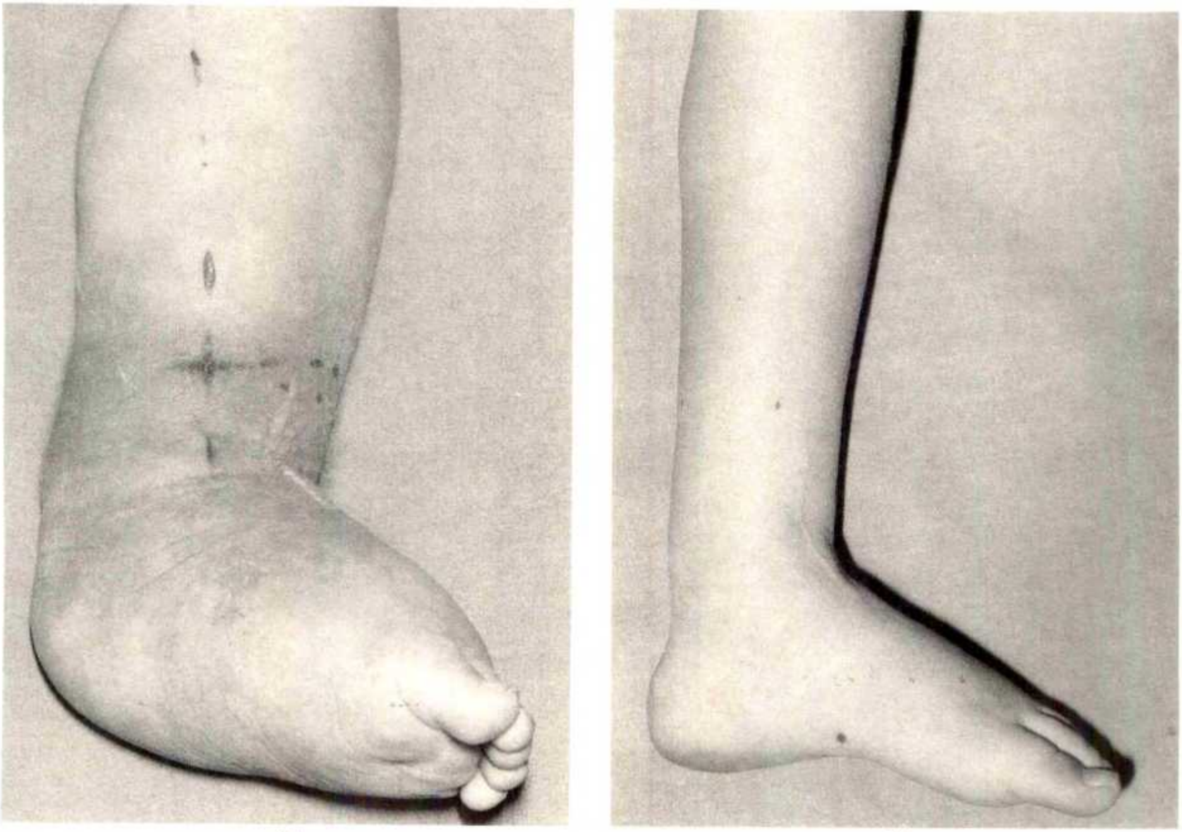
(a) (b)

Figure 3. *Case 2.* Photograph of left lower leg (a) before and (b) 4 years after radiotherapy and steroid therapy.

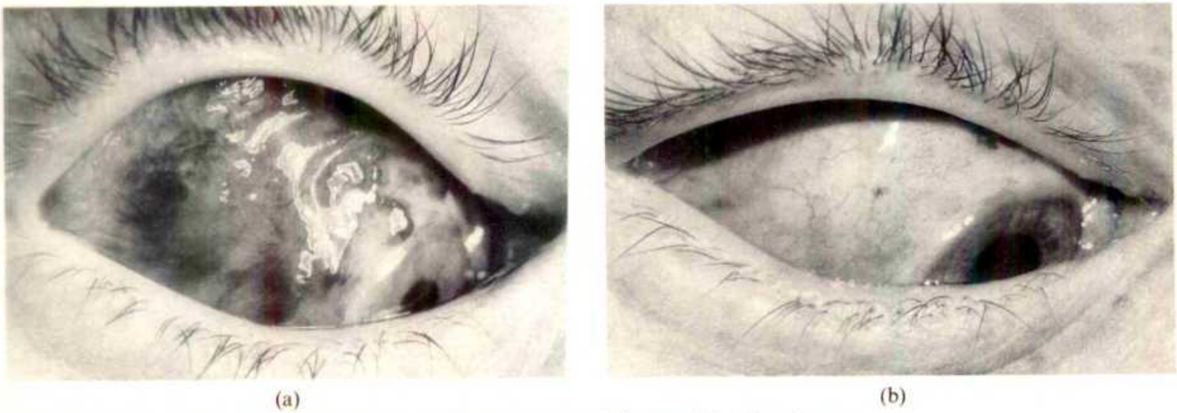

(a) (b)

Figure 4. *Case 4*. Conjunctival component of lymphangioma (a) before and (b) after therapy.

temporarily. Twelve days after admission, arteriography and embolization of the haemangioma with Ivalon particles was carried out, which decreased the size of the lesion and the degree of coagulopathy. Prednisolone was "tailed". Four days after embolization, her condition deteriorated, and a second embolization with Ivalon particles produced a temporary regression of the haemangioma. Five days later, owing to cyanotic episodes and extension of the lesion, further embolization was attempted and again 10 days later. This last embolization was complicated by ischaemia of the right arm and hand resulting in gangrene. The haemangioma had progressed to involve the neck, chest, right arm and abdominal wall, and cause SVCO; and she required intubation and ventilation. Radiotherapy was given: two opposed lateral 6 MV photon portals delivered 1200 cGy in 7 fractions over 13 days to a 11.5 cm × 11.5 cm field over the right chest. Radiotherapy resulted in a temporary improvement in ventilatory requirements, but the haemangioma continued to progress, and the anaemia, thrombocytopenia ($4–25 \times 10^9$/l) and prolongation of coagulation persisted. Two days after completion of radiotherapy she suffered a pulmonary haemorrhage and died. Limited biopsy post-mortem confirmed benign haemangioma.

Case 4

This otherwise healthy female was noted to have a pale swelling over the right side of the forehead and upper orbit at birth. Cavernous haemangioma was suspected, and no treatment was recommended. At 5 years of age the lesion had not regressed so it was surgically excised; histology demonstrated cavernous lymphangioma. She remained well until the age of 11, when she experienced periodic subconjunctival haemorrhages arising from haemangiomatous vessels underlying the right conjunctiva. These vessels were surgically removed at 16 years of age, and post-operatively she suffered an extensive subconjunctival haemorrhage and progression of the orbital lymphangioma. A CT scan demonstrated abnormal soft tissue surrounding the right globe extending intraconally and extraconally. On examination, she had grossly dilated blood vessels over the right lateral bulbar and palpebral conjunctiva, and superficial radiotherapy was given. The right lateral conjunctiva was treated with a double-sided, crescentic strontium β-ray plaque to a total dose of 1800 cGy in 2 fractions 7 days apart. A very good result was achieved with cessation of haemorrhages and atrophy of the conjunctival vessels within 3 months. She remained well without change in the orbital lymphangioma for 19 months, when she presented with subconjunctival haemorrhages due to abnormal vessels of the right medial canthus. In the same manner as before, a β-ray strontium plaque delivered 1800 cGy to the right medial canthus. Cessation of haemorrhages and a good cosmetic result was again obtained. She has been followed with yearly orbital CT scans which have demonstrated no change in the lymphangioma. Three years after her last treatment, she remains well with no recurrent haemorrhages or late radiation effects (Fig. 4).

Case 5

This otherwise healthy female was noted to have a right sided facial asymmetry at birth. A pale swelling was present from the right supraorbital ridge to the angle of the jaw with hypertrophy of soft tissues on the right. Combined haemangioma/lymphangioma was suspected, and no treatment was recommended. The right side of the face slowly increased in size and distortion over the next year and then became static. The right eye involvement resulted in blindness, conjunctival prolapse and repeated episodes of conjunctivitis. At 16 months of age the lesion was biopsied, and histology demonstrated vascular features of haemangioma and connective tissue features of hamartoma ("haemangiomatous hamartoma"). She underwent seven plastic surgery procedures over the next 6 years; however, the haemangioma remained essentially unchanged. At the age of 16, she presented with a cosmetic defect due to abnormal vessels involving the right superior orbit and conjunctiva. A CT scan demonstrated a mass medially

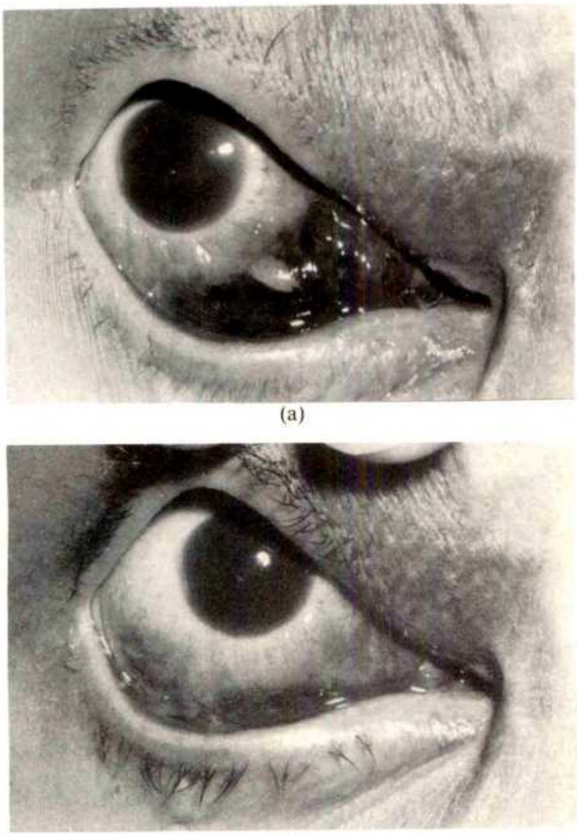

(a)

(b)

Figure 5. *Case 5.* Photograph of conjunctival haemangioma (a) before and (b) after strontium plaque therapy.

in the right orbit extending back beyond the equator of the globe and large vessels inside and outside of the conus. Right carotid angiography demonstrated dilated venous pockets with late filling and no arterio-venous shunting which suggested the angioma was unsuitable for embolization. A course of radiotherapy to the orbit was then given. A wedged pair of 6 MV photon portals was used to deliver a total dose of 3500 cGy in 20 fractions over 28 days to the right orbit. Six weeks after treatment, an excellent regression of the eyelid component of the haemangioma was noted. She proceeded to have β-ray treatment of the conjunctival component with a strontium plaque. A total of 1800 cGy was delivered in 2 fractions a week apart to the abnormal blood vessels of the right medial canthus. Excellent regression occurred (Fig. 5).

Case 6

This 15-year-old male patient with Sturge–Weber syndrome (coexisting port wine stain on the face and angioma of the central nervous system) presented with deteriorating vision in his right eye. He had no history of seizures. On examination, he was found to have a large circumscribed choroidal haemangioma associated with a greater than one-half inferior retinal detachment in the right eye. The retinal detachment was considered to be too expensive to re-attach by laser photocoagulation, therefore external beam radiotherapy was given. The technique used was lens-sparing external beam radiotherapy developed by our department at St Bartholomew's Hospital for the treatment of retinoblastoma (Harnett et al, 1987). Six MV photons were used to deliver a dose at depth of 4000 cGy in 20 fractions over 28 days to the right posterior globe. He completed treatment without complications. Seven weeks after the completion of radiotherapy, the haemangioma was still visible, but the sub-total retinal detachment appeared to have almost completely resolved. Unfortunately, he has been lost to follow-up in the year following radiotherapy treatment.

Case 7

This 12-year-old girl was born with a port wine stain over her right upper eyelid associated with vascular conjunctival and episcleral injection of that eye. However, the child's eyesight had been checked by an optician at age 7 years, and was said to have been good in both eyes. The child presented to an ophthalmologist at the age of 11 years because of decreased vision in the right eye. On examination, there was an upper right facial port wine stain with markedly dilated episcleral and conjunctival vessels. The right corneal diameter was greater than the left. The intraocular pressure was raised in the right eye. Retinoscopy showed +7 dioptres of hypermetropia in the right eye, and fundoscopy showed a serous detachment of the posterior retina including the macula and pericapillary area, with a probable underlying haemangioma. Visual acuity was reduced to counting fingers on the right. The left eye was normal.

The diagnosis was that of a variant of the Sturge–Weber syndrome, including a choroidal haemangioma and serous retinal detachment.

Using the same lens sparing external beam radiotherapy technique as described in Case 6 (above), and arguing from the success in Case 6 that a lower dose might be sufficient, a retinal dose of 1200 cGy was delivered in 8 fractions over 9 days.

Nine months later the retina was flat, the haemangioma smaller and the intra-ocular pressure reduced, but the visual acuity remained at counting fingers. The fluorescein angiograms demonstrate the improvement before and after radiotherapy (Fig. 6).

Case 8

This 17-year-old girl first presented aged 2.5 years with a left supraclavicular mass found to be contiguous with a left upper zone mass on chest radiography. Surgical exploration proved the histological diagnosis of benign thoracic haemolymphangioma but the lesion was unresectable due to envelopment of trachea, oesophagus and great vessels. The left phrenic nerve was sacrificed during the attempted thoracic inlet decompression. The child remained well until re-presenting at age 17 years with a 2-year history of worsening shortness of breath.

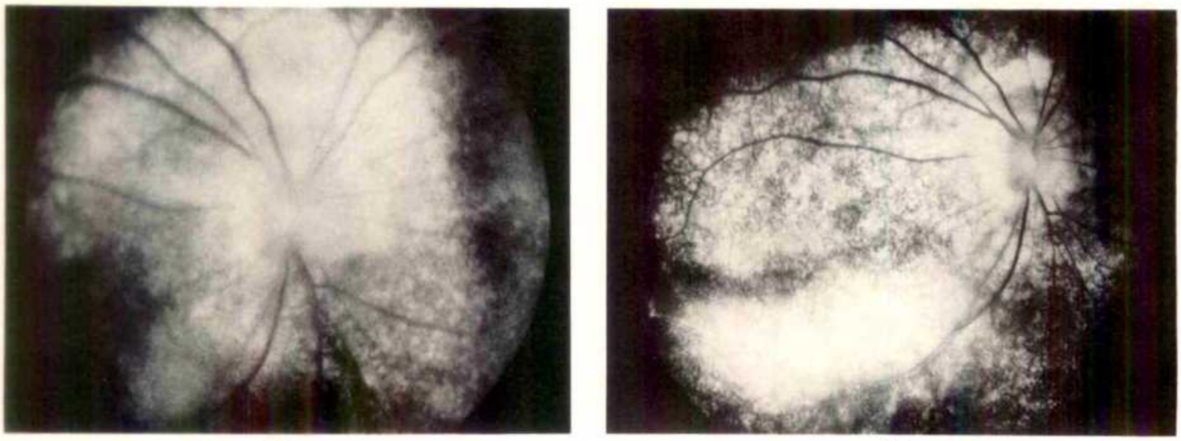
(a) (b)

Figure 6. *Case 7.* Fluorescein angiogram photographs. Both (a) and (b) represent the recirculation phase at 10 minutes following injection. (a) Photograph taken prior to radiotherapy showing clearing of the dye. (b) Photograph taken 6 months after radiotherapy: there is rapid clearing of the dye; the retina has flattened and become re-attached.

On examination, the girl had a marked scoliosis of the upper thoracic spine and poor expansion/aeration of the left chest. There was a hard mass in the left supraclavicular fossa extending into the thoracic inlet. A chest radiograph showed a very large left sided upper mediastinal mass with involvement of thoracic inlet with signs of compression and occupation of much of the upper left thorax. Scoliosis and adjacent rib deformities were demonstrated.

Through opposed anterior and posterior 6 MV X-ray portals the whole lesion received 3000 cGy (30 Gy) in 18 fractions over 24 days before midline structures were excluded to deliver a further 1000 cGy mid-plane dose in 5 fractions by a similar technique to the left upper chest.

One year later the patient is much less dyspnoeic and the palpable supraclavicular mass and radiological mass in the left chest are both much diminished.

Discussion

Historically, radiotherapy was the most popular method used to treat strawberry/cavernous haemangiomas. This was because haemangiomas are very radiosensitive, more so the earlier in life they are treated (Paterson & Tod, 1939; Strandquist, 1939; Ward & Covington, 1940; Thomas & Fjeldborg, 1953). Radiotherapy prior to 1960 was administered by means of radium/radon in plaques, moulds or glass capsules applied to the skin, implantation of radioactive seeds or needles, and application of low voltage X-rays (6–140 kV). Commonly, a combination of the above techniques was used to treat a single haemangioma.

Approximately 85% of haemangiomas treated with combined modality radiotherapy prior to 1960 completely resolved and 15% showed improvement. Residual haemangioma was associated with cavernous nature, larger lesions, and later onset of treatment (Ward & Covington, 1940; Apthomas, 1942). Although infrequently reported, some haemangiomas were resistant to irradiation even when treated early in life (Thomas & Fjeldborg, 1953). In addition, 6–15% of patients were left with scarring of the treated skin (sclerosis, atrophy, increased pigmentation, telangectasias). Permanent loss of hair from scalp, eyebrows and eyelashes was also reported (Ward & Covington, 1940; Pendergrass et al, 1948).

Superficial and megavoltage photons, electrons and radioactive implants are all used in the current radiotherapy treatment of complicated haemangiomas. Modern radiotherapists attempt to use the lowest possible dose of radiation necessary to control symptoms and induce regression of the lesion. For example, childhood hepatic haemangiomas, which can be life-threatening when associated with high-output cardiac failure, quickly regress in response to total radiotherapy doses as low as 400 cGy (Rotman, 1980). In addition to megavoltage photons, superficial electrons have been used successfully to treat these lesions (Corbella et al, 1983).

Subglottic haemangiomas necessitate treatment because of airway obstruction, and radiotherapy doses of 450 cGy to 1800 cGy provide prompt relief of stridor and slower resolution of the haemangioma over weeks to months (Holborow, 1958; Bek et al, 1980). Small initial fraction sizes (40–100 cGy) are used to treat subglottic lesions in the absence of intubation or tracheostomy to reduce the incidence of laryngeal swelling and respiratory distress that can occur with the initiation of radiotherapy (Ferguson & Flake, 1961).

Haemangiomas of the eyelids and conjunctiva have been successfully treated with superficial β-rays (1500 cGy) without causing damage to the globe or lens of the eye (Iliev & Chilova-Atanassova, 1985). The early treatment of these lesions is often indicated to prevent deprivation-amblyopia and other ocular complications (Plesner-Rasmussen et al, 1983).

Cavernous haemangiomas with thrombocytopenia (Kasabach–Merritt syndrome) respond to total radiotherapy doses of 700 cGy to 2000 cGy with regression of the haemangioma and coincident or delayed resolution of thrombocytopenia (Atkins et al, 1963; Yoshikawa et al, 1987). For example, platelet counts increased rapidly following radiation therapy in the cases reported by Southard and Scherz (Southard et al, 1951; Sherz et al, 1958). Conversely, Atkins reported two cases of Kasabach–Merritt syndrome in which radiotherapy produced prompt cessation of bleeding, although the patients remained thrombocytopenic for several months after the haemangioma apparently resolved (Atkins et al, 1963).

In addition to radiotherapy, steroid therapy plays a major role in the current treatment of childhod haemangiomas. Fost and Easterly first reported dramatic responses of strawberry/cavernous haemangiomas to oral prednisone in 1968. Many authors have since confirmed that prednisone (10–30 mg/day) induces regression of skin haemangiomas in up to 90% of cases after 2–3 weeks of therapy (Brown et al, 1972; Edgerton, 1976). The mechanism of action of steroids on regression of haemangiomas is not known.

Unfortunately, haemangiomas frequently progress when steroids are withdrawn, necessitating multiple courses of therapy (Fost & Esterly, 1968; Brown et al, 1972; Edgerton, 1976).

The excellent steroid response rate reported for skin haemangiomas has not been reported for subglottic, hepatic and Kasabach–Merritt haemangiomas.

The eight cases treated at this hospital by radiotherapy in the last 10 years illustrate important issues concerning the current treatment of childhood haemangiomas. Case 1 presented with stridor typical of subglottic haemangioma, and required urgent treatment for breathing difficulty. The total dose of 1065 cGy and the time course of resolution of the haemangioma is comparable to other cases reported in the literature.

Case 2 illustrates the phenomenon of "haemangiomatous gigantism" in which increased blood flow in a limb haemangioma results in overgrowth of the extremity. The main risk associated with irradiating the limb of an infant is growth retardation. It has generally been assumed that the radioresponsiveness of growing bones changes with aging. However, Gonzalez and Breur in 1983 found that, when the growth remaining after irradiation is taken into account, no differences in radioresponsiveness seem to exist with aging, the radiation dose being the major factor. The patient in Case 2 received 1840 cGy; the fact that the left leg was longer before treatment improved the final result, although given the same situation again a smaller radiotherapy dose would be considered, or a split course prescribed.

Case 2 is also an example of Kasabach–Merritt syndrome in which thrombocytopenia was present. The patient was treated with both radiotherapy and prednisolone simultaneously, so it is difficult to determine the effect of each on the thrombocytopenia. However, the time course of the increase in platelets 48 hours after prednisolone was started suggests steroids were responsible. The radiotherapy may have contributed to the maintenance of a normal platelet count after the short course of prednisolone was discontinued. The reason for the overshoot in platelet count above normal limits is unclear.

In contrast to Case 2, Case 3 represents a very aggressive variant of Kasabach–Merritt syndrome in which thrombocytopenia and consumption of fibrinogen caused a bleeding diathesis. The relentless growth of the haemangioma and the associated blood clotting abnormalities were resistant to prednisone therapy (10–25 mg/day for 21 days), embolization and radiotherapy. Unfortunately, steroid failures are well described in Kasabach–Merritt syndrome, and this appears to have been one such example.

Radiotherapy was also ineffective in shrinking the haemangioma. This is surprising because lesions treated in their growing stages, as this one was, are generally regarded as the most radiosensitive (Hodges et al, 1941). However, radiotherapy was given late in the clinical course to only a limited area of the haemangioma present at that time. Thoms and Fjeldborg in 1953 reported one case of radioresistant cavernous haemangioma despite early institution of treatment. A rare case of radioresistant haemangioma with benign histology and apparent malignant metastases was reported in 1936 by Robinson and Castleman.

Cases 4 and 5 are examples of orbital haemangiomas and Cases 6 and 7 examples of intraocular haemangiomas all successfully treated with radiotherapy. In Cases 4 and 5, abnormal vessels of the conjunctiva were treated with β rays (total dose 1800 cGy) delivered by a strontium plaque. Iliev used the same technique with excellent results (average dose 1500 cGy), and noted no late irradiation damage to the eye up to 7 years after treatment. Beta rays are ideal for treatment of superficial haemangiomas near radiosensitive organs because they penetrate only 1–3 millimetres. Strontium plaques are particularly useful for treatment of conjunctival lesions because they can be applied directly to the anaesthetized eye requiring only seconds per application. Intraocular lesions (Cases 6 and 7) are amenable to our lens-sparing external beam technique.

Cases 4 and 6 received relatively high external beam radiotherapy doses because of the expected more radioresistant nature of the angiomas. The haemangioma in Case 4 had a connective tissue component histologically which is associated with increased resistance to radiation (Ward & Covington, 1940). In addition, the patient was treated very late in childhood when haemangiomas are regarded to be less responsive to radiotherapy. The haemangioma in Case 5 (Sturge–Weber syndrome) was associated with a port wine stain which is known to be a radioresistant type of angioma (Ward & Covington, 1940). Therefore, we expected the choroidal haemangioma to exhibit a similar radioresistance, and treated to a higher dose. In fact, the good response led to the lower dose prescription which also proved successful in Case 7. In both Cases 6 and 7 the retina re-attached.

Case 8 is of interest as this child represents a considerably older child who nevertheless obtained an excellent response to radiotherapy to a longstanding thoracic haemolymphangioma. It was again argued that such lesions in older patients require higher radiation doses.

Before concluding on the role of radiotherapy in the current management of childhood haemangiomas, it is important to recognize the risks involved in using ionizing radiation to treat benign disease. The thousands of children routinely treated with radium and low voltage X-ray therapy for skin haemangiomas prior to 1960 have now reached adulthood, and the late effects of radiotherapy in childhood have been revealed. Breast hypoplasia, growth retardation and, most important, radiation-induced malignancies have all been reported. Furst and his colleagues studied cancer incidence in 18 000 patients treated with radiotherapy for haemangiomas in childhood, and found a significantly increased risk of breast cancer, brain tumours, papillary thyroid cancer and bone tumours (Furst et al, 1988). In view of the potential sequelae of ionizing radiation, radiotherapy has an important but limited role in the treatment of childhood haemangiomas. For example, radiotherapy is no longer appropriate for treatment of skin haemangiomas causing cosmetic problems due to rapid growth. A 2–3 week course of oral prednisone is the treatment of choice in those cases justifying therapeutic intervention.

In our experience, superficial β rays and lens-sparing external beam radiotherapy are useful in the treatment of certain ocular haemangiomas, producing significant benefit and incurring little risk (Plowman & Harnett, 1986). However, the major indication for use of radiotherapy in childhood haemangiomas is the treatment of complicated cavernous lesions posing a threat to function or life in which alternative therapies have failed.

In cases of complicated cavernous haemangiomas, the alternative therapies that must be considered prior to radiotherapy are steroid therapy, surgical excision and possibly embolization. Although the steroid response rate is not high in these haemangiomas, an initial trial of prednisone (10–25 mg/day) is advisable. However, radiotherapy should not be delayed more than a few weeks if a rapid steroid response is not forthcoming. In the case of Kasabach–Merritt syndrome, there is a rationale for combined steroid therapy and radiotherapy as they each appear to have a different mechanism of resolution of thrombocytopenia. Surgical excision of complicated haemangiomas may be feasible if prednisone has first induced regression, although the tumour is often inoperable. Our experience with embolization of cavernous haemangiomas is limited, but problems may be encountered (Case 3).

When radiotherapy is used to treat complicated cavernous haemangiomas, the lowest possible dose producing control of symptoms should be used (and the doses prescribed to several of the cases reported here were higher than we would currently practice), and the dose to adjacent radiosensitive structures minimized. In the Kasabach–Merritt syndrome in particular, it is important to use clinical status of the patient rather than platelet count as an index of the adequate dose of radiotherapy. In conclusion, radiotherapy used appropriately by experienced radiotherapists is a valuable technique in the current management of serious childhood haemangiomas resistant to other therapy.

Acknowledgments

We thank Miss T. Cocks for typing the manuscript and Mr D. Doughty for advice. We thank the Medical Illustration Department and Medical Photography Department of St Bartholomew's Hospital and the Medical Photography Department of Great Ormond Street Hospital for Sick Children for the preparation of photographs and diagrams.

References

APTHOMAS, I., 1942. Contact X-ray treatment of cavernous angioma in children. *British Journal of Radiology, 15*, 43–47.

ATKINS, H. L., WOLFF, J. A. & SITARZ, A., 1963. Giant hemangioma in infancy with secondary thrombocytopenic purpura. *American Journal of Roentgenology, 89*, 1062–1066.

BEK, V., ABRAHAMOVA, J., KOUTECKY, J., KOLIHOVA, E. & FAJSTAVR, J., 1980. Perinatal subglottic and hepatic hemangiomas as potential emergencies: effect of radiotherapy. *Neoplasma, 27*, 337–344.

BROWN, S. H., NEERHOUT, R. C. & FONKALSRUD, E. W., 1972. Prednisone therapy in the management of large hemangiomas in infants and children. *Surgery, 71*, 168–173.

CORBELLA, F., ARICO, M., PODESTA, A. F., VILLA, A., BELUFFI, G. & BIANCHI, E., 1983. Infantile hepatic hemangioendothelioma treated by radiotherapy. *Pediatric Radiology, 13*, 297–300.

DARGEON, H. W., 1960. In *Tumors of Childhood* (Paul B. Hoeber, Inc: Medical Division of Harper & Brothers), p. 368.

DEHNER, L. P. & ISHAK, K. G., 1971. Vascular tumors of the liver in infants and children. A study of 30 cases and review of the literature. *Archives of Pathology, 92*, 101.

EDGERTON, M. T., 1976. The treatment of hemangiomas with special reference to the role of steroid therapy. *Annals of Surgery, 183*, 517–532.

FERGUSON, C. F. & FLAKE, C. G., 1961. Subglottic hemangioma as a cause of respiratory obstruction in infants. *Annals of Otology, Rhinology, and Laryngology, 70*, 1095–1112.

FOST, N. C. & ESTERLY, N. B., 1968. Successful treatment of juvenile hemangiomas with prednisone. *Pediatrics, 72*, 351–357.

FURST, C. J., LUNDELL, M., HOLM, L. & SILFVERSWARD, C., 1988. Cancer incidence after radiotherapy for skin hemangioma: a retrospective cohort study in Sweden. *Journal of the National Cancer Institute, 80*, 1387–1392.

GONZALEZ, D. G. & BREUR, K., 1983. Clinical data from irradiated growing long bones in children. *International Journal of Radiation Oncology, Biology, Physics, 9*, 841–846.

HARNETT, A. N., HUNGERFORD, J. L., LAMBERT, G. D., HIRST, A., DARLISON, R., HART, B. L., TRODD, T. C. & PLOWMAN, P. N., 1987. Improved external beam radiotherapy for the treatment of retinoblastoma. *British Journal of Radiology, 60*, 753–760.

HODGES, F. M., SNEAD, L. O. & BERGER, R. A., 1941. Roentgen therapy of hemangiomata. *Radiology, 36*, 700–705.

HOLBOROW, C. A., 1958. Subglottic hemangiomas: two infants with laryngeal stridor. *Archives of Disease in Childhood, 33,* 210–211.

ILIEV, E. & CHILOVA-ATANASSOVA, B., 1985. Hemangioma on the eyelids and ocular conjunctiva. *Folia Medica, 27,* 27–34.

LISTER, W. A., 1938. The natural history of strawberry naevi. *Lancet, i,* 1429–1434.

PATERSON, R. & TOD, M. C., 1939. The radium treatment of angioma in children. *American Journal of Roentgenology, 42,* 726–730.

PENDERGRASS, E. P., KATTERJOHN, J. C. & BUTCHART, J. B., 1948. Some considerations in the treatment of hemangiomas in infants and young children. *American Journal of Roentgenology, 60,* 182–192.

PLESNER-RASMUSSEN, H., MARUSHAK, D. & GOLDSCHMIDT, E., 1983. Capillary haemangiomas of the eyelids and orbit. *Acta Ophthalmologica, 61,* 645–654.

PLOWMAN, P. N. & HARNETT, A. N., 1986. Radiotherapy in benign orbital disease. I: Complicated ocular angiomas. *British Journal of Ophthalmology, 72,* 286–288.

ROBINSON, J. M. & CASTLEMAN, B., 1936. Benign metastisizing hemangioma. *Annals of Surgery, 104,* 453–459.

ROTMAN, M., JOHN, M., STOWE, S. & INAMDAR, S., 1980. Radiation treatment of pediatric hepatic hemangiomatosis and coexisting cardiac failure. *New England Journal of Medicine, 302,* 852.

SCHERZ, R. G., LOURO, J. M. & GEPPERT, L. J., 1958. Giant hemangioendothelioma with associated thrombocytopenia. *Journal of Pediatrics, 52,* 212–216.

SOUTHARD, S. C., DESANCTIS, A. G. & WALDRON, R. J., 1951. Hemangioma associated with thrombocytopenic purpura. *Journal of Pediatrics, 38,* 732–737.

STRANDQUIST, M., 1939. Radium treatment of cutaneous cavernous haemangiomas using surface application of radium tubes in glass capsules. *Acta Radiologica, 20,* 185–211.

THOMS, J. & FJELDBORG, N., 1953. Radiation treatment of hemangiomas. *Acta Radiologica, 40,* 39–53.

WARD, G. E. & COVINGTON, E. E., 1940. Hemangiomas of the skin. *Journal of the American Medical Association, 114,* 2069–2075.

YOSHIKAWA, M., HAYASHI, T., SATO, T., AKIBA, T., WATARAI, J. & NAKAMURA, C., 1987. A case of pericardial hemangioma with consumption coagulopathy cured by radiotherapy. *Pediatric Radiology, 17,* 149–150.

1991, *The British Journal of Radiology*, *64*, 270–271

Technical note

An iridium-192 applicator for the treatment of stomal recurrence following tracheostomy for subglottic carcinoma

By R. D. Jones, MA, MRCP, FRCR, *D. G. Clarkson, BSc, MIEE, MInstP, R. P. Symonds, MD, FRCP, FRCR and S. G. McNee, PhD, MIPSM

Beatson Oncology Centre and *West of Scotland Health Board, Department of Clinical Physics and Bioengineering, Western Infirmary, Glasgow G11 6NT, UK

(*Received August 1990*)

Keywords: Stomal recurrence, Subglottic carcinoma, Tracheostomy

A 45-year-old man presented with a left-sided posterior triangle neck node and a history of sore throats for a year. At the time of presentation he had no other symptoms. An examination under anaesthetic was undertaken and revealed no abnormality of the larynx or pharynx but a suspicious area was seen in the nasopharynx. Biopsy of this region, however, was normal. Histology of the nodes dissected from the left side of the neck revealed anaplastic carcinoma and the appearances were in keeping with a primary from the nasopharynx or bronchus. Tonsillar biopsy was normal.

On clinical judgment the nasopharynx was thought to be the most likely primary site and so the patient was treated with radical radiotherapy to the neck and nasopharynx. The neck was treated with an anterior beam of 4 MV photons from a linear accelerator with midline shielding (2 cm wide, 6 cm thick) to reduce the dose to the spinal cord (Ho, 1978).

He remained well with no evidence of disease until 6 months following completion of radiotherapy when he developed hoarseness. Endoscopy at the time revealed a subglottic tumour which extended into the trachea, and he underwent laryngectomy for this. The excised specimen showed doubtful margins at the lower border. He developed evidence of stomal recurrence 1 month later.

Because of the previous irradiation the scope for further radiotherapy was limited. A technique was developed using radioactive iridium wires mounted on a tracheostomy tube to deliver a high dose to the stomal area while minimizing the radiation dose to the previously treated normal tissues.

The problem presented was to produce a device which would be tolerated by the patient and, most importantly, ensure that the radioactive wires could not be dislodged during treatment, with subsequent problems of retrieval from bronchus or lung. The largest tracheostomy tube feasible for this patient, a Shiley cuffless type size 8 (8CFS), was used. The normal insert was replaced by a size 4 insert onto which were attached eight iridium 192 wires varying in length from 47 to 53 mm and 0.3 mm in diameter (Amersham International, type ICW 1060), equally spaced around the outside of the insert (Fig. 1). This was achieved by bonding nylon tubing (Amersham International. type N253) along the length of the insert. The proximal ends of the nylon tubes were effectively closed by abutment with the collar of the insert. Iridium wires were cut to length and loaded into the distal ends which were then heat sealed using a soldering iron with a fine tip. Finally, adhesive heat-shrink sleeving was used in three places to keep the nylon tubes in place during use, the distal sleeve overlapping the nylon tube ends as an additional sealing measure. Two identical inserts were made so that if one had to be removed for cleaning it could be replaced by the other, thereby maintaining the intended dose schedule. The inserts were inspected for damage and cleaned between use in a protected radioiostope handling bench. Holding the insert under running tap water and then

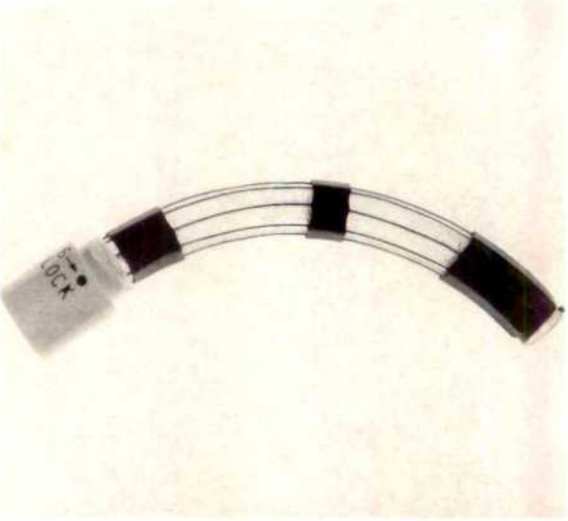

Figure 1. Photograph of the tracheostomy tube insert loaded with iridium.

Address correspondence to R. D. Jones, Beatson Oncology Centre, Western Infirmary, Glasgow G11 6NT, UK.

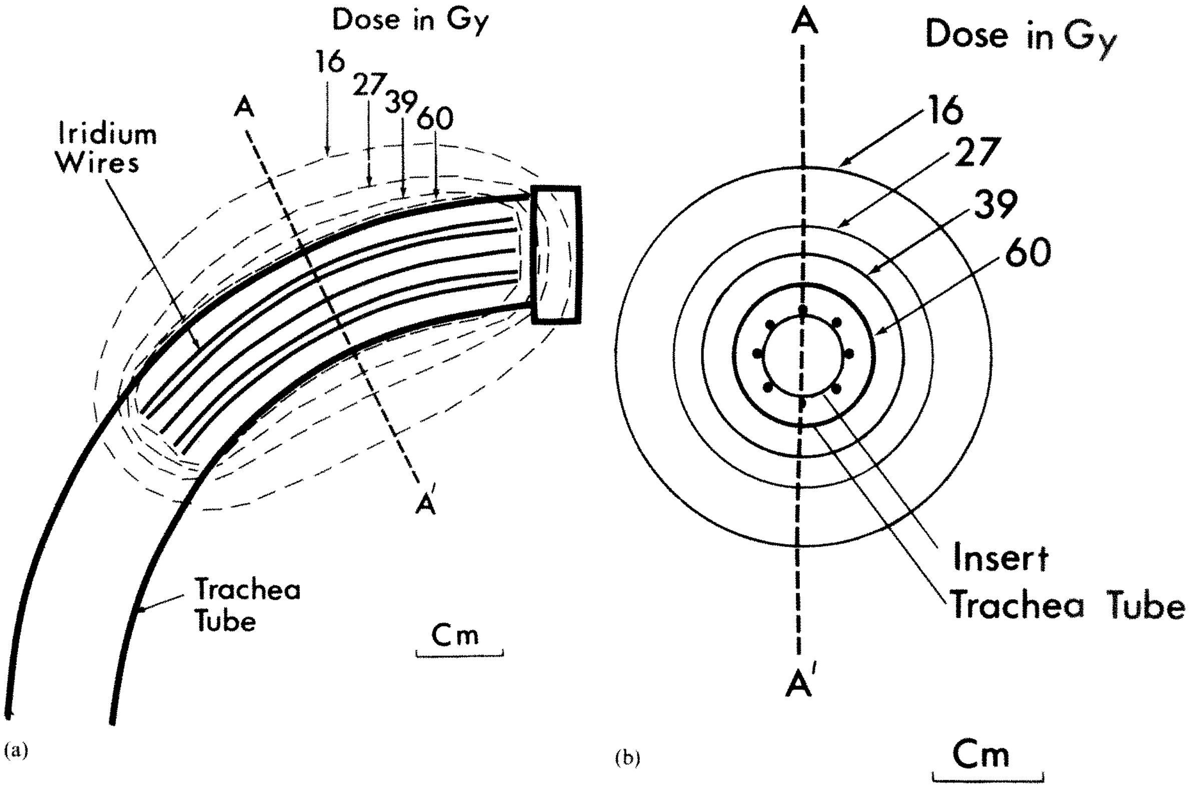

Figure 2. Dose contours: (a) longitudinal section, (b) cross-section.

rinsing it in saline were sufficient for cleaning. No damage was evident on either insert.

Dose rates were computed for tranverse and longitudinal planes using the supplied source of 0.234 μGy/h mm at 1 m. Doses of 60 Gy at the outer surface of the tracheostomy tube, 27 Gy at 5 mm depth in tissue and 16 Gy at 10 mm depth were achieved in an irradiation time of 64 hours (Fig. 2). Irradiation took place for about 9 hours per day on seven consecutive days. The patient himself was able to replace and remove the insert at the start and end of each day's treatment and at any interruption of treatment such as for visitors. The insert was stored and transported in a lead container on a wheeled trolley. This scheme minimized the doses to the ward staff.

The treatment was well tolerated and there were no acute problems.

By 1 month there was complete regression of the 2 cm ulcerated recurrence. Two months following the iridium therapy he developed neck nodes which were judged to be inoperable. He was treated with chemotherapy in the form of carboplatin and subsequently methotrexate, with some stabilization of disease. He died 14 months following the development of recurrent nodal disease but at that time the stomal disease remained controlled.

Provided radiation protection requirements are met, this technique for treatment of stomal recurrence using radioactive iridium is feasible and could be used as an alternative to or in combination with other modes of treatment. It may be particularly valuable in cases such as this where the patient has received previous radiotherapy.

Reference

Ho, J. H. C., 1978. An epidemiologic and clinical study of nasopharyngeal carcinoma. *International Journal of Radiation Oncology, Biology, Physics*, *4*, 181–198.

1991, *The British Journal of Radiology*, *64*, 272–275

Case reports

Hepatocellular carcinoma associated with polyarteritis nodosa with symptoms appearing after intra-arterial chemotherapy

By Kazuo Minakuchi, MD, Keiji Fujimoto, MD, Keiji Takada, MD, Sumio Takashima, MD, Kenji Nakamura, MD and *Takehiro Mitsuhashi, MD

Department of Radiology and *Second Department of Pathology, Osaka City University Medical School,
1-5-7 Asahimachi, Abeno-ku, Osaka 545, Japan

(*Received April 1990 and in revised form October 1990*)

Keywords: Hepatocellular carcinoma, Polyarteritis nodosa, Intra-arterial chemotherapy, Aneurysm, Angiography

Case report

A 57-year-old man presented with pain in his right hypochondrium. There was no history of blood transfusions, prolonged fever, or pain of the muscles or joints. The patient reported that he had never taken methamphetamine and had not taken sulphonamides or penicillins for a long time. The physical examination revealed a hard elastic mass in the right hypochondrium. Laboratory tests (Table I) showed the presence of a chronic liver disorder, but hepatitis B surface antigen and antibody were not detected. Serum α-fetoprotein (AFP) was 14 100 ng/ml. An ultrasound examination of the liver showed a large mass hypoechoic in parts and hyperechoic in other parts in the right lobe. Enhanced computed tomography (CT) revealed a large mass with a diameter of about 6 cm and a low density region in the anterior segment of the right lobe. There were multiple low density nodules throughout the right lobe and the medial segment of the left lobe, and a tumour thrombus in the portal vein and superior mesenteric vein. There was dilatation of intrahepatic bile ducts in other slices of the enhanced CT, and ascites elsewhere (Fig. 1). A first angiogram showed several aneurysms in the intrahepatic arteries, an encapsulated tumour stain with a diameter of about 6 cm in the right lobe, and multiple small tumour stains (Fig. 2). We diagnosed this patient as having advanced hepatocellular carcinoma (HCC) from the results of the imaging studies and because of the high AFP.

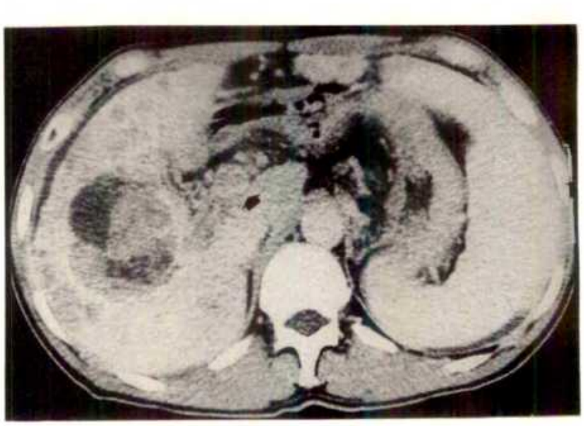

Figure 1. Enhanced CT scan taken before the first intra-arterial infusion of anti-cancer drugs. Large masses with a mosaic pattern and surrounding multiple small low density nodules are seen in the liver. A tumour thrombus (arrow) is visible in the portal vein.

Hepatic arterial embolization was not indicated, even though the left branches and the posterior inferior branches of the portal vein showed cavernous transformation, because there was a tumour thrombus in the portal vein. We performed intra-arterial chemotherapy with 20 mg of doxorubicin hydrochloride (Adriacin) and 10 mg of mitomycin C (MMC).

Table I. Laboratory data on admission

Haematology		Blood chemistry	
WBC	7200/mm^3	TP	7.7 g/dl
RBC	532×10^4/mm^3	TTT	> 8.0 U
Hb	14.6 g/dl	ZTT	> 20 U
Ht	44.7%	AAT	61 IU
Platelets	17.8×10^4/mm^3	ALT	37 IU
ESR	21 mm/h, 42 mm/2 h	CHE	0.50 ΔpH
Serology		Tumour markers	
HB$_s$ Ag	—	AFP	14 100 ng/ml
HB$_s$ Ab	—	CEA	0.7 ng/ml

About 1 week after this first chemotherapy, a slight intermittent fever of about 37.5°C appeared every evening, and a hard slightly sore subcutaneous nodule of 0.5 cm × 1 cm on the right forearm was reported by the patient. Similar nodules appeared in both arms thereafter. AFP decreased to 3130 ng/ml 14 days after the first chemotherapy. Enhanced CT done on day 17 showed that a solid portion of the main tumour was now of low density, and that the surrounding multiple nodules had become of lower density than before. The portal vein had recanalized as a result of the reduction in size of the tumour thrombus (Fig. 3).

A second session of intra-arterial chemotherapy was considered necessary. The same drugs and doses were used, and the injection was done 24 days after the first angiography. The patient developed an intermittent fever of 38.6°C or more every evening starting 10 days after the second angiography, and his temperature did not decrease even with administration of antibiotics and antifebriles. One of the subcutaneous nodules of the right forearm was resected, because both forearms had become

---

*Author for correspondence.

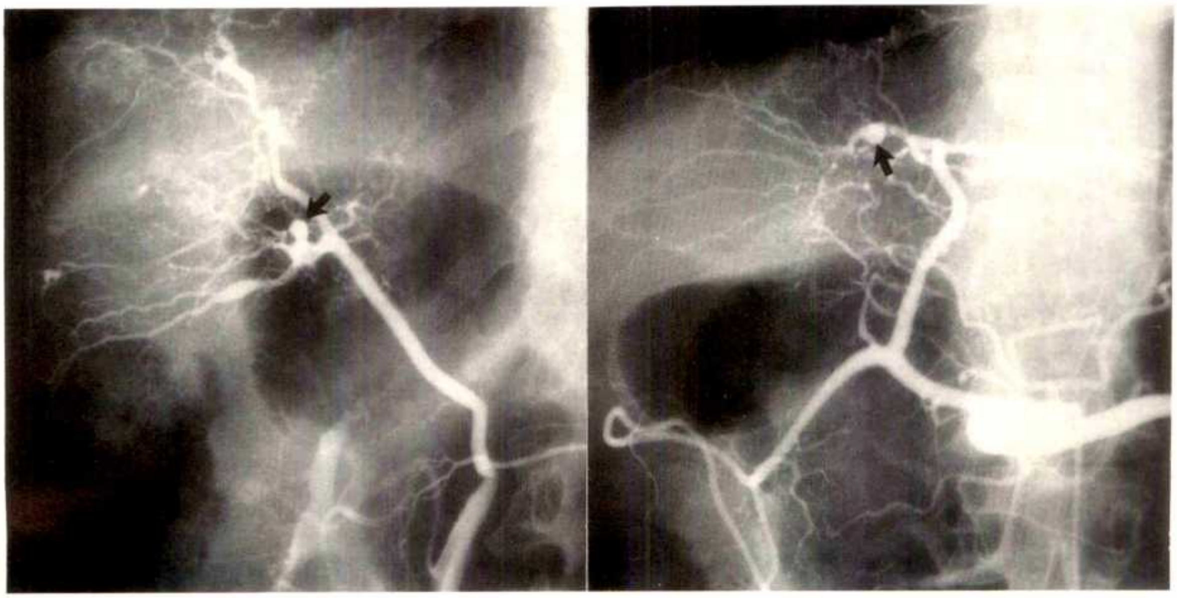

Figure 2. Arterial phase of angiography before the first chemotherapy. Aneurysms (arrows) are seen in the right hepatic artery with anomalous origin (right) and the left hepatic artery (left). Dilated and narrowed segments are visible in the arteries of the right lobe, and there is neovascularity.

swollen after the second chemotherapy and the number of subcutaneous nodules continued to increase gradually. The patient was diagnosed as having polyarteritis nodosa (PAN) associated with HCC, because the resected specimen showed exudation of serum protein and degeneration, and epithelioid cells existed in the intima and the media of the subcutaneous arterioles (Fig. 4). AFP was 19.4 ng/ml after 37 days of the second chemotherapy, and decreased to 5 ng/ml or less the day after resection of one nodule.

The patient was discharged when the tumour remained a low density mass, AFP stayed below 5 ng/ml, and the symptoms of PAN disappeared with antihistamine and steroid hormone treatment. He was hospitalized for follow-up about 8 months from discharge. At the second admission, AFP was less than 5 ng/ml and CT gave the same findings as before. Angiography revealed no aneurysms or tumour stain, but dilated or narrowed segments of the intrahepatic arteries were seen, as were decreased numbers of peripheral hepatic arterial branches. There was no obstruction of the portal vein, and the posterior inferior branch of the right first portal branch could now be seen, as a result of collateral circulation, in spite of the obstruction of the right first branch (Fig. 5). There were no aneurysms in the mesenteric arteries, splenic arteries, or both renal arteries. We performed a biopsy of the liver because imaging studies did not show whether the tumour was viable. The biopsy specimen was a necrotic mass without viable

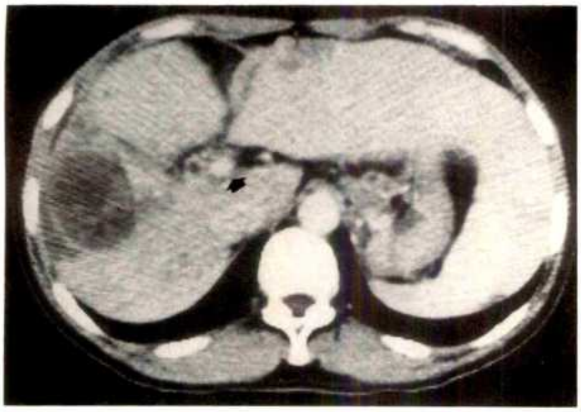

Figure 3. Enhanced CT scan 17 days after the first chemotherapy. The solid portions of the main tumour and surrounding multiple nodules have become lower in density, and the portal vein (arrow) can be seen by recanalization that resulted from reduction in the size of the tumour thrombus.

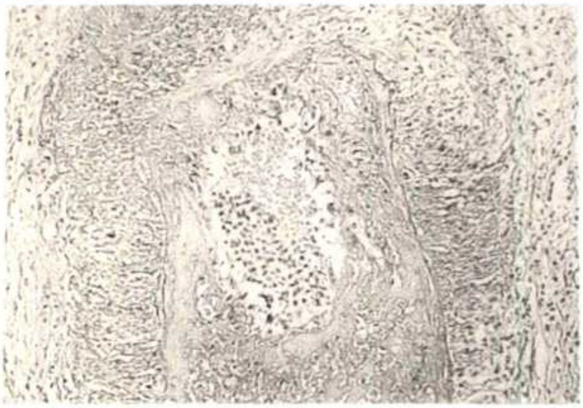

Figure 4. Histological findings of a subcutaneous nodule. This specimen shows exudation of serum protein, degeneration, and existence of epithelioid cells in the intima and the media of the subcutaneous arteriole.

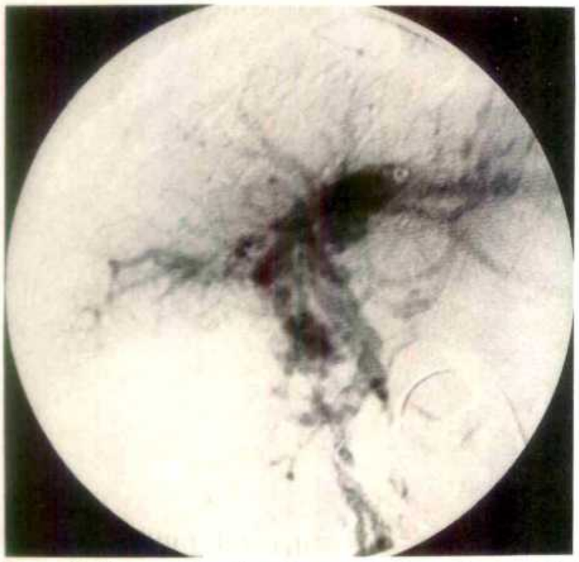

Figure 5. Portography after the second chemotherapy. The portal vein is not obstructed, and the posterior inferior branch of the right portal branch is visible because of collateral circulation, although the right first branch is obstructed.

tumour tissue. The patient has no symptoms of tumour recurrence at present, 25 months after the first admission.

Discussion

The aetiology of PAN is unknown, like that of the other angitis syndromes. Hepatitis B virus is particularly likely to be a cause (McMahon et al, 1989). However, the HCC of this patient did not seem to be caused by hepatitis B. Other possible causes, methamphetamine, sulphonamides, and penicillins, were not factors here.

PAN is a necrotizing angitis that invades small or medium-sized arteries throughout the body. The arterioles show exfoliation of the intima, oedema, and dysarrangement of the smooth muscle in the media, and develop perivascular oedema and fibrosis in the acute phase. Fibrinoid necrosis takes place, and disappearance of the internal and external elastic lamina occurs gradually in the arterioles. Stenosis of the vascular space and aneurysms finally form. As a rule, old and new lesions of the arterioles are found in the same place. PAN is well known for its characteristic and pathognomonic images by angiography, which shows much pathological change, including irregularities and microaneurysms of arteries supplying the central nervous system, kidney, heart, digestive system, and liver. Microaneurysms in the abdominal organs are found in 58% of patients with PAN examined in this way. Microaneurysms are most common in the renal circulation (93%), and are much less common in the coeliac circulation (24%). Mesenteric aneurysms are seen in only 14% of the patients examined. Generally speaking, angiographic abnormalities are correlated with clinical signs and symptoms (Tavers et al, 1979; Ewald et al, 1987). PAN seldom occurs as a primary liver disease affecting only that organ. There is danger of hepatic infarction and rupture of aneurysms, as arterial involvement of the liver is reported for 42–71% of subjects studied post-mortem. Angiography may have prognostic and therapeutic meaning in PAN, because it reveals hepatic arterial disorders clearly (Ahmed et al, 1986; Alleman et al, 1986; Haratake et al, 1988).

There has been one case report of PAN associated with nodular regenerative hyperplasia of the liver (Nakanuma et al, 1984). We have not found reports of PAN associated with HCC.

Stenosis, obstruction, and aneurysmal dilatation of the arteries sometimes result from arterial endothelial damage caused by intra-arterial infusion of anti-cancer drugs (Forsberg et al, 1978; Ueda et al, 1989). We feel sure that the aneurysms of this patient arose from the PAN and not from the anti-cancer drugs because angiography showed hepatic aneurysms before the drugs were used. The decrease in the numbers of intrahepatic arterial branches was probably caused partly by obstruction of the branches as a result of the progress of PAN as well as by arterial endothelial damage as a result of the chemotherapy. By CT, the main tumour and multiple metastatic nodules were seen to become low density masses, and the volume of the surrounding non-cancerous hepatic parenchyma decreased greatly after the two sessions of intra-arterial chemotherapy. These healing processes of HCC seen in the CT findings were mainly the result of hepatic arterial embolization rather than of the intra-arterial chemotherapy. Generally speaking, if intra-arterial chemotherapy is effective, reduction in the tumour size occurs, but the tumour does not always change into a low density mass. If transarterial embolization is effective, the tumour tends to change into a low density mass without reduction in size of the surrounding non-cancerous area (Tsubakimoto et al, 1988). We think that the ischaemic effects brought out by transarterial embolization occurred in this patient because of arterial obstruction caused by intra-arterial chemotherapy, as well as the obstruction caused by PAN.

Perhaps PAN that is latent will sometimes become clinically evident after intra-arterial chemotherapy. The possibility should be kept in mind that intra-arterial chemotherapy may make necrotizing angitis, especially PAN, worse.

References

AHMED, H. A., ARULAMBALAM, K. J. & NICKOLS, C. D., 1986. Polyarteritis nodosa of the liver: a case report and review of the literature. *Materia Medica Polona*, *18*, 231–234.

ALLEMAN, M. J. A., JANSSENS, A. R., SPOELSTRA, P. & KROON, H. M. J. A., 1986. Spontaneous intrahepatic hemorrhages in polyarteritis nodosa. *Annals of Internal Medicine*, *105*, 712–713.

EWALD, E. A., GRIFFIN, D. & MCCUNE, W. J., 1987. Correlation of angiographic abnormalities with disease manifestations and disease severity in polyarteritis nodosa. *Journal of Rheumatology*, *14*, 952–956.

1991, *The British Journal of Radiology*, *64*, 275–277

Forsberg, L., Hafstrom, L., Lunderquist, A. & Sundquvist, K., 1978. Arterial changes during treatment with intrahepatic arterial infusion of 5-fluorouracil. *Radiology*, *126*, 49–52.

Haratake, J., Horie, A., Furuta, A. & Yamato, H., 1988. Massive hepatic infarction associated with polyarteritis nodosa. *Acta Pathologica Japonica*, *38*, 89–93.

McMahon, B. J., Heyward, W. L., Templin, D. W., Clement, D. & Lanier, A. P., 1989. Hepatitis B associated polyarteritis nodosa in Alaskan Eskimos: clinical and epidemiologic features and long-term follow-up. *Hepatology*, *9*, 97–101.

Nakanuma, Y., Ohta, G. & Sasaki, K., 1984. Nodular regenerative hyperplasia of the liver associated with polyarteritis nodosa. *Archives of Pathology and Laboratory Medicine*, *108*, 133–135.

Tavers, R. L., Allison, D. J., Brettle, R. P. & Hughes, G. R. V., 1979. Polyarteritis nodosa: a clinical and angiographic analysis of 17 cases. *Seminars in Arthritis and Rheumatism*, *8*, 184–199.

Tsubakimoto, M., Nakamura, K., Matsuo, R., Murata, K., Takada, K., Usuki, N., Kaminoh, T., Manabe, T., Yamada, T., Takashima, S., Nakatsuka, H., Minakuchi, K. & Onoyama, Y., 1988. Evaluation by computed tomography of effects of transcatheter therapy for liver cancer. *Acta Hepatologica Japonica*, *29*, 1599–1604.

Ueda, E., Sako, M., Hirata, S., Hase, M., Hujii, M., Nagae, T., Kusumoto, M. & Kono, M., 1989. Experimental study of arterial damage induced by anti-cancer drug infusion. *Nippon Acta Radiologica*, *49*, 1430–1432.

Renal transitional cell carcinoma mimicking medullary sponge kidney

By M. Choong, MBBS, FRACR and G. W. L. Phillips, MA, MRCP, FRCR

Department of Radiology, Repatriation General Hospital Heidelberg, Banksia Street, West Heidelberg, 3081 Victoria, Australia

(Received May 1990 and in revised form October 1990)

Keywords: Renal carcinoma, Medullary sponge kidney

Transitional cell carcinoma (TCC) is the commonest neoplasm of the renal pelvis, usually appearing on intravenous urography (IVU) and retrograde pyelography as a filling defect in the pelvicalyceal system. We report a case of renal TCC which mimicked medullary sponge kidney (MSK) on IVU, an appearance not previously reported in the literature.

Case report

A 68-year-old man with no significant past history presented with macroscopic haematuria and right loin discomfort. Physical examination and plain abdominal X-ray were unremarkable.

Intravenous urography showed a 2 cm mass in the lower pole of the right kidney. Linear streaks of contrast were demonstrated within the mass, orientated in the direction of the collecting tubules of the papilla (Fig. 1). This appearance was interpreted as most likely due to focal MSK involving a single papilla in the right lower pole. Some coarse collections of contrast medium were seen within other papillae in this kidney and were thought to be most likely due to tubular stasis secondary to excessive ureteric compression.

However, urine cytology demonstrated degenerate transitional cells from well differentiated TCC or moderately severe dysplasia. On panendoscopy, fresh blood was seen coming from the right ureteric orifice but subsequent retrograde pyelogram did not show any abnormality (Fig. 2).

Contrast-enhanced computed tomography confirmed a solid 2 cm mass in the lower pole of the right kidney (Fig. 3). No contrast was seen within the mass.

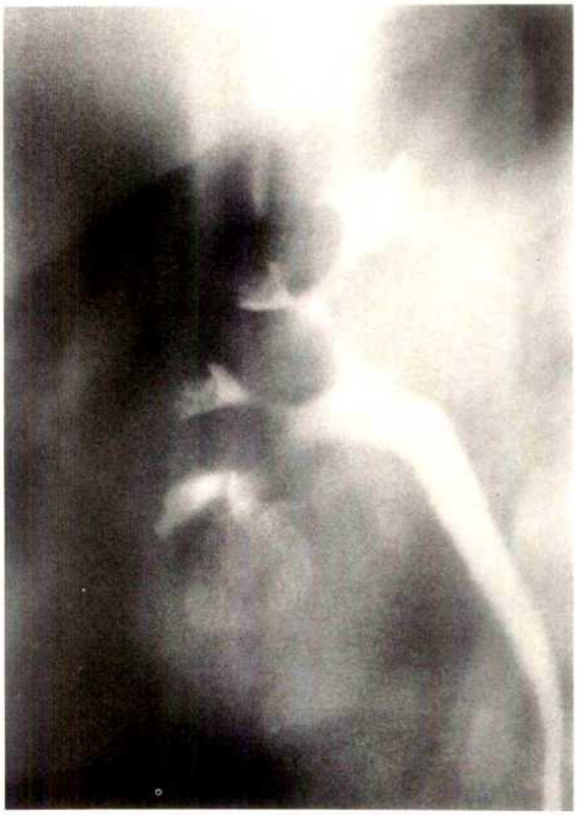

Figure 1. Intravenous urogram demonstrating linear streaky densities adjacent to the lower pole calyx, mimicking MSK.

Address correspondence to: G. W. L. Phillips, Department of Radiology (X-ray), Repatriation General Hospital Heidelberg, Private Bag 1, Heidelberg West 3081, Victoria, Australia.

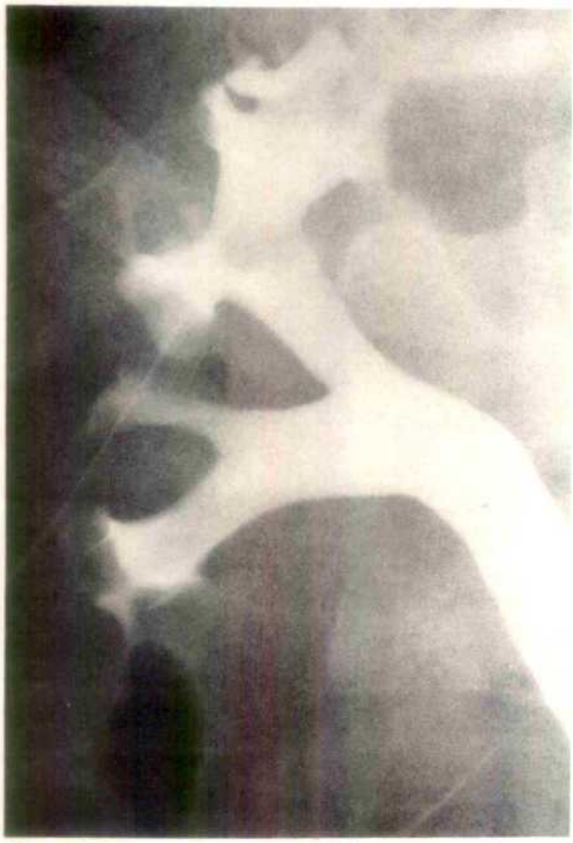

Figure 2. Retrograde pyelogram showing an apparently normal lower pole calyx.

In view of the cytology and radiological findings, partial nephrectomy of the right lower pole was performed. A 2 cm foliated mass was confirmed arising from the lower pole calyx. Histology was of a transitional cell carcinoma (Fig. 4). There was no histological evidence of MSK or papillary necrosis.

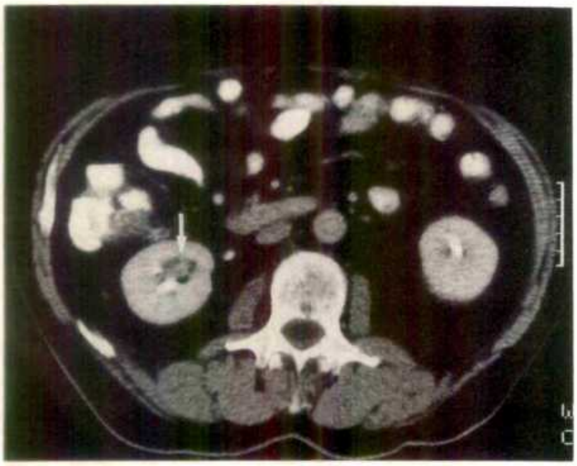

Figure 3. Contrast-enhanced computed tomography demonstrating a 2 cm soft tissue mass in the lower pole of the right kidney (arrow).

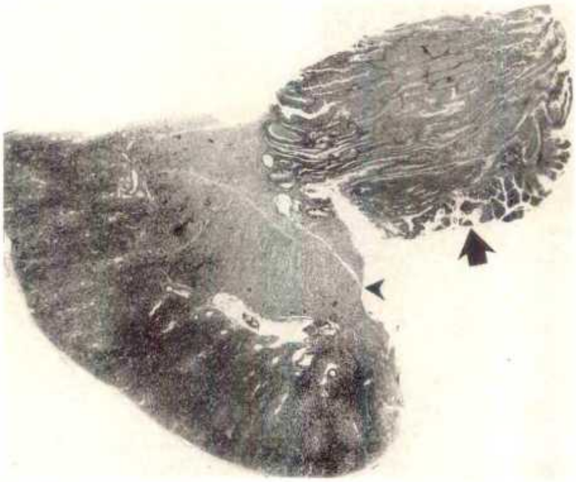

Figure 4. Microscopic histology of surgical specimen showing the TCC with multiple folds (arrow) arising from the renal medulla (arrowhead) and extending into the renal pelvis.

Discussion

Primary neoplasms of the renal pelvis account for less than 10% of kidney cancers. Transitional cell carcinoma is the commonest of these neoplasms. On IVU, a mass is recognized in 60–70% of cases. The lesion may be papillary or flat and broad based. The surface may appear smooth, irregular or lobular. Less commonly, a non-functioning kidney or a focal parenchymal mass is seen (Davidson, 1985; Goldman et al, 1987).

It is well recognized that some TCCs are frond-like tumours and have a stippled appearance on IVU due to contrast medium trapped within the interstices (Davidson, 1985; Goldman et al, 1987). In our case, the tumour had multiple, regular folds resulting in a foliated appearance. Contrast medium trapped between the folds mimicked contrast medium in dilated collecting tubules, as typically seen in MSK.

Retrograde pyelography usually offers better opacification of the renal collecting system, resulting in higher sensitivity and specificity for diagnosis of collecting system masses (Lowe & Roylance, 1976). However, it was unhelpful and misleading in our case since the tumour produced no significant distortion of the collecting system and there was no reflux of contrast into the folia of the tumour. Computed tomography and angiography are usually only of secondary importance in the evaluation of the collecting system lesions (Goldman et al, 1977; Gatewood et al, 1982).

The implications for treatment make the correct diagnosis of TCC and differentiation from MSK crucial. Medullary sponge kidney is usually asymptomatic and treatment is required only for complications such as infection or nephrolithiasis. Transitional cell carcinoma of the kidney requires nephro-ureterectomy. We conclude that TCC should be considered as a differential diagnosis when IVU shows striated densities apparently in a papilla.

Acknowledgments
We would like to thank Sophie Kalifatidis and Patricia Murnane for typing the manuscript.

References

DAVIDSON, A. J., 1985. *Radiology of the Kidney* (W. B. Saunders, Philadelphia, PA), pp. 453–468.

GATEWOOD, O. M. B., GOLDMAN, S. M., MARSHALL, F. F. & SIEGELMAN, S. S., 1982. Computed tomography in the diagnosis of transitional cell carcinoma of the kidney. *Journal of Urology*, *127*, 876–887.

GOLDMAN, S. M., BOHLMAN, M. E. & GATEWOOD, O. M. B., 1987. Neoplasms in the renal collecting system. *Seminars in Roentgenology*, *22*, 284–291.

GOLDMAN, S. M., MENG, C., WHITE, R. I. et al, 1977. Transitional cell tumour of the kidney. How diagnostic is the angiogram? *American Journal of Roentgenology*, *129*, 99–105.

LOWE, P. P. & ROYLANCE, J., 1976. Transitional cell carcinoma of the kidney. *Clinical Radiology*, *27*, 503–512.

Metastatic carcinoma to the male breast

By Lalitha Ramamurthy, MD and *†Richard A. Cooper, MD

Department of Radiology, Hines VA Hospital, Fifth Avenue and Roosevelt Road, Hines, Illinois 60141 and †Department of Radiology, Loyola University Medical Center, Foster G. McGaw Hospital, 2160 South First Avenue, Maywood, Illinois 60153, USA

(Received May 1990 and in revised form September 1990)

Keywords: Male breast carcinoma, Mammography

Metastatic carcinoma to the breast is relatively rare. In autopsy studies, metastatic tumours to the breast accounted for 1.7–6.6% of breast tumours (Abrams et al, 1950; Sandison, 1950). The clinically reported incidence of metastatic tumours to the breast ranges from 0.5–2% (Toombs & Kalisher, 1977; Egan, 1988a). Of primary breast cancers, 0.15–0.9% cancers occur in males (Kapdi & Parekh, 1983; Egan, 1988b). Metastatic tumours to the male breast are even rarer and this is the first such case reported in the literature. In this article, we report the clinical, radiographic and pathologic features of a case of metastatic prostate cancer to the male breast.

Case report

A 64-year-old black man had a 2-year history of Stage II prostate carcinoma. Histology showed infiltrating, moderate to poorly differentiated adenocarcinoma. The patient had radiation therapy and was continually treated with stilbesterol. His initial metastatic work-up was unremarkable. A bone scan 1 year prior to admission was positive in the axial skeleton. A repeat bone scan on the last admission showed progression of the disease. The patient presented with bilateral, painful gynecomastia secondary to oestrogen therapy which did not respond to radiation therapy. The right breast demonstrated a firm, palpable mass on clinical examination. Mammography (Fig. 1) revealed bilateral gynecomastia and multiple moderately well circumscribed, non-calcified masses in the lateral aspect of each breast. Fine needle aspiration biopsy (Fig. 2) of the right breast mass showed moderately well differentiated

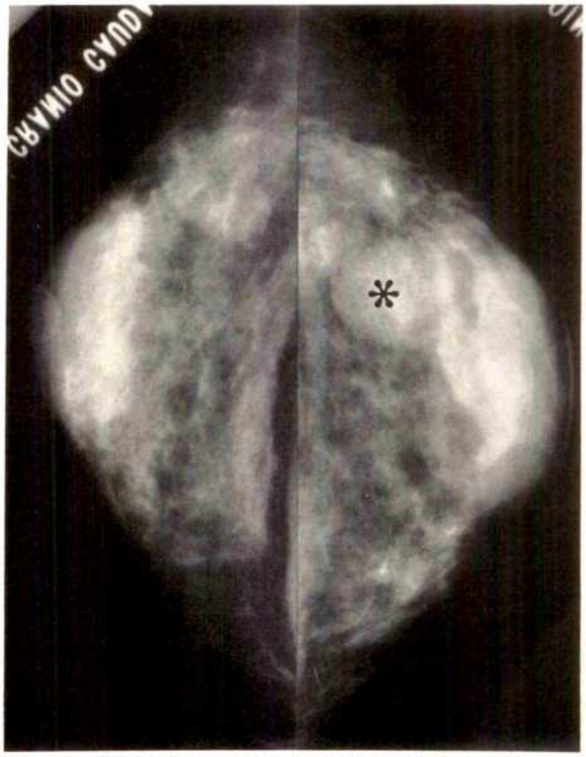

Figure 1. Bilateral gynecomastia with multiple well circumscribed masses. The largest mass (*) measured 1.75 cm in diameter and corresponded to the palpable mass. It was this mass that was biopsied.

---

* Author for reprint requests.

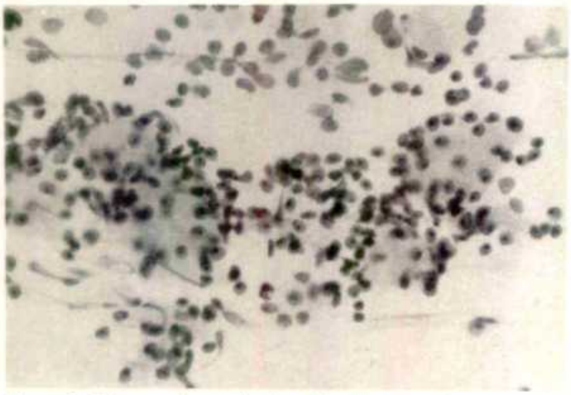

Figure 2. Fine needle aspiration biopsy smear demonstrating adenocarcinoma consistent with prostatic primary. Note the small acinar structures at the centre of the slide. Each nucleus contains a single prominent nucleolus characteristic of prostatic carcinoma. (Alcohol fixed Papanicolaou stained smear, × 92).

metastatic adenocarcinoma consistent with the primary prostatic lesion.

Immunochemistry revealed tumour positivity for prostate specific antigen. The patient did not receive treatment and died 4 months after discovery of the breast metastasis.

Discussion

Metastatic tumours to the male breast are extremely rare. The frequency of prostatic metastasis to the breast has been studied. Toombs & Kalisher (1977) reported nine prostate primaries out of 152 metastatic lesions to the breast. Salyer & Salyer (1973) examined histologically breast in 46 patients who died of metastatic prostate carcinoma. Metastases were found in 26% of these patients, none of whom had clinical evidence of breast metastasis. Earlier, many cases of metastatic carcinoma to the breast were wrongly diagnosed as primary carcinoma attributable to oestrogen therapy (Azzopardi, 1979). Salyer & Salyer (1973) found no increased incidence of primary breast cancer in their series of patients who died from metastatic prostate carcinoma. All their patients received oestrogen therapy and 95% had gynecomastia. Bland et al (1980) states that oestrogen causes proliferative changes in the breast with development of both ducts and periductal stroma. This may provide a more suitable environment for metastatic cancer. Mostofi and Price (1973) reported prostate cancer metastatic to the breast in patients without prior oestrogen therapy. Yet Toombs and Kalisher (1977) reported that oestrogen therapy was administered to eight out of nine patients with breast metastasis from adenocarcinoma of the prostate.

The prognosis after discovery of metastasis to the breast is poor. Our patient lived only 4 months after diagnosis.

Although one cannot always reliably differentiate metastatic lesions from primary breast cancer, Lo (1978) as well as Hajdu (1972) point to the absence of malignant cells within the ductal system as a sign of metastasis. Instead, in metastatic disease, there is a periductal distribution of tumour cells. Also, Charache (1953) noted that metastatic lesions are less fixed to the breast tissue and more likely to be encapsulated in subcutaneous fat. Azzopardi (1979) stresses not only the absence of ductal involvement but also the absence of elastosis as a salient feature of metastatic carcinoma to the breast. Specific diagnosis of metastatic prostate carcinoma has been obtained using immunochemical studies for prostate specific antigen (Nadgi et al, 1981).

Summary

A case of metastasis to the male breast from prostate carcinoma is reported. For proper treatment, it is important to differentiate primary from metastatic tumours.

Prostate-specific antigen screening should be strongly considered in all breast masses seen in patients with known prostatic carcinoma. One cannot assume that breast enlargement in these patients is solely due to oestrogen-induced gynecomastia.

References

Abrams, H. L., Spiro, R. & Goldstein, N., 1950. Metastases in carcinoma. *Cancer*, *3*, 74–84.

Azzopardi, J. G., 1979. *Problems in Breast Pathology* (W. B. Saunders, Philadelphia), p. 311–314.

Bland, K. I., Buchanan, J. B., Wiseberg, B. F., Hagan, T. A. & Gray, L. A., 1980. The effects of exogenous estrogen replacement therapy of the breast: Breast cancer risk and mammographic parenchymal patterns. *Cancer*, *45*, 3027–3033.

Charache, H., 1953. Metastatic tumors to the breast. *Surgery*, *3*, 385–390.

Egan, R., 1988a. *Breast Imaging* (W. B. Saunders, Philadelphia), p. 288.

——1988b. *Breast Imaging* (W. B. Saunders, Philadelphia), p. 295.

Hajdu, S. I. & Urban, J. A., 1972. Cancer metastatic to the breast. *Cancer*, *29*, 1691–1696.

Kapdi, C. C. & Parekh, N. J., 1983. The male breast. *Radiological Clinics of North America*, *21*, 137–148.

Lo, M. C., Chomet, B. & Rubinstone, A., 1978. Metastatic prostatic adenocarcinoma of the male breast. *Urology*, *11*, 641–646.

Mostofi, F. K. & Price, E. B., 1973. *Tumors of the Male Genital System* (Armed Forces Institute of Pathology, Washington DC), p. 239.

Nadjgi, M., Tabei, S., Castro, A., Chu, T. M. & Morales, A. R., 1980. Prostatic origins of tumours. An immunohistochemical study. *American Journal of Clinical Pathology*, *73*, 735–739.

Salyer, W. R. & Salyer, D. C., 1973. Metastases of prostatic carcinoma to the breast. *Journal of Urology*, *109*, 671–675.

Sandison, A. T., 1950. Metastatic tumours in the breast. *British Journal of Surgery*, *47*, 54–58.

Toombs, B. D. & Kalisher, L., 1977. Metastatic disease to the breast: Clinical, pathologic and radiographic features. *American Journal of Roentgenology*, *129*, 673–676.

1991, *The British Journal of Radiology*, 64, 279–280

Case of the month

There's more to it than meets the eye

By Sharon Evans, MB, BCh, FRCR

Department of Radiology, Walsgrave Hospital, Coventry, UK

(Received January 1990)

A 39-year-old Indian man presented to the Casualty Department with a 3-week history of headaches and nasal congestion, and a 3-day history of a painful swollen right eye. On examination, he was unwell and pyrexial with a sinus tachycardia. He had a tender right eye with a swollen upper eyelid and an obvious sixth nerve palsy with almost complete failure of abduction.

Computed tomographic (CT) head scan was performed which demonstrated the cause of his symptoms (Fig. 1). What is the diagnosis? How many abnormalities can you detect? What is the appropriate management?

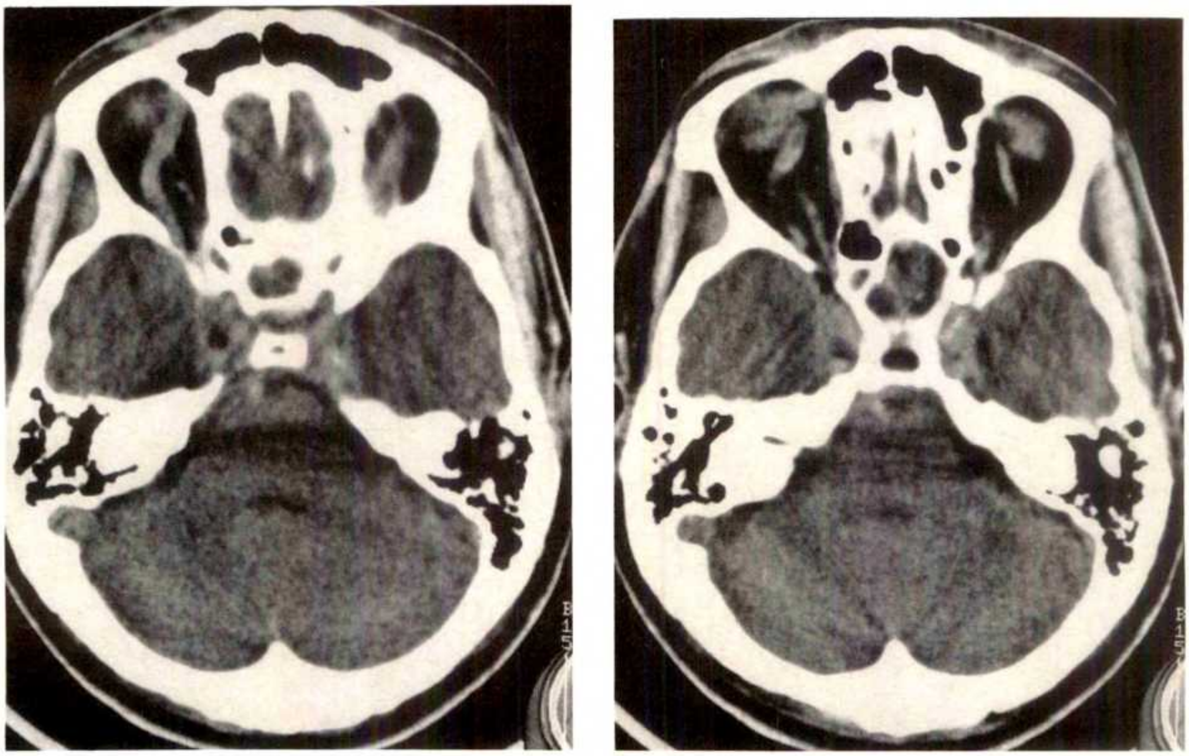

(a) (b)

Figure 1. Post-contrast 3 mm axial CT sections.

Address for correspondence: Department of Radiology, Neath General Hospital, West Glamorgan.

High resolution slices 3 mm thick before and after administration of contrast medium were obtained using an axial plane of section parallel to the orbitomeatal line. No reformatting was considered necessary.

An obvious right-sided cavernous sinus thrombosis is shown. There is enlargement and asymmetry of the right cavernous sinus with irregular filling defects within it, representing thrombus formation. Smaller regular filling defects are also seen in the left cavernous sinus and these represent normal structures and/or fat within the sinus (Kline et al, 1981). In addition, there is a marked engorgement of the right superior ophthalmic vein containing several thrombi. The sphenoid sinus is opaque and contains material of soft tissue density which denotes a sphenoid sinusitis.

Our patient had opacification of the right maxillary antrum and sphenoid sinus on admission which, taken together with his clinical presentation, suggested a tentative diagnosis of cavernous sinus thrombosis, duly confirmed by CT.

The patient was treated immediately with high dose intravenous antibiotics and nasal decongestants but had still not improved significantly after 48 hours. He was therefore referred to the Ear, Nose and Throat Department for bilateral sphenoid sinoscopy and washout, and right maxillary antrostomy. The right sphenoid sinus was found to contain much purulent debris, which after washout revealed a very hyperaemic mucosa and a blocked ostium. The left sinus appeared clear. Culture of the pus yielded a heavy growth of *Streptococcus pneumoniae*.

Within 24 hours of the procedure the patient had dramatically improved. His symptoms settled after a further 4 days of intravenous antibiotics, and by Day 10 his sixth nerve palsy had completely resolved.

Discussion

The cavernous sinus is a large, circular venous space which allows free drainage between the right and left compartments (Harrington, 1984). It contains several important vessels and nerves: the horizontal portion of the internal carotid artery running forward through the sinus, and the sixth cranial nerve passing between the artery and the lateral wall of the sinus. The third, fourth and firth nerves lie within the lateral wall separated from the venous blood by a thin fibrous sheath (Kline et al, 1981). Thus, the likeliest structures to be affected by thrombosis are the internal carotid artery and the sixth nerve. In severe cases of septic cavernous sinus thrombosis, third and fourth nerve palsies also occur. These may be unilateral, bilateral, or progress from one eye to the other (Harrington, 1984).

Septic cavernous sinus thrombosis is an uncommon condition, and can be life-threatening unless diagnosed and treated early (Yarrington, 1961). The most common predisposing factors are paranasal sinus, nasal or skin infection. The mechanism of spread from the paranasal sinuses to the cavernous sinus is attributed to a thrombophlebitic process. More seriously, a meningitic process may develop with or without generalized septicaemia.

This case highlights several important features of cavernous sinus thrombosis. First, the diagnosis is essentially a clinical one and is generally straightforward when clinical features are severe. Where orbital signs are mild or absent, high-resolution CT is invaluable for confirming the diagnosis as it can actually show the thrombus within the sinus (Clifford-Jones et al, 1982).

Secondly, having established the diagnosis of cavernous sinus thrombosis complicating acute sphenoid sinusitis, early and aggressive treatment with intravenous antibiotics should be instituted. Prompt surgical intervention is indicated if symptoms continue or complications arise (Urqhuart et al, 1989). Thirdly, cavernous sinus thrombosis remains a serious condition that is infrequently encountered and vigilance is required to ensure early diagnosis and rapid treatment. If left untreated, morbidity and mortality are high.

References

CLIFFORD-JONES, R. E., ELLIS, C. J. K., STEVENS, J. M. & TURNER, A., 1982. Cavernous sinus thrombosis. *Journal of Neurology, Neurosurgery and Psychiatry, 45*, 1092–1097.

HARRINGTON, P. C., 1984. Complications of sinusitis. *Ear, Nose and Throat Journal, 63*, 163–167.

KLINE, L. B., ACKER, J. D., POST, M. J. D. & VITEK, J. J., 1981. The cavernous sinus: a computed tomographic study. *American Journal of Neuroradiology, 2*, 299–305.

URQHUART, A. C., FUNG, G. & MCINTOSH, W. A., 1989. Isolated sphenoiditis: a diagnostic problem. *Journal of Laryngology and Otology, 103*, 526–527.

YARRINGTON, C. T., 1977. Cavernous sinus thrombosis revisited. *Proceedings of the Royal Society of Medicine, 70*, 456–459.

1991, The British Journal of Radiology, 64, 281

Correspondence

(The Editors do not hold themselves responsible for opinions expressed by correspondents)

The prognostic significance of radiologically detected knee joint effusions in the absence of associated fracture

The Editor—Sir,

If Maskell and Finlay (1990) had also studied the prognosis of patients whose radiographs did not show a knee joint effusion, then they might have produced a more meaningful, statistical conclusion concerning the prognostic significance of the presence of such an effusion, perhaps in terms of estimated relative risk. As presented, their data are uncontrolled.

Yours etc.,
P. Lord

Department of Radiology,
Fazakerley Hospital,
Liverpool L9 7AL
(Received December 1990)

Authors' reply

The Editor—Sir,

Our intention was simply to look at the clinical significance of a specific radiological sign, frequently seen in casualty X-ray film reporting. The data are uncontrolled, but to have obtained an adequate control group would have required a much greater undertaking with matching of clinical data etc., beyond the scope of our study.

Yours etc.,
T. Maskell
D. Finlay

Department of Radiology,
Leicester Royal Infirmary,
Leicester LE1 5WW
(Received January 1991)

Reference

Maskell, T. W. & Finlay, D. B. L. 1990. The prognostic significance of radiologically detected knee joint effusions in the absence of associated fracture. *British Journal of Radiology, 63*, 940–941.

Choroid plexus cysts and chromosomal defects

The Editor—Sir,

We read with interest the recent paper by Thorpe-Beeston et al describing their findings of a close association between choroid plexus cysts and trisomies. As they point out, theirs is one in a long series of such papers. Most however, including this paper, are flawed in being based on highly selected referred populations and not a general obstetric population. In this case patients were referred with both choroid plexus cysts and other gross anomalies from a variety of sources. Whether the criteria for referral were similar in all cases is doubtful, and, unless all choroid plexus cysts were referred, the potential incidence of trisomies in this condition is impossible to determine. Papers that are based on such high risk groups may therefore give a false impression of the frequency and associations of choroid plexus cysts. In addition, the paper shows a high incidence of other major anomalies *e.g.* exomphalos and diaphragmatic hernia in association with trisomy 18, the choroid plexus cyst being an incidental finding. In most centres the presence of an exomphalos would be a *de facto* indication for karyotyping. Conversely, none of the women with an isolated cyst appear to have had a trisomic fetus, and indeed only 25% underwent a karyotyping procedure.

Population based studies have shown an incidence of choroid plexus cysts of 0.18–0.8%, highly dependent on the quality of both ultrasound equipment and operator. Studies to date suggest an incidence of trisomies of around 5% in this group, the incidence being higher if the cysts are large, bilateral and persist beyond 22 weeks. Based on these criteria we detected 19 fetuses with choroid plexus cysts in the course of 4984 mid-trimester scans. None of these persisted, and no fetus in this group had a trisomy. These figures are of the same order of magnitude to other population based studies (Ostlere et al, 1989; Twining et al, 1989).

Trisomy 18 is a relatively rare condition, being seen in large numbers only in major referral centres. Conversely these centres are often unable to furnish large numbers of routine scans to assess the baseline incidence in the population. Whilst there is an undoubted association between trisomy 18 and choroid plexus cysts, the true relationship remains unclear. We would urge that publication of potentially confusing highly selected series cease, and that we all support and await the results of multi-centre trials such as that being run by Ostlere et al (Ostlere et al, 1989). Only in this way will the true incidence of the condition, associated trisomies and other anomales be established, and reliable guidelines laid down for karyotyping and management.

Yours etc.,
J. McHugo
G. Constantine
R. Rajah

The Birmingham Maternity Hospital,
Department of Ultrasound,
Edgbaston
Birmingham B15 2TG
(Received November 1990)

References

Ostlere, S. J., Irving, H. C. & Lilford, R. J., 1989. A prospective study of the incidence and significance of fetal choroid plexus cysts. *Prenatal Diagnosis, 9*, 205–211.

Thorpe-Beeston, J. G., Gosden, C. M. & Nicolaides, K. H., 1990. Choroid plexus cysts and chromosomal defects. *British Journal of Radiology, 63*, 783–786.

Twining, P., Zuccollo, J., Swallow, J. & Clewes, J., 1989. Choroid plexus cysts: a marker for trisomy 18. A prospective study and review of the literature. *BMUS Programme and Abstract Book, December 1989.*

Correction

In the letter from B. Sizer in *BJR* (January, 1991, p. 72), the sentence "Megavoltage irradiation was given to the mediastinum and adjacent lungfields using anterior and posterior parallel opposed fields, giving 12 Gy maximum permissible dose in 3 fractions in 1 week" should have been "Megavoltage irradiation was given to the mediastinum and adjacent lungfields using anterior and posterior parallel opposed fields, giving 12 Gy mid-plane dose in 3 fractions in 1 week"

Proceedings of the British Institute of Radiology

Treatment and measurement of tumour response to treatment

Abstracts of papers presented at an all day meeting held at the BIR, 36 Portland Place, London W1N 4AT, on Friday 9 November 1990

Chairman: R. S. Camplejohn

Predictive assays: why and how? by P. R. Twentyman
Comparison of MTT and clonogenic assays for assessment of *in vitro* radiosensitivity of human gliomas, by J. Ramsey, R. Ward and N. M. Bleehen
Resolution and reproducibility of surviving fraction at 2 Gy (SF_2) for cervical carcinoma, by S. E. Davidson, C. M. L. West and R. D. Hunter
Prediction of acute responses and likelihood of recurrence of tumours using a primary explant culture system, by C. Mothersill, C. Seymour, T. P. Hennessy and J. Bonnar
Mass culture techniques — is this the way to measure human tumour? by P. Price
Use of ^{31}P NMR to monitor treatment-induced changes in tumour metabolism in animal models, by J. C. M. Bremner, C. J. R. Counsell, J. Pearson, J. Samson, C. Thomas, P. J. Wood and G. E. Adams
Flow cytometric nucleoid analysis in the prediction of bladder cancer response to radiotherapy, by P. Anderson, T. H. Lynch, R. P. Beaney, D. M. A. Wallace, G. M. Kondratowicz and A. T. M. Vaughan
Response to radiotherapy assessed by flow cytometric analysis of sequential tumour biopsies, by J. E. D. Dyson
BrdUrd and Ki67 labelling in human tumour xenografts, by C. S Parkins, C. Bush, P. Price and G. G. Steel
Proliferation of human tumours measureed *in vivo* using BrdUrd: relation to outcome of radiotherapy, by G. D. Wilson, N. J. McNally, C. A. Whitsted, S. Dische, M. I. Saunders and K. Lochrin
The impact f S-phase fraction and tumour differentiation on response to adjuvant chemotherapy in node positive breast cancer, by S. M. O'Reilly, R. S. Camplejohn, R. R. Millis, R. D. Rubens and M. A. Richards
Measurement based sequential therapy in breast cancer, by A. E. Johnson
Commentary, by S. Dische

Predictive assays: Why and how?

Peter R. Twentyman
MRC Clinical Oncology and Radiotherapeutics Unit
Hills Road, Cambridge CB2 2QH, UK

It is well established that a variety of prognostic factors will furnish information regarding the likely radioresponsiveness of different tumours. For example, a small cell lung carcinoma is likely to be highly responsive whereas a squamous cell lung carcinoma much less so. In general, large tumours are less likely to be controlled than small tumours. Predictive assays are designed to extend this type of information from broad classes of tumours to ostensibly similar tumours in individual patients. Additionally, the possibility that patients likely to experience unusually severe or unusually modest normal tissue responses can be identified may allow for tailoring of total dose to the tolerance of the individual patient. In the foreseeable future, predictive tests are likely to produce answers in terms of probabilities rather than certainties. The value of predictive testing will lie mainly in situations where a variety of treatment options are available. Where surgery or radiotherapy are effective treatments, identification of tumours which are unlikely to respond to radiotherapy would allow immediate surgery to be selected. Similarly, identification of those tumours where unconventional radiation fractionation or use of hypoxic cell sensitization strategies are likely to be of particular value would be important. The radioresponsiveness of a tumour is determined by many factors including intrinsic cellular sensitivity, effect of intercellular contact, repair capacity, hypoxic fraction and potential doubling time. Although a surviving fraction at 2 Gy has been shown to predict for the clinical responsiveness of broad groups of tumours, its predictive importance in individual patients remains to be determined. A variety of approaches to the determination of this parameter may be used. The use of clonogenic assays with clinical specimens has the disadvantage of a relatively poor yield of successful assays, low plating efficiency and long assay time. Non-clonogenic assays, although producing an answer in a higher proportion of cases and in a shorter time, are complicated by the influence of stromal cells and the residual metabolism of sterilized cells. Use of anti-BrdUrd antibodies and flow cytometry to determine the potential doubling time of human tumours is likely to be a valuable tool for the identification of tumours where a short overall treatment time would produce better results. To date the use of radiolabelled nitroimidazoles to determine the *in situ* hypoxic fraction has been unsuccessful. The use of NMR may present a better option for the determination of this and related metabolic factors *in situ*. The ideal predictive assay would be cheap, convenient, rapid and 100% accurate. The complexities of tumour biology are such that expectations of progress in the immediate future must remain modest.

Comparison of MTT and clonogenic assays for assessment of *in vitro* radiosensitivity of human gliomas

J. Ramsay, R. Ward and N. M. Bleehen
MRC Clinical Oncology & Radiotherapeutics Unit, Hills Road, Cambridge, UK

Radiotherapy remains the main treatment modality for patients with malignant glioma but it is clear that only a proportion obtain significant benefit in terms of prolongation of survival. We have looked at the *in vitro* radiosensitivity of early passage cultures established from biopsies to see if this is a factor in determining survival. An important aspect of the work was to assess the value of the MTT assay in measuring radiosensitivity. Of 43 glioma biopsies obtained at time of neurosurgery 35 (81%) have been established in primary culture. Twenty-six out of 29 (90%) have been successfully tested using the MTT assay and 21 out of 29 (72%) with the clonogenic assay. Mean values for surviving fraction to 2 Gy were 0.57 (range 0.34–0.91) for MTT assay and 0.44 (range 0.12–0.66) for the clonogenic assay. While the difference in mean values for the two assays was significant ($p < 0.01$), there was reasonable qualitative agreement ($r = 0.79$). In 20 patients with follow up greater than 1 year, an analysis has been made to see if the results are of prognostic importance. For eight patients surviving greater than 1 year mean SF2 Gy/MTT was 0.51 compared with 0.64 for 12 patients surviving less than 1 year ($p = 0.5$). For the clonogenic assay the corresponding figures were 0.33 and 0.47 ($p = 0.06$). When patients were ranked in order of radiosensitivity of their tumours then the most sensitive third had a median survival of 17 months and the most resistant third 10 months ($p < 0.05$). These results suggest that differences in intrinsic radiosensitivity may be a factor in determining survival in this group of tumours. Also the MTT assay can be used to measure radiosensitivity and has some advantages over clonogenic assay in respect of proportion of cultures successfully tested and time to obtain a result. More patient data will be available after longer follow up.

Resolution and reproducibility of surviving fraction at 2 Gy (SF_2) for cervical carcinoma

*†S. E. Davidson, *C. M. L. West, and †R. D. Hunter
**Department of Radiobiology, Paterson Institute for Cancer Research and †Department of Radiotherapy, Christie Hospital and Holt Radium Institute, Manchester M20 9BX, UK*

Biopsies from 117 patients with cervical carcinoma were studied using a clonogenic assay to obtain values for the surviving fraction at 2 Gy (SF_2). Heterogeneity in intrinsic radiosensitivity was investigated by independently processing multiple biopsies from 18 tumours. No significant differences between intra tumour SF_2 values were demonstrated ($p = 0.3$). The results have shown that intra tumour heterogeneity is not a limitation to radiosensitivity testing using the Courtenay–Mills assay. A wide range of values (0.14–0.97) for SF_2 was obtained with a mean value of 0.44 (SD = 0.19) for 77 tumours (110 squamous cell carcinomas and seven adenocarcinomas). There were statistically significant differences between the individual tumours ($p < 0.001$). From analysis of variance of all the SF_2 results it appears to be the surviving fraction below about 0.4 and those above 0.7 which slow significant differences in radiosensitivity between pairs of tumours ($p = 0.05$). Also 36% of the values of SF_2 show significant differences from the mean SF_2 of all tumours. The storage of tumour cell suspensions in liquid nitrogen improved the colony forming efficiency but did not alter the radiosensitivity.

Prediction of acute responses and likelihood of recurrence of tumours using a primary explant culture system

C. Mothersill, C. Seymour, T. P. Hennessy and J. Bonnar
Department of Surgery & Obstetrics & Gynaecology, St James's Hospital, Dublin 8 and Radiobiology Research Group of the Nuclear Energy Board, Beggars Bush, Dublin 4

Tissue culture has been used to test the sensitivity of various cancers to chemotherapy agents and radiation both singly and in combination. A total of 52 samples have been cultured and 50 have given useful cultures. The two failures arose where the specimen provided was necrotic. Twenty-two ovarian cancers, 14 endometrial cancers, six cervical cancers and 12 oesophageal cancers have been examined. In most cases the results from the tissue culture were in agreement with the empirically established treatment, but in five cases resistance to the conventional or proposed treatment was detected in culture and an alternative treatment gave a good response. These cases are presented in detail. By incubating the cultures with tritiated thymidine at various time points post treatment, it is also possible to study repopulation rates. This is particularly useful in the case of radiation treatment. The results indicate that the use of tissue culture may aid treatment planning particularly where resistance to the conventional therapy occurs.

Mass culture techniques — is this the way to measure human tumour sensitivity?

Pat Price
Department of clinical Oncology, Hammersmith Hospital, London, UK

Measurement of the intrinsic radiosensitivity of human tumour cells may be the single most important factor in predicting radiocurability. Assays so far developed depend on the *in vitro* assessment of the primary cultures from tumour biopsies. Soft agar clonogenic assays have been the most successful. Growth in agar is the property of the malignant phenotype and clonogenic assessment of survival is both reliable and relevant as the regenerative capacity of the cells have been measured. Mass culture techniques involve growth of higher density of tumour cells with assessment of survival of the whole population, with a result often obtained quicker than with clonogenic assays. This is arguably a more physiological environment for the tumour cells, with cell attachment being encouraged. Also, the response of the whole population of cells to irradiation may be more representative of their response to irradiation than that of a small number of clonogenic cells. There are two requirements for the successful application of a mass culture assay to human biopsy material. (1) Establishment of cell growth. The physiological cell attachment matrix (CAM) has been evaluated. Successful growth on this matrix was achieved from 7 out of 22 human tumour biopsies. However, growth of fibroblasts precluded the evaluation of the radiosensitivity of the tumour cells. Overall more cell growth (both tumour and normal) was observed on CAM than on bare plastic but it appeared to offer no advantage over feeder cells of another attachment molecule, vitronectin. (2) Evaluation of cell kill. Out experience with cell lines has highlighted the requirements for accurate assessment of cytotoxicity from growth assays. Adequate cell numbers for multiple platings and radiation doses, careful choice of the time of assay and re-establishment of exponential growth after treatment are all needed.

Failure to take these into account can lead to very misleading measures of cell kill. Currently available mass culture techniques fall short on both of these requirements and therefore must be considered as unreliable. Until the preferential growth of tumour cells is possible the use of an agar clonogenic assay or DNA damage assays may be more suitable for predictive test on human tumour cells.

The use of ^{31}P NMR spectroscopy to monitor treatment-induced changes in tumour metabolism in animal models

J. C. M. Bremner, C. J. R. Counsell, J. Pearson, J. Samson, C. Thomas, P. J. Wood and G. E. Adams

^{31}P NMR has been used to observe *in vivo* metabolic changes occurring within tumours during growth or after application of treatments such as blood-flow modifiers, photodynamic therapy (PDT) and irradiation. NMR is non-invasive and is therefore useful in assessing the time-course of these changes within the same tumour for hours or days after the initiation of the treatment. Some work has been done where metabolic changes observed only hours after PDT have been used to predict the final response of tumours which do not occur until days after treatment. By altering blood flow to tumours it is possible to increase the effectiveness of various clinically applicable techniques. When it can be increased the radiosensitivity of tumours is also increased and when decreased the effectiveness of various bioreductive drugs may be enhanced as these agents are m ore toxic in the absence of oxygen. We have been using ^{31}P NMR spectroscopy, to monitor the metabolic response of many types of tumours to blood-flow modifiers. The degree of the changes incurred have been used to assess whether or not the radiobiological hypoxia has been altered significantly or if the modifier may be used in conjunction with bioreductive drugs to increase tumour toxicity. NMR can also detect other chemical nuclei such as carbon, fluorine and deuterium which may then be used in assessing cell damage, detecting hypoxia markers and measuring blood perfusion; all of which are experimentally and clinically relevant.

Flow cytometric nucleoid analysis in the prediction of bladder cancer response to radiotherapy

P. Anderson, T. H. Lynch, *D. M. A. Wallace, †G. M. Kondratowicz, R. P. Beaney and §A. T. M. Vaughan
*Departments of Immunology and *Pathology, University of Birmingham, †Department of Urology, Queen Elizabeth Hospital, Birmingham, and §Department of Radiotherapy, Loyola Medical School, Chicago, Illinois, USA*

Radical radiotherapy of patients with invasive bladder cancer has a local cure rate of 40–50%. There is no test which can accurately predict patient response to this treatment. It has been shown using a series of human squamous carcinoma and rodent cell lines that, following irradiation, radiosensitive cells contain DNA supercoils that are less effectively condensed by the DNA-intercalating dye ethidium bromide (EB). We have obtained single cell suspensions from either biopsy or urine samples of 105 patients with muscle invasive transitional cell carcinoma of the bladder. Cells were either irradiated with 12 Gy cobalt-60 gamma rays of left untreated. Cells were subsequently exposed to a 2M salt and detergent buffer producing intact DNA as supercoiled loops attached to the nuclear matrix, "the nucleoid". Condensation of nucleoids under the action of EB (50 μg/ml) was measured by laser light scatter from individual nucleoids within a flow cytometre. Nucleoids derived from irradiated cells were on average 15.5% larger than those from corresponding control cells (range −4.8 to +67%). Patients underwent a course of radical radiotherapy and residual disease was assessed by cystoscopic examination three months after completion of therapy. At present, data are available from 28 patients suitable for further analysis. These samples had an average of 58% nucleated cells of tumour origin. Of the patients studied, 2/12 (17%) with residual disease and 12/16 (75%) with no detectable disease at 3 months, gave nucleoids that were over 10% larger compared to unirradiated samples. These data indicate a correlation between immediate local tumour control and the behaviour of supercoiled DNA. Long term patient survival data is required to assess the usefulness of the technique as a predictive test of patients suitable for aggressive radiation treatment.

Response to radiotherapy assessed by flow cytometric analysis of sequential tumour biopsies

J. E. D. Dyson
Departments of Radiobiology and Radiotherapy, Tunbridge Building, Cookridge Hospital, Leeds LS16 6QB

Treatment-induced tumour cell death does not correlate well with tumour regression in the early stages of treatment due to the tumour stromal component. Assessment of tumour response to therapy by extent of regression can thus be misleading. In addition, therefore, to the prognostic value of flow cytometric analysis, its use to monitor response to radiotherapy by analysis of sequential biopsies during treatment has been investigated. Over 300 patients with cancer of the cervix uteri have been followed by weekly biopsies over the full 4–6 week treatment period. This has shown that both elimination of aneuploid peaks in death, can indicate tumour response to irradiation. The majority of aneuploid tumours show a consistently more rapid response to radiotherapy than diploid tumours, and this must betaken into account when judging response to treatment. By plotting changes in aneuploid cell content, and treatment induced cell death, as a function of radiation dose, and time of treatment, a profile representing the response of the tumour to therapy may be obtained. Comparison of such plots with histopathological assessment and clinical examination, carried out in parallel, has shown close agreement, but with the flow cytometric analyses on an earlier time scale.

Supported by the Yorkshire Cancer Research Campaign.

BUdR and Ki67 labelling in human tumour xenografts

C. S. Parkings, C. Bush, P. Price and G. G. Steel
Institute of Cancer Research, Sutton, Surrey, UK

Cell proliferation was measured in human tumour xenografts using *in vivo* bromodeoxyuridine (BUdR) labelling or Ki67 antibody staining. BUdR labelling was measured using either flow cytometry (FCM) or directly on tumour sections suing immunoperoxidase staining. Using the relative movement method of Begg et al (1986) the labelling index, S-phase duration (T_s) and potential doubling time (T_{pot}) were measured in cervix, breast and bladder tumour xenografts. Significant progression of BUdR-labelled cells occurred during the time after labelling, yielding average values of T_S from 7.4 to 9 hours and T_{pot} from 2.3 to 4.8 days. Measurement of BUdR-labelled cells on tumour sections yielded indices up to four times higher than from FCM. At present, it is uncertain if this discrepancy is due to under-estimation by FCM or over-estimation by peroxidase method. The discrepancy was not due to inclusion of newly divided BUdR-labelled cells appearing in the G_1 position. The potential doubling time would be reduced if these higher values of labelling index were used. Sub-optimal staining of the BUdR-labelled cells in the FCM or nonspecific labelling by Ki67 may contribute to this discrepancy. Cell proliferation was also measured using the Ki67 antibody, which recognizes a proliferation-related nuclear antigen. Ki67 indices were higher than BUdR labelling indices using either FCM or immunoperoxidase methods. Although the intertumour heterogeneity was large for each assay, it was possible to conclude that those tumours with low Ki67 indices had the longest T_{pot}. It is proposed that since Ki67 index shows ability to rank tumours of differing proliferation rates it should be included in those studies where BUdR labelling is currently being measured in isolation.

Proliferation of human tumours measured *in vivo* using BrdUrd: relation to outcome of radiotherapy

G. D. Wilson, N. J. McNally, C. A. Whitsed, S. Dische, M. I. Saunders and K. Lochrin.
Gray Laboratory and Marie Curie Research Wing, Mount Vernon Hospital, Northwood, Middlesex, UK

Proliferation is recognized to be one of the major factors contributing to the failure of conventional radiotherapy to cure some human tumours. Recently, there has been renewed interest in the use of altered fractionation schedules designed to exploit differences in the radiation response of early- and late-responding tissues. Compared with conventional fractionation, acceleration of treatment would be of particular benefit to patients whose tumours are capable of rapid proliferation. Until recently, the techniques available to estimate proliferation have been inadequate to fulfil the requirements to predict which treatment would be appropriate for a particular patient. A predictive assay is defined, in the context of radiotherapy, as a laboratory test predictive of the probability of tumour control in a patient treated with a given regime of radiotherapy independently of known clinical prognostic parameters. The assay should measure a biologically meaningful parameter rapidly and quantitatively, and it should inconvenience the patient as little as possible. The *in vivo* administration of BrdUrd to patients satisfies most of the requirements of a productive test. Using flow cytometry, both the L_I and the T_S can be calculated from a single biopsy taken several hours after an infection of 200 mg BrdUrd. From these parameters, the T_{pot} can be calculated. The T_{pot} is the shortest possible time a cell population can double its number taking into account the presence of dividing and non dividing cells but in the absence of any cell loss. Our results show that not only is there a wide variation in L_I among tumours of the same and different type but also that the T_S can be as variable as the L_I. Together these parameters produce T_{pot} values which show a wide range of heterogeneity within each tumour group. There appears to be a clear relationship between DNA aneuploid and proliferation parameters. diploid tumours have a shorter T_S and a lower L_I than aneuploid tumours. In head and neck tumours 65% of diploid tumours had a T_S less than the median value while 70% of aneuploid tumours had a T_S greater than this value. It is our belief that the L_I may be dictated by the T_S. The L_I may give an ambiguous measure of proliferation, when used alone, as a tumour with a low L_I but short T_S may possess the same T_{pot} as a tumour with a high L_I but long T_S. However, the overall measurement of proliferation, the T_{pot}, is shorter in aneuploid tumours. The median T_{pot} of diploid and aneuploid head and neck and lung tumours was 8.0 and 3.4 and 7.9 and 5.7 days, respectively. Although treatment will undoubtedly perturb the proliferation by the surviving cells in a tumour, it is our belief that the pre-treatment T_{pot} may be the best indication for the potential for proliferation during treatment. Bearing that in mind, 47% of all the tumours we have studied possess a T_{pot} of less than 5 days. Within the three major groups of tumours, 46% of head and neck tumour, 36% of lung tumours and 50% of cervix tumours possessed proliferative characteristics which may benefit from accelerating the treatment schedule. The prognostic significance of the parameters measured using this technique can only be assessed in a controlled, randomized clinical trial of conventional versus accelerated radiotherapy, in which the prediction that rapidly proliferating tumours do badly with longer treatment times can be properly assessed. *These studies are underway as part of the EORTC trial of accelerated fractionation and the multi-centre trial of CHART centred at Mount Vernon Hospital.*

The impact of S-phase fraction and tumour differentiation on response to adjuvant chemotherapy in node positive breast cancer

S. M. O'Reilly, *R. S. Camplejohn, †R. R. Millis, R. D. Rubens and M. A. Richards
*CRC Laboratories, Department of Medical Oncology, Charing Cross Hospital, London, *The Richard Dimbleby Department of Cancer Research, UMDS, St Thomas' Hospital, London SE1 7EH and †ICRF Clinical Oncology Unit, Guy's Hospital, London*

The influence of S-phase fraction (SPF), measured by DNA flow cytometry, and histological grade on outcome following adjuvant chemotherapy was analysed for 214 patients with node positive breast cancer. All patients were treated at Guy's Hospital as part of the Guy's/Manchester trial comparing combination chemotherapy with dyclophosphamide, methotrexate and 5-flourouracil (CMF) versus no adjuvant treatment. Adjuvant CMF significantly improved relapse free survival (RFS) for premenopausal patients whose tumours had an SPF $\leq$ 10% (control v. CMF, $p = 0.05$) and premenopausal patients whose tumours had an SPF > 10% (control v. CMF, $p = 0.003$). No significant improvement in RFS attributable to CMF was seen for either subgroup of post-menopausal patients (SPF $\leq$ 10%, $p = 0.2$; SPF > 10%, $p = 0.75$). When patients were divided into subgroups based on histological grade of tumour, an improvement in RFS attributable to CMF was seen for premenopausal patients with well differentiated (Grade 1 or 2) tumours (control v. CMF, $p = 0.03$) and premenopausal patients with poorly differentiated (Grade 3) tumours (control v. CMF, $p = 0.006$). Again, no improvement in RFS was noted for any sub-group of post-menopausal patients defined by tumour grade. These results extend our previous report that all sub-groups of premenopausal patients benefit from adjuvant CMF chemotherapy.

Measurement based sequential therapy in breast Cancer

A. E. Johnson
Mount Vernon Hospital, Northwood, Middlesex, UK

A new form of management of breast cancer has been developed in the Breast Study Centre at Mount Vernon Hospital: measurement based sequential therapy (MBST). All the standard forms of treatment are used with the proviso that the first management in every case should consist of short courses of single agent chemotherapy together with hormones. Frequent calliper measurements of the primary tumour during this initial systemic therapy have enabled the estimation of changing volumes in response to different treatments. Exponential regression lines have been fitted in relation to treatments. Earlier work form this centre has shown that, probably because of insufficient clonogenic cell kill by some schedules, the maximum possible steepness of slope is not always achieved. The slopes must therefore be interpreted in the light of histology obtained by needle biopsy (drill or Tru-Cut). The regression lines due to shrinkage, interpreted in the light of the histological appearances, have been used in a series of 102 patients in order to regulate management. The method of MBST is presented, illustrated by data from representative cases. The need for more than one predictive parameter is highlighted through examples. Preliminary results for a follow-up period from 3 to 11 years will be discussed in relation to both local control and long term survival. Pitfalls in the use of slopes owing to shrinkage to estimate growth rate and therefore to predict survival will be examined.

Prediction and measurement of tumour response to treatment — a commentary

S. Dische
Marie Curie Research Wing for Oncology, Mount Vernon Centre for Cancer Treatment, Northwood, Middlesex, UK

Predictive tests may influence the choice of treatment modality and alter the programming of the given management. Those discussed today, which may be performed prior to the decision as to treatment, include the determination of inherent radiosensitivity *in vitro* either by clonogenic mass of explant culture or by nucleoid production and the determination of the tumour cell kinetics using the cell sorter. During treatment the response may be assessed by flow cytometric analysis, NMR or clinical measurement. At this time some of the techniques, such as clonogenic cell assay, may seem impractical as predictors in clinical practice either because of the size of the sample required or because of the period of time which must elapse before the result is obtained. This should not deter in a thorough assessment in clinical trial for if shown to be of predicative value to is likely that modifications will be possible and the approach become, in time, a practical one. At this time it is probably an advantage not to be aware of the prediction at the time of commencement of treatment for the result would then not influence the choice and a fully unbiased assessment of the test can be made. We must recognize that there are many factors which influence the radiation response of a tumour and it is important that we bear all of them in mind when looking at predictors of response. For too long we regarded hypoxia as the dominant reason for radiation failure and in our efforts to correct hypoxia ignored other influences. At a time when repopulation and inherent radiosensitivity are the dominant interests we must not neglect hypoxia which has not been considered at this meeting today. Therefore all aspects of tumour biology must be considered in designing and programming treatment so as to give maximum tumour response and the minimum of change in normal tissues.

1991, *The British Journal of Radiology*, *64*, 287–288

Book reviews

Nonionizing Radiation Protection. Second Edition. Ed. by M. J. Suess and D. A. Benwell-Morison, pp. xiv + 346, 1989 (World Health Organization, Geneva), $34.40.
ISBN 92-890-1116-5

First published in 1982, this book was aimed at a professional readership to give guidance on a number of aspects of non-ionizing radiation sources. The book was intended to provide practical information on the health aspects of exposure to non-ionizing radiation and the scientific, hazard, protection, instrumentation and dosimetry information required for the establishment of a non-ionizing radiation control programme. The initial publication successfully met these aims and now, advanced in knowledge from research and experience, the author's have revised and republished this book as a second edition. All sections of this second edition have been revised, some more than others. Those dealing with radiofrequency radiation and low frequency electric fields have been retitled and rewritten.

The subject matter is divided into six sections: ultra violet radiation, both from solar and artificial sources; optical radiation, from one nanometre to one millimetre wavelength, with particular reference to lasers; infra-red radiation naturally occurring and that radiated from industrial processes; radio frequency radiation of 300 KHz to 300 GHz, a range that includes communications, navigation, industry and medicine; electric and magnetic fields at extremely low frequencies, 30–300 Hz, a range that contains the mains electricity supply frequency 50–60 Hz, which is covered in some detail; and, finally, the ultrasound section, a predominately medical section, dealing with the problems associated with both therapeutic and diagnostic ultrasound application.

Each section has been written by an international expert and reviewed prior to printing by a panel of experts. The result is a book in which, although the information on each type of non-ionizing radiation source is presented in an individual way, the standard of the information is consistently high. The variation in treatment of the subjects can be accounted for by the disparate nature of the sources, perceived degree of hazard and the individual styles of the authors. The presentation of the subjects in this way may introduce difficulties for the reader who is intending to use the book for comparative study of the various sources of non-ionizing radiation.

All sections cover, to a greater or lesser extent, previously identified key areas, physical aspects, biological processes, hazards, safety standards, protection, dosimetry and application of the source.

This is a worthwhile book not only for scientists or engineers, but also for any reader seeking an introduction to non-ionizing radiation. The information contained in each section is extensive, though it is summarized by the use of conclusions at the end of the section. Diagrams and tables have been used extensively to present the information in an understandable way.

The introduction to the book uses the wavelength, frequency and photon energy to define the radiation types covered in the book and a short discussion of the comparative hazards. However, the reader may feel the lack of a chapter addressing non-ionizing radiation as a single subject, though the book has been completed with a general chapter on regulations and enforcement procedures. A useful glossary of non-ionizing radiation terms is also included, as are the results of some extensive literature searching represented by some 650 references for further reading.

M. Davis

Advances in Cerebral Spect Imaging. Ed. by R. L. Van Heertum and R. S. Tikofsky, pp. 129, 1989 (Lea and Febiger, Philadelphia), £27.97.
ISBN 0-8121-1260-1

This is a small but very handy and useful 130 page book on the clinical utility of single photon emission computed tomography (CT) using I-123-labelled N-isopropyl-iodoamphetamine. The book contains sections on technique, normal and correlative anatomy, pitfalls, clinical disease states and an appendix covering radiopharmaceuticals and equipment, quality control and manufacturers' equipment protocols. A bibliography and an index are also available. The clinical disease entities that are discussed include cerebrovascular disease, dementias, seizure disorders, psychiatric disorders and a group of miscellaneous disorders. The main text of the book consists of the familiar structure of a case presentation, a selection of CT and cerebral blood flow maps, including a short discussion and a highlight of a particular teaching point.

This small book is a pleasure to read, contains a wealth of useful information and, despite the fact that the images are obtained with the older I-123-labelled blood flow tracers rather than the more modern ^{99m}Tc-labelled tracers, they are of consistently good quality. Most images are reproduced in black and white. There is some variation in the acquisition protocols of the clinical cases, since they come from a variety of authors who have contributed case material, but again this does not detract from the overall well edited and well organized presentation.

The book is well priced, and I believe deserves to be read by a wide audience including neurologists, psychiatrists, radiologists and nuclear medicine physicians. Most technicians and radiographers would also find this book very useful.

P. J. Ell

Guidelines for the Routine Performance Checking of Medical Ultrasound Equipment (Report 58), Ed. by R. E. Richardson, pp. 53, 1989 (Institute of Physical Sciences in Medicine), £9.80.
ISBN 0-904181-553

When clinical judgements depend on measurement, the accuracy of those measurements are of paramount importance. When alterations in image appearance are to be evaluated, then the highest possible image quality should be generated. This booklet explains how to ensure that ultrasonic diagnostic equipment performs so that measurements are accurate, and so that image quality is as high as possible. It is a practical handbook, informing the reader what quality assurance tools to buy, from whom and (at 1987 prices) the cost. The text is well supported by images showing examples of the results of the tests, and contains useful warnings of difficulties and errors that may be encountered.

The book provides excellent advice for those carrying out routine quality assurance tests on imaging equipment. It also includes guidance for the testing of both Doppler devices and physiotherapy machines. The authors clearly recognize some limitations in the text, and realize that, in such a rapidly developing area as clinical ultrasound, testing procedures need also to evolve, and such detailed information as is presented may quickly date (was the dollar exchange rate $1.30 to the pound so recently?). A second edition of the book should probably include further details about the use of hydrophones and acoustic power measurement in diagnostic beams, and perhaps also some guidance on measurement in extracorporeal lithotripsy. Nevertheless, the authors are to be congratulated on putting together a thoroughly practical guide, which will be useful to anyone whose responsibility includes the routine quality assurance of ultrasound equipment.

F. A. DUCK

Basic Principles of Radiographic Exposure. By D. C. DeVos pp. xi + 145, 1990 (Lea and Febiger, Philadelphia), £12.42.
ISBN 0-8121-1222-9

This is an American book on the basic principles of radiographic exposure and is in reality a set of lecture notes for student radiographers, covering the subject in great detail.

Each chapter starts with a list of objectives and ends with a set of self-assessment questions (answers at the back) and some most useful practical exercises. The majority of the chapters are short and all achieve their objectives. The early chapters on basic production and properties of X rays, exposure factors and inverse square law are aimed at readers with little mathematical knowledge, as the simple equations are worked out in detail. I would expect all student radiographers to have a considerably higher educational standard than that implied by these chapters.

Once past that hurdle, the book has chapters on contrast, unsharpness, filters, grids, film and beam defining devices. It continues with a chapter on geriatric and paediatric radiography, and one on the effects of pathology on exposures. Automatic exposure controls are included, and it closes with a chapter on preparing radiographic exposure charts and the interpretation of rating charts.

The text is illustrated with simple line diagrams well labelled and adequately serving their purpose. The radiographic reproductions were generally not of the same standard. They did not always demonstrate the point the text was making, and many were below publication standard with markers upside down and back to front. Given the difference in spelling, there are still some spelling mistakes, and I found the expression "exposure time in vulgar fractions" irritating.

There is a fundamental difference in approach to that taught in this country, in that they base tube potential settings on caliper measurements of patient thickness. However, any student who reads, learns and inwardly digests this book will never have any problem, in any circumstance, in deciding what exposure values to set.

In conclusion I think it would be a useful addition to any radiography school library for the practical exercises alone.

E. FORSTER

CT and MRI of the Liver and Biliary System. Ed. by P. M. Silverman and R. K. Zeman, pp. xii + 327, 1990 (Churchill Livingstone, New York), £55.00.
ISBN 0-443-08612-5

Professors Silverman and Zeman have succeeded in maintaining the very high standard of the "Contemporary Issues" series. They should be congratulated, along with the series editor Elliot Fishman. This latest offering tackles a difficult subject. The only pity is that ultrasound is not considered more, but at the outset it is acknowledged that computed tomography (CT) and magnetic resonance imaging (MRI) are principally used when ultrasound leaves unanswered questions.

The editors themselves prepared the excellent chapters on anatomy and technical aspects of CT, thus uniformity of message is ensured. I may even have to consider altering my own policy of a preliminary non-contrast examination as a routine. The authors do indicate a few areas where controversy still exists. The role of delayed CT imaging is also well aired.

I learnt a lot from the section on MRI of the liver. However, I remain to be convinced that there are all that many true indications given the pressure on MRI machine time in the UK. As with many such review chapters, each disease process is often discussed in isolation from the clinical problem. Thus it requires close reading to be reminded that the MRI appearances of an haemangioma are not pathognomonic; it is possible to be fooled by a simple cyst. Some overlap between chapters is inevitable, most is useful reinforcement. Occasionally inconsistencies proved annoying. For example, the proportion of patients with the diffuse (rather than solitary or multifocal) type of hepatocellular carcinoma is variously quoted between 5% and 25%. Such discrepancies are confusing for those studying for (or setting) multiple choice question examinations.

Benign masses of the liver proved an interesting section, particularly the discussion on focal nodular hyperplasia and hepatic cell adenoma. Diffuse liver diseases are well covered, with a particularly good discussion on the various features of cirrhosis and fat infiltration. However, while it is true that coexistent fat infiltration may reduce the CT attenuation of liver in Wilson's disease, the main reason that the attenuation is not elevated is that there are only a few micrograms of excess hepatic copper in this condition.

The chapter on the gallbladder and bile ducts provided a sensible approach to help establish the cause for an obstruction. I particularly liked the classification into three groups of diseases, namely those that usually, occasionally and seldom produce a mass. The final chapters covered paediatric and interventional topics; both were good.

This volume is well produced with few errors, and the figures have been well reproduced. It contains a plethora of recent (and useful) references and, at £55, is about par for such a book. All CT units should have access to this series; whether individuals will buy it for themselves remains to be seen.

ADRIAN K. DIXON

1991, *The British Journal of Radiology*, *64*, 479–484

VOLUME 64 NUMBER 762 JUNE 1991

The British Journal of Radiology

Quickscan: Doppler ultrasound emulation of angiography—its value prior to arteriography in peripheral vascular disease

By N. M. deSouza, MRCP, *D. H. King, DipPhys, *P. Pilgrim, BSc, *P. Bates, BSc, J. F. Reidy, FRCR and *R. G. Gosling, PhD

Departments of Radiology and Ultrasonic Angiology, Guy's Hospital, St Thomas' Street, London SE1 9RT, UK

(Received August 1990 and in revised form January 1991)

Keywords: Doppler ultrasound, Arteriography, Peripheral vascular disease

Abstract. The prevalence of peripheral vascular disease demands a quick, reliable, non-invasive technique for initial assessment. We have devised a new method which combines the two physical principles that (1) Doppler shift is proportional to blood velocity and (2) blood velocity is inversely proportional to arterial cross-section with the ability to track probe position using a non-contacting method. An image of the probe track and any arterial narrowing is shown superimposed on an outline of the patient. Pressure measurement, scan and graphics with final report take about 20 minutes. The accuracy of this system in peripheral vascular disease was evaluated. Thirty-one patients underwent quickscan (QS) and arteriography within an average time of 7 days. Abdominal aorta, common iliac–common femoral, superficial femoral and popliteal artery segments were graded independently as normal, significant stenosis (> 50% of diameter) or occluded by both techniques. Of 197 segments, QS correctly assessed 106 normal, 22 stenosed and 28 occluded segments. Four equivocal angiographic stenoses were normal on QS and three severe stenoses were graded occlusion. Fifteen segments on angiography and five on QS were not assessed. For the iliac and superficial femoral artery segments, sensitivity and specificity averaged 77% and 86%, respectively, for all grades. Aortic statistics were invalid (only one significant lesion). Six out of eight popliteal occlusions were correctly diagnosed by QS, but no popliteal stenoses were detected out of six shown on arteriography. Low numbers may contribute to this discrepancy but an improved popliteal scanning method may be necessary. We find initial QS an invaluable aid to direct percutaneous angiography and to indicate potential sites for angioplasty.

Arteriography is an invasive technique associated with a specific morbidity (Hessel et al, 1981), making it an unsuitable screening method in lower limb claudication. However, it is essential in the assessment of peripheral vascular disease before percutaneous angioplasty and surgery, and is held almost universally as the "gold standard", although some authors would disagree (Shearman et al, 1986). Lower limb arteriography restricted to a single view may overestimate or underestimate the significance of an assymetric plaque (Moore & Hall, 1971). Multiplane angiography has been used in cerebral and coronary assessment to reduce such errors, but lower limb arterial assessment is usually confined to single-plane studies, with occasionally an additional oblique view.

The resistance to flow of an isolated stenosis is primarily dependent on the reduction in luminal cross-sectional area and the effect of two or more stenoses is dominated by the lesion with the smallest cross-section, although other factors such as length of the lesion and degree of turbulence may contribute (Logan, 1975). Ultrasound scanning has, for several years, been used as an adjunct to arteriography. It commonly uses velocity ratio data to supply area information (Grigg et al, 1988). For some years we have been using hand-held continuous-wave (CW) Doppler before arteriography to separate stenosis from occlusion and to guide arteriographic approach. Our methods have undergone continuous refinement and evolution resulting in a simplified measurement protocol which we have called "Quickscan". This procedure records the Doppler frequency ratio from flow at adjacent points, read directly from a calibrated spectral display, and combines it with a video probe-tracking method designed to display lesions in their correct anatomical locations. Lesions are graded on the relative Doppler shifts from changes in flow-velocity and so emulate multiplane angiograms. In this paper, Quickscan is correlated prospectively with arteriography and with calf/brachial pressure indices to demonstrate its ability to detect significant lesions and to separate stenosis from occlusion, thus assessing its value before arteriography.

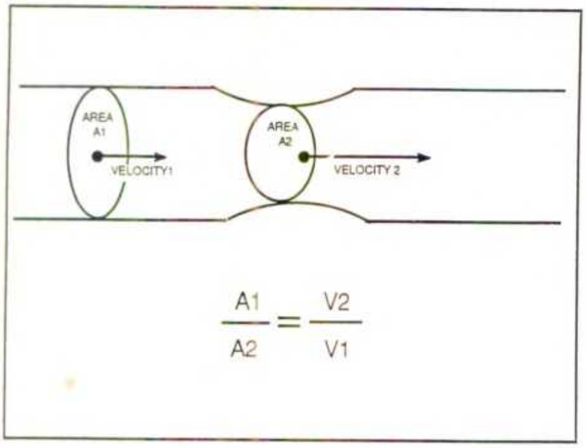

Figure 1. A diagrammatic vessel showing the relation of spatial mean velocity to luminal cross-sectional area.

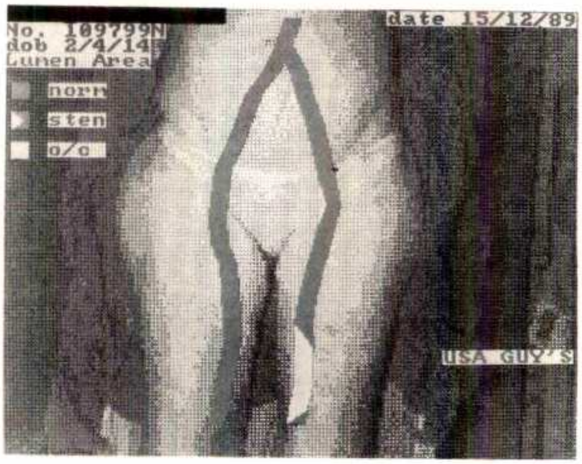

Figure 2. Quickscan with arterial pathways superimposed on an image of the patient; the white shaded area denotes stenosis.

Methods

Principles

Velocity ratio. In an idealized model of a stenotic artery where there are no side branches so that flow, Q, is constantly equal to $A \times V$ (Fig. 1), stenotic area ratio is inversely proportional to velocity ratio. Theoretically the most appropriate value of V would be the time-averaged mean of successive instantaneous spatially averaged velocities over one or more cardiac cycles. The velocity ratio would then be obtained from values within the stenosis as compared with an upstream reference value. However, in the presence of electronic noise and flow disturbance, peak systolic velocity is less prone to errors than mean velocity estimation, and peak velocity ratio has been favoured by a number of workers (Jager et al, 1985; Kohler et al, 1987), and is adopted in the Quickscan. An additional assumption has to be made in order to compute area ratio from such peak velocity data, *i.e.* that the velocity profile is unchanged when passing from the normal lumen to the stenosed region. Present evidence tends to support this assumption. Flat or blunt velocity profiles have been shown to exist in systole in normal calibre peripheral transit arteries (Keller et al, 1976) and flat velocity profiles have been predicted within a stenosis (Lew & Fung, 1970). However, under certain conditions and in small calibre vessels the velocity profile may become parabolic upstream and remain flat within the stenosis. In this case, area ratio may be underestimated by a factor of 2.

Frequency ratio. The CW Doppler probe used in the Quickscan method is calibrated only in terms of peak systolic frequency since the probe-vessel angle is unknown. However, if the probe is moved in sufficiently small increments along the vessel axis it can be assumed that the probe-vessel angle has not changed between successive samples, and thus frequency ratio should be equivalent to velocity ratio. In practice, by sampling at approximately 1 cm intervals, angle variation has relatively little effect on frequency ratio, and frequency ratio can be substituted for velocity ratio in the area ratio calculation.

Equipment

Quickscan emulates an arteriogram by superimposing arterial pathways over an anatomical outline of the patient (Fig. 2). The system has a number of features that make it particularly easy to use: (i) there are no mechanical constraints for the operator, (ii) probe position is tracked using a non-contacting video-tracking method, and (iii) peak frequency data and commands are passed to the computer (Commodore Amiga 500) by a voice recognition system (Marconi Macrospeak). Trailing microphone and earphone cables are avoided by using a short-range RF link (Azden Wireless Microphone System) and an ultrasound couplant is supplied direct to the probe tip via an infusion pump. These features allow the operator to concentrate on the scan process, leaving both hands free to guide the probe. In this way, optimum pressure can be maintained over the abdomen to smooth gas bubbles away from their location over the iliac arteries.

Scan process

Doppler probe position is monitored by placing a TV camera above the patient and tracking the position of a light emitting diode (LED) light source mounted on the probe tip (Fig. 3). Information on probe position and Doppler shift frequency is collected by a computer as the operator scans along the centre line of the artery. The probe is moved at approximately 1 cm increments along the expected path of the artery, from the adductor hiatus to the aorta, maximizing Doppler signal strength using small lateral movements of the probe. A sample is initiated by the operator each time the peak systolic frequency is read from a calibrated spectral display (Spectrascan Spectral Analyser, Doptek). If the patient is turned prone, Quickscan can demonstrate the popliteal and tibial arterial pathways.

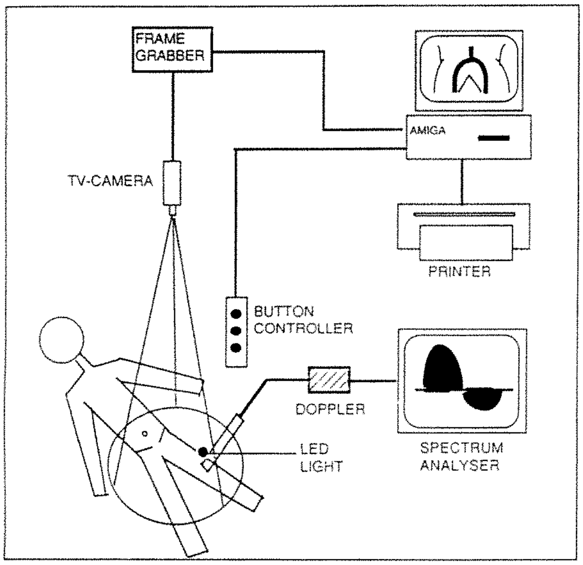

Figure 3. Diagrammatic representation of the Quickscan system.

Table I. The nine-level scale of area stenosis used in the Quickscan display

Yellow pixel Intrusion	1	2	3	4	5	6	7	8	9
Area stenosis	3:1	4:1 to 5:1	6:1 to 7:1	8:1 to 9:1	10:1 to 11:1	12:1 to 13:1	14:1 to 15:1	16:1 and >	Block

Normal arterial pathway is displayed as nine pixels wide in red. Area stenosis = Doppler frequency ratio, which is rounded up to the nearest whole number during the examination.

The artery is represented by a continuous red track of nine pixels width on the computer screen. When a localized Doppler shift increase greater than or equal to 3:1 is noted, the red track is overwritten with a contrasting yellow mark one pixel wide, indicating narrowing. The most severe grading of stenosis is for an area ratio reduction of 16:1 or more. This almost fills the lumen with eight yellow pixels. An occlusion completely overwrites the lumen in yellow. This "step" scale is indicated in Table I. It should be noted that a 3:1 area stenosis corresponds to about a 42% decrease in diameter.

The presence of occlusion can be reliably detected using one of two signs, alternating retrograde and antegrade flow patterns on spectral display, and absence of arterial signal when the vein can be clearly heard. When the scan is complete, a voice command turns on an overhead photoflood lamp which highlights skin tones, revealing the patient outline. This "snapshot" image is then frame grabbed, saved on disk and displayed on the computer screen. The approximate location of the aorta, iliac and common femoral boundaries are then located by marking skin crease and umbilicus co-ordinates on the screen using a mouse-driven cursor. The final image, together with an automatically written

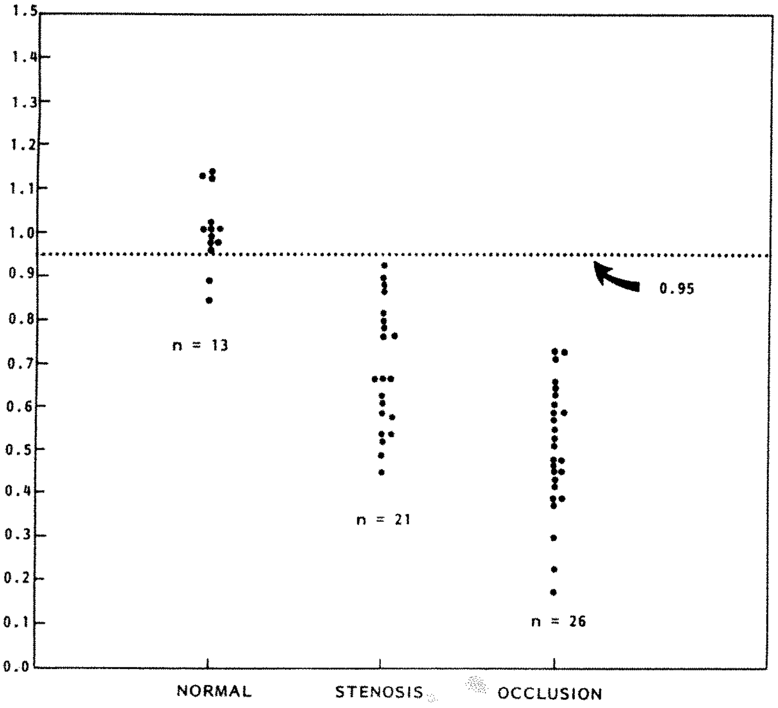

Figure 4. Values of CBI in normal limbs and in stenosis and occlusion.

report, is copied by a colour inkjet printer (Hewlett Packard Paintjet), ready for inclusion in the patient's notes.

Calf/brachial index

Quickscan has built into the hardware an arrangement that automates the measurement of calf/brachial pressure indices (CBI). This system is also voice controlled, the data being saved on disk for inclusion in the final report. In our laboratory the CBI was found to be 1.15 ± 0.10 in a sample of 40 normal limbs chosen at random from those working in the hospital. The CBI threshold for optimal separation between normal and abnormal was therefore set at two standard deviations below the mean, *i.e.* 0.95. This accords with the threshold for ankle/arm systolic pressure ratio at rest used by Laing (1984) in a much larger study. In diseased limbs, the CBI ranged from 0.18 to 0.94; CBI, however, does not separate significant stenosis from occlusion (Fig. 4).

Arteriography

Lumbar aortography involved an intra-arterial approach in all patients with a conventional film technique, which was supplemented with digital angiography and oblique views as necessary.

Assessment

Thirty-one patients (aged 39–92 years, mean 62 years) referred for arteriography for clinically suspected peripheral vascular disease were evaluated prospectively. They underwent Quickscan 1–42 days (mean 7 days) before arteriography. Arterial segments were divided into aortic, common iliac–common femoral, superficial femoral and popliteal, thereby assessing seven segments per patient. Each segment was graded normal, significant stenosis, occlusion, or not assessed by a single and different observer for each of the techniques. Significant stenosis was taken as a >3:1 frequency shift on Quickscan and a >50% reduction in arterial luminal diameter on angiography (<50% being normal). In our study it was shown that although peak frequency in the iliac pathway exceeded that in the superficial femoral artery by an average of 73%, the peak frequency ratio was only 17% higher in the iliac than the superficial femoral artery. In no case did the frequency ratio exceed a value of 2:1 in either pathway, and therefore a ratio of 3:1 was chosen as the threshold for abnormality. This is equivalent to a diameter stenosis of 42%, approximating to the commonly accepted threshold for haemodynamic significance of 50%. Occlusion on Quickscan was recognized by absence of arterial signal in the region where the vein was heard and by alternating retrograde and antegrade flow patterns on spectral display.

Table II. Correlation of angiography and Quickscan for each of the arterial segments

	Angiography			
Quickscan	Normal	Stenosis	Occlusion	Totals
Iliac/SFA				
Normal	48(30/18)	12(7/5)	1(1/0)	61
Stenosis	8(8/0)	21(10/11)	0(0/0)	29
Occlusion	2(0/2)	3(1/2)	22(3/19)	27
Totals	58	36	23	117
Popliteal				
Normal	28	6	2	
Stenosis	0	0	0	
Occlusion	7	1	6	

Kappa $\equiv (P_0 - P_C)/(1 - P_C) = 0.64$, where P_0 = diagnostic accuracy, *i.e.* $P_0 = \frac{48+21+22}{117} = 0.78$, and $P_C \equiv$ [sum of the cross-products of the totals]/[total number]^2. Thus $P_C = [(61 \times 58) + (29 \times 36) + (27 \times 23)]/(117)^2 = 0.38$.
Note: Kappa is a measure of the agreement between two methods or tests after chance agreement has been removed. Perfect agreement gives Kappa = 1.0 (Cohen, 1968).

Results

Of a potential 217 segments, 197 were satisfactorily examined by Quickscan and arteriography. There was only one aortic stenosis (which was correctly identified on Quickscan) and no aortic occlusions in this series, so aortic segments were not included in the statistical analysis. For the iliac–common femoral segments (60), there were four occlusions, 18 stenoses and 38 normal as assessed by angiography. For the superficial femoral artery (SFA) segments (57), there were 19 occlusions, 18 stenoses and 20 normal on angiography (Table II). Of the seven angiographic stenoses that were assessed as normal on Quickscan, four were considered equivocal lesions on review of the arteriograms. Three angiographically severe stenoses were graded occlusion on Quickscan.

In the popliteal segments, Quickscan correctly diagnosed six out of eight occlusions, but none of the six significant stenoses were detected. This was because

Table III. Sensitivity and specificity of Quickscan compared with angiography as the "Gold Standard"

	Sensitivity (%)	Specificity (%)
Iliacs		
Occlusion	75	98
Stenosis	56	81
Normal	79	64
SFA		
Occlusion	100	88
Stenosis	61	100
Normal	90	86
Popliteal		
Occlusion	75	81
Stenosis	0	100
Normal	80	88

popliteal artery imaging in the supine position was difficult. Popliteal scanning is time-consuming and, therefore, scanning in the prone position was reserved for those patients with evidence of tibial disease alone, whilst in the standard scan the popliteal area is examined in the supine position with the knee bent. This simple but limited technique is applied exclusively in the correlation shown here. However, a parallel study using the same protocol on femoro-popliteal grafts showed a higher sensitivity and specificity with Quickscan detecting three out of four distal popliteal graft stenoses. The overall comparison of Quickscan with angiography is shown in Table II together with the correction for agreement by chance: Kappa = 64%. It should be noted that this compares favourably with the Kappa value of 63% reported by Slot et al (1981) for corrected agreement achieved by two radiologists independently reading the same radiographs for >50% stenosis and occlusion. The sensitivity and specificity for each of the grades in the segments is shown in Table III. The overall sensitivity and specificity of Quickscan for all grades in both these segments averaged 77% and 86%, respectively.

Two separate sub-groups were selected from the correlation data. All limbs with either single-level stenoses or no disease as shown by (a) angiography ($n = 28$; iliac 7, femoro-popliteal 11, no disease 10) and (b) Quickscan ($n = 27$; iliac 10, femoro-popliteal 6, no disease 11) were then correlated with an independent standard—CBI. A threshold of 0.95 was used to differentiate normal from abnormal vessels. Sensitivities and specificities of Quickscan and arteriography compared with CBI as the standard are shown in Table IV. Angiography overscored by 30%, recognizing "significant stenosis" where there was no significant pressure drop, and missed 17% of significant lesions (CBI > 0.95), whereas Quickscan missed 12% of significant stenoses but had no false positives.

Discussion

In the critical assessment of the severity of peripheral vascular disease, the limitations of even detailed film arteriography with extra and oblique views are well known. In diffuse disease with irregular and eccentric stenoses and intraluminal plaques, attempts to quantify the degree of stenosis based on a comparison of stenotic diameter with that of normal adjacent artery are likely to be inaccurate, particularly when the stenosis is in the 50% range. The case for arteriography as the "gold standard" in all except occlusions, severe stenoses and unequivocally normal arteries is, therefore, poor.

Table IV. Sensitivity and specificity of Quickscan and angiography compared with CBI as the "Gold Standard" in 28 single-level angiographic stenoses

	Sensitivity (%)	Specificity (%)
X ray	83	70
Quickscan	88	100

The use of duplex Doppler scanning techniques to evaluate peripheral arteries has been demonstrated to be superior to other indirect methods (Kohler et al, 1987). Like duplex Doppler, Quickscan allows an assessment along the whole length of the artery from the aorta to the popliteal to detect focal areas of significant stenosis. Unlike the duplex method, where a single extremity takes up to an hour to examine and a complete study 2 hours or more (Kohler et al, 1987), Quickscan takes 20 minutes, which includes measuring simultaneous calf and brachial pressure indices and providing an instantaneous graphic print-out.

It is of interest that four of the seven iliac stenoses (as assessed by arteriography) were assessed as normal on Quickscan. On reviewing the arteriograms, the stenoses, though categorized as such, had all been assessed as borderline. Further evidence against assuming that arteriography is the "gold standard" comes from analysis of the 28 cases where there was a single-level stenosis in one limb. Comparison of Quickscan and arteriography using the CBI as the indicator of significant stenosis showed a similar sensitivity for both Quickscan and arteriography, but Quickscan produced no false positives compared with 30% by arteriography.

Jager et al (1985) demonstrated a sensitivity of 77% and a specificity of 98% of duplex Doppler compared with angiography for detecting a >50% stenosis. The results were not affected by multi-segment disease. Kohler et al (1987), in a prospective study of 32 claudicants, similarly showed a sensitivity of 82% and a specificity of 90% in the iliac and superficial artery segments. Our results with an overall sensitivity of 77% and specificity of 86% were very similar. Our popliteal artery results in stenotic disease were poor and initially a larger number of popliteal lesions needs to be assessed by Quickscan. It may be that a revision of popliteal scanning method viz. turning the patient prone may be necessary.

We have found Quickscan to be invaluable in the following circumstances. First, when the CBI is in the normal range and the Quickscan shows no evidence of haemodynamic abnormality, arteriography is not usually indicated and can be avoided. Secondly, Quickscan objectively assesses the severity of disease and provides a baseline study. Thirdly, Quickscan differentiates fairly effectively between stenotic and occlusive disease and demonstrates localized stenoses that are ideally suited for angioplasty and at risk of progressing to an occlusion. Angioplasty is then indicated with provisional arrangements being made for a short hospital admission. Some elderly patients with moderately severe claudication may only be candidates for angioplasty. If Quickscan suggests major occlusive disease, and if surgery is not considered an option, there would then be little indication for arteriography. Fourthly, Quickscan may focus attention on a particular area so that further views are obtained. Stenotic disease can sometimes be difficult to demonstrate even with detailed film arteriography. A lesion may be hidden by another artery (*e.g.* proximal SFA by the profunda), not clearly opacified or a particular segment (*e.g.* the common and external iliac) may not be optimally shown on arteriography. Normal findings on Quickscan may obviate the need for further views. Finally, we have found that Quickscan usefully directs angiographic approach, particularly in major aorto-iliac disease. Assessment of the femoral pulse may guide the angiographer but it is well known that this may be misleading. If the Quickscan suggests aortic or bilateral iliac occlusion, then an intra-arterial femoral study is not indicated and we would then advocate an intravenous digital study. Alternatively, if Quickscan shows major aortic or bilateral common-iliac stenotic disease, we would plan an intra-arterial study with a view to proceeding to angioplasty.

In conclusion, Quickscan cannot replace arteriography but supplements it by providing an inexpensive, quick, non-invasive screening technique for the initial assessment of peripheral vascular disease, for planning therapy and for subsequent follow-up. We believe that all patients who are being considered for arteriography should initially have a Quickscan or some similar Doppler study.

References

Cohen, J., 1968. Weighted Kappa. *Psychological Bulletin, 70*, 213–220.

Grigg, M. J., Wolfe, J. H., Tovar, A. & Nicolaides, A. N., 1988. The reliability of duplex derived haemodynamic measurements in the assessment of femoro-distal grafts. *European Journal of Vascular Surgery, 2*, 177–181.

Hessel, S. J., Adams, D. F. & Abrams, H. L. 1981. Complications of angiography. *Radiology, 138*, 273–281.

Jager, D. A., Phillips, D. J., Martin, R. L., Hanson, C., Roederer, G. O., Langlois, Y. E., Ricketts, H. J. & Strandness, D. E. Jr, 1985. Non-invasive mapping of lower limb arterial lesions. *Ultrasound in Medicine and Biology, 11*, 515–521.

Keller, H. M., Meier, W. E., Anliker, M. & Kumpe, D. A., 1976. Non-invasive measurement of velocity flow profiles and blood flow in the common carotid artery by pulsed Doppler ultrasound. *Stroke, 7* (4), 370–378.

Kohler, T. R., Nance, D. R., Cramer, M. M., Vandenburghe, N. & Strandness, D. E. Jr, 1987. Duplex scanning for diagnosis of aortoiliac and femoropopliteal disease: a prospective study. *Circulation, 76*, 1074–1080.

Laing, S., 1984. A one-minute exercise test in measurement of peripheral arterial disease. PhD Thesis, University of London.

Lew, H. S. & Fung, Y. C., 1970. Entry flow into blood vessels at arbitary Reynolds number. *Journal of Biomechanics, 3*, 23–38.

Logan, S. E., 1975. On the fluid mechanisms of human coronary artery stenosis. *IEEE Transactions on Biomedical Engineering, BME-22*, 327–334.

Moore, W. S. & Hall, A. D., 1971. Unrecognized aorto-iliac stenoses. A physiologic approach to the diagnosis. *Archives of Surgery, 103*, 633–638.

Shearman, C. P., Gwynn, B. R., Curran, F., Gannon, M. X. & Simms, M. H., 1986. Non-invasive femoro-popliteal assessment, is that angiogram really necessary? *British Medical Journal, 293*, 1086–1089.

Skidmore, R. & Woodcock, J. P., 1980. Physiological interpretation of Doppler-shift waveforms. II. Validation of the Laplace transform method for characterization of the common femoral blood velocity/time waveform. *Ultrasound in Medicine and Biology, 5*, 219–225.

Slot, H. B., Strijbosch, L. & Greep, J. M., 1981. Interobserver variability in single plane aortography. *Surgery, 90*, 497.

1991, *The British Journal of Radiology*, *64*, 485–488

Duplex sonography in splenomegaly

By *L. Jarvis, FRCR, ‡P. G. Cook, FRCR, *†C. M. James, MRCP, MRCPath, †M. Rose, MB, BS, †A. G. Prentice, FRCP, MRCPath and P. A. Dubbins, FRCR

Departments of Diagnostic Ultrasound and †Clinical Haematology, Plymouth Group Hospitals, Plymouth, UK

(*Received August 1990 and in revised form September 1990*)

Keywords: Doppler ultrasound, Spleen, Splenomegaly

Abstract. The aetiology of splenomegaly is seldom clear from either clinical or imaging assessment of the spleen. In the majority of cases sonographic assessment of the spleen produces a homogeneous enlargement of variable echodensity, but with very poor correlation with pathology. A study has been undertaken to assess the Doppler characteristics of the splenic artery in splenomegaly, excluding cases of portal hypertension in an attempt to provide further diagnostic information. Duplex assessment of 18 normal subjects and 10 patients with splenomegaly due to five different causes was undertaken. Analysis of waveform, peak frequency and pulsatility index were compared and failed to demonstrate any significant change. In the normal subject there is a broad systolic spectrum related to the tortuosity of the splenic artery, with persistence of forward flow throughout diastole, a reflection of the low peripheral resistance of the spleen. In splenomegaly the broad systolic spectrum is unchanged, since vessel tortuosity persists. Pathological and physiological assessment of the spleen in splenomegaly shows that a low resistance circulation persists, explaining maintenance of the diastolic flow pattern in splenomegaly. Increased blood flow to the spleen in splenomegaly occurs either as a result of an increase in vessel diameter or an increase in flow velocity, or a variable combination of the two which does not seem to be governed by specific pathology. An increase in peak frequency in some cases reflected some increase in flow velocity but provided no useful correlation. Analysis of the pulsatility index supported the above findings without adding further information.

Real-time ultrasound is now an established technique for the investigation of the intra-abdominal organs. The spleen is well seen in the majority of cases and the sonographic appearance of the normal spleen (Niederau et al, 1983) and the diseased spleen (Mittelstaedt & Partain, 1980; Kane & Katz, 1982; King et al, 1985) have been described. The clinical assessment of splenomegaly is non-specific, and in many cases sonographic assessment of the spleen gives no further clues to the cause of a diffusely enlarged spleen. The whole range of haemopoietic and myeloproliferative disorders producing splenomegaly may give identical appearances on ultrasound.

Developments in pulsed Doppler equipment have now made it possible to obtain non-invasive assessments of blood flow in major intra-abdominal vessels (Atkinson & Wells, 1977; Taylor et al, 1978; Gill, 1979) and characteristic time–velocity spectra for these vessels have been described (Taylor et al, 1985; Taylor & Burns, 1985). The blood flow through the spleen increases up to ten-fold in splenomegaly, with a consequent increase in flow through the splenic artery and vein and hepatic portal vein. The splenic vein and hepatic portal vein have been assessed by duplex ultrasound in cases of portal hypertension (Zoli et al, 1986; Ohnishi et al, 1985), but only in cases of chronic liver disease.

The purpose of this study is to assess the splenic artery and vein and the hepatic portal vein in patients with established splenomegaly, using duplex Doppler ultrasound to assess whether the time–velocity spectrum improves specificity of diagnosis.

Method

A prospective study was performed on 19 normal volunteers and 10 patients with known splenomegaly. The volunteers were all normal subjects, mostly members of staff of the Department of Diagnostic Radiology, aged from 20 to 79 years. Patients with splenomegaly were referred from the Department of Clinical Haematology, having been fully investigated with the cause of their disease established. Patients with splenomegaly and portal hypertension secondary to liver disease were excluded from the study. All subjects gave informed consent to the procedure.

Subjects were prepared as for a standard upper abdominal ultrasound examination. The upper abdomen was imaged using the Advanced Technology Laboratories Ultrasound Imager with the Advanced Technology Laboratories Pulsed Doppler Flow Analyser and 3.5 MHz or 5 MHz real-time sector transducers. In each case the spleen was imaged and the maximum length was measured. The splenic artery and vein and hepatic portal vein were imaged and the presence of variceal

---

Address for reprint requests to: Surgeon Commander L. J. Jarvis, RN, Department of Radiology, Royal Naval Hospital, Haslar, Gosport, Hampshire PO12 2AA, UK.

*Present address: Royal Naval Hospital, Haslar, Gosport, Hampshire, UK.

‡Present address: Royal Cornwall Hospital, Truro, Cornwall, UK.

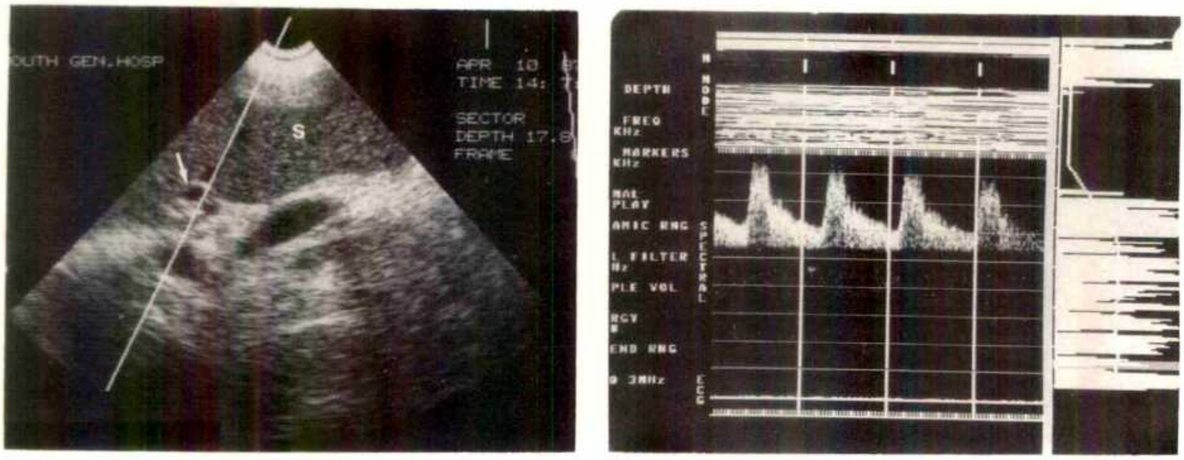

(a) (b)

Figure 1. (a) Longitudinal/oblique ultrasound image to the left upper quadrant, showing Doppler sampling from the splenic artery at the splenic hilum (arrow) (s = spleen). (b) Doppler spectral sonogram derived from the splenic artery at this site. The splenic bed is a low-resistance arterial system with continuous forward flow in diastole resulting in a relatively low pulsatility index. There is a wide spread of flow velocities in both systole and diastole, presumably as a result of flow disturbance in a tortuous vessel.

vessels was sought. The liver was assessed in an attempt to exclude primary hepatic pathology.

For duplex assessment of the splenic artery, the vessel was located on the real-time image at a point close to its origin from the coeliac axis, and again close to the splenic hilum. A cursor corresponding to the position of the sample to be assessed was moved into the area and the sample volume adjusted to encompass the width of the vessel. The angle between the axis of the ultrasound beam and the long axis of the vessel was adjusted to optimize Doppler signal. Duplex assessment of the hepatic portal vein at the porta hepatis was performed using a similar method.

For each patient the pulsatility index for the splenic artery Doppler waveform was calculated using the formula used by Gosling (Gosling & King, 1974).

Results

Spleen size and echo-pattern

The range of spleen size in the normal volunteers was within normal limits in all cases, *i.e.* an overall length of less than 11 cm with a homogeneous weakly echogenic reflectivity of similar density to the liver. The range of spleen sizes in the patients is given in Table I; in all cases there was a homogeneous echo pattern, without focal defects.

Doppler results

Normal subjects (Fig. 1). The spectral analysis of the splenic artery was similar in all subjects studied. There was a broad systolic spectrum, indicating multiple flow velocities within the vessel, which is probably related to the normal tortuosity of the splenic artery. The peak systolic frequency reached a maximum of 3.5 kHz. There was persistence of forward flow throughout diastole, which is a consequence of the low peripheral resistance in the spleen. Pulsatility indices were calculated for the normal subjects with a mean of 0.799, standard deviation 0.153. The normal portal veins demonstrated continuous flow throughout the cardiac cycle, directed towards the liver, with variation in flow related to respiratory movement.

Table I. Doppler waveform peak frequency and pulsatility indices related to pathology in splenomegaly

Diagnosis	Age	Spleen size (cm)	Peak frequency splenic artery	Splenic artery diameter	Pulsatility index
β-thalassaemia	17	21.7	4.5	0.6	0.56
Chronic myeloid leukaemia—on chemotherapy	51	12.0	3.5	0.3	0.63
Chronic myeloid leukaemia	77	21.4	3.5	0.8	0.71
Chronic myeloid leukaemia	60	16.3	5.0	0.3	0.81
Chronic myeloid leukaemia	59	19.0	7.0	1.4	0.93
Lymphoma—on chemotherapy	61	29.3	4.5	1.4	0.93
Lymphoma	73	23.5	6.0	0.9	1.06
Myelofibrosis	72	21.3	5.0	0.7	1.02
Myelodysplasia	68	31.2	4.0	1.1	1.09

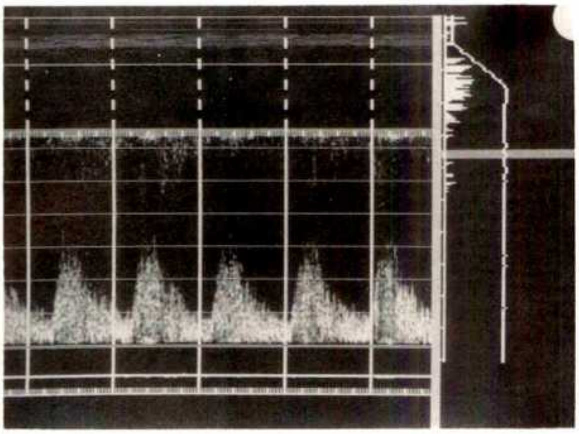

Figure 2. Spectral sonogram of the splenic artery at the splenic hilum in a 72-year-old woman with splenomegaly due to myelofibrosis. The flow pattern demonstrated is similar to that in a normal patient.

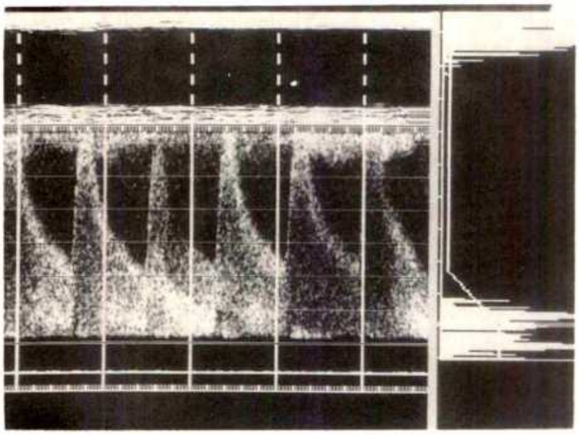

Figure 3. Spectral sonogram of the splenic artery in a 59-year-old woman with chronic myeloid leukaemia. Although there is an overall increase in flow velocities, the pulsability index does not differ significantly from the normal range.

Patients (Figs 2 and 3). Studies of the splenic vein and hepatic portal vein demonstrated flow directed towards the liver in all cases, with preservation of a slight variation in frequency, related to respiration. For the splenic artery, the spectral pattern in all 10 subjects with splenomegaly was similar to that seen in the normal subjects, with the characteristic broad spectrum in systole and continued forward flow in diastole; there was an increase in peak frequency in some but not all cases (Table I). The peak frequency did not bear any direct relationship to the size of the spleen—the largest spleen measured had a peak frequency of 4 kHz. The size of the splenic artery increased in proportion to the size of the spleen.

Pulsatility indices calculated for the patients with splenomegaly are shown in Table I. These values fall within 95% confidence limits for the indices calculated in normal subjects and are therefore considered to be statistically the same as the normal group.

Discussion

The poor correlation between splenic pathology and specific sonographic appearances provides persistent difficulty in clinical diagnosis. There may be some correlation with certain disease states, depending on the echodensity of the spleen and the presence or absence of focal defects (Mittelstaedt & Partain, 1980). However, in the large majority of patients with a homogeneously enlarged spleen a specific diagnosis cannot be made.

In splenomegaly the amount of blood flowing through the spleen and its flow rate may increase by five- to ten-fold and at the same time a certain proportion of the blood may be pooled in the cord spaces. Increased red cell pool is especially a feature of myeloproliferative and lymphoproliferative disorders. The normal red cell content of the spleen is 20–60 ml, or less than 5% of the red cell mass (Hegde et al, 1973), and the splenic blood flow represents about 5% of total blood volume per minute. With increasing splenomegaly the minute volume of the spleen is increased, but the irrigation coefficient, *i.e.* the blood flow per gram of splenic tissue, is unchanged or may even be reduced (Veda & Kitani, 1970).

Blood is brought to the spleen via the splenic artery and then through its branches, the trabecular arteries, into the central arteries sited in the white pulp. Circulation to the venous side is either directly through the sinuses and then via the collecting veins to the trabecular vein ("closed system"), or the blood passes into the cord spaces before joining up with the sinuses ("open system"). Because of the presence in the spleen of these two vascular systems there is both a rapid and a slow transit component in the splenic circulation. Both the vascular systems provide low resistance to the splenic arterial blood supply.

The spectral patterns in the splenic arteries in this study of patients with splenomegaly show no change from the normal. The broad spectrum remains, with continued forward flow in diastole, indicative of the turbulence in the splenic artery related to tortuosity of the vessel, and this would not be expected to alter. The diastolic component reflects a low-resistance organ, and again this finding corresponds to the state of the pathological splenic circulation described above. An increase in peak frequency in some cases may be a reflection of increased flow velocity through the vessel in these cases. However, in many cases increased size of the spleen was associated with increased diameter of the splenic artery. Although the volume of blood travelling to the spleen might be expected to increase in proportion to the size of the spleen, this volume increase appears to occur either predominantly as a result of increase in vessel diameter or increase in flow velocity, or a variable combination of the two that does not appear to be governed by specific pathology.

The pulsatility index has been developed to provide an index of the pulsatility of the maximum frequency waveform, whilst remaining independent of probe-vessel angle (Woodcock et al, 1972). This is important in evaluating the splenic artery. The course of the vessel is extremely tortuous, and accurate measurements of the angle of incidence of a Doppler beam are very difficult. Accurate measurement of velocity and volume of flow is therefore not currently realistic.

However, calculation of the pulsatility indices in both normal subjects and patients with splenomegaly has demonstrated no significant difference between the two groups. The spread of pulsatility index in both groups is wide, and while there is evidence from peak velocity measurements and from assessment of vessel size of increase in blood flow in splenomegaly, there are no features specific for a particular disease process.

In conclusion, the addition of pulsed Doppler analysis has failed to add any useful information to sonographic assessment of the spleen. Subjective interpretation of the spectral pattern in addition to calculation of pulsatility indices has shown no significant difference between normal subjects and patients with splenomegaly, although increase in volume flow is demonstrable in most cases. Patients have not been assessed progressively during therapy, and this remains an area where alteration in flow velocity may be found to indicate a response to treatment.

References

Atkinson, P. & Wells, P. N. T., 1977. Pulse-Doppler ultrasound and its clinical application. *Yale Journal of Biology in Medicine*, *50*, 367–373.

Gill, R. W., 1979. Pulsed Doppler with B-mode imaging for quantitative blood flow measurement. *Ultrasound in Medicine and Biology*, *5*, 223–235.

Gosling, R. G. & King, D. H., 1974. Arterial assessment by Doppler shift ultrasound. *Proceedings of the Royal Society of Medicine*, *67(b)*, 447–449.

Hegde, U. M., Williams, E. D., Lewis, S. M., Szur, L., Glass, H. I. & Pettit, J. E., 1973. Measurement of splenic red cell volume and visualization of the spleen with ^{99m}Tc. *Journal of Nuclear Medicine*, *14*, 769–771.

Kane, R. A. & Katz, S. G., 1982. The spectrum of sonographic findings in portal hypertension: a subject review and new observations. *Radiology*, *142*, 453–458.

King, D. M., Dawson, A. A. & Bayliss, A. P., 1985. The value of ultrasonic scanning of the spleen in lymphoma. *Clinical Radiology*, *36*, 473–474.

Mittelstaedt, C. A. & Partain, C. L., 1980. Ultrasonic–pathologic classification of splenic abnormalities: grey-scale patterns. *Radiology*, *134*, 697–705.

Niederau, C., Sonnenberg, A., Muller, J. E., Erckenbrecht, J. F., Scholten, T. & Fritsch, W. P., 1983. Sonographic measurements of the normal liver, spleen, pancreas and portal vein. *Radiology*, *149*, 537–540.

Ohnishi, K., Saito, M., Koen, H., Nakayama, T., Nomura, F. & Okuda, K., 1985. Pulsed Doppler flow as a criterion of portal venous velocity: comparison with cineangiographic measurements. *Radiology*, *154*, 495–498.

Taylor, K. J., Atkinson, P., De Graaff, C. S., Dembner, A. G. & Rossenfield, A. T., 1978. Clinical evaluation of pulse-Doppler device linked to gray scale B-scan equipment. *Radiology*, *129*, 745–749.

Taylor, K. J. & Burns, P. N., 1985. Blood flow in deep abdominal and pelvic vessels: ultrasonic pulsed Doppler analysis. *Radiology*, *154*, 487–493.

Taylor, K. J., Burns, P. N., Woodcock, J. P. & Wells, P. N. T., 1985. Duplex Doppler scanning in the pelvis and abdomen. *Ultrasound in Medicine in Biology*, *11*, 643–658.

Veda, H. & Kitani, K., 1970. Splenic blood flow in idiopathic portal hypertension in Japan measured by ^{85}Kr clearance method. *Acta Hepato-splenologica*, *18*, 28–40.

Woodcock, J. P., Gosling, R. G. & Fitzgerald, D. E., 1972. A new non-invasive technique for assessment of superficial femoral artery obstruction. *British Journal of Surgery*, *59*, 226–231.

Zoli, M., Marchesini, G., Cordiani, M. R., Pisi, P., Brunori, A., Trono, A. & Pisi, E., 1986. Echo-Doppler measurement of splanchnic blood flow in control and cirrhotic subjects. *Journal of Clinical Ultrasound*, *14*, 429–435.

1991, *The British Journal of Radiology*, *64*, 489–493

Focal myositis, a benign inflammatory pseudotumour: CT appearances

By *E. Moskovic, MRCP, FRCR, †C. Fisher, MA, MD, FRCPath, ‡G. Westbury, FRCS, FRCP and *C. Parsons, FRCS, FRCR

Departments of *Radiology, †Histopathology and ‡Academic Surgery, The Royal Marsden Hospital, Fulham Road, London SW3 6JJ, UK

(*Received May 1990*)

Keywords: Myositis, Soft tissue pseudotumour, CT scanning

Abstract. Focal myositis is a rare benign pseudotumour of skeletal muscle, of unknown cause. Clinically it presents as an enlarging mass within muscle, usually of an extremity, and is often mistaken for a soft tissue neoplasm. The diagnosis is made by biopsy which reveals characteristic histological changes of inflammation, focal degeneration and regeneration, and some evidence of denervation. The CT findings include irregularity and enlargement of the muscles involved, with diffuse, poorly defined fatty infiltration of the muscle planes, but no evidence of an associated mass. We present two cases of focal myositis of the calf, both of which mimicked a soft tissue neoplasm, and in which CT was helpful in determining the nature and extent of the abnormality, for needle biopsy, and follow-up.

Focal myositis was first described in 1977 by Heffner et al as an inflammatory lesion of skeletal muscle, and subsequently about 30 cases have been reported in the literature (Heffner et al, 1977; Liefeld et al, 1982; Shapiro et al, 1986; Azumo et al, 1987; Vercelli-Retta et al, 1988).

Occurring mainly in the lower limb, the condition has also been seen in the hand, forearm, back, abdominal wall, peri-oral musculature, neck and tongue. Sex distribution appears equal and the age range is from 7 to 67 years.

The usual presentation is with a mildly painful soft tissue mass within an extremity, steadily enlarging over a few months. Clinically the lesion is frequently misdiagnosed as a soft tissue neoplasm, and the correct diagnosis is only established following biopsy. At surgery, the muscles involved appear pale, enlarged and fibrotic, with a rubbery texture. Microscopically, the features are those of an inflammatory myopathy, with muscle cell necrosis, regeneration, and a lymphocytic infiltrate. Of unknown aetiology, the clinical course of focal myositis seems one of spontaneous regression, although very occasionally continuing symptoms and swelling within incompletely excised lesions need further definitive surgery (Heffner et al, 1977; Hansen et al, 1985).

The usefulness of CT scanning in the evaluation of both benign and malignant masses within the somatic soft tissues is well established (Hunter et al, 1979; Golding & Husband, 1982; Heiken et al, 1984). In general, its major advantages are accurate demonstration of a lesion, delineation of its extent and its relationship to surrounding structures, which are also valuable in planning surgical excision or percutaneous biopsy.

The appearances of focal myositis on CT have so far not been reported and we present two cases of this rare condition in which CT was a useful adjunct to both diagnosis and management.

Case reports

Case 1

A 43-year-old man presented in July 1985 with a 5 month history of increasing pain and weakness in his right calf, exacerbated by exercise. He felt that the calf was becoming swollen and noticed that after walking a hundred yards his right foot began to "flop" and the pain developed. He was otherwise well but his previous medical history included many years of intermittent lumbar backache, to which his current symptoms were thought to be related. On examination, some ill-defined tender swelling of the popliteal fossa and upper calf was noted; the circumference of the right calf was 3 cm greater than the left, with isolated weakness of the calf muscles which showed evidence of denervation on EMG. Reflexes and sensation were intact. Blood biochemistry and haematology were normal. Lumbar radiculography was subsequently performed which revealed a left-sided disc prolapse at the L5/S1 level, contralateral to the side of the symptoms, and thought to be unrelated. The possibility of a space-occupying lesion in the calf compromising both the muscles and the nerves was then raised and a CT scan of the calves was performed (Fig. 1). This revealed extensive disruption with fatty infiltration of both the gastrocnemius and soleus muscles proximally near the tendinous origins. No underlying bony abnormality was seen and the area involved was poorly defined and not encapsulated. Although not thought typical in appearance, the diagnosis of an adipose tumour such as a liposarcoma could not be excluded, and open exploration was undertaken. At surgery, the soleus and gastrocnemeus muscles were

---

*Address for correspondence: Dr E. Moskovic, Department of Radiology, Royal Marsden Hospital, Fulham Road, London SW3 6JJ.

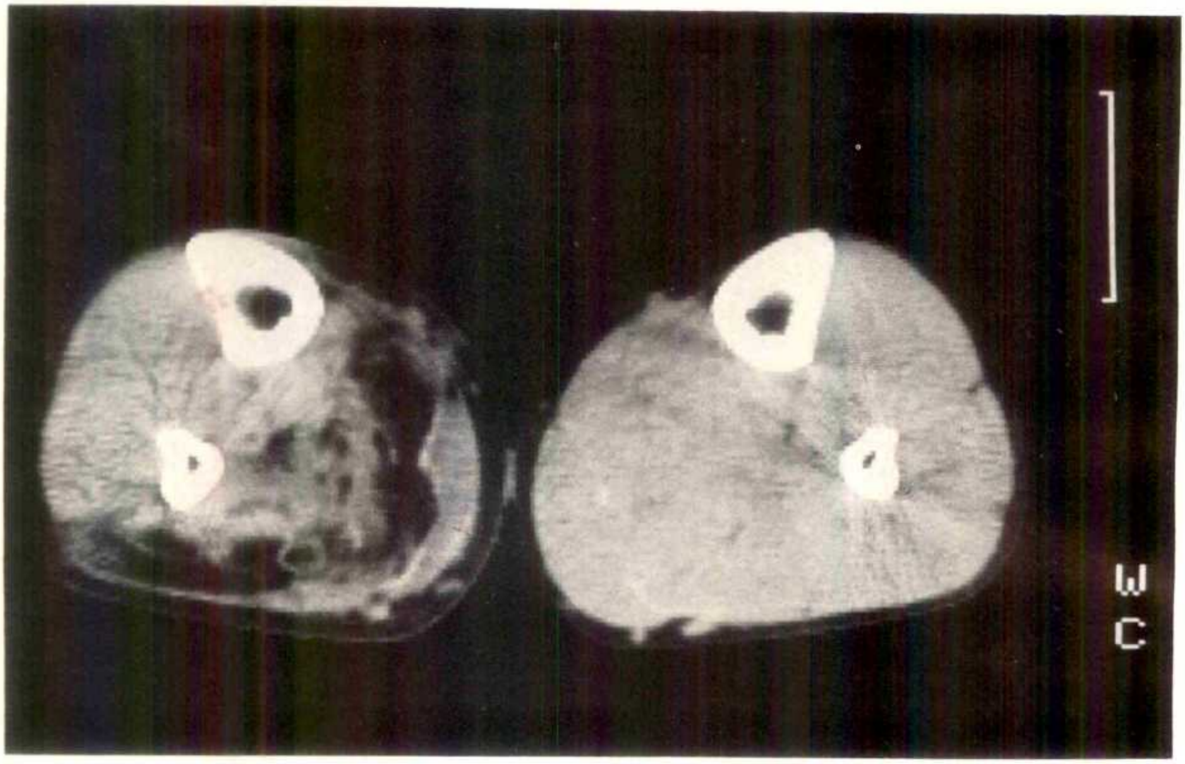

Figure 1. Computed tomographic scan through both calves of Case 1. The right calf shows poorly defined fatty change and disruption within the bellies of both gastrocnemius and soleus muscles.

found to be grossly abnormal, pale and fatty but with no discrete mass lesion. An extensive biopsy was performed. Histologically, this showed severe muscle damage, with scattered necrosis of muscle fibres, regeneration, fibrosis, fatty infiltration and focal perivascular inflammation, predominantly lymphocytic (Fig. 2). There was no evidence of malignancy, and the appearances were consistent with focal myositis. Following surgery, the patient's symptoms and signs did not progress, he remained well, and a follow-up CT scan 2 years later was unchanged in appearance.

Case 2

A 42-year-old man presented in August 1989 with a 6-month history of pain and swelling of the right calf for which there was no obvious cause. His previous medical history included an operation for a "slipped disc" 13 years previously. On examination, the right calf was mildly tender and swollen, measuring 2.5 cm more in circumference than the left, and the gastrocnemius and tibialis anterior muscles felt abnormally firm. The right ankle jerk was absent, but no other neurological abnormality was demonstrated. It was felt that the patient had evidence of both an old right S1 root lesion and in addition a co-existent abnormality within the right calf muscles which was either inflammatory or neoplastic. Routine blood tests were normal. A CT scan of the calves was performed (Fig. 3), which revealed a diffuse, ill-defined fatty infiltration of the right gastrocnemius and soleus muscles, which appeared atrophic, with no suggestion of a neoplastic mass lesion. A CT-guided needle biopsy of a representative part of the abnormality in the gastrocnemius was undertaken, which showed skeletal muscle infiltrated by fat with evidence of atrophy of muscle fibres, regeneration and perimysial fibrosis. Some inflammatory change, but less than in the previous case, was evident, with fibrosis being more marked. There was no evidence of malignancy. Unfortunately the patient's progress subsequently has not been documented as he returned abroad to work.

Discussion

The diagnosis of focal myositis is usually made by exclusion, following biopsy of a soft tissue mass thought clinically to be a tumour. Heffner et al (1977) first introduced this as a new entity, based on a study of 16 patients, all of whom had presented with an enlarging, variably tender muscle mass, usually within an extremity. Both that group of patients and those subsequently documented have shown a benign clinical course, with follow-up from between 2 and 6 years. Lesions that were totally excised have not recurred, and new sites of involvement or systemic disease have not developed. No abnormality of blood biochemistry, including muscle enzymes, or haematological abnormality has been seen at any stage of the disorder (Liefeld

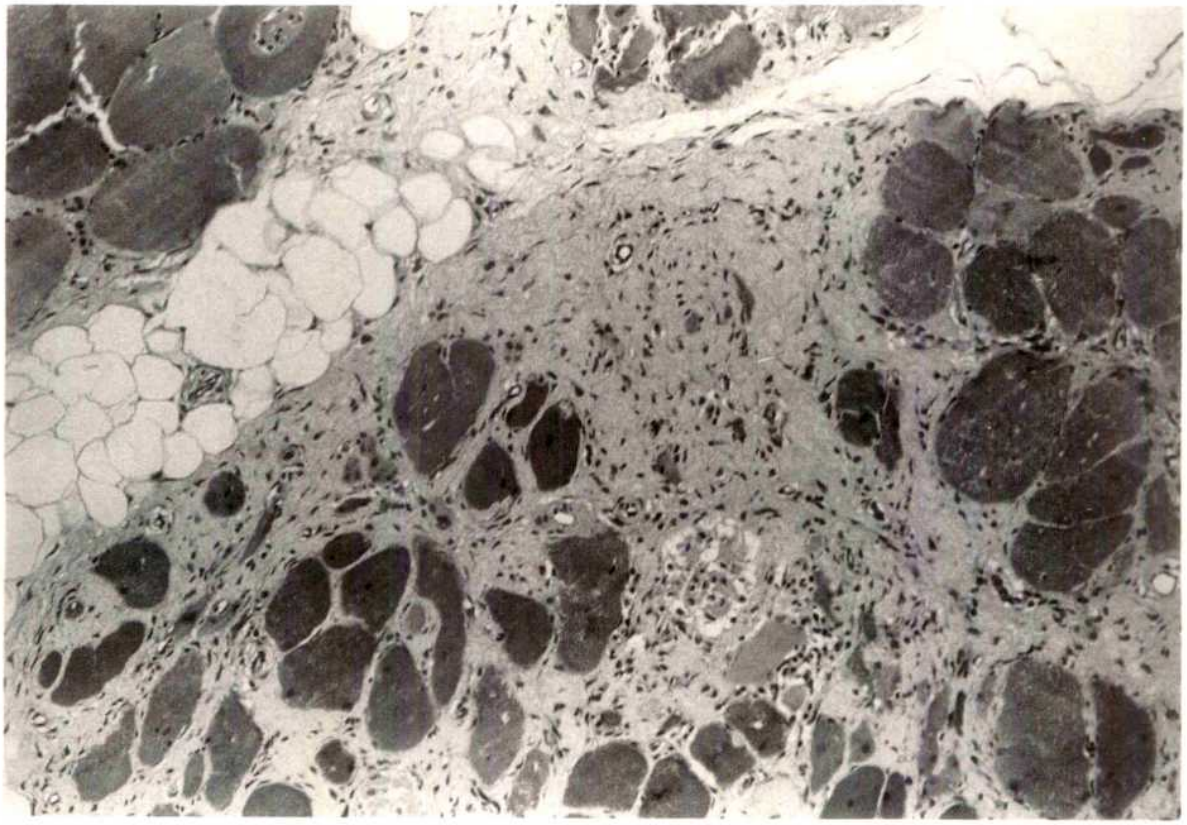

Figure 2. Biopsy from Case 1. Skeletal muscle showing patchy fibre atrophy, fibrosis, with a lymphocytic infiltrate, and fatty replacement. Haematoxylin and Eosin stain × 145.

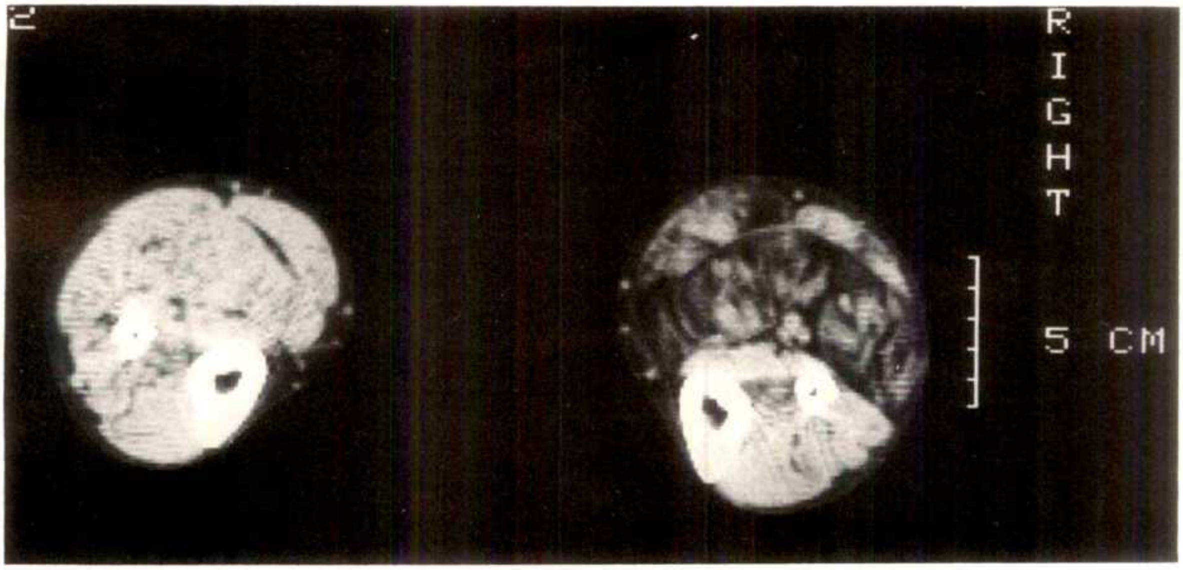

Figure 3. Computed tomographic scan through both calves of Case 2. The patient is lying prone. Diffuse fatty change is seen within the muscles of the right calf. No mass lesion is seen.

et al, 1982; Hansen et al, 1985; Shapiro et al, 1986; Azumo et al, 1987; Maguire et al, 1988; Vercelli-Retta et al, 1988).

Histologically, the characteristic changes of focal myositis are those of a severe myopathy with inflammation. Necrosis and regeneration of muscle fibres are seen against a background of predominantly lymphocytic infiltration of varying degree (Heffner et al, 1977). The muscle fibres themselves have different diameters and shapes; some are hypertrophic, while others are small and angulated. Necrotic fibres, which are randomly distributed rather than grouped, exhibit a vacuolar, hyalinized or fragmented sarcoplasm and regenerative changes elsewhere are seen to parallel the extent of necrosis. The degree of inflammation observed appears to reflect the age of the lesion. Earlier lesions display an abundant primarily lymphocytic response, whilst in older lesions an endomysial and perimysial fibrotic component is more conspicuous (Heffner et al, 1977; Hansen et al, 1985; Azumo et al, 1987). We observed this variation in our two patients; the second case described showed far less inflammation and more fibrosis.

While the aetiology of focal myositis remains obscure, proposals have included trauma, infection, denervation, and a localized manifestation of a systemic muscle disorder such as polymyositis. However, no history of trauma to the affected area has ever been elicited from these patients, and pathologically no areas of haemorrhage, calcification, or damage to underlying bone have been seen. Searches for an infective origin including tuberculosis, fungi and viral agents have been equally unrewarding. The disorder is not multifocal, systemic symptoms are never a feature, and it does not progress, differing completely from polymyositis and other generalized myopathic conditions. After his initial description of the condition, Heffner subsequently postulated that denervation might play a role in the pathogenesis of the disorder, since in some cases histological changes of denervation atrophy, with axonal swelling, demyelination and endoneurial fibrosis have been found (Heffner et al, 1977; Heffner & Barron, 1980). However, he concluded that the evidence to support this was insubstantial, since the presence of inflammatory infiltration is not typical of primary denervation, none of the patients described had any evidence of neurogenic disorder, and the grouping of the atrophic muscle fibres was inconsistent with chronic denervation. A more plausible explanation was that the changes of denervation seen were the effect of a primary inflammatory myopathic process rather than its cause, occurring as a consequence of local oedema, or entrapment of nerves by endomysial fibrosis. Interestingly, both of our patients had a previous history of lumbar disc prolapse, to which our first patient's symptoms were initially attributed, albeit erroneously.

To the surgeon, the gross appearance of a soft tissue sarcoma is that of a well demarcated tumour, with a "pseudocapsule" from which an inexperienced operator may attempt mistakenly to shell out the central mass. While clinically simulating a soft tissue sarcoma, the appearances of focal myositis on CT scanning are not typical of malignancy. The CT features of soft tissue sarcomas include the presence of an inhomogeneous mass lesion which is usually well demarcated, with mean attenuation values slightly lower than adjacent muscle and showing variable contrast enhancement (Golding & Husband, 1982). Good definition of the lesion is often due to the presence of surrounding soft tissue planes, and to the attenuation value of the tumour being significantly different from that of the surrounding soft tissues. Characteristically, low grade liposarcomas tend to be of low CT density owing to the presence of fat, but increasing malignancy and lack of differentiation within these tumours produces an increase in attenuation values, making CT prediction of histological type and grade difficult (DeSantos et al, 1981; Egund et al, 1981; Golding & Husband, 1982). Underlying bony involvement and the relationship of the tumour to neurovascular bundles and surrounding muscles is of course well demonstrated. Benign masses are often easier to classify using CT; they are often homogeneous, encapsulated, and in the case for example, of lipoma, have a characteristic appearance, being sharply defined and with attenuation values similar to that of normal body fat. The more aggressive infiltrating lipoma is also homogeneous on CT; its appearance is similar to that of the simple lipoma but demonstrates projections of fatty tissue into adjacent structures (Hunter et al, 1979; Heiken et al, 1984). However, an overlap clearly exists in the CT appearances of benign and malignant soft tissue tumours, and the specificity of CT in these circumstances is often poor (DeSantos et al, 1981; Golding & Husband, 1982; Heiken et al, 1984).

In the case of focal myositis, the CT appearances show no features to suggest malignancy; there is no discrete mass lesion, and no evidence of invasion of underlying bone or surrounding soft tissues. The findings are solely those of poorly defined disruption, enlargement and fatty infiltration of the muscles involved. Despite the appearances on CT, the presence of a steadily enlarging tender mass within an extremity alerts clinical suspicion of malignancy, and requires a firm diagnosis. In these circumstances, CT-guided biopsy of a representative area of the abnormality is adequate to reassure both clinician and patient of the benign nature of this rare disorder, thereby saving the patient from formal surgical exploration.

Acknowledgment

We wish to thank Dr R. Guiloff, Consultant Neurologist at the Westminster Hospital, for his help in the investigation of the first patient described (Case 1).

References

AZUMO, T., KOMORI, A. & NAGAYAMA, M., 1987. Focal myositis of the tongue. *Journal of Oral and Maxillofacial Surgery, 45*, 953–955.

DESANTOS, L. A., GINALDI, S. & WALLACE, S., 1981. Computed tomography in liposarcoma. *Cancer, 47*, 46–54.

EGUND, N., EKELUND, L., SAKO, M. & PERSSON, B., 1981. CT of soft tissue tumors. *American Journal of Roentgenology, 137,* 725–729.

GOLDING, S. J. & HUSBAND, J. E., 1982. The role of computed tomography in the management of soft tissue sarcomas. *British Journal of Radiology, 55,* 740–747.

HANSEN, L. B., BAEKGAARD, N. & RESKE-NIELSEN, E., 1985. Focal myositis of the rectus abdominal muscles. *Acta Chirurgica Scandinavica, 151,* 77–80.

HEFFNER, R. R., ARMBRUSTMACHER, V. W. & EARLE, K. M., 1977. Focal myositis. *Cancer, 40,* 301–306.

HEFFNER, R. R. & BARRON, S. A., 1980. Denervating changes in focal myositis, a benign inflammatory pseudotumor. *Archives of Pathology and Laboratory Medicine, 104,* 261–264.

HEIKEN, J. P., LEE, J. K. T., SMATHERS, R. L., TOTTY, W. G. & MURPHY, W. A., 1984. CT of benign soft-tissue masses of the extremities. *American Journal of Roentgenology, 142,* 575–580.

HUNTER, J. C., JOHNSTON, W. H. & GENANT, H. K., 1979. Computed tomography evaluation of fatty tumors of the somatic soft tissues: clinical utility and radiologic-pathologic correlation. *Skeletal Radiology, 4,* 79–91.

LIEFELD, P. A., FERGUSON, A. B. & FU, F. H., 1982. Focal myositis: a benign lesion that mimics malignant disease. *Journal of Bone and Joint Surgery (American Volumes), 64,* 1371–1373.

MAGUIRE, J. K., MILFORD, L. W. & PITCOCK, J. A., 1988. Focal myositis in the hand. *Journal of Hand Surgery, 13A,* 140–142.

SHAPIRO, M. J., APPLEBAUM, H. & BESSER, A. S., 1986. Cervical focal myositis in a child. *Journal of Pediatric Surgery, 21(4),* 375–376.

VERCELLI-RETTA, J., ARDAO, G. & DE CABRERA, M., 1988. Focal myositis and its differential diagnosis. *Annales de Pathologie, 8(1),* 54–56.

1991, *The British Journal of Radiology*, *64*, 494–497

Automated measurement of tumour extent in patients with colorectal liver metastases from X-ray computed tomography

By S. Perring, MA, *T. M. Hunt, FRCS, J. S. Fleming, PhD, FIPSM, †R. M. Blaquiere, FRCR and I. Taylor, MD, FRCS

Department of Medical Physics, *University Surgical Unit and †Department of Radiology, Southampton General Hospital, Tremona Road, Southampton, Hampshire, SO9 4XY, UK

(Received July 1990 and in revised form January 1991)

Keywords: Computed tomography, Liver metastases, Tumour staging

Abstract. Tumour burden is a significant prognostic factor in patients with colorectal liver metastases, and can be staged according to percentage hepatic replacement (PHR), but accurate measurements of PHR are difficult to obtain. We have used an automated computerized technique to isolate tumour and measure PHR from computed tomography images of 22 patients. Tumour identification was achieved by establishing local histogram-based thresholds at liver–tumour boundaries displaying clear bimodal histogram distributions. There was a significant association between measured PHR and independent visual estimates of PHR stage defined in quartiles ($p < 0.001$). When the measured value of PHR differed from the PHR stage, the visual estimate was always higher. The accuracy of PHR measurement was assessed on simulated liver computed tomography images. It seems likely that visual estimates of PHR from computed tomography images tend to overestimate tumour extent. The automated technique is probably more accurate and will be useful for assessing and monitoring patients.

Tumour burden in the presence of colorectal liver metastases can be staged according to the percentage hepatic replacement (PHR). Operative assessments of PHR have been shown to be a significant factor in assessing prognosis (Bengtsson et al, 1981; Finan et al, 1985). Visual PHR estimates from isotope scans (Mansfield et al, 1969), angiography (Lundstedt et al, 1985) or a variety of imaging techniques (Little & Hollands, 1987) have also been significantly associated with survival. There is, however, no "gold standard" of PHR estimation and estimates of PHR from different techniques vary widely, even when replacement is staged in quartiles (Hunt et al, 1989). The relative agreement between estimates from computed tomography (CT) and laparotomy suggests that CT may give the best visual estimate of PHR (Hunt et al, 1989). Since CT yields genuine three-dimensional volumetric information, it would be appropriate to apply automated image processing techniques to CT slice images to obtain accurate measured values of volumetric PHR.

We describe a semi-automated computerized method for obtaining precise measurements of PHR from sequential CT slice images of the liver.

Method

Twenty-two patients with colorectal liver metastases were studied. They received CT scans between June 1985 and November 1987.

Computed tomography was performed on a Siemens Somatom DR2 whole body scanner. Initial 8 mm slices were made at 16 mm intervals following iodinated oral contrast medium, and a further set of slices was taken at 10 mm intervals following at 50 ml intravenous contrast medium bolus. A further 50 ml of contrast medium was given as a rapid infusion during imaging to maximize contrast between healthy liver and tumour (Kemeny et al, 1986). Estimates were made of volumetric PHR by the reporting radiologist: stage 1, less than 25% tumour; stage 2, 25–50% tumour; stage 3, 50–75% tumour; stage 4, greater than 75% tumour.

Digital image processing of the CT images was performed on a DEC VAX 11-730 minicomputer and SIGMEX A7000 display processor, using the Southampton General Hospital Nuclear Medicine Department PICS image processing software (Fleming et al, 1987). Images acquired with intravenous contrast medium were transfered from the CT machine by floppy disk.

Each 256×256 pixel CT image within a study was displayed in turn. Within each CT image the liver was defined by a simple pixel intensity window technique with manual assistance, and isolated to form a liver image.

Sections of healthy liver and tumour were assessed for mean and standard deviation (SD) pixel intensity. Liver and tumour regions were defined at a distance greater than 10 pixels from a liver–tumour boundary to allow for beam hardening and the partial volume effect.

Since pixel intensity contrast between liver and tumour was found to be small when compared with pixel intensity noise, a large kernel median filter was applied to the liver images to reduce pixel noise while maintaining liver–tumour boundary definition. Linear movement artefacts were suppressed by the selective application of a line kernel median filter aligned perpendicular to the line artefact axis.

Automatic definition of tumour was performed using a local pixel intensity thresholding technique after that applied by Chow and Kaneko (1972) to the segmentation of cineangiograms. Square regions of width 32 pixels were superimposed on the liver image at 16 pixel intervals in the X and Y directions to ensure adequate overlap. Histograms were created for those squares centred within the liver and the histogram was tested for bimodality by comparing with a gaussian distribution of similar mean and SD. Those squares displaying adequate bimodality were assumed to straddle liver–tumour boundaries and were used to define a local threshold estimate for the centre of that square. Thresholds were defined by the iterative calculation of the following equation:

$$T = \frac{M_b + M_a}{2}$$

where T is the new estimate of the threshold, M_b is the mean value of the histogram elements below the old threshold (initially the mean of the whole histogram), and M_a is the mean value of the histogram elements above the old threshold.

The remaining pixels within the liver images were then awarded individual thresholds by interpolation from established thresholds to form a threshold map. Pixels in the liver image were then compared with their corresponding threshold, with tumour pixels identified as those which fell below their individual threshold.

By treating each pixel as expanded into the third dimension to fill the space between adjacent slices, the volume occupied by the whole liver and tumour was calculated and the PHR found.

The accuracy of volume and PHR measurements was assessed by testing on computer-generated CT images of isolated and grouped tumours under typical imaging conditions. The beam width was 8 mm and the interslice separation 10 mm, with the partial volume effect being modelled in software. The contrast in attenuation between liver and tumour was set at 27 HU and the pixel intensity gaussian noise over the image was set at an SD of 7 HU.

Results

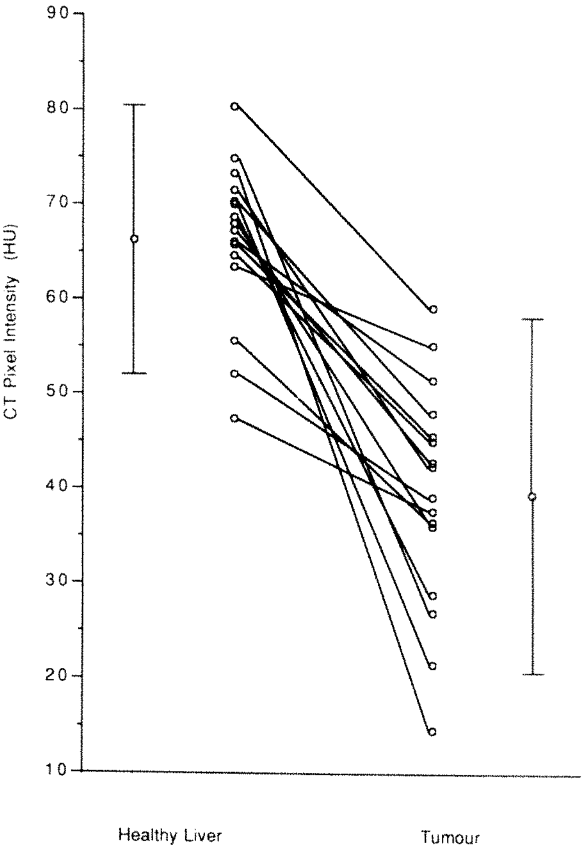

Figure 1. A comparison of the mean and spread of pixel intensity of CT image pixels lying within healthy liver and tumour for measurable cases of colorectal liver metastases. The error bars represent ±2 SDs from the mean for the average healthy liver and tumour.

Mean and SD pixel intensities for healthy liver and tumour are displayed in Fig. 1 for those studies where conditions for avoiding the effects of beam hardening and the partial volume effect were achieved. The results indicate that there is a clear pixel intensity contrast between liver and tumour, but that this contrast is insufficient without some form of image smoothing to prevent considerable overlap of liver and tumour pixel intensity distributions with consequent errors in tumour identification. Large kernel median filtering reduced the standard deviation of pixel intensity noise within uniform liver or tumour regions, to on average 40% of the unsmoothed standard deviation. Without intravenous contrast medium, the pixel intensity contrast between tumour and healthy liver was generally insufficient for automatic detection of tumour, even after median filtering.

The accuracy of volume and PHR estimates for computer-generated CT images of isolated and grouped tumours is indicated in Table I. The percentage error in volume estimate for small isolated tumours is considerable, but the corresponding error in PHR is not great owing to the low volumetric replacement that such tumours represent. Furthermore, the ability to identify small tumours by eye from CT images falls off rapidly with decreasing tumour diameter (Mittal et al, 1984). The error in PHR estimate for large isolated tumours or groups of small tumours is small.

The images of one patient proved to be too badly degraded by artefact to be assessed automatically. A comparison between measured PHR and the independent visual estimate of PHR stage for the remaining patients is displayed in Fig. 2. The association between measured PHR and visual PHR stage was found to be significant ($p < 0.001$) using analysis of variance with linear contrast. Where the visual estimate of PHR stage

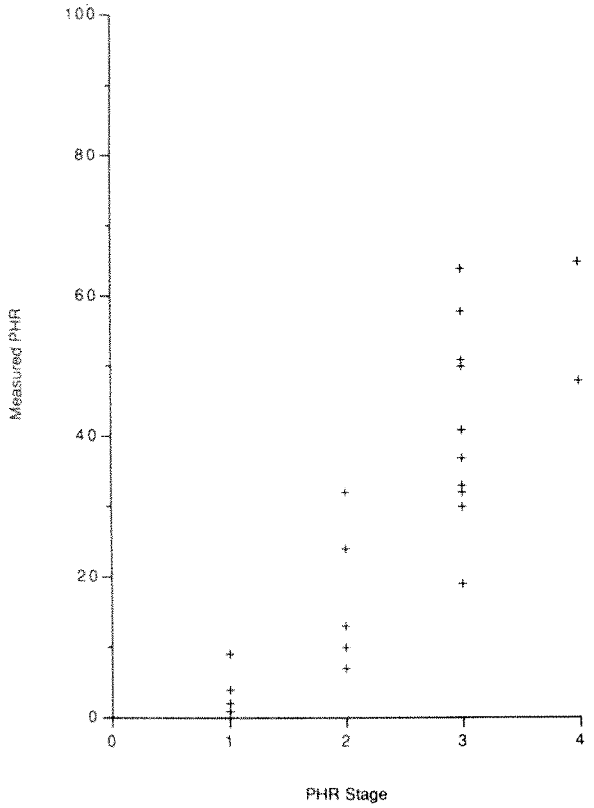

Figure 2. Comparison between the measured PHR and visual estimate of PHR stage from liver CT images.

differed from the measured PHR stage, the measured value was consistently lower.

The image processing required for this technique took approximately 3 min per CT slice presented.

Discussion

For any form of image segmentation and volumetric measurement to be clinically effective, the process must require little if any manual intervention by the user and must be relatively fast. The liver has been effectively identified by semi-automatic image processing software in abdominal CT images because of its large size and the uniformity of its internal structure. The identification of low attenuation features within an otherwise uniform liver image is a relatively simple procedure. The technique described has been used quickly and successfully to identify and measure metastatic liver involvement using a simple histogram-based thresholding technique without resorting to the more complex techniques of computer vision.

There is significant correlation between the measured values of PHR and visual estimates. It is likely that visual estimates of tumour replacement from CT in cases of colorectal liver metastases overestimate the volumetric PHR. Although survival does not greatly alter for different PHR stage in cases of untreated liver metastases, survival has been shown to be considerably improved with resection in cases of stage 1 metastatic involvement (Forster, 1978; Bengtsson et al, 1981). It is therefore hoped that efficient and accurate automated measurement of volumetric PHR from CT images will assist in the assessment of prognosis and subsequent management.

References

Bengtsson, G., Carlsson, G., Hafstrom, L. & Jonsson, P. E., 1981. Natural history of patients with untreated liver metastases from colorectal cancer. *American Journal of Surgery, 141*, 586–589.

Chow, C. K. & Kaneko, T., 1972. Automatic boundary detection of the left ventricle from cineangiograms. *Computers and Biomedical Research, 5*, 388–410.

Finan, P. J., Marshall, R. J., Cooper, E. H. & Giles, G. R., 1985. Factors affecting survival in patients presenting with synchronous hepatic metastases from colorectal cancer: a clinical and computer analysis. *British Journal of Surgery*, 72, 373–377.

Fleming, J. S., Britten, A. J., Blake, G. M., Gray, J. & Howlett, P. J., 1987. A general software system for the handling of medical images. *Nuclear Medicine Communications, 8(4)*, 270.

Forster, J. H., 1978. Survival after liver resection for secondary tumors. *American Journal of Surgery, 125*, 389–394.

Hunt, T. M., Ackery, D. M., Flowerdew, A. D. S., Blaquiere, R. M., Taylor, I. & Dewbury, K., 1989. A comparison of methods to measure the percentage hepatic replacement with colorectal metastases. *Annals of the Royal College of Surgeons of England, 71*, 11–13.

Table I. Assessment of the accuracy of automatic tumour volume measurement on computer-generated CT images of isolated and grouped tumours. The PHR was calculated for a liver of volume 1.64 l.

Tumour radii (mm)	Measured tumour volume (mm^3)	Actual tumour volume (mm^3)	Percentage volume error	Measured PHR	Real PHR
7	1050	1437	−26.9	0.06	0.09
10	4550	4189	8.6	0.28	0.26
15	14550	14137	2.9	0.89	0.86
20	33680	33510	0.5	2.06	2.05
30	114470	113098	1.2	6.99	6.90
45	384400	381704	0.7	23.46	23.30
33,25,16,11	228590	238714	−4.2	13.95	14.57
16,13,9,8,7	31950	32996	−3.2	1.95	2.01

KEMENY, M. M., GANTEAUME, B. A., GOLDBERG, M. D., HOGAN, J. M. & TERZ, J. J., 1986. Preoperative staging with computerised axial tomography and biochemical laboratory tests in patients with hepatic metastases. *Annals of Surgery*, *2*, 169–172.

LITTLE, J. M. & HOLLANDS, M., 1987. Hepatic resection for colorectal metastases—selection of cases and determinants of success. *Australian and New Zealand Journal of Surgery*, *57*, 355–359.

LUNDSTEDT, C., EKBERG, H., HALLDORSDOTTIR, A., TRANBERG, K. G. & STIGSSON, L., 1985. Angiography as a diagnostic, prognostic and therapeutic tool in liver metastases from a colorectal primary tumour. *Acta Radiologica, Diagnosis*, *26*, 373–380.

MANSFIELD, C. M., KRAMER, S., SOUTHARD, M. E. & MANDELL, G., 1969. Prognosis in patients with metastatic liver disease diagnosed by liver scan. *Radiology*, *93*, 77–84.

MITTAL, R., KOWAL, C., STARZL, T., VAN THEIL, D., BRON, K., IWATSUKI, S., SCHADE, R., STRAUB, W. & DEKKER, A., 1984. Accuracy of computerised tomography in determining hepatic tumour size in patients receiving liver transplantation or resection. *Journal of Clinical Oncology*, *2*, 637–641.

1991, *The British Journal of Radiology*, *64*, 498–504

Quantitative magnetic resonance imaging in cervical carcinoma: a report on 30 cases

By R. Santoni, MD, *M. Bucciolini, BSc, C. Chiostrini, MD, L. Cionini, MD and *R. Renzi, BSc

Radiation Therapy Unit and *Medical Physics Unit, Department of Clinical Physiopathology, University of Florence, Viale Morgagni 85, 50134 Firenze, Italy

(*Received July 1990 and in final form February 1991*)

Keywords: Cervical carcinoma, Radiation therapy, MRI, Tissue characterization

Abstract. T_1 and T_2 relaxation times were calculated, before radiation therapy, in 30 patients with cervical carcinoma. Eight healthy young women were submitted to magnetic resonance imaging (MRI) to determine T_1 and T_2 times of the normal cervix. Magnetic resonance imaging was repeated, in 22 patients, during radiation therapy and at follow-up. During treatment and follow-up, patients with complete tumour response showed a significant T_1 reduction compared with the pre-treatment values. With persistence of palpable or visible tumour, T_1 times showed a small decrease during therapy, and a marked increase at subsequent examinations. The results suggest that the modifications of T_1 relaxation times, during radiation therapy and follow-up, could be considered as a useful discriminant between patients with differing tumour response.

Several reports have shown that magnetic resonance imaging (MRI) can provide important information in patients with carcinoma of the uterine cervix (Powell et al, 1986; Togashi et al, 1986; Rubens et al, 1988; Waggenspack et al, 1988; Williams et al, 1989). In addition to morphological data, MRI has a potential for tissue characterization (Damadian, 1971; Bakker & Vriend, 1983; Bottomley et al, 1987). Tissue characterization and relaxation times are, however, regarded with great scepticism owing to the large variability of spin–lattice (T_1) and spin–spin (T_2) times among different tissues and in the same tissue with different pathology. Benign conditions such as oedema, inflammatory states and abscesses cannot be differentiated from tumours by the use of relaxation times. Nevertheless, relaxation times are modified during therapy and the size and characteristics of such modifications might be of some value to monitor and assess tumour response (Santoni et al, 1987; Nyman et al, 1987; Smith et al, 1988; Andersson et al, 1989). To explore the possibility of using relaxation times to monitor tumour response to radiation therapy, we analysed the long-term results in a group of 30 patients with cervical carcinoma, submitted to MRI before radiation therapy and during follow-up.

Methods

The analysis was performed on 38 female patients, eight of whom were healthy volunteers and 30 with squamous cell carcinoma of the uterine cervix.

Spin–lattice and spin–spin relaxation times of the normal uterine cervix were evaluated in eight healthy women. Four of these were nulliparous and four multiparous, with no evidence of gynaecological abnormality and aged between 25 and 40 years.

Thirty patients with squamous cell carcinoma of the uterine cervix, referred to the University and Hospital Department of Radiation Therapy of Florence, were submitted to MRI before, during and after radiation therapy at regular intervals.

Spin–lattice and spin–spin relaxation times of the tumour and of healthy tissues were evaluated.

The treatment in our department for carcinoma of uterine cervix is summarized in Table I.

Patients with disease confined to the cervix or limited extension to the fornices or parametria (IB, IIA and IIB) were submitted to MRI before intracavitary radiation therapy and immediately before surgery. Patients not suitable for surgery (IB and IIA barrel shape, IIB bulky disease, IIIA and IIIB) underwent MRI before external-beam radiation therapy, during treatment

Table I. Treatment options for carcinoma of the uterine cervix

Clinical stage	Radiation therapy	Surgery
IB, IIA, IIB	Pre-operative radiotherapy (50 Gy point A)	Radical abdominal or vaginal hysterectomy
IB, IIA, IIB (bulky disease) IIIA, IIIB	Exclusive radiation therapy (external-beam therapy; high-energy photons; box technique; 70 Gy to the pelvis)	No surgery

---

Address correspondence to: Dr R. Santoni, Radioterapia, Dipartimento di Fisiopatologia Clinica, Università degli Studi, Viale Morgagni 85, 50134 Firenze, Italy.

Table II. Category A patients (13 cases)

Patient	Age (years)	Clinical stage	Radiation therapy	Surgery	Status at last examination
1	61	IIIB	Alone	None	DOD
2	61	IIB	Alone	None	NED
3	65	IIB	Alone	None	DDM
4	50	IIIB	Alone	None	DDM
5	74	IIB	Alone	None	NED
6	60	IIB	Alone	None	NED
7	70	IIIB	Alone	None	NED
8	58	IIIB	Alone	None	DDM
9	43	IB	Pre-operative	RAH	NED
10	36	IIIB	Alone	None	NED
11	46	IB	Pre-operative	RAH	ADM
12	44	IB	Pre-operative	RAH	NED
13	42	IB	Pre-operative	RAH	NED

RAH = radical abdominal hysterectomy; DOD = dead, other disease; NED = no evidence of disease; DDM = dead, distant metastases; ADM = alive with distant metastases.

(usually after 30–40 Gy) and at regular intervals during follow-up.

Eight patients were submitted to MRI before surgery only and their data are not evaluated here.

Twenty-two patients with locally advanced disease completed the prescribed treatment programme and were submitted to MRI, according to the investigation schedule, to evaluate relaxation-time modifications induced by radiation therapy. Ninety-seven MRI examinations were performed in this group of patients. In four cases MRI was repeated more than once during external-beam radiation therapy to detect early T_1 and T_2 variations. All the patients had gynaecological evaluation before every MRI examination and the same staff (a physicist and a radiotherapist) performed each MRI examination in all the reported cases.

Patients were divided into two categories (A and B) according to their outcome.

Category A comprises all the subjects showing complete response to radiation therapy (no visible tumour or palpable evidence of pelvic tumour) maintained during follow-up.

Patients with persistent palpable or visible tumour 1 month after the end of treatment or presenting with local recurrence during follow-up were defined as Category B.

Thirteen patients were classified in Category A and nine in Category B. Their characteristics are shown in Tables II and III.

The results were analysed matching, for each patient, the T_1 and T_2 values found during radiation therapy and follow-up with their corresponding pre-treatment times.

Table III. Category B patients (nine cases)

Patient	Age (years)	Clinical stage	Radiation therapy	Surgery	Local failure	Status at last examination
14	58	IIB	Alone	None	CLPR	DLD
15	41	IIA	Pre-operative	RAH	CLPR	DLD
16	55	IIIB	Alone	None	LPR	DLDM
17	56	IIB	Alone	None	CLPP	DLD
18	56	IIIB	Alone	None	CLPP	DLD
19	66	IIIB	Alone	None	CLPR	DLD
20	32	IB barrel	Alone	None	CPP	DLDD
21	33	IIIB	Alone	None	CPP	DLDD
22	33	IIB	Alone	None	CPP	DLDD

RAH = radical abdominal hysterectomy; DLD = dead, local disease; DLDD = dead, local and distant disease; CLPR = central and lateral pelvic recurrence; LPR = lateral pelvic recurrence; CLPP = central and lateral pelvic persistence; CPP = central pelvic persistence.

Mean relaxation times were calculated in both Category A and B for each examination and the mean percentage variation from the pre-treatment number was determined. A Student's *t*-test, on paired observations, was used to quantify the significance of changes by comparison with the pre-treatment data. Differences were considered significant for $p < 0.05$.

Imaging technique

The MRI equipment was a 0.5 T superconductive magnet with a 50 cm body probe diameter. Data were acquired and processed on a 128×128 matrix that was interpolated to 256×256 when displayed. Slice thickness was 10 mm, field of view 400 mm and pixel size 3.12 mm. Images were obtained by averaging the signal from two successive sequences. The software allowed multislice imaging and automatic reconstruction of T_1 and T_2 values.

During the preliminary phase of the study, T_1 and T_2 times were derived by the use of an off-line multipoint fitting. The automatic facility for reconstruction of T_1 and T_2 times was, in fact, not sufficiently accurate to fit our requirements. Spin–lattice times were obtained by fitting the signal from a series of five inversion–recovery sequences with different interpulse times and a two-point parameter least-chi-square method. Spin–spin times were derived with a two-parameter least-squared method fitting the signal from a multi-echo sequence (GPMG sequence) with six successive echoes. The accuracy and reproducibility of the method was periodically checked by comparing T_1 and T_2 times of paramagnetic copper sulphate solutions, obtained by means of our off-line calculation (Bucciolini et al, 1986), with corresponding T_1 and T_2 spectrometric values.

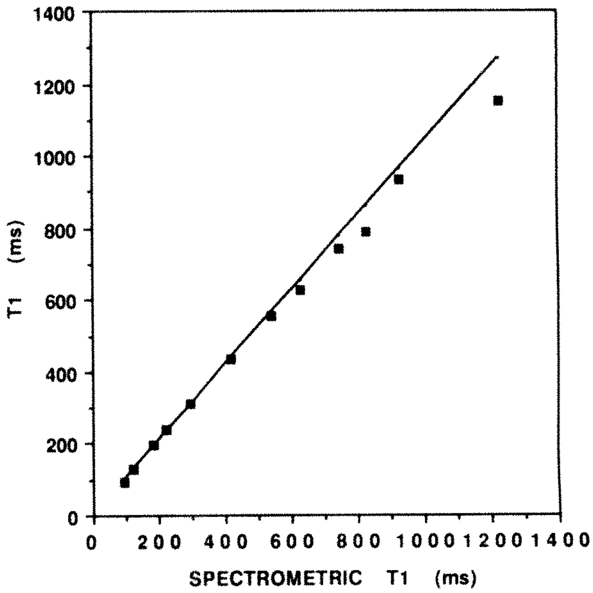

Figure 1. T_1 times obtained with a mixed sequence (■) and with fitting of the signal from inversion–recovery sequences (solid line) plotted against spectrometric data for samples of copper sulphate at different concentrations. Differences between the results of the two methods are within 9%.

During the course of the study an updated software version became available and T_1 measurements were

Table IV. Spin–lattice relaxation times for carcinoma of the cervix in 13 patients with local complete response to treatment (Category A)

Patient	T_1 Pre-radiotherapy	T_1 During radiotherapy	T_1 After radiotherapy (1–4 months)	T_1 After radiotherapy (5–8 months)	T_1 After radiotherapy (9–18 months)	T_1 After radiotherapy (> 18 months)
1	1002	723	819	673	—	—
2	607	504	663	—	612	611
3	809	635	619	—	610	679
4	779	—	802	705	446	—
5	598	549	650	738	680	565
6	574	322	781	561	560	620
7	731	662	578	680	685	670
8	764	727	618	—	—	—
9	754	822	663	—	—	—
10	788	763	598	—	—	—
11	747	—	653	—	—	—
12	574	—	598	—	—	—
13	1083	—	1071	—	—	—
Mean T_1	755	634	701	671	599	629
% T_1 variation		−16%	−7%	−11%	−21%	−17%
*p		0.026	0.141	0.437	0.236	0.308

**t*-statistic was performed on paired samples.

Table V. Spin–lattice relaxation times for carcinoma of the cervix in nine patients with residual pelvic tumour after radiation therapy or recurrence during follow-up (Category B)

Patient	T_1 Pre-radiotherapy	T_1 During radiotherapy	T_1 After radiotherapy (1–4 months)	T_1 After radiotherapy (5–9 months)
14	820	—	670	—
15	701	—	655	—
16	755	593	536	992
17	558	615	641	560
18	324	300	599	1035
19	620	562	777	794
20	470	710	903	—
21	677	716	855	—
22	794	770	900	—
Mean T_1	635	609	726	845
% T_1 variation	—	−4%	14%	33%
*p		0.843	0.221	0.161

*t-statistic was performed on paired samples.

then performed using the two-points ratio method with a mixed sequence, where inversion–recovery (IR) and spin–echo (SE) were consecutively combined in one cycle (Bucciolini et al, 1989). With the current method of T_1 automatic reconstruction, the real part of the inversion–recovery signal is replaced by the signed modulus (less sensitive to phase errors) (Bucciolini et al, 1989) with an overall increase in the quality of T_1 maps. Quality control of T_1 maps, ranging between 100 and 1200 ms, was performed using copper sulphate reference samples.

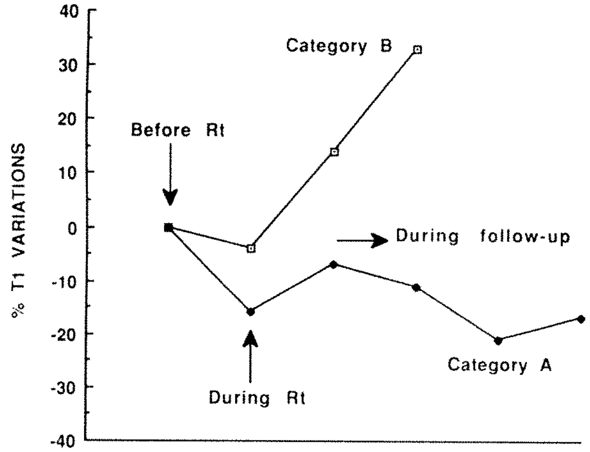

Figure 2. Percentage T_1 variations from the pre-treatment value in 22 patients with cervical carcinoma. (■) 13 patients with complete response after radiation therapy (Rt) and no recurrence during follow-up; (□) nine patients with residual disease after radiation therapy or recurrence during follow-up.

Figure 1 shows the comparison between T_1 times derived by the use of the "old" method (inversion–recovery sequences) and those obtained with the current method (mixed sequence). The good agreement between these data encouraged us to use this less time-consuming automatic T_1 reconstruction method during the second part of our study. T_2 calculated images were, however, still obtained by the standard CPMG sequence.

To calculate T_1 and T_2 times, initial siting scans were performed in orthogonal planes to identify the best site for data collection. The data were usually collected in a sagittal plane where the uterus is displayed along its longitudinal axis. Sagittal multislice images (5–7 slices) were obtained of the volume of interest, and SE and IR images produced of a representative section of the tumour. A 0.5 cm^2 region of interest (ROI) was used and T_1 and T_2 times calculated as a mean of these pixels. For repeat MRI scans, the representative section of the uterus where the T_1 and T_2 times were calculated was localized using the skin marks for positioning during external-beam therapy. Approximately 40–50 min were necessary for each investigation.

Results

The mean T_1 and T_2 values for the normal cervix of the eight healthy volunteers were found to be 617 ms (SD 136) and 145 ms (SD 27), respectively.

Absolute and mean T_1 values for patients with carcinoma of the cervix are reported in Tables IV (Category A) and V (Category B).

The pre-treatment T_1 values showed a high variability in both groups; the mean pre-treatment T_1 time for Category A patients (755 ms, SD 154) was longer than the mean value found in Category B cases (635 ms, SD 162), but this difference was not significant (p = 0.096).

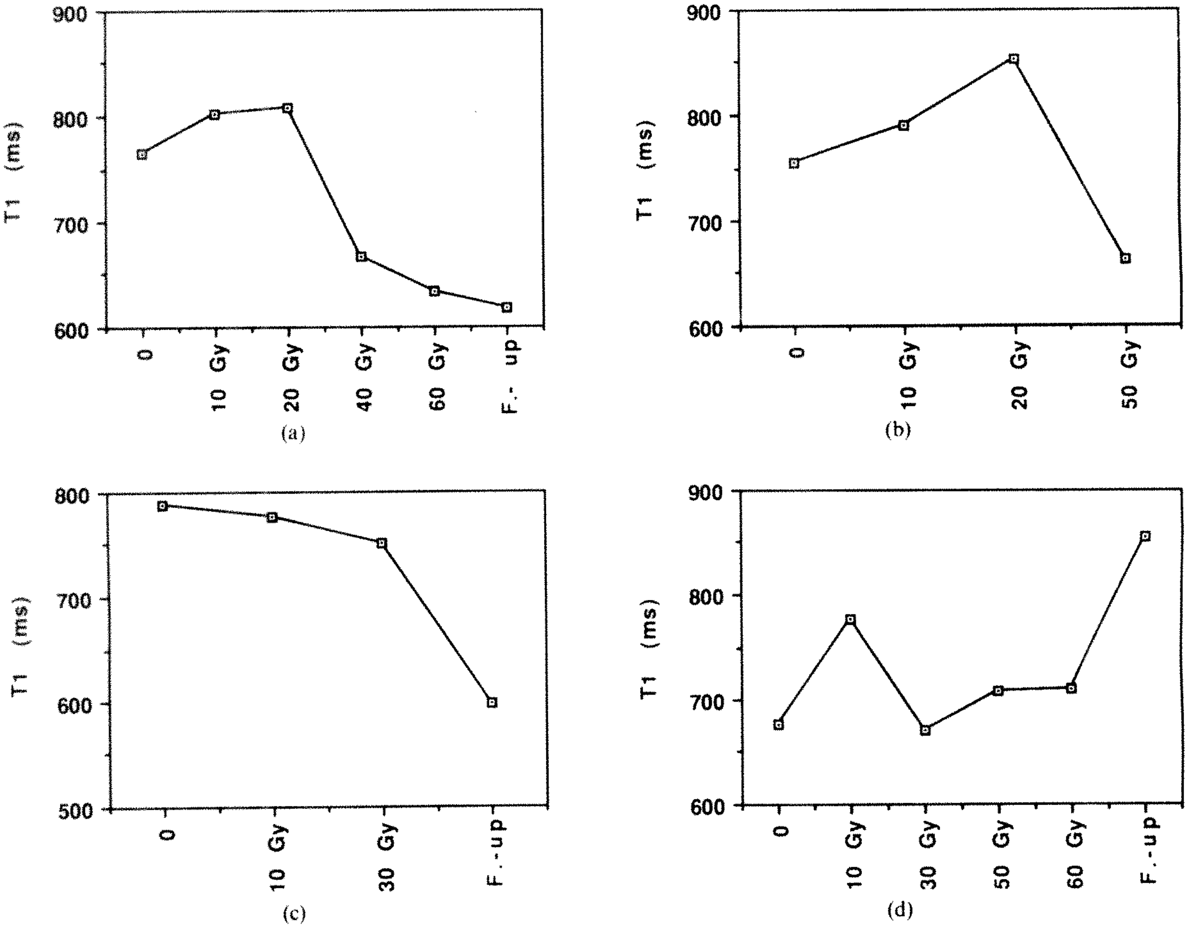

(a) (b) (c) (d)

Figure 3. T_1 changes in four patients during radiation therapy. (a), (b) and (c) (Category A patients) show a marked T_1 reduction at the end of radiation therapy. (d) (Category B patient) shows an increase in T_1 during treatment; at the first follow-up examination T_1 is longer than the initial value.

Patients in Category A showed a longer mean T_1 value (755 ms) than the healthy subjects (617 ms), but the difference was not significant ($p = 0.109$). No difference was found between the mean pre-treatment T_1 time in Category B patients (635 ms) and the normal subjects (617 ms).

At repeat examinations, the pattern of T_1 values was clearly different in the two patient categories.

In Category A most of the patients (8/9) showed, for the examinations performed during radiation therapy, a T_1 decrease by comparison with the pre-treatment values, and in all of them such a trend persists during follow-up (Table IV).

In Category A patients, T_1 reduction during therapy is significant ($p = 0.026$) compared with the initial value (Student's t-test on paired observations), while, on the contrary, no significance is evident matching column 1 data (Table IV) against columns 3–6. In Category B, T_1 times showed only a small and not significant variation (4%) from the examination performed during radiation therapy, and a marked T_1 increase was observed compared with the pre-treatment value during follow-up.

A comparison of the two different patterns is shown in Fig. 2 presenting the mean percentage variation of T_1 times with respect to the base-line pre-treatment values.

Four patients were repeatedly submitted to MRI during treatment (three in Category A and one in Category B). Figure 3 shows T_1 modifications during radiation therapy in these cases. An increase in spin–lattice time is evident after the first week of therapy (10 Gy) in three cases, followed by a decrease after the second week of treatment. At the end of radiation therapy, T_1 relaxation times are shorter than the initial value in all Category A patients (Fig. 3a, b, c). In the fourth case (Fig. 3d) with partial response to therapy and progression of the disease, T_1 times show, on the contrary, an increase after the third week of treatment and the first T_1 value during follow-up is higher than the pre-treatment figure.

For T_2, the mean pre-treatment value was found to be 116 ms (SD 25). No significant variation was detected during treatment and follow-up in any patient.

Discussion

Evaluation of the response of cervical carcinoma to radiation therapy can be performed by clinical examination, multiple biopsies of the cervix, ultrasonography and computed tomography. When a pelvic recurrence is suspected, a needle biopsy can distinguish tumour and non-neoplastic pelvic induration.

We have attempted, using quantitative MRI, to see if changes in the relaxation times T_1 and T_2, induced by radiation therapy in cervical carcinoma, could be correlated with the response of the tumour to therapy and to define the prognostic importance of these changes.

Our results suggest that a spin–lattice time decrease during treatment and at the end of radiation therapy may be correlated with tumour regression. On the contrary T_2 values do not allow evaluation of local tumour response.

The number of patients included in both Category A and B is not high and the statistical limitations are recognized. It is, however, difficult to submit a large number of patients to quantitative MRI over a long period of time. Nevertheless, this is probably the first study documenting, with a long-term follow-up, a relationship between variations of T_1 relaxation times and response of the tumour to therapy.

All the pre-treatment T_1 times were calculated on a representative section of the pelvis where bulky disease was present; during treatment it was still easy to find a section were tumour was clearly visible. During follow-up, when tumour regression was complete (Category A patients), measurements were performed on that connective tissue, which progressively replaces the neoplastic mass, and this can be appreciated at a gynaecological examination in patients submitted to radical external-beam radiation therapy. T_1 variation observed in patients with complete tumour regression may depend on the different characteristics of neoplastic and fibrous tissue.

The observation that fibrous pelvic masses have T_1 times significantly shorter than tumour tissue has been made on patients with recurrent carcinoma of the rectum (Johnson et al, 1987), and supports our explanation for T_1 reduction in Category A patients. Other authors (Glazer et al, 1985; Ebner et al, 1988) have concluded similarly.

All Category B cases showed rapid tumour growth during follow-up and all died within 1 year of radiation therapy. The longer T_1 values of rapidly growing tumour can probably be attributed to a greater total water content and to the fact that less water is bound to macromolecules (Bakker & Vriend, 1983).

As a wide variability was found among the pre-treatment T_1 values in both Category A and B patients, no predictive or prognostic significance can be given to the initial T_1 time in any single patient. Our results suggest that the degree of T_1 reduction, by comparison with the pre-treatment value, is more reliable than the absolute T_1 value in predicting the likelihood of tumour control.

As T_1 times increase during early treatment, it does not seem useful to perform MRI too early during radiation therapy; more reliable information can be obtained during the second half of external-beam radiation therapy. Moreover, when a significant T_1 decrease is noted during and after radiation therapy, it does not seem useful to repeat MRI frequently during follow-up. Magnetic resonance imaging should probably be restricted to selected cases with abnormal or suspicious clinical pelvic examinations. In these cases, MRI may differentiate between fibrosis or recurrent tumour (Johnson et al, 1987).

We conclude that even if our results are not definitive, they are suggestive of a significant trend in mean values of relaxation times in each of our two groups of patients when considered as a whole. Larger numbers of patients are needed to evaluate tissue characterization and to explore the predictive role of MRI in tumour response over longer periods of time.

References

ANDERSSON, T., ERICSSON, A., ERIKSSON, B., HEMMINGSSON, A., LINDH, E., MYMAN, R. & OBERG, K., 1989. Relative proton density and relaxation times in liver metastasis during interferon treatment. *British Journal of Radiology, 62*, 433–437.

BAKKER, C. J. G. & VRIEND, J., 1983. Proton spin–lattice relaxation studies of tissue response to radiotherapy in mice. *Physics in Medicine and Biology, 28*, 331–340.

BOTTOMLEY, P. A., HARDY, C. J. & ALLEN-MOORE, G., 1987. A review of ^{1}H nuclear magnetic resonance relaxation in pathology: are T_1 and T_2 diagnostic? *Medical Physics, 14*, 1–37.

BUCCIOLINI, M., CIRAOLO, L. & LEHMANN, B., 1989. Simulation of biologic tissues by using agar gels at magnetic resonance imaging. *Acta Radiologica, 30*, 667–669.

BUCCIOLINI, M., CIRAOLO, L. & RENZI, R., 1986. Relaxation rates of paramagnetic solutions: evaluation by nuclear magnetic resonance imaging. *Medical Physics, 13*, 298–303.

DAMADIAN, R., 1971. Tumour detection by nuclear magnetic resonance. *Science, 171*, 613–618.

EBNER, F., KRESSEL, H. Y., MINTZ, M. C., CARLSON, J. A., COHEN, E. K., SCHIEBLER, M., GEFTER, W. & AXEL, L., 1988. Tumour recurrence versus fibrosis in the female pelvis: differentiation with MR imaging at 1.5 T. *Radiology, 166*, 333–340.

GLAZER, H. S., LEE, J. K. T., LEVITT, R. G., BALFE, D. M., EMANI, R., WASSERMAN, T. H. & MURPHY, W. A., 1985. Radiation fibrosis: differentiation from recurrent tumour by MR imaging. *Radiology, 156*, 721–726.

JOHNSON, R. J., JENKINS, J. P. R., ISHERWOOD, I., JAMES, R. D. & SCHOFIELD, P. F., 1987. Quantitative magnetic resonance imaging in rectal carcinoma. *British Journal of Radiology, 60*, 761–764.

NYMAN, R., REHN, S., GLIMELIUS, B., HAGBERG, H., HEMMINGSSON, A. & JUNG, B., 1987. Magnetic resonance imaging for assessment of treatment effects in mediastinal Hodgkin's disease. *Acta Radiologica, 28*, 145–151.

POWELL, M. C., WORTHINGTON, B. S., SOKAL, M., WASTIE, M., BUCKLEY, J. & SYMONDS, E. M., 1986. Magnetic resonance imaging—its application to cervical carcinoma. *British Journal of Obstetrics & Gynaecology, 93*, 1276–1285.

Rubens, D., Thornbury, J. R., Angel, C., Stoler, M. H., Weiss, S. L., Lerner, R. M. & Beecham, J., 1988. Stage IB cervical carcinoma: comparison of clinical, MR and pathologic staging. *American Journal of Roentgenology, 150*, 135–138.

Santoni, R., Bucciolini, M., Cionini, L., Ciraolo, L. & Renzi, R., 1987. Modifications of relaxation times induced by radiation therapy in cervical carcinoma: preliminary results. *Clinical Radiology, 38*, 569–573.

Smith, F. W., Sarkar, T. K. & Hewitt, J. B., 1988. Monitoring of bladder neoplasia by low-field magnetic resonance imaging. *British Journal of Radiology, 61*, 166–169.

Togashi, K., Mishimura, K., Itoh, K., Fujisawa, I., Asato, R., Nakano, Y., Itoh, H., Torizula, K., Ozasa, H., & Mori, T., 1986. Uterine cervical cancer: assessment with high-field MR imaging. *Radiology, 160*, 431–435.

Waggenspack, G. A., Amparo, E. G. & Hanningan, E. V., 1988. MR imaging of uterine cervical carcinoma. *Journal of Computer Assisted Tomography, 12*, 409–414.

Williams, M. P., Husband, J. E., Heron, C. W., Cherryman, G. R. & Koslin, D. B., 1989. Magnetic resonance imaging in recurrent carcinoma of the cervix. *British Journal of Radiology, 62*, 544–550.

1991, *The British Journal of Radiology*, *64*, 505–509

Fetal blood sampling from the intrahepatic vein for rapid karyotyping in the second and third trimesters

By Peter Nicolaidis, MD, *Umberto Nicolini, MD, Nicholas M. Fisk, FRACOG,
Yuen Tannirandorn, MD, Hassan Nasrat, MRCOG and Charles H. Rodeck, FRCOG

Royal Postgraduate Medical School, Institute of Obstetrics and Gynaecology, Queen Charlotte's and
Chelsea Hospital, Goldhawk Road, London W6 0XG, UK

(Received June 1990 and in revised form November 1990)

Keywords: Fetal blood sampling, Karyotype, Fetal malformations, Fetal growth retardation

Abstract. One hundred and twelve fetuses with structural anomalies ($n = 84$), intrauterine growth retardation ($n = 21$) or amniotic fluid volume disorders ($n = 7$) detected by ultrasound underwent blood sampling from the intrahepatic vein for rapid karyotyping. The procedure was successful in 95.5%. 12.5% of the fetuses had an abnormal karyotype. Fetal bradycardia was observed in two fetuses (1.8%) and intraperitoneal bleeding in three (2.7%). There were three procedure-related losses but these were not due to the intrahepatic vein sampling itself. Fetal blood sampling is the method of choice for rapid karyotyping in the second and third trimesters, and the intrahepatic vein is an alternate site when access is difficult or failure to sample occurs at the placental cord insertion. Additional advantages of fetal blood sampling at the intrahepatic vein include absence of cord complications, reduced risk of fetal blood loss and fetomaternal haemorrhage, and the lack of need to confirm the fetal origin of the sample.

Assessment of fetal karyotype is widely recommended following ultrasound diagnosis of fetal structural malformations, intra-uterine growth retardation (IUGR) or amniotic fluid abnormalities (Nicolaides et al, 1986; Palmer et al, 1987; Williamson et al, 1987). There are several reasons for this. First, unnecessary Caesarean section and intra-uterine treatment are avoided in non-viable fetuses. In addition, recent evidence suggests that parental psychological trauma is reduced by advanced knowledge that they have an abnormal fetus, even in the third trimester of pregnancy when termination of pregnancy is no longer an option (Clark & DeVore, 1989). Finally, if intra-uterine death occurs, the problem of failed cytogenetic culture on post-mortem tissue is avoided, so that appropriate assessment of the reproductive risk in subsequent pregnancies can still be achieved.

Tissue for karyotyping can be obtained by amniocentesis, chorionic villous sampling, and fetal blood sampling (FBS). Amniocentesis, although technically simpler, and associated with a lower risk than FBS, requires 3–4 weeks to obtain chromosomal analysis. Chorionic villous sampling in the second half of the pregnancy does not seem to be safer than FBS (Holzgreve et al, 1990), and it yields false positive results (Simoni et al, 1987; Callen et al, 1988). Therefore, FBS in the second half of the pregnancy is the method of choice as, in addition, it provides knowledge of acid–base status, haematological and metabolic changes (Nicolaides et al, 1986) and allows diagnosis of fetal infection (Daffos et al, 1985; Hobbins et al, 1985; Forestier, 1987). All these parameters are clearly important in the further management of the pregnancy, besides the presence or absence of chromosomal abnormalities.

Fetoscopy for FBS has been replaced by the relatively simplier, easier and safer technique of ultrasound guided needling. The usual site of sampling is from the umbilical cord vessels at the placental cord insertion, and the word "cordocentesis" has become synonymous for this technique. Difficulties may arise, however, in approaching the placental cord insertion in the presence of abnormal amniotic fluid volume, maternal obesity or when the fetus obscures a posterior placenta.

We have previously suggested a flexible approach to FBS, and proposed the intrahepatic vein (IHV) as an alternate site of sampling (Nicolini et al, 1988a). Here we present our experience of IHV sampling for rapid karyotyping.

Patients and methods

One hundred and twelve patients underwent FBS from the IHV for rapid karyotyping, following ultrasound detection of IUGR ($n = 21$), structural anomalies ($n = 84$) and unexplained amniotic fluid volume disorders (oligohydramnios ($n = 6$), polyhydramnios ($n = 1$)), between August 1986 and March 1990. Gestational age at FBS was 16–20 weeks in 38 patients, 21–24 weeks in 29, 25–28 in 20, 29–32 in 16 and 33–36 in 9.

Some of these patients have been included in a previous report of IHV samplings and transfusions for a variety of indications, dealing with safety and technical aspects (Nicolini et al, 1990).

The fetal IHV was electively chosen as site of

---

* Author for correspondence.

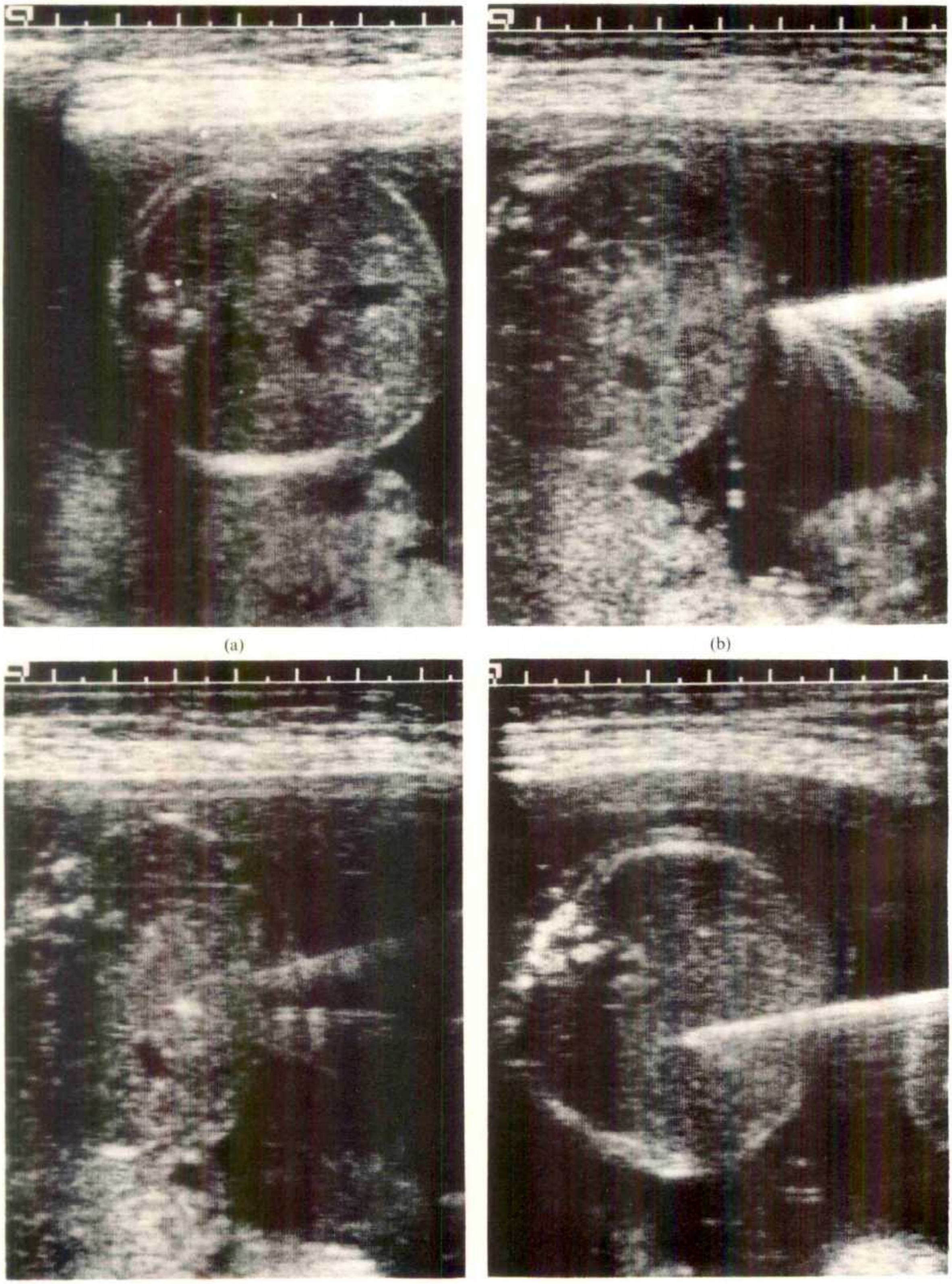

(a) (b)

(c) (d)

Table I. Indication for rapid karyotyping, frequency of abnormal chromosomes and outcome

Indication	No.	%	Abnormal karyotype	A+W	P/N losses	TOP
IUGR	21	18.7	—	13	8	—
Abnormal amniotic fluid volume	7	6.3	—	3	3	1
Fetal anomalies						
Non-immune hydrops	14	12.5	4 47,XX,+21 (1) 47,XY,+13 (1) 45,XO (2)	3	6	5
Hydrocephalus/intracranial	4	3.6	—	4	—	—
Urogenital	37	33.0	1 46,XY,inv.6	20	7	10
Gastrointestinal	5	4.5	1 47,XY,+21	3	1	1
Multiple	10	8.9	6 47,XY,+18 (4) 47,XX,+21 (1) Triploidy (1)	—	2	8
Cardiac	4	3.6	2 47,XX,+18 Transloc. 11	1	—	3
Others	10	8.9	—	5	4	1
Total	112	100	14 (12.6%)	52	31	29

A+W = alive and well; P/N = perinatal; TOP = termination of pregnancy; IUGR = intrauterine growth retardation.

sampling on 104 occasions, whereas the remaining eight procedures were secondary attempts after a failed attempt at the placental cord insertion. The criteria for elective choice of the IHV were (a) poor visualization of, or difficult approach to, the placental cord insertion, (b) concern about feto-maternal haemorrhage in Rh negative patients (Nicolini et al, 1988b) and (c) selective blood sampling in twin pregnancies where attribution of the placental cord insertion was uncertain.

Fetal IHV sampling was performed as an outpatient procedure and maternal sedation was not used. No direct medication was given to the fetus.

The procedure, which has been described in detail elsewhere (Nicolini et al, 1988a, 1990), was performed under sterile conditions, with the patient in the wedged supine position. The transducer was placed in a sterile plastic bag; sterile mineral oil was used for the acoustic coupling on the maternal abdomen. The fetal IHV was identified by ultrasound scanning with a linear transducer (Acuson Mountain View, CA), in the same cross-sectional view of the fetal abdomen as used for the standard abdominal circumference measurement (Fig. 1a).

Local anaesthetic was infiltrated prior to the insertion of a 20 gauge, 15 cm long, spinal needle which was introduced "free hand" under ultrasound guidance into the fetal abdominal wall, which was approached either anteriorly near the midline or from left or right hypochondrium, and then advanced through the liver parenchyma into the craniodorsal continuation of the umbilical vein (Figs 1b, 1c, 1d). The needle was then left, allowing it to move freely, minimizing the risk of dislodgement caused by fetal or maternal movements, and avoiding fetal visceral damage. 2–3 ml of blood were then aspirated. Unlike FBS at the placental cord insertion, there was no need to confirm the fetal origin of blood.

Whenever fetal bradycardia, tachycardia or evidence of intraperitoneal bleeding was observed, cardiotocogram and ultrasound were performed, until these resolved.

Results

Fetal blood sampling was successful (>1 ml obtained) on 107 occasions (95.5%). Five failures occurred: three were primary attempts, and two were secondary attempts following failure of sampling at the cord insertion. All but one of the five failures had subsequent successful sampling from the cord insertion, and rapid karyotyping was achieved in 111/112 (99.1%) patients.

The karyotype was abnormal in 14 fetuses (12.5%). All 14 abnormalities were in the 84 fetuses with structural malformations (16.7%). There were 12 aneuploidies: three trisomies 21, five trisomies 18, one trisomy 13, two Turner's syndrome and one triploidy, and two chromosome rearrangements (Table I). In the 21 growth retarded fetuses and in the seven cases complicated by

Figure 1. Scheme of intrahepatic vein sampling: (a) cross-section of fetal abdomen (24 weeks) at the level of the intrahepatic vein; (b) needle approaching the fetal abdomen; (c) needle within the fetal abdomen; (d) needle tip in the intrahepatic vein.

amniotic fluid volume abnormalities there were no chromosomal anomalies.

Fetal bradycardia lasting longer than 2 min was observed on two occasions (1.8%). Of these, one infant is alive and well, while a fetus with non-immune hydrops died in the neonatal period. In three fetuses (2.7%) in which ultrasonic findings of intraperitoneal bleeding were documented, the intra-abdominal echo-free area disappeared within 48 h; one underwent termination of pregnancy for multiple abnormalities and the remaining two were delivered in good condition.

Pregnancy outcome in relation to the indication for FBS is shown in Table I. In this series there were three fetal losses (2.7%) clearly attributable to the procedure. Two were spontaneous abortions which occurred in two twin pregnancies 3 weeks after FBS. In both sets of twins, FBS was performed in one fetus at the IHV, and in the co-twin at the placental cord insertion. The remaining loss was an intra-uterine death 1 week following a failed attempt at both the IHV and the cord insertion.

Discussion

We have previously reported the safety of FBS from the IHV (Nicolini et al, 1990) after the initial description of the technique by Bang et al in 1982. Other reported series are too small to draw conclusions about the efficacy and safety of this alternative to cordocentesis for FBS (Hsieh et al, 1987; Koresawa et al, 1987). Our experience of 112 cases confirms that IHV sampling is an efficient and safe method for obtaining blood for fetal karyotyping.

The reported incidence of chromosomal abnormalities associated with structural malformations detected by ultrasound ranges from 10 to 50% (Gosden et al, 1985; Nicolaides et al, 1986; Williamson et al, 1987; Eydoux et al, 1989; Rosendahl & Kivinen, 1989). These frequencies are higher in multiple malformations (Eydoux et al, 1989), whereas in cases of isolated abnormalities or IUGR the reported frequency is 7% or 10% respectively (Benacerraf et al, 1988; Wladimiroff et al, 1988; Eydouz et al, 1989). The overall incidence of 12.5% in this series is in agreement with published series. However, in contrast with other series, no chromosomal anomalies were found in cases of IUGR or abnormal amniotic fluid volume. Careful study of fetal anatomy in cases of IUGR or amniotic fluid volume disorders, using intra-amniotic or intraperitoneal infusion of normal saline to improve visibility (Nicolini et al, 1989; Fisk et al, 1990) excluded minor structural anomalies from these two groups of fetuses. This might explain the lower incidence of chromosomal anomalies than previously reported.

The IHV approach represents not only an alternative to, but also has specific advantages over, needling the placental cord insertion. The fetal origin of the sample does not require laboratory confirmation and contamination with amniotic fluid is avoided as the sampling site is within the fetal abdominal cavity. In addition, differentiation of fetuses in multiple pregnancy is ensured.

The safety of inserting a 20 gauge needle under continuous sonographic control into the fetus is well documented in fetal intraperitoneal transfusions (Barss et al, 1986). We found that by leaving the needle unheld, the possibility of intraperitoneal trauma is reduced as the needle moves freely with maternal and fetal movements (Nicolini et al, 1988a). Needle dislodgement using this technique for fetal intravascular transfusions has been reported to be 8% (Nicolini et al, 1990) and compares favourably with studies at the placental cord insertion (Berkowitz et al, 1987; Ronkin et al, 1989). Intra-amniotic bleeding from cord sampling has been reported to be as high as 40% (Daffos et al, 1988; Bovicelli et al, 1989), and the incidence of feto-maternal haemorrhage was found to be approximately 70% in samplings from an anterior placenta. In contrast, these complications occur less frequently when the IHV is sampled (Nicolini et al, 1988b). Although intra-peritoneal bleeding may occur (2.7% in this series), the blood loss from the fetal circulation is reabsorbed within a few days (Harman et al, 1983).

This study does not permit comment on fetal or neonatal outcome, as it was a very high risk group of fetuses. However, all three procedure related losses (two of which were twin pregnancies) following sampling at the IHV had also undergone additional sampling at the placental cord insertion so that it was not possible to determine which of the two procedures was the likely cause.

Advances in prenatal diagnosis and improvements in ultrasound imaging technology should increase the number of fetuses in whom chromosomal analysis is indicated.

This study supports a role for sampling at the IHV for rapid karyotyping as an alternate site when difficulties arise or failure occurs at the placental cord insertion.

References

BANG, J., BOCK, T. E. & TROLLE, D., 1982. Ultrasound-guided fetal intravenous transfusions for severe rhesus haemolytic disease. *British Medical Journal*, *284*, 373–374.

BARSS, V. A., BENACERRAF, B. R., GREENE, M. F. & FRIGOLETTO, F. D., 1986. Use of a small-gauge needle for intrauterine fetal transfusions. *American Journal of Obstetrics and Gynecology*, *155*, 1057–1058.

BENACERRAF, B. R., BARSS, V. A., SALTZMAN, D. H., GREENE, M. F., PENSO, C. A. & FRIGOLETTO, F. D., 1988. Fetal abnormalities: diagnosis or treatment with percutaneous umbilical blood sampling under continuous ultrasound guidance. *Radiology*, *166*, 105–107.

BERKOWITZ, R. L., CHITKARA, U., WILKINS, I., LYNCH, L. & MEHALEK, K. E., 1987. Technical aspects of intravascular intrauterine transfusions: lessons learned from thirty-three procedures. *American Journal of Obstetrics and Gynecology*, *157*, 4–9.

BOVICELLI, L., ORSINI, L. F., GRANNUM, P. A. T., PITTALIS, M. C., TOFFOLI, C. & DOLCINI, B., 1989. A new funipuncture technique: two-needle ultrasound and needle biopsy-guided procedure. *Obstetrics and Gynecology*, *73*, 428–431.

CALLEN, D. F., KORBAN, G., DAWSON, G., GUGASYAN, L., KRUMINS, E. J. M., EICHENBAUM, S., PETRASS, J., PURVIS-SMITH, S., SMITH, A., DEN DULK, G. & MARTIN, N., 1988. Extra embryonic fetal karyotypic discordance during diagnostic chorionic villus sampling. *Prenatal Diagnosis, 8*, 435–460.

CLARK, S. L. & DE VORE, G. R., 1989. Prenatal diagnosis for couples who would not consider abortion. *Obstetrics and Gynecology, 73*, 1035–1037.

DAFFOS, F., CAPELLA-PAVLOVSKY, M. & FORESTIER, F., 1985. Fetal blood sampling during pregnancy with use of needle guided by ultrasound: a study of 606 consecutive cases. *American Journal of Obstetrics and Gynecology, 153*, 655–660.

DAFFOS, F., FORESTIER, F., CAPELLA-PAVLOVSKY, M., THULLIEZ, P., AUFRANT, C., VALENTI, D. & COX, W. L., 1988. Prenatal management of 746 pregnancies at risk of congenital toxoplasmosis. *New England Journal of Medicine, 318*, 271–275.

EYDOUX, P., CHOISET, A., LE PORRIER, N., THEPOT, F., SZPIRO-TAPIA, S., ALLIET, J., RAMOND, S., VIEL, J. F., GAUTIER, E., MORICHON, N. & GIRARD-ORGEOLET, S., 1989. Chromosomal prenatal diagnosis: a study of 936 cases of intrauterine abnormalities after ultrasound assessment. *Prenatal Diagnosis, 9*, 255–268.

FISK, N. M., TANNIRANDORN, Y,. NICOLINI, U., TALBERT, D. G. & RODECK, C. H., 1990. Amniotic pressure in disorders of amniotic fluid volume. *Obstetrics and Gynecology, 76*, 210–214.

FORESTIER, F., 1987. Some aspects of fetal biology. *Fetal Therapy, 2*, 181–187.

GOSDEN, C., RODECK, C. H., NICOLAIDES, K. H., CAMPBELL, S., EASON, S. & SHARP, J. C., 1985. Fetal blood chromosome analysis: some new indications for prenatal karyotyping. *British Journal of Obstetrics and Gynaecology, 92*, 915–920.

HARMAN, C. R., BIEHL, D. R., POLLOCK, R. T., BOWMAN, J. M. & MANNING, F. A., 1983. Intrauterine transfusion: kinetics of absorption of donor cells in fetal lambs. *American Journal of Obstetrics and Gynecology, 145*, 830–835.

HOBBINS, J. C., GRANNUM, P. A., ROMERO, R., REECE, E. A. & MAHONEY, M. J., 1985. Percutaneous umbilical blood sampling. *American Journal of Obstetrics and Gynecology, 152*, 1–6.

HOLZGREVE, W., MINY, P. & SCHLOO, R., 1990. 'Late CVS' international registry compilation of data from 24 centres. *Prenatal Diagnosis, 10*, 159–167.

HSIEH, F. H., CHANG, F. M., KO, T. M. & CHEN, H. Y., 1987. Percutaneous ultrasound-guided fetal blood sampling in the management of non-immune hydrops fetalis. *American Journal of Obstetrics and Gynecology, 157*, 44–49.

KORESAWA, M., INABA, J. & IWASAKI, H., 1987. Fetal blood sampling by liver puncture. *Acta Obstetrica Gynaecologica Japonica, 39*, 395–399.

NICOLAIDES, K. H., RODECK, C. H. & GOSDEN, C. M., 1986. Rapid karyotyping in non-lethal fetal malformations. *Lancet, i*, 283–287.

NICOLINI, U., SANTOLAYA, J., OJO, O. E., FISK, N. M., HUBINONT, C., TONGE, M. & RODECK, C. H., 1988a. The fetal intrahepatic vein as an alternative to cord needling for prenatal diagnosis and therapy. *Prenatal Diagnosis, 8*, 665–671.

NICOLINI, U., KOCHENOUR, N. K., GRECO, P., LETSKY, E., JOHNSON, R. D., CONTRERAS, M. & RODECK, C. H., 1988b. Consequences of fetomaternal haemorrhage after intrauterine transfusion. *British Medical Journal, 297*, 1379–1381.

NICOLINI, U., SANTOLAYA, J., HUBINONT, C., FISK, N. M., MAXWELL, D. & RODECK, C. H., 1989. Visualization of fetal intra-abdominal organs in second trimester severe oligohydramnios by intraperitoneal infusion. *Prenatal Diagnosis, 9*, 191–194.

NICOLINI, U., NICOLAIDIS, P., FISK, N. M., TANNIRANDORN, Y. & RODECK, C. H., 1990. Fetal blood sampling from the intrahepatic vein: analysis of safety and clinical experience with 214 procedures. *Obstetrics and Gynecology, 76*, 47–53.

PALMER, C. G., MILES, J. H., HOWARD-PEBLES, P. N., MAGENIS, R. E., PATIL, S. & FRIEDMAN, J. M., 1987. Fetal karyotype following ascertainment of fetal anomalies by ultrasound. *Prenatal Diagnosis, 7*, 551–555.

RONKIN, S., CHAYEN, B. & WAPNER, R. J., 1989. Intravascular exchange and bolus transfusions in the severely isoimmunized fetus. *American Journal of Obstetrics and Gynecology, 160*, 407–411.

ROSENDAHL, H. & KIVINEN, S., 1989. Antenatal detection of congenital malformation by routine ultrasonography. *Obstetrics and Gynecology, 73*, 947–951.

SIMONI, G., FRACCARO, M., GIMELLI, G., MAGGI, F. & BRICARELLI, D., 1987. False positive and false negative findings on chorionic villus sampling. *Prenatal Diagnosis, 7*, 671–672.

WILLIAMSON, R. A., WEINER, C. P., PATIL, S., BENDA, J., VARNER, M. W. & ABU-YOUSEF, M. M., 1987. Abnormal pregnancy sonogram: selective indication for fetal karyotype. *Obstetrics and Gynecology, 69*, 15–20.

WLADIMIROFF, J. W., SACHS, E. S., REUSS, A., STEWART, P. A., PIJPERS, L. & NIERMEIJER, M. F., 1988. Prenatal diagnosis of chromosome abnormalities in the presence of fetal structural defects. *American Journal of Medical Genetics, 29*, 289–291.

1991, *The British Journal of Radiology*, *64*, 510–515

Assessment of the psychological impact of a breast screening programme

By A. R. Bull, MRCGP, MFCM and *M. J. Campbell, PhD

Yorkshire Regional Health Authority, Park Parade, Harrogate, HG1 5AH, UK and *Department of Medical Statistics and Computing, Southampton General Hospital, Southampton SO9 4XY, UK

(*Received January 1990 and in revised form May 1990*)

Keywords: Psychological effects, Mammographic screening

Abstract. In order to assess the psychological effect of mammographic screening, questionnaires (which included psychometric tests) were sent to 750 women at invitation and, 6 weeks after screening, to 420 women normal after the first mammograph, to 240 women normal after special assessment, and to 68 women normal after open biopsy. Increasing degree of the investigation was associated both with increasing frequency of breast self examination (10% were practising breast self-examination at least once a week before screening compared with 24% for women after special assessment and 35% of women who had had an open biopsy ($p < 0.001$)), and with greater confidence that any malignancy in the breast would have been found. Psychometric scores showed no increase of general levels of anxiety or depression in the screened groups. For anxiety, percentages abnormal were 5, 4, 2 and 6 for the four groups, respectively, and for depression the percentages abnormal were 5, 4, 4 and 6, respectively; 10% of screened women were more anxious about having breast cancer as a result of the screening. At least 10% of women proceeding to open biopsy of benign lesions require professional counselling and support. Psychological ill effects were not detected by the psychometric test among women who did not proceed to this final investigation. Behavioural changes did suggest a raised awareness or fear of potential cancer among the screened population.

Several authors have suggested that screening for breast cancer could raise the level of cancerophobia and general anxiety in the screened population (Gravelle et al, 1982; Maguire, 1983; Roebuck, 1986). In 1983, Maguire claimed that the introduction of a breast cancer screening programme in Manchester had led to an increased number of women presenting with cancerophobia, who "are extremely anxious, constantly fearful about cancer of the breast, and frequently attend their doctor's surgery or hospital clinics with alleged lumps" (Maguire, 1983). He recommended that screening programmes should try to determine the extent of associated psychological complications.

In 1988, Salisbury and Southampton Health Districts introduced a mammography screening programme, according to the recommendations of the Forrest report (Forrest, 1986). We decided to assess the psychological effects on well women of participation in the screening process.

Methods

Four stages of the screening programme were identified as Stage A: the invitation to attend; Stage B: routine mammography; stage C: attendance at a special clinic for investigation of mammographic abnormality by ultrasound, further radiography, or fine-needle cytology; and Stage D: attendance for surgical biopsy of a probably malignant lesion.

Women at Stage A were selected by taking the first 125 women listed for each of the first six general practices involved in the programme (Group A). The first 420 of these women who were found to be normal at

Table I. Age distribution by group

	Group							
	A		B		C		D	
Age (years)	*n*	(%)	*n*	(%)	*n*	(%)	*n*	(%)
50–54	122	(22.6)	76	(22.9)	66	(32.3)	10	(20.4)
55–59	154	(28.5)	113	(34.1)	54	(26.5)	18	(36.7)
60–64	185	(34.2)	105	(31.7)	54	(26.5)	16	(32.7)
65–70	40	(7.4)	26	(7.9)	15	(7.4)	4	(8.2)
Unknown	40	(7.4)	11	(3.3)	15	(7.4)	1	(2.0)
Total	541		331		204		49	

Table II. Frequency of breast self-examination compared with before screening frequency

	Group							
	B				C		D	
	Also in A		Not in A					
	n	(%)	*n*	(%)	*n*	(%)	*n*	(%)
More often	35	(15)	15	(14)	75	(37)	22	(45)
As often	148	(65)	71	(68)	101	(49)	20	(41)
Less often	34	(15)	12	(12)	24	(12)	5	(10)
No response	10	(4)	6	(6)	4	(2)	2	(4)
Total	227		104		204		49	

Stage B were identified as the second study group (Group B). The first 240 of all women found to be normal at Stage C, and the first 68 of all women normal at Stage D, formed Groups C and D, respectively, regardless of whether they had been part of Group A. The numbers were chosen to give a 95% power at the 5% significance level of detecting an increase in the prevalence of depression from 10 to 20% comparing Group A with Group D.

A short questionnaire was posted to all women in

Table IIIa. Frequency of breast self-examination by group

	Group											
	A				B				C		D	
	Not in B		Also in B		Also in A		Not in A					
	n	(%)	*n*	(%)	*n*	(%)	*n*	(%)	*n*	(%)	*n*	(%)
Never	56	(18)	63	(28)	68	(30)	22	(22)	24	(12)	7	(14)
< Once/month	155	(50)	94	(41)	44	(19)	23	(23)	34	(17)	7	(14)
Once/month	69	(22)	54	(24)	85	(37)	47	(46)	97	(48)	18	(37)
Once/week	25	(8)	15	(7)	24	(11)	10	(10)	41	(20)	12	(25)
> Once/week	6	(2)	3	(1)	5	(2)	0	—	8	(4)	5	(10)
No response	1	(0)	0	—	3	(1)	0	—	0	—	0	—
Total	311		229		229		102		204		49	

Table IIIb. Frequency of breast self-examination before and after screening

	After screening					
	Never	< Once/ month	Once/ month	Once/ week	> Once/ week	Total
Before screening						
Never	48	8	5	1	0	62
< Once/month	19	34	34	5	0	92
Once/month	0	2	44	6	2	54
Once/week	1	0	1	10	3	15
> Once/week	0	1	0	2	0	3
Total	68	45	84	24	5	226

$\chi^2 = 15.2$, d.f. = 1, $p < 0.001$.

Table IVa. Psychometric score (depression) by group

	Group											
	A				B				C		D	
	Not in B		Also in B		Also in A		Not in A					
	n	(%)	*n*	(%)	*n*	(%)	*n*	(%)	*n*	(%)	*n*	(%)
Normal	232	(75)	186	(83)	187	(84)	95	(91)	168	(83)	43	(88)
Borderline	52	(17)	26	(12)	23	(10)	7	(7)	25	(12)	3	(6)
Abnormal	26	(8)	10	(4)	12	(5)	2	(2)	9	(4)	3	(6)
Total	310		222		222		104		202		49	

$\chi^2 = 11.2$, d.f. $= 6$, $p = 0.083$.

Table IVb. Psychometric score (depression) before and after screening

	After screening			
	Normal	Borderline	Abnormal	Total
Before screening				
Normal	176	8	2	186
Borderline	11	11	4	26
Abnormal	0	4	6	10
Total	187	23	12	222

McNemar $\chi^2 = 0$, d.f. $= 1$, $p = 1.0$.

Group A with their letter of invitation to attend for screening. A similar questionnaire was posted to all women of Groups B, C and D, 6 weeks after a normal result was declared. No reminders were sent.

The questionnaire asked for demographic information, family history of breast cancer, habits of self-examination and impressions of the screening programme. It incorporated the Hospital Anxiety and Depression Scale (Zigmond & Snaith, 1983), which has been validated against other such instruments (Aylard et al, 1987) and was designed for use in both outpatient and community settings (R. P. Snaith, personal communication). The scale comprises two sets of seven questions, one testing for anxiety, the other for depression, none of which refer to somatic symptoms. The maximum (worst) score for each set is 21.

Statistics

Group B will contain a group of women who completed a questionnaire before screening in Group A, and a group of women who failed to complete the questionnaire before screening. Thus, Groups A and B will have some women in common and a comparison of Groups A, B, C and D by an analysis of variance or non-parametric Kruskal–Wallis test is not strictly valid since the observations were not all independent. This was borne in mind, and a paired comparison of these women who appeared in both Groups A and B was made using a paired *t*-test or a Wilcoxon rank sum test.

Results

Five-hundred and forty-one (72%) replies were received to 750 questionnaires sent to Group A, 331 (79%) to 417 sent to Group B, 204 (85%) to 240 sent to Group C, and 49 (72%) to 68 sent to Group D. Not every questionnaire was entirely complete. Of the 331 in Group B only 229 (69%) had completed a questionnaire before screening. Table I compares the age distribution in each of the four groups and shows that it was similar, apart from an increase in 50–54 year olds in Group C, which is consistent with the low specificity of single-view mammography in younger age groups (Maguire, 1983).

Table II shows the response to the question "Compared with what you did before you were screened, do you examine your breasts for lumps". Ranking the three categories "less often", "as often" and "more often" by 1, 2, 3, respectively, we find mean ranks of 2.0, 2.3 and 2.4 for Groups B, C and D, respectively, differences that are most unlikely to have arisen by chance (Kruskal–Wallis $\chi^2 = 28.6$, d.f. $= 2$, $p < 0.001$), suggesting that women in Groups C and D now examine their breasts more often.

Table IIIa quantifies the frequency of breast self-examination for all four groups. Within Groups B, C and D, there was a significant correlation (Spearman's $r = 0.24$, $p < 0.001$) between increasing intensity of the investigation and increasing frequency of subsequent breast self-examination. For the 226 women who answered the question in both Groups A and B (Table IIIb), 64 had increased breast self-examination and 26 had decreased ($\chi^2 = 15.2$, d.f. $= 1$, $p < 0.001$).

The mean scores (range) for the set of psychometric questions that tested for depression were, for Groups A, B, C and D, respectively, 5.0 (0–19), 4.23 (0–15), 4.25 (0–16) and 3.82 (0–18). There was a significant difference between the four groups (Kruskal–Wallis $\chi^2 = 19.0$, d.f. $= 3$, $p = 0.0003$). However, a multiple-comparison test indicated that this was entirely due to

Table Va. Psychometric score (anxiety) by group

	Group											
	A				B				C		D	
	Not in B		Also in B		Also in A		Not in A					
	n	(%)	n	(%)	n	(%)	n	(%)	n	(%)	n	(%)
Normal	253	(81)	186	(85)	184	(84)	91	(88)	174	(86)	42	(86)
Borderline	40	(13)	27	(12)	25	(11)	10	(10)	24	(12)	4	(8)
Abnormal	20	(6)	6	(3)	10	(5)	2	(2)	4	(2)	3	(6)
Total	313		219		219		103		202		49	

$\chi^2 = 5.09$, d.f. $= 6$, $p = 0.053$.

Table Vb. Psychometric score (anxiety) before and after screening

	After screening			
	Normal	Borderline	Abnormal	Total
Before screening				
Normal	173	12	1	186
Borderline	11	12	4	27
Abnormal	0	1	5	6
Total	184	25	10	219

McNemar $\chi^2 = 0.5$, d.f. $= 1$, $p = 0.8$.

Group A scoring higher than the others, and a comparison of Groups B, C and D was not significant (Kruskal–Wallis $\chi^2 = 1.9$, d.f. $= 2$, $p = 0.4$). For the second set, which tested for anxiety, the scores were, respectively, 4.97 (0–20), 4.43 (0–17), 4.32 (0–15) and 4.27 (0–14). Again there was a significant difference between the groups (Kruskal–Wallis $\chi^2 = 10.7$, d.f. $= 3$, $p = 0.014$) that was entirely due to Group A scoring higher than the others, and a comparison of Groups B, C and D was not significant (Kruskal–Wallis $\chi^2 = 0.7$, d.f. $= 2$, $p = 0.7$).

When the psychometric scores were grouped into ranges of normal (0–7), borderline (8–10) and abnormal (> 10), there was no significant difference between the groups (Tables IVa and Va). In Table IVb, 14 people became more depressed after screening and 15 less so. In Table Vb, 15 people became more anxious and 12 less so. When asked "has the screening left you more anxious about having breast cancer, less anxious or unchanged", of all responders in Groups B, C and D, 57 (10%) said that screening had left them feeling more anxious about having breast cancer, 232 (41.2%) were less anxious, and 273 (48.5%) were unchanged. For depression, those who were more anxious scored 70%, 28% and 2% for normal, borderline and abnormal, respectively; those who were less anxious scored 85%, 10% and 5% for normal, borderline and abnormal, respectively; and those who were unchanged scored 89%, 8% and 3% for normal, borderline and abnormal, respectively. For anxiety, more anxious scored 65%, 26% and 8%, less anxious scored 84%, 10% and 5% and unchanged scored 90%, 7% and 3% for normal, borderline and abnormal, respectively. There is a highly significant difference in the scores for both anxiety ($p < 0.001$) and depression ($p < 0.01$).

Table VI shows an increasing confidence in the sensitivity of the screening process with degree of investigation ($\chi^2 = 48.3$, d.f. $= 3$, $p < 0.001$), with 96% of those in Group D confident that the screening programme was very likely to or would always detect a malignancy, compared with 81% of Group A. A total of 21 women were less confident after screening than before and 49 more confident (Table VIb). When asked, "Do you think that a woman has a good chance of being cured from breast cancer, 97.8% of all women replied "only if the cancer is caught early enough". There was no difference between the groups. Only two women (in Group A) replied 'never'.

Remarks made in the space on the questionnaire for open comment were categorized by ARB. A total of 349 (85.7%) of Groups B, C and D said that the programme was very good or of clear personal benefit. Six per cent of women had found it a threatening or frightening experience, and 4% remarked that it had been physically uncomfortable but made no other comment.

Discussion

The greater the exposure to screening procedures, the more likely were women subsequently to have increased the frequency of breast self-examination for lumps (Table II). This could be a beneficial effect of the programme provided that such an increase did not denote obsessional behaviour.

Table IIIa suggests that for Group B and C, breast self-examination increased in the short-term from never or less than once a month to once a month or once a week. Table IIIb suggests it is particularly women going

Table VIa. "If a woman has breast cancer, how likely is the breast screening programme to find it?"

	Group											
	A				B				C		D	
	Not in B		Also in B		Also in A		Not in A					
	n	(%)	*n*	(%)	*n*	(%)	*n*	(%)	*n*	(%)	*n*	(%)
Always	27	(9)	31	(14)	36	(16)	16	(16)	48	(24)	15	(31)
Very likely	233	(75)	147	(64)	170	(74)	74	(73)	137	(67)	32	(65)
Quite likely	48	(15)	47	(21)	21	(9)	7	(7)	15	(7)	2	(4)
Unlikely	1	(0)	0	—	—		—		0		0	
Missing	2	(1)	4	(2)	2	(1)	5	(5)	4	(2)	0	
Total	311		229		229		102		204		49	

Pooling "unlikely" with "quite likely" and omitting "missing", $\chi^2 = 48.3$, d.f. = 6, $p < 0.001$.

Table VIb. Change in opinion before and after screening

	After screening			
	Always	Very likely	Quite likely	Total
Before screening				
Always	15	15	1	31
Very likely	17	125	5	147
Quite likely	4	28	15	47
Total	36	168	21	225

McNemar $\chi^2 = 10.4$, d.f. = 1, $p < 0.001$.

from less than once a month to once a month. Such behaviour is normal and acceptable, although perhaps paradoxical, since having been declared clear by the screening process, many women might be expected to have seen no further need for *any* self-examination. Indeed, increasing exposure to the screening process did convince many women that if a cancer were present it would have been found (Table VI). The increased frequency of breast self-examination suggests that screening did raise awareness of potential malignancy in the breast for Groups B and C, although not to a pathological degree. Whether or not these changes in frequency of examination persist can only be assessed by long-term follow-up.

In Group D, however, there was a significant increase (to over 10%) in women examining themselves for lumps more often than once a week (Table III). Since Group D is expected to comprise 1% of women screened (Forrest, 1986), the number of women who appear to have been precipitated into excessive self-examination is 0.1% of those screened, or 0.07% of those invited to screen. These figures suggest that at least 10% of women proceeding to open biopsy of benign lesions may require professional counselling or support.

The questionnaires were completed by women who had received a normal result, since the study was designed specifically to assess the psychological cost to those women without breast pathology. It is very likely that a greater degree of anxiety occurs during the period before the result is known. For this reason, the Southampton and Salisbury screening programme gives great importance to the full and rapid provision of information and quick progression from one stage to the next, which will have contributed significantly to containing the anxieties of the clients (Fentiman, 1988). An interval of 6 weeks from last examination to questionnaire was chosen to detect prolonged psychological effect in normal women. No reminders were sent to non-responders because to do so would have included them at a different interval from that of the majority of the study population. A response rate of over 75% is acceptable and was similar for each of the six general practices used. It is possible that those whose anxiety had been raised by screening were less likely to respond than those who were not affected, although the response rate in each of the four study groups was similar suggesting that anxiety was not an important factor of non-response. Whether or not this is the case requires further study.

An increased consciousness of, and examination for, lumps in the breast may lead to an increase, even if by only a small percentage, in presentations to the local general practitioner. The level of such presentations would be worth monitoring.

The majority of women commented favourably on the programme. It is perhaps not surprising that, with exposure to the more thorough investigation of successive stages, there was increasing confidence in the ability of the programme to detect any malignancy (Table VI), although this is at odds with the increased frequency of self-examination for lumps among women in Groups C and D (Table III), a paradox that could be explained by a feeling of reassurance that no cancer already existed, but increased concern about the possibility of developing a breast lump.

The mean anxiety and depression scores on the HAD scale were not raised following screening—indeed, among the screened groups they were reduced, although when grouped into ranges of normal, borderline and abnormal there was no difference between the groups. Nevertheless, 10% of those who had attended reported that the programme had made them more anxious, a figure similar to that of 8% at 6 months reported in Edinburgh (Dean et al, 1986). The HAD scores showed that this 10% showed greater levels of anxiety and depression than the remainder.

The fact that the HAD scale did not indicate an overall increase in anxiety or depression may be due to their occurrence at a subclinical level. The studies that have validated the HAD scale have done so on its ability to detect clinically significant anxiety and depression (Zigmond & Snaith, 1983; Aylard et al, 1987). The frequency of breast self-examination following screening shows that such levels of anxiety were provoked only in a small minority of those women who proceeded to open biopsy. Both the HAD scale and habits of self-examination show that the overall prevalence of clinically significant emotional disturbance was not increased by screening, which contradicts the allegations of Maguire (1983).

Nevertheless, there does appear to have been an increase in awareness of, or anxiety about, breast cancer among the screened population, albeit at a subclinical level, reflected in an increase in self-examination (which may in itself be seen as a beneficial consequence) and by self-reported anxiety in 10% of women.

We conclude that the psychological effects of breast cancer screening, though detectable, are small in the general population, but of note in those who proceed to open biopsy of a benign lesion.

Acknowledgment

This study could not have been done without the support of the staff in the Breast Screening Unit office under Miss Sue Terry. We also thank Miss Jo Scott for typing and printing the questionnaires and Miss Alison Lee for typing the manuscript.

References

Aylard, P., Gooding, J., McKenna, P. & Snaith, R., 1987. A validation study of three anxiety and depression self assessment scales. *Journal of Psychosomatic Research, 31,* 261–268.

Dean, C., Roberts, M., French, K. & Robinson, S., 1986. Psychiatric morbidity after screening for breast cancer. *Journal of Epidemiology and Community Health, 40,* 71–75.

Fentiman, I., 1988. Pensive women, painful vigils: consequences of delay in assessment of mammographic abnormalities. *Lancet, i,* 1041–1042.

Forrest, P., 1986. *Breast Cancer Screening,* (HMSO, London).

Gravelle, H., Simpson, P. & Chamberlain, J., 1982. Breast cancer screening and health service costs. *Journal of Health Economics, 1,* 185–207.

Maguire, G., 1983. Possible psychiatric complications of screening for breast cancer. *British Journal of Radiology, 56,* 284 (Abstr.).

Roebuck, E., 1986. Mammography and screening for breast cancer. *British Medical Journal, 292,* 223–226.

Zigmond, A. & Snaith, R., 1983. The Hospital Anxiety and Depression scale. *Acta Psychiatrica Scandinavica, 67,* 361–370.

1991, *The British Journal of Radiology*, *64*, 516–519

Stage distribution of breast cancer: a basis for the evaluation of breast screening programmes

By A. Bull, MFCM, *L. Mountney and *H. Sanderson, FFCM

Public Health Medicine, Yorkshire Health, Queen Building, Park Parade, Harrogate HG1 5AH, UK and
*Wessex Cancer Intelligence Unit, Royal South Hants Hospital, Graham Road, Southampton SO9 4PE, UK

(*Received June 1990 and in revised form January 1991*)

Keywords: Breast cancer, Screening, Evaluation, Cancer stage

Abstract. Stage at presentation can be predictive of future mortality rates. A change in stage distribution will be indicative of the effect of a programme. All registrations for 1985 aged over 50 years were staged from case notes and, to assess whether a stage drift is already occurring, cases that presented in 1975 were also staged. The accuracy and completeness of the Wessex Cancer Register for this particular cancer was assessed and further sources of registration identified. There was a significant difference between 1975 and 1985 stage distributions. If the Southampton and Salisbury service achieves the same success as the Gavleborg County trials, 4.61 deaths will be prevented at 5 years for each annual cohort of cases. For individual breast screening programmes, effectiveness is better monitored by analysis of stage distribution than of mortality rates.

To evaluate the efficacy of a screening programme it is necessary to assess the effect of that programme on the target disease within the community that is served. The intention of the breast screening programme is to reduce mortality from breast cancer. That the screening technique can be effective in doing so has been demonstrated by research programmes (Collette et al, 1984; Tabar et al, 1985; Aron & Prorock, 1986). Whether this effect is also achieved by routine screening programmes must be assessed.

The difficulties of demonstrating a reduction in mortality are demonstrated by the UK trial (UK Breast Cancer Group, 1988) in which, after 7 years, a 20% reduction in mortality of the study group of 45 841 women just failed to reach statistical significance. Knox has also shown that mortality changes would not be measurable by single districts even in the medium term and he suggests that groups of 10 or 20 health districts would be required for productive evaluation (Knox, 1988). Breast screening is now underway for the health districts of Salisbury and Southampton. An early indication of any likely effect of the programme on mortality would be the effect of screening on the distribution of cancer stage at first presentation. The correlation of tumour size, lymph node metastasis and distant metastasis with survival time has been shown in various analyses (Haybittle et al, 1982; Todd et al, 1987), and it was felt that a change in stage distribution could, with care, be extrapolated to a change in mortality. Where a large, multicentre trial (UK Breast Cancer Group, 1988) is required to monitor changes in mortality, the difficulties of obtaining uniformity in assessment of stage are such that, in this regard, a smaller study may have the advantage, and a single centre may be able to evaluate its performance.

The publicity associated with the programme is likely to increase awareness of the disease and, perhaps independently of the actual screening, to encourage earlier presentation of breast lumps, the majority of which (in the absence of screening) are first detected by patients (Senie et al, 1981). It is also important to assess the effect of screening on the whole of the target population, and not just on those who take up the invitation to screen. Accordingly, it was decided to describe the stage distribution at presentation in 1985 rather than to use concurrent controls such as those who decline the invitation. To test whether a stage drift is already occurring (for which an allowance will have to be made in any future analysis of the screening programme), the stage at presentation in 1975 is also described.

When screening is introduced, registration of cancers detected is likely to be more complete than registration of cancers presenting in other ways. If screening does detect cancer at an earlier stage than otherwise (Collette et al, 1984; Tabar et al, 1987), then this imbalance of registration would distort the true effect on the overall pattern of stage distribution. This study also provided an opportunity to assess the completeness and accuracy of the Cancer Register and to make recommendations for its improvement.

Method

A list was obtained of women born in 1935 or earlier who were first registered as having breast cancer in 1985 while resident in Southampton or Salisbury Health District. A similar list was obtained for women born in 1925 or earlier and first registered in 1975. Identification of cases not registered was made from several sources.

1. A Tamoxifen trial conducted in 1985.
2. A randomized trial of therapy conducted during 1975.
3. Research records of all cases handled by the Southampton Professorial Unit in 1985.

Table I. Breast cancer stage at presentation: women aged 50 years and over (%)

	Stage I/CIS	Stage II	Stage III	Stage IV	Total
1975	30 (27.3)	30 (27.3)	33 (30.0)	17 (15.4)	110 (100)
1985	46 (22.0)	94 (45.4)	37 (17.9)	30 (14.5)	207 (100)
					($p < 0.01$)

4. The Register of patients treated at the Southampton Radiotherapy Unit.

The research records contained details of staging and the clinical notes of these patients were not re-inspected. In all other cases, staging was undertaken from the hospital notes, using pathology reports when available (which was in the great majority of cases). A pilot survey was undertaken to compare stages described from a sample of case notes by this researcher with those described by the responsible surgeon. There was close agreement. Staging was according to the TNM system approved by the American Joint Committee on Cancer.

Results

In 1985, 259 women were registered. Fifty-one (20%) were found to have presented prior to that year and were registered because of death, crisis or coincidental admission; 39 (15%) sets of notes could not be traced. From other sources, 39 cases of breast cancer were found that presented in 1985 but were not on the Register for that year. Of these, 28 were identified from the Radiotherapy Unit, seven from the Tamoxifen trial and four from the Professorial research records.

Of 124 women on the Register for 1975, 23 (18.4%) had presented previously, two had developed cancer subsequently, one had a different form of cancer. Thirty-seven sets of notes could not be traced and 49 cases were found to have presented that year but not registered. Of these, 41 were identified in the Radiotherapy Unit and eight from the randomized trial.

For 1985, 207 cases were studied and for 1975, 110. The overall TNM distribution is shown in Table I. The significant difference ($p < 0.01$) between the 2 years is mostly accounted for by a reduction in Stage III and an increase in Stage II.

The distributions of stage for those registered and those not registered are compared in Table II, and the distributions for women aged between 50 and 65 years in Table III. For neither comparison was there a statistically significant difference. The distribution in 1985 for women aged 50–64 years was similar to the distribution for all women of 50 years and over.

Discussion

The success of the programme depends on altering the mortality rate of the overall population. This early attempt to predict such an effect using stage at diagnosis must describe the pattern of stage of all who present in a given year, not just those who attend for screening. To that end, it is of concern that the register has been shown to be incomplete (and so open to bias). At present, registration is made from hospital discharge data, or notification of death. The latter source means that many women are registered for a year in which their cancer was not incident, and this negates the value of registration data for analysis of trends of the disease. A method of notification is being implemented that would include using radiotherapy department records and pathology department reports. This will make the coverage of breast cancer as complete as possible.

Introduction of screening will provide a complete registration of breast cancer discovered by the programme. Comparisons of this with the disease as registered by less efficient methods (as in earlier years) must be made with caution, because of the bias that such different methods of sampling may introduce.

Despite the search of various sources for breast cancer cases, it is unlikely that these data are a complete analysis. Nevertheless, there is no difference in stage distribution between those registered and those not registered, whether for 1975, 1985 or both years combined. This suggests that the results are a valid representation of the true picture. The large increase in numbers detected is not due to an increase in the denominator population. It may be due to either more

Table II. Breast cancer stage according to whether registered (%)

	Stage I/CIS	Stage II	Stage III	Stage IV
1985				
Registered	45 (23.4)	84 (43.8)	35 (18.2)	28 (14.6)
Not registered	6 (15.4)	19 (48.7)	7 (17.9)	7 (17.9)
1975				
Registered	19 (31.0)	14 (23.0)	17 (27.9)	11 (18.0)
Not registered	11 (22.4)	16 (32.7)	16 (32.7)	6 (12.2)

Table III. Breast cancer stage in women aged between 50 and 65 years of age (%)

	Stage I/CIS	Stage II	Stage III	Stage IV
1975	20 (34.5)	17 (29.3)	14 (24.1)	7 (12.1)
1985	22 (23.1)	43 (45.3)	16 (16.8)	14 (14.7)

efficient case registration or increased incidence. The proportion of stages within the total gives a better indication of changed sensitivity of detection than would the absolute rate of advanced cancers, since there is nothing to indicate what would have happened to the latter had there been no change in the sensitivity of detection.

This study suggests that a change to earlier stage at diagnosis has occurred over the last decade. The reasons for this are not clear. Some studies have shown that breast self-examination leads to earlier diagnosis, others have not (Senie et al, 1981; O'Higgins, 1986). It is possible that greater awareness of the significance of breast lumps, and perhaps greater faith in their curability (Hobbs et al, 1980), has led women to come forward more promptly.

The comparison of stage distribution described here with that described in other studies is difficult. There is a wide variation in clinical detection of lymph node metastases (Yorkshire Breast Cancer Group, 1977) and it is clear that pathological detection of such metastases depends on whether and how extensively the lymph nodes are sampled. It has been suggested that tumour size is a reliable surrogate for TNM stage (O'Higgins, 1986; Day et al, 1988). The standard classification of tumour size, however, takes T_1 as less than or equal to 2 cm. Other papers have used T_1 as less than 2 cm (Yorkshire Breast Cancer Group, 1977; Senie et al, 1981; Tabar et al, 1987). With the propensity to round numbers up, this is an important distinction. The problems of staging consistency in this study were minimized by using pathology reports (available in nearly all cases), and by conducting a validation exercise of retrospective case note staging against the stages allocated in an academic surgical study. It is interesting to note (Table IV) that before screening was introduced in Gavleborg County the proportion of stages at diagnosis was 11% Stage I, 80% Stage II and III and 9% Stage IV. After screening the proportions were, respectively, 70%, 26% and 4% (Lundgren, 1986). Tabar et al (1987) reported that in their trial 34% of their study population against 57% of their controls had tumours of 2 cm or more; 27% of their study population and 34% of their controls had lymph node metastases at diagnosis.

There are many difficulties in the assessment of a screening programme by stage of tumour (Day, 1988). Most important, perhaps, are the lead and length time biases (Aron & Prorock, 1986). Essentially, bias is introduced because screening detects tumours before they would otherwise have presented. Even though the women in whom those tumours are diagnosed might live no longer than they would otherwise have done, their survival time from diagnosis is increased. Stage distribution is affected in a similar way. If tumour volume is but a proxy for time (Atkinson et al, 1986), then earlier detection will automatically reduce stage. That this reduction will also reduce mortality depends both on the assumption that there is no behavioural difference between screen-detected and self-presented tumours, and on successful treatment.

An increased incidence of breast cancer has been shown in study populations. This may in part be due to early-stage, slow-growing tumours that would not have presented because of an intervening death by other cause. In one study (Aron & Prorock, 1986) there was an initial excess of 44% which disappeared at 7 years. In the Two County study (Tabar et al, 1985) there was a 21% excess which persisted at 6 years, which is similar to the results observed in Malmö (Anderson et al, 1988).

These factors are allowed for in the predictions of the effect of changing stage distribution on future mortality (Table V). Wessex registration rates of breast cancer

Table IV. Stage at diagnosis

	Stage I/CIS		Stage II/III	Stage IV
Southampton/Salisbury 1975	27.3%		57.3%	15.4%
Southampton/Salisbury 1985	22.0%		63.3%	14.5%
Gavleborg before screening	11.0%		80.0%	9.0%
Gavleborg after screening	70.0%		26.0%	4.0%
	<2 cm	>2 cm	LNM	No LNM
Tabar et al (Study group	66.0%	34.0%	27.0%	73.0%
Tabar et al (Control group)	43.0%	57.0%	34.0%	66.0%

LNM = lymph node metastases.

Table V. Numbers of deaths at 5 years

Stage	5-year survival	78 women at 1975 Distribution	78 women at 1985 Distribution	93.6 women at Gavleborg Distribution
I	75.1%	5.32	4.33	16.38
II	62.1%	8.09	13.46	12.17
III	38.1%	14.5	8.64	
IV	11.1%	10.73	10.06	3.33
Total		38.64	36.49	31.88
		36.49 − 31.88 = 4.61		

during 1981–83, for the age range 50–64 years, were 173.3 per 100 000. Since the Salisbury and Southampton female population of that age is 45 000, 78 cases of breast cancer are expected in any one year.

The mean relative 5-year survival rates described by the Christie and South Thames registers for 1970–3 (CRC, 1982) are 75% for Stage I, 62% Stage II, 38% Stage III and 11% Stage IV. If these are applied to 78 women at the 1975 stage distribution, 38.64 women would have died at 5 years. Applied to 79 women at the 1985 stage distribution, 36.49 women would have died—an improvement of 2.15 women still alive at 5 years.

Assuming a 20% increase in incidence when screening is introduced (and a 100% uptake of screening), 93.6 cases are expected. Using the distribution described for Gavleborg County after screening, 31.88 of these would have died at 5 years, which is 4.61 deaths less than calculated using the 1985 distribution. These predictions are in close agreement with the results for Malmö (Anderson et al, 1988). Thus, if the Southampton and Salisbury programme matches the success of the Swedish, 4.61 deaths will be prevented at 5 years for each annual cohort of cases—clearly a figure too small to be detected at a local level. In order to have a 70% power of detecting the difference in mortality induced by the two stage distributions, using a test at 0.05 level, 1560 cases would have to be observed in the unscreened distribution and 1872 after screening. For the Salisbury and Southampton programme this would take 20 years.

Pooling data for the six screening programmes planned in Wessex Region would still require 4.5 years of screening and 5 years of follow-up to detect a change in mortality. Surveillance of stage at diagnosis will therefore be an important part of any interim evaluation.

References

Anderson, I., Aspegren, K., Janzon, L., Landberg, T., Lindholm, K., Lindell, F., Ljungberg, O., Ranstam, J. & Sigfusson, B., 1988. Mammographic screening and mortality for breast cancer. *British Medical Journal, 297,* 943–948.

Aron, J. & Prorock, P., 1986. An analysis of the mortality effect in a breast cancer screening study. *International Journal of Epidemiology, 15,* 36–43.

Atkinson, E., Brown, B. & Montague, E., 1986. Tumour volume, nodal status, and metastasis in breast cancer in women. *Journal of the National Cancer Institute, 76,* 171–178.

CRC, 1982. *Trends in Cancer Survival in Great Britain,* CRC, 1970–73.

Collette, H., Rombach, J., Day, N. & De Waard, F., 1984. Evaluation of screening for breast cancer in a non-randomised study (the DOM Project) by means of a case-controlled study. *Lancet, i,* 1224–1226.

Day, N. E., 1988. Self examination of the breast. *British Medical Journal, 297,* 624.

Day, N., Williams, D. & Khaw, K., 1988. Breast cancer screening programmes: the development of a monitoring and evaluation system. Paper 88 (16) NP 132 (Advisory Committee on Breast Cancer Screenings).

Haybittle, J., Blamey, R., Elston, C., Johnson, J., Doyle, P., Campbell, F., Nicholson, P. & Griffiths, K., 1982. A prognostic index in primary breast cancer. *British Journal of Cancer, 45,* 361–366.

Hobbs, P., Smith, A., George, W. & Selwood, R., 1980. Acceptors and rejectors of an invitation to undergo breast screening compared with those who referred themselves. *Journal of Epidemiology and Community Health, 34,* 19–22.

Knox, E. G., 1988. Evaluation of a proposed breast cancer screening regime. *British Medical Journal, 297,* 650–654.

Lundgren, B., 1986. Mammographic breast cancer screening. Should we, could we, how? Proceedings of a Conference, Marie Curie Memorial Foundation, London, 11 November 1986 (Marie Curie Memorial Foundation, London).

O'Higgins, N., 1986. Reducing the mortality from breast cancer. *British Journal of Hospital Medicine, 36,* 404–408.

Senie, R., Rosen, P., Lesser, M. & Minnie, D., 1981. Breast self examination and medical examination related to breast cancer stage. *American Journal of Paediatric Haematology, 71,* 583–589.

Tabar, L., Duffy, S. & Krusemo, U., 1987. Detection method, tumour size and node metastasis in breast cancers diagnosed during a trial of breast cancer screening. *European Journal of Cancer and Clinical Oncology, 23,* 959–962.

Tabar, L., Gad, A., Holberg, L. H., Ljungquist, U., Fagerberg, C., Baldetorp, L., Grontoft, O., Lundstrum, B., Manson, J., Eklund, G., Day, N. & Petterson, F., 1985. Reduction in mortality from breast cancer after mass screening with mammography. *Lancet, i,* 829–832.

Todd, J. H., Dowle, C., Williams, M., Elston, C., Ellis, I., Hinton, C., Blaney, R. & Haybittle, J., 1987. Confirmation of a prognostic index in primary breast cancer. *British Journal of Cancer, 56,* 489–492.

UK Breast Cancer Group, 1988. First results on mortality reduction in the UK trial of early detection of breast cancer. *Lancet, ii,* 411–416.

Yorkshire Breast Cancer Group, 1977. Observer variation in recording clinical data from women presenting with breast lesions. *British Medical Journal, 2,* 1196–1199.

1991, *The British Journal of Radiology*, *64*, 520–523

The effect on pulmonary function of tangential field technique in radiotherapy for carcinoma of the breast

By May Brit Lund, MD, Kurt Inge Myhre, MD, *Haakon Melsom, MD and Bjørn Johansen, MD

University of Oslo, Department of Thoracic Medicine, Rikshospitalet, The National Hospital, and
*The Norwegian Radium Hospital, Oslo, Norway

(*Received September 1990*)

Keywords: Respiratory function tests, Radiation injuries, Breast neoplasms

Abstract. Twenty-five patients treated by lumpectomy and radiotherapy for Stage I breast cancer were enrolled in a prospective study to measure the effects of tangential field irradiation on pulmonary function. Fractional doses of 2 Gy to a total of 50 Gy were administered with the tangential technique. An additional 10 Gy (2 Gy × 5) was given as direct booster. Dynamic and static lung volumes, distribution of ventilation and gas transfer were measured before irradiation and at varying intervals up to 1 year after the completion of therapy. There was a small, but statistically significant decrease in the forced vital capacity (mean 63 ml) and the forced expiratory volume in 1 second (mean 79 ml) measured 3 months after irradiation ($p < 0.05$). These changes were reversed within 1 year. The reduction in total lung capacity (mean 240 ml) after 3 months was nearly significant ($p = 0.06$). The remaining variables did not change to a significant degree. We conclude that a slight restrictive ventilatory impairment may occur when a combined tangential and direct booster technique is applied. The changes are, however, small and reversible, and imply no clinical importance.

The traditional choice in treating breast cancer has been mastectomy. Recent studies, however, have convincingly demonstrated that acceptable long-term survival can be obtained if conservation surgery (lumpectomy) of small breast tumours is followed by radiotherapy (Montague et al, 1984). Such breast-preserving treatment can be offered to women with small solitary tumours (diameter < 2 cm), and without clinical evidence of lymph node involvement or tumour infiltration outside the breast, *i.e.* carcinoma of the breast Stage I ($T_1N_0M_0$).

Lung injury induced by radiation is well documented (Rubin & Casarett, 1968) and the clinical and radiographic syndrome has been thoroughly investigated and described (Gross, 1977). In breast-preserving treatment, radiotherapy is usually given as a small booster dose directly to the tumour area while the larger fraction is administered as two opposing tangential fields. Even with this precaution, some part of the underlying lung will invariably be included in the radiation field. To determine to what extent, if any, lung tissue is affected by breast-preserving radiotherapy, we have studied pulmonary function in patients before and at varying intervals after such treatment.

Patients and methods

Patients

Patients with Stage I disease who had been treated with lumpectomy at a general hospital and subsequently referred to the Norwegian Radium Hospital for post-operative radiotherapy were invited to participate in the study. They were not included if they had a history of productive cough, dyspnoea or wheezing. Between January 1986 and May 1987, 28 consecutive patients were enrolled and gave their informed consent. After the first examination, two patients did not want to take part, and one was excluded because her lung function values were below the lower normal limits.

The remaining 25 patients were 35–75 years old (mean 46.7 years).

Methods

Radiotherapy was started 2–4 weeks after surgery and was given as two opposing tangential fields with a 5 MeV linear accelerator. Fractions of 2 Gy were given 5 days a week to a total dose of 50 Gy. The tumour bed was then boosted with 10–12 MeV electrons at 2 Gy daily for 5 days.

Pulmonary function tests included dynamic spirometry and measurements of static lung volumes, distribution of ventilation and gas transfer. Each patient was examined on four occasions: immediately before radiotherapy, and 1 week, 3 months and 1 year after completion of the therapy. All measurements were taken before 12 a.m.

Standing spirometry was performed on a Med-Science wedge spirometer, model 570, which was calibrated daily. At least three forced expirations were required, of which two were selected according to the criteria of the ATS (American Thoracic Society, 1979). The average FVC (forced vital capacity) and the average FEV_1 (forced expiratory volume in 1 second) were recorded, both in absolute values and as a percentage of the predicted (Gulsvik et al, 1979). Functional residual capacity (FRC) and vital capacity (VC) were measured

---

Address correspondence to Dr May Brit Lund, Department of Thoracic Medicine, Rikshospitalet, N-0027 Oslo 1, Norway.

in a constant-volume body plethysmograph (Siemens Siregnost FD 91). Total lung capacity (TLC) was defined as the sum of FRC and the inspiratory reserve capacity (IRC) obtained during the same manoeuvre. Residual volume (RV) was obtained by subtracting VC from TLC. Duplicate values of TLC and RV were averaged and recorded. Figure 1 illustrates the relationships between static lung volumes.

Distribution of ventilation was determined by the single-breath nitrogen washout test according to recommended criteria (National Heart and Lung Institute, 1973). We used a Hewlett-Packard nitrogen analyzer (47302A). The slope of Phase III and closing volume were determined by computer analysis (modified after Craven et al, 1976). Duplicate tests were averaged and recorded.

Gas transfer was examined with the Hewlett-Packard 47404 Single Breath Diffusion System. Average values for TLCO (transfer factor of the lung for carbon monoxide) and kCO were recorded; kCO is TLCO divided by alveolar volume. The latter is determined by helium dilution. Owing to technical breakdown, gas transfer values from the fourth examination were incomplete and omitted from the analysis. A few patients were unable to complete some of these tests.

We performed all statistical analyses with the StatGraphics Version 2.0 statistical computing package on an IBM AT personal computer. For each lung function variable, the individual difference between pre- and post-treatment values was chosen as test statistic. As these differences were normally distributed, we used the paired *t*-test, at a one-tailed probability level of 0.05, to determine whether their means differed from zero. We calculated the power of the present study to be at least 95% for detecting a difference of 10% from pre-therapy values of FVC and FEV_1, and at least 90% for detecting a 20% change in TLC and TLCO. The probability of detecting differences in RV, Phase III and kCO was rather low (Altman, 1980).

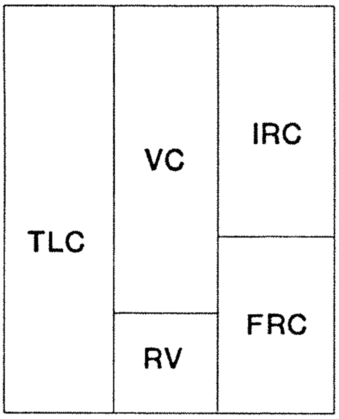

Figure 1. Relationships between static lung volumes. Total lung capacity (TLC) = FRC + IRC; it also equals VC + RV (see text).

Results

Table I presents the changes in FVC (mean and SD) at the three post-radiotherapy examinations. A small, but statistically significant reduction appeared after 3 months (at visit 3), but disappeared within 1 year. When the values are adjusted for the change in age, the reduction at 3 months persists (Table II).

Table III shows that FEV_1 is significantly reduced, both after 3 months and after 1 year. Figure 2 presents graphically the decrease in the latter variable. When these differences are age-adjusted, the reduction after 1 year disappears, while it persists at 3 months (Table IV). There were no significant deviations in any of the remaining variables, either in absolute or in age-adjusted terms. However, the total lung capacity was reduced after 3 months to a near-significant degree (Table V).

Discussion

The present study demonstrates a small, but statistically significant decrease in ventilatory lung function, measured approximately 3 months after tangential field irradiation. We found no evidence of persistent reduction after 1 year.

Pathological changes in lung tissue following thoracic irradiation have been recognized as a clinical entity for many years. In a comprehensive review, Gross (1977) thoroughly discussed the pulmonary effects of radiation therapy. The biological aspects and histopathology of radiation damage were described and summarized, and the clinical features including characteristic changes in pulmonary function and radiographic appearance were dealt with. The syndrome has two phases: an acute transient phase, radiation pneumonitis, that occurs 6–12 weeks after radiotherapy, and a second phase, radiation fibrosis, that may subsequently develop within the following 6–12 months.

Lung injury is thought to be a direct consequence of irradiation, the incidence and severity being directly related to the volume of lung irradiated, the total dose and the rate of delivery (Rothwell et al, 1985; Rubinstein et al, 1988). Changes have also been documented in the non-irradiated lung, which suggests the possibility of an additional hypersensitivity mechanism (Gibson et al, 1988).

Table I. Paired *t*-test analysis of differences in FVC (ml) between first and subsequent visits

	Visit		
	1–2 ($n = 25$)	1–3 ($n = 24$)	1–4 ($n = 23$)
Mean	48	−63	−49
SD	210	158	266
SEM	42	32	55
p	0.13	0.032	0.19

SD = standard deviation; SEM = standard error of the mean.

Table II. Paired *t*-test analysis of differences in FVC between first and subsequent visits (FVC given as % of predicted value)

	Visit		
	1–2 ($n = 25$)	1–3 ($n = 24$)	1–4 ($n = 23$)
Mean	1.5	−1.6	−0.7
SD	6.2	4.5	8.1
SEM	1.2	0.9	1.7
p	0.11	0.048	0.33

Table III. Paired *t*-test analysis of differences in FEV_1 (ml) between first and subsequent visits

	Visit		
	1–2 ($n = 25$)	1–3 ($n = 24$)	1–4 ($n = 23$)
Mean	−32	−79	−71
SD	144	128	116
SEM	29	26	24
p	0.14	0.003	0.004

Table IV. Paired *t*-test analysis of differences in FEV_1 between first and subsequent visits (FEV_1 given as % of predicted value)

	Visit		
	1–2 ($n = 25$)	1–3 ($n = 24$)	1–4 ($n = 23$)
Mean	−1.1	−2.6	−1.3
SD	5.1	4.8	4.3
SEM	1.0	1.0	0.9
p	0.15	0.007	0.075

Table V. Paired *t*-test analysis of differences in TLCO, Phase III and TLC between visit 1 and visit 3

	TLCO (mmol/kPa/min)	Phase III ($\%N_2/l$)	TLC (l)
Mean	−0.20	−0.09	−0.24
SD	1.52	0.83	0.62
SEM	0.32	0.17	0.15
p	0.27	0.30	0.06

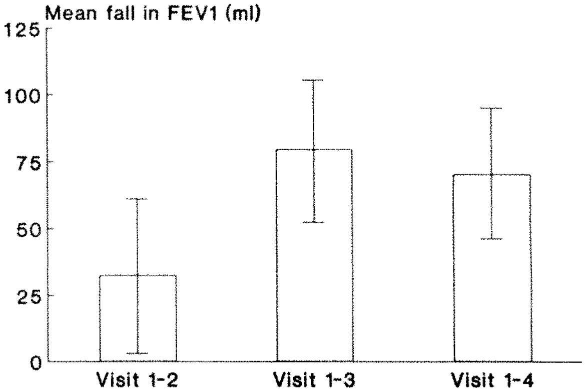

Figure 2. Decrease in FEV_1 between first and subsequent visits (mean and standard error of the mean).

In the first systematic study on effects of irradiation on pulmonary function, Emirgil and Heinemann (1961) found that TLC, RV, TLCO and pulmonary compliance decreased in their 15 patients, most of them treated for inoperable carcinoma of the breast. The static lung volumes remained reduced while TLCO values returned to normal with time. There was no change in the distribution of inspired air. Høst and Vale (1973) studied lung function after mantle field irradiation in 17 patients with extrathoracic Hodgkin's disease. They too found a restrictive ventilatory impairment with lung volumes reduced by approximately 10%. The initial reduction in TLC appeared to be due to a decrease in VC only, whereas later RV also slightly decreased. They found this type of irradiation to have no apparent influence on the pulmonary gas exchange.

Three months after the completion of radiotherapy, Groth et al (1986) compared the effects of tangential and direct irradiation on global and regional lung function in 22 patients treated with simple mastectomy. The dose delivered to the lungs was less than 5 Gy in the tangential field group (eight patients) and up to 20 Gy in the other. They concluded that there was no impairment of ventilation or perfusion in the group treated with the tangential technique, but a reduction in both indices in those treated with direct radiation. Ventilatory lung function was not measured prior to irradiation and only predicted values were applied when the effects were evaluated. The two groups differed significantly in their smoking habits which may explain some of the observed differences. Kaufman et al (1986) studied the effects of radiation therapy on lung function in 21 patients with breast cancer. Treatment included a modified radical mastectomy followed by radiation to ports overlying the respective upper lobe of the lung, the mediastinum and the chest wall. The dose to the chest wall (50 Gy) was delivered with opposing non-angulated tangential portals. The irradiation of the ipsilateral internal mammary and supraclavicular lymph nodes (affecting the mediastinum and the upper lobe) was administered as direct beam. They found a small, but statistically significant decline in FVC, FEV_1 and the ratio of FEV_1 to FVC within the first 3 months following irradiation. There was no evidence of reversibility after 1 year.

Our results confirm the previous findings that the tangential field technique has a much less damaging effect on the lungs than direct irradiation. In the study of Groth et al (1986), the dose delivered to the lungs was small. We have not calculated the exact dose to the lungs of our patients, but presumably it is larger than

5 Gy. This may be one reason why we found a small ventilatory impairment and Groth et al did not. Actually, what they found was a difference between the two modes of treatment. The design of their study does not permit any conclusions regarding the temporal effect of tangential irradiation *per se*. The findings of Kaufman et al (1986) are more in accord with ours, with the exception that lung function was persistently reduced in their patients. This may be explained by larger radiation doses and a different irradiation technique. They also calculated the volume of lung that received direct radiation to be nearly five times larger than the portion receiving the tangential beams. Even if the direct dose is considerably less than the tangential one, injury caused by the former may be partly responsible for the observed effects on pulmonary function. Whether "pure" tangential radiation affects lung function remains to be seen.

It is conceivable that the reduced vital capacity reflects a restrictive defect even if the concurrent decrease in FEV_1 suggests an obstructive element as well. The nearly significant reduction in total lung capacity supports this view. The restriction may be due not only to structural changes in the lung parenchyma, but also to altered elastic properties of the chest wall caused by radiation. The findings of Høst and Vale (1973) that vital capacity but not residual volume initially decreased agree with this. The fact that Kaufmann et al (1986) did not find any correlation between X-ray changes and lung function also supports this view. It has recently been shown by Bell et al (1988) that radiation also causes shrinkage of pulmonary vessels, especially when the hilum and mediastinum are included in the field.

It may seem surprising that the more sophisticated lung function variables did not change. While these tests almost exclusively reflect the properties of the lung itself, lung volumes are also dependent on the function of the chest wall. If damage of the latter contributes to the reduced vital capacity, one should not expect changes in transfer factor and gas distribution. An additional explanation is that the number of patients is too small to detect true differences in these test variables owing to their larger variability. The power of the applied statistical test in this case is too low.

Our findings and those cited above do not support the suggestion that hypersensitivity mechanisms play a role in radiation-induced lung injury. The magnitude of the decrease in ventilatory lung function seems to be correlated to the amount of irradiated tissue *per se*. Structural changes, however small, due to hypersensitivity and hence affecting larger lung regions, would possibly be reflected by changes in transfer factor and distribution of ventilation.

Shielding of the chest wall and underlying lung is important to avoid radiation damage. We have shown that such damage may also occur when the tangential field technique, including a direct component, is applied. The observed changes are small and of no clinical importance. One must therefore conclude that this technique is a safe procedure in breast-preserving treatment.

Acknowledgments

The technical assistance of Else-M. Blix, Hanne Gohn and Kristin Bjerke Aas is highly appreciated. This work was initiated by the late Professor Jon R. Vale.

References

American Thoracic Society, 1979. ATS Statement—Snowbird workshop on standardization of spirometry. *American Review of Respiratory Disease, 119*, 831–838.

Altman, D. G., 1980. Statistics and ethics in medical research. III. How large a sample? *British Medical Journal, 281*, 1336–1338.

Bell, J., McGivern, D., Bullimore, J., Hill, J., Davies, E. R. & Goddard, P., 1988. Diagnostic imaging of post-irradiation changes in the chest. *Clinical Radiology, 39*, 109–119.

Craven, N., Sidwall, G., West, P., McCarthy, D. S. & Cherniack, R. M., 1976. Computer analysis of the single-breath nitrogen washout curve. *American Review of Respiratory Disease, 113*, 445–449.

Emirgil, C. & Heinemann, H. O., 1961. Effects of irradiation of chest on pulmonary function in man. *Journal of Applied Physiology, 16*, 331–338.

Gibson, P. G., Bryant, D. H., Morgan, G. W., Yeates, M., Fernandez, V., Penny, R. & Breit, S. N., 1988. Radiation-induced lung injury: a hypersensitivity pneumonitis? *Annals of Internal Medicine, 109*, 288–291.

Gross, N. J., 1977. Pulmonary effects of radiation therapy. *Annals of Internal Medicine, 86*, 81–92.

Groth, S., Zaric, A., Sørensen, P. B., Larsen, J., Sørensen, P. G. & Rossing, N., 1986. Regional lung function impairment following post-operative radiotherapy for breast cancer using direct or tangential field techniques. *British Journal of Radiology, 59*, 445–451.

Gulsvik, A., Johansen, B. & Vale, J. R., 1979. Spirometric variables. Precision of measurement and values in an asymptomatic population. In *Obstructive Lung Disease in an Urban Population*, ed. by A. Gulsvik (Department of Thoracic Medicine, Rikshospitalet, University of Oslo), pp. 88–119.

Høst, H. & Vale, J. R., 1973. Lung function after mantle field irradiation in Hodgkin's disease. *Cancer, 32*, 328–332.

Kaufman, J., Gunn, W., Hartz, A. J., Fisher, M., Hoffman, R. G., Schlueter, D. P. & Komanduri, A., 1986. The pathophysiologic and roentgenologic effects of chest irradiation in breast carcinoma. *International Journal of Radiation Oncology, Biology, Physics, 12*, 887–893.

Montague, E. D., Ames, F. C., Schell, S. R. & Romsdahl, M. M., 1984. Conservation surgery and irradiation as an alternative to mastectomy in the treatment of clinically favorable breast cancer. *Cancer, 54*, 2668–2672.

National Heart and Lung Institute, Division of Lung Diseases, 1973. Suggested standardized procedures for closing volume determinations (nitrogen method) (National Heart, Lung and Blood Institute, Bethesda).

Rothwell, R. I., Kelly, S. A. & Joslin, C. A. F., 1985. Radiation pneumonitis in patients treated for breast cancer. *Radiotherapy and Oncology, 4*, 9–14.

Rubinstein, J. H., Richter, M. P., Moldofsky, P. J. & Solin, L. J., 1988. Prospective prediction of post-radiation therapy lung function using quantitative lung scans and pulmonary function testing. *International Journal of Radiation Oncology, Biology, Physics, 15*, 83–87.

Rubin, P. & Casarett, G. W., 1968. *Clinical Radiation Pathology* (W. B. Saunders, Philadelphia).

1991, *The British Journal of Radiology*, *64*, 524–528

The reduction in radiation dose for intra-oral radiographs by the use of thin K-edge filters

By D. S. MacDonald-Jankowski, MSc, FDSRCPS, DDRRCR and *C. P. Lawinski, BSc, MSc, MPhil

Department of Dental Radiology, King's College School of Medicine and Dentistry, Denmark Hill, London SE5 9RS and *Department of Medical Physics and Medical Engineering, King's College Hospital, Denmark Hill, London SE5 9RS, UK

(*Received July 1990 and in revised form November 1990*)

Keywords: Dental radiography, Filtration, Radiation dosage

Abstract. The aim of this investigation was to reduce the radiation dose to patients undergoing intra-oral dental radiography by using thin K-edge filters in addition to the existing aluminium filter. The subject was a head phantom (a human skull embedded in tissue-equivalent material), which was exposed to X rays over a range of tube voltages (50–90 kVp) for each of the four filter systems. These were 2.7 mm aluminium alone (the existing total filtration) or with added 0.1 mm erbium, 0.1 mm yttrium or 0.05 mm niobium. The radiation dose was measured at four selected sites along the primary beam. These were the entrance skin dose, the exit skin dose and intra-orally both in front and behind the dental film packet. The exposure times and radiation doses required to produce an equivalent density (degree of blackening) on a radiograph of an upper molar tooth were determined. Within the usual diagnostic range of 60–80 kV the use of the thin K-edge filter resulted in a doubling of the exposure time (owing to the additional attenuation of the added filters). However, the skin dose and the total dose imparted to the patient were significantly reduced.

There is no known minimum radiation dose threshold below which radiation-induced malignant tumours or genetic deformities cannot occur. Therefore, in general, the radiation dose to the patient should be as low as reasonably achievable (ALARA) (ICRP, 1977). In addition to careful collimation of the X-ray beam, the use of faster film or film–screen combinations, optimal processing and the implementation of quality-control programmes, a reduction in dose can in part be achieved by the use of suitable beam filtration.

In the majority of diagnostic X-ray units the added filter is aluminium, which preferentially absorbs the low-energy photons from the beam. The thicker the filter the greater the proportion of low-energy photons removed and the smaller the skin dose. However, if the thickness of aluminium is too great the total intensity of the X-ray beam will fall off markedly. This can result in an increase in the exposure time, which could increase the chance of movement unsharpness (especially with children). A thick aluminium filter is therefore not the most ideal way to reduce skin dose.

Several materials (in the form of thin foils) have been suggested as supplements to the existing aluminium filtration in an X-ray tube. These materials are chosen as they exhibit absorption edges (K-edge) at suitable energy values to shape the X-ray spectrum and to remove more effectively the low-energy radiation. The materials are: (i) yttrium (K-edge at 17 keV); (ii) niobium (K-edge at 19 keV); and (iii) erbium (K-edge at 58 keV).

With yttrium (atomic number 39) and niobium (atomic number 41) the K-edge is towards the lower end of the X-ray spectrum and more efficiently removes the unwanted low-energy radiation than aluminium alone (K-edge at 1.5 keV).

In the case of erbium, owing to its higher atomic number (68), a substantially increased proportion of the low-energy photons are absorbed by the photoelectric effect. This might be expected to result in an increase in the mean energy of the spectrum. However, the K-edge, towards the higher end of the spectrum, results in the increased absorption of high-energy photons (also by the photoelectric effect) maintaining the mean energy of the spectrum at the required level.

In conventional dental radiography, two rare-earth filter materials, samarium (Richards et al, 1970; Gelskey & Baker, 1981; Kircos et al, 1989) and erbium (Horner et al, 1988; Ponce et al, 1988; Kircos et al, 1989), have been examined. Both materials demonstrated a marked reduction in skin dose. Farman and his co-workers (1989) reported a reduction in dose by using yttrium filtration.

The aim of this study was to examine and compare the effect on radiation dose to the patient of the addition of three commercially available thin metal filters to a typical dental X-ray unit. Additionally, the effect on image quality was subjectively assessed and the effect on the shape of the X-ray spectrum was investigated.

Materials and methods

A General Electric GE1000 dental X-ray unit with a total filtration equivalent to 2.7 mm of aluminium (0.5 mm aluminium-equivalent inherent filtration and

2.2 mm aluminium added filtration) was employed for all measurements made. The tube voltages could be varied between 50 and 90 kV and two settings of tube current, 10 and 15 mA, were available.

The calibration of tube voltage was checked using an RMI type 230 digital kVp meter (supplied by Vinten Instruments Ltd). All set values were correct to within ±1 kV.

For all exposures the unit was operated at 15 mA. Collimation of the beam was provided by a 36 cm open-ended cylindrical long cone with a diameter of 6 cm. This was used in conjunction with a dental X-ray film holder/tube locator (Rinn) to produce a consistent 50 cm focus–film distance.

Kodak E-speed (Ektaspeed) non-screen dental film (4.1 cm × 3.1 cm) was used. All radiographs were processed in a Siemens Pantomat P10 automatic processor (running at a developer temperature of 24°C, processing time approximately 5 minutes) with chemistry by Champion Photochemistry International Limited. Consistent processing was ensured by daily sensitometric monitoring.

The following filter systems were investigated.

1. The existing 2.7 mm aluminium-equivalent filtration alone (referred to as aluminium).
2. 0.1 mm erbium foil (Reactor Experiment Inc.) in addition to the 2.7 mm aluminium-equivalent filtration (referred to as erbium).
3. 0.05 mm niobium foil (Niobex Inc.) in addition to the 2.7 mm aluminium-equivalent filtration (referred to as niobium).
4. 0.1 mm yttrium foil (Yttro Corporation) in addition to the 2.7 mm aluminium–equivalent filtration (referred to as yttrium).

The additional foils were affixed to the added aluminium filter (accessible through the tube port) on the side facing the patient.

The radiation spectra of the four systems were computed using the methods of Birch et al (1979). The half-value layer (HVL) in millimetres of aluminium of all four filter systems was measured at 75 kVp using a series of pure aluminium foils. These allowed the total filtration of each system to be estimated using the data provided in Wachsmann and Drexler (1976).

The effect of the added filters on exposure time was investigated. The upper molar area (on a DXTTR phantom) was selected as the "target" site for this investigation as this was considered the site most likely to allow a typical radiographic technique to be closely followed.

With the aluminium filtration alone an exposure time of 0.25 seconds at 75 kV was found to give the optimum quality radiograph of the target area. This was taken to be the "standard radiograph", to which those obtained with the other filter systems could be compared.

For ease of experimental reproducibility (particularly in terms of positioning) a step wedge technique was used to obtain an objective measure of the relative exposure time for each filter system. An image of an aluminium step wedge (with 1 mm steps) was produced using the exposure factors for the "standard radiograph". The optical density under each step was measured using a densitometer (Victoreen Inc.). The density under the fifth step (5 mm of aluminium) was found to be 1.2, which was taken as the "standard density". A series of images of the step wedge was then produced for each of the four filter systems over a range of exposure times and over a range of tube voltages (from 55 to 85 kV at 5 kV intervals). For each radiograph the optical density was plotted against the exposure times for each kVp used. Thus, the exposure time to produce an optical density of 1.2 (the "standard density") for each of the four filter systems at each value of kV could be determined.

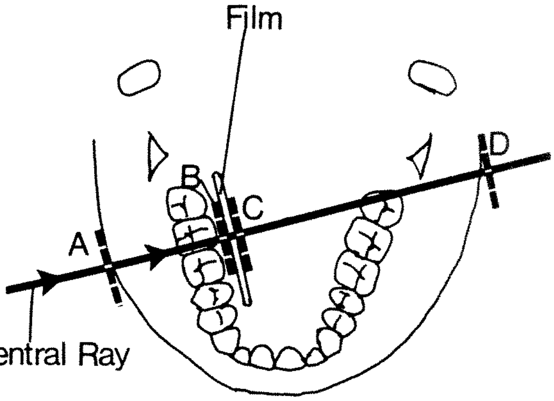

Figure 1. Sites of dose measurement in a horizontal section through the level of the upper teeth.

Radiation dose measurements for each filter system were made on a head phantom with the mouth in the open position. A 37D exposure meter system with a 3.5 cm^3 volume ionization chamber (supplied by Vinten Instruments Ltd) was used. This chamber was chosen as it was small enough to be placed into the oral cavity of the phantom.

A non-screen intra-oral dental film packet incorporating a lead foil backing (Kodak, Ektaspeed or E speed) was placed palatal to the upper right molar teeth in the usual manner.

A focal film distance of 50 cm (defined by a cylindrical long cone 6 cm in diameter) and a tube current of 15 mA with a 1 second exposure time were employed.

The radiation exposure was measured at four sites along the central beam axis for a series of kV values (55, 65, 75 and 85 kV) for each of the four filter systems. The sites of selected dose measurement were the entrance skin dose (right side, A in Fig. 1), the exit skin dose (left side, D) and intra-orally, both in front of the film (B) and behind the film (C).

The measured exposures were then converted to absorbed dose and adjusted by the relative exposure time factors to give the doses for each filter system approximating to the "standard" radiograph, and are presented graphically.

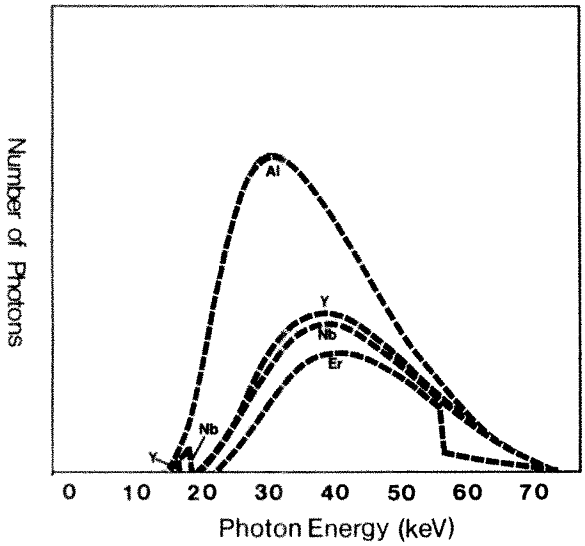

Figure 2. Computed beam spectra for the four filter systems.

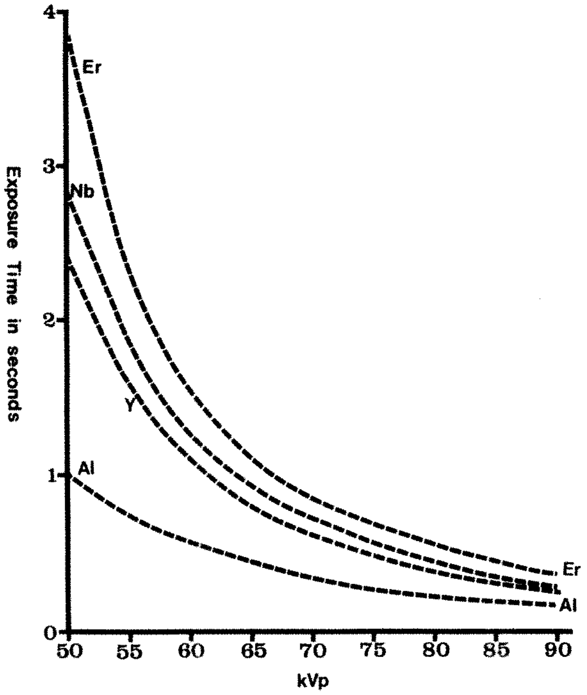

Figure 3. Variation in exposure time to produce the "standard density" on the film.

Results

The computed spectra for the four filter systems at a tube voltage of 75 kV are shown in Fig. 2. The shaping of the spectra resulting from the additional thin K-edge filters is clearly illustrated. The calculated mean energy of each filter system is shown in Table I. HVL and derived total filtration of the four filter systems is given in Table II. All values of filtration are within the minimum requirements given in the notes for *Guidance Notes for the Protection of Persons against Ionising Radiations Arising from Medical and Dental Use* (NRPB, 1988).

The exposure times for each filter system to achieve the same optical density on the processed film are illustrated graphically in Fig. 3. The relative exposure (the factor by which the exposure time must be increased) for each filter to achieve the same optical density can be derived from these curves. The data for radiation dose are presented in Figs 4–7.

As expected, for all the filter systems the higher the kVp the lower the entrance skin dose due to the higher penetration of the beam (Fig. 4). In comparing the filter systems the aluminium filter alone (with a lower mean photon energy) delivered a higher dose to the skin than the other filter systems. The results for these are close, with the erbium system delivering the least dose. As the kV is increased the differences between the aluminium and the other three filter systems decreases.

Figure 5 demonstrates that the film dose of the four filter systems is similar. This is to be expected as the sensitivity of the film has only slight dependence on the energy of the radiation. The film dose exhibits a gradual increase in dose delivered with increase in kVp, which is consistent with a fall in the sensitivity of the film with increasing kVp. This time the highest to lowest order was niobium, yttrium, erbium and then aluminium, possibly because of the relationship between the spectrum of radiation produced with each filter system and the spectral sensitivity of the film.

The post-film dose (Fig. 6) and exit skin dose (Fig. 7) show a more marked increase in dose with increasing kVp. This is consistent with the higher-energy radiation delivering a greater depth dose. The doses for the additionally filtered systems are higher than for the

Table I. Mean energies of the four filter systems

Filter system	Mean energy (keV)
2.7 mm aluminium alone	37.9
Al + 0.1 mm yttrium	42.9
Al + 0.05 mm niobium	43.1
Al + 0.1 mm erbium	43.1

Table II. Half-value layers and equivalent filtration

Filter system	HVL 75 kVp (mm Al)	Filtration (mm Al)
2.7 mm aluminium alone	2.6	2.7
Al + 0.1 mm yttrium	4.0	6.0
Al + 0.05 mm niobium	4.3	7.0
Al + 0.1 mm erbium	4.8	9.0

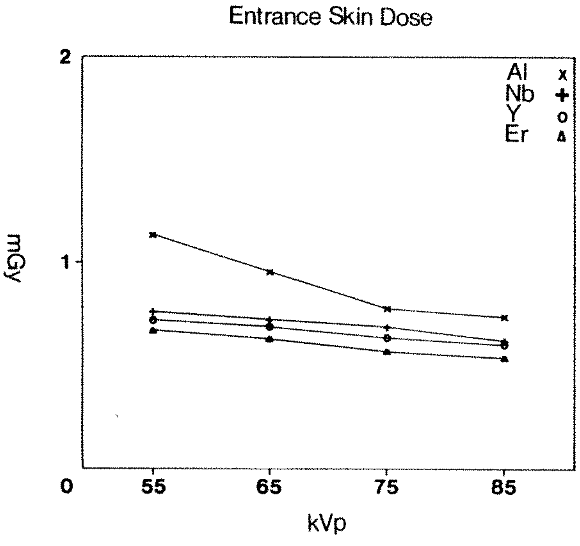

Figure 4. Entrance skin dose for the four filter systems.

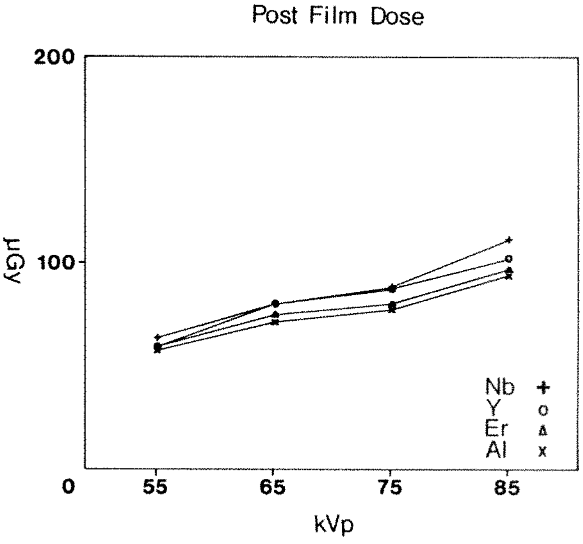

Figure 6. Post-film dose for the four filter systems.

aluminium alone. This is consistent with the higher mean energy (greater penetration) of each of the K-edge filtered beams.

An examination of the errors involved in the experimental methods used suggested typical errors of ±5% in the measurements of radiation dose and ±1 kV in tube voltage (Figs 4–7).

Discussion

The results of the spectral analysis demonstrates that the addition of the thin K-edge filters results in a narrower energy range than that obtained with aluminium alone. For the three materials (yttrium, niobium, erbium) the modified spectrum is well matched to the spectral sensitivity of dental X-ray film (peaking at between 32 and 47 keV; MacDonald et al, 1987). There is a substantial reduction in the number of X-ray photons both at the low- and high-energy ends of the spectrum, which do not significantly contribute to the production of the image and are primarily dose producing.

With yttrium and niobium, the K-edge is towards the lower end of the X-ray spectrum, whereas with erbium the K-edge is towards the higher end of the spectrum.

As expected the addition of the thin K-edge filters results in a considerable increase in HVL (owing to their

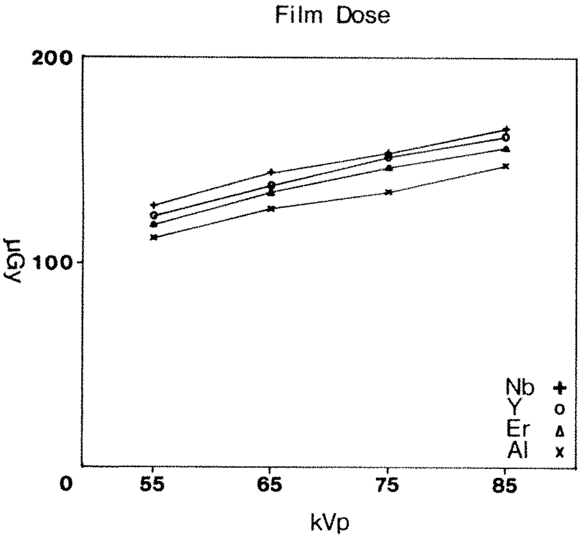

Figure 5. Film dose for the four filter systems.

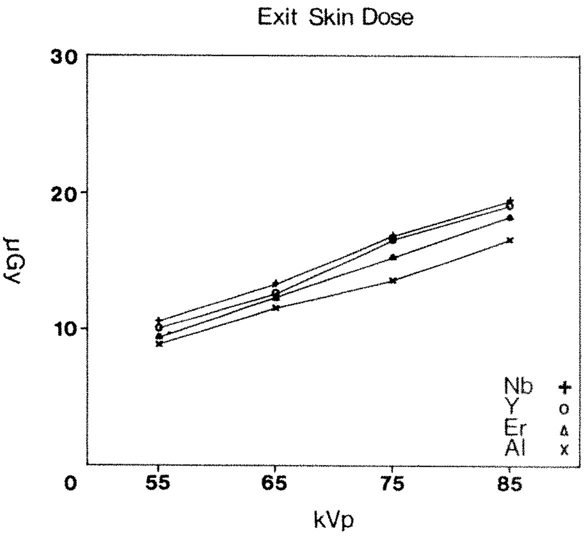

Figure 7. Exit skin dose for the four filter systems.

comparatively high atomic number) with a consequent increase in the required exposure time. The effect on total filtration is even more marked with, in the case of erbium, an increase of over three times.

Within the usual diagnostic range of 60–80 kV the use of the thin K-edge filters required, on average, an increase in exposure time of a factor of 2. This could increase the risk of movement unsharpness and may have some repercussion in terms of life of the X-ray tube. However, in many cases this may be compensated for by the use of E speed rather than D speed film (E speed film typically requires half the radiation dose when compared to D speed film). An alternative solution may be to use smaller thicknesses of aluminium and the K-edge filter material to reduce the HVL. This would allow a reduction in dose with an appreciably smaller increase in exposure time.

The K-edge filter systems deliver a substantially lower entrance skin dose than aluminium alone, especially at lower kVp values. This is due to the spectral shaping by the K-absorption edges with a significant reduction in the low-energy component of the X-ray beam with a resultant increase in penetration. The exit doses are higher for the thin K-edge filters, again because of the increased penetration.

Image quality

During the progress of this study, the opportunity was taken to produce a series of clinical images with each of the filter systems. An initial subjective examination suggested no significant change in the diagnostic image quality when using the thin K-edge filters. A fuller discussion of image quality will form the subject of a future publication.

Conclusions

In summary, when compared with aluminium filtration alone, thin K-edge filter systems exhibit a significantly smaller entrance dose. Additionally, the exit dose with the thin K-edge filters is larger, from which it can be concluded that the overall dose absorbed by the patient is less.

Acknowledgments

We would like to thank Dr K. Cranley of the Royal Victoria Hospital, Belfast, for computing the spectra and Mrs Lorna Vassell for preparing the typescript.

References

Birch, R., Marshall, M. & Ardran, G. M., 1979. *Catalogue of Spectral Data for Diagnostic X-rays* (Hospital Physicists' Association), Scientific Report Series No. 30.

Farman, A. G., Perez, C., Jacobson, A. & Kelly, M. S., 1989. Evaluation of aluminium–yttrium filtration for intra oral radiography. *Oral Surgery, Oral Medicine, Oral Pathology, 67*, 224–226.

Gelskey, D. E. & Baker, C. G., 1981. Energy selective filtration of dental X-ray beams. *Oral Surgery, Oral Medicine, Oral Pathology, 52*, 565–567.

Horner, K., Lawinski, C. P. & Smith, N. J. D., 1988. Erbium filtration for dose reduction in dental radiography. *British Journal of Radiology, 61*, 609–612.

ICRP, 1977. International Commission on Radiological Protection Publication 26. *Recommendations of the International Commission on Radiological Protection. Annals of the ICRP*, No. 3.

Kircos, L. T., Staninec, M. & Chou, L., 1989. Rare earth filters for intraoral radiography: exposure reduction as a function of kV(p) with comparisons of image quality. *Journal of the American Dental Association, 118*, 605–609.

MacDonald, J. C. F., Reid, J. A. & Luke, M., 1987. The spectral sensitivity of dental X-ray films. *Dento Maxillo Facial Radiology, 16*, 29–32.

NRPB, 1988. National Radiological Protection Board, Health and Safety Executive and Health Departments, 1988. *Guidance Notes for the Protection of Persons against Ionizing Radiations Arising from Medical and Dental Use* (HMSO, London).

Ponce, A. Z., McDavid, W. D. & Langland, O. E., 1988. The use of added erbium filtration in intra oral radiology. *Oral Surgery, Oral Medicine, Oral Radiology, 66*, 513–517.

Richards, A. G., Barbor, G. L., Bader, J. D. & Hale, J. D., 1970. Samarium filtration in dental radiology. *Oral Surgery, Oral Medicine, Oral Pathology, 29*, 704–715.

Wachsmann, F. & Drexler, G., 1976. *Graphs and Tables for Use in Radiology*, 2nd edn (Springer-Verlag, Berlin).

1991, *The British Journal of Radiology*, *64*, 529–536

Quantitative assessment of a new dental imaging system

By A. Walker, MSc, BSc, *K. Horner, MSc, FDS, DDRRCR, J. Czajka, BSc, †A. C. Shearer, MSc, BDS, FDS and †N. H. F. Wilson, PhD, MSc, FDS

North Western Medical Physics Department, Christie Hospital and Holt Radium Institute, Wilmslow Road, Manchester M20 9BX, *Unit of Radiology, Department of Oral Medicine, and †Unit of Conservative Dentistry, Department of Restorative Dentistry, University Dental Hospital of Manchester, Higher Cambridge Street, Manchester M15 6FH, UK

(*Received September 1990 and in revised form January 1991*)

Keywords: Dental radiography, Digital techniques

Abstract. The "Radiovisiography" dental imaging unit (Trophy UK Ltd) is a digital system using an intensifying screen and charge-coupled device in an intra-oral sensor. This paper presents a description of the system and an assessment of the original model in terms of patient dose (relative to film systems), resolution (limiting resolution and modulation transfer function), distortion and image noise (amplitude). The system does offer the possibility of reduced patient exposure and minimal distortion, although resolution and latitude are inferior to standard dental film.

Since the first machine-wrapped dental film packet was introduced by Kodak in 1919, X-ray sensitive film has remained virtually unchallenged as the image receptor for intra-oral film radiography. The introduction of double-sided emulsion in 1924 and progressive increases in film speed over the years have resulted in a lowering of the radiation dose. Film remains a cheap and reliable method of obtaining images in dental radiography and is universally used by dental surgeons. Attempts to introduce alternatives such as xeroradiography have generally been unsuccessful, while film/screen combinations for intra-oral work remain in the research stage. A new alternative to film has recently been developed. It is known under the trade name of "Radiovisiography" (RVG) and is presently being marketed by Trophy (UK) Ltd. Radiovisiography is a digital imaging system using an intra-oral sensor in place of the radiographic film packet, the image being immediately displayed on a TV screen.

The aim of this independent study was to undertake physical measurements on the first commercially available model of the RVG system for comparison with other imaging techniques and to provide baseline data for the evaluation of future developments of the system. The findings of an assessment of the clinical performance of this system are published elsewhere (Horner et al, 1990).

System description

The RVG system comprises four components (Fig. 1): the X-ray set with timer, an intra-oral sensor, the display/processing unit and a printer (Mouyen et al, 1989). The model available to us for assessment (and described below) was the first one to be commercially marketed. A new version is now on the market, although the original model is still available.

The X-ray set

The X-ray tube and generator are of conventional design but with an electronic timer ("CCX") capable of giving the reduced exposures required for RVG and of providing a control signal to the processing unit to initiate retrieval of the image from the sensor. The timer can also be used for conventional film radiography.

The X-ray unit used was a Novelix 708 (70 kVp, 8 mA, 20 cm long cone) model. The X-ray beam is circular with a nominal 6 cm diameter. This was verified using a film cassette placed at the cone end.

Although nominally 70 kVp this unit has a pronounced "pre-heat" period of approximately 0.2 s. During this time the full kilovoltage is not applied to the tube and the output is roughly a third of full operation. After this "pre-heat" period the kVp rises to the nominal 70 kVp (Fig. 2).

The intra-oral sensor

The radiation detector within the sensor is a rare-earth intensifying screen (25 mm × 16 mm), which is optically coupled to an array of charge-coupled devices (CCDs). The optical layer between screen and CCD also acts as a radiation absorber protecting the CCD. The CCD has an array size of 288 (horizontal) by 384 (vertical) nominally covering an area of 26 mm × 17 mm. There are two modes of operation of the sensor, which have to be selected before an exposure. In the "normal" mode the image from the whole sensor is used; in "zoom" mode only the top half of the image from the sensor is processed and displayed.

The sensor (Fig. 3) is enclosed in a plastic casing of dimensions 40.6 mm long, 22.8 mm wide and 14 mm thick, which can be opened for cleaning the intensifying screen. A lead connects the sensor to the display unit. In clinical use the sensor is protected by a rubber sheath

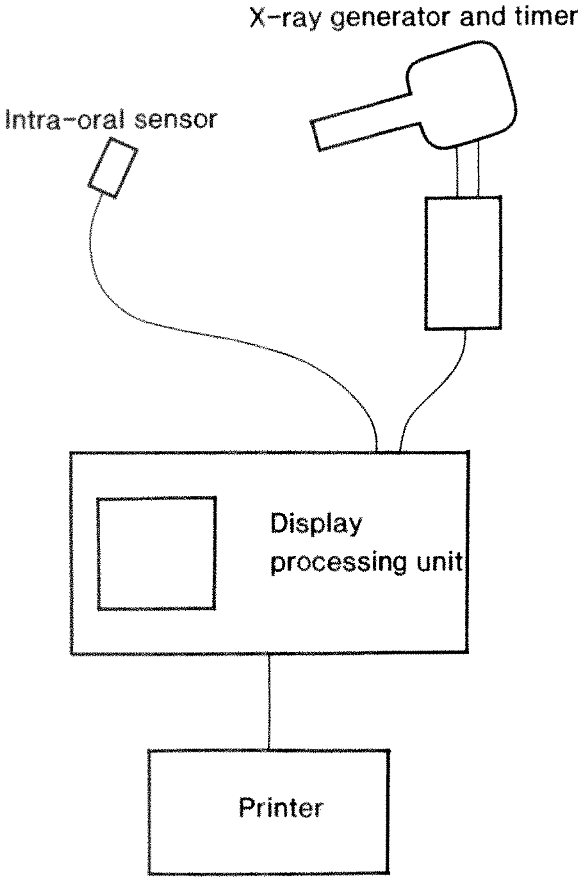

Figure 1. Diagram of the total RVG system.

for infection control and to prevent contamination of the contents of the sensor by saliva.

Processor/display unit

The analogue signal from the intra-oral sensor is digitized to a depth of 8 bits (256 levels) and is stored in either a 192 × 288 array ("normal" mode) or 284 × 288 ("zoom" mode) array. The image is displayed on a small monitor (312 lines) incorporated into the unit. In the "normal" mode the images of the two preceding exposures are displayed at once, although in the "zoom" mode only the image of the last exposure is displayed over the whole of the screen.

The unit offers limited image manipulation although with a digital system there is obvious potential for future development. Contrast enhancement and grey-scale reversal are available. Normally areas of high exposure are displayed black, as in film. The original data remain in the store and can be redisplayed if required.

Printer

A separate printer can be attached to the processing unit to produce a permanent record of the image. The system supplied with the RVG was a Dry Silver Imager (3M UK PLC). Alternatively, thermal printers can be used or a polaroid photograph taken directly from the TV screen.

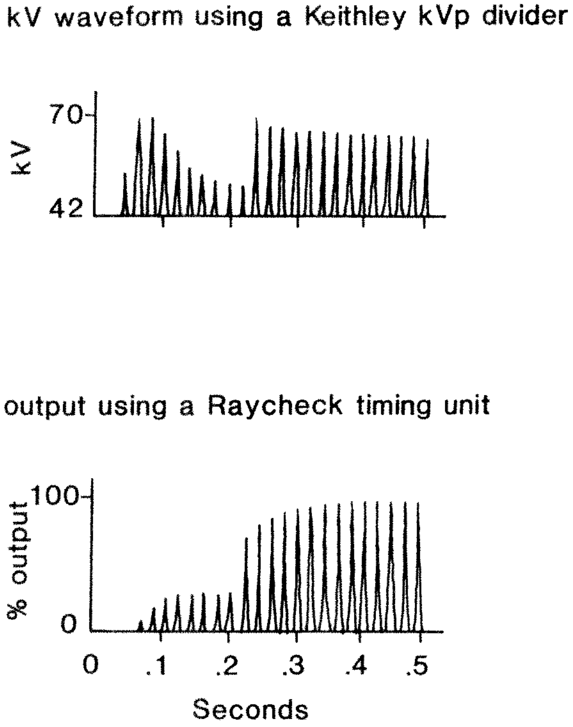

Figure 2. Tube kilovoltage and output characteristics of the Novelix 708 dental X-ray tube.

It is envisaged that the diagnosis will mainly be made from the TV screen and that the permanent record will only be required for the patient's records. The assessment results described here were made from the TV image where appropriate and the printer has not been included.

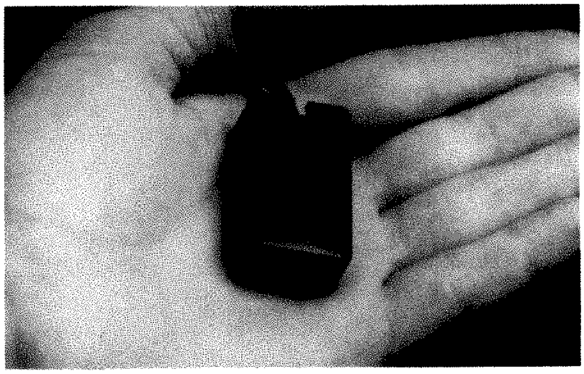

Figure 3. The intra-oral sensor.

Method

Radiation dose, contrast and latitude

A simple comparison of the patient dose, between RVG and conventional intra-oral film, was obtained by measuring the air kerma at both RVG and film settings. The dependence of both screen luminance and the video voltage, supplied to the TV monitor from the processing unit, on radiation dose to the sensor was also investigated. The video signal was displayed on an oscilloscope using a delayed trigger to isolate a single line, and the variation of voltage level with air kerma measured at the sensor position determined for both the "normal" and the "zoom" modes. The effect of the "enhancement" control was also assessed in this way. A Hagner photometer was used to measure screen luminance for a range of video signal levels.

Field size and distortion

The image size and the image distortion introduced into the final image by the sensor and processing were assessed by imaging a small-spaced regular wire mesh placed directly on the sensor.

Resolution

The response of the system to high-contrast detail was assessed using resolution test gratings. Two test gratings were used: a Huttner type 538 which spans 0.25–6 lp/mm and that incorporated within the TOR(MAX) mammography test phantom (Hay et al, 1981), which has a spatial frequency range of 1–20 lp/mm. The correct exposure was judged by viewing the video signal and ensuring that the maximum amplitude was obtained without exceeding the "black" or "white" video voltage levels.

The limiting resolution, which was taken to be the highest line pair frequency that still maintained a separate line pair identity, was judged by eye from the screen. The resolution patterns were aligned both horizontally and vertically, and with the diagonal of the image.

By measuring the video voltage peak-to-peak response to the square wave signal generated by the gratings for the different frequencies, the square wave response function (SWRF) was obtained. Obviously this will only give the SWRF in the horizontal direction of the video scan. This measurement was not performed with the image enhancement facility. Since the voltage is linearly related to the incident exposure (as shown in Fig. 5) no correction needs to be made for system linearity. The modulation transfer function (MTF), or sine wave response function, was calculated from the SWRF using the Coltman series correction (Barnes, 1979; Evans, 1981).

Noise

The oscilloscope trace of a video line is not even but clearly exhibits a random fluctuation caused by noise within the system. The peak-peak amplitude of this fluctuation was measured to give an index of system noise.

Results and discussion

Radiation dose, contrast and latitude

The X-ray unit and timer of the RVG system can be used to produce images with the RVG sensor and with standard intra-oral film. Clinically acceptable film images of the correct density were obtained using the recommended film speed setting with the same technique setting as for RVG images. It was therefore assumed that the unit is thus correctly set for both RVG and film and that comparison of the air kerma at these settings would give a good indication of difference in patient dose.

From this simple measurement it was determined that the RVG in "normal" mode of operation required 0.40 (±0.03) times the exposure of E-speed film and 0.23 (±0.02) times that of D-speed film. When used in the "zoom" mode the air kerma was the same as for D-speed film.

The exposure times required by the RVG unit are typically 0.25 s to 0.35 s, which means that a major section of the exposure is in the "preheat" phase with a subsequent lower effective kV. This difference in the beam quality is equivalent to a change in half-value layer (HVL) from 1.6 mm Al to 2 mm Al (RVG to film). Using published data of HVL variation with kV (Hospital Physicists' Association, 1977) such a change is roughly equivalent to 6 kV. We understand a dental X-ray tube without the "pre-heat" period is under development by Trophy.

Clearly, use of RVG in the "normal" mode leads to a significant reduction in patient dose compared with the intra-oral film in common use. The patient dose saving, in terms of total absorbed dose, might well be slightly greater than the in-beam air kerma measurements indicate, given that with the present X-ray tube the effective kV is some 6 kV less when used with the RVG setting when compared with the film setting.

The luminance of the TV screen is dependent on the video voltage level supplied to it. A linear relationship is usually assumed and this was confirmed for the present system (Fig. 4). With this information, measurement of the video signal dependence on sensor dose (Fig. 5) can be used to assess the total system response to different exposure levels at the sensor.

The relationship between luminance and dose is equivalent to that between film transmittance and radiation dose. However, film density is more commonly used to show the characteristic response of film to dose. Density is preferred rather than transmittance or opacity principally because the physiological response of the eye to differences in light intensities is logarithmic rather than linear (Christenson et al, 1978). Thus, differences in a logarithmic quantity such as density give a better guide to the perceived contrast than differences in a linear quantity such as transmittance.

For comparison of RVG characteristics with that of film, an analogous quantity to density was required. Density is defined as $\log I_0/I$ where I_0 is the incident illumination and I the transmitted. Parallel quantities for the RVG are $\log V_w/V$ and $\log L_w/L$, where V is the

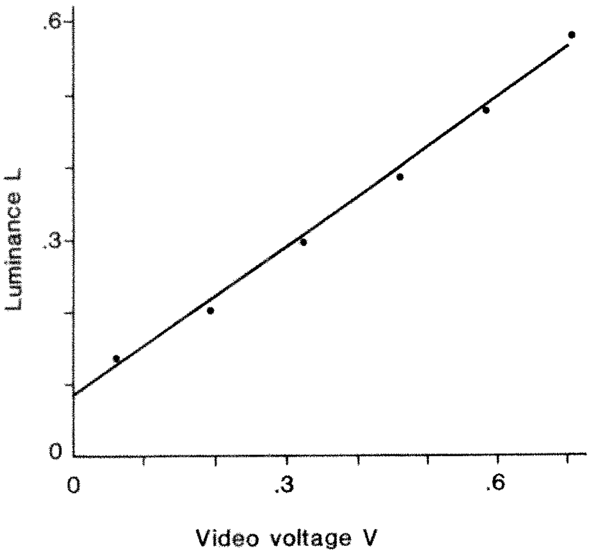

Figure 4. Dependence of screen luminance on video voltage.

video voltage amplitude and L the TV screen luminance, V_w and L_w referring to the "white level" values of these two quantities. Log V_w/V will give information about the contrast and latitude available at the video signal level whereas log L_w/L will show how this information is reproduced on the screen in the TV image. The two quantities differ because the screen luminance is not zero when the video amplitude is zero, as shown in Fig. 4.

Results for both quantities are presented. Log L_w/L is clearly the relevant quantity for the screen image but log V_w/V gives useful information if other display systems such as the printer are used. Both quantities plotted against log exposure are shown in Fig. 6a, and Fig. 6b gives the characteristic curves of Kodak E- and D-speed film for comparison.

One of the most noticeable features seen when comparing these two graphs is the limited range of log V_w/V when compared with film density. This means that the visual contrast range available on an RVG image is less than film, in the same way that print is inferior to transparencies for viewing X-ray images because of the restricted maximum density (Christenson et al, 1978).

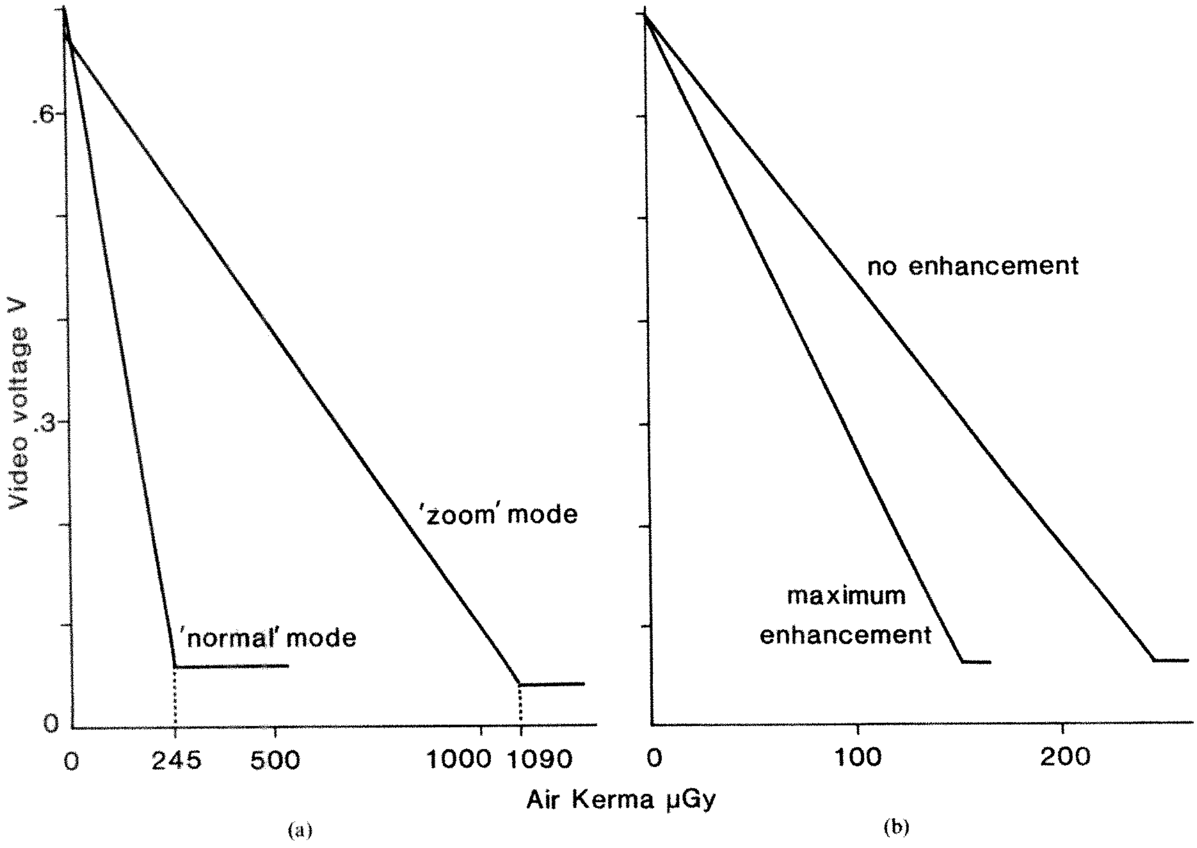

(a)

(b)

Figure 5. Dependence of video voltage on air kerma at the sensor: (a) in both normal and zoom modes and (b) in normal mode with and without enhancement.

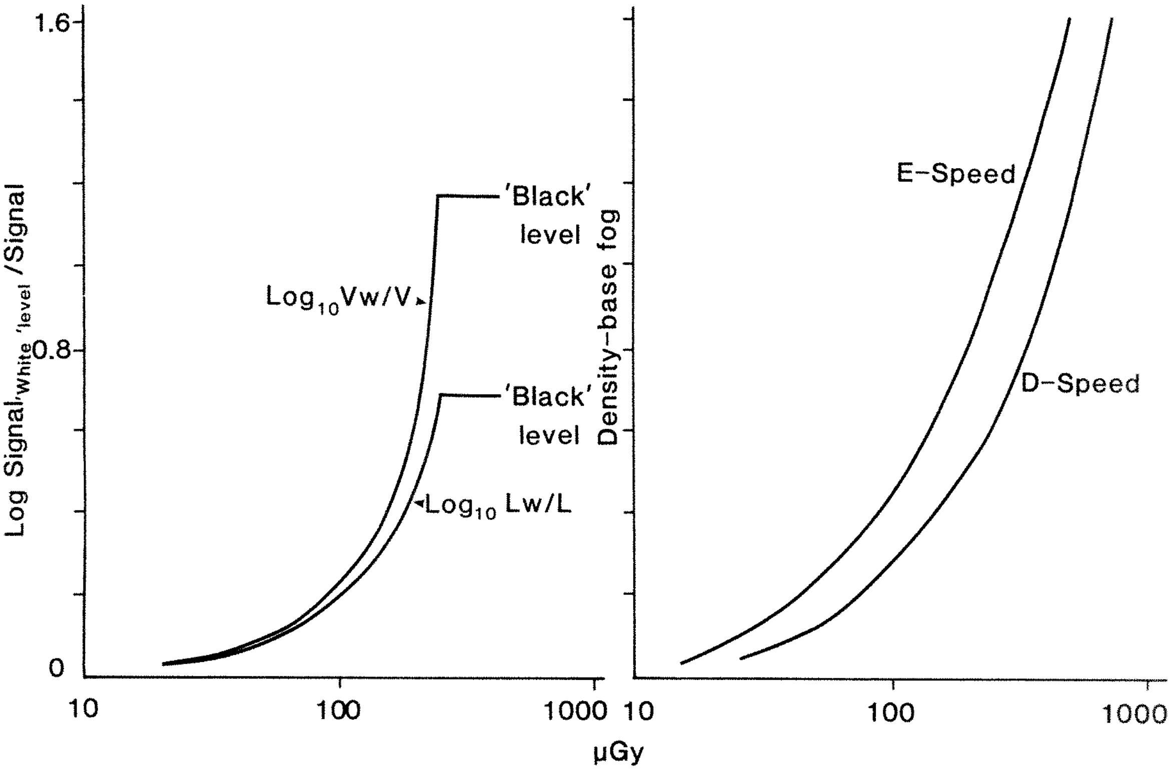

(a) (b)

Figure 6. RVG and dental film characteristic curves.

Owing to the relationship between video voltage level and screen luminance there is a further reduction in contrast range in the transition of the image from the video signal to TV screen. This limited contrast range can be compensated for by using the "enhancement" facility to ensure that maximum contrast is obtained in the structures in the image of particular interest. However, this will lead to loss of information in other parts of the image.

Another feature of the RVG characteristic is the sharp cut-off at the "black" level exposure. Exposures greater than this will not give rise to any further difference in video voltage level and will appear uniformly black on the image. Consequently, on overexposure no information will be recorded, unlike film where information in the denser areas of the image can often be revealed with a brighter light source. This may prove to be a significant problem in clinical practice. For example, the crest of the interdental alveolar bone is often thin and of low mass density. Correct assessment of the position of the crestal bone relative to the tooth is important in diagnosis of periodontal disease. The limitations of RVG with respect to overexposure suggest that the information might be lost and the degree of crestal bone destruction in periodontal disease overestimated.

In the light areas of the RVG image, the contrast (indicated by the gradient of the lower part of the curve of Fig. 6), is similar to that of film. For the darker areas the gradient of the RVG curve is considerably greater than that of film. Use of the enhancement facility to position the maximum contrast region can be used to improve the visualization of a particular area of the image. Therefore, the actual contrast is as good as, if not better than, film for the greater portion of the image. However, as explained above, the actual range of contrasts visible on a single image is far less.

Paradoxically, a clinical trial (Horner et al, 1990) found that a significant minority of clinical images, all performed in the "normal" mode, showed inadequate contrast. However, clinical experience indicated that such images could be improved by increasing X-ray exposure. This suggests that the timer settings allocated on the CCX for RVG use may be too low for some patients and that in these cases the system is functioning on the low-exposure/lower-contrast portion of the RVG curve.

Field size and distortion

The area of mesh imaged was 25 mm × 16 mm in "normal" mode and 12.5 mm × 16 mm in "zoom" mode, which agree closely with the nominal values in

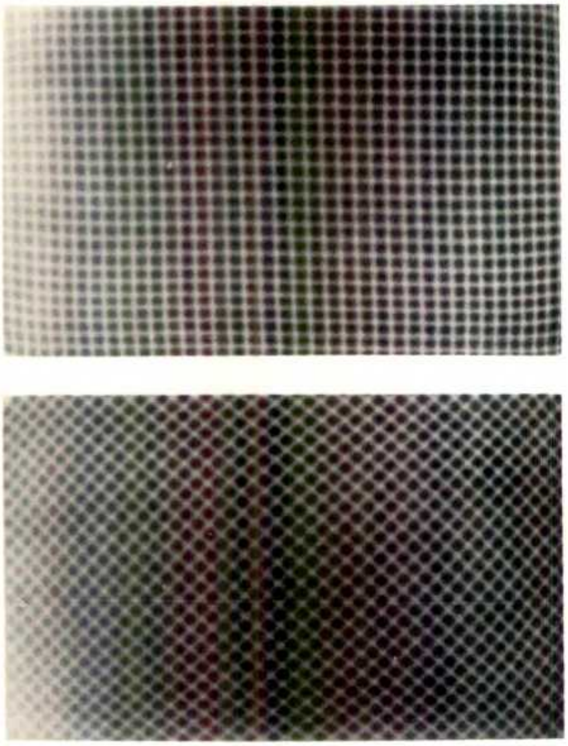

Figure 7. Wire mesh images.

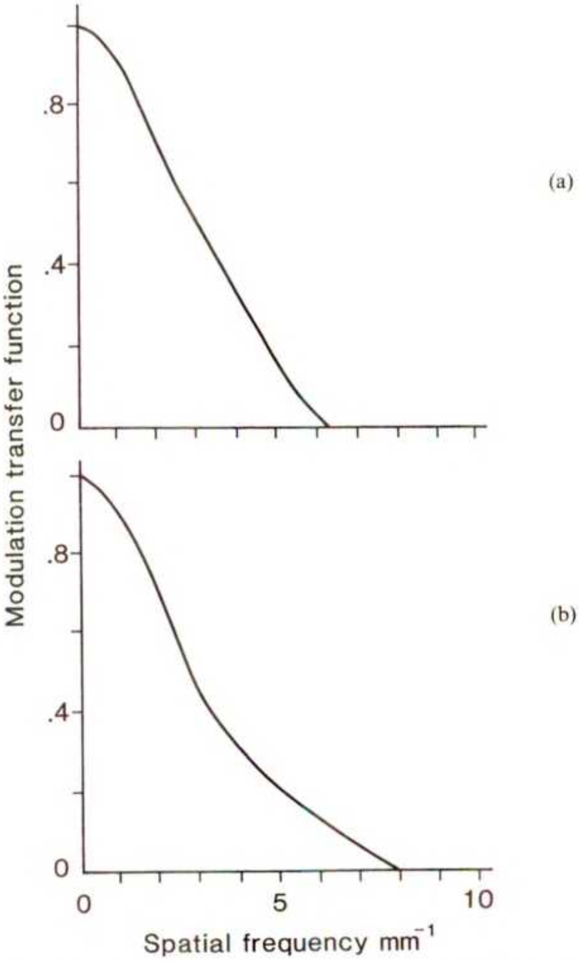

Figure 8. Modulation transfer functions in (a) normal and (b) zoom RVG modes.

the Radiovisiography manual, and are slightly less than the CCD dimensions. The image on the TV screen represents a four-fold magnification when used in "normal" mode, and an eight-fold magnification when in "zoom" mode.

A mismatch between the circular X-ray beam and rectangular detector is normal in dental radiology, the extra latitude this allows being necessary because of the uncertainty involved in positioning using the bisecting angle technique. Rectangular collimation is a possibility only when more accurate alignment with the X-ray tube is permitted by the use of film holders incorporating beam aiming devices (Pitts, 1984).

Nevertheless, it should be possible to reduce the beam size for RVG work from the present standard 6 cm diameter beam. Adult intra-oral film has a diagonal of 5 cm, which leads to the X-ray beam being some 56% larger than the area of the detector. The sensor of RVG is considerably smaller than film, having a diagonal of some 3 cm, leading to the area of the RVG sensor being only 16% of the total area irradiated. A significantly smaller beam size for use with RVG, perhaps 4 cm diameter, should not greatly increase positioning errors and could lead to a valuable dose reduction. We understand that such a collimator is now available from Trophy for use with RVG, but it was not available at the time of this study.

The image area is smaller than that normally used in dental radiography and typically only accommodates one molar tooth or two incisor teeth. This is considerably smaller than the area of the standard periapical dental film. One consequence of this is that two or more RVG examinations are necessary to image the same anatomical area as a conventional radiograph. This has important implications for radiation dose comparisons of RVG with film radiography. Furthermore, the small size of the receptor indicates accurate positioning of the sensor is necessary to ensure adequate images are produced (Horner et al, 1990).

The wire mesh images, illustrated in Fig. 7, indicate a very slight amount of pincushion type distortion towards the corners of the image. The image of straight lines is also slightly curved across the image. However, the rigid nature of the sensor removes the distortion often produced in dental film radiography caused by bending of the film packet. The inherent distortion introduced by the sensor and electronic processing, demonstrated by the wire mesh images, is small and unlikely to cause any problems in diagnosis.

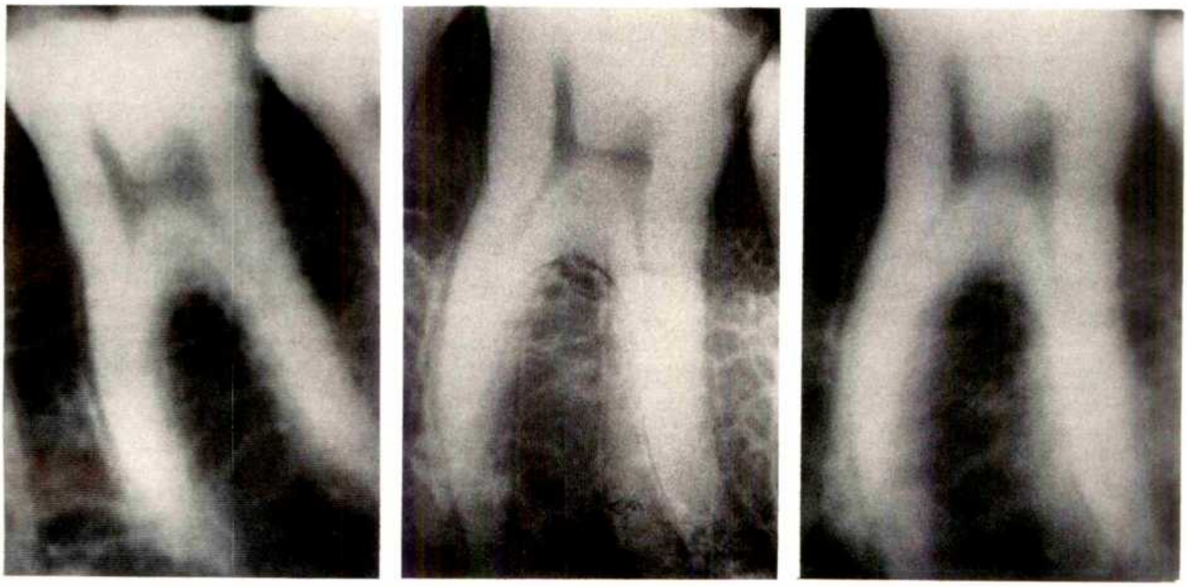
(a) (b) (c)

Figure 9. Images of the same tooth obtained with (a) RVG, (b) Kodak E-speed intra-oral film and (c) Fuji G4 intensifying screens with HR-G Fuji film.

Resolution

The limiting resolution, judged by eye from the screen, was found to be 6.0 lp/mm in the "normal" mode and 8.5 lp/mm in the "zoom" mode, with the bar test patterns aligned in the horizontal and vertical directions. The limiting resolution was slightly lower with the bar pattern in a diagonal orientation, measuring not greater than 5.0 lp/mm in the "normal" mode and 7.0 lp/mm in the "zoom" mode. The measured MTFs for both the "normal" and "zoom" modes are given in Fig. 8.

The resolution of the system will be limited by (a) the resolution of the screen used to convert the X-ray photons to light, (b) the collecting optics, and (c) the spacing of the individual CCD detectors which form the detecting array.

We understand from the manufacturers that the screen used is a fast rare-earth type. Such screens, when used in conjunction with film, typically have limiting resolutions of between 5 and 7 lp/mm (DHSS 1981, 1983, 1985). It is possible that the RVG system could have a slightly better resolution capability than a film/screen combination as only a single screen is used and the collecting optics might reject scattered light with a greater efficiency than film.

The storage array size is 192×288 (horizontal × vertical) for the nominal CCD size of 17 mm × 26 mm in "normal" mode and 384×288 when only using half the CCD (13 mm × 17 mm) in "zoom" mode. The Nyquist frequency, $N = 1/2\Delta x$ (Harrison, 1988) gives the resolution limit of a digital system, where Δx is the sampling interval. In both horizontal and vertical orientations the Nyquist frequency is 5.6 mm^{-1} in "normal" mode and 11.3 mm^{-1} in "zoom" mode.

In the "normal" mode the expected limiting resolutions from considerations of both screen type and sampling interval are within the range of 5–6 mm^{-1}, which was experimentally determined. For the "zoom" mode the limiting resolution was experimentally determined as 7–8.5 lp/mm, which is less than the prediction based on sampling interval, suggesting that the unsharpness in the intensifying screen is the limiting factor in the resolution of the system in this mode rather than the spatial sampling of the signal.

Overall, the resolution of the system is similar to that of a fast film/screen combination, and is clearly inferior to that obtained by the standard non-screen film, which has a limiting resolution of well over 20 mm^{-1}. This can be subjectively demonstrated by comparing RVG, conventional dental (non-screen) film and standard film/screen combination images of the same tooth (Fig. 9). Whether RVG provides adequate image sharpness will depend on the use that is made of the image obtained. It is our opinion that the system will give adequate representation of small detail for most dental radiological applications. However, it is probable that it will not be suitable for applications where fine detail of small structures, *e.g.* bone trabeculae, is required.

Noise

The peak-to-peak random fluctuation on the video signal is independent of the signal level, remaining constant throughout the exposure latitude. The peak-peak amplitude was 0.02 V in both "normal" and "zoom" modes, which is some 3% of the maximum video signal amplitude ("white" level).

By referring to Fig. 5a it can be deduced that the amplitude of the noise (measured as 0.02 V) is equivalent to a difference of 8 μGy exposure to the sensor (normal mode). As the noise amplitude remains constant throughout the range of signal levels, the signal-to-noise ratio varies from approximately 35 : 1 at the "white" level to 3 : 1 at the "black" level.

Conclusion

Radiovisiography offers the possibility of reduced patient dose compared with conventional non-screen intra-oral radiography. The use of the enhancement facility does allow contrast to be improved. However, as is to be expected, the system resolution and latitude are inferior to standard non-screen dental film and could well be the factors that limit the use of this technique in some areas of dental radiology.

References

BARNES, G. T., 1979. The use of bar test pattern objects in assessing the resolution of film screen systems. In *Physics of Medical Imaging: Recording System Measurements and Techniques*, ed. by A. G. Haus (American Institute of Physics, New York).

CHRISTENSON, E. E., CURRY, T. S. & DOWDEY, J. E., 1978. *An Introduction to the Physics of Diagnostic Radiology*, 2nd edn (Lea and Febiger, Philadelphia).

DHSS STB/3/81, 1981. *Measurements on Dupont Screen-film Systems* (Department of Health and Social Security, London).

DHSS STB/4/83, 1983. *Measurements on Kodak Screen-film Systems* (Department of Health and Social Security, London).

DHSS STB/6E/85/26, 1985. *Physical Evaluation of Imaging Performance of Agfa Gevaert Screen-film Systems* (Department of Health and Social Security, London).

EVANS, A., 1981. *The Evaluation of Medical Images, Medical Physics Handbook 10* (Adam Hilger Ltd, Bristol).

HARRISON, R. M., 1988. Digital radiography. *Physics in Medicine and Biology, 33*, 751–784.

HAY, G. A., CLARKE, O. F., COLEMAN, N. J., COWAN, A. R. & CRAVEN, D. M., 1981. Test equipment for quality control in diagnostic radiology, particularly for image intensifier–television systems (Department of Medical Physics, University of Leeds).

HOSPITAL PHYSICISTS' ASSOCIATION, 1977. *The Physics of Radiodiagnosis (Scientific Report Series 6)*, (The Hospital Physicists' Association, London).

HORNER, K., SHEARER, A. C., WALKER, A. & WILSON, N. H. F., 1990. Radiovisiography: an initial assessment. *British Dental Journal, 168*, 244–248.

MOUYEN, F., BENZ, C., SONNABEND, E. & LODTER, J. P., 1989. Presentation and physical evaluation of Radiovisiography. *Oral Surgery, Oral Medicine, Oral Pathology, 68*, 238–242.

PITTS, N. B., 1984. Film-holding, beam aiming and collimating devices as an aid to standardization in intra-oral radiography—a review. *Journal of Dentistry, 12*, 36–46.

1991, *The British Journal of Radiology*, *64*, 537–538

Ovarian ablation failures by radiation: a comparison of two dose schedules

By S. F. Leung, MBBS, FRCR, S. Y. Tsao, MBBS, FRCR, DMRT, Peter M. L. Teo, MBBS, FRCR, DMRT, Peter H. K. Choi, MBBS, FRCR, DMRT and Wesely C. T. Shiu, MD, FRCP

Department of Clinical Oncology, Prince of Wales Hospital, Hong Kong

(*Received October 1990 and in revised form January 1991*)

Keywords: Breast cancer, Menopause, Ovary, Radiotherapy

Abstract. Sixty Chinese breast cancer patients underwent ovarian irradiation with one of two dose schedules: 12 Gy/4 fractions/4–6 days or 14 Gy/4 fractions/4–6 days. The ovarian ablation failure rates were 14% and 0% respectively in patients above 40 years of age. The overall ablation failure rate in younger patients was unacceptably high at 35%. The significance of the findings is discussed.

Ablation of ovarian function by radiation is widely used as a means of endocrine manipulation in the treatment of breast cancer in therapeutic and prophylactic settings. A low dose level such as 4.5 Gy in one fraction was known to be associated with a significant ablation failure rate (Cole, 1968). Although a fractionated dose of 10–20 Gy has been reported to give very high success rates (Peck et al, 1940; Meakin et al, 1977; Tobias, 1986; Dembo, 1989), there is uncertainty regarding the optimal dose within this dose range. Ideally, the minimum effective dose should be used to minimize the potential risk of carcinogenesis when the treatment is given in a prophylactic setting (Norris & Taylor, 1965; Smith & Doll, 1976). This retrospective study of two dose schedules serves to supplement clinical data on the low-dose side of this range.

Method and materials

From April 1984 to December 1989, 74 Chinese breast cancer patients seen at the Department of Clinical Oncology, Prince of Wales Hospital, Hong Kong were given ovarian irradiation for prophylatic or therapeutic treatment of metastatic disease. Fourteen of the 74 patients were excluded from this retrospective study because of the presence of menstrual disturbance or amenorrhoea before ovarian irradiation or hormone treatment or chemotherapy given very soon after ovarian irradiation. The remaining 60 patients were studied, including four patients who persistently had regular menstruation after previous treatment by Tamoxifen or chemotherapy. Patient characteristics are summarized in Table I and their age distribution detailed in Fig. 1. All the 60 patients had regular menstrual periods before ovarian irradiation. Ovarian irradiation was carried out using an anterior–posterior opposing pair of portals averaging 13×9 cm^2 with the lower border at the obturator foramina. Photons of energy 6 MeV from a linear accelerator were used with the dose prescribed at the midplane of the field centre. A dose schedule of 12 Gy/4 fractions/4–6 days was used from April 1985 to April 1987. By the end of this period an appreciable failure rate of ovarian ablation was noted and a dose schedule of 14 Gy/4 fractions/4–6 days was used thereafter. Failure of ovarian ablation is defined as persistence of menstruation for more than 6 months after irradiation or return of menstruation at any time on follow-up. All patients were observed for more than 2 years except for four patients with shorter follow-up times of 9–21 months and another three patients who were censored from observation at 6, 10, 21 months after ablation due to commencement of chemotherapy (all these patients had successful ablation and remained amenorrhoeic after chemotherapy).

Table I. Patient characteristics

	12 Gy group	14 Gy group
Mean age of patients (age <40)	34.6	36.1
Mean age of patients (age >40)	45.1	44.2
Number of patients with previous hormone treatment or chemotherapy	0	4[a]
Ablation failure rate (age <40)	6/15	6/19
Ablation failure rate (age >40)	2/14	0/12

[a] These four patients were aged 30, 32, 40 and 50; all had successful ablation.

Address for correspondence: Dr S. F. Leung, Department of Clinical Oncology, Prince of Wales Hospital, Shatin, Hong Kong.

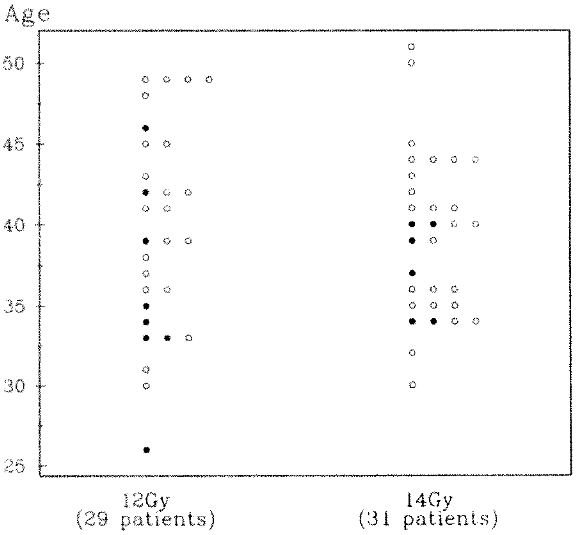

Figure 1. Outcome of ablation with the two dose schedules according to age: ○ successful ablations; ● ablation failures.

Results

Effects of radiation dose and age

The results are summarized in Table I and Fig. 1. The patients above 40 years of age had less ablation failures with the 14 Gy/4 fractions/4–6 days schedule than the lower dose schedule (0% and 14% respectively) although the difference is not statistically significant ($p = 0.28$, Fisher's exact test). For patients at or below age 40 the failure rates were similarly high for both schedules (32% and 40% respectively). The overall failure rate in this age group was significantly higher than that in older patients (35% *versus* 8% respectively, $p = 0.02$, χ^2 test).

Patterns of alteration in menstruation in patients with failed ablation

Half of the patients with ablation failure had persistent menstruation after irradiation, the other half had initial amenorrhoea followed by return of menses at 5–10 months after irradiation. Thus persistent amenorrhoea at 10 months can be taken as an indicator of successful ovarian ablation. The pattern of alteration in menstruation was not related to the dose schedule or age.

Discussion

There are cost implications of failed ovarian ablation in addition to the need to repeat the ablation procedure. The achievement of therapeutic effects may be delayed, as is the administration of alternative systemic treatment in the case of non-response of the disease to endocrine manipulation. The return of menstruation after apparent menopause poses the diagnostic problem of per vaginal bleeding which necessitates further investigations to exclude alternative causes such as malignancy of the genital tract. In view of the prevalence of breast cancer, optimization of dose-fractionation for ovarian ablation has significant cost-effectiveness implications. The ablation failure rate of 35% in patients at or below age 40 in the present series is unacceptably high. This is in contrast to the experience of Peck et al (1940) who observed a failure rate of less than 5% in women under 40 years of age using 5–10 Gy only. Our results are also in discordance with Dembo's (1989) description of a near 100% success rate with a dose of 10–15 Gy in 4 or 5 fractions. In contrast, Ribeiro (1985) has expressed doubt about the permanence of irradiation menopause with a dose of 15 Gy/4 fractions/4 days and recommends oophorectomy in patients aged 40 years or less. Tobias (1986) also recommends a higher dose of 20 Gy over 8–10 days for young patients. Thus there is still discordance in the clinical data regarding the optimal dose within the 10–20 Gy range for ovarian ablation in young patients. Given the data mentioned already, it seems reasonable to use a dose on the high side of the range, such as 20 Gy, for management of metastatic disease in young patients when certainty of ablation is important and carcinogenesis is not a relevant consideration. For patients above 40 years of age, the present study suggests that a schedule of 14 Gy/4 fractions/4–6 days is optimal.

Acknowledgments

We would like to thank Mr Joseph Lau for statistical advice, Mr Kai-kwong Man for preparing the figure and Ms Carmen Wong for secretarial assistance. This study is supported by the Chinese University of Hong Kong Research Fund.

References

COLE, M. P., 1968. Supression of ovarian function in primary breast cancer. *Proceedings of the First Tenovus Symposium, Cardiff, 1967.* In *Prognostic Factors in Breast Cancer*, ed. by A. P. M. Forrest & P. B. Kunkler (E & S Livingstone, Edinburgh), pp. 146–156.

DEMBO, A. J., 1989. The ovary. In *Radiation Oncology: Rationale, Technique, Results*, ed. by W. T. Moss & J. D. Cox (Mosby, St Louis), p. 582.

MEAKIN, J. W., ALLT, W. E. C., BEALE, F. A., BROWN, T. C., BUSH, R. S., CLARK, R. M., FITZPATRICK, P. J., HAWKINS, N. Y., JENKIN, R. D. T., PRINGLE, J. F. & RIDER, W. D., 1977. Ovarian irradiation and prednisone following surgery for carcinoma of the breast. In *Adjuvant Therapy of Cancer*, ed. by S. E. Salmon & S. E. Jones (North-Holland, Amsterdam), pp. 91–95.

NORRIS, H. J. & TAYLOR, H. B., 1965. Post-irradiation sarcomas of the uterus. *Obstetrics and Gynecology, 26*, 689–694.

PECK, W. S., MCGREER, J. T., KRETSCHMAR, N. R. & BROWN, W. E., 1940. Castration of the female by irradiation. *Radiology, 34*, 176–186.

RIBEIRO, G. G., 1985. Breast. In *The Radiotherapy of Malignant Disease*, ed. by E. C. Easson & R. S. Pointon (Springer-Verlag, Berlin), p. 274.

SMITH, P. G. & DOLL, R., 1976. Late effects of X-irradiation in patients treated for metropathia haemorrhagica. *British Journal of Radiology, 49*, 224–232.

TOBIAS, J. S., 1986. Breast cancer. In *Radiotherapy in Clinical Practice*, ed. by H. F. Hope-Stone (Butterworths, London), p. 87.

1991, *The British Journal of Radiology*, *64*, 539–546

Estimation of doses to patients from "complex" conventional X-ray examinations

By A. Calzado, PhD, E. Vañó, PhD, P. Morán, PhD, *C. Castellote, PhD, S. Ruiz, MD and L. González, PhD

Cátedra de Física Médica, Universidad Complutense de Madrid, Facultad de Medicina, Pabellón II, Planta 4ª, Ciudad Universitaria, 28040 Madrid, and *Departamento de Radiología, Hospital Militar Central "Gómez Ulla", Glorieta del Ejército, s/n, 28047 Madrid, Spain

(*Received July 1990 and in revised form October 1990*)

Keywords: Dosimetry, Radiodiagnostics, Phantom, Monte Carlo, Radiation protection

Abstract. A numerical method has been developed to estimate the organ doses and effective dose-equivalent for patients undergoing three "complex" examinations (barium meal, barium enema and intravenous urography). The separation of radiological procedures into a set of standard numerical views is based on the use of Monte Carlo conversion factors and measurements within a Remab phantom. The radiation doses measured in a phantom for such examinations have been compared with the predictions of the "numerical" method. Dosimetric measurements with thermoluminescent dosemeters attached to the patient's skin along with measurements of the dose–area product during the examination have enabled us to derive organ doses and to estimate the effective dose-equivalent. Mean frequency weighted values of dose–area product, energy imparted to the patient, doses to a set of organs and effective dose-equivalent in the area of Madrid are reported. Comparisons of the results with those from similar surveys in other countries have been made.

Some of the examinations performed with conventional X-ray equipment can be considered as "complex". It is quite usual to find significant shifts in techniques and procedures in their acquisition. These differences depend in part on the examination routine followed by each individual radiologist or team in a given centre (Rowley et al, 1987). The main characteristics of this group of examinations are a high but variable number of exposures with very different film sizes for each exposure, and the use of typically some few minutes of screening time during the examination.

To assess the health detriment caused by radiological examinations, it is useful to obtain the values of absorbed dose in organs of the patient and make an estimation of the effective dose–equivalent caused by them. The values of these parameters can be obtained relatively easily when the X-ray examination is "simple", since the examination involves the obtaining of two or three views and there are different procedures to derive organ doses from the entrance dose for each exposure. Among them, as is known, the conversion coefficients obtained with mathematical phantoms and by the Monte Carlo (MC) method (Drexler et al, 1984; Jones & Wall, 1985; Rosenstein, 1988) are widely used.

In "complex" examinations, the assessment of the organ or tissue doses of individual patients can turn out to be more complicated. Apart from the aforementioned variations in techniques and protocols, a significant contribution to the dose to patients may also come from fluoroscopic screening, which makes it difficult to simulate—via calculations either with mathematical phantoms or measurements in anthropomorphic ones—the actual examination to each individual patient. Therefore, for the types of examination identified under the "complex" category, numerical methods appear to be more attainable than simulative measurements in a phantom for the assessment of doses to organs of each individual patient, as has been pointed out by some authors (Ranniko et al, 1987).

In the present paper, the procedures to classify three "complex" X-ray examinations—barium meal (BM), barium enema (BE) and intravenous urography (IVU)—into a number of calculation standard views are described. The calculation protocol allows organ dose values to be estimated and an estimation to be made of the effective dose-equivalent value for each individual patient undergoing such examinations. These three examinations account for more than 50% of the collective effective dose-equivalent from radiodiagnostic examinations in the area of Madrid (Vañó et al, 1989a). As this work is part of a project to assess the risks associated with diagnostic radiology in the area of Madrid (Vañó et al, 1989b), average values of organ dose and effective dose-equivalent for the examinations mentioned above in the region of Madrid have also been calculated.

Method

The method has been devised to calculate the contribution of the X-ray examinations to the organ doses and the effective dose-equivalents to the patient. The standard views included in the calculation protocol are intended to cover all possible procedures (exposures and fluoroscopic screening) involved in each of the three types of examination.

The first step has been the selection of a set of tables associated with standard views giving the dose to organs per entrance skin-dose conversion factors with inputs for different kVp and total filtration values. Once the calculation protocol has been established, dosimetric measurements and technical data recording during the irradiation of the patient were performed to obtain the input parameters needed for its effective application.

Calculation protocol

The calculation protocol consists of the standard views selected from the exposure included in each examination type. The tables of conversion factors obtained by MC methods and mathematical phantoms have been included in the protocol, provided that the standard view (irradiated area, field size and projection) corresponds to those already published. When this condition was not fulfilled, additional tables have been derived by comparing the results from MC calculations for a similar irradiated anatomical area (same projection but different field size) with that obtained from measurements with thermoluminescent (TL) dosemeters in an anthropomorphic phantom (Remab system). The changes were mainly made for those organs remaining partially in the radiation field during the actual exposure. Finally, some tables were worked out from direct in-phantom measurements when no MC comparable views were found.

The contribution from screening has been calculated by means of the same standard view used for the calculation of the subsequent exposure. This can lead to uncertainties, but it is not unusual for the radiologist to gather information from fluoroscopic screening of the region of interest before making an exposure. When information about the entrance dose during each separate screening period was not available, the cumulative dose from screening during the whole examination was divided into the number of standard views used to calculate organ doses for the examination.

The standard views included in the calculation protocol for BM, BE and IVU examinations together with the calculation table sources are presented in Table I. The IVU examination appears to be the most feasible for calculation with MC conversion coefficient factors except when longitudinal tomography is present as part of the examination (30% of the total cases in the Madrid area). The contribution of tomograms to the total doses has been assigned, for simplicity of calculation purposes, to the antero-posterior (AP) abdominal view. In a similar way, all the oblique (O) views were calculated, when needed, from coefficient tables derived from the comparison between O lumbar spine MC factors and results from dosimetric measurements within the phantom.

In the BE examination, as indicated in Table I, the contribution from both the right anterior oblique (RAO) and the left anterior oblique (LAO) colon projections were calculated using the half sum of the AP and O lumbar spine MC factor tables. For BM examinations, the conversion coefficients associated to the standard view of oesophagus has been obtained from in-phantom measurements.

Irradiation conditions

The operating conditions during each examination (applied potential, number of exposures and films, screening time, field size, focal spot to film distance)

Table I. Standard views included in the calculation protocol for each type of examination

Examination					
Barium meal		Barium enema		Intravenous urography	
Standard view	Source	Standard view	Source	Standard view	Source
AP Abdomen	Jones & Wall (1985)	AP Abdomen	Jones & Wall (1985)	AP Abdomen	Jones & Wall (1985)
PA Abdomen	Jones & Wall (1985)	PA Abdomen	Jones & Wall (1985)	AP Kidneys	Jones & Wall (1985)
Lat Abdomen	Rosenstein (1988)	Lat Abdomen	Rosenstein (1988)	AP Bladder	Jones & Wall (1985)
O Oesophagus	Remab	O Colon	Remab	O Kidneys	Jones & Wall (1985)
AP Stomach	Remab Jones & Wall (1985)	RAO Colon LAO	Jones & Wall (1985)[a]	Lat Kidneys	Remab
				Tomograms	Jones & Wall (1985)[b]
O Stomach and Duodenum	Remab Jones & Wall (1985)				
O Duodenum	Remab Jones & Wall (1985)				
AP Upper Abdomen (Erect)	Jones & Wall (1985) Remab				

[a] Average of MC calculated conversion factors for AP and O Lumbar spine.
[b] MC calculated factors for AP Abdomen.

were collected. Data concerning the patient (age, sex, height and weight) as well as the total filtration of the unit and the focus to skin distance were also recorded.

Dosimetric measurements

Dosimetric measurements were made during examination performance at two levels. On one hand, separate values of dose–area product for exposures and screening intervals have been measured and, on the other hand, TL dosemeters have been used for estimating doses to some organs of the patient.

Measurements of the dose–area product were made using a Diamentor system (PTW, Freiburg, Germany). These measurements give absorbed dose in muscle at the entrance for both single exposure and fluoroscopic screening intervals. The value of dose–area product for the whole examination is also useful to derive the energy imparted, which can be considered as a relative radiation risk parameter (Shrimpton et al, 1984).

TLD 100 chips (LiF, Harshaw) were used to measure the cumulative doses for each complete examination on the patient's skin at six anatomical sites. One TLD was attached to the patient's throat (to estimate the dose to the thyroid). Two pairs of chips were attached to the front and back of the thorax (to derive the dose to breasts, lungs and the output dose) and another TLD was placed on the groin (to estimate the testes dose).

Patient samples

Patient samples have been taken at random in four hospitals and some outpatient centres in the area of Madrid. Collected information was as described in previous paragraphs and all the data have been computed, so that all the relevant parameters can be calculated and correlated.

Doses to organs estimation

The doses to all relevant organs were estimated via the calculation protocol described above, except for thyroid, breasts, testes and lungs, using the entrance dose values for each standard view included in the complete examination as input data. As is known, some of these organs are usually located near the boundaries of the radiation field, making it acceptable, as a practical approach, to estimate mean doses to them from direct TLD measurements during the examination. This is why a strategy was adopted similar to the one described in detail by Shrimpton et al (1986a) for estimating doses to thyroid, breasts, testes and lungs.

According to these criteria, the absorbed dose measured by the TL dosemeters located on the patient's throat and groin was assumed to represent the mean dose to the thyroid and testes, respectively. For BM and IVU examinations, mean dose to the breasts was estimated as half the average reading of the two TL dosemeters on each breast surface; the dose to the lungs was estimated as the mean value of the four front and back dosemeter readings. When PA and O projections are dominant, as for BE examination, the mean doses to the breasts and lungs were estimated by taking the maximum value between that estimated from TLD readings and that calculated from the protocol.

Remab measurements

As was mentioned previously, some measurements were performed by using TL dosemeters and a water-filled plastic phantom containing a human adult male skeleton (Remab).

Apart from the aforementioned measurements needed for the calculation protocol tables, simulations in the phantom of the three complete examinations under study were performed to compare the experimental results with those calculated via the protocol. To perform such measurements, the technical conditions as well as the number of exposures and films and the screening time were fixed for each type of examination according to the most probable values observed in the centres involved in the study.

Although the phantom characteristics have already been described (Poretti, 1985), it may be worth remarking that it contains isolated plastic compartments simulating the organs of interest, without special sites for the dosemeters to be placed in, although it does allow the use of contrast media.

During the irradiation of the phantom in order to simulate the X-ray examinations or views, about 100 TLD chips were used to estimate the dose delivered to the organs. Chips were placed in plastic tubes (3 mm inner diameter) before inserting them into the organ cavities. Some dosemeters were attached to the surface (thyroid, breasts, back and entrance at different points of the radiation field).

Mean organ doses to the phantom were estimated to be the average value of the absorbed dose measured by the dosemeters inserted in them, except for breast, skin, red bone marrow and bone. The procedure for estimating the mean absorbed dose to the breasts from TLD readings was the same as for patients described above. For the mean dose to skin estimation, the fractions of the total surface area given for adult Reference Man (ICRP, 1975) were taken into account. The mean red bone marrow (RBM) dose was estimated using the percentage distribution in weight in the different bones (Ellis, 1961; Cristy, 1981), and for the estimation of bone dose, the fractions of total bone volume were taken into account.

The X-ray unit used to perform all the irradiations of the phantom was an MSX (12-pulse) GE generator with a Maxiray-100 X-ray tube (tungsten/rhenium molybdenum backed anode; 11° angle; 0.6 mm × 1.5 mm focal spot size; 1.1 mm equivalent inherent filtration) and a Telegem II supporting system. The unit was equipped with a fixed grid (12:1; 36 lines/cm). The cassette used was a Curix Universal rare-earth system with a rated speed of 400. The film used was Agfa-Gevaert RP-2. The image intensifier was a GE Fluorigem system with a resolution of 3.8 line pairs/mm. The measured dose-in-air rate during fluoroscopy at the patient's entrance for 100 kV and 1 mA was 12.2 mGy/min.

Effective dose-equivalent

The effective dose-equivalent (H_E) for all the examinations was obtained using the expression (ICRP, 1977):

$$H_E = \Sigma w_i \; H_i$$

where w_i is the weighting factor for organ i and H_i the corresponding dose-equivalent for organ i.

Since the introduction of this quantity, its meaning and interpretation has been discussed. When irradiation is not uniform, as in the case of patients undergoing X-ray examinations, it has been pointed out that the suitable quantity to use for the estimation of individual or collective radiation risks should be the expected detriment (Drexler et al, 1985). It has been also indicated by some authors (Ranniko et al, 1987; Huda & Sandison, 1988) that the average contribution of the "remainder" dose computed, following the ICRP recommendations, to the resultant H_E is higher than expected in terms of risk. As a consequence of the discussions and problems associated with the use of the "effective dose-equivalent" to deduce the severity in non-uniform irradiations, the ICRP published a draft version of its recommendations for radiological protection, which is at present under discussion (Clarke, 1990). Since the final text is expected to be published in the first quarter of 1991, it was decided to obtain the effective dose-equivalent following the recommendations of the ICRP expressed in 1977, although provisions were made to adapt the calculation method to the new ICRP w_i values.

Results and discussion

In-phantom measurements

Table II summarizes the procedures followed to simulate the complete X-ray examinations on the phantom. The measured dose–area product values and the calculated energy imparted during phantom irradiation are also indicated in the last two columns of the table. For BM examination, irradiations have been performed with and without contrast medium in the stomach of the phantom. In the simulation of BE examination, the tubes in the phantom representing the rectum sigma, descending and transverse colon were filled with conventional contrast barium solution. The first consequence of using a barium compound and automatic exposure control during fluoroscopy is the increase in the Diamentor readings and, subsequently, of the energy imparted to the phantom.

Measured and calculated Remab organ doses and effective dose-equivalents derived for the three examinations analysed are presented in Table III. The measured results compare favourably with the ones obtained from the calculation protocol, except in the case of BM using contrast medium. For this simulation, the differences between calculated and measured doses are larger than expected for absorbed dose in kidneys, urinary bladder, ovaries and uterus. These differences can, to a large extent, be explained by the lack of contrast medium effects in the MC calculations. Other significant differences, as in the case of red bone marrow, can be explained by the difficulties already mentioned (Huda & Sandison, 1984; Poretti, 1985) in measuring absorbed doses in this tissue.

The relatively good agreement between calculated and measured results for the IVU simulation can be explained by the lack of fluoroscopy screening during its performance.

Uncertainties associated with such results are not included in the table owing to the difficulty in estimating them from the calculated values. The coefficients of variation associated with phantom measurements can be estimated as ranging between 8 and 60% of the mean values according to the organ size and its location in the radiation field, as well as the number and position of dosemeters used to estimate the absorbed dose in the organ. It is also important to bear in mind that fluoroscopy screening contributes up to 77% of the examination energy imparted for BM examinations using contrast medium, and to take into account the difficulty in reproducing the screening irradiation in simulations of the same examination type (Rowley et al, 1987). On the other hand, it must be emphasized that the time and work needed in the measurements within a Remab phantom lead to a limitation of the number of X-ray simulations that are performed with it.

Table II. Values of number of exposures and films, screening time, applied potential, dose–area product and energy imparted for the simulation of examinations

Examination	Remab simulations					
	No. exposures	No. films	Screening time (seconds)	Applied potential (kV)	Dose–area product (cGy.cm^2)	Energy imparted (mJ)
Barium meal	15	6	240	120	1137	138
					3145	428[a]
Barium enema	10	10	180	100	4050	420[a]
IVU	7	7	—	67	2245	144

[a] With contrast.

Table III. Measured and calculated Remab organ doses (mGy) and effective dose-equivalents (EDE) in mSv

Organ	Examination							
	Barium meal				Barium enema		IVU	
	Without contrast		With contrast		With contrast			
	Measured	Calculated	Measured	Calculated	Measured	Calculated	Measured	Calculated
Breasts	2.88	2.88	2.40	2.40	0.48	0.48	0.18	0.18
Stomach	8.81	8.56	29.1	30.4	8.55	8.94	3.94	5.05
Small intestine	3.49	3.16	10.6	11.7	7.83	8.71	2.81	3.70
Upper large intestine	4.03	3.97	11.6	14.3	9.66	9.30	3.46	4.60
Lower large intestine	1.62	1.56	4.32	4.54	5.10	6.27	2.23	2.75
Kidneys	1.90	1.63	7.16	4.46	11.6	9.60	0.91	0.82
Liver	4.73	5.45	16.1	20.5	6.71	6.24	2.87	2.80
Lungs	5.90	5.10	14.2	12.3	0.83	0.92	0.23	0.20
Ovaries	2.15	2.21	2.41	6.17	5.18	7.53	2.87	2.45
Pancreas	5.24	4.91	17.1	13.2	5.45	5.88	1.82	1.87
Skin	1.08	1.14	3.25	3.47	2.88	2.58	1.51	1.35
Testes	1.24	1.24	0.25	0.25	0.75	0.75	7.08	7.08
Thyroid	2.07	2.07	0.34	0.34	0.15	0.15	0.16	0.16
Urinary bladder	2.81	2.80	2.86	5.47	4.96	7.50	6.43	6.02
Uterus	2.42	2.51	3.02	6.33	5.73	7.80	3.91	3.40
Bone	1.4	1.27	4.03	3.58	3.35	3.21	0.72	0.61
Red bone marrow	1.28	0.96	3.78	2.80	4.77	2.80	0.65	0.41
EDE (mSv)	3.40	3.25	8.05	8.50	4.25	4.32	2.64	2.68

Sample of patients

The frequency weighted mean values (with the standard error of the mean in parentheses) of dose–area product and energy imparted derived from the sample of patients for each type of examination, along with the size of the sample, the weighted average values of number of exposures, films and screening time, are shown in Table IV.

The mean of the dose–area product measurements is very similar to the value obtained in Italy (Padovani et al, 1987) for BM and BE examinations. When comparing our results with those estimated in England, it is found that for BM our value is larger than published (2202 R.cm^2) by Shrimpton et al (1986b) and for BE and IVU examinations our values (4889 cGy.cm^2 and 3237 cGy.cm^2) are close to their respective values (4817 R.cm^2 and 3445 R.cm^2).

The frequency weighted mean organ doses and effective dose-equivalents calculated from the adult patients' data collected in the centres are presented in Table V. As data were obtained during the 1988–89 period, the average number of such explorations performed in each centre during this period was used to weight the mean values. Values in parentheses represent standard errors and are larger for some tissue doses, especially for those derived from TLD measurements or located close to the edges of the radiation field.

These results can be compared with others that recently appeared in the United Nations Scientific Committee on the Effects of Atomic Radiations Report

Table IV. Mean values (with standard errors in parentheses) of number of exposures and films, screening time, applied potential dose–area product and energy imparted from measurements on patients' random sample

Examination	Sample size	Patient's sample					
		No. exposures	No. films	Screening time (seconds)	Applied potential (kV)	Dose–area product (cGy.cm^2)	Energy imparted (mJ)
Barium meal	117	16.7 (1.0)	7.9 (0.5)	282 (34)	110 (2)	4495 (1112)	264 (52)
Barium enema	124	11.6 (0.6)	9.5 (0.4)	234 (23)	101 (3)	4889 (443)	388 (45)
IVU	129	6.5 (0.4)	6.5 (0.4)	29 (6)	64 (2)	3237 (561)	218 (43)

Table V. Mean frequency weighted organ doses (in mGy) and effective dose-equivalents from the patients' sample. Values in parentheses are the associated standard errors

Organ	Examination		
	Barium meal	Barium enema	IVU
Breasts	3.86 (1.15)	1.58 (0.54)	1.70 (0.32)
Stomach	16.7 (3.2)	10.4 (1.6)	14.9 (3.1)
Small intestine	4.56 (0.76)	14.3 (2.6)	10.5 (2.1)
Upper large intestine	5.93 (1.06)	13.3 (2.3)	13.8 (2.7)
Lower large intestine	1.93 (0.38)	12.7 (2.4)	9.73 (2.03)
Kidneys	3.00 (0.57)	31.7 (6.8)	2.19 (0.47)
Liver	11.4 (2.5)	9.19 (1.62)	9.01 (1.79)
Lungs	10.0 (3.3)	2.64 (0.67)	0.35 (0.07)
Ovaries	2.82 (1.65)	15.5 (4.3)	8.42 (3.66)
Pancreas	7.79 (1.59)	10.6 (2.0)	6.16 (1.27)
Skin	1.56 (0.28)	5.10 (0.83)	3.81 (0.71)
Testes	1.14 (0.38)	11.2 (3.4)	6.00 (1.45)
Thyroid	4.10 (1.82)	0.17 (0.05)	$< 10^{-3}$ mGy
Urinary bladder	2.10 (0.56)	13.0 (1.9)	20.8 (4.1)
Uterus	1.85 (0.36)	14.7 (4.3)	12.6 (5.3)
Bone	1.58 (0.31)	8.45 (1.74)	2.13 (0.43)
Red bone marrow	1.18 (0.23)	7.92 (1.82)	1.37 (0.29)
EDE (mSv)	5.49 (0.84)	9.70 (1.53)	6.66 (1.35)

(UNSCEAR, 1988). For the mean effective dose-equivalent and BM examination, a value of 9.27 mSv has been estimated in Italy by Padovani et al (1987). The same authors have estimated a mean effective dose-equivalent of 8.97 mSv caused by BE examinations; meanwhile Maccia et al (1988) estimated 9.96 mSv for the mentioned examination (only radiographic contribution) in France, Nikitin et al (1986) estimated 17.95 mSv in the USSR and a value of 4.06 mSv has been estimated in the US (NCRP, 1989). From the same references in the different countries and for the IVU examination, mean values of effective dose-equivalent of 10.42 mSv were estimated in France, 7.07 mSv in Italy, 2.51 in the USSR and 1.58 mSv in the USA.

Values of mean organ dose are very difficult to compare because in some cases it is difficult to find estimates for all of the tissues reported here. It is worth emphasizing the high value obtained for mean ovary dose for IVU examinations (8.42 mGy) compared with 6.71 mSv in France (Maccia et al, 1988); a value of 5.7 mSv was estimated in Germany by Hinz et al (1978), 3.58 mSv in England (Wall et al, 1980), 2.27 mSv in Finland (Rannikko et al, 1987) and 5.50 mSv in Italy (Padovani et al, 1987). One of the explanations for such a high mean value may be the high number of tomograms included in IVU examinations in some of the hospitals.

As an example of the differences between the mean values obtained in the centres, the mean organ doses (in mGy) and the effective dose-equivalents (in mSv) distributed by centres, along with their respective frequency

Table VI. Mean organ doses (in mGy) and effective dose-equivalents distribution by centres and associated frequency weighting factors from the sample of patients undergoing barium enema examination

Organ	Hospital 1 wf = 0.205	Hospital 2 wf = 0.407	Hospital 3 wf = 0.106	Hospital 4 wf = 0.038	Outpatient centres wf = 0.244
Breasts	1.18 (0.15)	2.69 (0.80)	0.09 (0.03)	0.70 (0.20)	0.88 (0.32)
Stomach	8.92 (0.60)	16.1 (2.3)	0.86 (0.15)	6.28 (2.45)	6.87 (1.06)
Small intestine	13.1 (0.9)	22.0 (3.9)	1.25 (0.21)	7.80 (1.92)	9.15 (1.26)
Upper large intestine	11.9 (1.1)	20.5 (3.3)	1.14 (0.19)	7.43 (2.17)	8.61 (1.26)
Lower large intestine	11.9 (0.8)	19.4 (3.6)	1.12 (0.19)	5.76 (1.09)	8.10 (1.11)
Kidneys	34.1 (2.6)	46.7 (10.2)	3.09 (0.52)	14.6 (1.6)	19.9 (2.9)
Liver	8.80 (0.60)	13.9 (2.4)	0.81 (0.13)	5.19 (1.62)	5.92 (0.84)
Lungs	3.52 (0.64)	3.47 (0.75)	0.25 (0.15)	0.39 (0.12)	1.91 (0.75)
Ovaries	13.6 (1.1)	24.6 (6.6)	1.02 (0.28)	8.96 (1.47)	9.12 (1.40)
Pancreas	10.8 (0.8)	15.8 (3.0)	0.97 (0.16)	5.19 (1.40)	6.68 (0.91)
Skin	5.70 (0.38)	7.24 (1.21)	0.48 (0.07)	3.68 (0.44)	3.28 (0.48)
Testes	33.5 (7.9)	9.41 (3.25)	0.28 (0.06)	1.39 (0.28)	1.59 (0.89)
Thyroid	0.48 (0.06)	0.03 (0.01)	0.004 (0.002)	0.006 (0.001)	0.23 (0.09)
Urinary bladder	11.2 (0.8)	20.4 (2.8)	1.08 (0.19)	5.05 (0.95)	8.76 (1.41)
Uterus	12.0 (1.0)	23.8 (6.5)	0.99 (0.23)	7.54 (1.60)	8.98 (1.47)
Bone	8.85 (0.66)	12.5 (2.6)	0.81 (0.13)	4.55 (0.49)	5.32 (0.76)
Red bone marrow	7.20 (0.58)	12.3 (2.8)	0.71 (0.12)	4.42 (0.42)	4.95 (0.67)
EDE (mSv)	10.7 (0.8)	14.1 (2.2)	0.78 (0.12)	5.52 (1.00)	6.17 (0.92)

weighting factors (w_f) for the BE examination, are shown in Table VI. The considerable differences between hospital 3 outcomes and the rest (mainly hospitals 1 and 2) are probably due to a combination of procedures, equipment, imaging systems and operator training differences (Rowley et al, 1987). When compared with the rest of the centres involved in the work, hospital 3 is superior in almost all aforementioned aspects, as became clear when representative levels of exposure for patients undergoing common types of X-ray examinations in Madrid were established (Vañó et al, 1989b). The other centres have comparable figures although the maximum values are encountered in the largest hospitals (with highest w_f values). A progressive improvement of the working conditions (via obsolete equipment replacement, quality assurance and quality-control programmes) should yield significant dose savings in the future.

Conclusions

The method described to estimate organ doses and effective dose-equivalents can be considered as a useful way to assess the individual and collective risk to the population arising from "complex" conventional X-ray examinations. However, some remarks should be made about the limits and inconveniences of its application.

First of all, obtaining the complete data needed to apply the method can become rather complicated and tedious for radiographers and radiologists, leading to errors at any stage of the data collection. These errors can affect the reliability of dose estimates for some individual patients and influence the final results for samples of a small size. As an alternative, a simplification of the data collection can be advisable, although it may imply a lack of precision in the estimation of the doses to tissues closer to the limits of irradiated areas and an untrue assignment of the fluoroscopy contribution to the doses.

Moreover, the estimates of mean dose for some tissues, such as lungs, testes, thyroid and breasts, can have larger uncertainties than the others, because of the simplified way of deriving them.

Finally, the mean organ dose values and effective dose-equivalent for the three types of conventional X-ray examination presented in this paper can be considered representative of the average doses received by the adult patient undergoing that examination in the area of Madrid during the period 1988–89. Estimates of the radiation risk to the average patient will be presented in a future paper using the results of the present survey in the Madrid area.

Acknowledgments

We wish to thank the radiologists and radiographers at the centres involved in the work: San Carlos University Hospital, Doce de Octubre Hospital, "Gómez Ulla" C. M. Hospital, La Princesa Hospital, Hermanos Miralles Outpatient Centre and Avda. Portugal Outpatient Centre. We acknowledge the assistance of M. J. Ruiz and A. Velasco in the data recording. We are also grateful to M. Marco for TLD treatment and calibration, to J. M. Fernandez Soto for computer assistance and to V. Delgado for statistical analysis of the data.

This study was partially supported by the CEC (contract BI6-214-EA), the General Directorate of Technical and Scientific Research (ref. C86-0006), the Department of Health and Consumer Affairs and the Nuclear Safety Council.

References

Clarke, R. H., 1990. A summary of the draft recommendations of ICRP, 1990. *NRPB Radiological Protection Bulletin No. 111*, 5–8.

Cristy, M., 1981. Active bone marrow distribution as a function of age in humans. *Physics in Medicine and Biology*, *26*, 389–400.

Drexler, G., Panzer, W., Widenman, L., Williams, G. & Zankl, M., 1984. *The Calculation of Dose from External Photon Exposures using Reference Human Phantoms and Monte Carlo Methods. Part III: Organ Doses in X-ray Diagnosis* (Gesellschaft für Strahlen-und Umweltforschung GSF-Bericht, S–1026, München).

Drexler, G., Williams, G. & Zankl, M., 1985. The meaning and the principle of determination of the effective dose equivalent in radiation protection. *Radiation Protection Dosimetry*, *12*, 95–100.

Ellis, R. E., 1961. The distribution of active bone marrow in the adult. *Physics in Medicine and Biology*, *5*, 255–258.

Hinz, G., Kramer, R. & Platz, L., 1978. Aktuelle fragen des strahlenschutzes bei untersuchungen im beckenbereich. *Roentgen Ber*, *7/2*, 170–183.

Huda, W. & Sandison, G. A., 1984. Estimation of mean doses in diagnostic radiology from Rando phantom measurements. *Health Physics*, *47*, 463–467.

Huda, W. & Sandison, G. A., 1988. Computing remainder dose equivalent for H_E. *Health Physics*, *55*, 1011–1013.

Huda, W., Sandison, G. A., Palser, R. F. & Savoie, D., 1989. Radiation doses and detriment from chest X-ray examinations. *Physics in Medicine and Biology*, *34*, 1477–1492.

ICRP, 1975. *Report of the Task Group on Reference Man.* Publication 23. *Annals of the ICRP*, *1* (Pergamon Press, Oxford).

ICRP, 1977. *Recommendations of the International Commission on Radiological Protection.* Publication 26. *Annals of the ICRP*, *1* (Pergamon Press, Oxford).

Jones, D. G. & Wall, B. F., 1985. *Organ Doses from Medical X-ray Examinations Calculated using Monte Carlo Techniques*, NRPB Report NRPB R–186 (HMSO, London).

Maccia, C., Benedittini, M., Lefaure, C. & Fagnani, F., 1988. Doses to patients from diagnostic radiology in France. *Health Physics*, *54*, 397–408.

NCRP, 1989. *Exposure of the U.S. Population from Diagnostic Medical Irradiation*. NCRP Report No. 100 (NCRP, Bethesda, Maryland).

Nikitin, V. V., Ermakov, I. A., Zerbin, E. A., Ivanov, E. V., Komarof, E. I., Masarskij, L. I., Ramzaev, P. V., Saltykova, L. M. & Chervjakov, A. M., 1986. *The Assessment of Population Doses from X-ray Examinations in the USSR:* (1970–1980), (USSR State Committee on the Use of Atomic Energy/USSR National Commission on Radiation Protection), Moscow, 1986 (in Russian).

Padovani, R., Contento, G., Fabretto, M., Malisan, M. R., Barbina, V. & Gozzi, G., 1987. Patient doses and risks from diagnostic radiology in North-east Italy. *British Journal of Radiology*, *60*, 155–165.

Poretti, G. G., 1985. Radiation exposure of a population due to diagnostic X-ray examinations: some critical remarks. *Physics in Medicine and Biology*, *30*, 1017–1027.

RANNIKO, S., SERVOMAA, A., ERMAKOV, I., MASARSKII, L., SALTUKOVA, L., RAZUMNAYA, M. & NIKITIN, V., 1987. Calculations of the estimated collective effective dose equivalent (S_E) due to X-ray diagnostic examinations: estimate of S_E in Finland. *Health Physics, 53*, 31–36.

ROSENSTEIN, M., 1988. *Handbook of Selected Tissue Doses for Projections Common in Diagnostic Radiology*, HHS Publication (FDA) U.S. Department of Health and Human Services, Maryland. 89–8031.

ROWLEY, K. A., HILL, S. J., WATKINS, R. A. & MOORES, B. M., 1987. An investigation into the levels of radiation exposure in diagnostic examinations involving fluoroscopy. *British Journal of Radiology, 60*, 167–163.

SHRIMPTON, P. C., WALL, B. F., JONES, D. G. & FISHER, E. S., 1984. The measurement of energy imparted to patients during diagnostic X-ray examinations using the Diamentor exposure-area product meter. *Physics in Medicine and Biology, 29*, 1199–1208.

SHRIMPTON, P. C., WALL, B. F., JONES, D. G., FISHER, E. S., HILLIER, M. C. & KENDALL, G. M., 1986a. *A National Survey of Doses to Patients Undergoing a Selection of Routine X-ray Examinations in English Hospitals*, NRPB Report NRPB R-200 (HMSO, London).

SHRIMPTON, P. C., WALL, B. F., JONES, D. G., FISHER, E. S., HILLIER, M. C., KENDALL, G. M. & HARRISON, R. M., 1986b. Doses to patients from routine diagnostic X-ray examinations in England. *British Journal of Radiology, 59*, 749–758.

UNSCEAR, 1988. *Sources, Effects and Risks of Ionizing Radiation*, UNSCEAR Report (United Nations, New York).

VAÑO, E., GONZALEZ, L., CALZADO, A., MORAN, P. & DELGADO, V., 1989a. Some indicative parameters on diagnostic radiology in Spain: first dose estimations. *British Journal of Radiology, 62*, 20–26.

VAÑO, E., GONZALEZ, L., CALZADO, A., DELGADO, V. & MORAN, P., 1989b. Some results of a patient dose survey in the area of Madrid. In *Optimization of Image Quality and Patient Exposure in Diagnostic Radiology, BIR Report 20* (British Institute of Radiology, London), pp. 180–185.

WALL, B. F., FISHER, E. S., SHRIMPTON, P. C. & RAE, S., 1980. *Current Levels of Gonadal Irradiation from a Selection of Routine Diagnostic X-ray Examinations in Great Britain*, NRPB Report NRPB R-105 (HMSO, London).

1991, *The British Journal of Radiology*, *64*, 547–548

Technical note

Assessment of a radiotherapy beam analyser

By J. A. Mills, PhD and P. Martin-Smith, MSc

Department of Clinical Physics and Bioengineering, Radiotherapy Centre, Walsgrave Hospital, Coventry
CV2 2DX, UK

(*Received June 1990 and in revised form October 1990*)

Keywords: Beam analyser, Flatness monitor, Output check

A Protea Systems Corporation Radiation Beam Analyser (RBA-3) was acquired by this department with a view to providing non-Physics personnel with an easy-to-use system to monitor both photon and electron output. The manufacturer describes the RBA-3 as not only fulfilling the above requirement reliably but also as providing a check on field flatness and symmetry. It is one of several commercially available systems for this type of application.

Having acquired the RBA-3 and made appropriate Perspex build-up, its performance was assessed. The accuracy and precision of the RBA-3 was compared with the standard routine calibration facilities used in the department.

Standard checking procedures

Standard dosimetry calibrations and output checks are made using both NE 2570 and NE 2500/IONEX electrometers with NE 2571 graphite chambers. Machine calibrations are maintained in accordance with uncertainties specified in ICRU 24 and are done in the standard manner. A 10 cm × 10 cm field is set at a source–skin distance (SSD) equal to the source to axis distance (SAD) of high energy machines. The chamber is placed 5 cm deep in a closed water phantom which has been cross calibrated against an open water phantom. Field symmetry is monitored weekly using the closed water phantom and monthly using a full field in-air scanner. The flatness of the accelerators at Coventry are in compliance with the IEC specification (1979) which concerns the uniformity variation across a field area defined geometrically relative to field edges determined at 50% of the central axis dose. Field profiles are taken along diagonal and major axes through the machine isocentre at a depth of 10 cm in water. Points are determined on each axis which are a distance d_d in from the 50% edge on the diagonal axes and a distance d_m in from the 50% edge on the major axes. Straight lines joining these points define the "flattened area". The distances to define the area and the limiting ratio of maximum to minimum doses are given in Table I.

Table I. IEC displacements and dose ratios for use in specifying beam flatness

Field dimension (F) (cm)	d_m cm	d_d cm	Maximum/minimum Dose ratio limit
5–10	1	2	1.06
> 10–30	0.1F	0.2F	1.06
> 30–maximum	3	6	1.10

Description of RBA-3

The RBA-3 consists of an array of five identical 0.2 cm³ parallel plate ionization chambers (Fig. 1). One chamber is placed centrally with two other chambers placed symmetrically on either side of it along each major axis of the beam. Each chamber is contained within a 50 mm diameter Perspex drum and mounted onto a 4 mm thick Perspex sheet which forms the incident surface of the 25 cm × 25 cm phantom. Build-up

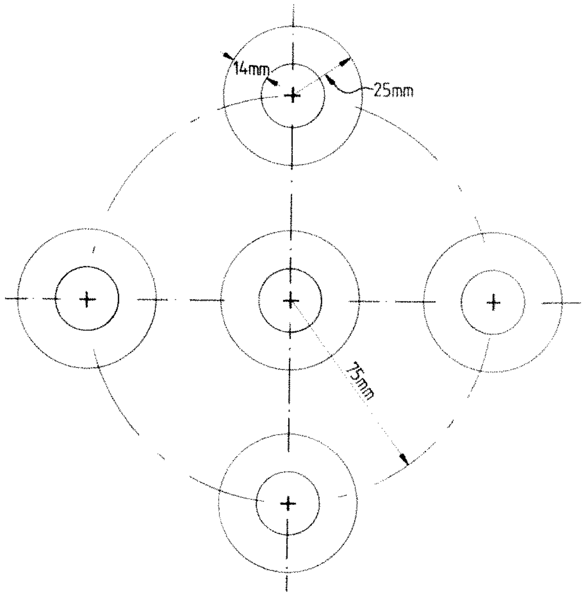

Figure 1. RBA-3 chamber configuration. Chamber centres are indicated with + and the 14 mm lateral Perspex surrounding the chambers is shown.

material can be added onto this surface to give an appropriate depth. The central chamber is used to monitor machine output while the surrounding chambers indicate flatness and symmetry variations. Pressure and temperature detectors within the phantom are utilized to correct the chamber signal response. This correction is performed by an electronic signal processor and can be inhibited if required. The readings from the chamber electrometers and signal processor are displayed on a liquid crystal display (LCD) attached to the phantom and outside the radiation beam.

Dosimetry assessment

Reproducibility of the central chamber reading was assessed by exposing the RBA-3 in a cobalt beam. For a series of 10 exposures the standard deviation was ±0.23% of the mean reading with maximum deviation of +0.26% and −0.4%.

Linearity of the RBA-3 was assessed by exposures of between 0.1 and 0.8 minutes in a cobalt beam. This resulted in a mean reading per minute which had a standard deviation of ±0.08% and for reading versus exposure time a regression coefficient of 0.999.

The consistency of the central chamber response without temperature and pressure correction was assessed by determining the ratio between that chamber reading and the uncorrected standard dosimetry check reading over a period of 6 days on a linear accelerator. The consistency of the central chamber's temperature and pressure corrected reading was similarly assessed by activating the correction facility of the RBA-3 and taking the ratio with the corrected standard dosimetry reading.

Without temperature and pressure correction, the mean ratio was 11.172±0.33%, (maximum deviation +0.4% and −0.4%). With the correction present the mean ratio was 14.973 ±0.26%, (maximum deviation +0.4% and −0.3%). The reason for the difference in the actual mean value between corrected and uncorrected ratios was the sensitivity of the RBA-3 not being set to give any specific value.

Following this comparison, a sequence of readings was taken of the output of a Siemens Cobalt-60 unit over a period of 30 days. Taking source decay into account this gave a set of temperature and pressure corrected readings with mean of 0.8470 ±0.48%, (maximum deviation +0.6% and −0.5%).

Linearity and reproducibility were very good. The precision of the mean ratios obtained on the linear accelerator for both conditions of temperature and pressure correction in the RBA-3 indicate good agreement with the standard calibration measurement variation. The readings taken over the extended period on the Cobalt-60 with temperature and pressure correction also show good precision.

Flatness and symmetry assessment

It is claimed by the manufacturer that the RBA-3 is a sensitive field flatness detector and as such it can detect energy variation, resulting in flatness changes, and that this is more sensitive than depth dose measurements. This, of course, does not take into account flatness variations due to target spot distortion and, with a maximum field size of 20 cm × 20 cm, it was not anticipated that the system would be particularly sensitive. The energy and hence the flatness of a 6MV Philips SL75-5 linear accelerator was altered by detuning the frequency control system and producing a significant change in the flatness in water. A ±2% change at the IEC reference depth positions on a 10 cm × 10 cm field was obtained. Although the energy variation was not determined, the above change was sufficient to take the field out of specification, but because of the chamber configuration the RBA-3 gave no indication of this. For no additional build-up the corresponding maximum change detected was −0.5% while with additional build-up of 13 mm and 26.2 mm of Perspex the maximum flatness variations detected were −0.1% and −0.185%, respectively. Symmetry change was not assessed but these variations are not significant enough to adequately assess the field. In order to detect uniformity changes, attention needs to be given to the placement of chambers in relation to the specification used. Only in cases of gross non-uniformity or assymmetry would a significant change be detected, and in the case of Philips 75 and 25 machines the internal flatness monitoring system would operate.

RBA-3 in daily use

The RBA-3 was used routinely over a period of 16 weeks by physics personnel for routine output checks. Flatness and symmetry were not assessed but output and wedge factor were checked and assessed against predetermined tolerances based on ±2%. A total of 37 measurements were made and an "out of tolerance" result occurred in eight. In these cases the standard checks were undertaken. Of the eight "out of tolerance" cases, three were output only and one was wedge factor only while the remaining four involved both. Of these eight in only one case was adjustment of the machine dosimetry system required. This results in a false fault rate of 88% which was unacceptable.

Conclusion

Under test conditions the reproducibility and pressure-temperature correction of the RBA-3 was acceptable. It was unsatisfactory for flatness and field symmetry assessment. In practice the number of false fault detections arising for tolerance limits of ±2% was unacceptably high. With relaxation of the tolerances this could be overcome but in the context of a quality control programme aimed at maintaining dosimetry within required tolerances the RBA-3 is inappropriate.

References

ICRU, 1976. *Report 24. Determination of Absorbed Dose in a Patient Irradiated by Beams of X or Gamma Rays in Radiotherapy Procedures* (International Commission on Radiation Units and Measurements, Maryland, USA).

IEC, 1979. *Draft Performance Specifications* (International Electro-technical Committee).

1991, *The British Journal of Radiology*, *64*, 549–551

Case reports

Positioning for plain spinal radiography producing paraplegia in a patient with ankylosing spondylitis

By S. S. Upadhyay, D Orth, MS Orth, DM, *E. K. W. Ho, FRCS, FRACS and *L. C. S. Hsu, FRCS, FACS

Duchess of Kent Children's Hospital and University of Hong Kong, 12 Sandy Bay Road, Hong Kong, and *Department of Orthopaedic Surgery, University of Hong Kong, Hong Kong

(Received April 1990 and in revised form January 1991)

Keywords: Ankylosing spondylitis, Pseudarthrosis, Paraplegia, Neurological recovery

In the later stages of ankylosing spondylitis the spine is prone to fracture even with minor trauma (Resnick & Niwayama, 1988), because it is rigid, deformed and osteoporotic. Following a trivial injury the patient usually complains of mild back pain. The radiographic findings may not be helpful as the quality of radiographs is often poor owing to severe osteoporosis. A misdiagnosis is not uncommon, nor is the development of neurological symptoms due to displacement of previous fractures. As far as we know, no case has been reported where the patient becomes paraplegic while being positioned for plain radiographs of the spine. We report such a case.

Case report

A female aged 75 years with a history of ankylosing spondylitis for over 40 years consulted a local "bonesetter" for back pain a few days after a minor incident when she twisted her back at home. While positioning her for plain radiographs of the spine a crack was heard and she developed weakness in both lower limbs, and was unable to walk. She also became incontinent of urine.

Three months later the patient was referred to the Duchess of Kent Children's Hospital at Sandy Bay, Hong Kong. Clinical examination revealed a localized tenderness over the midlumbar area of her kypho-scoliotic spine. She had impaired sensation in both lower limbs. The motor power was MRC grade 0 for hip and knee muscles, and grade 1 for ankle and foot muscles. Knee and ankle tendon reflexes were absent. The Babinski sign was extensor on the left side and she had lax anal tone.

Radiographs at the time of the accident were of poor quality, but a hairline fracture of the third lumbar vertebra was visible. Plain radiographs of the spine obtained 3 months after the injury showed gross changes of ankylosing spondylitis and a shear type fracture of the L3 vertebral body (Fig. 1), seen more clearly on tomograms (Fig. 2). A computed tomographic scan demonstrated the fracture to extend into the ossified posterior elements (Fig. 3).

As her spine was grossly unstable, she underwent posterior surgical exploration of her spine, confirming a pseudarthrosis of the hypertrophic type through the body of third lumbar vertebra, which was excised and the gap filled with iliac crest bone graft. The spine was stabilized with internal fixation using Luque instrumentation. Elsewhere we have reported the details of surgical techniques for this patient (Ho et al, 1991). She made excellent progress in the post-operative period with progressive neurological recovery. Three months after operation, she was able to walk with a rolator and her muscle

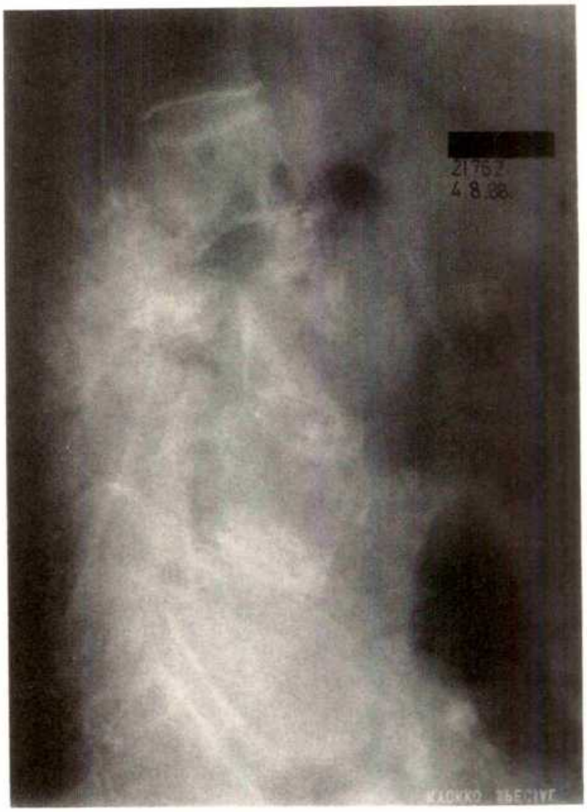
[redacted]

Figure 1. Plain lateral radiograph of the lumbo-sacral spine showing gross changes of ankylosing spondylitis and an ununited fracture through the body of third lumbar vertebra.

Author for correspondence: Dr S. S. Upadhyay, Duchess of Kent Children's Hospital, 12 Sandy Bay Road, Hong Kong.

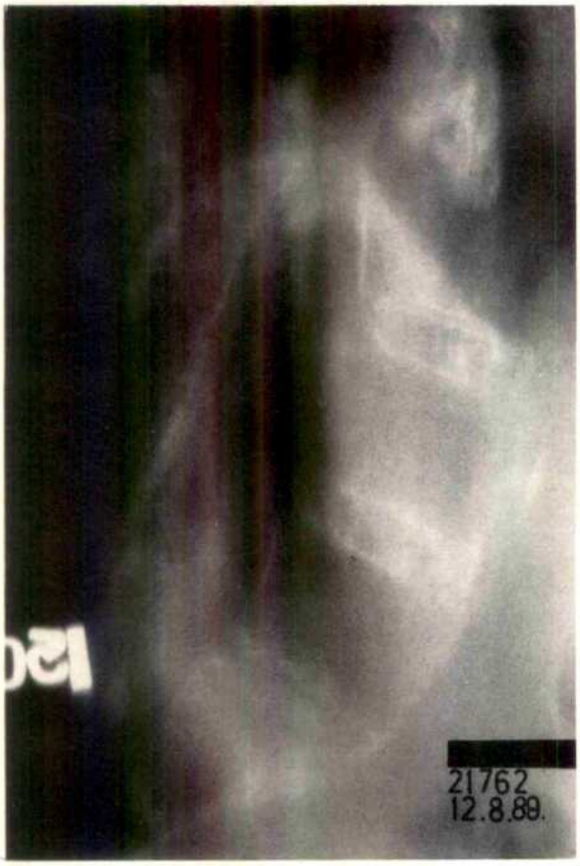

Figure 2. Tomogram of lumbo-sacral spine showing fracture (pseudarthrosis) through body of third lumbar vertebra and posterior elements.

strength had improved by at least two grades. Her fracture healed normally within 6 months.

Discussion

Minor neurological deficit may occur in stress fractures in patients with ankylosing spondylitis (Grisolia et al, 1967; Hansen et al, 1967; Hunter & Dubo, 1983; Weinstein et al, 1982). Stress fracture or fracture with minimum force may occur in these patients (Resnick & Niwayama, 1988), usually resulting from a hyperextension injury, typically in the lower cervical segment. However, fractures in the thoracic and lumbar spine are often clinically unrecognized (Little et al, 1974; Thorngren et al, 1981; Resnick & Niwayama, 1988).

The radiographic appearance of a pseudarthrosis of the spine resembles that which is observed in infection or neuroarthropathy, although a soft tissue mass is common in infective spondylitis and rare in pseudarthrosis (Karlstrom & Olerud, 1981). Similarly this patient did not show any significant soft tissue mass at the pseudarthrosis.

A severe neurological accident during the positioning for plain spinal antero-posterior radiography has not been reported as far as we know. In this case the circumstances were unusual, in that the person supervising the radiograph was untrained; but it could have happened in normal circumstances. Great care must be taken when positioning such a patient for antero-posterior radiographs as the spine is rigid, deformed (kyphotic) and osteoporotic, and a supine position may exert a hyperextension force leading to a fracture which starts anteriorly and propagates posteriorly towards the posterior elements and ossified ligaments.

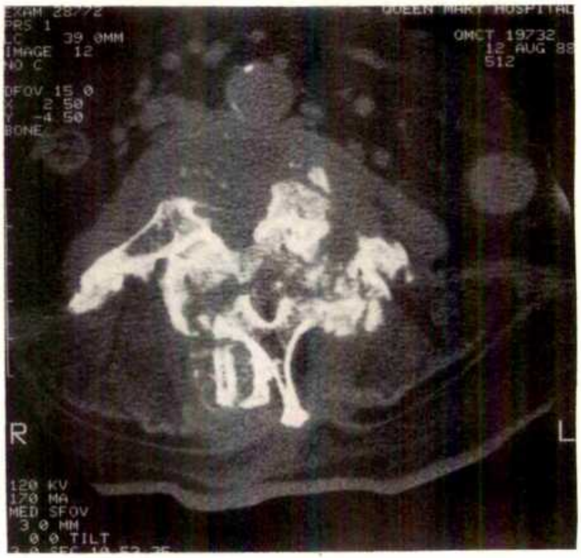

Figure 3. Computed tomographic scan at the level of third lumbar vertebra showing the fracture extending into the posterior element.

References

GRISOLIA, A., BELL, R. L. & PELTIER, L. F., 1967. Fractures and dislocations of the spine complicating ankylosing spondylitis. *Journal of Bone and Joint Surgery*, *49A*, 339–344.

HANSEN, S. T., TAYLOR, T. K. F., HONET, J. C. & LEWIS, F. R., 1967. Fracture-dislocations of the ankylosed thoracic spine in rheumatoid spondylitis. *Journal of Trauma*, *7*, 827–837.

HO, E. K. W., CATABAGAN, A. B., UPADHYAY, S. S. & LEONG, J. C. Y., Complete recovery after surgical stabilisation from paraplegia of three months duration in a fractured ankylosing spondylitic spine. *Clinical Orthopaedics and Related Research*, in press.

HUNTER, T. & DUBO, H., 1983. Spinal fractures complicating ankylosing spondylitis. *Arthritis and Rheumatism*, *26*, 751–759.

KARLSTROM, G. & OLERUD, S., 1981. Spinal pseudarthrosis with paraplegia in ankylosing spondylitis. *Archives of Orthopaedic and Traumatic Surgery*, *98*, 297.

LITTLE, H., UROWITZ, M. B., SMYTHE, H. A. & ROSEN, P. S., 1974. Asymptomatic spondylodiscitis: an unusual fracture of ankylosing spondylitis. *Arthritis and Rheumatism*, *17*, 487–493.

RESNICK, D. & NIWAYAMA, G., 1988. Ankylosing spondylitis. In *Diagnosis of Bone and Joint Disorders*. Ed. by D. Resnick and G. Niwayama (W. B. Saunders Co., Philadelphia) pp. 1118–1136.

THORNGREN, K. G., LIEDBERG, E. & ASPELIN, P., 1981. Fractures of the thoracic and lumbar spine in ankylosing spondylitis. *Archives of Orthopaedic and Traumatic Surgery*, *98*, 101.

WEINSTEIN, P. R., KARPMAN, R. P., GALL, E. P. & PITT, M., 1982. Spinal cord injury, spinal fracture and spinal stenosis in ankylosing spondylitis. *Journal of Neurosurgery*, *57*, 609–616.

Atypical skeletal tuberculosis mimicking neoplasm

By Ibrahim Fikry Abdelwahab, MD, *Samuel Kenan, MD, George Hermann, MD, *Michael Lewis, MD, †Michael Klein, MD and Jack G. Rabinowitz, MD

Departments of Radiology, *Orthopaedics and †Pathology of The Mount Sinai Medical Center, CUNY, New York, USA

(*Received October 1990 and in revised form December 1990*)

Keywords: Skeletal tuberculosis, Infection, Bone, Computed tomography, Magnetic resonance

Although the radiographic features of skeletal tuberculosis are well described, little has been written regarding tuberculous involvement of the shaft of tubular bones. In general, para-articular regions are mainly affected. Only 10% of cases spare the joint, and the majority of these are metaphyseal. Diaphyseal disease is rare and the radiographic features are variable and at times confusing. Pulmonary tuberculosis with subsequent skeletal tuberculosis is being encountered with increasing frequency (DHHS, 1988). Our recent experience with two unusual presentations prompted this report.

Methods

Two patients, both women, were diagnosed with focal bone tuberculosis. The lesion involved the left tibia in a 40-year-old woman of Chinese extraction and the pubic ramus in a 46-year-old black woman. Conventional radiography, bone scanning and computed tomography (CT) were performed on both patients. In addition, angiography and magnetic resonance imaging (MRI) were also performed on the second patient. The diagnosis was established in both patients by open biopsy. Paraffin sections were stained with haematoxylin and eosin as well as with acid-fast and fungal stains. Smears were made of the fresh material in each case for both Gram's and acid-fast staining. Some of the fresh material from each case was cultured for organisms, including acid-fast bacilli and fungi. Although the sections did not reveal acid-fast organisms, culture for acid-fast bacilli was positive in the two patients.

Case reports

Case 1

A 40-year-old Asian woman presented with a 3-month history of pain and gradually increasing swelling of her left leg. Previous medical history was unremarkable.

Physical examination revealed a woman in severe distress, limping and having difficulty walking. There was swelling with skin erythema over the anteromedial aspect of the middle part of the left leg. The overlying skin was hot and tender. There was

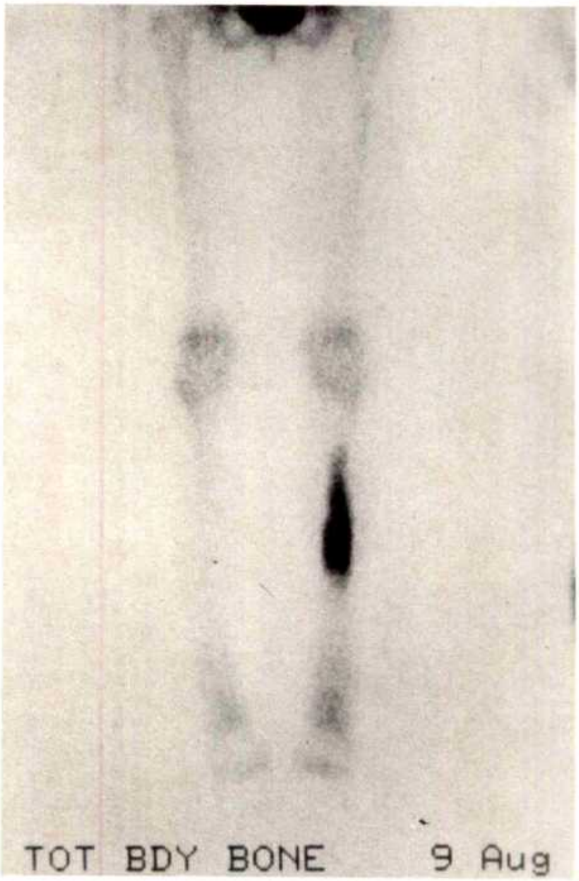

Figure 1. Radionuclide scanning by $^{99}Tc^{m}$-methylene diphosphonate showing increased uptake of the radioisotope in the mid shaft of the left tibia.

Address correspondence to: Dr I. Fikry Abdelwahab, Box 1234, Department of Radiology, Mount Sinai Medical Center, One Gustave L. Levy Place, New York, NY 10029-6574, USA.

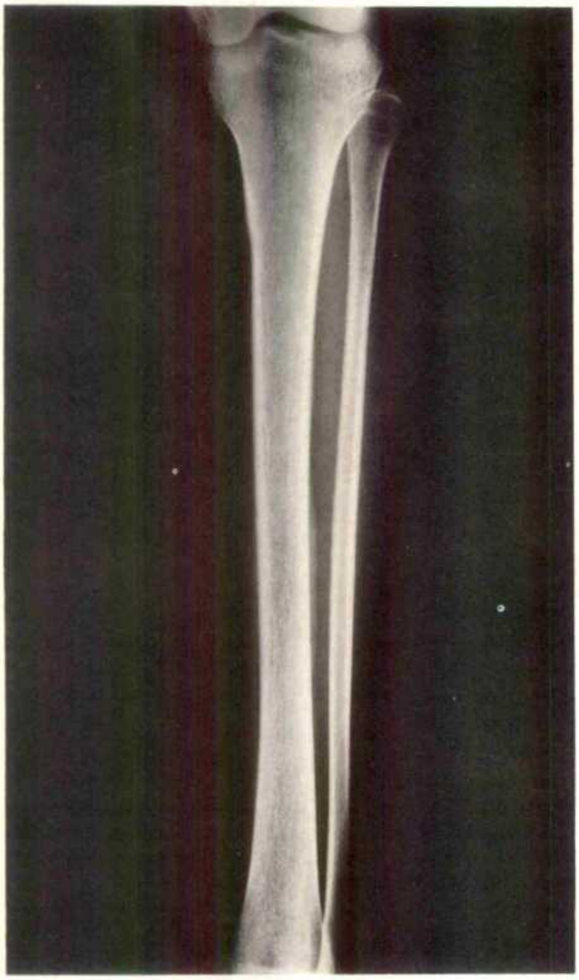

Figure 2. Frontal view of the left leg. This view shows minimal osteolytic changes of the mid shaft of the tibia with localized solid periosteal thickening.

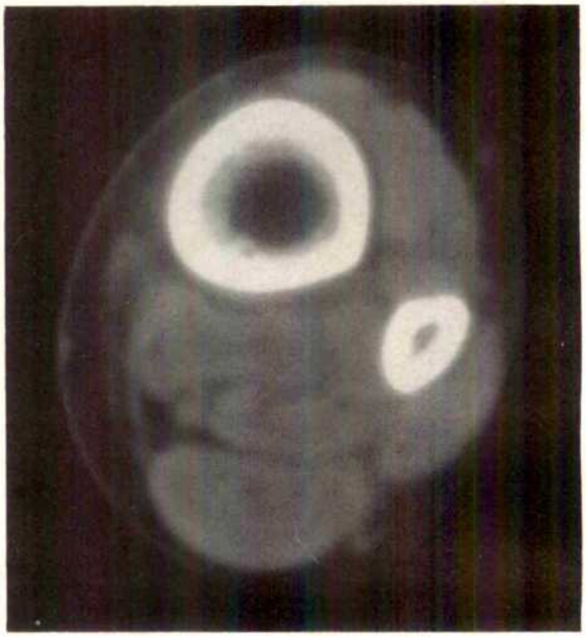

Figure 3. A CT scan of the mid shaft of the tibia. Minimal periosteal thickening is seen on the lateral cortex. There is no soft-tissue mass. There is infiltration of the marrow.

no neurovascular deficit. The chest radiograph was unremarkable. Laboratory studies showed an increased erythrocyte sedimentation rate, neutropenia and lymphocytosis. A bone scan (Fig. 1), plain radiography (Fig. 2) and computed tomography (Fig. 3) demonstrated a lesion in the mid shaft of the left tibia with localized periosteal reaction. Histological features from an open biopsy were compatible with tuberculosis. Direct smears of the biopsy material and special stains failed to demonstrate the acid-fast bacilli. However, cultures revealed *Mycobacterium tuberculosis*. The patient then received anti-tuberculous therapy and radiographs performed 6 months after treatment revealed marked improvement. There were no osteolytic changes, and the solid periosteum blended with the cortex (Fig. 4).

Case 2

A 46-year-old native black woman presented with pain over the left groin associated with low-grade fever. Three months earlier, she had undergone open biopsy for a left groin mass in another hospital, revealing necrotizing granulomata. Smears and special stains for acid-fast bacilli and fungus from the biopsy material were negative. On the assumption that these caseating granulomata were tuberculous, she received anti-tuberculous therapy for 3 months. Because of partial relapse of pain and the possibility of an occult tumour, the patient was referred to our hospital. Physical examination revealed a soft-tissue mass in the left groin. There were no skin changes or neurovascular deficits and the left hip had full range of motion. The chest radiograph was unremarkable. The laboratory studies showed an increased erythrocyte sedimentation rate and relative lymphocytosis. A bone scan, plain radiography, angiography, CT and MRI revealed a destructive lesion of the superior ramus of the left pubic bone associated with a huge soft-tissue mass (Figs 5–8). Another open biopsy was performed and again demonstrated caseating granulomata. Cultures were again negative and the anti-tuberculous therapy was stopped. Six months after the initial biopsy, the patient underwent exploration of the left lower pelvis to drain an intrapelvic abscess and debride the necrotic tissue. Fresh tissue was cultured and this time grew *Mycobacterium tuberculosis*. Anti-tuberculous therapy was resumed and the patient is presently being followed-up in the orthopaedic clinic.

Discussion

With the introduction of anti-tuberculous antibiotics, the incidence of tuberculosis both in Europe and North America underwent a marked decline. However, there has been a recent rise in the number of cases encountered (DHHS, 1988). The organism mainly responsible for the disease is *Mycobacterium tuberculosis*, which usually affects the lung as a primary site. Bone involvement is usually secondary and the result of bacterial emboli. However, the incidence of coexisting active pulmonary tuberculosis is less than 30% (Chapman et al, 1979). In our case no evidence of pulmonary

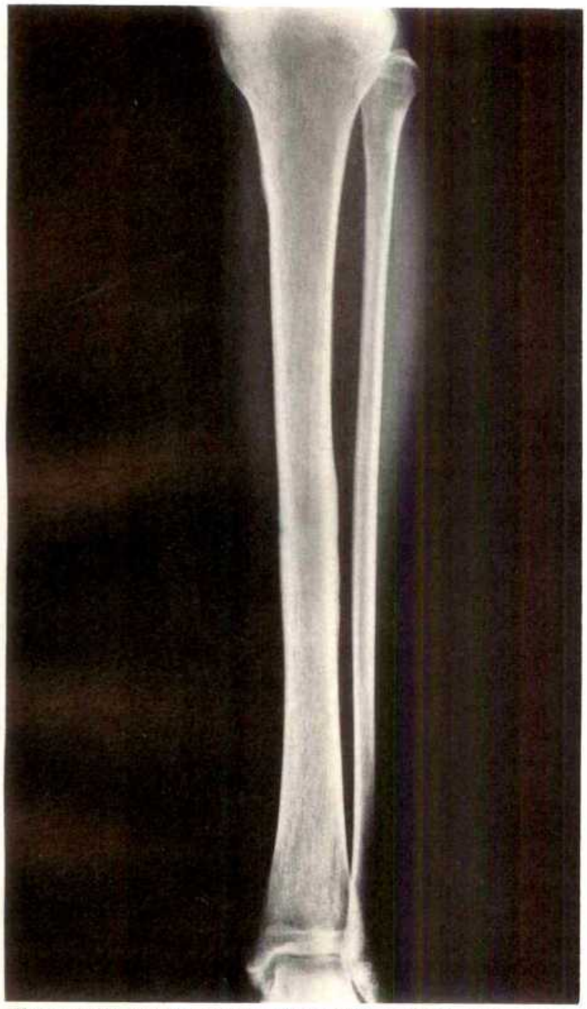

Figure 4. Frontal view of the left leg. This radiograph was taken 6 months after anti-tuberculous therapy and shows no bone osteolysis. Note that the dense periosteum has blended with the cortex causing localized cortical thickening. The lucent bony defect is the site of the previous open biopsy.

tuberculosis or other sources could be found. Diaphyseal involvement may be caused by a tuberculous embolus that remains lodged in the nutrient vessel because of thrombus or other reasons and therefore fails to spread to the metaphyseal region, the common site of involvement.

Tuberculosis in adults typically involves the end of a bone and the adjacent joint. The subarticular margin, which is normally sharp, becomes blurred and eventually destroyed. Secondary marginal erosions follow and, in due course, destruction of the articular cartilage leads to narrowing of the joint space. Characteristically, no reactive sclerosis, sequestration or periosteal reaction occurs (Davidson & Horowitz, 1970; Golding, 1971; Chapman et al, 1979). This so-called typical radiographic appearance is not always encountered among non-whites. Marginal sclerosis, sequestration and periosteal reaction are seen more frequently. In addition, the location of the infection appears more variable. The end of a long bone with preservation of the articular

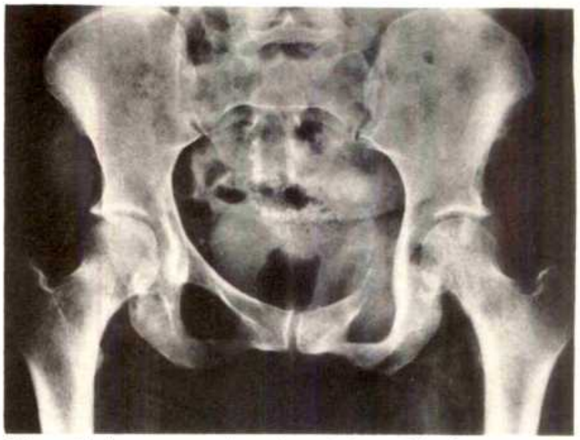

Figure 5. Antero-posterior view of the pelvis demonstrating destruction of the superior ramus of the left pubic bone. Note the osteoporosis of the proximal femur, scattered sequestra in the soft-tissue mass, the sharp bony margin of the lesion and the reactive sclerosis of the acetabular rim.

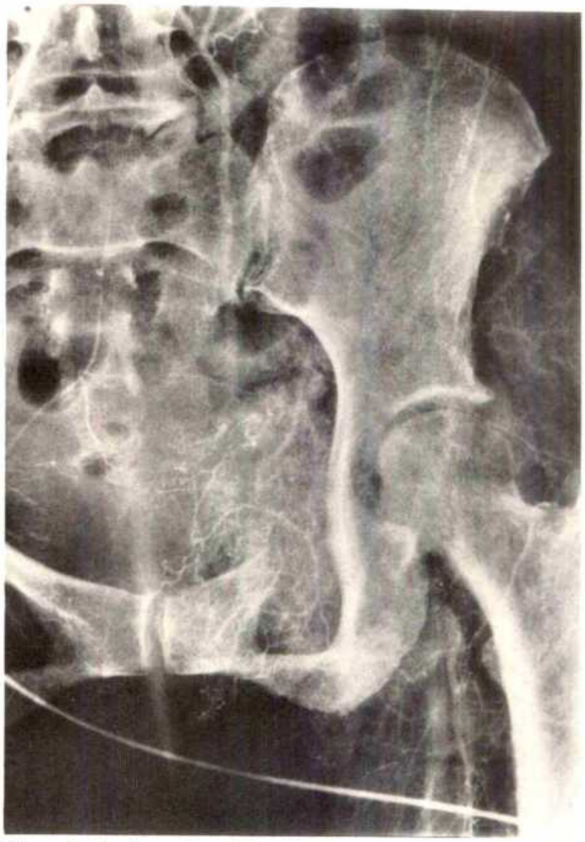

Figure 6. Angiography of the left side of the pelvis reveals the vascular soft-tissue mass.

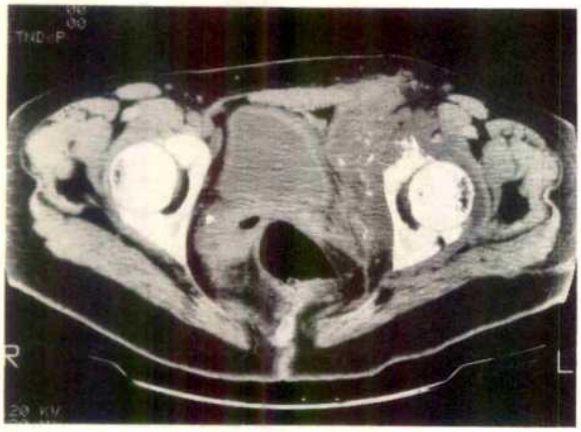

Figure 7. A CT scan demonstrating scattered tiny sequestrae in a large intrapelvic soft-tissue mass, extending to the left groin. There is some destruction of the anterior column and minimal destruction of the posterior column of the acetabulum.

margin and cartilage space in major joints, such as the hip and knee, is now being encountered (Jacobs, 1964; Goldblatt & Cremin, 1978; Chapman et al, 1979; Abdelwahab et al, 1986, 1987). Non-articular tuberculosis tends to involve bony prominences (*e.g.* the greater trochanter).

Tuberculosis of the shaft of the tubular bones makes up less than 1% of all cases of skeletal tuberculosis but surprisingly was noted commonly in individuals of Chinese extraction (Hsieh, 1934; Resnik & Niwayama, 1988). Various radiographic types of tuberculous involvement of the shaft have been described: a periosteal form, a solitary metaphyseal form simulating a Brodie's abscess, and an infiltrative form (Hsieh, 1934). In our patient, the lesion demonstrated diffuse osteolysis of the tibial shaft associated with a dense periosteal reaction overlying an intact cortex. Our second patient demonstrated an extensive lesion that broke through the cortex of the pubic ramus producing a large soft-tissue mass. Although no periosteal bone formation could be detected, multiple sequestrae were present in the mass. Moreover, the margin of the lesion was sharply defined and reactive sclerosis was apparent in the adjacent acetabular rim.

Although the lesions were first thought to be neoplastic, retrospective analysis of the radiographic features offered some clues to the more benign nature of the process. The dense periosteum, reactive sclerosis and the sharp margin are all features suggesting a chronic inflammatory process.

Involvement of the mid shaft of long bones and the pubic rami are rare. Amongst 30 cases of atypical skeletal tuberculosis in non-white immigrants in the United Kingdom, only two cases involved the shaft of long bones and both cases were not solitary. In one, a 31-year-old man from Aden, the left tibial shaft was infected by spread from tuberculous arthritis of the left ankle. The second patient, a 21-year-old Indian woman, had disseminated disease (Jacobs, 1964).

Involvement of the pubic ramus by tuberculosis is even more unusual. Goldblatt and Cremin (1978) reported 21 cases of tuberculosis of the pelvis, none involving the pubic ramus. Chapman et al (1979) in their discussion of osseous tuberculosis noted that the pubic rami are occasional sites but did not include radiographs. Tuberculous involvement of the pubic ramus and shaft of long bones has not been found in caucasians (Jacobs, 1964).

The inability to demonstrate tuberculous organisms in sections with special stains is not an unexpected finding assuming random dispersion of organisms in a tissue sample in which 5 μm thick histological sections are examined (Abdelwahab et al, 1986); a culture is far more sensitive. Since tuberculous lesions are often mistaken for neoplasms, a small amount of fresh tissue should always be sent for culture, even if a clinical diagnosis of a tumour seems certain. Our experience suggests that any confusing bone lesion in a non-white patient may prove to be tuberculous.

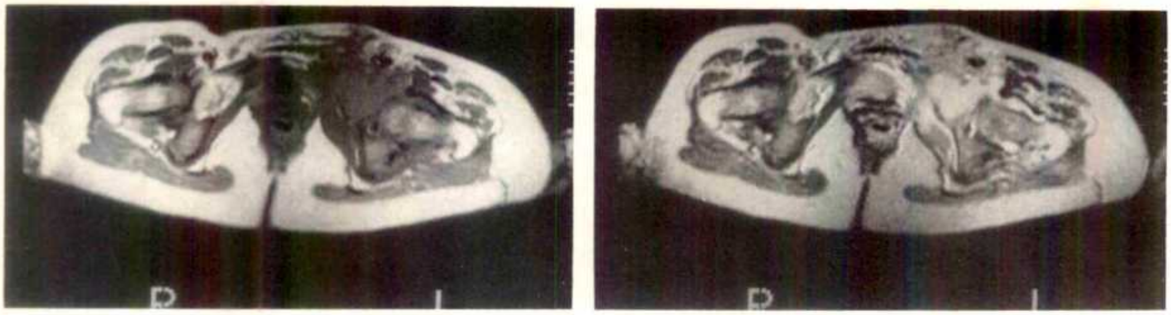

(a) (b)

Figure 8. Axial MR scan of the left pubic ramus. (a) T_1-weighted image (SE 600/30); (b) T_2-weighted image (SE 2200/80). The soft-tissue mass has an isointense signal in the T_1-weighted image and heterogeneous high-intensity signal in the T_2-weighted image.

1991, *The British Journal of Radiology*, *64*, 555–557

References

ABDELWAHAB, I. F., PRESENT, D. A. & KLEIN, M. J., 1986. Tuberculous pseudotumor of the proximal end of the right tibia without obvious synovial involvement. *Skeletal Radiology*, *15*, 652–656.

ABDELWAHAB, I. F., PRESENT, D. A., ZWASS, A., KLEIN, M. J. & MAZZARA, J., 1987. Tumor-like tuberculous granulomas of bone. *American Journal of Roentgenology*, *149*, 1207–1208.

DHHS, 1988. *Annual Summary 1988. Reported Morbidity and Mortality in the United States* (Department of Health and Human Services, Public Health Service, Atlanta).

CHAPMAN, M., MURRAY, R. O. & STOKER, D. J., 1979. Tuberculosis of the bone and joints. *Seminars in Roentgenology*, *24*, 266–282.

DAVIDSON, P. T. & HOROWITZ, I., 1970. Skeletal tuberculosis. A review with patient presentation and discussion. *American Journal of Medicine*, *78*, 77–84.

GOLDBLATT, M. & CREMIN, B. J., 1978. Osteoarticular tuberculosis, its presentation in colored races. *Clinical Radiology*, *29*, 669–677.

GOLDING, F. C., 1971. *A Textbook of X-ray Diagnosis*, 4th edn (Lewis, London), pp. 293–316.

HSIEH, C. K., MILTNER, L. J. & CHANG, C. P., 1934. Tuberculosis of the shaft of the large long bones of the extremities. *Journal of Bone and Joint Surgery*, *16*, 545–563.

JACOBS, P., 1964. Osteoarticular tuberculosis in colored immigrants. A radiological study. *Clinical Radiology*, *15*, 59–69.

RESNIK, D. & NIWAYAMA, G., 1988. *Diagnosis of Bone and Joint Disorders* (W. B. Saunders, Philadelphia), p. 2674.

Demonstration of intramedullary tuberculomas by magnetic resonance imaging: a report of two cases

By A. Jena, DRM, DNBE(NM), *A. K. Banerji, MS(Surg), MS(Neuro), R. P. Tripathi, MD, P. K. Gulati, MD, R. K. Jain, BSc, S. Khushu, MSc and M. L. Sapra, MD

NMR Research Centre, Institute of Nuclear Medicine and Allied Sciences, Lucknow Marg, Delhi 110054 and *Neuro Centre, All India Institute of Medical Sciences, Ansari Nagar, New Delhi 110016, India

(*Received August 1990 and in revised form December 1990*)

Keywords: Spinal cord, Infection, Tuberculosis, MRI

Intramedullary tuberculomas are rare (Arseni & Samitca, 1960; Dastur, 1972; Compton & Dorsch, 1984) but have been demonstrated either at surgery or at autopsy. The appearance of tuberculomas in the brain on magnetic resonance imaging (MRI) has been reported (Gupta et al, 1988). However, the image morphology of intrinsic cord tuberculomas has not been described. We present the MR findings in two patients with tuberculomas of the cervical cord diagnosed on the basis of positive therapeutic response to antituberculous therapy (ATT).

Two young patients with clinical and radiological evidence of intramedullary pathology, who were referred for MRI study with possibility of tuberculous myelitis, are described. Magnetic resonance imaging of the cervicodorsal spine was performed with a 1.5 T (MAGNETOM, Siemens) system using spin echo sequences (repetition time (TR), 2000 ms and echo time (TE), 69–90 ms for T_2 images; TR, 700–800 ms and TE, 17–22 ms for T_1 images) in axial and sagittal planes. Images were acquired on 256×256 matrix and 1.2 gradient zooming with 5 mm contiguous slices. Follow-up studies in both cases were taken after 4 months and after 1 year in Case 2.

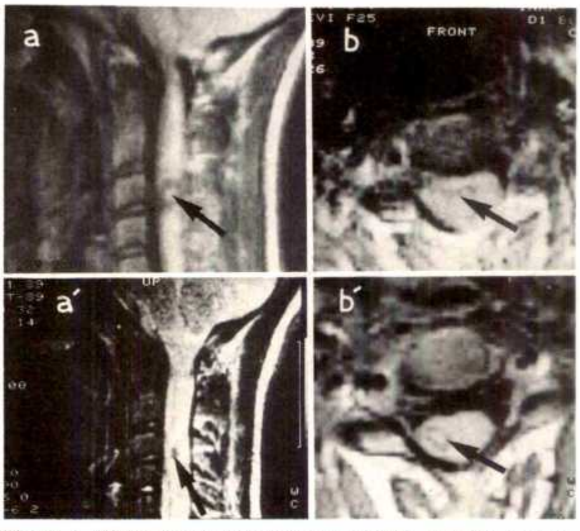

Figure 1. Magnetic resonance images of the cervical spine in Case 1. (a) Sagittal T_2 image with TR: 2000 ms/TE: 69 ms showing a well defined hypointense lesion with central hyperintensity (arrow). (b) Axial T_1 image with TR: 700 ms/TE: 22 ms at the same level showing the lesion to be heterogenously low to isointense (arrow). (a') Sagittal T_2 image with TR: 2000 ms/TE: 90 ms, 4 months following antitubercular therapy (ATT) showing marked regression in the size of the cord lesion (arrow). (b') Axial T_1 image with TR: 800 ms/TE: 22 ms showing the residual focal lesion in the cord (arrow).

Address correspondence and reprint requests to: Lt. Col. A. Jena, DRM, DNBE (NM), Head, NMR Research Centre, Institute of Nuclear Medicine and Allied Sciences, Lucknow Marg, Delhi 110054, India.

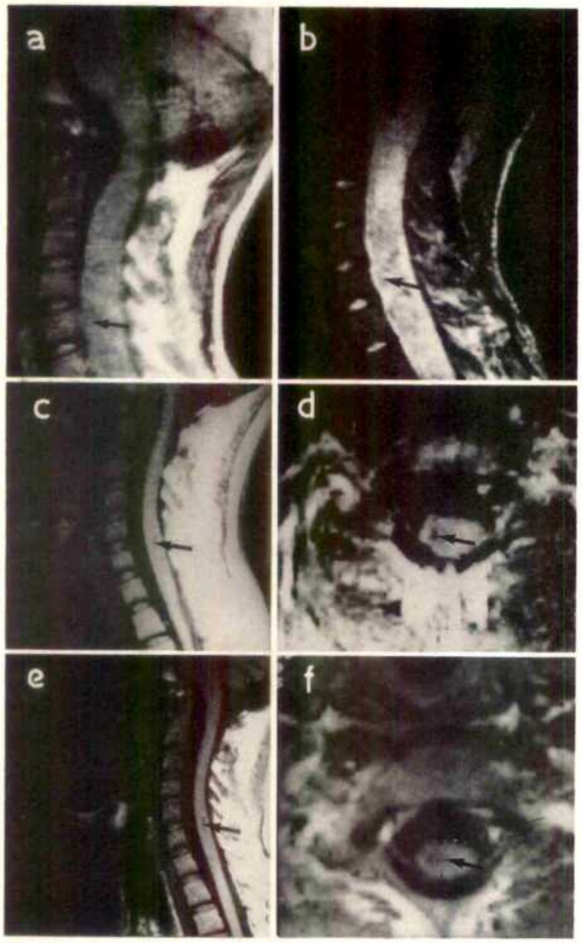

Figure 2. Sagittal and axial MR images of the cervical spine in Case 2. (b) Sagittal T_2 image with TR: 2000 ms/TE: 90 ms before treatment, showing diffuse expansion of the cord with multiple low intensity lesions in the cord (arrow). (a) T_1 sagittal image with TR: 700 ms/TE: 17 ms showing obliteration of arachnoid space and heterogenously low intense lesions in the cord (arrow). (c) & (d) Sagittal and axial T_1 images with TR: 700 ms/TE: 17 ms of the same patient 4 months after showing marked reduction of lesions in the cord and better visualization of the intradural space (arrow). (e) & (f) Sagittal and axial T_1 images after 1 year of ATT showing residual lesion in the cord (arrow).

Case reports

Case 1

A 25-year-old woman was admitted complaining of a 3-month history of progressive weakness of the right side of the body. On examination, she was found to have wasting of the right upper limb, exaggerated tendon jerks and 50% sensory loss involving the lateral and posterior column below C6 level. Routine laboratory investigations and chest radiography were essentially normal. Cerebro-spinal fluid (CSF) examination showed 225.2 mg/dl protein and 18 lymphocytes/HPF. Contrast myelography showed widening of the cord at the C2–C4 levels. Magnetic resonance imaging showed a well defined intramedullary lesion measuring 9.2 × 9.2 mm at the C3/C4 level on the right with diffuse expansion of the cord from C2 to C5/C6 (Figs 1a & b). The extradural space and vertebral bodies were found to be normal. The lesion appeared to be hypointense in its periphery with central hyperintensity on T_2-weighted images and low to isointense on T_1 images. The patient showed remarkable relief of her symptoms over a period of 4 months with ATT. Regression of cord swelling was associated with reduction in the size of the lesion to 3 × 3 mm on the follow-up study (Figs 1a′ & b′). The residual lesion confined to the lateral and posterior column at C3/C4 level persisted and this explained the neurological deficit in the right upper limb.

Case 2

A 23-year-old man presented with a 4-month history of progressive weakness, fasciculation of right upper limb, associated low grade fever and anorexia. On examination, he was found to have bilateral axillary lymphadenopathy, grade III to IV power in the right upper limb and no sensory loss. Routine laboratory investigations showed a raised erythrocyte sedimentation rate (28 mm in first hour) and leucocytosis with lymphocyte predominence and positive sputum for acid-fast bacilli (AFB). A chest radiograph showed patchy parenchymatous lesions in the upper zone of right lung suggestive of tuberculosis. Contrast myelography showed an intramedullary lesion involving the C2–D1 levels. A lymphnode biopsy (axillary) showed granulomatous lymphadenitis with areas of caseous necrosis consistent with tuberculosis. Magnetic resonance imaging showed diffuse expansion of the cord with poor definition of subarachnoid space extending from C2 to D2 levels. In the T_2 images, multiple focal low intensity lesions were seen in the cord substance and intradural space (Figs 2a & b). The vertebral bodies were found to be normal. A follow-up study after 4 months' antitubercular treatment showed regression in the cord expansion (Figs 2c & d). After 1 year, a small residual/healed focus on the right side of the cord was all that remained (Figs 2e & f).

Discussion

The role of MRI in the spine is well documented and has been shown to offer advantages in the delineation and better characterization of lesions. Intracranial tuberculomas have been described as low intensity rings with or without central hyperintensity (because of the varying amount of caseous necrosis) on T_2 images and low to isointense on T_1 images (Gupta et al, 1988).

Dastur and Shah (1968) documented gross and microscopic features in a tuberculoma of cord as focal caseating necrosis with a rim of transluscent granulation tissue consisting of epitheloid cells, Langhan's giant cells and fibroblasts. The MR findings in our cases correspond to the above morphological description and are similar to the characteristic appearance of tuberculomas of brain shown by magnetic resonance imaging. The highly suggestive clinical picture and positive therapeutic response confirmed the diagnosis of intramedullary tuberculomas in both of our cases.

We conclude that spinal cord tuberculomas could be demonstrated on MR and their appearance is similar to that described for tuberculomas in brain.

Acknowledgments

We would like to thank Mr H. S. Bist and Mr Y. C. Gupta for secretarial assistance.

1991, *The British Journal of Radiology*, *64*, 557–558

References

ARSENI, C. & SAMITCA, D. C., 1960. Intraspinal tuberculous granuloma. *Brain*, *83*, 285–292.

COMPTON, J. S. & DORSCH, N. W. C., 1984. Intradural extramedullary tuberculoma of the cervical spine. *Journal of Neurosurgery*, *60*, 200–203.

DASTUR, H. M., 1972. A tuberculoma review with some personal experiences. Part II: Spinal cord and its coverings. *Neurology India*, *20*, 127–131.

DASTUR, H. M. & SHAH, M. D., 1968. Intramedullary tuberculoma of spinal cord. *Indian Pediatrics*, *5*, 468–471.

GUPTA, R. K., JENA, A., SHARMA, A., GUHA, D. K., KHUSHU, S. & GUPTA, A. K., 1988. MR imaging of intracranial tuberculomas. *Journal of Computer Assisted Tomography*, *12*, 280–285.

Oesophageal atresia and other disorders with a similar antenatal presentation

By A. C. Havard, MB, BS, FRCR and L. M. MacDonald, MB, BS, FRCR

Department of Radiology, St Thomas' Hospital, London SE1 7EH, UK

(*Received September 1990 and in revised form October 1990*)

Keywords: Oesophageal atresia, Fetal ultrasound, Fetal stomach

Oesophageal atresia without distal tracheo-oesophageal fistula is a recognized cause of the absence of fluid in the fetal stomach seen on serial ultrasound examinations. It is rare not to demonstrate fluid in the fetal stomach after 15 weeks gestation. There have been several reports of the antenatal diagnosis of oesophageal atresia by ultrasound, the earliest by Farrant (1980).

Oesophageal atresia occurs once in every 1500 live births and 90% of these are associated with a tracheo-oesophageal fistula. The fistula is usually to the distal oesophageal segment but rarely are a distal and proximal fistula found. In 1%, an H-type tracheo-oesophageal fistula is present without an associated oesophageal atresia. In cases of oesophageal atresia with tracheo-oesophageal fistula to the distal segment, fluid in the lungs and major airways may reach the fetal stomach by way of the fistula in spite of oesophageal interruption. Polyhydramnios may still be present. When oesophageal atresia occurs in isolation (10%) or when a single fistula is present to the proximal oesophagus (1%), no fluid can enter the stomach and none will be seen on serial ultrasound examinations.

The purpose of this report is to review other abnormalities that may produce a similar appearance and to document two cases presenting in this manner, which, to our knowledge, have not been previously reported.

Case reports

Case 1

A 31-year-old gravida 5 para 3 in her 32nd week of gestation was examined to assess the placental position. A live fetus was present in the vertex position. Mild polyhydramnios was present. The patient was rescanned at 34, 35 and 36 weeks by which time she had experienced recurrent episodes of premature labour and had noticed reduced fetal movements. In addition to a Grade 1 placenta previa, breech presentation and increasing polyhydramnios, the scans showed no fetal stomach or fluid-filled bowel loops and no evidence of spontaneous swallowing activity. Oesophageal atresia was suspected.

The patient went into spontaneous labour at 36 weeks but was delivered by a Caesarian section for fetal distress. The live male baby weighed 2.64 kg. The Apgar scores at 1, 5 and 10 min were 5, 8 and 4 respectively. He was hypotonic and cyanosed with shallow respirations. A tube was passed which confirmed oesophageal patency. At 4 hours the baby was still profoundly hypotonic and showed no spontaneous movements. The baby required tube feeding. A congenital neuromuscular (probably nemaline) myopathy was postulated. He died a few weeks later.

In this case the absent fluid in the fetal stomach and polyhydramnios seen antenatally were undoubtedly due to an inability to swallow efficiently even though the oesophagus was patent.

Case 2

A 36-year-old gravida 3 para 2 presented late in pregnancy for her first antenatal appointment. An ultrasound examination estimated the gestational age at 32 weeks. In addition to polyhydramnios there was no demonstrable fluid in the fetal stomach. She was admitted at 36 weeks following spontaneous rupture of membranes and draining blood-stained liquor. An emergency Caesarian section was performed for interpartum haemorrhage and fetal distress, and a live male infant weighing 2.3 kg was delivered. The Apgar scores at 1 and 5 min were 8 and 9. A nasogastric tube failed to pass into the stomach and coiled in the proximal part of an atretic oesophagus. Radiographs showed gas in the upper intestines. At surgery a fistula was found from the right main bronchus to the distal oesophageal segment. In addition, the stomach was found to be hypoplastic. Subsequent ultrasound and angiographic examinations revealed a very small spleen and a sequestered upper lobe in the right lung. The infant died aged 12 months.

Address correspondence to: Dr A. C. Havard, Department of Radiology, Charing Cross Hospital, Fulham Palace Road, London W6 8RF, UK.

Discussion

The finding of polyhydramnios and the absence of fluid in the fetal stomach on antenatal ultrasound examinations should alert the examiner to the possibility of oesophageal atresia. However, other conditions may also give this appearance as in our first case where neuromuscular incoordination prevented the ingestion of normal amounts of fluid and no fluid was present in the fetal stomach on serial antenatal scans. We believe that this is the first such case reported. It has been shown that in polyhydramnios fetal swallowing activity may be increased. Bowie and Clair (1982) studied the swallowing activity of 20 babies *in utero*, of whom seven had associated polyhydramnios. Five of these seven showed distinct pharyngeal swallowing whereas only two of the 13 babies with normal amounts of amniotic fluid showed similar movements. Interestingly, two-thirds of the cases of oesophageal atresia with tracheo-oesophageal fistula showed apparent active regurgitation whilst one-third showed no increased swallowing. Therefore, the lack of spontaneous swallowing in our first case might have alerted us to the correct diagnosis.

The second case presented antenatally with polyhydramnios, absent fluid in the fetal stomach on serial ultrasound examinations and no swallowing abnormality. Oesophageal atresia with proximal tracheo-oesophageal fistula or without associated fistula was suspected. In fact, a broncho-oesophageal fistula was present.

The occurrence of oesophageal atresia with a broncho-oesophageal fistula is very rare. Most broncho-oesophageal fistulae are of the H-type with an intact oesophagus and, to our knowledge, neither type has been reported as causing abnormalities on an antenatal scan.

There have been cases of oesophageal atresia and tracheo-oesophageal fistula where no fluid was seen in the fetal stomach. The first reported case of oesophageal atresia detected on antenatal scanning (Farrant, 1980) did have a tracheo-oesphageal fistula to the distal oesophageal segment. The reason no fluid could be detected in the fetal stomach was the presence of a coexistant tracheal atresia proximal to the fistula limiting passage of fluid to the stomach.

In other cases (Weinberg & Diakoumakis, 1985; Rahmani & Zalev, 1986), the fistula may have been too small to allow passage of fluid into the stomach, was plugged by extraneous material or was narrowed by impingement of adjacent structures. This mirrored our second case where the fistula was found in association with many other thoracic abnormalities and a microgastria. A small fetal stomach is also a significant finding (Kurjak et al, 1984).

Oesophageal atresia with tracheo-oesophageal fistula can therefore be present with absence of fluid in the fetal stomach, but, conversely, there has been at least one report of an isolated oesophageal atresia where a fluid-filled stomach was seen on the antenatal scans (Claiborne et al, 1986) due to co-existent atresia of the gastric antrum and retained gastric secretions. Isolated oesophageal atresia cannot be excluded when fluid is seen in the fetal stomach. Up to 5% of infants with oesophageal atresia will have other atresias in the upper gastrointestinal tract (Martin & Alexander, 1985).

We conclude absent or reduced fluid in the fetal stomach should suggest the possibility of an oesophageal lesion. Other malformations may be present and absence of fluid in the stomach does not rule out an associated fistula. Even with an isolated oesophageal atresia, fluid may be present in the stomach if there is a second atresia in the stomach or duodenum.

It is important to assess swallowing activity where an oesphageal lesion is suspected, as it may be increased where oesphageal interruption exists. The absence of swallowing activity may differentiate between an obstruction and neurological abnormality.

When a suspected diagnosis of an oesophageal lesion is made in the antenatal period, provision can be made to allow delivery at a suitable hospital.

References

Bowie, J. D. & Clair, M. R., 1982. Fetal swallowing and regurgitation: observation of normal and abnormal activity. *Radiology*, *144*, 877–878.

Claiborne, A. K., Blocker, S. H., Martin, C. M. & McAlister, W. H., 1986. Prenatal and postnatal sonographic delineation of gastrointestinal abnormalities in a case of Vater syndrome. *Journal of Ultrasound in Medicine*, *5*, 45–47.

Farrant, P., 1980. The antenatal diagnosis of oesophageal atresia by ultrasound. *British Journal of Radiology*, *53*, 1201–1203.

Kurjak, A., Gogolja, D., Kogler, A., Latin, V. & Rajhvajn, B., 1984. Ultrasound diagnosis and perinatal management of surgically correctable fetal malformations. *Ultrasound in Medicine & Biology*, *10*, 443–455.

Martin, L. W. & Alexander, F., 1985. Esophageal atresia. *Surgical Clinics of North America*, *65*, 1099–1113.

Rahmani, M. R. & Zalev, A. H., 1986. Antenatal detection of esophageal atresia with distal tracheoesophageal fistula. *Journal of Clinical Ultrasound*, *14*, 143–145.

Weinberg, B. & Diakoumakis, E. E., 1985. Three complex cases of foregut atresia: prenatal diagnosis with radiographic correlation. *Journal of Clinical Ultrasound*, *13*, 481–484.

1991, *The British Journal of Radiology*, *64*, 559–560

Case of the month

A dense problem

By D. O'Keeffe, MRCP1, FRCR and J. E. Adams, FRCP, FRCR

Department of Diagnostic Radiology, Stopford Building, University of Manchester Medical School, Oxford Road, Manchester M13 9PT, UK

(*Received March 1990*)

A 30-year-old woman with infertility and endometriosis, who was about to commence ovarian suppression therapy with a gonadotrophin releasing (GnRH) agonist, Nafarelin, was referred for measurement of bone mass by quantitative computed tomography (QCT) as a participant in a research study assessing the effects of GnRH agonists on bone.

The patient was asymptomatic; the only past history of note was an isolated episode of unexplained left loin pain 3 years previously. Investigations performed at that time, including an intravenous urogram, had been reported as normal. Her father was hypertensive.

An abnormality was noted on the CT sections obtained for bone mass measurement and consequently a formal CT examination of the abdomen was performed. Figure 1 is a transaxial section from that examination; what abnormalities are present, what diagnosis would you consider and what would you do next?

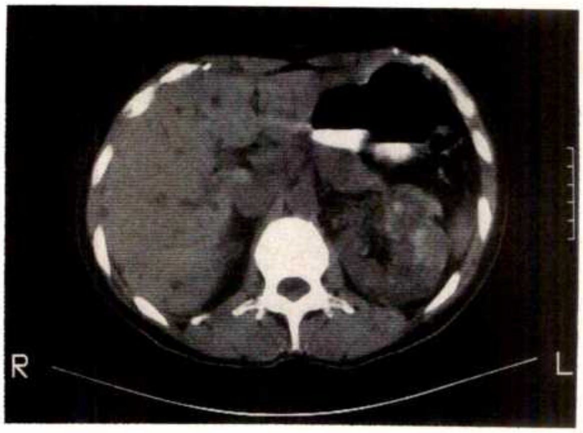

Figure 1. Transaxial section from formal CT examination of the abdomen.

Keywords: Autosomal dominant polycystic kidney disease, Computed tomography

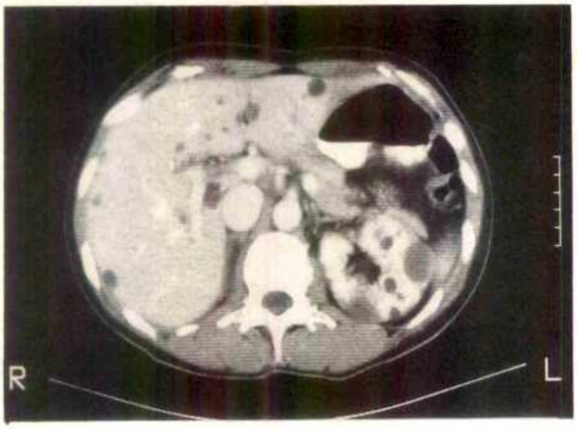

Figure 2. Transaxial CT section during intravenous contrast enhancement, at a slightly higher level than Fig. 1.

Figure 1 shows multiple areas of high attenuation (59–72 HU) and of varying size within the parenchyma of the left kidney. Within the right kidney there was a well defined, rounded region of low attenuation (5 HU). Multiple low attenuation areas are seen in the liver.

The differential diagnosis of the abnormality in the right kidney is either a renal cyst or a small renal tumour. The high attenuation areas in the left kidney may represent haemorrhagic simple cysts, calcified cyst walls, calcification in a renal neoplasm, diffuse unilateral high attenuation infiltration (*e.g.* amyloid) or nephrocalcinosis. Although unilateral nephrocalcinosis is unusual, it may occur in 25% of cases of medullary sponge kidney (Lalli, 1982), in papillary necrosis *in situ* and in chronic granulomatous infection such as tuberculosis or xanthogranulomatous pyelonephritis. In some cases of polycystic kidney the cysts may contain high attenuation material on CT. To characterize the abnormality further, contrast enhancement is required.

Figure 2 is a transaxial CT section, at a slightly higher level than Figure 1, performed during intravenous contrast medium injection (100 mls Omnipaque 300 (Nycomed U.K.) at 2 ml/s via Medrad pump). Figure 3a is a magnification of a selected part of Figure 2 set beside a comparable pre-contrast section through the left kidney (Fig. 3b).

There are multiple non-enhancing, low attenuation (5–10 HU) areas in the left renal parenchyma and in the liver (Fig. 2). Similar lesions were present in the pancreatic tail. The low attenuation area in the right kidney also failed to enhance. The areas of high attenuation within the left kidney on the initial examination are shown on post-contrast scans to be of two distinct types. They lie either in the centre of a region of lower attenuation than the surrounding enhancing renal parenchyma, or are related to the margins of a low attenuation area (Figs 3a & b). Measurement of attenuation of these areas of apparent "low" attenuation within the left kidney shows that they are unchanged from pre-contrast values (59–72 HU); they merely appear lower in attenuation when compared with the surrounding enhanced renal parenchyma.

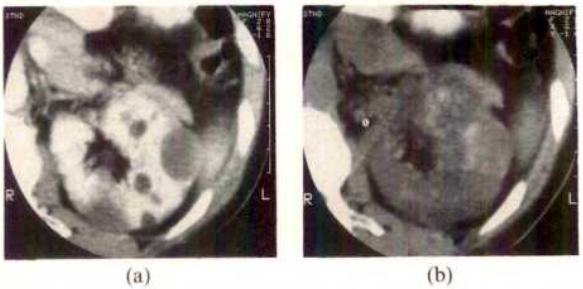

(a) (b)

Figure 3. (a) Magnified section of left kidney following IV contrast medium as in Fig. 2 with (b) comparable pre-contrast image.

This combination of well defined, low attenuation, non-enhancing renal, pancreatic and hepatic lesions is characteristic of autosomal dominant polycystic kidney disease (ADPKD). The high attenuation of the cysts in the left kidney are unusual, but has been described in up to 43% of patients with ADPKD (Levine & Grantham, 1985). Acute haemorrhage will cause an increase in the attenuation of the cyst contents (Meziane et al, 1986). The attenuation falls as the clot liquifies. Paradoxically, as the clot retraction progresses, concentration of the blood contents increases attenuation values. It is now established that the protein content of the clot contributes most to the high CT attenuation value, not the iron rich haem (which accounts for between 7–10% of the total attenuation (New & Aronow, 1976)).

When high attenuation cysts are encountered in ADPKD they are most often bilateral (Levine & Grantham, 1985). When unilateral they are more common on the left than the right. This left-sided preponderance is thought to be the result of the left kidney being less well protected than the right and, consequently, more liable to minor trauma (Meziane et al, 1986). In this patient it is possible that the previous episode of loin pain represented a spontaneous haemorrhage into the cyst. The patient was referred for a nephrological opinion and genetic counselling.

Acknowledgments

We would like to thank Professor M. Elstein for permission to report this case.

References

Lalli, A. F., 1982. Renal parenchyma calcifications. *Seminars in Roentgenology*, *17*, 101–112.

Levine, E. & Grantham, J. J., 1985. High density renal cysts in autosomal dominant polycystic kidney disease demonstrated by CT. *Radiology*, *154*, 477–482.

Meziane, M. A., Fishman, E. K., Goldman, S. M., Friedman, A. C. & Siegelman, S. S., 1986. Computed tomography of high density renal cysts in adult polycystic disease. *Journal of Computer Assisted Tomography*, *10*, 767–770.

New, P. F. & Aronow, S., 1976. Attenuation measurements of whole blood and blood fractions in computed tomography. *Radiology*, *121*, 635–640.

1991, *The British Journal of Radiology*, *64*, 561–564

Correspondence

(The Editors do not hold themselves reponsible for opinions expressed by correspondents)

Irregular-shaped fields in electron radiotherapy

The Editor—Sir,

We read with interest the technical note describing an irregular field technique for electrons, (Plane & Usher, 1990). On our SL 25, at Coventry, we have used a similar technique for over a year with satisfactory results.

On our SL 25, no modification to the applicator is required which makes this technique readily applicable. Perhaps more importantly the shielding alloy we use is MCP 69, and the accessories are cast in an aluminium moulding tray of a size specific to the applicator used. No pre-heating or forced cooling is required making the casting process simpler and possible without special equipment in addition to the moulding trays.

The aluminium moulds are constructed in such a way as to allow the reproduction of the registration holes in the SL 25 endplate. This is done by drilling the base in the appropriate position and the insertion of steel pegs (Fig. 1). These are removable so that blank plugs can be used to give the code of choice for each individual patient. There is a tapered peg in the centre of the baseplate to hold the polystyrene irregular shape. A 10 cm deep aluminium border is fitted to contain the MCP 69 metal when it is poured. This is fixed in position by 8 x 2 BA screws allowing the border to be removed so that the finished shape can be easily taken away. A polycarbonate plate with two holes of 20 mm diameter to facilitate pouring is fitted. The plate ensures a consistent thickness of 10 mm and a smooth finish.

Before pouring the mould is warmed briefly in hot water and dried. After pouring the metal is allowed to form a skin and then plunged into cold water, this means that the irregular shape can be ready for use in approximately 1 h.

The trays include removable coding holes to make the cast endplates compatible with the verification system of the SL 25. The plates are 10 mm thick and transmissions at energy up to 20 MeV are not significantly greater than for lead, the material which has been replaced.

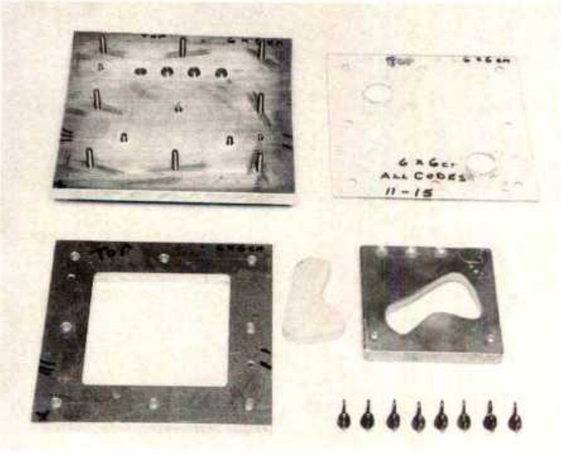

The authors describe application of the technique to flat surfaces. We are still evaluating the use of these plates for situations involving stand-off, wax build-up and curvature.

Yours, etc.,
P. B. Smith

Department of Radiotherapy Physics,
Walsgrave Hospital,
Clifford Bridge Road,
Walsgrave,
Coventry CV2 2DX, UK

(*Received January 1991*)

References

Plane, J. H. & Usher, C., 1990. A rapid method of production of irregular-shaped fields for use with patients receiving electron radiotherapy. *British Journal of Radiology*, *63*, 882–883.

Perfomance of a commercially available field flatness device

The Editor—Sir,

Hermes, a commercially available field flatness device (manufactured by Precitron AB, UK agents Graytech Ltd), has been used to measure the value of field flatness of radiotherpay treatment fields including γ-rays (cobalt 60), X rays (55 kV to 8 MV) and electrons (5 MeV to 14 MeV). A secular variation has been observed over a period of 12 months use. It is postulated that this may be partly attributable to radiation damage.

The device contains 10 P type semiconductor diode detectors, nine of which are strategically placed for the measurement of field flatness and one for measurement of depth dose. The detectors are mounted in a polystyrene phantom. Polystyrene build-up plates are used to vary the depth of measurement. The signals from the detectors are connected to a remote display which is battery operated. Each detector has its own integrating electrometer, scale factor adjustment potentiometer and digital display. The device is calibrated on the day of use by exposing each diode in turn to cobalt 60 γ-rays using a small field. The sensitivity of each diode is adjusted to give an absolute reading of radiation dose. A 250 x 250 mm radiation field (the maximum dimension of the calibration block) is then used to measure field flatness. The device is transported to the range of treatment units used in this centre. The block is allowed to reach thermal equilibrium. The value of field flatness for each energy and modality is measured.

The value of field flatness is defined as the ratio of maximum dose within the beam to the minimum dose within the flattened area (IPSM, 1988).

Cobalt 60 radiation was chosen for calibration purposes because the radiation output is predictable and field flatness is less likely to change as might be the case for X-ray units. Midway through this study the source of cobalt was removed and replaced with one of higher activity. The value of field flatness did not change as a result and was reproducible (mean 1.044, standard deviation (SD) 0.009).

However, this was not typical. At low X-ray energy the observed value of field flatness decreased with time (maximum range 100 kV: 1.214 to 1.017). For photon energies above cobalt 60 the observed value of field flatness increased with time (maximum range 8 MV: 1.042–1.100). For each electron energy the observed value of field flatness increased with time (maximum range 5MeV: 1.050–1.150).

For comparison purposes, measurements were carried out at 4 MV and 8 MV using a custom made device which drives a diode across a major field axis independent of the above. In contrast to the commercial flatness device these measurements did not reveal a secular increase at either energy (*e.g.* 8 MV maximum range 1.049 –1.059). Indeed, the reproducibility of flatness was good (*e.g.* 8 MV mean 1.053 SD 0.003).

It is recognized that the device calibration is strictly only valid in terms of absolute dose for cobalt 60 radiation. Nevertheless relative readings at other beam qualities are expected to be constant if field flatness does not change. The calibration procedure ensured that the cobalt 60 sensitivity of each diode and its associated electronics remained constant.

The observation that measured field flatness is changing with time at other energies suggests that the sensitivity of the diodes is changing. A well known effect of radiaiton damage is loss in radiation sensitivity. This may be attibuted to an increased number of defects in the crystal structure after irradiation which act as additional traps for minority carriers. Whilst this may cause a decrease in sensitivity it did not result in an increase in dark current (Rikner, 1983).

Hermes can be and is used for other quality assurance tests in a quality assurance programme (WHO, 1988). In this centre it is not used as a field flatness device without reference to an independent system. The manufacturer cautions users about the need for calibration and reference to independent measurements of field flatness. The above observations suggest that this caution is justified and may therefore be of interest to other users and potential users of the equipment.

Yours, etc.,
J. H. Plane

Regional Medical Physics Department,
South Cleveland Hospital,
Marton Road Middlesbrough,
Cleveland TS4 3BW, UK

(Received January 1991)

References

IPSM, 1988. *Commissioning and Quality Assurance of Linear Accelerators. Report 54* (IPSM, York).
Rikner, G., 1983. PhD Thesis, University of Uppsala.
WHO, 1988. *Quality Assurance in Radiotherapy*, (WHO, Geneva), pp. 15–37.

Choroid plexus cysts and chromosomal defects

Authors' reply

The Editor—Sir,

McHugo et al (1991) raise a number of important points. Our study (Thorpe-Beeston et al, 1990) did not attempt to investigate the incidence of choroid plexus cysts, and whilst we too eagerly await the results of prospective trials, the detection of choroid plexus cysts at ultrasonography presents a management dilemma now.

The criteria for referral to our centre were indeed dissimilar, the precise reasons being stated in the methods section. However, our results do not state, as is suggested, the incidence of trisomies in fetuses with choroid plexus cysts. We do, however, record that 59% of fetuses with choroid plexus cysts and additional malformations were karyotypically abnormal and conclude that the identification of choroid plexus cysts at routine ultrasonography should stimulate the search for additional malformations. Choroid plexus cysts are particularly useful markers because they can not easily be missed even by the relatively inexperienced sonographer, since they present in the standard biparietal view.

In the absence of other malformations it would appear that the prognosis is good, although this has not been the experience of all researchers, (Ostlere et al, 1989) and indeed since publication of our article we have detected a case of trisomy 21 in a fetus undergoing fetal blood sampling for the prenatal diagnosis of toxoplasmosis, choroid plexus cysts being the only observed abnormality.

Although exomphalos is a bigger malformation and McHugo et al (1991) state that this is a defacto indication for karyotyping, exomphalos is not dissimilar to choroid plexus cysts in its association with chromosomal defects. Thus, in our series of 97 cases with exomphalos, 40 (41%) had chromosomal defects, but none of the 36 fetuses, in whom exomphalos was the only malformation, were chromosomally abnormal.

Before multicentre trials can be undertaken, observations have to be made and these may frequently be at specialist centres. Whilst awaiting the outcome of multicentre trials we have suggested a management plan to inform fully the parents of the existing dilemmas and allow them to be involved in the decision making process.

Yours, etc.,
J.G.Thorpe-Beeston
K.H.Nicolaides

Harris Birthright Research Centre for Fetal Medicine,
Department of Obstetrics and Gynaecology,
King's College School of Medicine and Dentistry,
Denmark Hill,
London SE5 8RX, UK

(Received November 1990)

References

McHugo, J., Constantine, G. & Rajah, R., 1991. Choroid plexus cysts and chromosomal defects. *British Journal of Radiology, 64*, 281.
Ostlere, S. J., Irving, H. C. & Lilford, R. J., 1989. A prospective study of the incidence and significance of choroid plexus cysts. *Prenatal Diagnosis, 9*, 205–211.
Thorpe-Beeston, J. G., Gosden, C. M. & Nicolaides, K. H., 1990. Choroid plexus cysts and chromosomal defects. *British Journal of Radiology, 63*, 783–786.
Walkinshaw, S. A., Hebish, G. & Hey, E., 1989. The diagnosis of anterior abdominal wall defects—How good is routine ultrasound? *BMUS Programme and Abstract Book*, December 1989.

cGy *vs* Gy

The Editor—Sir,

The radiation oncology practice has a prolonged history of using the rad as a unit. With the introduction of the SI system, the Gy came into being. It is fortunate that the Gy has a metric relation to the rad, such that 1 rad = 0.01 Gy or 1 cGy. The literature is having a mixture of use of Gy as well as cGy. It makes sense to be consistent. To use the cGy rather than the Gy may be preferable for the following reasons.

1. The ear which had prolonged experience with the rad will hear familiar figures with the cGy. Radiation oncologists and other specialists reading old literature or discussing current cases will find it easier and faster to comprehend doses expressed in cGy than in Gy.

2. It is generally preferable to use figures without fractions than with fractions. Thus, a physician expresses the size of a node as 2 cm rather than 0.02 m. We prescribe 4 mg of a drug and not 0.004 g. It is similarly easier to say 180 cGy per fraction than 1.80 Gy per fraction.

3. For every day practice in radiation oncology, prescriptions in cGy without fractions are less likely to lead to errors than prescriptions in Gy with possible fractions.

I advocate using the cGy instead of the Gy in radiotherapy practice. For the sake of consistency, I also encourage scientific writing in journals, protocols and presentations to do the same. For example, a communication about the dose of radiation from an X-ray imaging procedure is expressed as 0.6 cGy rather than 0.006 or 6×10^{-3} Gy.

Yours, etc.,
RUSHDY ABADIR

Department of Oncology,
University of Missouri,
Columbia, Mo. 65203 USA

(*Received January 1991*)

Energy imparted to the patient during fluoroscopy using magnified fields of view

THE EDITOR—SIR,

Most textbooks on radiological equipment contain the information that the gain of an X-ray image intensifier is proportional to the ratio of the areas of its input and output phosphors, but the practical implications of this in terms of dose to the patient appear to be less well known.

For the normal practice of performing fluoroscopy under automatic dose rate control, when switching to a magnified field of view the dose rate would be expected to increase in inverse proportion to the change in gain of the intensifier if a constant signal-to-noise ratio in the image is to be maintained. At the same time an automatic change in collimation should take place so that the radiation beam size is restricted to cover only the active portion of the intensifier input phosphor (NRPB, 1988). This will reduce the area of the entrance surface of the patient being directly irradiated by the same proportion. Since the irradiated area has decreased in inverse proportion to the dose rate increase, the overall effect is to maintain a constant dose rate-area product.

The integrated dose-area product is recognized as a valuable practical measure of energy imparted to the patient (ICRP, 1970; Shrimpton et al, 1984), leading to the conclusion that the energy imparted for a given duration of fluoroscopy when using magnified fields of view should be identical to that imparted when using the full field of view provided that the automatic dose rate control is operating correctly and that automatic collimator settings are used with all the fields of view being compared. Despite the fact that the energy imparted ignores the different radiosensitivities of the various organs within the body, there is a reasonable correlation between this quantity and effective dose equivalent and radiation risk (Shrimpton et al, 1986).

To examine the effect of intensifier field size selection on dose rate in actual practice, the results from 26 routine commissioning and end-of-warranty tests on multi-field image intensifier systems were analysed to find the relationship between the change in active input phosphor area and the corresponding change in automatic dose rate. The tests were conducted by measuring the dose rate at the input surface of the intensifier whilst screening a 1 mm copper filter placed on the collimator housing to provide an essentially X-ray scatter free measurement, and also a 17 cm thick Perspex phantom at the position of the patient to provide a more realistic scatter situation. The active phosphor diameters for the various field sizes were measured using the "M1" matrix test object from the set of Leeds test objects (HPA 1981) placed at the intensifier input surface. The results are plotted as a scatter diagram in Figure 1a (without X-ray scatter) and Figure 1b (with X-ray scatter), where R_a is the ratio of active input phosphor areas and R_d is the ratio of measured automatic dose rates, for the magnified and full fields of view. If the automatic dose rate controls were set up to provide a constant signal-to-noise ratio, and hence, by the argument above, a constant dose rate-area product across all field sizes, then a direct proportionality between R_d and $1/R_a$ would be expected (dotted lines). In fact most of the points for both the scatter free and scatter inclusive cases fall on the lower dose rate side of the line, the trend being particularly pronounced for the highest magnifications.

In overall conclusion, it appears that magnified fields of view can be used in fluoroscopy under automatic dose rate control with no additional dose penalty, although it is likely that the highest magnifications will tend to give the poorest image quality in terms of signal-to-noise performance due to the way that the automatic dose rates are set up in practice. This result, which is based on a comparison using automatic collimator settings is not, however, intended to suggest a relaxation of the constraint of always using the minimum practicable X-ray beam size regardless of the intensifier field of view.

Yours, etc.,
C. J. KOTRE
N. W. MARSHALL
K. FAULKNER

Regional Medical Physics Department,
Newcastle General Hospital,
Newcastle-upon-Tyne,
NE4 6BE, UK

(*Received November 1990 and in revised form February 1991*)

References

HPA, 1981. *Measurement of the Performance Characteristics of Diagnostic X-ray Systems Used in Medicine: Part 2, X-ray Image Intensifier Systems.* Document TGR 32, (Hospital Physicists Association, York).

ICRP, 1970. *Protection of the Patient in X-ray Diagnosis*. Publication 16, (Pergamon, Oxford).

NRPB, 1988. *Guidance Notes for the Protection of Persons Against Ionising Radiations Arising from Medical and Dental Use*, HMSO.

SHRIMPTON, P.C., WALL, B.F., JONES, D.G. & FISHER, E.S., 1984. The measurement of energy imparted to patients during X-ray examinations using the Diamentor exposure-area product meter. *Physics in Medicine and Biology, 29*, 1199–1208.

SHRIMPTON, P.C., WALL, B.F., JONES, D.G., FISHER, E.S., HILLIER, M.C., KENDALL, G.M. & HARRISON, R. M., 1986. *A National Survey of Doses to Patients Undergoing a Selection of Routine X-ray Examinations in English Hospitals.* National Radiological Protection Board Report, NRPB-R200, HMSO.

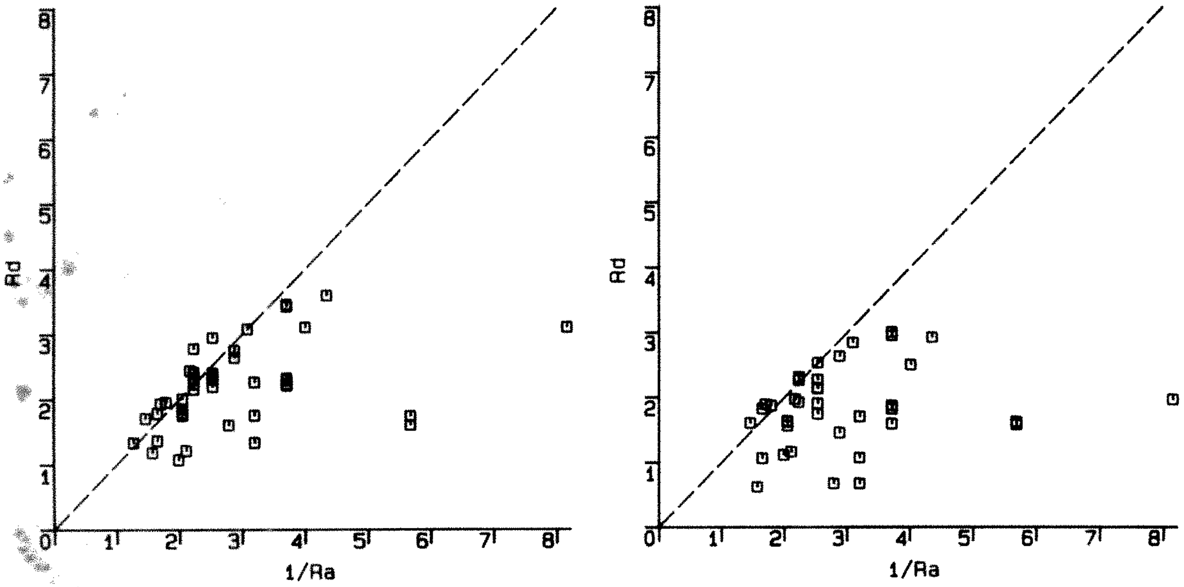

(a)

(b)

Figure 1. Scatter diagrams showing the relationship between R_d, the ratio of measured automatic dose rates for magnified and full fields of view for an X-ray image intensifier, and $1/R_a$, where R_a is the corresponding ratio of active input phosphor areas, for 26 routine test of image intensifier systems. (a) is for the X-ray scatter free case and (b) the scatter inclusive case. The dotted lines indicate the direct proportionality that would be expected if the automatic dose rates were set to maintain a constant signal-to-noise ratio in the image.

Haematopoiesis in the liver: the role of ^{99}Tc^m

The Editor—Sir,

We read with interest the case report of Bradley and Metreweli (1990), describing the ultrasound appearances of extramedullary haematopoiesis in the liver. However we are surprised that they omitted to include the role of isotope liver scanning using ^{99}Tc^m labelled millimicrospheres in suggesting the diagnosis of this condition. The haemopoietic tissue will appear as an area of increased or normal uptake in contrast to all other hepatic lesions with the exception of focal nodular hyperplasia (Rhys Davies, 1987). This simple imaging technique should be considered before following the author's suggestion of performing ultrasound guided needle biopsy which can be hazardous in this condition.

Yours, etc.,
M. Abboud
S. K. Morcos

Department of Diagnostic Imaging,
Northern General Hospital,
Sheffield S5 7AU, UK

(*Received December 1990*)

References

Bradley, M. J., & Metreweli, C., 1990 Ultrasound appearances of extramedullary haematopoiesis in the liver and spleen. *British Journal of Radiology, 63*, 816–818.

Rhys Davies, E., 1987. *Radio-isotope imaging. A Text Book of Radiology and Imaging, Vol. II, 4th edn.* Ed by D. Sutton, (Churchill Livingston, Edinburgh), pp 1739–1773.

Authors' reply

The Editor—Sir,

We would like to thank Dr Abboud and Dr Morcos for pointing out the value of ^{99}Tc^m labelled millimicrospheres. However, the aim of this paper was to document some common ultrasonographic appearances of liver lesions with the unusual diagnosis of extradmedullary haematopoiesis, which is a rare liver condition with only one ultrasound documented case in the literature.

These sonographic appearances have a wide differential diagnosis, including focal nodular hyperplasia in one of our cases. Dr Abboud and Dr Morcos admit that this may cause diagnostic confusion with this scintigraphic technique and so this was not the preferred diagnostic pathway.

We have performed several thousand ultrasound guided percutaneous biopsies in our department without any serious complications and view this procedure as a safe, quick and definitive diagnostic aid in the investigation of such liver lesions, obviating the need in many instances for further radiation based investigations.

Yours, etc.,
M. Bradley
C. Metreweli

Rotherham District General Hospital,
Moorgate Road,
Oakwood,
Rotherham S60 2UD, UK

(*Received December 1990*)

1991, *The British Journal of Radiology*, *64*, 565–566

Book reviews

Hyperthermic Oncology 1988. Vol. 1. Summary Papers. Proceedings of the 5th International Symposium, Japan. Ed. by T. Sugahara and M. Saito, pp. vi+970, 1989 (Taylor and Francis, London), £80.00.
ISBN 0-85066-791-7

These two volumes represent the proceedings of the 5th International Symposium on Hyperthermic Oncology held in Kyoto in September 1988. There is an enormous amount of information here, with over 1700 pages and more than 400 presentations from the most basic, through clinical experience to the physics of hyperthermia.

Volume 1 contains a vast number of summary papers, up to three pages in length, on all aspects of hyperthermia. Only the really dedicated "hyperthermist" will find this volume of value. For him there will be many nuggets to find, although it may be hot work to extract them!

Volume 2 is probably of more general interest and may stand the test of time better than the first. It contains the special plenary lectures, plenary lectures and symposium papers, and workshop summaries. The first special lecture by Professor Sugahara has the fascinating title "Hyperthermia and hot springs: scientific and cultural considerations". After a brief review of the development of hyperthermia research in Japan, Professor Sugahara tells us that the Japanese like hot spa baths at 43–45°C, whereas Caucasians prefer 34–35°C. There follow papers on engineering approaches to hyperthermia (Saito), clinical hyperthermic oncology in Japan (Matsuda), biological aspects (Hall), hyperthermic physics (Cetas) and clinical aspects (Stewart). There are plenary sessions on physics, clinical applications and hyperthermia biology. The 33 symposia cover all aspects of hyperthermia, from mechanisms of cell kill to heat shock proteins, vascular effects, thermotolerance, use of magnetic resonance spectroscopy, physiological effects, clinical applications, whole body hyperthermia, different methods of heating, etc.

The papers are presented as camera-ready copy, but overall the presentation is good. It is inevitable that the proceedings of such a large and extensive meeting will be very variable in quality. Nevertheless, no group seriously involved in the clinical uses of hyperthermia should be without these volumes. The general reader, however, may find all this information too indigestible and more specific reviews or textbooks will be of greater value to him.

N. J. McNally

Radiation Exposure and Occupational Risks. Ed. by E. Scherer, C. Streffer and K. Trott, pp. v+150, 1990 (Springer-Verlag, Berlin), DM148.
ISBN 3-540-51174-1

This relatively slim volume is in Springer's "Medical Radiology" series, and is therefore presumably aimed at practising medical imagers and radiation oncologists—a group who *should* know about radiation risks, but who, at least in the UK, are remarkably un-informed if not positively ill-informed! Sadly, however, although this volume is an updated version of an excellent 1985 German edition and has tremendous value as a source book, it is not sufficiently "user friendly" for radiologists to *want* to read it. The absence of "executive summary" of the major points made in each of the five otherwise excellent chapters, is a crucial structural omission.

Although multi-authored, the text has a commendable uniformity of style, which I suspect is imposed by the discipline of translation. The first chapter on natural radiation exposures is a splendid overview and has the virtue of a good summary at the end of the chapter. It comes up with an annual effective dose equivalent approximately half that in the UK. This is because of the higher average contribution to the UK population from radon—although the effect of our apparent preoccupation with energy conservation, and consequent reduction in building air-flows, and its effect on *increasing* indoor radon concentration is highlighted. The second chapter, on occupational risks and the handling of radioactive substances, covers the demonstrated hazards to the earlier radiation workers and the evolution of occupational dose limitation. It is interesting for the reader with a UK bias to see a quite different set of continental primary references. The latter part of the chapter loses its way somewhat, and the section on measurements of and statistical statements on occupational radiation exposures overlaps considerably with the subsequent chapter on occupational radiation carcinogenesis. Once again, however, the extensive bibliography makes this a useful source.

Two chapters on occupational radiation carcinogenesis, and medical aspects of radiation accidents form the main "meat", and are both outstandingly comprehensible. A minor niggle is that, for the latter, the references are largely the previous compendia or relatively inaccessible sources.

The final chapter on chemical radio-protection is probably the least satisfactory in that, while it catalogues much good science, it gives no indication of the extent to which chemical radio-protection may actually be useful in man in real-life situations. Again, it suffers from the lack of any "bringing together". However, the extensive bibliography is an excellent source catalogue.

In summary, this well produced but expensive book will be a valuable tool for the few radiologists, radiation oncologists and radiobiologists for whom it can serve as an annotated bibliography to the whole range of literature sources on biological effects of occupational radiation exposure. It should certainly be on the shelves of every radiological library, but is unlikely to find a place on the bedside table of the practising radiologist—an area for which there is still a yawning gap between the National Radiation Protection Board's excellent and simply written *Living with Radiation* and this specialist source book.

R. J. Berry

Year Book of Diagnostic Radiology 1990. Ed. by D. G. Bragg, W. R. Hendee, T. E. Keats, J. A. Kirkpatrick, F. J. Miller, A. G. Osborn and W. M. Thompson, pp. xvi+569, 1990 (Wolfe Publishers, London), £44.00.
ISBN 0-8151-1131-2

Another year, another Year Book. Cynical senescent apathy? No, just the reappearance of a faithful friend. This is the last yearbook of which Dr David Bragg will be Editor in Chief after 8 years of maintaining an excellent, readable and informative review of diagnostic radiology literature.

The current selection of topics by Dr Bragg and his colleagues remains instructive, stimulating and as comprehensive as a book of this size can reasonably be. As usual there is a considerable preponderance of North American authors and journals but in some ways this is an advantage for those who already subscribe to British Journals.

The series remains a good way of keeping up with specific papers and for many this is very satisfactory. There may be some, however, who prefer regular broader views of the radiological literature for whom this series will not be quite so well suited. This particular volume, however, maintains the general excellence of the series.

D. SHAW

Nuclear Medicine Annual 1989. Ed. by Leonard M. Freeman and Heidi S. Weissmann, pp. xii + 307, 1989 (Raven Press, New York), $122.50.
ISBN 0-88167-517-2

This is the 1989 incarnation of the popular annual series. The book follows the established pattern of its predecessors and consists of some 290 pages split into eight main subject areas. The quality of production is high and, in particular, the images are sufficiently well produced to allow all the points made within the text to be clearly illustrated. The first topic is that of thyroid scanning in the management of thyroid disease. It provides an up-to-date overview of the available methods of investigation within the nuclear medicine department of the thyroid and their applicability to clinical management.

The next topic is that of ageing and dementia demonstrated by a variety of methods, including magnetic resonance imaging (MRI), computed tomography (CT) and positron emission tomography (PET). This topic is a little in the way of being a "Cinderella" within mainstream brain imaging and it is interesting to see comparison between these three modalities, even if their routine clinical applicability is not fully proven. Quality assurance is a topic which haunts all of us and the way in which SPECT imaging needs to be monitored is well outlined, with much useful information for both the practising nuclear medicine physician as well as the physicist.

The two topics relating to the skeleton are the scintigraphy of injury and a comparison between different imaging methods in the diagnosis of a variety of bone diseases. Both chapters produced coherent arguments in favour of their chosen modality and in doing so make interesting reading. A review of renal studies in paediatric practice in nuclear medicine allows some of this perhaps unclear area to be rationalized and therefore makes the task of requesting an investigation for good clinical reasons an easier one. The last two chapters relate to less clinical and more management orientated topics and discuss decision making on a fairly formal basis including the application of Bayes' theorem and various other statistical mechanisms for deciding which treatment or investigation is correct. The final chapter on management in nuclear medicine is a delight to read and on its own is more than enough reason to buy this book.

In conclusion this current offering from an established series follows its predecessors in the quality of its content providing contemporary comment on topics of interest to both nuclear medicine personnel and clinicians.

G. HUNTER

Ultrasound in Neurosurgery. By J. M. Rubin and W. F. Chandler, pp. xi + 205, 1989 (Raven Press, New York), $124.00.
ISBN 0-88167-549-0

Intraoperative ultrasound (US) has been available since the early eighties, but increasingly sophisticated equipment and more adventurous interventional techniques have allowed a recent expansion of its applications. This compact, well presented volume is aimed mainly at neurosurgeons and radiologists with little experience of US in theatre, although radiographers performing US will also find it of interest.

The first chapter, written by a radiologist, deals mainly with the physics of US. Whilst not making ideal bedtime reading, a difficult topic is dealt with lucidly and in appropriate detail. The merits of various different shapes, sizes and frequencies of available probes are explored, this is useful for departments considering purchase, but the authors do not make firm recommendations. The theory of pulsed and colour flow Doppler is explained. The techniques section at the end is useful, particularly in the localization and biopsy of cerebral lesions.

The second chapter, written by a neurosurgeon, deals with the practical aspects of cranial surgery and US. He draws on his experience to provide examples of the major commonly encountered pathologies, which are well illustrated with US images and the corresponding computed tomograms (CT). Low grade gliomas can be difficult to detect on CT and their borders difficult to define on magnetic resonance imaging (MRI), therefore, it is very encouraging that US can define these lesions as areas of high echogenicity. One particularly instructive case illustrates the evolution of a post-biopsy haematoma by US, showing the changing echogenicity of blood and its post operative appearance on CT. The section on arteriovenous malformations (AVMs) and colour flow Doppler (with colour illustrations) is stimulating. However, until the technique becomes more widely available in this country, we are a long way from the author's declaration that intra-operative US imaging ". . . should be available at all times".

The third chapter goes into techniques of scanning and illustrates normal and pathological appearance of the spinal cord by high quality images obtained with a 10 megaHertz probe. Much of the section is of great practical use, although the parts on disc prolapse and AVMs are mainly of theoretical consequence.

The fourth chapter deals with the authors' special interest, the Arnold-Chiari malformations. A complex subject is dealt with clearly with the aid of US illustrations, post-mortem specimens, line drawings and intra-operative photographs. The great difficulties encountered at surgery of US interpretation in some cases are presented and the ability of US, in experienced hands, to elucidate problematic cases is shown.

In conclusion, it is an excellent book on an exciting technique which will encourage its wider use.

B. M. MCGANN and A. R. VALENTINE

1991, *The British Journal of Radiology*, *64*, 567–568

VOLUME 64 NUMBER 763 JULY 1991

The British Journal of Radiology

Editorial

The Guidance Notes revisited: advice to patients leaving hospital after diagnostic nuclear medicine

Recently the Radiation Protection Committee of the British Institute of Radiology conducted an informal survey of the practices adopted concerned with the method and level of information given to patients leaving hospital after administration of a radiopharmaceutical for *diagnostic purposes* only. There is a wide variation in practice, which does not always follow the advice of the "Guidance Notes for the Protection of Persons against Ionising Radiation Arising from Medical and Dental Use" (National Radiological Protection Board, 1988). It seems appropriate to examine the logic of the relevant regulations and the derived guidance with regard to the non-conformity of standards practised.

Schedule 6 of the Ionising Radiations Regulations 1985 (HMSO, 1985) requires an employer to designate as "controlled" an area in which the dose rate is likely to exceed 7.5 μSv/h. This value of dose rate was originally obtained by dividing 15 mSv by 2000 h. A dose equivalent of 15 mSv is three-tenths of the relevant annual dose limit for workers, and the figure of 2000 (being 40×50) is an upper estimate of the number of hours in a working year. A worker must be "classified" if he is likely to receive more than three-tenths of a relevant dose limit. The definition of "controlled area" is based on the concept of ensuring that a non-classified worker who is *constantly exposed for the whole of the working year* does not receive more than three-tenths of the annual dose limit.

The same schedule provides for an equivalent definition of a "controlled area" in terms of the local quantity of a γ emitting radioactive substance: an area must be controlled if the product of activity and total γ energy per disintegration ("the product") exceeds 50 MBq MeV. A relaxation of this figure is given for situations where the radioactivity is distributed in the human body; the product must not exceed 150 MBq MeV. In both cases these values of the product correspond to an exposure rate at 1 m from the source which would just give a worker three-tenths of the dose limit *if the same exposure rate were maintained constantly during a 2000 h working year*.

The Regulations also define a "supervised area" as one in which the dose rate might be more than one-third of the level which would require it to be "controlled".

Patients who have received doses of radioactive substances may constitute a source of γ radiation during the time that they retain radioactivity. The quantity of activity will, in every case, diminish by dint of physical decay and biological elimination. Nevertheless the concept of a "controlled" (or a "supervised") area around the patient is useful when considering the potential effects on *hospital workers, e.g.* technicians, nurses, porters, who may come into contact with such patients on a regular basis. For these workers the fact that the radioactivity in any one patient may be short-lived is irrelevant because there may be a constant supply of patients each with "fresh" radioactivity.

When the patient leaves hospital and goes home or back to his own workplace then the situation is completely different, because the radioactive substance brought into the home or workplace constitutes a single event which is unlikely to be repeated. The question of significance to members of the patient's family or to colleagues at work is not "what annual dose would I receive if I were constantly exposed to radioactivity at this level?" but rather "what dose will I receive from this event?". The worst possible situation representing the highest conceivable absorbed dose that any other person might receive (the "third party dose") is the dose absorbed by a frequently cuddled child of the patient. This dose can be calculated on the basis of a suitably conservative biokinetic model (even recognizing physical decay alone) without resorting to the absurdity of postulating a constant exposure rate throughout the year. Such calculations have been made (Mountford, 1987) and have shown that the total absorbed dose equivalent to cuddled infants following disgnostic radionuclide administration to the mother does not approach 1 mSv for any diagnostic technique with the single exception of ^{111}In-labelled leucocytes. The highest such dose from other diagnostic techniques has been estimated as 240 μSv.

The National Radiological Protection Board (1986) has recommended an annual dose limit for members of the public of 1 mSv. There is a suggestion that this should be lowered, but if it is more than halved then the figure will be well within the range of changes in natural background radiation (currently estimated as an average of 2.4 mSv annually in the UK). It is clear that no nuclear medicine diagnostic technique can give rise to a third party dose which could exceed an annual dose limit for members of the public or, indeed, which could be greater than one-tenth of the average annual natural background radiation in the UK.

The UK Guidance Notes, published in 1986, provide general guidance to medical and dental workers on "good practice", consistent with regulatory requirements. However, the guidance given in Chapter 12 ("Patients leaving hospital after administration of radioactive substances") is based on an unnecessarily rigid premise. The authors had to determine what levels of radioactivity in patients might give rise to "significant" exposure to third parties. (This requirement is identified in paragraph 33 of part 2 of the Approved Code of Practice (Health and Safety Commission, 1985)). In determining what levels might lead to significant exposures, the authors have used critical values of "the product", thus extending the concept of "controlled" and "supervised" areas outside the workplace. They have apparently failed to note that this concept is based upon the need to ensure that a worker who is *constantly exposed for the whole working year* does not exceed his annual dose limit. It is wholly inappropriate to the consideration of third party doses from nuclear medicine patients. Such doses can and have been estimated as the consequence of individual events and can be shown (see above) to be quite "insignificant" for almost all diagnostic nuclear medicine.

The Guidance Notes advise that instructions should be given to certain patients on reducing close contact with other persons, and especially on "avoiding unnecessary contact with children". We consider this advice to be inappropriate and unhelpful to patients who have received *diagnostic quantities* of radionuclide. Patients who come to hospital for tests are often anxious and one aspect of our care for them must be to help them to keep the problems in perspective. The maximum conceivable dose to a cuddled infant will be of the same order as variations in annual natural background and the reduction in the child's annual dose achieved by avoiding "non-essential contact" with his mother will be even less than these insignificant amounts. The advice to "avoid non-essential contact" may well raise levels of anxiety further and would, therefore, be "unreasonable" in the context of ALARA or ALARP. By the same token, doses to people other than the patient's children will be even smaller, and the advice recommended in the Guidance Notes will be even less reasonable.

The Guidance Notes draw attention to the possibility that radioactive excreta might cause contamination problems, but state "Normal sanitary arrangements should suffice. The use of bed pans should be avoided if possible". Such advice may be considered gratuitous. It is unfortunate that the justifiable concern over potential hazards following large therapeutic administrations should here be confused with the negligible hazards associated with diagnostic procedures.

The Guidance Notes also recommend advice to a patient to notify his employer if his work might be affected by radiation. This is no doubt well meant, but is not required by any regulation. The patient's work may be considered in two categories: (a) work with materials (*e.g.* photographic film) which happen to be radiosensitive, and (b) work involving radiation (*e.g.* in assays or dosimetry). In the first category it is extremely unlikely that the patient could have any significant effect on the materials (remembering that the calculated maximum dose to a cuddled infant is of the order of geographic changes in natural background). In the second category the employer will already have taken precautions against fluctuations in background, will already have appropriate local rules and should have instructed his employees in appropriate precautions. These instructions should, if appropriate, include the exercise of care following nuclear medicine, and are obviously best determined by the employer. Sensitive radiation-detection alarms can be triggered by workers who have undergone nuclear medicine examinations; this must be understood by those using the radiation detectors but it does not constitute a hazard.

We conclude that patients leaving hospital after receiving *diagnostic* nuclear medicine administrations do not generally present any external radiation hazard to other persons, and that *no special instructions are necessary*. The single known exception is that of ^{111}In-labelled leucocytes, when special advice may be necessary for mothers of babies (and the dose administered to such mothers should be restricted to less than 10 MBq of ^{111}In).

The foregoing does *not*, of course, apply to the potential *internal* radiation hazard associated with *breast-feeding*, and special advice may be necessary for nursing mothers (Mountford & Coakley, 1986, 1989). Such advice will be based upon whether the estimated dose to the infant is likely to exceed 1 mSv. Similarly the foregoing does *not* apply to *therapeutic* administrations. It should be noted, in particular, that a potential hazard might exist for other persons following the administration to a patient of more than 30 MBq of ^{131}I. Appropriate instructions should then be given.

R. A. SHIELDS
for the Radiation Protection Committee
of the BIR

References

HEALTH AND SAFETY COMMMISSION, 1985. *Approved Code of Practice. The Protection of Persons against Ionising Radiation arising from any Work Activity* (HMSO, 1985).

HMSO, 1985. *The Ionising Radiations Regulations 1985 (Statutory Instrument 1985 No. 1333)* (HMSO, London).

MOUNTFORD, P. J., 1987. Estimation of close contact doses to young infants from surface dose rate on radioactive adults. *Nuclear Medicine Communications, 8*, 857–863.

MOUNTFORD, P. J. & COAKLEY, A J., 1986. Guidelines for breast-feeding following maternal radiopharmaceutical administration. *Nuclear Medicine Communications, 7*, 399–401 (Editorial).

—— 1989. A review of the secretion of radioactivity in human breast milk: data, quantitative analysis and recommendations. *Nuclear Medicine Communications, 10*, 15–27.

NATIONAL RADIOLOGICAL PROTECTION BOARD, 1986. *Dose Limits for Members of the Public* (NRPB-GS4) (HMSO, 1986).

—— 1988. *Guidance Notes for the Protection of Persons against Ionising Radiations arising from Medical and Dental Use* (HMSO, London).

1991, *The British Journal of Radiology*, *64*, 569–575

Lymphoproliferative disorders of the thyroid gland: radiological appearances

By K. Kasagi, MD, H. Hatabu, MD, Y. Tokuda, MD, *H. Yamabe, MD, A. Hidaka, MD, K. Yamamoto, MD, Y. Iida, MD, T. Misaki, MD, †T. Mori, MD, K. Endo, MD and J. Konishi, MD

Department of Radiology and Nuclear Medicine, *Laboratory of Anatomic Pathology and †Department of Internal Medicine, Kyoto University School of Medicine, 54 Kawahara-cho, Shogoin, Sakyo-ku, Kyoto 606, Japan

(*Received August 1990 and in revised form January 1991*)

Keywords: Lymphoma, Plasmacytoma, Thyroid, Hashimoto's thyroiditis

Abstract. Images of lymphoproliferative disorders of the thyroid by ultrasonography (US), computed tomography (CT), $^{99}Tc^{m}$ and ^{67}Ga scintigraphy were analysed in eight patients (two men and six women, aged 42–83 years). Seven patients were diagnosed as having primary lymphoma and one plasmacytoma. Ultrasound revealed a solid mass with homogeneous and very low echogenicity clearly distinguishable from residual thyroid tissue in five patients, diffuse hypoechoic goitre in one and multiple irregular hypoechoic nodules in both lobes in the patient with plasmacytoma (Case 8). Computed tomography demonstrated a focal low-density area in six cases of lymphoma and decreased density throughout the gland in the other two patients. $^{99}Tc^{m}$ scintigraphy showed hemilobar enlargement with decreased and uneven trapping, cold area or complete lobar defect in six patients with lymphoma and no trapping in the case of plasmacytoma. ^{67}Ga scintigraphy demonstrated high accumulation in lymphoma and faint accumulation in the case of plasmacytoma. Radiological manifestations with a focal lesion were considered typical and diagnostic of primary thyroid lymphoma, while in one case with diffuse infiltration through the whole gland, the differential diagnosis from Hashimoto's thyroiditis could not be made. In the final case, cells infiltrated diffusely to form islands with patchy distribution among well preserved follicles, correlating with the multiple hypoechoic areas observed by US.

Primary malignant lymphoma of the thyroid is uncommon, contributing 2.2–2.5% of lymphomas (Aozasa et al, 1986a) and 0.6–5.0% of all thyroid malignancies (Walfish, 1986). Most patients tend to be older, over 50 years of age. Like Hashimoto's thyroiditis, malignant lymphoma is a disease that affects females more than males with a ratio of 3–5:1 (Compagno & Oertel, 1980; Hamburger et al, 1983; Rasbach et al, 1985; Aozasa et al, 1986a; Walfish, 1986). Presentation is frequently with a rapidly enlarging thyroid mass, which may cause obstructive symptoms such as hoarseness, dysphagia and dyspnoea.

Plasmacytoma of the thyroid is exceedingly rare, with an incidence of 2.6% among patients with multiple myeloma (Macpherson et al, 1981) and less than 40 cases have been reported in the world literature (Chen et al, 1986; Aozasa et al, 1986b; Salazar et al, 1987). Plasmacytomas of the thyroid have been shown to have many features in common with malignant lymphomas, including a strong association with Hashimoto's thyroiditis.

Although the number of reported lymphomas and plasmacytomas involving the thyroid has been increasing, detailed descriptions of their radiological appearance are limited. There are very few cases in which comparative studies with ultrasonography (US), computed tomography (CT) and radionuclide scanning have been performed (Takashima et al, 1989). The present study was designed to analyse the radiological appearances of malignant lymphoma and of plasmacytoma by US, CT and scintigraphy with $^{99}Tc^{m}$ and ^{67}Ga in relation to histological findings observed in eight patients.

Patients and methods

Seven patients with primary thyroid lymphoma (one male and six female, aged 42–83 years) and one patient with primary thyroid plasmacytoma (a male, aged 72 years) were studied. Table I summarizes the clinical, laboratory and pathological data of seven cases of malignant lymphoma (Cases 1–7) and one case of plasmacytoma (Case 8). All patients had had an enlarging mass in the thyroid for a duration of from 1 month to 2 years. Common presenting symptoms were dysphagia, hoarseness, choking and discomfort in the neck.

Cases 4, 6 and 7 had been given a clinical diagnosis of Hashimoto's thyroiditis 3, 5 and 2 years before the final diagnosis, respectively, on the basis of diffuse goitre, positive antimicrosomal antibody titres or primary hypothyroidism. Of the eight patients, five were hypothyroid and six had detectable antibodies against thyroid microsomal antigens at the time of diagnosis. Antithyroglobulin antibodies were not detected.

Histological diagnosis of malignant lymphoma, determined according to Working Formulation (The Non-Hodgkin's Lymphoma Pathologic Classification Project, 1982), revealed diffuse, large, non-cleaved cells in three cases (Cases 1–3), diffuse mixed small and large

Table I. Clinical, laboratory and pathological findings in eight patients with lymphoproliferative disorders of the thyroid

Case	Age (years)/ Sex	Duration of thyroid enlargement	Presenting abnormalities	Thyroid function (TSH)*	Antithyroid antibodies*	Pathology
1	69/f	10 months	Diffuse goitre with enlargement of right lobe; R axillary lymph node swelling	Mild hypothyroidism (14 μU/ml)	Negative	Diffuse large non-cleaved cell (open biopsy)
2	67/f	5 months	Diffuse goitre	Mild hypothyroidism (13.7 μU/ml)	Positive anti-M, 1280	Diffuse large non-cleaved cell (needle biopsy)
3	64/f	3 months	Right lobe thyroid mass	Euthyroidism (0.8 μU/ml)	Positive anti-M, 1280	Diffuse large non-cleaved cell (needle biopsy)
4	42/f	4 months	Diffuse goitre with enlargement of right lobe	Mild hypothyroidism (25.8 μU/ml)	Negative	Diffuse mixed small and large cell (needle biopsy)
5	83/m	1 month	Right lobe thyroid mass	Euthyroidism (5.6 μU/ml)	Positive anti-M, 1600	Follicular, predominantly small cleaved cell with diffuse areas (open biopsy)
6	70/f	3 months	Diffuse goitre with enlargement of right lobe	Euthyroidism (3.4 μU/ml)	Positive anti-M 6400	Follicular, predominantly small cleaved cell with diffuse areas (operation)
7	55/f	2 years	Diffuse goitre	Hypothyroidism (15.9 μU/ml on 200 μg T4)	Positive anit-M 6400	Diffuse mixed small and large cell (operation)
8	72/m	1 year 2 months	Diffuse goitre	Mild hypothyroidism (2.0 μU/ml on 50 μg T4)	Positive anti-M 6400	Plasmacytoma (operation)

Anti-M; antithyroid microsomal antibody.
* Normal range; TSH = 0.4–3.9 μU/ml; anti-M = < 100.

cells in two (Cases 4 and 7) and follicular, predominantly small cleaved cells with diffuse areas in two (Cases 5 and 6). There was no case of Hodgkin's disease. Lymphoma was staged as IIE in one patient (Case 1) and as I in six patients (Cases 2–7). Patient 8 had enlarged and palpable regional lymph nodes, later found to be due to involvement with plasmacytoma.

The patients were carefully examined by CT, US and scintigraphy with ^{99}Tc^{m} and ^{67}Ga with the exceptions of Cases 1 and 7, who did not undergo US and ^{99}Tc^{m} scintigraphy. The ultrasound equipment used consisted of an electronic linear array real-time scanner and 7.5 MHz transducer (Yokogawa U-SONIC, RT-2800). Images were obtained using a water-bath technique according to the method developed by Sacker et al (1977). Computed tomography was performed with an 8800 CT/T scanner (General Electric, Milwaukee), with the patient in the supine position. Scans were obtained through the neck and thyroid masses with contiguous 5 mm slices and with contrast medium enhancement. A large-field-of-view gamma camera (Gammaview-F, Hitachi, Tokyo) was used for both ^{99}Tc^{m} and ^{67}Ga scanning. ^{99}Tc^{m} scintigraphy was performed 30 min after intravenous administration of 148 MBq (4 mCi) ^{99}Tc^{m}-pertechnetate with a low-energy parallel hole collimator and a window setting of 140 KeV. Isotope scanning was undertaken before CT in all cases. ^{67}Ga scintigraphy was performed 3 days after intravenous administration of 111 MBq (3 mCi) ^{67}Ga-citrate with three energy window settings (93, 184 and 296 keV) and a medium-energy parallel hole collimator.

Results

Ultrasonography revealed a solitary nodule with homogeneous and very low internal echogenicity clearly demarcated from residual thyroid tissue in five patients (Cases 2–6, Fig. 1a,b), diffuse hypoechoic goitre in one (Case 7, Fig. 1C) and multiple irregular hypoechoic areas in both lobes in one (Case 8, Fig. 1d). Computed tomography demonstrated a focal low-density area surrounded by residual thyroid tissue in six patients (Cases 1–6, Fig. 2a) and diffuse goitre with decreased density in two (Cases 7 and 8, Fig. 2b). In Case 1, a central low-density area was observed in the tumour, suggesting necrosis. Deviation or compression of the trachea was demonstrated in four patients (Cases 1, 2, 3 and 5). ^{99}Tc^{m} scintigraphy showed lobar enlargement with decreased and uneven trapping in four patients

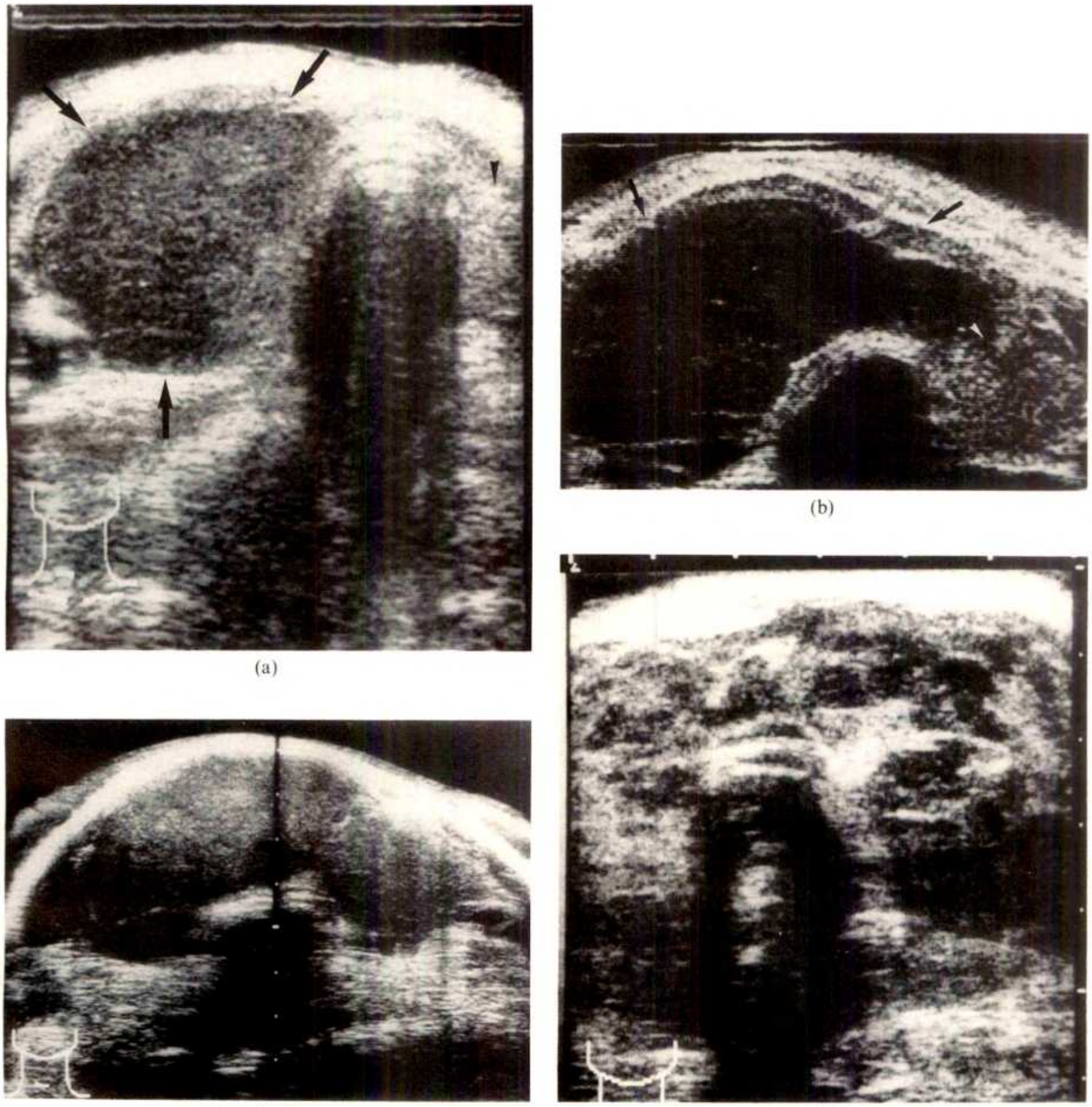

(a) (b) (c) (d)

Figure 1. Transverse sonographic scanning of the thyroid shows an hypoechoic mass (arrow) in the right lobe and the isthmus in Case 4(a), and a well defined hypoechoic mass (arrow) in the right lobe in Case 5(b), both clearly demarcated from residual thyroid tissue (arrowhead). Diffuse hypoechoic goitre is shown in Case 7(c), and heterogeneity of internal echo pattern with multiple irregular hypoechoic nodules in Case 8(d).

(Cases 2, 3, 5 and 6, Fig. 3), a cold area in one (Case 4), complete lobar defect in one (Case 1) and no trapping in one (Case 8). ^{67}Ga scintigraphy demonstrated high accumulation in seven patients (Cases 1–7, Fig. 4a,b) and faint accumulation in one (Case 8, Fig. 4c). Extension of the disease to the thorax was shown by ^{67}Ga scintigraphy in Case 1.

Histological findings disclosed lymphoma cells infiltrating diffusely with sparse atrophic follicles in Cases 1–6 (Fig. 5a). A compressed rim of thyroid tissue was visible along a portion of the periphery of the tumour in the operated specimen of Case 6, while the lymphoma cells infiltrated through the whole gland in Case 7. In Case 8, plasmacytoma cells infiltrated diffusely forming islands with patchy distribution among well preserved follicles (Fig. 5b).

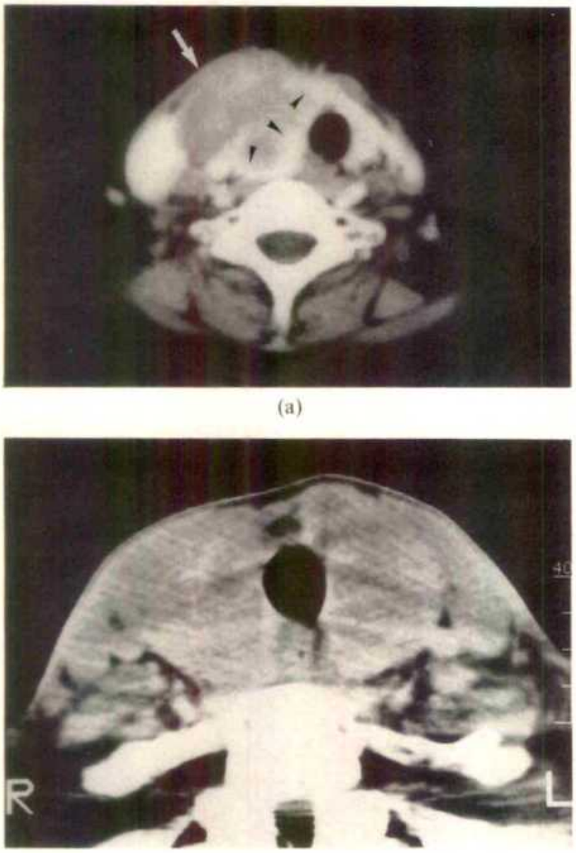
(a)

(b)

Figure 2. Contrast-enhanced CT scanning of the thyroid shows a localized low-density area (arrow) surrounded by residual thyroid tissue (arrowhead) with deviation of the trachea in Case 3(a) and diffuse goitre with decreased density in Case 8(b).

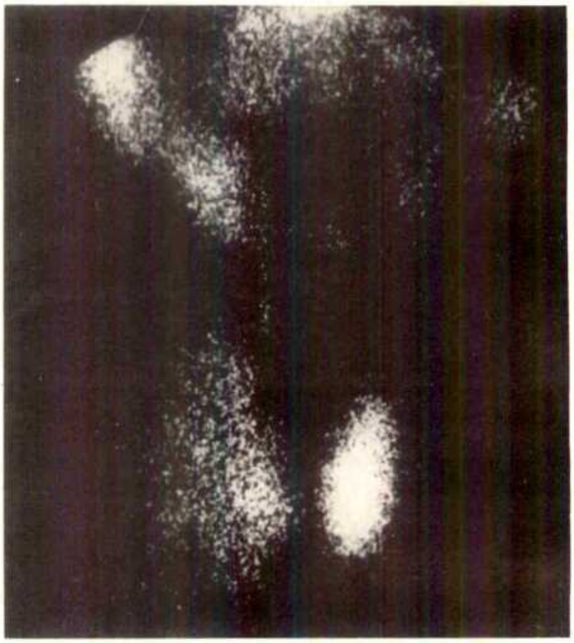

Figure 3. A $^{99}Tc^{m}$ scintigram revealed hemilobar enlargement with decreased and uneven trapping in Case 5.

Discussion

The clinical and histological findings of tumour in our patients are all similar to those previously reported (Shimkin & Sagerman, 1969; Sirota & Segal, 1979; Compagno & Oertel, 1980; Macpherson et al, 1981; Hamburger et al, 1983; Lopez et al, 1983; Rasbach et al, 1985; Aozasa et al, 1986a,b; Chen et al, 1986; Walfish, 1986; Salazar et al, 1987; Takashima et al, 1988).

The sonographic appearance observed in most of the cases (2–6), of a solitary lesion with homogeneous and very low echogenicity clearly demarcated from residual thyroid tissue, is similar to that previously reported by Solbiati et al (1985) (four cases), Perulekar and Katzman (1986) (one case) and Takashima et al (1989) (12 of 16 cases), and seems typical of primary lymphoma. One patient (Case 7) showed diffuse hypoechogenicity in the whole gland. Similar US findings were reported by Hayashi et al (1986) in patients with advanced Hashimoto's thyroiditis and by Takashima et al (1989) in one of their 16 cases of primary thyroid lymphoma. Case 8 with plasmacytoma showed heterogeneity of the internal echo pattern with multiple hypoechoic nodules. To our knowledge, there has been no report describing US findings in patients with thyroid plasmacytoma.

Takashima et al (1988) recently analysed and classified CT appearances of primary thyroid lymphoma into three patterns: solitary nodule (type 1, 12/15); multiple nodules (type 2, 2/15); and diffuse goitre (type 3, 1/15). The CT features observed in our patients (Cases 1–6) seemed to be type 1. The generally decreased density in the whole gland observed in Cases 7 and 8 cannot be differentiated from that in other diffuse thyroid diseases such as Hashimoto's thyroiditis and Graves' disease (Iida et al, 1983). Gruber et al (1987) and Salazar et al (1987) reported CT features in plasmacytoma of the thyroid similar to those in Case 8 (type 3).

Thyroid imaging with $^{99}Tc^{m}$ or radioactive iodine has resulted in variable findings such as cold nodules, patchy uptake and inadequate visualization of the thyroid in patients with thyroid lymphoma (Shimkin & Sagerman, 1969; Hamburger et al, 1983). In the present study, cold nodules including complete lobar defect were observed in two patients. Four patients showed lobar enlargement with low and uneven trapping, less frequently seen in thyroid cancer, suggesting the heterogeneous nature of lymphoma cell infiltration. As for plasmacytoma, Lopez et al (1983) reported that thyroid lesions were cold on ^{131}I scanning in two cases, while according to studies by Aozasa et al (1986b), hot and cold nodules were demonstrated by ^{131}I scintigraphy in

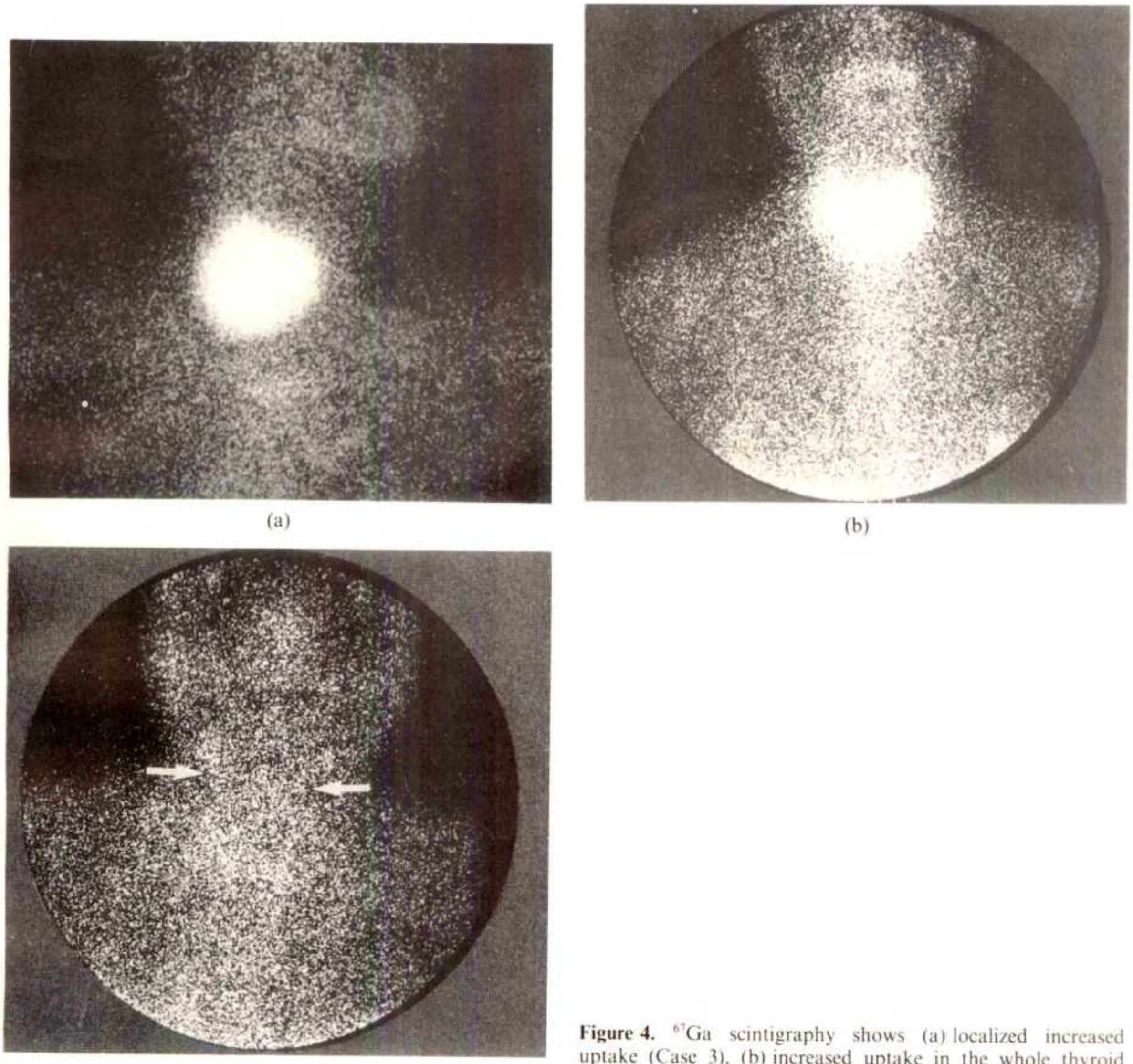

Figure 4. ^{67}Ga scintigraphy shows (a) localized increased uptake (Case 3), (b) increased uptake in the whole thyroid gland in Case 7 and (c) faint accumulation in Case 8 (arrow).

two and four cases, respectively. Case 8 in the present study displayed inadequate visualization of the thyroid, probably because of low uptake in the enlarged thyroid with relatively high background levels of ^{99}Tc^{m}. Higashi et al (1981) reported that 12 of 14 patients with malignant lymphoma but only one of 26 patients with differentiated thyroid cancer were positive with ^{67}Ga scanning. They also reported high positive rates in anaplastic carcinoma (28/31) and Hashimoto's thyroiditis (6/9). There was an intense accumulation in the region of the tumour in all seven patients with primary thyroid lymphoma. ^{67}Ga has the additional advantage of occasionally detecting distant metastasis, as with Case 1, and may be useful for staging. However, it offers little help in making the differential diagnosis from Hashimoto's thyroiditis in cases involving diffuse infiltration of lymphoma cells throughout the gland, as seen in Case 7. The patient with plasmacytoma was negative with ^{67}Ga scanning. Further studies are needed of ^{67}Ga scanning in plasmacytoma.

From a diagnostic viewpoint, the "solitary nodule" type (Cases 2–6, and probably Case 1 without additional US findings) is easily recognizable. Cold areas or decreased and uneven trapping on ^{99}Tc^{m} scintigraphy; localized, increased accumulation with or without extrathyroidal uptake of ^{67}Ga; a solitary hypoechoic area on US images and low-attenuation mass on CT images occasionally accompanied by deviation or compression of the trachea, are all typical and characteristic of primary malignant lymphoma, in patients

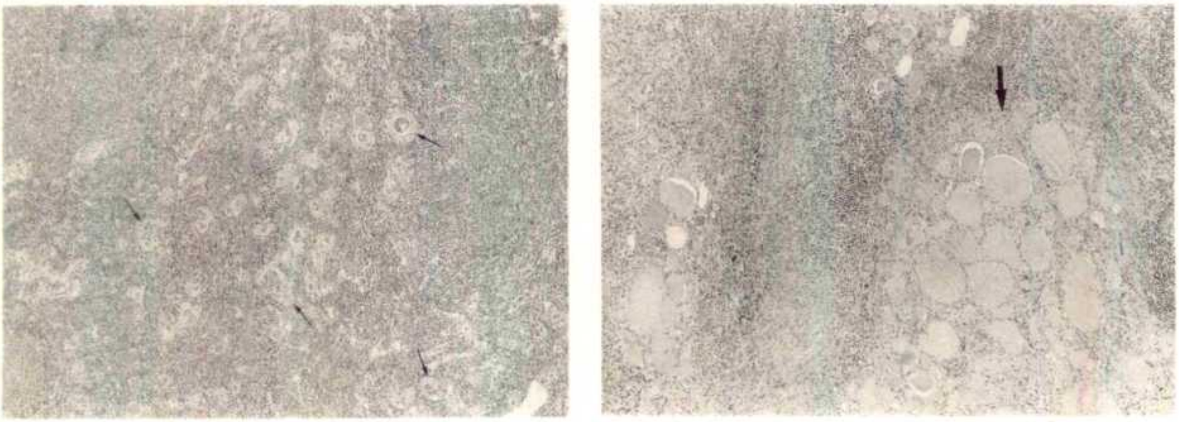

Figure 5. Histology of the thyroid shows (a) diffuse infiltration of lymphoma cells with sparse atrophic follicles (arrow) (Case 6) and (b) patchy and diffuse infiltration of plasmacytoma cells among well preserved follicles (arrow) (Case 8) (H & E, original magnification × 100).

previously diagnosed as having Hashimoto's thyroiditis. Differential diagnosis with subacute thyroiditis or acute suppurative thyroiditis is sometimes required, because patients with these diseases are known to have hypoechoic areas and ^{67}Ga uptake in the region of the thyroid (Grove et al, 1973; Higashi et al, 1981; Clair et al, 1983; Tokuda et al, 1990). However, patients with subacute thyroiditis usually have pain and tenderness in the region of the thyroid, fever and mildly thyrotoxic symptoms. Furthermore, patients without such clinical features display chemical thyrotoxicosis and absence of radioiodine or ^{99}Tc^{m} uptake by the thyroid in the acute phase of the disease. Patients with acute suppurative thyroiditis have a very tender mass, fever, leukocytosis and pyriform sinus fistula often detected by barium study (Takai et al, 1979). Although a solitary hypoechoic lesion is seen in many carcinomas (Solbiati et al, 1985), the internal echogenicity in malignant lymphoma is rather homogeneous and extremely low (Perulekar et al, 1986; Takashima et al, 1989). Furthermore, the differentiation from differentiated thyroid cancer can easily be made on the basis of positive ^{67}Ga scanning (Higashi et al, 1981) and the rather rapid growth of the tumour. On the other hand, it is sometimes impossible to make the differential diagnosis from anaplastic carcinoma, requiring histological diagnosis, although this has no strong relationship with Hashimoto's thyroiditis. A relatively high frequency of coexistent calcification compared with the findings for thyroid lymphoma (Takashima et al, 1988) and heterogeneity of internal echogenicity with irregular and obscured margins (Hayashi et al, 1986) were reported in patients with anaplastic carcinoma.

Ultrasonography seems the most appropriate as a screening test in view of its excellent cost-effectiveness. However, Takashima et al (1989) reported that CT findings were positive, though US findings were negative in one of their 16 cases. Computed tomography is also superior to US in the definition of intrathoracic tumour extension (Takashima et al, 1989). ^{99}Tc^{m} scintigraphy is performed in all patients with thyroid disease in our thyroid clinic, and ^{67}Ga scanning sometimes provides a definite diagnosis. The combination of all these images is recommended when lymphoma or plasmacytoma is strongly suspected.

Although the "solitary nodule" type of lymphoma is most common and its radiological appearance is typical, radiologists should be aware of other types of appearances as demonstrated in Cases 7 and 8. Acute onset of the enlargement of the thyroid gland, which is unresponsive to suppressive thyroid hormone therapy, should lead to a strong suspicion of lymphoma or plasmacytoma. In such patients, even with no positive radiological findings supporting the diagnosis, pathological examination including immunohistochemical studies using monoclonal antibodies (Faure et al, 1988), known to be useful for the differential diagnosis from anaplastic carcinoma and Hashimoto's thyroiditis, should be performed to ensure a prompt and accurate diagnosis.

Acknowledgment

The authors thank Miss Tomoko Maeda for secretarial assistance.

References

AOZASA, K., INOUE, A., TAJIMA, K., MIYAUCHI, A., MATSUZUKA, F. & KUMA, K., 1986a. Malignant lymphomas of the thyroid gland. Analysis of 79 patients with emphasis on histologic prognostic factors. *Cancer*, *58*, 100–104.

AOZASA, K., INOUE, A., YOSHIMURA, H., MIYAUCHI, A., MATSUZUKA, F. & KUMA, K., 1986b. Plasmacytoma of the thyroid gland. *Cancer*, *58*, 105–110.

CHEN, T. K. T., BAUER, V. & BAUER, F., 1986. Localized thyroid plasmacytoma. *Journal of Surgical Oncology*, *32*, 220–222.

CLAIR, M. R., MANDELBLATT, S., BRAIM, R. S., PERKES, E. & GOODMAN, K., 1983. Sonographic features of acute suppurative thyroiditis. *Journal of Clinical Ultrasound, 11*, 222–224.

COMPAGNO, J. & OERTEL, J. E., 1980. Malignant lymphoma and other lymphoproliferative disorders of the thyroid gland. A clinicopathologic study of 245 cases. *American Journal of Clinical Pathology, 74*, 1–11.

FAURE, P., CHITTAL, S., WOODMAN-MEMETEAU, F., CAVERIVIERE, P., GORGUET, B., VOIGT, J. J. & DELSOL, G., 1988. Diagnostic features of primary lymphomas of the thyroid with monoclonal antibodies. *Cancer, 61*, 1852–1861.

GROVE, R. B., PINSKY, S. M., BROWN, T. L., BRAAMER, S. R. & JOHNSON, M. C., 1973. Uptake of ^{67}Ga-citrate in subacute thyroiditis. *Journal of Nuclear Medicine, 14*, 403.

GRUBER, B., GOLDMAN, M. & RECANT, W., 1987. Plasmacytoma of the thyroid. *Otolaryngology–Head and Neck Surgery, 97*, 567–571.

HAMBURGER, J. I., MILLER, J. M. & KINI, S. R., 1983. Lymphoma of the thyroid. *Annals of Internal Medicine, 99*, 685–693.

HAYASHI, N., TAMAKI, N., KONISHI, J., YONEKURA, Y., SENDA, M., KASAGI, K., YAMAMOTO, K., IIDA, Y., MISAKI, T., ENDO, K., TORIZUKA, K. & MORI, T., 1983. Sonography of Hashimoto's thyroiditis. *Journal of Clinical Ultrasound, 14*, 123–126.

HAYASHI, N., TAMAKI, K., YAMAMOTO, M., SENDA, M., YONEKURA, Y., MISAKI, T., IIDA, Y., KASAGI, K., ENDO, K., KONISHI, J., TORIZUKA, K., MORI, T. & MAKIMOTO, K., 1986. Real-time ultrasonography of thyroid nodules. *Acta Radiologica Diagnosis, 27*, 403–408.

HIGASHI, T., ITO, K., MIMURA, T., OHI, T., NISHIKAWA, Y. & WILCOX, J. R., 1981. Clinical evaluation of ^{67}Ga scanning in the diagnosis of anaplastic carcinoma and malignant lymphoma of the thyroid. *Radiology, 141*, 491–497.

IIDA, Y., KONISHI, J., HARIOKA, T., MISAKI, T., ENDO, K. & TORIZUKA, K., 1983. Thyroid CT number and its relationship to iodine concentration. *Radiology, 147*, 793–795.

LOPEZ, M., LAURO, L. D., MAROLLA, P. & MADONNA, V., 1983. Plasmacytoma of the thyroid gland. *Clinical Oncology, 9*, 61–66.

MACPHERSON, T. A., DEKKER, A. & KAPADIA, S. B., 1981. Thyroid gland plasma cell neoplasma(plasmacytoma). *Archives of Pathology and Laboratory Medicine, 105*, 570–572.

THE NON-HODGKIN'S LYMPHOMA PATHOLOGIC CLASSIFICATION PROJECT, 1982. National Cancer Institute sponsored study of classifications of non-Hodgkin's lymphomas. Summary and description of a working formulation for clinical usage. *Cancer, 49*, 2112–2135.

PERULEKAR, S. G. & KATZMAN, R. A., 1986. Primary malignant lymphoma of the thyroid: sonographic appearance. *Journal of Clinical Ultrasound, 14*, 60–62.

RASBACH, D. A., MONDSCHEIN, M. S., HARRIS, N. L., KAUFMAN, D. S. & WANG, C., 1985. Malignant lymphoma of the thyroid gland: a clinical and pathologic study of twenty cases. *Surgery, 98*, 1166–1170.

SACKER, J. P., PASSALAQUA, A. M., BLUM, M. & AMOROCHO, L., 1977. A spectrum of disease of the thyroid gland as imaged by gray scale water bath sonography. *Radiology, 125*, 467–472.

SALAZAR, J. E., NELSON, J. F. & WINER-MURAM, T. W., 1987. Extramedullary plasmacytoma of the thyroid. *Journal of the Canadian Association of Radiologists, 38*, 136–138.

SHIMKIN, P. M. & SAGERMAN, R. H., 1969. Lymphoma of the thyroid gland. *Radiology, 92*, 812–816.

SIROTA, D. K. & SEGAL, R. L., 1979. Primary lymphomas of the thyroid gland. *Journal of the American Medical Association, 242*, 1743–1746.

SOLBIATI, L., VOLTERRANI, L., RIZZATTO, G., BAZZOCCHI, M., BUSILACCHI, P., CANDIANI, F., FERRARI, F., GIUISEPPETTI, G., MARESCA, G., MIRK, P., RUBALTELLI, L. & ZAPPASODI, F., 1985. The thyroid gland with low uptake lesions: evaluation by ultrasound. *Radiology, 155*, 187–191.

TAKAI, S., MIYAUCHI, A., MATSUZUKA, F., KUMA, K. & KOSAKI, G., 1979. Internal fistula as a route of infection in acute suppurative thyroiditis. *Lancet, i*, 751–752.

TAKASHIMA, S., IKEZOE, J., MORIMOTO, S., ARISAWA, J., HAMADA, S., IKEDA, H., MASAKI, N. & KOZUKA, T., 1988. Primary thyroid lymphoma: evaluation with CT. *Radiology, 168*, 765–768.

TAKASHIMA, S., MORIMOTO, S., IKEZOE, J., ARISAWA, J., HAMADA, S., IKEDA, H., MASAKI, N., KOZUKA, T. & MATSUZUKA, F., 1989. Primary thyroid lymphoma: comparison of CT and US assessment. *Radiology, 171*, 439–443.

TOKUDA, Y., KASAGI, K., IIDA, Y., YAMAMOTO, K., HATABU, H., HIDAKA, A., KONISHI, J. & ISHII, Y., 1990. Sonography of subacute thyroiditis: changes in the findings during the course of the disease. *Journal of Clinical Ultrasound, 18*, 21–26.

WALFISH, P. G., 1986. Miscellaneous tumors of the thyroid. In *The Thyroid,* ed. by S. H. Ingbar & L. E. Braverman (Lippincott Co, Philadelphia), pp. 1363–1376.

1991, *The British Journal of Radiology*, *64*, 576–579

Fibrous dysplasia of the skull: disease activity in relation to age

By *M. L. Davies, FRCR and P. Macpherson, FRCP, FRCR

Department of Neuroradiology, Institute of Neurological Sciences, Southern General Hospital, Glasgow, UK

(*Received August 1990 and in revised form November 1990*)

Keywords: Fibrous dysplasia, Skull, Age, Progression

Abstract. Eighteen of 19 patients with histologically confirmed fibrous dysplasia of the skull seen at the Institute of Neurological Sciences, Glasgow, in the past 20 years have been reviewed and recent radiographs obtained. Sex, age at presentation and at follow-up were recorded, in addition to the site, type and extent of cranial involvement. The findings have been related to disease activity and progression. In comparison with other reports we found the proportion of patients with activity in adulthood to be relatively high (37%). Overall, there was an equal sex distribution, but of seven patients presenting as adults, six were female as were six of seven patients with evidence of disease activity in adulthood.

Although fibrous dysplasia is a well known entity, very few series of patients with skull involvement have been reported. It is a developmental anomaly in which the normal bone architecture is replaced by fibrous tissue containing bony elements. The radiological appearances vary from lytic to sclerotic depending on the proportions of these tissues. The cranio-facial bones are affected in 10% of patients with monostotic disease and rates are quoted from 50 to 100% for the polyostotic form (Windholz, 1947; van Tilburg, 1972). Distressing symptoms due to disfiguring deformity and/or pressure on cranial nerves may occur.

Although there is a generally held view that the disease tends to affect young people and that progression ceases at about bone maturity, the radiological and pathological literature is rather vague and inconsistent on these points (Table I). In particular, reports of the age at which the disease arrests range from puberty to early middle age (van Tilburg, 1972; Henderson, 1973; Rothman & Allan, 1977). Having encountered patients in whom there was progression in adulthood, we were stimulated to survey all patients with fibrous dysplasia of the skull seen at the Institute of Neurological Sciences, Glasgow, during the last 20 years.

Patients and methods

Patients with fibrous dysplasia were identified by two methods: through Neuroradiology department records, and through Neuropathology department records of biopsy results which were available from 1964 onwards.

The age at presentation, sex, relevant clinical features and follow-up, if any, were noted and radiographs were traced. Review of patients no longer attending the Institute was sought by sending an explanatory letter and questionnaire to the patient's general practitioner. Information was requested regarding the current clinical state of the patient and up to date radiography was obtained by asking for attendance at either the Institute or the local hospital.

Nineteen patients were identified and only one of these failed to attend for follow-up examination. All the patients had presented with symptoms directly attributable to their fibrous dysplasia. In none had it been an incidental finding during investigation.

We regarded 20 years as the age of bone maturity.

Of the 18 patients reviewed, nine were female and nine were male. Age at presentation was in the range 11–73 years (Table II). The average age at presentation was 16.5 years for males and 29.9 years for females. A further four patients with probable but unconfirmed fibrous dysplasia were excluded from the study. One was a 19 year old male and two were adult females. Clinical or radiological surveillance for periods of 1–3 years had detected no change in the condition. The fourth patient was also female, but no details are available apart from one radiological report from 1972.

Results

Radiological categories

The vault alone was affected in six patients, the base in eight and both vault and base in four. Where the base was involved it was always sclerotic. The vault was affected in a total of 10 patients, three were solely sclerotic, two were purely lytic and five showed a mixed pattern.

Clinical categories

The patients fell into three broad clinical groups (Table II).

(1) Patients whose clinical and radiological state remained static throughout follow-up (numbers

---

*Present address: Department of Radiology, Western Infirmary, Glasgow, UK.

Table I. Literature review

Author	Year	Age at onset	Age at presentation	Progression
van Tilburg	1972	Early life	—	Generally to a standstill before puberty
Rothman & Allan	1977	Early life	Early life	Lack of progress beyond puberty helps diagnosis
Patton	1986	—	—	Activity ceases with skeletal maturity
Paul & Juhl	1965	Childhood	—	Grows slowly or not at all after adulthood
Pugh	1962	Childhood	Later years of growth	Slow progression or not at all in adult life, rare acceleration after maturity
Edeiken	1981	Young, often infancy	Young to adult	—
Leeds & Seaman	1962	—	—	Progresses during years of growth
Grossman	1984	10–20 years	May be much later	Mostly arrested when growth stops
Henderson	1973	Average 10 years	Juvenile and adolescent	Most active 10–30 years, then usually slows down
Vickers	1981	—	25–35 years	—

Table II. Clinical and radiological features of fibrous dysplasia

Number	Sex	Age at presentation	Follow-up (years)	Age at follow-up (years)	Site	Lytic/sclerotic	Progress
1	M	41[a]	14	55	Vault	sclerotic/mixed	NC
2	F	73[a]	2	75	Base	Sclerotic	NC
3	F	25[a]	3	28	Base	Sclerotic	NC
4	F	32[a]	14	46[b, c]	Vault and base	Lytic Sclerotic	CE NC
5	M	11	12	23	Vault	Lytic	CE
6	M	16	5	22	Vault	Sclerotic/lytic[d]	CE CE
7	M	15	9	24	Base	Sclerotic	CE
8	M	18	12	30	Vault	Sclerotic	CE
9	M	12	3	15	Base	Sclerotic	CE
10	F	33[a]	8	41[b]	Vault	Sclerotic/lytic[d]	CE
11	M	13	2	15	Base	Sclerotic	Slight residual
12	F	12	9	21[b]	Base	Sclerotic	Progress
13	M	12	3	15	Base	Sclerotic	Progress
14	F	13	4	17	Base Vault	Sclerotic Mixed	Progress Progress
15	M	11	19	30[b]	Vault	Sclerotic	Progress
16	F	14	12	26[b]	Vault and base	Sclerotic	Progress
17	F	20[a]	11	31[b]	Vault and base	Mixed Sclerotic	 Progress
18	F	47[a]	2	49[b]	Base	Sclerotic	Progress

[a] Presenting in adulthood.
[b] Activity in adulthood.
[c] Excision of vault lesion at age 41 years.
[d] Predominant feature.
NC, no change; CE, complete excision.

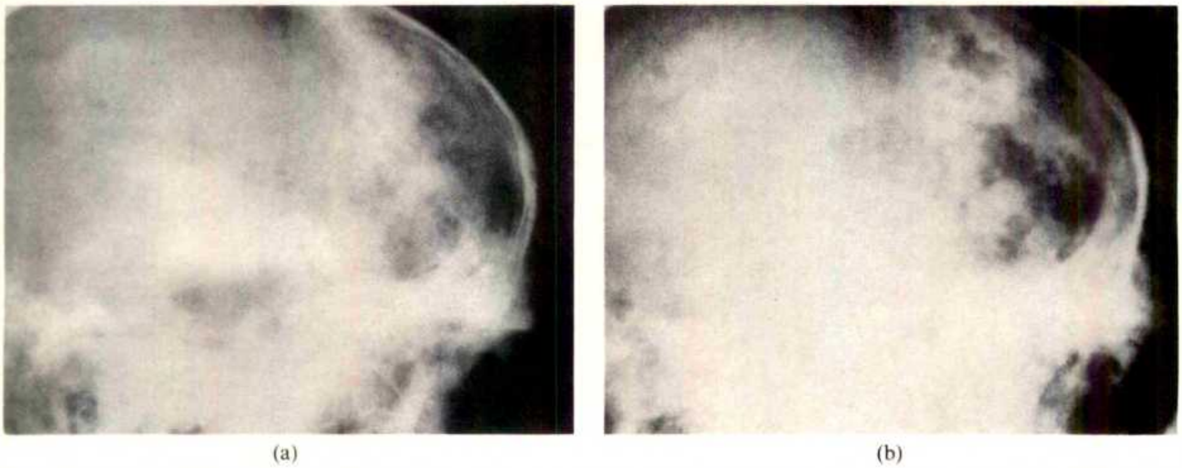
(a) (b)

Figure 1. Patient number 17. (a) At presentation aged 20 years, showing extensive sclerosis of the skull base and orbit, and a mixed sclerotic and lytic lesion involving the frontal bone. (b) Despite orbital decompression at age 22 years, her clinical features advanced and the radiological changes progressed to the state shown at age 31 years.

1–3). All had presented in adulthood with symptoms due to fibrous dysplasia but in none were these serious enough to merit surgery beyond biopsy.

(2) Patients whose disease was progressive and who required radical surgery for the relief of symptoms and in whom complete excision was possible (numbers 4–11). With two exceptions (numbers 4 and 10), all of this group were in their teens. Patient 4 was 32 years old when she presented with a parietal swelling shown to be lytic fibrous dysplasia on removal. She also had slight sclerotic changes in the skull base which have not changed throughout follow-up. Patient 10 is a female who presented at the age of 33 years with extensive changes in the temporal region and radical excision of the abnormal bone was required. Complete excision in all these cases has resulted in eradication of diseased tissue with no evidence of recurrence or of the disease arising in previously unaffected bone.

(3) Patients with advancing disease in whom complete resection was not possible or in whom surgery is not yet necessary (numbers 12–18). Of the seven patients in this group, five were teenagers at presentation (numbers 12–16). At recent follow-up two are still in their teens but one is now 21 years old and another is 30 years. Patient 16 underwent partial excision at the age of 14 years and she continues to have symptoms and evidence of radiological progression despite now being 26 years of age. Patients 17 (Fig. 1) and 18 were adults at presentation and although both have undergone partial excision the fibrous dysplasia is still progressing.

In this series fibrous dysplasia was most active during the teenage years, when there was a preponderance of male patients, eight males to three females. The site and extent of involvement did not seem to have any bearing on disease activity, although it may influence outcome by limiting operability, especially when the orbit is involved. Of the seven patients in whom there was evidence of progression in adulthood (numbers 4, 10, 12, 15, 16, 17, 18), all but one were female, as were six of the seven patients presenting in adulthood. Two cases are known to have evidence of fibrous dysplasia in bones other than the cranio-facial skeleton (numbers 13 and 17), but no attempt was made to assess the possibility of polyostotic disease in the other patients, none of whom had clinical features referable to the remainder of the skeleton.

Discussion

Fibrous dysplasia of the skull is a surprisingly rare condition, only 19 confirmed cases have been seen in 20 years at the Institute of Neurological Sciences, Glasgow. In our series the majority of cases conform to previous reports of site, radiological appearance and age at presentation. Where surgical excision is not required or possible the disease usually becomes less active and can be expected to arrest altogether in most cases, although further follow-up would be required to establish this in all our patients. As yet, with one exception all patients presenting as teenagers have either had radical resection or are continuing to progress. Patient 11 is the exception with slight residual, apparently inactive disease. Complete excision, when needed and possible, offers the only guarantee of cure and we have found no evidence of occurrence in previously unaffected bone.

However, our study has revealed several interesting features of fibrous dysplasia of the skull. While most reports state that the disease progresses slowly or not at all after bone maturation, the range in the literature is wide, from no progression beyond puberty (Rothman &

Allan, 1977) to occurrence in old age (Olmsted, 1981). Most references we have quoted are from textbooks, because of the paucity of reported series. An exception is the series from Leeds and Seaman (1962) who studied a total of 46 patients but did not detail age at presentation, although the range was 2–68 years. They followed 15 patients for between 6 and 39 years and found appreciable progression in only two, aged 8 and 12 years at presentation, and 13 and 25 years respectively at follow-up.

We did not find presentation in adulthood to be rare: 39% of our patients were adults. Although we had an equal sex distribution overall, all but one presenting as adults were female. In addition, our series indicates that the disease is more active in adulthood than previously suggested. Progression occurred in four out of seven patients who presented in adult life, and in three who presented as teenagers the disease continues to advance into adulthood. All but one of those showing progression as adults were female.

The site, extent and radiological type did not seem to influence disease activity and we have been unable to elicit any distinctive histological type associated with progression.

In summary, fibrous dysplasia of the skull is an active process, not only in young patients but also in a proportion of affected adults and, as such, should not be dismissed as an incidental finding but should be followed up clinically and radiologically.

Acknowledgment

We would like to thank Professor D. I. Graham for his help in tracing the histology of patients in this study.

References

EDEIKEN, J., 1981. Fibrous dysplasia. In *Roentgen Diagnosis of Diseases of Bone*, 3rd edn. ed. by J. Edeiken (Williams and Wilkins, Baltimore, MD), pp. 1021–1025.

GROSSMAN, M. E., 1984. The normal teeth and jaws. In *Textbook of Radiological Diagnosis*, ed. by G. H. du Boulay (H. K. Lewis, London), p. 426.

HENDERSON, J. W., 1973. Fibrous connective tissue tumours. In *Orbital Tumours*, ed. by J. W. Henderson (W. B. Saunders Philadelphia, PA), pp. 215–223.

JACOBS, P. & RENTON, P., 1987. Fibrous dysplasia. In *A Textbook of Radiology and Imaging*, ed. by D. Sutton (Churchill Livingstone, Edinburgh), p. 26.

LEEDS N. & SEAMAN, W. B., 1962. Fibrous dysplasia of the skull and its differential diagnosis. *Radiology*, *78*, 570–582.

OLMSTED, W. N., 1981. Some skeletogenic lesions with common calvarial manifestations. *Radiologic Clinics of North America*, *19* (4), 703–713.

PAUL, L. W. & JUHL, J. H., 1965. Anomalies and dysplasias of the skeleton. In *The Essentials of Roentgen Interpretation*, 2nd edn. ed. by L. W. Paul & J. H. Juhl (Harper and Row, New York), pp. 52–53.

PUGH, D. G., 1962. Fibrous dysplasia of bone. In *Roentgenological Diagnosis of Diseases of Bone*, ed. by D. G. Pugh (Williams and Wilkins, Baltimore, MD), pp. 426–432.

ROTHMAN, S. L. G. & ALLEN, W. E., 1977. Congenital and developmental abnormalities of the orbit. In *Orbital Roentgenology*, ed. by P. H. Arger (John Wiley and Son, New York), p. 50.

VAN TILBURG, W., 1972. Fibrous dysplasia. In *Handbook of Clinical Neurology*, ed. by P. J. Vinken and G. W. Bruyn (North-Holland, Amsterdam), Vol. 14, pp. 163–212.

VICKERS, R. A. & ROSAI, J., 1981. Mandible and maxilla. In *Ackerman's Surgical Pathology*, 6th edn. ed. by J. Rosai (C. V. Mosby, St. Louis, MD), pp. 177–178.

WINDHOLZ, F., 1947. Cranial manifestations of fibrous dysplasia of bone. *American Journal of Roentgenology*, *58*, 51–63.

1991, *The British Journal of Radiology*, 64, 580–583

The extrapleural fat in empyema: CT appearance

By Julie E. Takasugi, MD, *J. David Godwin, MD and Sharlene A. Teefey, MD

Department of Radiology (114), Seattle VAMC, 1660 South Columbian Way, Seattle, WA 98108, USA and
*Department of Radiology, SB-05, University of Washington Medical Center, Seattle, WA 98195, USA

(Received August 1990 and in revised form February 1991)

Keywords: Empyema, CT, Chest wall, Extrapleural fat, Pleural effusion

Abstract. Pleural empyema can be accompanied by changes in the adjacent chest wall. We examined the chest wall on computed tomographic scans in 24 patients with pleural effusions. Eighteen patients had pleural empyema and six had transudative effusions. Of the 18 empyema patients, 13 had abnormally high attenuation in the extrapleural tissues. In 12 of these 13, the high attenuation was probably caused by reaction to the pleural infection. In two, it was probably caused by haematoma (one patient had haematoma and empyema). In five patients there was either no clear abnormality in the extrapleural space or an insufficient amount of fat to permit detection of an abnormality, or the parietal pleura could not be distinguished from the pleural fluid because intravenous contrast medium was not given. Of the six patients with proven transudative pleural effusions, all had extrapleural fat which appeared normal. Abnormally high attenuation in the extrapleural tissues can be expected to accompany exudative pleural effusion, particularly empyema, but not transudative effusion.

When an empyema is present, changes may occur in the adjacent chest wall reflecting the pleural infection. Oedema or inflammatory cells can infiltrate the fat of the extrapleural compartment between the parietal pleura and the ribs. Although thoracic surgeons are familiar with the chest wall oedema which can accompany empyema, there has only been one radiological description (Waite et al, 1988; Waite et al, 1990). It is important that radiologists be familiar with this condition, since the increased attenuation of the extrapleural fat on chest computed tomography (CT) may cause the fat to be mistaken for a pleural fluid collection. Therefore, we undertook a combined retrospective and prospective study to determine how frequently this finding was present in patients with empyema and whether it was also present in patients with transudative effusions.

Materials and methods

From January 1987 to December 1989, 18 patients with empyema were studied with chest CT at our hospital. Six patients had more than one scan. Eight cases were evaluated retrospectively, and 10 cases prospectively. For comparison, CT scans of an additional six patients, with thoracentesis-proved transudative pleural effusions, were also reviewed.

Medical records were reviewed in all cases. The diagnosis of empyema was established in 16 patients by the presence of bacteria on Gram stain or culture. In two patients in whom pleural fluid bacteria could not be demonstrated, the pleural fluid protein, the lactate dehydrogenase (LDH) and the white cell count were elevated and rising, and therefore empyemas were presumed. All patients with empyema were treated with tube thoracostomy in addition to antibiotics. In 13 of the 18 patients, the diagnosis of empyema had been established before CT scanning and the scan was performed to identify any undrained fluid collection as the cause of persistent fever. In the remaining five patients, the scan was performed before the results of thoracentesis were known. Eleven of the 13 empyema patients with abnormalities in the extrapleural tissues had or had already had tube thoracostomy at the time of CT scanning. Three of the five patients with empyema who did not have any visible extrapleural abnormality had thoracostomy tubes in place. None of the patients with transudative effusions had or had already had tube thoracostomy at the time of CT scanning.

All CT scans were performed using a Picker 1200SX scanner. Thirteen of the 18 patients with empyema and one of the six patients with simple effusion were scanned following intravenous contrast medium administration (170 cm^3 Conray 60% as a bolus and drip infusion). Intravenous contrast medium was not administered in 10 patients because of renal failure (three patients) or poor venous access (two patients), or because it was considered unnecessary at the time of scanning (five patients). Scans were performed using 10 mm collimation at 10 mm (22 patients) or 30 mm (two patients) intervals. Lung (width 2000 Hounsfield units (HU), level −700 HU) and mediastinal (width 500 HU, level 50 HU) windows were examined. The thicknesses of the visceral and parietal pleura were measured in cases where these structures were distinguishable from the adjacent pleural effusion and extrapleural tissues. The thickness of the extrapleural compartment was measured as the distance between the enhancing parietal pleura and the innermost cortex of the adjacent rib. In patients with empyema the contralateral normal hemithorax was used as a control for measuring the pleural

---

Address correspondence to Dr Julie E. Takasugi.

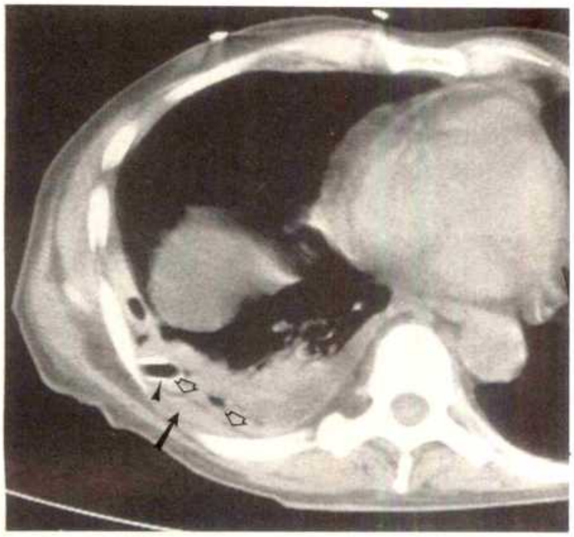

Figure 1. Patient with *Eikenella corrodens* empyema and band of extrapleural high attenuation (arrow), representing haematoma, at thoracostomy tube (arrowhead) site. Note normal extrapleural fat (open arrow) separating haematoma from parietal pleura. Intact fat plane argues against extension of infection from pleural space into chest wall.

and extrapleural thicknesses. The attenuation coefficient of the extrapleural fat was measured in 10 patients with empyema and in two patients with transudative pleural effusions. The attenuation of the fat in the remaining eight patients with empyema and four patients with transudative effusions could not be measured since CT data were no longer available.

Results

In 13 of the 18 patients with proven empyema, the extrapleural fat had abnormally high attenuation visible on simple inspection of images made at mediastinal window settings. In one of the 13 patients, the abnormal attenuation was probably caused by haematoma from a thoracostomy tube (Fig. 1). In another patient, abnormal attenuation was probably caused by haematoma related to a thoracotomy with rib fracture (Fig. 2a). This latter patient also had an empyema due to an oesophagopleural fistula and subsequently developed high attenuation in extrapleural fat at sites remote from the thoracotomy incision on a follow-up CT scan 3 days later (Fig. 2b).

In the remaining 11 patients, and in the one post-thoracotomy patient mentioned above, high attenuation in the extrapleural tissues was not explained by tube insertion but was attributed to extension of the inflammatory process or oedema into the chest wall. In most patients, the abnormality in the extrapleural space was patchy; normal fat attenuation was present on CT images near areas of abnormal attenuation (Fig. 3). In two patients, extrapleural fat which was normal on initial CT scans became abnormal on follow-up scans 3 and 8 days later, respectively (Figs 2 and 4).

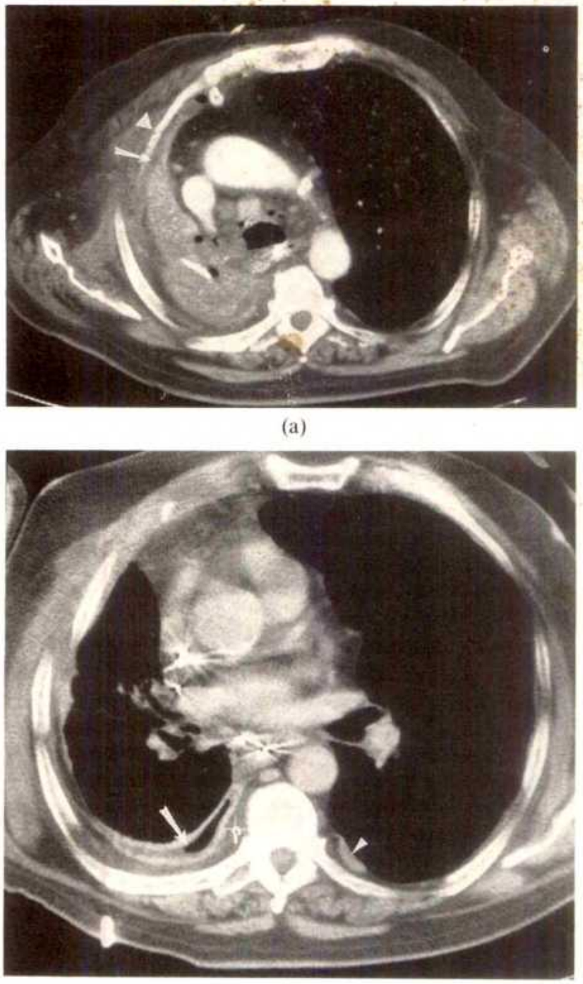

(a)

(b)

Figure 2. (a) Patient with empyema and pneumomediastinum caused by oesophago-pleural fistula following mediastinoscopy and right upper lobectomy for lung cancer. Note extrapleural soft tissue representing haematoma (arrow) associated with fractured rib (arrowhead). The right lung was collapsed. (b) Same patient 3 days later. Right-sided pyopneumothorax (arrow) surrounded by thickened and enhancing pleura. Increased attenuation (−20 HU) of extrapleural fat (cursor) at site distant from haematoma and rib fracture. Left sided pleural plaque (arrowhead) surrounded by normal extrapleural fat (−100 HU).

In those patients in whom intravenous contrast medium was used, the visceral and parietal pleural thickness could be measured in the abnormal and normal hemithoraces (Table I). On the normal side, the mean combined thickness of visceral and parietal pleura was 1.5 mm, ranging from 0 to 2 mm. On the side of the empyema, the thickness of the visceral pleura ranged from 3 to 6 mm, and the parietal pleura from 3 to 7 mm.

In patients with empyema, the thickness of the extrapleural compartment of the normal contralateral

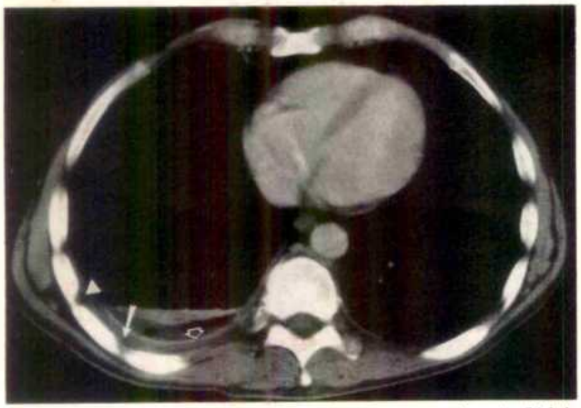

Figure 3. Patient with culture-negative empyema. Band of high attenuation in extrapleural tissues (arrow) immediately adjacent to normal extrapleural fat (arrowhead). Note air and fluid in pleural cavity and thick, enhancing parietal pleura (open arrow).

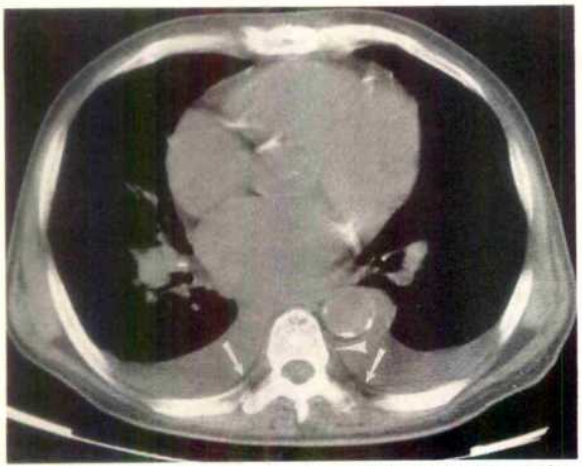

Figure 5. Patient with congestive heart failure and transudative pleural effusions. Note normal size and attenuation of extrapleural fat (arrows). Normal fat separates intercostal veins (arrowhead) and muscles from pleura.

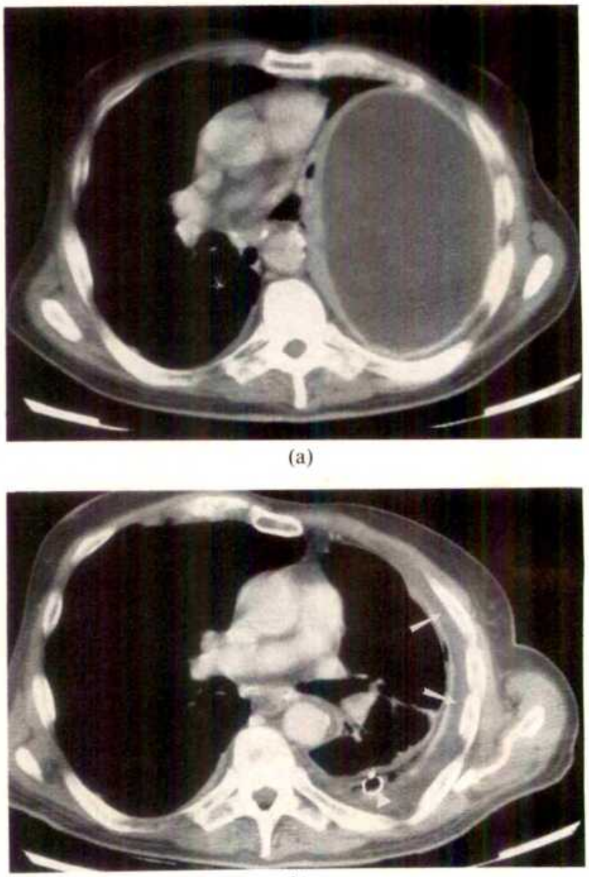

(a)

(b)

Figure 4. (a) Patient with *Streptococcus pneumoniae* empyema with large left pleural effusion compressing left lung. Note mediastinal shift to right. (b) Same patient 8 days later after thoracostomy drainage. Note high attenuation (arrows) and thickening of extrapleural compartment, which could be mistaken for a pleural fluid collection. Thoracostomy tube (arrowhead) can be seen between two layers of thickened pleura. Mediastinum now shifted to left.

Table I. CT measurements of pleural and extrapleural tissues in empyema and transudative pleural effusions

Patient diagnosis	Ipsilateral				Contralateral		
	EPC	EPFA	PP	VP	P	EPC	EPFA
Empyema							
Range	4–15	−40 to +34	2–7	0–6	0–2	1–6	−100 to −51
x	10.6	3.8	4.7	3.6	1.4	3.9	−84.5
σ	3.1	24	1.4	1.8	0.8	1.6	14.1
n	15	10	14	11	13	18	10
Transudate							
Range	3–5	−96 to −83	1	0	1	3–5	−85 to −84
x	3.8	−89.5	—	—	—	3.8	−84.5
σ	0.8	9.2	—	—	—	0.8	0.7
n	6	2	1	1	1	6	2

x = mean; σ = sample standard deviation; n = sample size.

EPC = extrapleural compartment thickness (mm); EPFA = attenuation coefficient of extrapleural fat (HU); PP = parietal pleural thickness (mm); VP = visceral pleural thickness (mm); P = pleural thickness (parietal + visceral) (mm).

hemithorax ranged from 1 to 6 mm (Table I). The attenuation of the extrapleural fat was similar to that of fat elsewhere in the body (−50 to −100 HU). The thickness of the extrapleural compartment of the abnormal hemithorax ranged from 8 to 15 mm. The attenuation of the extrapleural fat varied from fat density (−40 HU) to soft tissue density (+34 HU), but was always higher than the attenuation of the normal contralateral extrapleural fat (Table I).

Of the six patients with proved transudative pleural effusions, two had cirrhosis, ascites and pleural effusions, three had congestive heart failure with pleural effusions, and one, with pneumonia, had a sympathetic effusion. Although intravenous contrast medium was administered in only one of the six patients, the extrapleural fat was clearly distinguishable from the pleural effusion. None of these patients had high attenuation in the extrapleural space and the extrapleural compartment was thinner (ranging from 2 to 5 mm) (Fig. 5) than in patients with empyema (Table I). There was no thickening of the visceral or parietal pleura in the one patient who received intravenous contrast medium.

Discussion

The normal components of the extrapleural compartment include fat, the endothoracic fascia, the innermost intercostal muscle, intercostal fat and vessels and intercostal muscles (Im et al, 1989). Even with 10 mm collimation, we found the intercostal veins and internal intercostal muscles were visible in the extrapleural compartment. The intercostal vein runs in the extrapleural fat, between the parietal pleura and rib, and drains into the azygos or hemiazygos veins. The internal intercostal muscle stretches between adjacent ribs. Both of these normal structures are separated from the parietal pleura by extrapleural fat, with the typical low attenuation of adipose tissue anywhere in the body. The normal structures become indistinguishable from each other when the attenuation of the extrapleural fat is increased by reaction to an adjacent empyema.

Intravenous contrast medium enhances the pleura, providing more precise identification of its location and thickness. Normally, the combined thickness of the visceral and parietal pleura is 2 mm or less (Im et al, 1989). When intravenous contrast medium was not used in patients with empyema, it was difficult to distinguish the parietal pleura and the abnormal extrapleural fat because they had the same attenuation. In three of the five patients in whom contrast medium was not used, extrapleural abnormalities could not be identified because of these difficulties. In one patient, increased attenuation in the extrapleural space was detected even though contrast medium was not injected, because, for unknown reasons, the attenuation of the parietal pleura was greater than the adjacent pleural fluid and extrapleural tissues. The final patient had no discernible extrapleural abnormalities. Besides aiding in locating the parietal pleura, intravenous contrast medium also helped to identify the thickening of the visceral and parietal pleura which accompanied pleural infection. The thickness of the pleural layers in cases of empyema ranged from three to seven times that of the contralateral normal side. When the parietal pleura was visible, the thickness of the extrapleural compartment could be measured. The thickness of the extrapleural compartment increased by a factor of 2–3 in the presence of empyema.

The attenuation of the extrapleural fat can be increased to an extent where the fat can be mistaken for a pleural fluid collection (Fig. 4b) unless its relationship to the parietal pleura is recognized. It is essential to distinguish this abnormal fat from pleural fluid, since tube thoracostomy is indicated only when pleural effusion is actually present.

Our experience shows that the majority of empyemas that have been drained by tube thoracostomy are associated with increased attenuation of the extrapleural fat and increased thickness of the visceral and parietal pleura and extrapleural tissues. It is doubtful that the increased attenuation in the extrapleural space is due to the tube thoracostomy itself since the changes were present at sites remote from the tube and were also present in patients who had not had a tube inserted.

We believe that the abnormally high attenuation of the extrapleural fat is caused by oedema, lymphatic distension, and infiltration with inflammatory cells or granulation tissue in the extrapleural compartment and pleura. The composition of the infiltrate in the extrapleural compartment would vary with the stage of the empyema (exudative, fibropurulent or organizing (Light, 1985)). These findings of chest wall oedema and thickening are well known to thoracic surgeons. Associated histologic changes have not, to our knowledge, been described since patients with empyemas do not routinely undergo biopsy of the extrapleural tissues.

The extrapleural compartment was normal in the patients with transudative pleural effusions due to congestive heart failure, cirrhosis and ascites. It was also normal in the one patient with a sympathetic effusion, a finding which may be explained if diagnosis and treatment is instituted in the exudative stage (Light, 1985), when pleural fluid cell count, LDH, glucose and pH levels may be normal.

We conclude that high attenuation in the chest wall commonly accompanies empyema. In our experience it does not accompany transudative pleural effusion.

References

Im, J. G., Webb, W. R., Rosen, A. & Gamsu, G., 1989. Costal pleural: appearances at high-resolution CT. *Radiology*, *171*, 125–131.

Light, R. W., 1985. Parapneumonic effusions and empyema. *Clinics in Chest Medicine*, *6*(1), 55–62.

Waite, R. J., Carbonneau, R. J., Balikian, J. P., Umali, C. B. & Pezzella, T. A., 1988. Extrapleural reaction in pulmonary empyema (Abstract). *Investigative Radiology*, *23*(S1), S33.

Waite, R. J., Carbonneau, R. J., Balikian, J. P., Umali, C. B., Pezzella, T. A. & Nash, G., 1990. Parietal pleural changes in empyema: appearances at CT. *Radiology*, *175*(1), 145–150.

1991, *The British Journal of Radiology*, *64*, 584–586

The ocular effects of hyoscine-*n*-butylbromide ("Buscopan") in radiological practice

By G. R. J. Sissons, MRCP, FRCR, *A. McQueenie and †M. Mantle, MRCP, FRCR

Department of Diagnostic Radiology, *University Hospital of Wales, Heath Park, Cardiff CF4 4XW, UK and
†Department of Diagnostic Radiology, Queen Elizabeth Hospital, Edgbaston, Birmingham B15 2TH, UK

(*Received October 1990 and in revised form January 1991*)

Keywords: Accommodation, Ocular, Butylscopolammonium bromide, Scopolamine derivatives

Abstract. "Buscopan" (hyoscine-*n*-butylbromide, HBB) is a smooth muscle relaxant regularly used in radiological and endoscopic procedures. One unwanted effect is temporary impairment of visual accommodation. Near and distance vision were assessed in 100 patients undergoing barium meal and barium enema studies. Visual testing was performed prior to the examination and repeated immediately before leaving the radiology department. Completed data was obtained in 90 patients. Of these, 37 were given a conventional 20 mg intravenous dose of HBB, 37 were given glucagon and 16 received no drug. No patient showed any impairment of distance vision. Minor abnormalities of near vision were observed in five patients. All had been given HBB. They were aged 50 years or less and had been retested 12–21 min after administration of the drug. It is suggested that the degree of visual impairment observed is not sufficient to impair driving ability. Routine questioning concerning history of glaucoma is unlikely to be of value; more appropriate would be a warning to seek urgent medical advice if eye pain or visual loss is experienced.

Hyoscine-*n*-butylbromide (HBB, Boehringer Ingelheim) is a smooth muscle relaxant regularly used in radiological and endoscopic procedures to temporarily abolish bowel peristalsis. It is a useful and well tolerated drug (Hüpscher & Dommerholt, 1984). One unwanted effect is temporary impairment of visual accommodation owing to paralysis of the ciliary muscle. This leads to an increase in the near point of vision. In young healthy volunteers this effect is maximal at 15 min and has resolved by 40 min after a conventional intravenous dose of 20 mg (Herxheimer & de Groot, 1977). This study was performed to determine whether any significant alteration in vision is present in patients leaving the radiology department after undergoing barium studies.

Patients and methods

One-hundred consecutive adult patients undergoing barium meal and barium enema examinations were studied over a 2 week period. Visual tests were performed before the procedure and again just before leaving the department. The tests performed (on each eye) were:

(a) visual acuity — Snellen test (6 m);

(b) reading charts — published by Clement Clarke Ltd ($\frac{1}{3}$ m);

(c) near point of vision — RAF near point rule (Clement Clarke Ltd).

The equipment used is illustrated in Fig. 1. In (a) and (b) a change of more than one line of print size in both eyes was considered significant. In test (c), performed by moving a block of print along a rule balanced on the patient's nose and recording the point at which it becomes blurred, a change of greater than 5 cm was

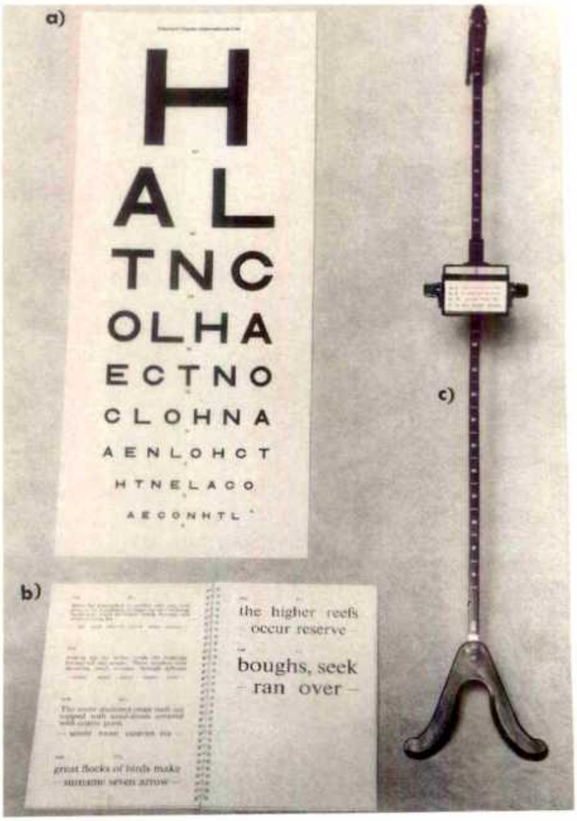

Figure 1. (a) Snellen chart; (b) reading charts; (c) near point rule.

Table I. Completed studies

Drug (+ dose)	Number of patients and examination	Mean age/years (+ range)	Mean interval between drug and re-testing (+ range)/min	Number of patients with change in distance vision	Number of patients with change in near vision
HBB 20 mg intravenous	14 meals	48 (28–85)	20 (10–69)	0	5
	23 enemas	56 (20–83)	36 (19–70)	0	0
Glucagon 0.1 mg intravenous	36 meals	55 (17–85)	19 (7–85)	0	0
	1 enema	29 (—)	20 (—)	0	0
No drug	16 meals	47 (19–74)	20 (8–71)	0	0

considered significant. Pupillary diameter was also recorded using a millimetre ruler.

Patients were asked to wear their usual spectacles, though five did not comply and were tested uncorrected. The tests were performed in the same enclosed room under standard lighting conditions by the same observer (A. McQueenie, student orthoptist).

Patients were given HBB, glucagon or no drug according to the practice of the radiologist performing the investigation. No attempt was made to randomize the patients under study. Details of drug type and the time and mode of administration were recorded independently by the radiographer supervising the procedure in the fluoroscopy room.

No patient gave a history of glaucoma.

Results

Of the 100 patients who agreed to be tested the data were incomplete in 10. The main results are presented in Table I. 37 patients were given HBB 20 mg intravenously (14 barium meals and 23 barium enemas); 36 patients (barium meals) were given glucagon 0.1 mg intravenously and one enema patient was given 0.25 mg; 16 patients (all barium meals) were given no drug. The mean interval between the drug administered (or the start of the procedure if no drug was given) and the second set of visual tests was approximately 20 min in all barium meal patients. The mean interval in the barium enema patients was 36 min.

On Snellen testing there was no change in visual acuity of more than one line in any patient.

Tests of near vision revealed measurable changes in five patients. All showed an increase in near point of greater than 5 cm in both eyes, but in no case did the near point exceed 37 cm. Of these five patients, three showed impairment on reading chart testing of more than one line in both eyes. All five patients were in the barium meal group given HBB. The mean age of these patients was 43 years (range 38–50) and they were retested 12–21 min after receiving the drug.

Only one of the five patients reported a change in near vision on direct questioning; he volunteered that he could not focus on the small print in his newspaper.

Two patients showed a change in pupil diameter of more than 1 mm in both eyes. Both were in the HBB group and both showed an increase of 2 mm in both eyes. Only one of these showed a change in near vision.

Of the 100 patients, 23 were driving; all were undergoing barium meals. Of these, seven were in the HBB group including two patients with a measurable change in near vision.

Discussion

Five out of 37 patients (13.5%) receiving 20 mg of HBB intravenously showed a measurable change in near vision when retested 12–21 min after receiving the drug. This falls within the range reported in other series, which have often used different doses, modes of administration and means of assessment (Ayre-Smith, 1976; Herxheimer & de Groot, 1977; Stevenson et al, 1980; Hüpscher & Dommerholt, 1984).

In our series, the patients with impaired near vision were all in the barium meal group. The shorter duration of this investigation is the likely cause as patients were retested after a mean interval of 20 min. In contrast, barium enema patients were retested at a mean of 36 min, though the range was wide (19–70 min).

Each patient with a measurable change in near vision was aged 50 years or less. Near point is known to increase with age and these changes will mask the action of the drug. The greatest near point values recorded (over 40 cm) were observed in elderly patients tested without their spectacles.

Referring to HBB and another anticholinergic drug probanthine, Kreel (1975) stated that these drugs "should not be used on out-patients who have to drive themselves home as they cause failure of accommodation".

Current UK driving regulations specify that a driver must be able to read a vehicle registration plate (print size 3 in) at 20.5 m with both eyes open. On Snellen testing this corresponds to 6/10 vision. The ability to perform this test was not affected by HBB in the patients studied.

Mehlfeld and Bleichert (1986) describe the potential for impairment of distance vision in long-sighted individuals driving without corrective lenses whose vision would then be dependent upon accommodation. As a rule, only minor degrees of long-sightedness remain undetected in adults and even a small degree of accommodation is sufficient for focusing on distant objects.

As regards near vision, the effects observed were of a minor nature. The instrument panel in a range of vehicles examined lies at least 50 cm from the driver's head—well beyond the greatest near point recorded (42 cm).

Similarly, pupillary dilatation did not appear to be a significant problem. It should be noted that marked and prolonged pupillary dilatation, seen with more potent mydriatics such as atropine, can lead to excessive glare.

Anticholinergic drugs are a recognized precipitating cause of an acute rise in intraocular pressure in individuals with a shallow anterior chamber or narrow-angle glaucoma. This is present in 0.1% of those over 50 years (Kilker & Heatherington, 1976), but is less common than chronic glaucoma whose prevalence is estimated to be 0.28% (Hollows & Graham, 1966). Acute glaucoma following HBB is uncommon. Doran et al (1987) describe one patient who developed acute glaucoma within 12 h of the administration of HBB as part of a barium meal examination. However, it should be remembered that the low light intensity in the fluoroscopy room and patient anxiety are other stimuli to mydriasis which can lead to a rise in intraocular pressure in predisposed individuals. The condition also has a natural incidence and these factors may be difficult to separate from the effects of the drug alone.

Conclusions

In the patients under study:

(1) No patient showed any change in distance vision.

(2) Small but measurable effects on near vision were observed in five out of 37 patients given HBB. All were aged 50 years or less and were retested 12–21 minutes after receiving the drug.

(3) Pupillary changes, when observed, were of a minor nature. Excessive glare should not be a problem.

In summary, whilst driving ability is unlikely to be affected, a brief explanation about the possible effects of HBB is appropriate (particularly in younger patients) to allay any possible anxiety if symptoms are experienced.

Routine questioning for glaucoma is unlikely to prevent any cases of acute glaucoma and could be substituted by a warning to seek early medical advice if eye pain or loss of vision develops in the first few hours following administration of HBB.

References

Ayre-Smith, G., 1976. Hyoscine-*n*-Butylbromide (Buscopan) as a duodenal relaxant in tubeless duodenography. *Acta Radiologica Diagnosis, 17*, 701–713.

Doran, R. M. L., Gray, R. & Virjee, J. P., 1987. Buscopan and glaucoma. (Letter). *British Journal of Radiology, 60*, 417.

Herxheimer, A. & de Groot, 1977. Some effects of injected hyoscine butylbromide: a versatile class experiment in human pharmacology. *British Journal of Clinical Pharmacology, 4*, 337–342.

Hollows, F. C. & Graham, P. A., 1966. Intra-ocular pressure, glaucoma and glaucoma suspects in a defined population. *British Journal of Ophthalmology, 50*, 570–586.

Hüpscher, D. N. & Dommerholt, O., 1984. Action and side effects of small doses of Buscopan in gastroduodenal radiography. *Diagnostic Imaging in Clinical Medicine, 53*, 77–86.

Kilker, A. & Heatherington, J., 1976. *Becker–Schaffer's diagnosis and management of the glaucomas*, 4th edn (C. V. Mosby Company, St Louis), p. 183.

Kreel, L., 1975. Pharmaco-radiology in barium examination with special reference to glucagon. *British Journal of Radiology, 48*, 691–703.

Mehlfeld, G. & Bleichert, A., 1986. The effect of anticholinergic drugs on the inner eye muscles. *Graefe's Archive for Clinical and Experimental Ophthalmology, 224*, 92–95.

Stevenson, G. W., Somers, S. & Virjee, J., 1980. Routine double contrast barium meal: appearance of normal duodenal papillae. *Diagnostic Imaging, 49*, 6–14.

1991, *The British Journal of Radiology*, *64*, 587–590

A comparison between iotrolan, a non-ionic dimer, and a hyperosmolar contrast medium, Urografin, in hysterosalpingography

By *Candice Brokensha, FRCR and Graham Whitehouse, FRCP, FRCR
Department of Diagnostic Radiology, Royal Liverpool Hospital, Liverpool L7 8XP, UK

(*Received October 1990 and in revised form December 1990*)

Keywords: Iotrolan, Urografin, Contrast media, Hysterosalpingography

Abstract. For hysterosalpingography, there were no significant differences between the non-ionic dimeric contrast medium iotrolan (300 mgI/%) and Urografin (370 mgI/%) with regard to ease of application or radiographic quality, and both agents were equally suitable. There were no significant differences between two groups of patients with regard to pain due to instrumentation, pain at the time of injection and pain up to 2 h after the procedure. There was a significant difference ($p = 0.04$) between the two groups with respect to delayed pain, when iotrolan was associated with a lower incidence and decreased severity of delayed pain. There were no differences in the incidence of nausea, vomiting, headache and syncope. No allergic phenomena were seen in either group.

Iotrolan is a new, non-ionic, water-soluble, dimeric, hexa-iodinated radiographic contrast medium which, in a concentration of 300 mgI/ml, is almost isotonic with blood. This low osmolality, together with the high viscosity (Table I), should theoretically be advantageous when iotrolan is used in hysterosalpingography (HSG). A comparative study of iotrolan and Urografin 370, the standard contrast medium used for HSG in this centre, was performed with special regard to image quality, ease of application and side-effects.

Materials and methods

Patients

A double-blind, randomized, single-centre study was performed on 70 patients who were being investigated for primary infertility. Having given their informed consent, patients were allocated iotrolan (300 mgI/ml) or Urografin (370 mgI/ml) according to a randomization list. Hysterosalpingography was performed towards the end of the first week after the menstrual period. Patients with a history of pelvic infection within the previous 6 months, active vaginitis or cervicitis, or with a history of allergy to iodinated contrast medium, were excluded from the study.

Technique

A standard balloon catheter method was used to perform the HSG (Yoder, 1988). One gynaecologist carried out all the HSGs, which were reported by the same radiologist. A third party drew up 20 ml of the contrast medium which had been assigned from the randomization list. The appropriate amount of contrast medium required to delineate the fallopian tubes was determined by fluoroscopic control during the injection. Two radiographs were taken during the procedure: one primarily to demonstrate the uterine cavity and the other to depict the fallopian tubes. A third radiograph was taken at 20 min after the investigation in order to demonstrate the pattern of peritoneal spillage.

Ease of application

The operator assessed (1) the ease of injection, graded as free, moderate or hard, and (2) leakage around the cannula, graded as absent, slight, moderate or marked in extent.

Radiographic quality

The radiologist assessed the following features.

(1) Pathology demonstrated in the uterus and fallopian tubes.
(2) Quality and density of uterine delineation, graded as poor, moderate, good or excellent.
(3) Quality and density of fallopian tube delineation, graded as poor, moderate, good or excellent.
(4) Peritoneal spillage and ease of spread, graded as poor, moderate, good or excellent.

Side-effects

Pain. The patient was interrogated by an independent observer. The severity of pain was evaluated on a scale of 0 to 3 (0 = absent, 1 = slight, 2 = moderate and 3 = severe pain) with regard to:

(1) The insertion of the cannula and inflation of the balloon.

---

* Present address: Kalgoorlie Hospital, Kalgoorlie, 6430, Western Australia.
Address correspondence to: Professor G. H. Whitehouse, University Department of Radiodiagnosis, Royal Liverpool Hospital, PO Box 147, Liverpool L69 3BX, UK.

Table I. Physiochemical properties of iotrolan and Urografin

	Iodine concentration (mg/ml)	Viscosity (mPa @ 37°C)	Osmolality (mOsm kg^{-1} H_2O @ 37°C)
Blood	—	3.1–3.8	290
Iotrolan	300	9.2	360
Urografin	370	8.9	2150

(2) The injection of the contrast medium, assessed immediately after the procedure.
(3) During the first 2 h after the HSG.
(4) More than 2 h after the HSG. These data were recorded by the patient and obtained at the follow-up visit 2 weeks later.

Other symptoms. The occurrence of nausea, vomiting, headache and syncope after HSG was specifically evaluated 2 h after the procedure.

Allergic phenomena. The presence of any urticaria, pruritis, asthma or laryngeal oedema following HSG was noted.

Results

Thirty-seven patients received iotrolan and 33 received Urografin. The mean age of the women was 28.2±0.81 years in the iotrolan group and 28.9±0.75 years in the Urografin group.

Ease of application (Table II)

Data were obtained for 69 patients.

Ease of injection. There were no statistically significant differences in the scores for either group. Approximately 73% of injections in the iotrolan group and 66% of injections in the Urografin group were rated as "free".

Leakage around cannula. There were no statistical differences between the scores of both groups. Approximately 59% of injections in both groups resulted in some leakage around the cannula, but marked leakage was present in only one case in each group.

Radiographic quality (Table III)

Pathology demonstrated. HSG resulted in the demonstration of uterine pathology in three patients within the iotrolan group (two cases of endometrial polyps and one bicornuate uterus) and in one patient within the Urografin group (subseptate uterus). Fallopian tube obstruction or para-ampullary loculation was found in eight patients in the iotrolan group and three patients in the Urografin group. These differences were not statistically significant.

Table II. Ease of application (figures are numbers of patients)

	Iotrolan	Urografin	Probability > χ^2
Ease of injection			
Free	27	21	
Moderate	7	7	0.77
Hard	3	4	
Leakage around cannula			
Absent	22	19	
Slight	10	5	0.50
Moderate	4	7	
Marked	1	1	

Symptoms (Table IV)

Pain at the time of injection. The majority of patients in both groups experienced some pain. Approximately two-thirds of patients in each group complained of moderate or severe pain at the time of contrast medium injection. These differences were not statistically significant.

Table III. Radiographic quality (figures are numbers of patients)

	Iotrolan	Urografin	Probability > χ^2
Uterine pathology demonstrated			
Yes	3	1	0.33
No	33	32	
Tubal pathology demonstrated			
Yes	8	3	0.12
No	27	30	
Uterine density			
Excellent	27	26	
Good	9	6	0.39
Moderate	0	1	
Delineation of uterine body			
Excellent	31	26	
Good	5	5	0.21
Moderate	0	2	
Delineation of fallopian tubes			
Excellent	26	18	
Good	6	12	0.17
Moderate	0	2	
Peritoneal spill and ease of spread			
Excellent	25	21	
Good	7	8	0.71
Moderate	1	2	

Table IV. Pain (figures are numbers of patients)

	Iotrolan	Urografin	Probability $> \chi^2$
Pain at time of instrumentation			
Absent	27	25	
Slight	8	4	0.26
Moderate	2	2	
Severe	0	2	
Pain at time of injection			
Absent	6	4	
Slight	7	6	0.96
Moderate	12	12	
Severe	12	11	
Pain within 24 h of examination			
Absent	17	16	
Slight	6	2	
Moderate	7	4	0.6
Severe	4	4	
Not recorded	3	7	
Delayed pain up to 2 weeks after examination			
Absent	17	12	
Slight	6	5	
Moderate	10	4	0.04
Severe	0	4	
Not recorded	4	8	

Pain within 2 h of the examination. Seventeen patients in the iotrolan group and 10 in the Urografin group experienced pain within 2 h of the examination, but this was only severe in four cases within each group. There were no statistical differences between the two groups.

Delayed pain up to 2 weeks after the examination. Approximately half of all patients experienced delayed pain. In the iotrolan group six had slight pain, 10 reported moderate pain but none complained of severe pain. In the Urografin group, five patients reported slight pain while four had moderate pain and four complained of severe pain. These differences were statistically significant ($p = 0.04$) in that there was a higher incidence of absent and moderate pain in the iotrolan group and a higher incidence of severe pain in the Urografin group.

Other symptoms. The incidence of side-effects other than pain was small. Nausea was reported by 14 patients (6 iotrolan, 8 Urografin), vomiting by only two patients (iotrolan), headache by three patients (2 iotrolan, 1 Urografin) and syncope by one patient (Urografin). Side-effects were regarded as "slight" in all cases. There were no statistically significant differences between treatment groups in the incidence or severity of nausea, vomiting, headache or syncope.

No allergic reactions were reported.

Discussion

The ideal contrast medium for HSG would have the following characteristics (Whitehouse, 1988). (1) It should be sufficiently radiopaque to delineate the uterine cavity and fallopian tubes, yet not so opaque as to obscure mucosal detail and small filling defects. (2) The viscosity should be sufficient to allow retention of the contrast medium in the uterine cavity and fallopian tubes long enough to obtain a radiographic record and to prevent flooding of the contrast medium into the peritoneal cavity with resultant obscuring of the fallopian tubes. On the other hand, the viscosity must not be so high that there are difficulties in handling and injecting the contrast medium or a long delay in spillage from the tubal ampullae into the peritoneal cavity. A viscosity of 8–12 mPas is considered to be the optimum (Dietz, 1952). (3) There should be rapid and total excretion. (4) No damage should occur to the uterus and adnexa, the peritoneal cavity or any other structures along the excretion pathway of the contrast medium. (5) The contrast medium should cause no discomfort to the patient.

None of the available contrast media are totally satisfactory with regard to these criteria. The viscosity of currently used contrast media in HSG is achieved by virtue of their large molecular size or high concentration. Agents containing viscogenic additives have generally fallen into disuse. The diatrizoates and iothalamates have been found to be generally acceptable contrast media for HSG. Urografin 370, for instance, gives a satisfactory contrast density and has sufficient viscosity, but causes pain in most cases (Whitehouse & Sausman, 1981). Pain during HSG can be reduced by the use of a Foley catheter, rather than a rigid cannula with the use of volsellum forceps (Yoder, 1988). The presence and severity of pain during the injection of contrast medium depends on the volume and rate of injection (Whitehouse, 1981). However, the pain that occurs after completion of the injection may be due to the direct irritant effect of contrast medium on the pelvic peritoneum (Woltz et al, 1958). Hyperaemia has been induced in peritoneum of the rat following direct contact with contrast media used in HSG (Scila et al, 1962).

The injection of a hyperosmolar agent would theoretically be considered more likely to cause peritoneal irritation than would a low-osmolar contrast medium. This has not been found in practice when the non-ionic contrast medium metrizamide and hyperosmolar agents of the same concentration caused no significant differences in discomfort and pain during and after HSG (Stiris & Andrew, 1979; Cold et al, 1983). Russell and Maguire (1979) reported no difference between the same concentrations of metrizamide and Dimer X, an early mono-acid dimeric contrast medium, with regard to pain after injection, radiographic quality or ease of injection. Comparing the low-osmolar but ionic mono-acid dimer Hexabrix with methyl glucamine diatrizoate, Winfield et al (1984) found no difference in the degree of discomfort during the injection of contrast medium or within the next 30 min. More patients experienced delayed discomfort at 24 h with the hyperosmolar diatrizoate than with Hexabrix, although this trend showed no statistically significant difference. Davies et al (1985) also compared Hexabrix (320 mgI/ml) and a hyperosmolar agent, meglumine iothalamate (280 mgI/ml), and found no difference in abdominal pain during contrast medium injection, at 10–15 minutes after the examination or during the 6 days following HSG. This assessment of delayed pain showed that this symptom was most frequent and severe during the evening after the investigation.

The non-ionic dimer iotrolan has already been found to be a well tolerated contrast medium in peripheral arteriography (Hagen & Wenzel-Hora, 1989), myelography (Hammer & Deisenhammer, 1985) and selective bronchography (Morcos et al, 1989). Iotrolan has a satisfactory viscosity, when warmed to body temperature, as reflected by the relative ease of injection and the lack of vaginal back flow.

The viscosity of iotrolan (300 mgI/ml) is 16.4 mPas at 20°C, a value that is appreciably higher than the optimal range of viscosity for hysterosalpingographic contrast media. Warming the contrast medium to body temperature before injection into a body cavity is widely regarded, mainly on hypothetical grounds, to be an appropriate procedure. In the case of HSG, the warmer contrast medium may possibly reduce the chance of inducing smooth muscle spasm in the uterus and fallopian tubes.

One small series, comparing iotrolan with the non-ionic agent iohexol and an ionic diatrizoate in HSG, found little difference in the incidence of pain but a significantly greater intensity of pain with the diatrizoate than with both the low-osmolar agents (Wolf & Fitzal, 1989). The pain with iotrolan and iohexol lasted no more than 3 min. In a few of the diatrizoate cases the pain lasted for 4 min or more but, as with the other two contrast media, the duration of pain was for no more than a minute in the majority of cases.

The only significant difference between iotrolan and Urografin 370 in the present study was in the reduced incidence and decreased severity of delayed pain, probably related to the very low osmolality of iotrolan.

Acknowledgments

We are grateful to Schering Health Care Ltd, and especially to Dr E. C. Carter, for supplying the contrast media used in this study.

References

COLD, A. S., HASEN, K. F., PEDERSEN, P. R. & PEDERSON, J., 1983. Biviskinear of Urografin of Amipaque ved hysterosalpingographie. *Ugeskr. Laeger*, *145*, 1304–1306.

DAVIES, A. C., KEITHLEY, A., BORTHWICK-CLARKE, A. & WALTERS, H. L., 1985. The use of a low-osmolality contrast medium in hysterosalpingography: comparison with a conventional contrast medium. *Clinical Radiology*, *36*, 533–536.

DIETZ, W., 1952. Hysterosalpingography with water soluble contrast media. *Forschritte auf dem Gebiete der Röntgenstrahlen*, *77*, 224–229.

HAGEN, B. & WENZEL-HORA, B. I., 1989. Initial experience with a non-ionic, dimeric contrast medium (iotrolan) in direct and indirect arteriography: a randomized, intraindividual double-blind study in 60 patients. In *Recent Developments in Non-ionic Contrast Media*, ed. by V. Taenzer & S. Wende (Georg Thieme Verlag, Stuttgart & New York), pp. 54–60.

HAMMER, B. & DEISENHAMMER, E., 1985. Iotrol, a new water soluble non-ionic dimeric contrast medium for intrathecal use. *Neuroradiology*, *27*, 337–341.

MORCOS, S. K., BAUDOUIN, S. V., ANDERSON, P. B. BEEDIE, R. & BURY, R. W., 1989. Iotrolan in selective bronchography via a fibreoptic bronchoscope. *British Journal of Radiology*, *62*, 383–385.

RUSSELL, J. G. B. & MAGUIRE, B. G., 1979. Metrizamide in hysterosalpingography. *British Journal of Radiology*, *52*, 421–422.

SCILA, P., GRONROOS, M., KAVPPILA, O. & PYKONEN, L., 1962. Water soluble, viscosized water soluble and iodized oily contrast media in hysterosalpingography. *Acta Radiologica, Supplement 218*.

STIRIS, G. & ANDREW, E., 1979. Hysterosalpingography with Amipaque. *Radiology*, *130*, 795–796.

WHITEHOUSE, G. H., 1981. *Gynaecological Radiology* (Blackwell Scientific Publications, Oxford & London), p. 23.

WHITEHOUSE, G. H., 1988. Contrast media in gynaecology and obstetrics. In *Contrast Media*, ed. by D. H. Carr (Churchill Livingstone, Edinburgh & London), pp. 202–211.

WHITEHOUSE, G. H. & SAUSMAN, C., 1981. A comparison between two hysterosalpingographic contrast media—Urografin 370 and Isteropac. *British Journal of Radiology*, *54*, 429–430.

WINFIELD, A. C., MAXSON, W. S., HARDING, D. R., DIGGS, J. & WENTZ, A. C., 1984. Hexabrix as a contrast agent for hysterosalpingography. *Investigative Radiology*, *19*, 5389–5390.

WOLF, G. & FITZAL, P., 1989. Hysterosalpingography with a new contrast medium. In *Recent Developments in Non-ionic Contrast Media*, ed. by V. Taenzer & S. Wende (Georg Thieme Verlag, Stuttgart & New York) pp. 190–194.

WOLTZ, J. H. E., BRADFORD, W. Z., BRADFORD, W. B. & MCCOY, J. B., 1958. Complications of hysterosalpingography. *Journal of Obstetrics and Gynaecology*, *76*, 736–741.

YODER, I., 1988. *Hysterosalpingography and Pelvic Ultrasound: Imaging in Infertility and Gynaecology* (Little, Brown & Co., Boston & Toronto), pp. 7–15.

1991, *The British Journal of Radiology*, *64*, 591–595

Real-time digital contrast enhancement and magnification in the assessment of acute elbow injuries

By P. Holland, FRCR, A. M. Davies, FRCR, E. Morris, FRCR, J. Fowler, FRCR,
R. Wellings, FRCR and P. N. M. Tyrrell, MRCP

Department of Radiology, Birmingham General Hospital, Birmingham, UK

(*Received November 1990*)

Keywords: Digital image, Enhancement, Magnification, Elbow injury

Abstract. The elbow is a common site of injury and missed fractures may lead to disability and litigation. An assessment was made of a commercially available desk-top digital contrast enhancement and magnification unit (DETECT system) in a series of 320 patients with an acute elbow injury. Five radiologists of varying experience independently viewed elbow radiographs on a conventional light-box, and subsequently using the digitizer, indicating the presence or absence of a fracture. The overall results demonstrated no difference in performance when using the unit, though small improvements in the confidence with which a definite diagnosis was made were observed. Assessment of soft tissues with the digitizer was less reliable.

Plain film radiography remains the mainstay of imaging in acute elbow trauma despite the introduction of alternative imaging techniques. Computed tomography (CT) in patients with an elbow fracture can provide useful information and change management (Franklin et al, 1988). Soft-tissue changes in particular are easier to assess. Arthrography (Eto et al, 1975; Pavlov et al, 1979; Hudson, 1981; Blane et al, 1984) and CT arthrography (Singson et al, 1986) have been used, but are most useful in the post-traumatic assessment of loose bodies, osteochondral fractures and ligamentous damage. Ultrasound (Dias et al, 1988; Miles & Lamont, 1989) is of limited use. Supplementary radiography such as the radial head-capitellum view is said by some to improve the diagnosis of elbow fractures (Greenspan et al, 1984; Greenspan & Norman, 1987), but its routine use is probably not justified (Hall-Craggs et al, 1985; Page, 1986). Any potential means of improving fracture detection would thus be useful. This study aimed to assess the performance of radiologists using a desk-top digital image enhancement unit, DETECT (Damon Corporation, Massachusetts) in the detection of elbow fractures.

Patients and methods

The radiographs of 320 patients presenting with an acute elbow injury to the Birmingham General Hospital were extracted from files. Criteria for entry to the study were a history of acute elbow trauma and adequate antero-posterior and lateral radiographs of the elbow. A definitive diagnosis of normal or fracture was made by a radiologist using all radiographs available, including additional views such as the radial head-capitellum view, and any follow-up radiographs.

Five radiologists with 2, 3, 4, 6 and 10 years radiological experience, respectively, separately assessed each patient's antero-posterior and lateral radiographs using a conventional light-box, a bright light and a magnifying glass as required. Each recorded the presence or absence of a joint effusion and of a fracture; the latter was also assigned a "degree of confidence", either definite normal, equivocal normal, equivocal abnormal or definite fracture. The site of suspected or definite fracture was noted.

At a later date, the same five radiologists, unaware of their original observations, repeated the exercise using a digitizing unit, the DETECT system (Damon Corporation, Massachusetts). This system uses a high-resolution video camera to view the radiographs, allowing up to × 10 magnification. The video signal is digitally processed and displayed on a television monitor in a 525 × 480 matrix with a dynamic range of over 2000 grey levels. The image is displayed in real time, there being a screen refresh rate of 30 times per minute. The unit allows for background subtraction, contrast enhancement and chromatic reversal (Wetzner & Newberg, 1988). An example is shown in Fig. 1.

Statistical analysis was performed to ascertain the performance of each radiologist with and without the digitizer.

Results

The group of 320 patients comprised 178 males and 142 females, with ages ranging from 6 to 73 years. There were 103 fractures, 83 (80.6%) of which were at the radial head or neck. Other fractures were supracondylar (6), medial epicondyle (2), lateral epicondyle (2), capitellum (1), olecranon (4) and coracoid (5). Of the radial head fractures, 35 were undisplaced fissure fractures, 38 impaction fractures, nine displaced fissure fractures and

---

Address correspondence to: Dr P. Holland, Senior Registrar, Department of Radiology, Birmingham General Hospital, Steelhouse Lane, Birmingham B4 6NH, UK.

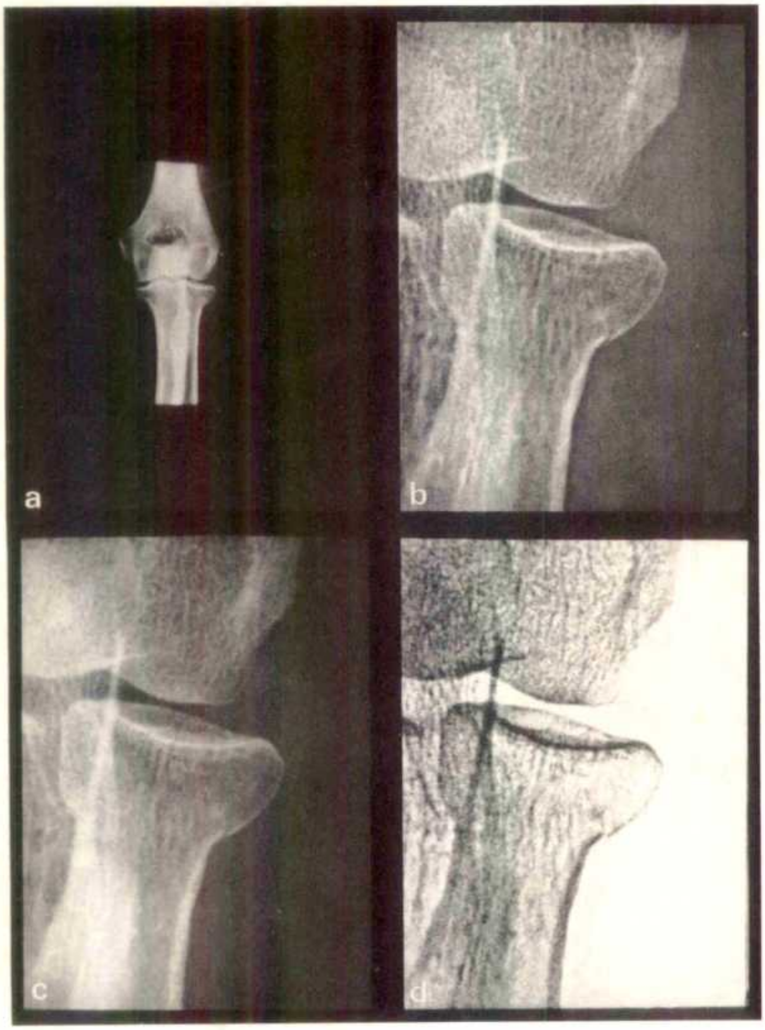

Figure 1. Antero-posterior projection of a subtle fracture in the head and neck of the radius. (a) Unenhanced/unmagnified image; (b) unenhanced × 5 magnification relative to (a); (c) contrast-enhanced × 5 magnification relative to (a); (d) contrast-enhanced × 5 magnification chromatic reversal relative to (a).

one greenstick fracture of the neck. Of the 103 fractures present, 12 had no visible joint effusion; eight of these were radial head or neck injuries.

The results for each radiologist and the combined group, based on the actual presence or absence of a fracture, are summarized in Fig. 2. To produce these figures, the radiologists equivocal and definite normal results were combined to produce a single normal category, and the equivocal abnormal and definite fracture observations added to give a single fracture category.

No significant differences were identified in the overall accuracy of each radiologist with and without the digitizer. The less experienced radiologists (A, B and C) showed either no change or minimal improvement in performance. Of the more experienced radiologists, one (D) performed slightly worse with the digitizer, whilst the other (E) performed slightly better. The combined results, however, show no overall change in performance, with virtually identical values for true positive, true negative, false positive, false negative, sensitivity, specificity, positive predictive value and negative predictive value (Fig. 2).

Although no differences were observed when results were expressed simply as fractured or normal, small differences were apparent when the definite observations were separated from the equivocal. All but one radiologist (B) identified a higher proportion of true elbow fractures as definite fractures using the digitizer compared with radiographs alone. The digitizer improved the definite true positive pick-up rate by a mean of 5.3% (range −2.9% to 9.7%) and the definite true negative pick-up rate by 4.3% (range −8.3% to 14.6%). This increased confidence in identifying definite results, however, was at the expense of correctly identifying fractures in the case of four radiologists (A, B, C, E) and of correctly identifying normality in one (D). Overall, there was a 7% (range 0.3–14.6%) shift of results from the equivocal to the definite categories using the

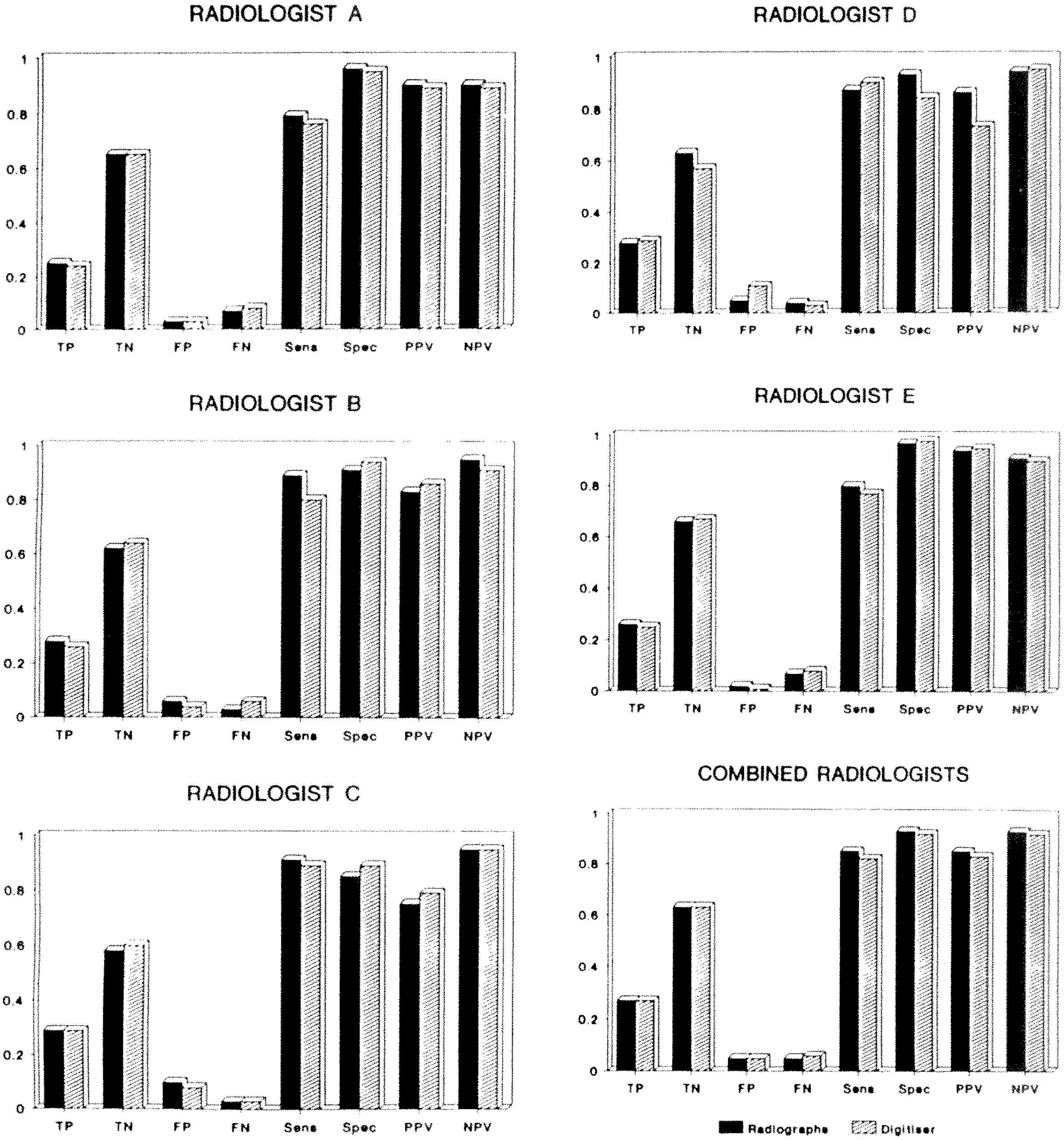

Figure 2. Accuracy of the radiologists' performance in assessing elbow injuries. The radiologists (A–E) are listed in ascending order of radiological experience. (TP = true positive; TN = true negative; FP = false positive; FN = false negative; Sens = sensitivity; Spec = specificity; PPV = positive predictive value; NPV = negative predictive value).

digitizer, with the least experienced radiologist showing the greatest change.

The most frequent fracture site was the radial head or neck. Overall, 84% (range 78–89%) of these fractures were correctly identified from the plain radiographs, but this detection rate decreased by 2.2% with the digitizer. Individually, this represented no change in two (A and C), a reduction in two (B and E, 12% and 3.7%, respectively) and an improvement in only one (D, 4.5%).

The radiologists as a group identified a joint effusion, as indicated by elevation of the anterior and posterior fat pads, in 39% of joints when viewing the radiographs on the light-box. Use of the digitizer resulted in a 2% decrease in this mean figure.

Discussion

Digital radiography is likely to be more widely available in the future (Dawood, 1990), but, at present, installing such a system is hampered by cost, image quality and a rapidly evolving technology. As these systems become more popular, however, it is important that radiologists be as confident in interrogating digital images as they are in interpreting plain radiographs. Several studies have compared the accuracy of digital images with conventional images produced in chest radiography (Fajardo et al, 1989; Hayrapetian et al, 1989; Sheline et al, 1989), mammography (Chan et al, 1987), gastrointestinal radiography (Kastan et al, 1987) and musculoskeletal radiography (Bramble et al, 1989; Murphey, 1989; Wegryn et al, 1990). These show that digital imaging at present can be as accurate, but no more so, as conventional radiographs in terms of diagnostic image quality (Murphey et al, 1990; Slasky et al, 1990).

This study used a table-top digitizing unit, which allows a radiograph to be examined in real time. Advantages of this system are that it is cheap, compact, independent and has the ability to magnify the radiograph before digital processing, thereby improving the resolution. Its main disadvantage is that a radiograph has to be taken and retained.

Our results show that in terms of sensitivity and specificity, the initial plain radiograph is accurate in identifying elbow fractures, and that overall performance was not altered by the digitizer, though the confidence with which each radiologist made a definite diagnosis was increased, albeit at the expense of identifying fractures in the majority. There were slight improvements in the definite true positive and definite true negative pick-up rates.

In a previous study using the digitizer to assess scaphoid fractures (Davies et al, 1990), the more experienced radiologists performed marginally better with the unit, although, as with this study, the combined results demonstrated no change. It too showed an increased confidence with which a definite diagnosis of fracture was made, but for the less experienced radiologists this was at the expense of identifying normality. A possible explanation for this was that the magnification and enhancement of the radiograph might accentuate normal anatomical features that the less experienced radiologist may interpret as an injury. The results of this study seem to suggest that normality was easier to identify and that fracture identification may be impaired in some way. Part of the problem may be our own perception of the visual data presented (Hendee, 1989). Detection of visual information is thought to occur very quickly, but the brain can be tricked into mistakes and illusions unless cognitive processes provide plausible interpretations of the perceptual hypotheses formed during the detection process. The introduction of a less familiar form of visual presentation, digitally enhanced images, may well disturb this detection-cognition process sufficient to produce poorer results, at least initially.

In a patient presenting with elbow trauma, a joint effusion is a strong indication that a fracture is likely to be present (Norrell, 1954; Bledsoe & Izanstark, 1959; Bohrer, 1970). Moorwood (1987) showed that of patients with an elbow effusion but no visible fracture at presentation, 29% were subsequently shown to have radial head or neck fractures, and so advocated follow-up radiographs in such a situation. This is considered unnecessary by some (Nutton, 1987; Wray, 1987) as the treatment remains the same whether or not a subtle fracture is visible, and current management would advocate early active mobilization (Rockwood & Green, 1984; Holdsworth et al, 1987). However, it could be dangerous to assume a fracture, without attempting to identify it, especially in a child's elbow where, for instance, an epicondylar injury can be overlooked with disastrous consequences.

In this study, 30 patients had effusions without evidence of a fracture. Most had supplementary views, but only a few were followed up. To our knowledge, none have since presented with evidence of a missed fracture. Perhaps more interesting are the 12 patients in whom a fracture was identified but no joint effusion was visible. Eight of these injuries involved the radial head or neck. Kohn (1959) observed that failure to see the fat pads where an intracapsular effusion must be present occurred relatively commonly (13%). Sub-optimal radiography might be in part responsible for this, and the slightly poorer performance shown in this study in identifying effusions with the digitizer suggests that the unit may not help overcome this technical problem. Davies et al (1990) showed an apparent loss of accuracy with the digitizer when assessing wrist fat planes, though this seemed to be in favour of accentuation rather than obliteration of these planes.

Conclusion

In a series of patients presenting with acute elbow trauma, we have shown no significant difference in the overall rate of fracture detection when the radiographs are viewed alone and with a desk-top contrast enhancer and magnifier. A small improvement in the confidence with which fractures were correctly identified was observed, but this was at the expense of missing some fractures. Assessment of soft tissues with the unit appears marginally impaired.

Acknowledgments

We are grateful to Mrs E. M. Davies for performing the statistical analysis, Mrs D. Gregory for extracting films and Draeger Ltd, Hemel Hempstead, for the loan of the DETECT system.

References

Blane, C. E., Kling, T. F., Andrews, J. C., DiPietro, M. A. & Hensinger, R. N., 1984. Arthrography in the post-traumatic elbow in children. *American Journal of Roentgenology, 143*, 17–21.

Bledsoe, R. C. & Izenstark, J. L., 1959. Displacement of fat pads in disease and injury of the elbow. *Radiology, 73*, 717–724.

Bohrer, S. P., 1970. The fat pad sign following elbow trauma. Its usefulness and reliability in suspecting "invisible" fractures. *Clinical Radiology, 21*, 90–94.

Bramble, J. M., Cook, L. T., Murphey, M. D., Martin, N. L., Anderson, W. H. & Hensley, K. B., 1989. Image data compression in magnification hand radiographs. *Radiology, 170*, 133–136.

Chan, H. P., Vyborny, C. J., MacMahon, H., Metz, C. E., Doi, K. & Sickles, E. A., 1987. Digital mammography: ROC studies of the effects of pixel size and unsharp-mask filtering on the detection of subtle microcalcifications. *Investigative Radiology, 22*, 581–589.

Davies, A. M., Morris, E., Manns, R. A., Fowler, J. & Wellings, R. M., 1990. Real-time digital contrast enhancement and magnification in the assessment of scaphoid and other wrist injuries. *British Journal of Radiology, 63*, 934–939.

Dawood, R., 1990. Editorial. Digital radiology—a realistic prospect? *Clinical Radiology, 42*, 6–11.

Dias, J. J., Lamont, A. C. & Jones, J. M., 1988. Ultrasonic diagnosis of neonatal separation of the distal humeral epiphysis. *Journal of Bone and Joint Surgery, 70B*, 825–828.

Eto, R. T., Anderson, P. W. & Harley, J. D., 1975. Elbow arthrography with the application of tomography. *Radiology, 115*, 283–288.

Fajardo, L. L., Hillman, B. J., Pond, G. D., Carmody, R. F., Johnson, J. E. & Ferrell, W. R., 1989. Detection of pneumothorax: comparison of digital and conventional chest imaging. *American Journal of Roentgenology, 152*, 475–480.

Franklin, P. D., Dunlop, R. W., Whitelaw, G., Jacques, E., Blickman, J. G. & Shapiro, J. H., 1988. Computed tomography of the normal and traumatized elbow. *Journal of Computer Assisted Tomography, 12*, 817–823.

Greenspan, A. & Norman, A., 1987. Radial head-capitellum view: an expanded imaging approach to elbow injury. *Radiology, 164*, 272–274.

Greenspan, A., Norman, A. & Roser, H., 1984. Radial head-capitellum view in elbow trauma: clinical application and radiographic–anatomic correlation. *American Journal of Roentgenology, 143*, 355–359.

Hall-Craggs, M. A., Shorvon, P. J. & Chapman, M., 1985. Assessment of the radial head-capitellum view and the dorsal fat pad sign in acute elbow trauma. *American Journal of Roentgenology, 145*, 607–609.

Hayrapetian, A., Aberle, D. R., Huang, H. R., Fiske, R., Morioka, C., Valantino, D. & Boechst, M. I., 1989. Comparison of 2048 line digital display format and conventional radiographs: a ROC study. *American Journal of Roentgenology, 152*, 1113–1118.

Hendee, W. R., 1989. The perception of visual data: a summary of the ACR meeting on visualisation sciences in engineering, computing and medicine. *American Journal of Roentgenology, 152*, 1313–1315.

Holdsworth, B. J., Clement, D. A. & Rothwell, P. N. R., 1987. Fractures of the radial head—the benefit of aspiration: a prospective controlled trial. *Injury, 18*, 44–47.

Hudson, T. M., 1981. Elbow arthrography. *Radiological Clinics of North America, 19*, 227–241.

Kastan, D. J., Ackerman, L. V. & Feczko, P. J., 1987. Digital gastrointestinal imaging: the effect of pixel size on detection of subtle mucosal abnormalities. *Radiology, 162*, 853–856.

Kohn, A. M., 1959. Soft tissue alterations in elbow trauma. *American Journal of Roentgenology, 82*, 867–874.

Miles, K. A. & Lamont, A. C., 1989. Ultrasonic demonstration of the elbow fat pads. *Clinical Radiology, 40*, 602–604.

Moorwood, D. J. W., 1987. Incidence of unsuspected fractures in traumatic effusions of the elbow joint. *British Medical Journal, 295*, 109–110.

Murphey, M. D., 1989. Digital skeletal radiography: spatial resolution requirements for detection of subperiosteal resorption. *American Journal of Roentgenology, 152*, 541–546.

Murphey, M. D., Bramble, J. M., Cook, L. T., Martin, N. L. & Dwyer, S. J., 1990. Nondisplaced fractures: spatial resolution requirements for detection with digital skeletal imaging. *Radiology, 174*, 865–870.

Norrell, H. G., 1954. Roentgenologic visualisation of the extracapsular fat, its importance in the diagnosis of traumatic injuries to the elbow. *Acta Radiologica, 42*, 205–210.

Nutton, R. W., 1987. Incidence of unsuspected fractures in traumatic effusions of the elbow joint (letter). *British Medical Journal, 295*, 329.

Page, A. C., 1986. Critical examination of the radial head-capitellum view in elbow trauma. *American Journal of Roentgenology, 146*, 81–82.

Pavlov, H., Ghelman, B. & Warren, R. F., 1979. Double contrast arthrography of the elbow. *Radiology, 130*, 87–95.

Rockwood, C. A. & Green, D. P., 1984. *Fractures in Adults*, 2nd edn. (Lippincott, Philadelphia), pp. 559–652.

Sheline, M. E., Brikman, I., Epstein, D. M., Mezrich, J. L., Kundel, H. L. & Arenson, R. L., 1989. The diagnosis of pulmonary nodules: comparison between standard and inverse digitised images and conventional chest radiographs. *American Journal of Roentgenology, 152*, 261–263.

Singson, R. D., Feldman, F. & Rosenberg, Z. S., 1986. Elbow joint: assessment with double contrast CT arthrography. *Radiology, 160*, 167–173.

Slasky, B. S., Gur, D., Good, W. F., Costa-Greco, M. A., Harris, K. M., Cooperstein, L. A. & Rockette, H. E., 1990. Receiver operating characteristic analysis of chest image interpretation with conventional, laser-printed, and high-resolution workstation images. *Radiology, 174*, 775–780.

Wegryn, S. A., Piraino, D. W., Richmond, B. J., Schluchter, M. D., Uetani, M., Freed, H. A., Meziane, M. A. & Belhobek, G. A., 1990. Comparison of digital and conventional musculoskeletal radiography: an observer performance study. *Radiology, 175*, 225–228.

Wetzner, S. M. & Newberg, A. M., 1988. Digitally enhanced radiography. Presented as "Work in progress" at the RSNA Chicago Meeting, November 1988. *Radiology, 169* (Suppl.), 374.

Wray, C. C., 1987. Incidence of unsuspected fractures in traumatic effusions of the elbow joint (letter). *British Medical Journal, 295*, 329.

1991, *The British Journal of Radiology*, *64*, 596–602

Clinical application of an electronic imaging device for assisting patient set-up in radiotherapy

By *J. Penelope Wade, BSc, MSc and David Nicholas, BSc, PhD

Radiotherapy Physics Department, Norfolk and Norwich Hospital, Norwich, UK

(*Received October 1990 and in revised form December 1990*)

Keywords: Radiotherapy, Treatment verification, Digital imaging, Portal imaging

Abstract. As radiotherapy treatment set-ups are becoming more complicated and a greater emphasis is placed on accuracy, there is an increasing need to verify and record the actual treatments being given. A direct electronic imaging device is currently marketed by Varian (the DYNARAY ID), which uses the latest technology in detection and image processing to obtain digital images of the patient's anatomy using the actual treatment beam. At Norwich we have been using a prototype machine in a busy district radiotherapy centre and have examined over 50 patients. We have found the images easy to obtain and the technique superior to the standard practice of using verification radiographs. The role of this device lies in aiding quality assurance of treatments whilst generating a permanent record of the actual treatment given.

Commercial availability of linear accelerators with complex treatment beam collimation and computer-controlled movements permits the delivery of complex dose distributions within the patient to a high degree of accuracy. Such accuracy is only relevant provided the radiation field relative to the treatment volume can be monitored to a similar degree of accuracy, once the patient has been set-up on the treatment machine. Any verification method must provide images that are capable of resolving the anatomy necessary for the observer to decide confidently on the presence of a field or shielding block placement error.

For most radiotherapy centres the established methods for verifying a treatment are limited. The most common procedure is to place photographic film in the way of the beam exiting from the patient, adopting either a double-exposure technique or leaving long-exposure film in position for the whole of one treatment exposure (AAPM, 1988). The disadvantages of these verification radiography are the limited contrast and poor sharpness, the cost of the film and the delay in image availability due to film processing. There have been numerous attempts at increasing the contrast in verification radiographs by designing special cassettes (Droege & Bjarngard, 1979), digitizing films using densitometers (Meertens, 1985) or laser-scanned microdensitometers (Powlis et al, 1988) to enable the use of digital enhancement techniques, or gamma multiplication (Reinstein & Orton, 1979). Unfortunately none of these provide rapid image availability.

More recent technological developments have concentrated on imaging devices using either fluoroscopy combined with an analogue system (Bailey et al, 1980), or digital image processing (Leong, 1986; Suit et al, 1988). Other imaging devices are being developed that consist of arrays of detectors tracking across the treatment field (Taborsky et al, 1982; Lam et al, 1986); these systems tend to have long scanning or processing times that can exceed the treatment duration, although more recent work (Morton & Swindell, 1987) suggests that these times can be reduced. Currently there is a need for a digital imaging device that is simple to use and set up, provides the necessary contrast and spatial resolution and produces an image with sufficient speed for appropriate action to be taken when necessary. At Norwich, a practical assessment has been undertaken of a system that appears to fulfill these criteria.

Imaging device and methods

At the Netherlands Cancer Institute a technique has been developed that uses a matrix ionization chamber as the detector (Meertens et al, 1985; van Herk & Meertens, 1987, 1988). The imaging device is commercially available from Varian (formerly from Asea Brown Boveri) and named the DYNARAY ID. We have been evaluating a prototype machine for the past 6 months at the Norfolk and Norwich Hospital. The imaging device consists of a cassette, which holds the detector, connected by a single lead to a personal computer (Fig. 1). The detector is a flat, liquid-filled ionization chamber with the cover plates divided into strips forming a matrix of 256 × 256 cells. The physical area of the detector is 325 × 325 mm, which makes each cell 1.27 mm square. The detector is set into a cassette with dimensions 520 mm × 520 mm × 50 mm, which also contains all the amplifiers and switching electronics. The cassette is quite portable as it weighs less than 5 kg.

Address for correspondence: Department of Radiotherapy Physics, Norfolk and Norwich Hospital, Brunswick Road, Norwich, Norfolk NR1 3SR, UK.

*Present address: East Anglian Regional Radiation Protection Service, Addenbrookes Hospital, Hills Road, Cambridge CB2 2QQ, UK.

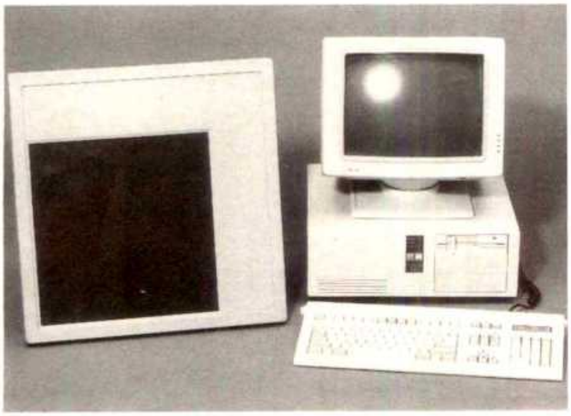

Figure 1. Studio view of the imaging device.

The computer compiles, processes and displays the image using the information received from the detector. The software is written in "C" and runs under the standard MSDOS operating system. The operating procedures are controlled by single stroke "function keys", which enable ease of use. The software package controlling the device is divided into five sections: image acquisition, image processing, image management, calibration/control and digitization from camera. The last section was introduced in a software update in order to compare images with digital information from an alternative source, and was not considered during the present clinical evaluation. The "calibration/control" mode gives the user the opportunity to select and set up parameters for a particular treatment machine. This is necessary for linear accelerators where the timing of data acquisition needs to be synchronized to the pulsed radiation and the cells are read while the radiation is on. Any corrections for dose-rate can also be incorporated at this stage. Parameters for up to four treatment machines may be stored and the machine currently selected is always displayed on the screen. The "processing" mode allows the user to enhance certain aspects of the image by adjusting the contrast, grey-scale display or spatial detail by using the various software filters available. The images are stored on 1.2 Megabyte, 5.25 in floppy disks, which can hold a total of nine images; image compression is not yet used. The images are displayed on a colour monitor where the size of the image on the screen corresponds to the whole detector area. There is also the option to support a video printer to obtain hard copies.

The DYNARAY ID imaging device has been used primarily with a Radiation Dynamics 5.4 MeV linear accelerator, and occasionally used on a Mobatron F100 cobalt treatment machine. The detection cassette should ideally be mounted as close to the patient as possible for maximum resolution and supported at any angle so that all fields can be imaged. Two simple support frames were constructed, using DEXION Speedframe$_R$, one to hold the detection cassette horizontally and the other to hold it vertically. This enabled us to take images of treatment fields at gantry angles of 0°, 90° and 270°. It has been suggested that the detection cassette could either be supported in a primary beam stopper, or separately attached to the gantry of the treatment machine. As the detection cassette is currently free-standing it is positioned after the patient is set up for treatment. The detection cassette in its stand is still relatively light so it can be carried and positioned by one person, who would normally be a therapy radiographer. Alignment of the detection cassette with the treatment field was aided by marks on the floor and the existing patient alignment lasers. A distance of 1.5 m between the focus of the linear accelerator and the detection cassette was chosen for both horizontal and vertical set-ups. There has only been one patient out of the 56 imaged who could not be accommodated within this set-up.

The image acquisition time is very fast, as the imaging device takes only 5 seconds to actually record an image. This is then displayed directly from memory on to the colour monitor. The image is therefore available during the treatment exposure and it is also feasible to use a short radiation exposure to check positioning before the main treatment is delivered. For a dose-rate of 3.5 Gy/min, an image can be obtained during an exposure of 0.4 Gy, which includes a time allowance for the dose-rate build-up. This acquisition time may vary, depending on the machine in use and its reliability. The short acquisition time allows multiple images to be taken during a treatment exposure to monitor patient movement. The device will automatically record an image every 5 seconds, then these images are displayed as either four images at quarter size or one full image on the monitor.

At Norwich we have been taking the images during the patient's normal treatment and exposing a verification film of the treatment field at the same time, thus enabling direct comparison of the two techniques to be made. A number of patients were imaged on different days during their course of treatment thus enabling any shifts in set-up to be studied. The verification film used was Kodak X-omat V film, which required an exposure of 0.8–1.0 Gy, so that it could be left in position during the whole treatment exposure and the patient's position need not be disturbed until afterwards. At this centre the technique of using metal screens for enhancing a film image has never been used, so that only those verification films which are in close contact with the patient provide adequate contrast. As a consequence verification films that were exposed during lateral treatment fields were of very poor quality. As our intention is not to provide a full physical assessment of the imaging device, comparison with optimal film techniques were not performed.

Results

Over 90 images of patient treatments were recorded on the two treatment machines, with 88 images to date taken on the linear accelerator. The reasons for the

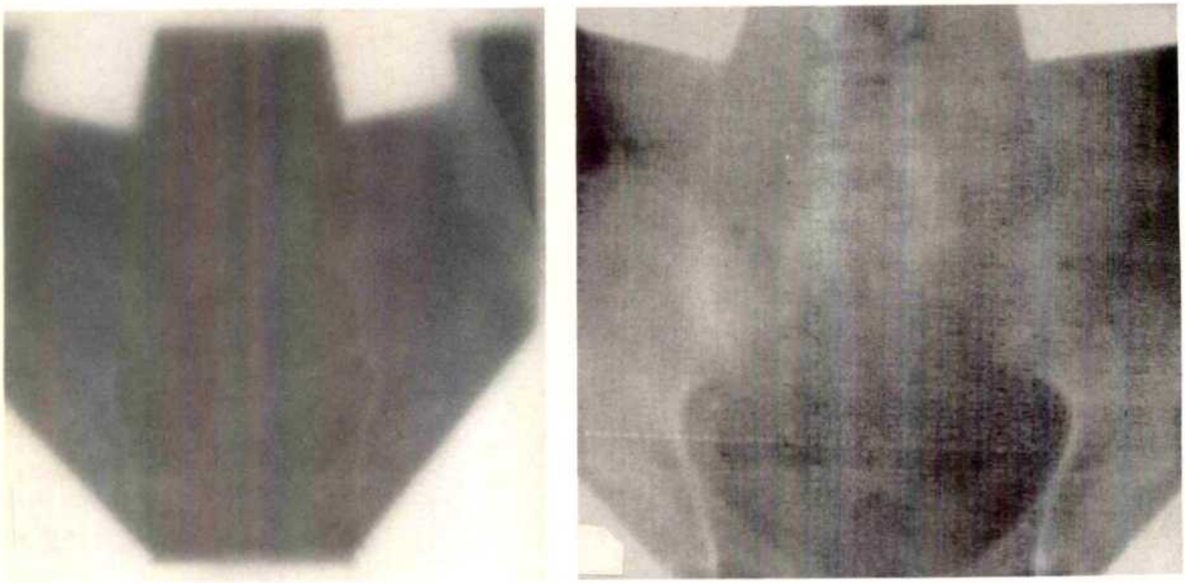
(a) (b)

Figure 2. Anterior pelvic views obtained by (a) convential verification radiograph and (b) Dynaray ID.

small number of images recorded on the cobalt machine were the unsuitability of the set-ups and the range of gantry angles for the beams being used (because of the way the workload is divided in the department). A wide range of anatomical sites have been imaged from the head to the pelvis (Table I). Positioning of the device was accurate to within ±2 mm; however, as intra-comparison of the fields and anatomy is only being considered, this is not of great significance.

Thirty-seven anterior fields and five lateral fields to sites in the pelvis, including uterus, bladder and prostate, have been imaged on 19 different patients, 12 of whom had their treatment monitored on more than one day. Several of these images demonstrated a shift in the positioning of the treatment field compared with anatomical details and in two cases this shift was 2 cm or more. Conversely, four images recorded from one patient all showed excellent reproducibility. Each shift in positioning of the field is easily quantified by noting the change in cell co-ordinates for a particular anatomical feature. The lateral pelvic views were more difficult to study as they were of smaller dimensions and contained fewer anatomical features. All the anterior images were compared with the verification radiographs produced in the same exposure and also localization radiographs obtained on the simulator. An example of the DYNARAY ID image and verification radiograph image of a pelvis is shown in Fig. 2.

Table I. Range of treatment fields imaged

Field definition	No. of patients	No. of views	Cobalt
Pelvis AP	15	31	1
Pelvis lateral	3	5	
Abdominal bath	2	3	
Hip AP	3	3	
Dog leg	1	3	
Chest AP	4	4	
Bronchus AP	5	5	1
Spine PA	2	4	
Breast peripheral	4	9	2
S/Clavical	4	5	
Mantle	1	2	
Neck AP	5	6	1
Neck lateral	3	6	
Head AP	1	1	
Head lateral	3	6	
Total	56	93	5

Nine images were recorded of thoracic sites, including oesophagus, sternum and bronchus. Because these treatment fields included lung as well as skeletal structures it is much easier to assess any errors in positioning. This set of digital images showed good contrast with very little need for image enhancement. In a further nine images involving peripheral breast fields, lead blocks were used to shield the lung, oesophagus and/or humerus heads. The device allowed a clear assessment of the positioning of the shielding blocks and the adequacy of their function. Unfortunately the humerus bones could not be resolved on the verification radiographs so the positioning of the blocks shielding the humerus heads could not be confirmed, as shown in Fig. 3. One digital image demonstrated that the oesophageal shielding was not correctly placed which was not apparent on the verification radiograph.

Only one "mantle" patient has been treated during our trial period with the DYNARAY ID imaging device. This patient was treated at a focus–skin

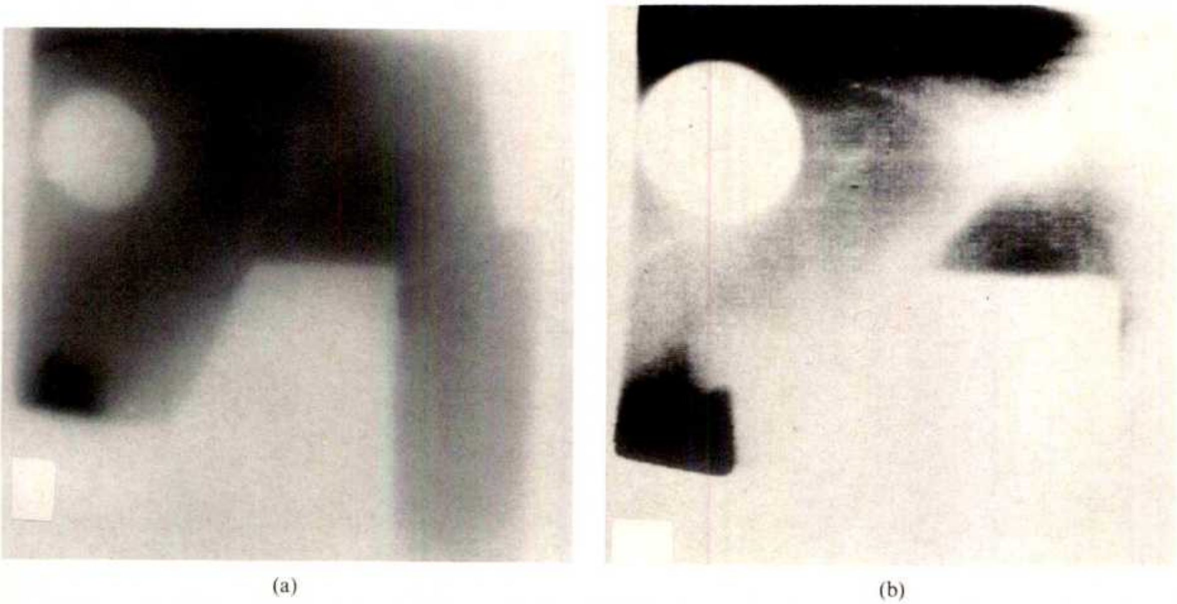
(a) (b)

Figure 3. Images obtained from a peripheral breast treatment incorporating shielding to the head of the humerus and lung; (a) conventional verification radiograph, (b) Dynaray ID.

distance of 1.4 m with the detector cassette placed at 1.79 m from the focus. Despite using the standard set-up machine parameters on the computer, no loss in picture quality was detected due to the increased distances and lower dose-rate involved. Again the digital images contained greater contrast than the corresponding verification radiographs.

A total of 17 different lateral treatment fields have been imaged, including the five pelvic fields mentioned above, with none of these fields repeated on subsequent days. The other 12 images have been of treatment fields used to treat head and neck sites. Only half of these images had corresponding verification radiographs taken owing to the exceedingly poor image quality being obtained. For fields treating the whole brain the imaging device displayed only a limited amount of information, namely the edge of the skull and the pituitary fossa. The images of the treatment fields for the pituitary were small so that it was difficult to identify any anatomical structures.

In the simulator views the edges of the fields are marked with wires to distinguish the treatment volume from the surrounding structures. Similar surrounding anatomical information would also be useful when looking at small fields with the imaging device on the treatment machine. If the detector on the DYNARAY ID device is calibrated to image a small treatment field then it is still possible to image structures surrounding the treatment field, as the detector area outside the beam will respond to a different dose range to the detector area inside the beam and should be sensitive enough to record the smaller doses in these areas. We have been able to do this on phantoms but not on a patient as yet, because of the very low dose-rates involved.

The images of lateral treatment fields for treating the larynx are particularly good, as the tongue, trachea, jaw, vallecula and epiglottis can all be seen. A digital image together with a corresponding simulator image are shown in Fig. 4. Most of the anatomy in this treatment field is soft tissue, where it is inherently much harder to obtain contrast variation. There are no verification radiographs of these fields for comparison because of their total unsuitability.

The radiographers demonstrated a great deal of interest in using this device, and they were encouraged to suggest patients to be imaged, particularly where it would be of benefit to have feedback on the field set-up. They also found it reassuring when a difficult set-up, such as one involving a patient with mobile marks, was confirmed to be correct.

The short acquisition time allowed the images to be viewed before the end of the treatment exposure. We found that it was easier to have one person dedicated to operating the DYNARAY ID imaging device, controlling the image acquisition, the input of patient identifiers and the storage of images, while other radiographers continued with the routine of patient treatment.

Discussion

The verification of treatment fields in a busy radiotherapy department requires careful planning. Whether verification should include all treatment fields on the first day of a course of treatment, or just selected sites and techniques, such as all fields using beam blocks, will

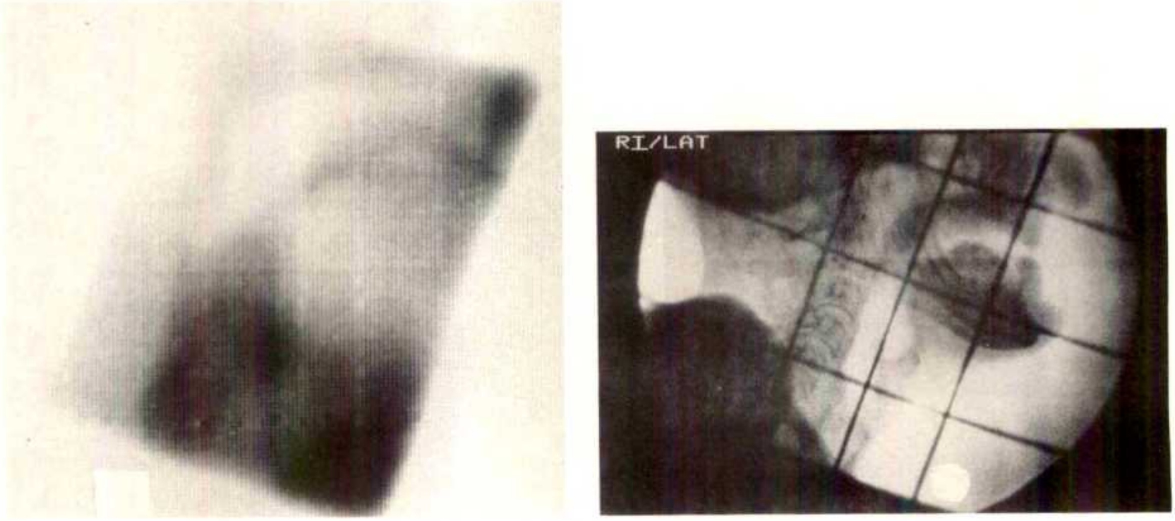

(a) (b)

Figure 4. Lateral view of a treatment of the larynx obtained by (a) Dynaray ID and (b) the simulator localization image.

be determined by the department's needs. There are a number of papers already written to aid this decision (Marks et al, 1976; Byhardt et al, 1978; Griffiths & Pearcey, 1986). In our department it is felt that priority should be given to verifying those treatments incorporating shielding blocks.

Radiotherapists and radiographers are familiar with anterior and lateral views for most treatment sites and so can readily identify anatomical features when seen in simulator and verification images. When it comes to oblique fields the task is more difficult and there is a greater need to have simulation radiographs of all the treatment fields being verified, so that an accurate comparison of positioning can be made. Future support systems for the detection cassette must enable the device to be used in most machine configurations. An attachment to the machine gantry or "beam stopper" appears to be the most promising solution. Currently some of the characteristics of the detector change slightly with orientation, requiring the detector to be recalibrated for every change in orientation. In practice this means that the anterior and lateral fields cannot both be imaged on a patient during a single treatment session, as the patient would have to leave the treatment room for recalibration to take place. We have been assured that this problem will not occur on the production model of the detector.

Treatment sites in the head, neck and thorax lend themselves to verification as the presence of air and dense bone produce large contrast variations. At the energies used in radiotherapy treatment, the X-rays are highly penetrating, which means that much smaller changes in contrast have to be detected than in diagnostic imaging. For example, at 6 MeV a 4% attenuation could be produced by 9 mm of tissue or 6 mm of bone. For an equivalent attenuation at 100 kVp, only 1.1 mm of tissue or 0.3 mm of bone are required. The problem of producing images displaying adequate contrast appears to have been resolved by the DYNARAY ID where the information content available is considerably better than that provided by a verification radiograph.

The tolerance for errors in positioning of fields is another area to be addressed if verification is to be used sensibly in a department. The accuracy of the patient set-up may be of more importance for some tumour sites than others, a subject that has been investigated by several authors (Pearcey & Griffiths, 1985; Rabinowitz et al, 1985). Actual treatment field placement errors were easily detected and quantified. With the current software it is also possible to display the most recently acquired image beside a stored image. This facility makes visual comparison between set-ups on different days or changes within an on-going treatment easy to note. One such comparison is shown in Fig. 5; the images are of a "dog-leg" technique (used in the treatment of seminoma) and recorded on consecutive days. The shielding blocks are positioned using skin marks. It can be seen from the two images that there has been a change in the area treated; this was within acceptable limits and no modification to the patient's treatment was necessary.

There is a problem with small fields that contain few recognizable anatomical features. Here, information on structures outside the treatment field would be useful as would the ability to expand the image to fill the screen. We understand that these facilities will also be available on the production model.

Additional software facilities enable various image

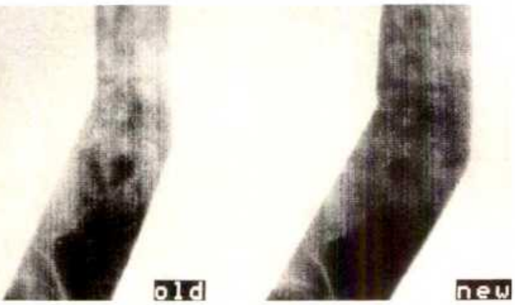

Figure 5. Comparison of two Dynaray ID images taken on different days for the same patient undergoing a "dog-leg" treatment technique.

enhancement techniques to be applied to the raw image. Figure 6 shows an original image and three enhanced versions. Specific details of the filters have not been released to date; however, the combined filter does improve the soft-tissue/air boundary definition without detracting from the general soft-tissue contrast. Further details relating to the software will be reported elsewhere.

Conclusions

The DYNARAY ID imaging device heralds a new generation of equipment available to radiotherapy centres, and as awareness of the need for quality assurance increases so the use of verification will increase. Previous concern about the use of verification techniques was due primarily to the poor image quality of film; this has been greatly improved with this device. We have found the device easy to use, the detector cassette easy to position and the software straightforward to follow. Departments that use techniques such as dynamic or conformation therapy should find such a device invaluable for providing a record of the treatment actually given to the patient, since multiple images can be taken throughout a single treatment exposure. The same advantages would apply equally where any beam modifiers are used. The short image acquisition and display time coupled with the image-enhancement software currently available gives the DYNARAY ID imaging device many advantages over conventional verification radiograph techniques.

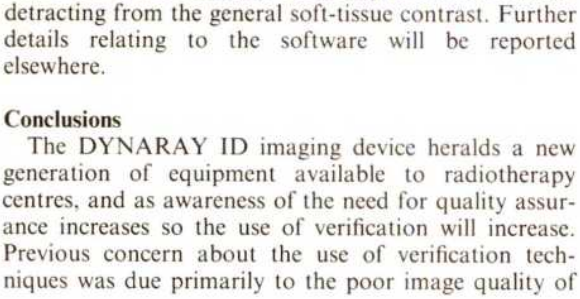

Figure 6. The raw image of a bronchus treatment field with three filter-enhanced images. The "sharp" filter used is a Laplace filter, the "edge" filter is a simple edge enhancement filter and the "edge and smooth" is a combined filter.

Acknowledgments

We wish to thank Asea Brown Boveri for making this imaging device available to us and especially the assistance of Dr Sutter. Our thanks are also due to the radiographers and consultant staff at the Norfolk and Norwich Hospital who allowed us to integrate with their busy schedules.

References

AAPM, 1988. *American Association of Physics in Medicine Report No. 24, Portal Imaging* (AAPM, New York).

BAILEY, N. A., HORN, R. A. & KAMPP, T. D., 1980. Fluoroscopic visualisation of megavoltage therapeutic x-ray beams. *International Journal of Radiation Oncology, Biology, Physics, 6,* 935–939.

BYHARDT, R. W., COX, J. D., HORNBURG, A. & LIERMANN, G. F., 1978. Weekly localisation films and detection of field placement errors. *International Journal of Radiation Oncology, Biology, Physics, 4,* 881–887.

DROEGE, R. T. & BJARNGARD, B. E., 1979. Influence of metal screens on contrast in megavoltage x-ray imaging. *Medical Physics, 6,* 487–493.

GRIFFITHS, S. E. & PEARCEY, R. G., 1986. The daily reproducibility of large, complex-shaped radiotherapy fields to the thorax head and neck. *Clinical Radiology, 37,* 39–41.

LAM, K. S., PARTOWMAH, M. & LAM, W. C., 1986. An on-line electronic imaging system for external beam therapy. *British Journal of Radiology, 59,* 1007–1013.

LEONG, J., 1986. Use of digital fluoroscopy as an on-line verification device in radiation therapy. *Physics in Medicine and Biology, 31,* 985–992.

MARKS, J. E., HAUS, A. G., SUTTON, H. G. & GRIEM, M. L., 1976. The value of frequent treatment verification films in reducing localisation error in the irradiation of complex fields. *Cancer, 37,* 2755–2761.

MEERTENS, H., 1985. Digital processing of high-energy photon beam images. *Medical Physics, 12,* 111–113.

MEERTENS, H., VAN HERK, M. & WEEDA, J., 1985. A liquid ionisation detector for the digital radiography of therapeutic megavoltage photon beams. *Physics in Medicine and Biology, 30,* 313–321.

MORTON, E. J. & SWINDELL, W., 1987. A digital system for the production of radiotherapy images. *Proceedings of the 9th International Conference on the Use of Computers in Radiation Therapy*, pp. 375–377.

PEARCEY, R. G. & GRIFFITHS, S. E., 1985. The impact of treatment errors on post-operative radiotherapy for testicular tumours. *British Journal of Radiology, 58,* 1003–1005.

Powlis, W. D., Brikman, I., Seshadri, S. B. & Block, P., 1988. Portal radiographs: digital enhancement of contrast. *Radiology, 169,* 839–841.

Rabinowitz, M. D., Broomberg, J., Goitein, M., McCarthy, K. & Leong, J., 1985. Accuracy of radiation field alignment in clinical practice. *International Journal of Radiation Oncology, Biology, Physics, 11,* 1857–1867.

Reinstein, L. E. & Orton, C. G., 1979. Contrast enhancement of high-energy radiotherapy films. *British Journal of Radiology, 52,* 880–887.

Suit, H. D., Becht, J., Leong, J., Stracher, M., Wood, W. C., Verhey, L. & Goitein, M., 1988. Potential for improvement in radiation therapy. *International Journal of Radiation Oncology, Biology, Physics, 14,* 777–786.

Taborsky, S. C., Lam, W. C., Sterner, R. E. & Skarda, G. M., 1982. Digital imaging for radiation therapy verification. *Optical Engineering, 21,* 888–889.

van Herk, M. & Meertens, H., 1987. A digital imaging system for portal verification. *Proceedings of the 9th International Conference on the Use of Computers in Radiation Therapy,* pp. 371–374.

van Herk, M. & Meertens, H., 1988. A matrix ionisation chamber imaging device for on-line patient set-up verification during radiotherapy. *Radiotherapy and Oncology, 11,* 369–378.

1991, *The British Journal of Radiology*, *64*, 603–607

An innovative method for neuraxis radiotherapy using partial transmission block technique

By P. N. Plowman and *D. Doughty

Radiotherapy Department, St Bartholomew's Hospital, London EC1 and *Oncology Department, The Hospital for Sick Children, Great Ormond Street, London WC1, UK

(*Received November 1990 and in revised form January 1991*)

Keywords: Craniospinal radiotherapy, Partial transmission block technique, Daily fractions size

Abstract. Whole CNS (neuraxis) radiotherapy is an important part of therapy for certain CNS tumours which seed via the CSF. Many, if not the majority, of these predominantly young patients are cured but the neuropsychometric, neuroendocrine and growth morbidity of neuraxis radiotherapy on children by conventional methods may be considerable; patients receiving such therapy at an early age often are eventually in the educationally subnormal category. Recent radiobiological data support the concept that all aspects of CNS radiation tolerance are heavily dependent on daily fraction size. We describe a new radiotherapy technique that allows lower daily fraction sizes to be delivered to the neuraxis without prejudicing the total dose to the neuraxis or primary area and without prolonging the overall treatment time. Published radiobiological data support the concept that all the major morbidities attributed to conventional neuraxis radiotherapy will be reduced by the currently described technique without reducing tumour control rates.

Medulloblastoma and the similar primitive neurectodermal tumour (PNET) of the CNS are tumours which have a propensity to seed via the CSF and which are radiosensitive. Total neuraxis radiotherapy is standard treatment in all patients and survival is seriously compromised in patients who do not receive such treatment (Brown et al, 1977; Barrer et al, 1984; Heideman et al, 1989). Many workers have demonstrated the need for total doses of at least 5000 cGy to the posterior fossa for optimal local control in medulloblastoma (Brown et al, 1977; Cumberlin et al, 1979; Berry et al, 1981; Silverman & Simpson, 1982). However, the total prophylactic dose to the whole neuraxis is a topic of great contemporary interest and controversy. In the past, total neuraxis doses of 3500–4000 cGy have been delivered, but, particularly with recently appreciated prognostic presentation features (and in younger patients), many groups including ourselves have reduced the total neuraxis prescription doses to 2500–3000 cGy in children (3000–3500 cGy in adults) (Plowman, 1991b). Current data from several centres do not suggest that the selective dose reductions significantly increase relapse risk (Brown et al, 1977; Cumberlin et al, 1979; Allen, 1985; Heideman et al, 1989) although the current Societé Internationale Oncologie Pédiatrique (SIOP) trial results do not wholly support this view in an unselected patient group. The neuraxis dose prescription is of great current interest because of increasing reports of significant intellectual (Cohen & Duffner, 1984; Silverman et al, 1984; Janoun & Bloom, 1990; Walterhouse & Meadows, 1991), neuroendocrine (Blacklay et al, 1986; Grossman, 1991), and non-endocrine growth morbidity in the late follow-up of survivors, and a safe reduction in the total neuraxis dose received would be a sure way of reducing this morbidity. All these remarks have application to other radiosensitive tumours with a propensity to CSF seeding and for which neuraxis radiotherapy has a standard therapeutic role (*e.g.* PNET, high grade ependymoma, intracranial germ cell tumours, pineoblastoma).

However, there is another aspect to the radiotherapy dose prescription which has recently been appreciated to have a considerable bearing on late CNS morbidity quite separate from the total dose administered; this is the daily fraction size. Reducing the daily dose fraction size to the whole brain of a child from conventionally sized doses towards 100 cGy will be predicted to reduce disproportionately any "expected" morbidity due to the logarithmic power weighting found to be attributable to fraction size/number in isoeffect equations of CNS radiation tolerance (Sheline, 1980, Thames & Hendry, 1987). These remarks are applicable to all "late responding" tissues (*i.e.* applicable to the radiation tolerance/morbidity of CNS, lung, kidney, liver, heart, etc.).

This recent appreciation of the disproportionately increased morbidity to late responding normal tissues from large daily dose fractions, together with the radiobiological data suggesting good "cell kill" from low daily dose fractions, has led us to abandon many classic "shrinking field techniques" traditionally used for paediatric radiotherapy in favour of partial transmission block (PTB) techniques (Plowman, 1989, 1991a).

For neuraxis radiotherapy, the advantage of PTB

Address requests for reprints to Dr P. N. Plowman, Radiotherapy Department, St Bartholomew's Hospital, London EC1.

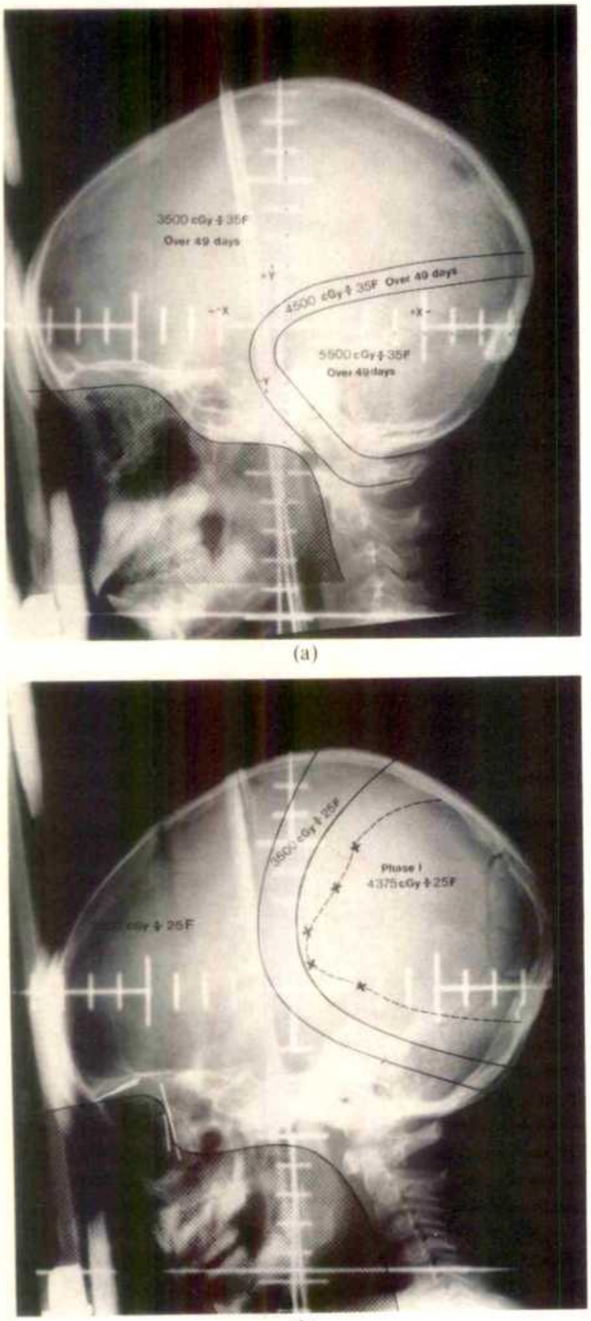

(a)

(b)

Figure 1. Radiotherapy simulator radiographs showing the position of the total protection and PTBs. (a) For cerebellar medulloblastoma radiotherapy. (b) For occipital PNET radiotherapy.

technique is that, during simultaneous irradiation, a dose rate differential between the whole cranium (prophylactic area) and the primary site (high dose volume) is achieved. The daily dose (fraction size) to the whole neuraxis is kept low but the overall treatment time is not increased. It is predicted that serial neuropsychometric studies will show reduced late sequelae (Plowman & Janoun, in preparation). It is also predicted that spinal growth will be less retarded and that neuroendocrine sequelae will be reduced; these aspects too are under serial study at these centres.

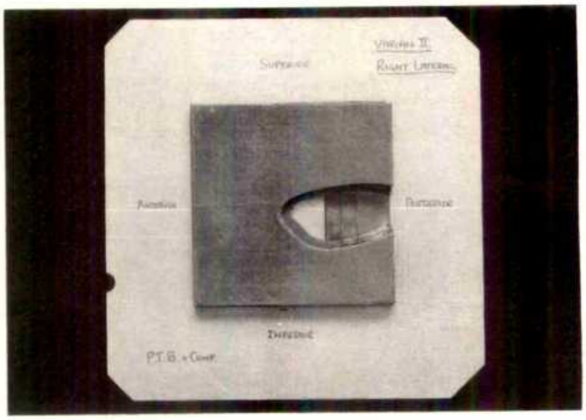

Figure 2. A PTB made from laminated lead sheets attached to an aluminium plate. Note the addition of missing tissue compensation.

In this manuscript we describe the PTB technique, introduced at St Bartholomew's Hospital and the Hospital for Sick Children, for tumours requiring a prophylactic dose to the whole cerebrospinal fluid volume.

Methods

The physical method for the deliberate introduction of dose gradients during external beam radiotherapy, by the use of PTBs, is based broadly on existing remote tissue compensation (RTC) technology which is available for use on our 6 MV (Varian 6/100) accelerators. The required thickness of lead, calculated by empirical methods to produce the prescribed dose differential, is mounted at the front face of the accelerator head. Typical dose rate differentials range from 100 to 175 cGy per fraction. Both the dosimetric and positional accuracy of individual patient's blocks are checked on the therapy machine prior to treatment.

The cranial part of routine craniospinal irradiation is performed at 6 MV using parallel opposed lateral portals with the patient prone in an individually constructed head shell. These lateral isocentric cranial portals are rotated caudally by approximately 7° in order that the inferior field border "matches" the diverging superior border of the spinal portal. "Total" shielding blocks (approximately six half-value layers) for the protection of eyes, mouth and face are individually constructed from low melting point alloy, their shape having been defined on simulator radiographs. These shaped blocks are mounted on Perspex plates suitable to access the standard shadow shield tray slide of the accelerator. When PTBs are additionally required, their shapes and positions are also marked on the simulator films (Fig. 1). PTBs are "built up" from sheet lead (0.5, 1.0 or 2.0 mm thick) to the required thickness and shape and mounted using double sided tape to an aluminium plate (Fig. 2). A pantograph technique is used to provide the exact demagnified shape. Manufacture of the PTBs would add approximately 1 h to the initial planning process for each patient. The plate holding the laminated lead PTB is designed to locate positively in the accelerator head moulding, just above the external wedge, at 40 cm distance from the source. As others have observed (ICRU, 1976), lead is the most suitable material considering the space limitation and ease of manufacture.

Dosimetry

With remote missing tissue compensation the thickness of any given attenuating material required to reduce the dose is energy, field size and depth dependent (Wilks & Casebow, 1969). Similar physical criteria apply to PTB techniques. However, as the necessary dose reduction is usually greater than with RTC, so will be the thickness of the attenuator, thus increasing the potential for anomalies.

Our standard transmission data used to design individual PTBs were measured with an ionization chamber at a depth of 7 cm in water substitute material. The measurements were made off axis using a typical field size of 20.0 × 20.0 cm, approximately one quarter of which was "totally" (*vide supra*) blocked to simulate orbital/facial protection. When these transmission data are used to calculate PTB thickness, the patient surface (at maximum lateral separation) is assumed in the first instance to be flat and normal to the beam axis. As this, in practice, will result in an enhanced dose in the areas where the separation is less (*e.g.* changing contour of the skull in the posterior fossa region) RTC can be added to the PTB as seen in Fig. 2.

In-phantom ionization measurements are performed on each PTB before the start of treatment. These measurements have shown, over a range of patients, that when standard transmission data alone are used to calculate block thickness, absorbed dose errors of $\pm 3\%$ may occur. However, following the initial measurements, "fine tuning" is possible by adding (or subtracting) 0.5 mm sheets of lead; 0.5 mm approximates to a 3% change in dose at depth.

Verification of the PTB position in the beam is eloquently achieved by portal films on the linear accelerator (Fig. 3) and these are standard check procedures.

Clinical radiotherapy aspects

We have argued elsewhere that paediatric tumour control will not be prejudiced by reducing daily dose fractions towards 100 cGy (Plowman, 1989) and yet the gain in terms of reduced CNS morbidity will be great. The presently described PTB neuraxis technique is currently used to deliver doses to the neuraxis of 100–120 cGy per day whilst the primary site will receive a daily dose of about 175 cGy as in previous techniques.

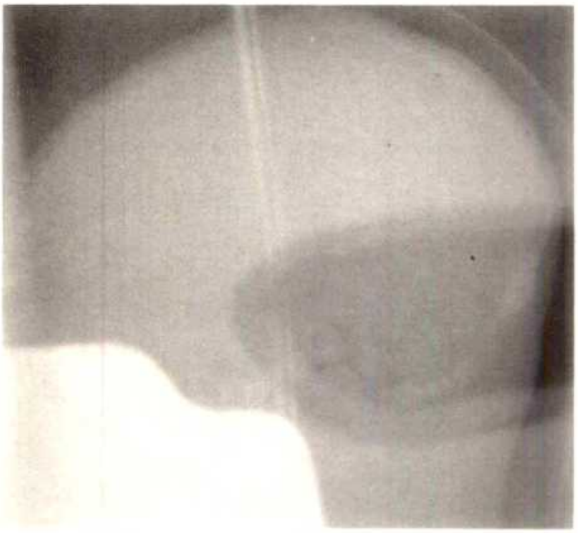
(a)

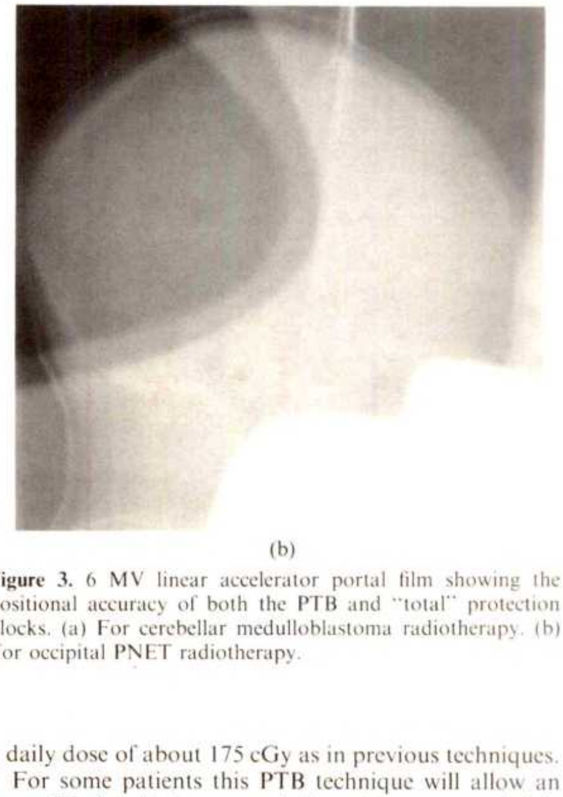
(b)

Figure 3. 6 MV linear accelerator portal film showing the positional accuracy of both the PTB and "total" protection blocks. (a) For cerebellar medulloblastoma radiotherapy. (b) For occipital PNET radiotherapy.

For some patients this PTB technique will allow an unmodified radiotherapy technique from start to finish. Thus, the patient illustrated in Figs 1a and 3a is an older child who presented with disease infiltrating the brainstem incompletely resected and with free floating blast cells found on CSF cytology, *i.e.* a high risk case. For such a high risk child the total neuraxis dose recommended at these centres is 3500 cGy. For this case, using PTB neuraxis technique, the posterior fossa received 5500 cGy in 35 fractions over 49 days whilst the neuraxis received 3500 cGy in 35 fractions over 49 days—same technique throughout.

However, for other patients, a phase II or "boost" phase may still be required as we have not taken the neuraxis daily dose below 100 cGy (for reasons to do with uncertainty of the flexure dose, Df, for paediatric tumours (Plowman, 1989)). The patient illustrated in Figs 1b and 3b has been chosen to exemplify this. This 3-year-old child had a radically resected supratentorial PNET, and computed tomography (CT) head scan, myelography and CSF cytology staging procedures were negative, *i.e.* low risk case. During this child's PTB neuraxis technique, and whilst the neuraxis received 2500 cGy in 25 fractions over 35 days, the primary area received 4375 cGy in 25 fractions over 35 days before a wedge pair of 6 MV X-ray portals were used to deliver a boost to the primary tumour bed of 1100 cGy in six fractions over 8 days. Although a second phase of treatment was necessary, the fact that the primary tumour bed was irradiated at orthodox daily dose size fractions during the first/PTB phase of treatment allowed us to complete the treatment in a time period and total number of treatments equivalent to a conventional treatment course.

Discussion

If paediatric tumours such as medulloblastoma and primitive neurectodermal CNS tumour (PNET) respond well (*i.e.* have a low quasithreshold (Dq) and radiosensitivity parameter (Do) radiobiologically (Hall, 1978)) to low fraction size doses of radiotherapy, and if CNS morbidity is fraction size related (Sheline, 1980), then syllogistic reasoning demands that PTB technique will be an improved treatment method for neuraxis radiotherapy in these diseases. In support of the first point comes the radiobiological data on the homologous tumour: neuroblastoma (Deacon et al, 1985). We have reviewed data in favour of a higher Df for tumours than for late responding normal tissues (Plowman, 1989). The importance of the latter point is underlined by the growing literature concerning the intelligence, learning and intellectual stunting and retardation following neuraxis radiotherapy by conventional techniques, particularly in young children (Cohen & Duffner, 1984; Silverman et al, 1984; Janoun & Bloom, 1990). The major advantage of the PTB neuraxis technique described here is that, without prolonging the overall treatment time or changing the total dosage to either the neuraxis or primary site, the lower daily dose/fraction size delivered to the whole CNS may be predicted to be less "morbid" than the same total dose delivered by conventional techniques. Prospective studies of survival and neuropsychometric sequelae following PTB neuraxis therapy are ongoing at these hospitals and will form the basis of later publications. However, there are already some data suggesting that centres employing more fractionated treatment schemes for medulloblastoma (Janoun & Bloom, 1990) or acute lymphoblastic leukaemia prophylaxis (Janoun, personal communication) find less severe neuropsychometric sequelae.

A recent publication from our group (Douek et al, 1991) has demonstrated clearly the high response rate of medulloblastoma, PNET, pineal germ cell tumours and pineoblastomas to platinum/epipodophyllotoxin/vinca alkaloid chemotherapy. The success of these studies has prompted us to introduce such chemotherapy into the primary treatment scheme for all of these tumours. The well known problem with chemo-radiotherapy for these diseases is that both the chemotherapy and the neuraxis radiotherapy are myelosuppressive and the combination of the two may prejudice full doses of one or other modality. Arguing from experience with other paediatric tumours, we have introduced the chemotherapy first (*i.e.* neoadjuvantly) but encountered more marked myelosuppression during the subsequent neuraxis radiotherapy. Our initial observations with neuraxis radiotherapy by the new PTB technique suggest that bone marrow tolerance will be better preserved.

The technique described in this manuscript is relatively simple to introduce on any linear accelerators with a head moulding incorporating both wedge and accessory tray slides. Although some attachment modifications would be necessary for machines possessing "internal" wedge(s), implementation of this technique would be possible by most radiotherapy departments supported by radiation physics expertise and workshop facilities. The method we have adopted for our PTB technique is no more than a variant of our tissue compensator construction technique; a "shrinking fraction" technique would be a simple method of attaining the same goal (*i.e.* treating a wide volume to 100–120 cGy before shrinking fields to complete the fraction—each day). We believe such techniques will become standard practice for all tumours requiring whole neuraxis prophylactic radiotherapy and that the adverse sequelae of previous conventional techniques will be much reduced by the adoption of this St Bartholomew's/Great Ormond Street method.

References

ALLEN, J. C., 1985. Childhood brain tumours: current status of clinical trials in newly diagnosed and recurrent disease. *Pediatric Clinics of North America, 32*, 633–651.

BARRER, S. J., SCHUT, L., SUTTON, L. N., 1984. Re-operation for recurrent brain tumours in children. *Child's Brain, 11*, 375–386.

BERRY, M., JENKIN, D., KEEN, C., 1981. Radiation treatment for medulloblastoma: a 21 year review. *Journal of Neurosurgery, 55*, 43–51.

BLACKLAY, A., GROSSMAN, A., SAVAGE, M., PLOWMAN, P. N. & BESSER, G. M., 1986. Cranial irradiation in children with cerebral tumours—evidence for a hypothalamic defect in growth hormone release. *Journal of Endocrinology, 108*, 25–29.

BROWN, R., GUNDERSON, L. & PLENK, H., 1977. Medulloblastoma: a review of the LDS Hospital experience. *Cancer, 40*, 56–60.

COHEN, M. E. & DUFFNER, P. K., 1984. Ependymomas. In *Brain Tumours in Childhood: Principles of Diagnosis and*

Treatment, ed. by M. E. Cohen and P. K. Duffner (Raven Press, New York), pp. 136–155.

CUMBERLIN, R., LUK, K. & WARD, W., 1979. Medulloblastoma treatment results and effect on normal tissues. *Cancer, 43*, 1014–1020.

DEACON, J. M., WILSON, P. A. & PECKHAM, M. J., 1985. The radiobiology of human neuroblastoma. *Radiotherapy and Oncology, 3*, 201–211.

DOUEK, E., KINGSTON, J. E., MALPAS, J. S. & PLOWMAN, P. N., 1991. Platinum based chemotherapy for recurrent CNS tumours in young patients. *Journal of Neurology Neurosurgery and Psychiatry*, (in press).

GROSSMAN, A., 1991. Endocrine morbidity of cancer treatment. In *The Complications of Cancer Management*, ed. by P. N. Plowman, A. Meadows and T. J. McElwain (Butterworths/Heinemann, London) pp. 412–422.

HALL, E. J., 1978. *Radiobiology for the Radiologist* (Harper & Row, New York), pp. 33–35.

HEIDEMAN, R. L., PACKER, R. J., ALBRIGHT, L. A., FREEMAN, C. & RORKE, L. B., 1989. Tumors of the central nervous system. In *Pediatric Oncology*, ed. by P. A. Pizzo and D. G. Poplack (J. B. Lippincott Co, Philadelphia), pp. 505–553.

INTERNATIONAL COMMISSION ON RADIATION UNITS AND MEASUREMENTS, 1976. Determination of absorbed dose in a patient irradiated by beams of X or gamma rays in radiotherapy procedures. *ICRU Report 24*, Washington DC 20014, pp. 39–41.

JANOUN, L. & BLOOM, H. J. G., 1990. Long term psychological effects in children treated for intracranial tumours. *International Journal of Radiation Oncology Biology Physics, 18*, 747–753.

PLOWMAN, P. N., 1989. Partial transmission block (PTB) technique: the logical successor to shrinking field technique in paediatric radiotherapy. *Proceedings Sixth Varian European User's Meeting* (Varian, Zug, Switzerland) pp. 146–149.

—— 1991a. Minimising the morbidity from radiotherapy. In *The Complications of Cancer Management*, ed. by P. N. Plowman, A. Meadows and T. J. McElwain (Butterworths/Heinemann, London) pp. 474–486.

—— 1991b. CNS tumours. In *Controversies in Paediatric Oncology* (Chapman & Hall, London). In press.

SHELINE, G. E., 1980. Irradiation injury of the human brain: a review of clinical experience. In *Radiation Injury to the Nervous System*, ed. by H. A. Gilbert and A. R. Kagan (Raven Press, New York), pp. 39–58.

SILVERMAN, C. & SIMPSON, J., 1982. Cerebellar medulloblastoma: the importance of posterior fossa dose to survival and patterns of failure. *International Journal of Radiation Oncology Biology Physics, 8*, 1869–1876.

SILVERMAN, C. L., PALKES, H., TALENT, B., KORNAR, E., CLOUSE, J. W. & THOMAS, P. R., 1984. Late effects of radiotherapy on patients with cerebellar medulloblastoma. *Cancer, 54*, 825–829.

THAMES, H. D. & HENDRY, J. H., 1987. *Fractionation in Radiotherapy* (Taylor and Francis, London).

WALTERHOUSE, D. O. & MEADOWS, A. T., 1991. Late effects of childhood cancer therapy. In *The Complications of Cancer Management*, ed. by P. N. Plowman, A. Meadows and T. J. McElwain (Butterworths/Heinemann, London) pp. 95–113.

WILKS, R. & CASEBOW, M. P., 1969. Tissue compensation with lead for 60Co therapy. *British Journal of Radiology, 42*, 452–456.

1991, *The British Journal of Radiology*, 64, 608–624

Dose to red bone marrow from natural radon and thoron exposure

By R. B. Richardson, BSc, MSc, J. P. Eatough, BSc and D. L. Henshaw, BSc, PhD

H. H. Wills Physics Laboratory, University of Bristol, Tyndall Avenue, Bristol BS8 1TL, UK

(*Received June 1990 and in final form January 1991*)

Keywords: Radon, Thoron, Dosimetry, Red bone marrow

Abstract. The age-dependent radiation dose to the haematopoietic tissue of bone marrow has been calculated for exposure to radon, thoron and their daughter products. The component of dose due to pure radon is dependent on the fat content of the marrow, since the solubility of radon in fat is about 16 times that in tissue. The mean dose equivalent μSv to the total active marrow is estimated for a range of fat cell diameters from 25 to 200 μm, taking account of the percentage cellularity and distribution of active marrow as a function of age. Similarly, the dose due to the inhalation of short-lived radon daughters was estimated, based on measurements in blood and marrow, modified to allow for the greater deposition of daughter products expected in children. An estimate of the age-dependent dose from long-lived radon daughters was made from uranium miner and natural exposure data. Dose estimates were made for the average UK indoor exposure to radon gas of 20 Bq/m^3 and an equilibrium equivalent thoron concentration of 0.3 Bq/m^3. The annual radon and thoron derived dose to the active marrow of the newborn was calculated as 30 and 40 μSv, respectively. For a 10-year-old child, the radon and thoron derived annual dose are 70 and 40 μSv, and for a 40-year-old adult 90 and 30 μSv, respectively. The above values exhibit wide range limits due principally to uncertainties in the accumulation of ^{210}Pb in bone, and ^{210}Po in marrow. These data indicate that at the average UK exposure, the alpha-particle dose to active marrow is dominated by that derived from inhaled radon and thoron compared with dietary intake. In infants the dose is dominated by thoron daughters. At the UK radon Action Limit of 200 Bq/m^3, the radon and associated thoron derived dose is similar to that from all low LET sources. This work shows that the dose to red bone marrow from radon and thoron is significant, and that the possibility of leukaemia induced by these radiation sources warrants further investigation.

Research into the effects of radon exposure has been dominated by the observed relation between radon exposure and lung cancer in uranium miners (BEIR IV, 1988). Computer modelling has shown that the majority of the radiation dose from radon to the lung is delivered by radon short-lived daughter nuclei (Jacobi & Eisfeld, 1980; James, 1988). The radiation dose to other organs, compared with lung, has been considered to be negligible, when individual organ doses are expressed in terms of whole body effective dose equivalent (UNSCEAR, 1988). However, for UK children aged 0–14 years, there are no deaths due to lung cancer, but 175 annually due to leukaemia; and the 15 to 29 age group have 14 times as many mortalities from leukaemia as from lung cancer (OPCS, 1985). There is increasing epidemiological evidence that radon exposure of the population is associated with leukaemia in children and adults (Lucie, 1989; Alexander et al, 1990; Henshaw et al, 1990). It is therefore important to calculate the dose to the tissues where radiation induced leukaemia may originate.

In the case of leukaemia the haematopoietic stem cells have been considered to be the cells at risk. The dose to bone marrow from radon and its daughter products has been previously considered to be small and was generally neglected (Black, 1984), except in the pioneering work of Austrian researchers (Pohl & Pohl-Rüling, 1967; Hofmann et al, 1979). In this paper, we show that the combination of several previously unconsidered yet widely published factors contribute to the haematopoietic stem cell dose from radon and radon daughters inhaled by the general population (Richardson et al, 1990a).

In order to estimate the dose contribution from radon to the haematopoietic stem cells, we need to consider the part played by radon itself, then that of the short- and long-lived daughters (Fig. 1). Radon, an inert gas, rapidly diffuses across the alveolar membrane of the lung, and is transported by the blood to all parts of the body, where, by diffusion, it is taken up by the organs (Peterman & Perkins, 1988). Transport times in the body are generally short compared with the physical half-life of radon. In view of the relatively high flow rate of blood in bone marrow, we have assumed radon equilibrium, such that the uptake is governed by radon solubility in that particular tissue. Radon solubility in body tissues was measured by Nussbaum and Hursh (1957, 1958). They found values of 0.4 and 6.3 mBq/kg per Bq/m^3 radon exposure, in blood and human fat, at 37°C, respectively. A review of radon solubility measurements in biological systems is given by Clever (1979). The high value in fat has important consequences for the radiation dose to haematopoietic tissue in marrow.

A dosimetric model has been developed which has taken into account the transfer of radon to bone marrow. Bone marrow consists of various cellular components, mainly haemotopoietic cells and fat. In the newborn, nearly all the bone marrow contains active red haematopoietic tissue with negligible fat content. In the growing child, the red bone marrow is gradually replaced by yellow marrow, beginning in the central

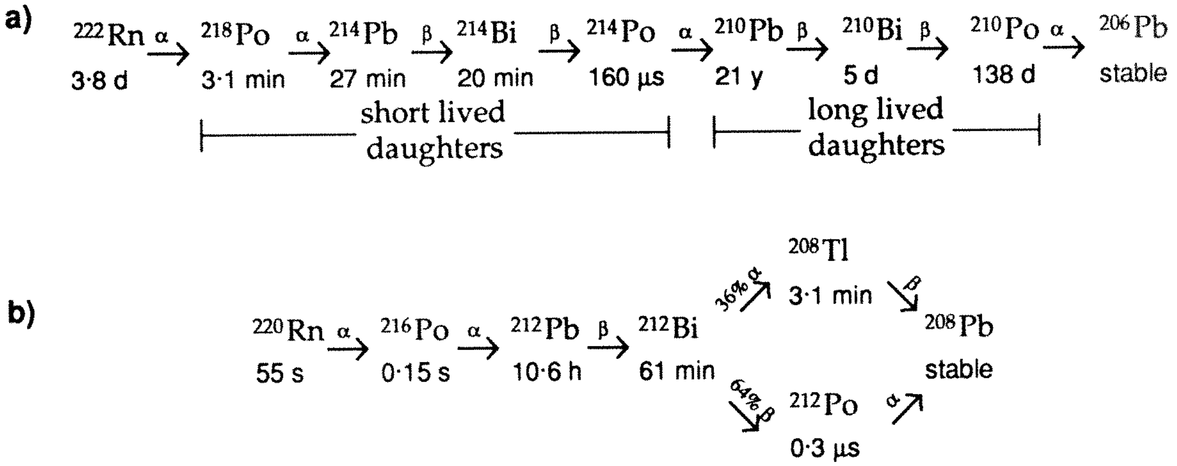
a)
222Rn α 218Po α 214Pb β 214Bi β 214Po α 210Pb β 210Bi β 210Po α 206Pb
3·8 d 3·1 min 27 min 20 min 160 µs 21 y 5 d 138 d stable
short lived daughters
long lived daughters
b)
208Tl
3·1 min
36% α
β
220Rn α 216Po α 212Pb β 212Bi
55 s 0·15 s 10·6 h 61 min
208Pb
stable
64% β
212Po
α
0·3 µs

Figure 1. Decay products of radon (^{222}Rn) and thoron (^{220}Rn), and their half-lives. (a) Uranium-238 decays via a series of intermediate steps to radium-226 (not shown). Radon is then produced by the alpha-decay of radium-226. Owing to the short half-lives of the daughter nuclei down to ^{210}Pb, three alpha-particles are associated with the decay of radon. The decay-chain then "brakes" at ^{210}Pb, with a half-life of 21 years. Lead-210 decays via ^{210}Bi to alpha-emitting ^{210}Po. (b) Thorium-232 eventually decays to ^{220}Rn. In considering dose to body tissues, ^{212}Pb is the important precursor to the alpha-emitting daughters ^{212}Bi or ^{212}Po.

portions of the long bones and extending both distally and proximally. Similarly, the percentage of active haematopoietic tissue gradually decreases with age in the axial skeleton of the child and adult. The fraction of haematopoietic marrow in a given bone may be expressed in terms of a cellularity fraction. The cellularity of bone and the contribution to the total active marrow of the skeleton were derived by Cristy (1981) for all major haematopoietic bones of the newborn to 40-year-olds.

The fat in marrow is in the form of adipocytes (fat cells) which are composed predominantly of triglyceride (Hiragun, 1985). Bone marrow adipocytes are morphologically similar to extramedullary white adipose tissue, but dissimilar in origins and functions. The number of bone marrow adipocytes fluctuates with the state of haematopoiesis and increases in physiologically or pathologically hypoplastic marrow (Weiss, 1970). Recent studies have investigated extensively the fat cell size in human subcutaneous fat (Hausman, 1985), with less known of medullary fat cell size. The fat cell is the largest cell in the whole body with a mean extramedullary diameter of approximately 50 µm (Gray's Anatomy, 1980). The size of extramedullary fat cells ranges from 50 to 80 µm in the fetus, and from 25 to 200 µm in the adult (Hiragun, 1985). Isolated cells assume a spherical morphology but when in close proximity assume a polyhedral form (Sjöström et al, 1971). The maximum diameter of medullary fat cells in animals and cultured human cells have been measured as being 140–160 µm (Tavassoli, 1976) and 80–100 µm (Zucker-Franklin et al, 1978), respectively.

The short- and long-lived radon daughters are radionuclides of the elements lead, bismuth and polonium, therefore their general physical, biochemical uptake and excretion properties in the body are important considerations in relation to dose to bone marrow. Lead, bismuth and polonium are heavy metals, but with polonium having many of the characteristics of rare-earth elements. The short half-lives of ^{214}Po and ^{218}Po means that they have relatively short times for biochemical effects to occur, unlike the long-lived daughter ^{210}Pb giving rise to ^{210}Po. Therefore, the characteristics of short-lived daughter products, both from soluble radon and direct inhalation, will be dominated by the properties of lead and bismuth, with physical mean lifetimes of 39 and 28 minutes.

Approximately 30% and 50% of radon and thoron short-lived daughter nuclei when inhaled, cross the alveolar membrane of the lung (Pohl & Pohl-Rüling, 1977). In the blood, lead binds rapidly to red cells, with 95% of vascular lead binding to red cell membranes in minutes (Watanabe & Yana, 1953), while polonium is taken up more slowly, with maximum binding to red cells occurring in hours (Thomas, 1964). Bismuth in blood binds readily to serum proteins (Russ et al, 1975). Bismuth and polonium are both associated with proteinaceous material (Szymańska et al, 1981), with both exhibiting non-specific protein binding. Lead binds non-specifically to lipids and lipoproteins in the cell membranes (Waldron & Stöfen, 1974). The fraction of total plasma lead and polonium (and presumably bismuth) that is not bound was assumed by Stover (1959) to be in ionic form, and in equilibrium with body tissues and plasma proteins. Animal experiments with carrier-free lead showed two thirds of the administered activity to be in blood at 1 hour after administration. The transport of the short-lived daughters into fat can be assumed to be negligible, as the biological rate of uptake of lead and polonium from blood has been given by ICRP (1979, 1980) as 8 hours. The uptake of radiobismuth in fat, 1 hour after intravenous administration, has been reported to be minimal (Richardson et al, 1990b). The longer half-lives of ^{210}Pb, ^{210}Po and ^{212}Pb point to homogeneous distribution in fatty marrow being more likely (Casarett, 1964).

In this paper we have considered first the exposure from pure radon gas to the critical tissue in leukaemia induction. This has been estimated from the solubility of radon in the fat and haematopoietic tissues of bone marrow, and the bone marrow's changing composition with an individual's age. Secondly, we have considered the absorbed dose to haematopoietic marrow due to the inhalation of short-lived daughters for radon exposure and occupancy typical of UK homes. This has been estimated from the detailed measurements of radon daughters in the blood of Austrian spa workers by Pohl (1964). Thirdly, we have estimated the dose contribution from ^{210}Po following protracted radon exposure using data of Clemente et al (1984), and others for uranium miners and radon spa area inhabitants.

These data have been used to provide dose estimates appropriate to domestic exposures in the UK at the population-weighted mean radon concentration of 20 Bq/m^3 indoors (Wrixon et al, 1988) and 4 Bq/m^3 outdoors (Hughes et al, 1988). Finally, the dose to marrow from thoron has been considered since the thoron and its daughter concentrations are often elevated in the presence of high radon concentrations (Schery, 1985; Martz et al, 1990). The relative biological effectiveness (RBE) for alpha-particles at natural exposure levels is a matter of debate (Peto, 1990). Throughout this work we have used a quality factor of 20 for the alpha-particle and expressed our dose values in dose equivalent units of μSv.

Theoretical methods

Basis of the dosimetric model

A model is developed which considers the absorbed dose to haematopoietic tissue from radon and its alpha-emitting daughters situated both in the tissue itself and also in fat cells distributed within marrow. In this dosimetric model, fat cells are considered to be randomly distributed spheres of pure fat, that are homogeneously distributed in marrow. This is a simplification of the actual distribution, with different cell types having varying concentration across the trabeculae (Lord & Schofield, 1980). Haematopoietic stem cells have a much smaller diameter (~ 5 μm) than fat cells (ICRP, 1975). In children and adults, haematopoietic marrow lies mainly in cavities of trabecular bone, whose size varies with age (Spiers, 1966, 1988), with a cellularity-weighted skeletal average of 0.49 and 0.88 mm for the newborn and 40-year-old, respectively. Since the trabecular cavity size is large compared with fat cell sizes, edge effects at the bone/marrow interface were considered to be negligible.

The model must consider both the possibility that alpha-particles emitted from a fat cell terminate in haematopoietic marrow, and also that the alpha-particle may traverse the haematopoietic tissue to enter another fat cell. In this model, each spherical fat cell of radius r_s is considered to be surrounded by a representative annulus of active marrow whose external radius is r_c. It has been assumed that the fraction of fat Z present in bone marrow is equal to the ratio of the representative volume of a fat cell to that of the cavity plus fat cell, whereby

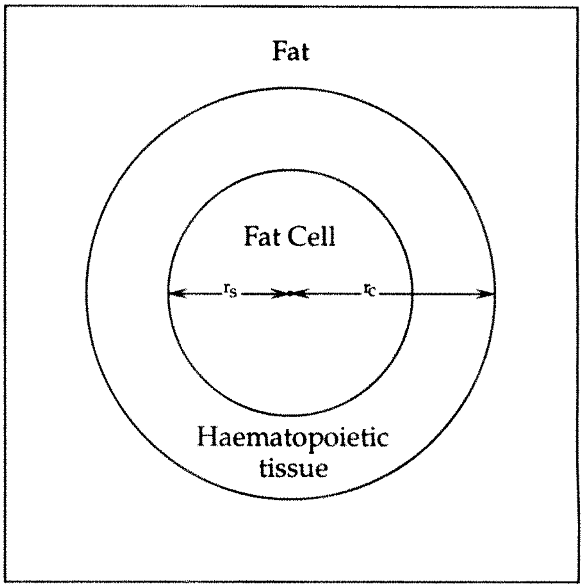

Figure 2. Theoretical representation of a spherical fat cell within a spherical cavity in fat, representing adipocytes in haematopoietic marrow.

$$r_s = r_c . Z^{1/3} \quad (1)$$

Pluripotent stem cells are estimated as ~ 1 per 500 bone marrow cells (Lord & Schofield, 1980). They are assumed to be homogeneously distributed in active marrow as recommended by ICRP (1979), and to lie between and to be irradiated by the inner spherical fat cell and the outer spherical fat cavity (Fig. 2). The dose to active marrow is therefore the sum of the dose from the inner spherical fat cell and the fat from beyond the representative annulus of active marrow.

The absorbed dose per second at a point in a haematopoietic tissue element, which is adjacent to fat uniformly loaded with an alpha-emitter, may be expressed, based on the work of Charlton and Cormack (1962), as

$$D_\alpha(x) = \frac{C . E_\alpha . u . S(x) . Q}{n} \quad (2)$$

where $D_\alpha(x)$ is the absorbed dose equivalent per second at a distance x from the fat/haematopoietic tissue interface, from alpha-particles of initial energy E_α in MeV. The activity concentration C is the disintegrations per second emitted per unit mass of fat; Q is the quality factor, taken as 20 for alpha-particles; u is the ratio of densities of the emitter and irradiated tissue and n is the

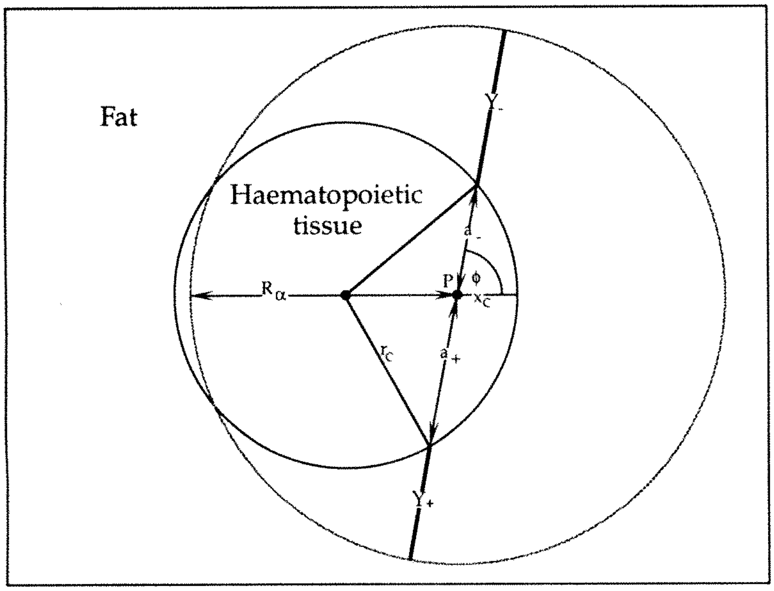

Figure 3. The geometry used in calculating the energy dissipation at point P inside an irradiated spherical cavity of radius r_c.

ratio of the ranges in the irradiated and the emitter tissue. $S(x)$ is the geometrical function (≤ 1), at distance x, and is the ratio of the apparent activity of the irradiated haematopoietic tissue to the activity of the alpha-emitter in fat. $S(x)$ depends on the shape of the interface and on the form of the alpha-particle range–energy relationship. For alpha-particles of energy between 1 and 10 MeV, the relationship between residual range R and energy E may be expressed by

$$R = \mathrm{v}\,.\,E^{\mathrm{w}} \tag{3}$$

where v and w are empirical constants which can be found from experimental data. Charlton and Cormack (1962) took a value of 1.5 for w.

Spherical cavity in fat. It is assumed that alpha-particles are emitted isotropically, that the activity is constant throughout the fat, that alpha-particles travel in straight paths with range R_α. Linear energy transfer (LET) can be estimated by differentiation. For a spherical interface of radius r_c, where x_c is the shortest distance between the point P and the interface, it has been shown by Howarth (1965) that the geometric factor $S_c(x_c)$ has the form

$$S_c(x_c) = \frac{1}{2}\int\left(1-\frac{a}{R_\alpha}\right)^{1/\mathrm{w}} \sin\phi\,\mathrm{d}\phi \tag{4}$$

where, by Fig. 3,

$$r_c^2 = (r_c - x_c)^2 + a^2 - 2a(r_c - x_c)\cos\phi \tag{5}$$

Solving the quadratic equation for a gives

$$a = (r_c - x_c)\cos\phi \pm\sqrt{(r_c - x_c)^2\cos^2\phi - [(r_c - x_c)^2 - r_c^2]} \tag{6}$$

Let the two solutions be a_+ and a_-. The dose to point P is the sum of two contributions Y_+ and Y_-, which are shown in Fig. 3. Let j = lesser of a_+ and R_α, and k = lesser of a_- and R_α. Therefore

$$S_c(x_c) = \frac{1}{2}\int_0^{\pi/2}\left[\left(1-\frac{j}{R_\alpha}\right)^{1/\mathrm{w}} + \left(1-\frac{k}{R_\alpha}\right)^{1/\mathrm{w}}\right]\sin\phi\,\mathrm{d}\phi \tag{7}$$

Spherical fat cell. Equation 4 has been extended and applied to irradiation of point P from outside a spherical cell (Fig. 4) to give a geometric factor $S_s(x_s)$ at a radial distance x_s from the fat cell where

$$r_s^2 = (r_s + x_s)^2 + a^2 - 2a(r_s + x_s)\cos\phi \tag{8}$$

$$a = (r_s + x_s)\cos\phi \pm\sqrt{(r_s + x_s)^2\cos^2\phi - [(r_s + x_s)^2 - r_s^2]} \tag{9}$$

$$S_s(x_s) = \frac{1}{2}\int_0^{\phi_{\max}}\left[\left(1-\frac{j}{R_\alpha}\right)^{1/\mathrm{w}} - \left(1-\frac{k}{R_\alpha}\right)^{1/\mathrm{w}}\right]\sin\phi\,\mathrm{d}\phi \tag{10}$$

The condition for $\phi_{\max}$ occurs when $a_- = a_+$ and

$$\phi_{\max} = \sin^{-1}\left(\frac{r_s}{r_s + x_s}\right) \tag{11}$$

Summing the contributions from the spherical cavity in fat and fat cell gives

$$S(r) = S_c(x_c) + S_s(x_s) \tag{12}$$

where $x_c = r_c - r$ and $x_s = r - r_s$. Therefore

$$S_\alpha = \frac{\displaystyle\int_{r_s}^{r_c} S(r)\,.\,4\pi r^2\,\mathrm{d}r}{\displaystyle\int_{r_s}^{r_c} 4\pi r^2\,\mathrm{d}r} \tag{13}$$

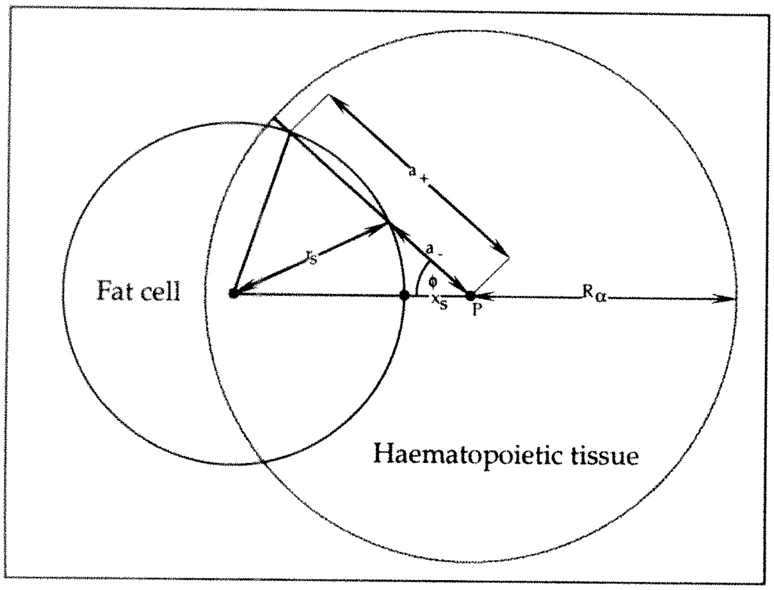

Figure 4. The geometry used in calculating the energy dissipation at point P outside an irradiating spherical cell of radius r_s.

The mean dose to a small volume of haematopoietic tissue is the sum of the contributions of alpha-radiation from the spherical fat cell and spherical fat cavity (Eqn 12). Consider a shell at radius r of volume $dv = 4\pi r^2\,dr$, with a position-dependent geometric factor $S(r)$. The latter was computed with steps of dr equal to 0.005 μm. The mean geometric factor S_α for the representative annulus of active marrow, for alpha-particle α, was estimated by iterative computation over the limits of the integrals of $S_c(x_c)$ and $S_s(x_s)$, with steps of $d\phi$ of 0.001 radian.

Contribution from pure radon

Radon-222 upon decay emits a 5.5 MeV alpha-particle with a range in water of about 42.8 μm. The short-lived daughter products of radon, ^{218}Po and ^{214}Po, emit alpha-particles of energy 6.0 and 7.7 MeV, respectively, with ranges in water of 49.5 and 74.2 μm (Fews, 1982). Alpha-particle ranges were assumed to be that in water as ranges in haematopoietic tissue and fat calculated by the data of Ziegler (1977) were within ±5% of that in water. The average densities of red and yellow marrow are given by ICRP (1975) as 0.97 and 1.03 g/cm^3. The parameter u/n was assumed to be unity. The atomic recoil of ^{222}Rn, ^{218}Po and ^{214}Po in tissue is negligible, with a recoil kinetic range of the order of 0.1 μm (Bossus, 1984). It has been assumed that radon and its short-lived daughters produce a three alpha-particle point decay, as the effect of diffusion and other forms of transcellular transport of heavy metals, in the large central lipid droplet of the fat cells, is probably small during the short lifetimes of the daughter products.

The activity concentration in fat C_f and haematopoietic tissue C_h were taken to be 6.33 mBq/kg and 0.4 mBq/kg, respectively, for air inhaled with a radon concentration of 1 Bq/m^3 (Nussbaum & Hursch, 1957, 1958). The effective activity concentrations $C_h(i, t, \alpha)$ of the short-lived daughters in haematopoietic tissue at age, t, for a particular bone, i, were calculated by Eqn 14:

$$C_h(i, t, \alpha) = C_h + [(C_f - C_h) . S_\alpha . Z(i, t)] \qquad (14)$$

Geometric dose factors S_α were computed by Eqn 13, for a given alpha-particle α, fat fraction $Z(i, t)$, and fat cell diameter $2r_s$ (25–200 μm). The active marrow in bone i at age t is expressed as a fraction of the total active marrow in the skeleton and denoted by $M(i, t)$. The mean effective activity concentration $\bar{C}_h(t, \alpha)$, per Bq/m^3, to the total haematopoietic marrow of the skeleton at age t is the sum of effective activity concentration $C_h(i, t, \alpha)$ for a particular bone i, weighted by $M(i, t)$.

$$\bar{C}_h(t, \alpha) = \sum_i \bar{C}_h(i, t, \alpha) . M(i, t) \qquad (15)$$

The mean dose equivalent per year $\bar{D}_h(t)$ in μSv to the haematopoietic marrow of the whole skeleton is the sum of the three alpha-particle point decays (radon and two short-lived daughters), and is given by

$$\bar{D}_h(t) = \sum_\alpha \left[\bar{C}_h(t, \alpha) . \left(\frac{E_\alpha . u . Q . Y}{n} \right) \right] \qquad (16)$$

where Y is the number of seconds in 1 year.

Contribution from the inhalation of radon short-lived daughters

The activities of short-lived daughter products in blood or marrow are dependent on the "equilibrium-equivalent" decay-product concentration, which is the amount of each decay product necessary to collectively have the same potential alpha-energy concentration that is actually present (Nero, 1988). The ratio of the equilibrium-equivalent decay-product concentration to radon concentration is defined as the equilibrium factor F. On the basis of Pohl's (1964) animal experiments, it has been assumed that when inhaling radon daughters, under normal domestic conditions, the dose to blood is mainly derived from ^{214}Po in equilibrium with ^{214}Bi, with the precursor daughters of ^{214}Po contributing a much smaller dose. Pohl (1964) found the activity of ^{214}Bi (and hence ^{214}Po) in blood to be 4.2, 3.0 and 0.45 mBq/kg for F factors of 0.87, 0.51 and zero (pure radon), respectively, per Bq/m^3 radon concentration, in atmospheres at 24°C and 70% humidity. UNSCEAR (1988) has assigned F factors of 0.4 and 0.8 for indoor and outdoor atmospheres, for which we estimate blood activity values of 2.2 and 3.6 mBq/kg per Bq/m^3. For the UK, the average indoor and outdoor radon concentrations are 20 and 4 Bq/m^3. We have taken into account a UK occupancy factor at all ages of 0.9, for the portion of time spent indoors (Francis, 1987), in calculating a constant activity concentration for ^{214}Bi in blood of 40 mBq/kg, under average UK conditions.

Because of uncertainties in radon daughter transport in the body, lower, mean and upper activity ratios of the radon daughter ^{214}Bi, and hence ^{214}Po, in red bone marrow to blood A_h/A_B have been estimated. The rate of change of activity dA_α/dt of radionuclide α in tissue T can be described by Eqn 17. The uptake factor f_{T_α} of a given tissue defines the fraction of activity, of the short-lived daughters ^{218}Po, ^{214}Pb, ^{214}Bi, that is eliminated from blood, translocated and retained in the tissue. Jacobi and Eisfeld (1980) have shown that the equilibrium activity in tissue A_{T_α} is related to the activity A_{B_α} of ^{218}Po, ^{214}Pb, ^{214}Bi in blood. A_{T_α} is also dependent on the physical and biological rate constants λ_{p_α} and λ_{T_α} of the three alpha-emitters:

$$\frac{dA_\alpha}{dt} = f_{T_\alpha} . \lambda_{T_\alpha} . A_{B_\alpha} - \lambda_{p_\alpha} . A_{T_\alpha} \tag{17}$$

In the steady state $dA_\alpha/dt = 0$, then summing each radionuclide:

$$A_{T_\alpha} = \sum_\alpha f_{T_\alpha} . \frac{\lambda_{T_\alpha}}{\lambda_{p_\alpha}} . A_{B_\alpha} \tag{18}$$

In accordance with the recommended values of f_{T_α} and λ_{T_α} by the ICRP (1979, 1980), the contribution from ^{214}Bi dominates. We consider the activity in other organs, apart from the bone, liver, kidneys, spleen and adipose tissue (assuming no uptake in fat) to be homogeneous and to include the active marrow. The activity A_h per unit mass of ^{214}Bi in active marrow is C_h and the mass ratio of blood to that of other organs is approximately 0.13, at all ages (ICRP, 1975). It can be shown that the ratio C_h/C_B including 6% vascularity is approximately 0.16. An activity ratio of 0.32 was obtained from animal experiments by Pohl-Rüling et al (1982) with similar values found in other investigations (Pohl & Pohl-Rüling, 1967). We have considered the theoretical and animal activity ratios of 0.16 and 0.32 to be lower and upper limits, and have taken a mean value of 0.24.

As the short-lived daughter half-lives are in total less than an hour, it is assumed that little intra-cellular uptake occurs in fat cells. Binding of radon daughters to the cell membranes can be expected to be largely non-specific and mainly dependent on the cell surface area of the haematopoietic and blood cells, as the fat cells contribute only about 6% of the total cell surface area of the adult's marrow at 60% cellularity (ICRP, 1975). On this basis the radon daughter products free in plasma or extra-vascular fluid, or bound to intra- and extra-vascular cell membranes have been assumed to be homogeneously distributed among the stem cells, with the activity of whole marrow dependent on the cellularity. Therefore, by the radiation reciprocity theorem, the effective ^{214}Po activity concentration $C_h(i, t)$ in the haematopoietic marrow of bone i, at age t, may be derived from Eqn 14 and given by

$$C_h(i, t) = C_h[1 - S_\alpha . Z(i, t)] \tag{19}$$

The mean effective activity concentration $\bar{C}_h(t)$ and mean annual dose $\bar{D}_h(t)$ to the haematopoietic tissue of the whole skeleton have been computed in a similar manner to Eqns 15 and 16. Since changes with age in the anatomy and physiology of the respiratory tract cause variation in the deposition of daughter products in the lung and the rest of body, an age-dependent dose modifying factor for bone marrow $K_m(t)$ has been employed. The factors, $K_m(t)$, and for bone $K_b(t)$, are the product of the relative deposition in the alveolar-interstitium, as determined by James et al (1990) and the ratio of the organ mass (Cristy & Eckerman, 1987) of an adult to that of a child, at age t (Table I).

$$\bar{D}_h(t) = \frac{\bar{C}_h(t) . E_\alpha . u . Q . Y . K_m(t)}{n} \tag{20}$$

Contribution from radon long-lived daughters

Clemente et al (1984) gives the results of regression analyses of the cumulative lung exposure due to radon

Table I. Age-dependent modifying factors based on relative deposition in the alveolar-interstitium by James et al (1990)

Age-dependent modifying factor	Age (years)					
	0	1	5	10	Female adult	Male adult
Alveolar-interstitium	0.057	0.28	0.54	0.70	0.79	1.00
Bone marrow $K_m(t)$	1.36	2.12	1.88	1.28	0.84	1.00
Bone $K_b(t)$	2.04	2.85	2.45	1.76	1.16	1.00

Table II. The percentage fat in marrow **(bold type)** and distribution of active marrow for various bones showing variation with age, from Cristy (1981) and extended for age greater than 40 years

Bone	Age (years)							
	0	1	5	10	15	25	40	70
Vertebrae, sternum, ribs	**0**	**5**	**15**	**20**	**25**	**28**	**30**	**42**
	23.4	27.6	33.9	41.7	52.2	58.3	61.4	61.4
Skull, scapulae	**0**	**5**	**20**	**35**	**45**	**58**	**62**	**75**
	32.2	30.2	20.2	15.6	13.4	11.4	11.2	11.2
Clavicles	**0**	**5**	**21**	**27**	**48**	**63**	**67**	**81**
	0.8	0.8	0.9	0.9	1.0	0.8	0.8	0.8
Upper half femora and humeri	**0**	**5**	**23**	**40**	**55**	**70**	**75**	**90**
	6.0	6.5	9.2	11.9	12.3	9.9	9.0	9.0
Lower half femora and humeri	**0**	**11**	**29**	**61**	**90**	**100**	**100**	**100**
	6.0	6.2	8.5	7.7	2.7	0	0	0
Tibiae, fibulae, patellae, ulnae and radii	**0**	**11**	**43**	**77**	**100**	**100**	**100**	**100**
	10.5	11.2	11.0	6.6	0	0	0	0
Ankle, foot, wrist and hand bones	**0**	**50**	**80**	**100**	**100**	**100**	**100**	**100**
	11.9	6.6	3.4	0	0	0	0	0
Os coxae	**0**	**5**	**21**	**28**	**36**	**42**	**52**	**63**
	9.2	11.1	13.1	15.6	18.5	19.5	17.5	17.5

and the resulting ^{210}Pb concentration, based on ^{210}Po measurements, in bone or teeth from studies of uranium miners and domestic radon exposure. Mainly linear relationships were found ranging from 0.03 Bq/kg of ^{210}Pb in bone to 1.2 Bq/kg in teeth per working level months (WLM) exposure. These extremes are taken as the basis of the lower and upper dosimetric estimates for radon-derived ^{210}Po. Our mean value of 0.1 Bq/kg per WLM was estimated from three studies of the levels of ^{210}Pb in the bones of uranium miners (Black et al, 1968; Blanchard et al, 1969; Holtzman, 1970). A linear correlation was assumed and the studies results were weighted by the number of miners involved. A ^{210}Po/^{210}Pb ratio of 0.8 was assumed for bone (UNSCEAR, 1988).

At average UK radon exposures the annual exposure of an adult is 0.1 WLM (Wrixon et al, 1988). At these exposures, the majority of the inhaled ^{210}Pb body burden is estimated to originate from ^{210}Pb and radon short-lived daughters, rather than radon soluble in tissues (Holtzman, 1963; Fisher, 1969). The greater part of ^{210}Pb is deposited in the skeleton. We have assumed that a child's annual exposure is the product of 0.1 WLM and age-dependent dose modifying factors for the bone $K_b(t)$ (Table I). Account has been taken of the physical decay of ^{210}Pb occurring after its initial uptake, both for UK citizens and for uranium miners who were on average exposed to an elevated radon atmosphere over a 20-year period. Allowance has been made for the growth of the skeleton, pre- and post-natally, which dilutes the ^{210}Pb accumulation in bone from previous exposure. The concentration of ^{210}Po in the bone of newborn is estimated, assuming that ^{210}Pb, like calcium (Walters, 1989), is derived wholly from the maternal system. A mean reproductive age of 30 years is assumed. The placental transfer of bismuth (Richardson et al, 1990b) and polonium is relatively poor compared to that of lead (Sikov, 1987). Allowance has been made for the ingrowth of ^{210}Po from ^{210}Pb, and the lower calcium concentration in fetal compared with the maternal bone (Dickerson, 1962) reducing the potential uptake of lead.

The dose to the active marrow of bone i, at age t, has been taken as the sum of the doses, from the alpha-particles originating from ^{210}Po in marrow $D_m(i, t)$ and bone $D_b(i, t)$ (Eqn 21). The 5.3 MeV alpha-particles were calculated to have ranges in adult marrow and bone of about 40 and 26 μm, with the elemental composition of bone given by Woodard (1962). It has been assumed that ^{210}Pb and ^{210}Po, with mean physical lifetimes of 30 years and 195 days, will be redistributed homogeneously in marrow by intracellular transport, bone remodelling and perhaps fat cell turnover (Van, 1985). The distribution of ^{210}Po in the marrow and bone volume have been assumed to be independently homogeneous, though at different activities. The estimated activity of ^{210}Po in bone has been reduced by a factor of 22 (UNSCEAR, 1988) to obtain an estimate of the activity in bone marrow. To estimate the dose to marrow from ^{210}Po it has been assumed that the large majority of active marrow lies within spherical cavities in trabecular bone: this is a good approximation, particularly in adults. The dose to marrow from ^{210}Po in marrow $D_m(i, t)$ has been estimated considering the ^{210}Po, in the trabecular cavity, as a spherical source. The geometric factor for the spherical source was calculated using Eqn 13, considering the contribution from $S_s(x_s)$ only.

$$\bar{D}_h(t) = \sum_i [D_m(i, t) + D_b(i, t)] \,.\, M(i, t) \qquad (21)$$

The dose from ^{210}Po from bone $D_b(i, t)$, to the whole marrow cavity has been calculated using Eqns 2 and 13, where r_s was considered to be minimal size (infinitely small). The spherical trabeculae cavities were assumed to have a mean cavity size as given by Spiers (1966) and ICRP (1975) for different bones of the skeleton. The percentage variation of the mean cavity size with age was based on Spiers' (1966) measurements for the vertebrae. Estimates of the elemental composition, density and alpha-particle range, R_α, were made for bone at different ages, based on the measurements of Dickerson (1962) and the methods of Robinson (1960), Woodard (1962) and Ziegler (1977). The age variation of the dosimetric parameter, $u.S_\alpha/n$ (Eqn 2 modified) was found to be dependent mainly on changes in S_α, with u/n remaining virtually constant. The mean annual dose $\bar{D}_h(t)$ to the total haematopoietic marrow of the skeleton was calculated as the summed dose to the marrow, of bones i, of age t, weighted by the fraction of skeletal marrow, $M(i, t)$.

Contribution from thoron and its daughters

Finally, the contribution from radon-220, normally referred to as thoron, and its daughter products have been taken into account. The results of regional surveys (Green et al, 1985) indicate that the mean equilibrium equivalent thoron concentration in UK homes is about 0.3 Bq/m^3 (Hughes et al, 1988). In outdoor air, a few available measurements, world-wide, of thoron decay products (UNSCEAR, 1982) point to an average ^{212}Pb/^{222}Rn activity ratio of about 0.04 (UNSCEAR, 1988). The UK average annual dose to the adult's red bone marrow from thoron and its daughter products has been estimated at 30 μSv (no range given), with about 90% of the dose coming from the thoron daughters (Stather et al, 1986). Dose factors for the inhalation of thoron (Peterman & Perkins, 1988), and indoor and outdoor thoron decay products, by members of the public are given by UNSCEAR (1988), adapted from the calculations of Jacobi & Eisfeld (1980, 1982). We have modified the value for the UK dose to an adult's marrow by the deposition factor $K_m(t)$ to give an estimate for different ages. It was assumed that the thoron daughter, ^{212}Pb ($T_{1/2} = 10.6$ hours) has time to become homogeneously distributed in marrow, with negligible changes of dose with cellularity.

Results

Basis of the dosimetric model

The age-dependent percentage of fat in marrow and the distribution of active marrow in bones of the skeleton are given in Table II for ages 0–70 years. For ages greater than 40 years the distribution of active marrow in the skeleton was assumed to remain the same as that at age 40. The fat fractions for ages greater than 40 were estimated by extending Cristy's (1981) data using the age patterns of the vertebrae, sternum and ribs given by Custer and Ahlfeldt (1932). Similarly, the age patterns for the anterior iliac crest by Hartsock et al (1965) were applied to the os coxae and the remaining 20% of active marrow of the skeleton, which also have a relatively high fat content.

Contribution from pure radon

The geometric factors S_α were determined for the radon point decay of ^{222}Rn, ^{218}Po and ^{214}Po. The greatest differences in the geometric factors of the three alpha-emitters occurs for intermediate fat fractions, where the different ranges of the alpha-particles have most effect (Table III, Fig. 5).

The mean dose to haematopoietic tissue from the point decay of ^{222}Rn, ^{218}Po and ^{214}Po has been estimated for variable fat fraction and fat cell diameters, for 1 Bq/m^3 radon concentration in inhaled air (Fig. 6). The

Table III. A comparison of the geometric factors S_α for alpha-particles of ^{222}Rn, ^{218}Po and ^{214}Po analysed for variable fat fractions Z and a constant fat cell diameter of 25–200 μm

Alpha-emitter	Range (μm)	Fat cell diameter (μm)	Fat fraction				
			0.1	0.3	0.5	0.7	0.9
^{222}Rn	42.8	25	0.667	0.835	0.900	0.944	0.986
		50	0.444	0.671	0.792	0.882	0.962
		100	0.238	0.482	0.657	0.797	0.926
		150	0.160	0.351	0.551	0.726	0.897
		200	0.120	0.265	0.462	0.663	0.869
^{218}Po	49.5	25	0.721	0.860	0.915	0.952	0.989
		50	0.489	0.703	0.814	0.895	0.963
		100	0.274	0.526	0.691	0.818	0.934
		150	0.185	0.399	0.592	0.758	0.917
		200	0.139	0.307	0.509	0.696	0.883
^{214}Po	74.2	25	0.827	0.910	0.944	0.969	0.995
		50	0.615	0.803	0.883	0.935	0.978
		100	0.397	0.637	0.769	0.867	0.953
		150	0.274	0.526	0.690	0.818	0.934
		200	0.207	0.437	0.624	0.774	0.915

Table IV. The mean annual dose μSv to haematopoietic tissue due to the point decay of ^{222}Rn, ^{218}Po and ^{214}Po, from radon dissolved in fat cells at different ages and fat cell diameters, for 1 Bq/m^3 radon concentration in air

Fat cells diameter	Age (years)							
	0	1	5	10	15	25	40	70
Minimal size	0.78	1.8	3.5	4.6	4.8	5.2	5.6	7.0
25 μm	0.78	1.6	3.2	4.2	4.4	4.8	5.2	6.6
50 μm	0.78	1.4	2.8	3.7	4.0	4.3	4.7	6.1
100 μm	0.78	1.2	2.3	3.2	3.4	3.7	4.1	5.5
150 μm	0.78	1.1	2.0	2.8	2.9	3.3	3.6	5.0
200 μm	0.78	1.1	1.8	2.5	2.6	2.9	3.3	4.6

dose is significantly reduced for large fat cell sizes compared with that for homogeneous mixing of haematopoietic marrow and fat. The latter is represented by a fat cell of minimal size (infinitely small). The age-dependent mean dose per year to haematopoietic marrow, for a range of fat cell diameters, was calculated for ages 0–70 years, inhaling a pure radon concentration of 1 Bq/m^3 (Table IV). Similarly, the mean annual dose to haematopoietic marrow at ages 0–70 years, accounting for cellularity and skeletal distribution, is shown in Fig. 7 for exposures at the average UK radon indoor concentration of 20 Bq/m^3. The mean annual dose increases 6-fold or more, with increasing fat cell size, from age 0–70 years.

Contribution from the inhalation of short-lived daughters

Taking into account age-dependent modifying factors (Table I), the mean dose to haematopoietic tissue from ^{214}Po has been calculated per unit Bq/m^3 radon exposure for different ages and fat cell diameters (Table V). The mean dose to active marrow from inhaled radon daughters shows a peak at around 1 year of age, due to respiratory deposition, with the dose falling off in the elderly, as shown in Fig. 7 for average UK exposures.

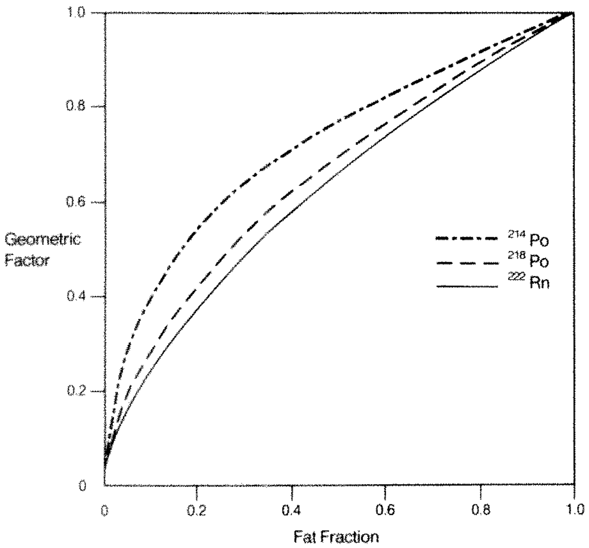

Figure 5. A comparison of the geometric factors S_α for the alpha-particles of ^{222}Rn, ^{218}Po and ^{214}Po for variable fat fractions Z and a fat cell diameter of 100 μm.

Contribution from radon long-lived daughters

The mean dose to active marrow from ^{210}Po, derived from the cumulative exposure to radon and daughter products, was calculated (Table VI, Fig. 7) for average UK radon exposures. The majority of the dose to the newborn marrow is from the ingrowth of ^{210}Po from

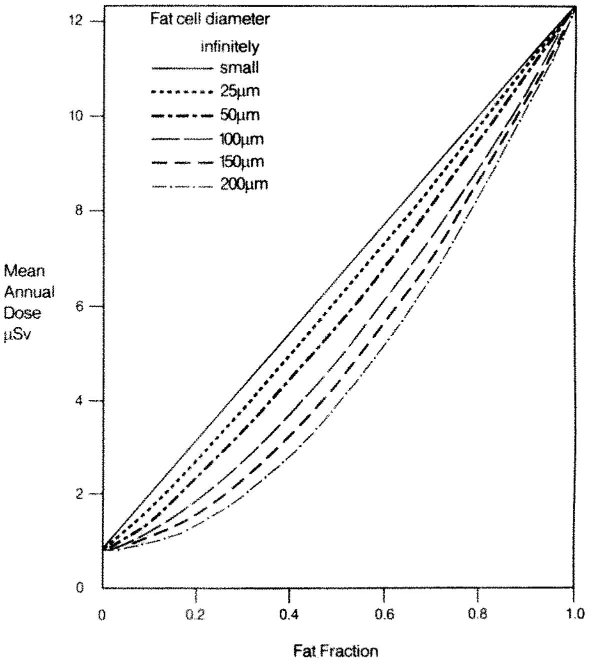

Figure 6. The mean annual dose to haematopoietic tissue for the point decay of ^{222}Rn, ^{218}Po and ^{214}Po, estimated for variable fat fraction Z and fat cell diameters of minimal size to 200 μm, for 1 Bq/m^3 radon concentration in inhaled air.

Table V. The mean annual dose μSv to haematopoietic tissue, from ^{214}Po per Bq/m^3 indoor ($F = 0.4$) radon exposure, at different ages and fat cells diameters up to 200 μm. Age-dependent deposition factors $K_m(t)$ have been employed. To convert to outdoor dose per Bq/m^3 it is necessary to multiply by the ratio of the activity values given in the section "Contribution from the inhalation of radon short-lived daughters" under "Theoretical methods"

Fat cells diameter	Age (years)							
	0	1	5	10	15	25	40	70
Minimal size	0.59	0.84	0.62	0.37	0.29	0.25	0.23	0.18
25 μm	0.59	0.85	0.64	0.39	0.30	0.26	0.24	0.19
50 μm	0.59	0.87	0.67	0.40	0.31	0.27	0.26	0.21
100 μm	0.59	0.88	0.70	0.43	0.33	0.29	0.28	0.23
150 μm	0.59	0.89	0.72	0.45	0.35	0.30	0.29	0.24
200 μm	0.59	0.90	0.73	0.46	0.36	0.31	0.30	0.25

^{210}Pb ($\sim 30\%$ of the ^{210}Pb activity), transferred from the mother's accumulated ^{210}Pb. The mean annual dose from ^{210}Po rises over 4-fold from 0 to 40 years, but increases only by a further 25% to 70 years of age. For the newborn, the child aged 10 years and the adult aged 40 years, the percentage of haematopoietic dose from ^{210}Po situated in marrow $D_m(t)$ is estimated at 42%, 46% and 57%, respectively, of the total dose to haematopoietic marrow $D_h(t)$ from ^{210}Po in both marrow and bone.

Total radon-derived and thoron-derived doses

A range of dose estimates to haematopoietic marrow for radon-derived exposure is given in Table VI and the mean value only illustrated in Fig. 8. The lower, mean and upper estimates for pure radon assume fat cell diameters of 150, 100 and 50 μm, respectively. Similarly, for radon daughters, fat-cell diameters of 50, 100 and 150 μm, and variation in C_h/C_B, have been assumed. At average UK exposures, the total radon-derived (^{222}Rn and daughters) dose per year rises continually with age, whereas the thoron-derived (^{220}Rn and daughters) dose reaches a maximum in infants at 1 year of age. The total radon and thoron-derived annual dose at average UK exposures in the newborn is around 70 μSv and rises rapidly in childhood, with a peak of 120 μSv at 5 years of age. This peak in marrow dose occurs principally because of the relatively high respiratory deposition in infants. The annual dose falls to a minimum of 110 μSv

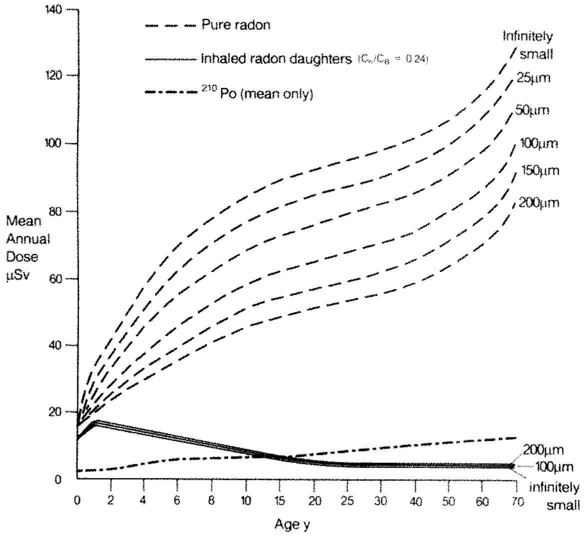

Figure 7. Comparison of the mean annual dose to haematopoietic marrow, fat cell size up to 200 μm, from the inhalation of pure radon, short-lived daughters, and radon-derived ^{210}Po, for 0–70 years of age at the mean UK radon exposure.

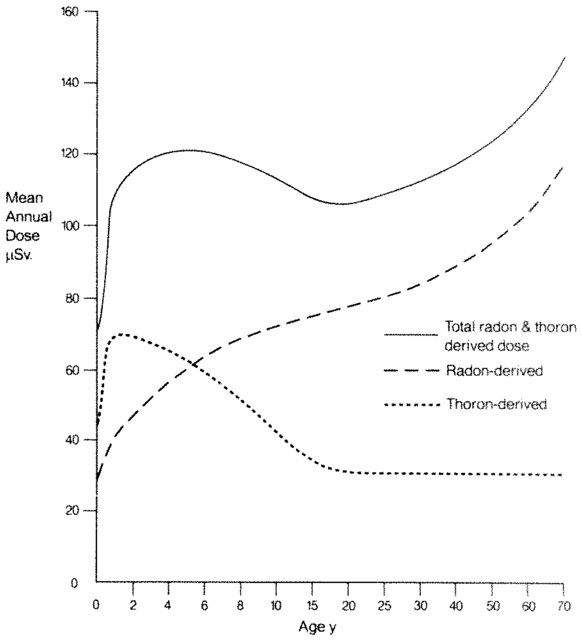

Figure 8. The mean values of the total dose to haematopoietic marrow from radon-derived (^{222}Rn and daughters) and thoron-derived (^{220}Rn and daughters) at average UK exposure, estimated from birth to 70 years of age. No range values are depicted; uncertainty limits are discussed in the text.

Table VI. The radon-derived (^{222}Rn and daughters) and thoron-derived (^{220}Rn and daughters) dose to haematopoietic marrow at the average UK exposure, from birth to 70 years of age. Mean annual doses in μSv are given, with the values in parentheses representing lower and upper limits

	Age (years)					
	0	5	10	15	40	70
^{222}Rn annual dose	14 (14)	42 (36–51)	58 (51–69)	62 (54–73)	75 (66–86)	101 (92–113)
^{222}Rn daughters annual dose	11 (7–15)	13 (11–22)	8 (5–11)	6 (4–9)	5 (3–7)	4 (3–6)
^{210}Po annual dose	2 (0.7–30)	4 (1–50)	5 (2–70)	5 (2–70)	9 (3–110)	12 (4–140)
Radon-derived annual dose	28	59	72	73	89	117
Radon-derived cumulative dose	0	220	620	900	2900	5900
Thoron-derived annual dose	44	60	42	33	30	30
Total radon and thoron-derived annual dose	72	120	113	106	119	147
Total radon and thoron-derived cumulative dose	0	540	1100	1700	4500	8400

for the 15–20-year-olds before rising again with age, having rounded values of 120 and 150 μSv at 40 and 70 years, respectively. The dose accumulated from birth to age 40 years is estimated at around 3 mSv derived from radon, and 4.5 mSv including thoron.

Discussion

Estimates of the mean dose to haematopoietic stem cells will have uncertainties due to the distribution of cellularity for a particular bone, and the large variations in the skeletal marrow of individuals which is reflected in the wide range of measurements obtained from different workers for cellularity and distribution data (Cristy, 1981). Variation in mean diameter or the effects of a distribution of sizes will lead to changes in the mean dose to haematopoietic marrow. The development period of adiopocytes is about 5 weeks (Emery & Follet, 1964; Tavassoli, 1976) and can be assumed to be short compared with their mean life-time, although definitive values are not available. For this reason we have treated fat cell sizes as constant with age. To improve the dosimetry more knowledge is required of fat cell size and their skeletal distribution. This is the subject of further work in this laboratory.

Previous estimates of the annual dose to bone marrow of an adult from the inhalation of pure radon were 0.71 and 0.78 μSv per Bq/m^3, estimated by Pohl and Pohl-Rühling (1977) and Peterman and Perkins (1988). This is similar to the estimate given here for fat-free marrow of the newborn. Our mean annual dose value per Bq/m^3 of 4.1 μSv and a range of 3.6–4.7 μSv to a 40-year-old adult's haematopoietic marrow is higher, mainly owing to allowance made for fat in marrow and the greater solubility of radon in fat relative to other tissues. The range given for the dose from radon gas (Table VI) takes no account of the uncertainties of radon solubility in fat. The Ostwald radon solubility coefficient measured for various fats, *in vitro* at 37°C, is generally in the range of 4 to 7, although some higher values have been reported for oils (Clever, 1979). Exhalation experiments in humans have been used to model uptake and solubility (Bernard & Snyder, 1975). In addition, whole body counting of γ-rays confirms, *in vivo*, the high solubility of radon in fat (Lykken et al, 1991).

Calculations of dose were also made that considered the variation of density and alpha-particle range in fat and haematopoietic tissue, rather than assuming these tissues to have the physical properties of water. The small change in dose estimates of $<5\%$ was not thought to warrant the additional theoretical complexity. Minor errors will arise from neglecting to consider the reduction in dose from radon due to edge effects at the marrow/bone interface of the trabecular cavities. However, calculation shows that the dose lost is about 5%. The additional dose contribution from radon in bone is negligible, since radon activity in bone is approximately 0.07 mBq/kg per Bq/m^3 (Peterman & Perkins, 1988). In the limit of low fat concentrations the marrow dose is dominated by radon in haematopoietic tissue, rather than in fat. However, it is interesting to note that total irradiation of the stem cell population from radon dissolved in fat within a trabecular marrow cavity occurs at comparatively low fat concentrations of marrow. For example, for fat cells of diameter 100 μm, a concentration within marrow of only 5% is sufficient for the entire stem cell population to be within range of alpha-particles emitted from radon and daughter nuclei within fat cells.

The dose to marrow from short-lived daughter products has been estimated in this work from measured activities in blood and the activity ratio of blood to that in marrow. Although this dosimetric study employed marrow to blood activity ratios in the range 0.16 to 0.32, it would appear that in animals the highest ratio is about 0.5 (Pohl & Pohl-Rüling, 1967). However, subtraction of a contribution from pure radon dissolved in fat in marrow may influence this value downwards. The mean annual dose to an adult's bone marrow due to domestic inhalation of radon daughters was estimated as 0.47 μSv per Bq/m^3 radon concentration by Pohl and Pohl-Rüling (1977), based on experimental data from man and animals and allowing for $F = 0.5$. This value is similar to that based on the modelling of Jacobi and Eisfeld (1980), but greater than the mean annual dose of 0.28 μSv Bq/m^3 to a 40-year-old adult's haematopoietic marrow for 100 μm diameter fat cells estimated in this paper. This is mainly because of assumed confinement of radon short-lived daughters to the haematopoietic tissue, causing a reduction in activity to the whole marrow and an increased loss of dose to fat cells with age.

Account has been taken of the age-dependent variation in the deposition of inhaled radionuclides in the lung, and hence in other organs, as developed by Hofmann et al (1979, 1982) and James et al (1990). The relative deposition data of Hofmann et al, shows a maximum at 6 years of age for the dose to bone marrow from the inhaled daughter products of radon and thoron. This compares with a peak at 1 year of age by James et al, where recent advances in the understanding of the infant's lung development, and other factors, have been taken into account.

The range of dose estimated to marrow for radon-derived ^{210}Po is very large, and reflects the uncertainty of ^{210}Pb and ^{210}Po activities in bone marrow (Fisher, 1969; Raabe, 1970), for different ages exposed to varying domestic radon concentrations. The upper limit relies on a ratio of unity for the ^{210}Po activity in teeth to that of bone (Clemente et al, 1984), and is perhaps overestimated. This dosimetric analysis can only give an order of magnitude to the ^{210}Po activity and mean dose to haematopoietic marrow. As yet, direct measurements are not available for activity in bone (rather than teeth) and marrow, correlated with domestic radon exposures. Some use has been made of uranium miner data; however, the atmospheric conditions in homes and mines can differ in factors such as the activity medium aerodynamic diameter (AMAD) of aerosols and the quantity of airborne dust. Smoking may be another factor, increasing ^{210}Pb and ^{210}Po activities in tissues (Radford & Hunt, 1964; Hill, 1965; Parfenov, 1974).

For marrow, at the average levels of indoor radon exposure estimated for the temperate world of 50 Bq/m^3, the mean radon-derived ^{210}Po activity of 25 mBq/kg estimated here for a 40-year-old is a significant proportion of the 110 mBq/kg ^{210}Po total activity given by UNSCEAR (1988). The remainder of the ^{210}Po comes mainly from ^{210}Pb in the diet (Hill, 1965; Smith-Briggs & Bradley, 1984). There is data showing the accumulation of ^{210}Po in bone with age in children (Czeglédi, 1987) and more activity in adult bone than that of children (Henshaw et al, 1988). Accumulation of ^{210}Po in teeth increases with all ages (Clemente et al, 1984), although this process in adult bone is less than certain (Holtzman, 1963; Hunt et al, 1963). Surprisingly, the long-term accumulation of ^{210}Pb in teeth from spa workers and "normal" populations have shown a higher accumulated activity concentration, in mBq/kg per WLM exposure, than the shorter term exposures for uranium miners. The ^{210}Pb and ^{210}Po bone concentrations have been observed to correlate with ^{210}Pb and ^{210}Po in blood and soft tissue organs (Blanchard & Moore, 1971). The bone to marrow ^{210}Po activity ratio used in this work is 22:1 from UNSCEAR (1988), but lower ratios have been recorded (Parfenov, 1974), including 10:1 by Ladinskaya et al (1973). A lower ratio would result in a higher dose to marrow; however, this has not been taken into account in our derivation of range limits for dose. There is also evidence suggesting a smaller bone to soft tissue Pb ratio in children than adults (Barry, 1975). To improve the reliability of the radon-derived ^{210}Po dose to marrow, further work is needed to determine ^{210}Pb accumulation in bone, and ^{210}Po in the marrow, for the general public.

Estimates of the dose from long-lived alpha-radionuclides in marrow are largely based on measurements confined to bone. Natural and artificial alpha-emitting radionuclides such as radium-226 and plutonium-239 selectively irradiate the proportion of marrow close to bone surfaces. Radium-226 is traditionally regarded as a bone-volume seeker (Spiers, 1988). Consequently, at natural levels of exposure, the marrow dose from ^{226}Ra in bone will be negligible (Fisenne et al, 1981). It should be noted that even in samples from West Cumbria, man-made actinides such as plutonium and americium represent less than 0.1% of the activity present from natural long-lived alpha-emitters in marrow and bone (Burkinshaw et al, 1987; Henshaw et al, 1988). In the UK, generally, it would be expected to be even lower. Unlike bone-seeking radionuclides, alpha-radiation from radon and thoron daughters irradiates the whole marrow volume. Spiers (1988) has argued that complete irradiation of the stem cell population has a potentially greater cancerous effect than does partial irradiation. Therefore the lower dose contribution from artificial alpha-radionuclides in bone may, in any case, be less effective than that derived from natural radon and thoron.

The annual UK radiation dose to red bone marrow from potassium-40, medical X-rays, nuclear fall-out and all other low LET sources is estimated as approximately 1 mSv (Stather et al, 1986), at all ages (Richardson & Henshaw, 1990). Potassium-40 resides mainly in fat-free tissue. Our calculations, not reported here, show an increased dose, world-wide, from potassium-40 to the active marrow of children compared with adults. The mean dose contribution from medical X-rays, in the UK, increases about 20-fold from children less than 15 years old to adults more than 64 years old. There is a much wider variation in the radon exposure of individuals. Average indoor radon concentrations vary nationally from between 9 and 150 Bq/m^3 (UNSCEAR, 1988). It is estimated that between 75 000 (NRPB, 1990) and 350 000 (IEHO, 1988) homes in the UK have radon concentrations in excess of the UK Action Limit of 200 Bq/m^3. Our calculations show that at this limit the radon and thoron-derived absorbed dose in the haematopoietic tissue of the adult is similar to that from low LET sources.

An important result from this work is that the dose derived from radon and thoron represents the largest contribution to marrow from alpha-radiation, even at UK mean exposures. It is interesting to note the role of the thoron-derived dose to active marrow. Thoron occurs in association with radon and we have shown here that for young children the radon dose to marrow is dominated by thoron daughters. This highlights the importance of thoron exposure in the home. Many passive type detectors used in national surveys detect radon only. From the point of view of accurate assessment of child dose, detectors designed specifically for the long-term measurement of thoron and its daughter nuclei should be employed. Thoron gas and progeny concentrations are often associated with radon gas and progeny concentrations (Schery, 1985; Martz et al, 1990) with elevated doses to red bone marrow from these sources in areas of high radon concentration. The half-life of thoron gas (55 seconds) is much less than that of radon gas (3.8 days), with thoron less able than radon to reach bone marrow. However, the relatively low concentrations of the inhaled thoron daughter ^{212}Pb, with a 10.6-hour half-life, irradiates marrow more effectively than the higher concentrations in air of the shorter-lived radon daughters.

The high incidence of lung cancer from radon exposure among uranium miners is well documented (BEIR IV, 1988) with less evidence or negative correlations for domestic dwellings (Haynes, 1988; Cohen, 1989; Blot et al, 1990; Butland et al, 1990). There is little evidence for the induction of leukaemia from radon among uranium miners, although Radford (1990) has shown an excess of multiple myeloma in iron miners. There are important, yet generally understated, differences in the radon and thoron-derived exposure of miners and the normal population. Besides the different atmospheric conditions, miners are male adults that are subjected to comparatively short-term exposures. For the general population, exposure occurs in the fetus and at all ages thereafter. For acute exposures, the fetus and child are known to be more radiation sensitive than adults (Richardson, 1990a). Radiation exposure of the father (Gardner et al, 1990) and the mother may lead to a higher risk of contracting leukaemia in their children.

Henshaw et al (1990) have suggested that, for radon levels in the dwellings of temperate countries, significant correlations exist between incidences of childhood and adult leukaemia and other cancers, including osteosarcoma. The bone stem cells, the critical tissue for osteosarcoma induction, will also have a radon dose elevated because of the presence of fat cells in marrow. If the observations of Henshaw et al (1990) are indicative of cause and effect, then the authors estimate that 6–12% of the incidence of myeloid leukaemia in the UK is associated with radon exposure. Within the UK, the association with leukaemia has been examined in detail by Alexander et al (1990). They also find significant correlations with radon exposure, the greatest effect being with acute lymphoblastic leukaemia in children.

In conclusion, this work has shown that, by considering the contribution from radon dissolved in fat, from inhaled radon and thoron daughters and accumulated ^{210}Po, the radon- and thoron-derived dose to active marrow is considerably greater than previously thought. These basic conclusions are unaffected by the wide range of dose limits owing principally to uncertainties in the accumulation of ^{210}Po in bone and marrow, and indicate useful areas of further research. Even at an indoor radon concentration of 20 Bq/m^3, the alpha-radiation dose to an adult's active marrow is dominated by radon exposure and in infants the dominant dose is from thoron daughters. At the UK Action Limit of 200 Bq/m^3, the dose to active marrow derived from radon and associated thoron exposure is similar to that from all low LET radiations. This work shows that the dose to red bone marrow from radon and thoron is significant, and that the possibility of leukaemia induced by these radiation sources warrants further investigation.

Acknowledgments

It is a pleasure to acknowledge the useful advice on theoretical methods from Drs J. H. Hannay and R. R. Hillier, Department of Physics, University of Bristol and Mr G. Staddon, Department of Medical Physics, Bristol General Hospital. We are very grateful to Dr A. C. James for discussions and data on the age-dependent deposition of inhaled radionuclides. We thank the NRPB for providing advice and radiation exposure data for the UK. We would like to thank Mr Y. M. Wong and Mr P. Cox for their excellent help in the preparation of the illustrations. This work is supported financially by MRC programme grant PG8319972II, by the Department of Health and the United Kingdom Coordinating Committee for Cancer Research (UKCCCR).

Table of symbols and units used in the model

Symbol	Unit	Meaning
Z	—	Fraction of fat in bone marrow
r_c	μm	Radius of cavity in fat
r_s	μm	Radius of spherical fat cell
x	μm	Distance from interface
$D_\alpha(x)$	μSv/s	Dose equivalent, for alpha-particle α at a distance x from a fat/haematopoietic tissue interface
C	Bq/kg	Activity concentration

Symbol	Unit	Meaning
E_α	MeV	Initial energy of alpha-particle α
u	—	Ratio of densities of the emitter and irradiated tissue
$S(x)$	—	Geometrical function, at distance x
Q	—	Quality factor
n	—	Ratio of the ranges in the irradiated and the emitter tissue
R	μm	Residual range of alpha-particle
E	MeV	Residual energy of alpha-particle
v and w	—	Empirical constants
R_α	μm	Range of alpha-particle α
P	—	Point at distance x from interface
x_c	μm	Shortest distance between cavity interface and point P
x_s	μm	Shortest distance between spherical interface and point P
ϕ	radian	Angle between alpha-emitter contribution and radial line through P
Y_- and Y_+	—	Dose contributions
a	—	Solutions of quadratic equation
a_- and a_+	—	Solutions of quadratic equation
j	—	Lesser of a_+ and R_α
k	—	Lesser of a_- and R_α
$S_c(x_c)$	—	Geometrical factor inside cavity at a radial distance x_c
$S_s(x_s)$	—	Geometrical factor outside sphere at a radial distance x_s
r	μm	Radial distance of "shell" in haematopoietic tissue from centre of fat cell
$S(r)$	—	Geometrical factor for haematopoietic volume at r
S_α	—	Mean geometrical factor for representative annulus of active marrow, for alpha-particle α
$Z(i, t)$	—	Fraction of fat for bone i at age t
C_f	Bq/kg	Activity concentration in fat
C_h	Bq/kg	Activity concentration in haematopoietic tissue
$C_h(i, t, \alpha)$	Bq/kg	Effective activity concentration in haematopoietic tissue, for bone i, age t, and alpha-particle α
$M(i, t)$	—	Fraction of skeletal active marrow in bone i at age t
$\bar{C}_h(t, \alpha)$	Bq/kg	Mean effective activity concentration in haematopoietic tissue, for age t and alpha-particle α
Y	—	Number of seconds in a year
$\bar{D}_h(t)$	μSv	Mean annual dose equivalent to haematopoietic marrow
F	—	Equilibrium factor
A_h	Bq	Activity in haematopoietic tissue
A_B	Bq	Activity in blood
C_B	Bq/kg	Activity concentration in blood
$\mathrm{d}A_\alpha/\mathrm{d}t$	Bq/s	Rate of change of activity for radionuclide α for tissue T
f_{T_α}	—	Uptake factor of tissue T, for α
A_{T_α}	Bq	Equilibrium activity in tissue T, for α
A_{B_α}	Bq	Equilibrium activity in blood, for α
λ_{p_α}	s^{-1}	Physical rate constant, for α
λ_{T_α}	s^{-1}	Biological rate constant, for tissue T, for α
$C_h(i, t)$	Bq/kg	Effective activity concentration of ^{214}Po in haematopoietic marrow of bone i at age t
$\bar{C}_h(t)$	Bq/kg	Mean effective activity concentration of ^{214}Po in haematopoietic marrow of skeleton at age t
$\bar{D}_h(t)$	μSv	Mean annual dose equivalent to the haematopoietic marrow of the skeleton at age t
$K_m(t)$	—	Age-dependent modifying factor for marrow
$K_b(t)$	—	Age-dependent modifying factor for bone
$D_m(i, t)$	μSv	Dose equivalent from ^{210}Po in marrow, irradiating the marrow of bone i at age t
$D_b(i, t)$	μSv	Dose equivalent from ^{210}Po in bone, irradiating the marrow of bone i at age t

References

ALEXANDER, F. E., McKINNEY, P. A. & CARTWRIGHT, R. A., 1990. Radon and leukaemia. *Lancet*, *i*, 1336–1337.

BARRY, P. S. I., 1975. A comparison of concentrations of lead in human tissues. *British Journal of Industrial Medicine*, *32*, 119–139.

BEIR IV, 1988. *Health Risks of Radon and Other Internally Deposited Alpha-emitters* (National Academy Press, Washington).

BERNARD, S. R. & SNYDER, W. S., 1975. *Metabolic Models for Estimation of Internal Radiation Exposure Received by Human Subjects from the Inhalation of Noble Gases* (ORNL Report 5046), pp. 197–204.

BLACK, D., 1984. Investigation of the possible increased incidence of cancer in West Cumbria. In *Report of the Independent Advisory Group* (Chairman: Sir Douglas Black) (HMSO, London).

BLACK, S. C., ARCHER, V. E., DIXON, W. C. & SACCOMANNO, G., 1968. Correlation of radiation exposure and lead-210 in uranium miners. *Health Physics, 14*, 81–93.

Blanchard, R. L., Archer, V. E. & Saccamanno, G., 1969. Blood and skeleton levels of ^{210}Pb-^{210}Po as a measure of exposure to inhaled radon daughter products. *Health Physics, 16*, 585–596.

Blanchard, R. L. & Moore, J. B., 1971. Body burden, distribution and internal dose of ^{210}Pb and ^{210}Po in a uranium miner population. *Health Physics, 21*, 499–518.

Blot, W. J., Xu, Z.-Y., Boice, J. D., Zhao, D.-Z., Stone, B. J., Sun, J., Jing, L.-B. & Fraumeni, J. F., 1990. Indoor radon and lung cancer in China. *Journal of the National Cancer Institute, 82*, 1025–1030.

Bossus, D. A. W., 1984. Emanating power and specific surface area. *Radiation Protection Dosimetry, 7*, 73–76.

Burkinshaw, L., Bayhreyni-Toossi, M. T. & Spiers, F. W., 1987. Plutonium content of tissues of members of the general public. *Journal of the Society of Radiological Protection, 7*, 27–32.

Butland, B. K., Muirhead, C. R. & Draper, G. J., 1990. Radon and leukaemia. *Lancet, i*, 1338–1339.

Casarett, L. J., 1964. Autoradiographic observations after inhalation of polonium-210 in rats. *Radiation Research, Suppl. 5*, 187–204.

Charlton, D. E. & Cormack, D. V., 1962. A method for calculating the alpha-ray dosage to soft tissue-filled cavities in bone. *British Journal of Radiology, 35*, 473–477.

Clemente, G. F., Renzetti, A., Santori, G., Steinhäusler, F. & Pohl-Rüling, J., 1984. Relationship between the ^{210}Pb content of teeth and exposure to Rn and Rn daughters. *Health Physics, 47*, 253–262.

Clever, H. L., 1979. *Krypton, Xenon and Radon (Gas Solubilities). Solubility Data Series, Vol. 2* (Pergamon Press, Oxford).

Cohen, B. L., 1989. Expected indoor ^{222}Rn levels in counties with very high and very low lung cancer rates. *Health Physics, 57*, 897–907.

Cristy, M., 1981. Active bone marrow distribution as a function of age in humans. *Physics in Medicine and Biology, 26*, 389–400.

Cristy, M. & Eckerman, K. F., 1987. *Specific Absorbed Fractions of Energy at Various Ages from Internal Photon Sources. I. Methods.* (ORNL/TM-8381/V1) (NTIS, Springfield, Virginia).

Custer, R. P. & Ahlfeldt, F. E., 1932. Studies on the structure and function of bone marrow. II. Variations in cellularity in various bones with advancing years of life and their relative response to stimuli. *The Journal of Laboratory and Clinical Medicine, 17*, 960–962.

Czeglédi, P., 1987. Natural contents of Ra-226, Pb-210 and Po-210 in young human bones and teeth. *Isotopenpraxis, 23(7)*, 272–277.

Dickerson, J. W. T., 1962. Changes in the composition of the human femur during growth. *Biochemistry Journal, 82*, 56–61.

Emery, J. L. & Follett, G. F., 1964. Regression of bone-marrow haemopoiesis from the terminal digits in the foetus and infant. *British Journal of Haematology, 10*, 485–489.

Fews, A. P., 1982. *A Study of Alpha Particle Tracks in CR-39 Plastic* (PhD thesis, University of Bristol).

Fisenne, I. M., Keller, H. W. & Harley, N. H., 1981. Worldwide measurement of ^{226}Ra in human bone: estimate of skeletal α dose. *Health Physics, 40*, 163–171.

Fisher, H. L., 1969. A model for estimating the inhalation exposure to radon-222 and daughter products from the accumulated lead-210 body burden. *Health Physics, 16*, 597–616.

Francis, E. A., 1987. *Patterns of Building Occupancy for the General Public (NRPB-M129)* (NRPB, Chilton).

Gardner, M., Snee, M. P., Hall, A. J., Powell, C. A., Downes, S. & Terrell, J. D., 1990. Results of case-control study of leukaemia and lymphoma among young people near Sellafield nuclear plant in West Cumbria. *British Medical Journal, 300*, 423–429.

Gray's Anatomy, 36th edn, 1980. Ed. by P. L. Williams & R. Warwick (Churchill Livingstone, London).

Green, B. M. R., Brown, L., Cliff, K. D., Driscoll, C. M. H., Miles, J. C. H. & Wrixon, A. D., 1985. Surveys of natural radiation exposure in UK dwellings with passive and active measurement techniques. *Science of the Total Environment, 45*, 459–466.

Hartsock, R. J., Smith, E. B. & Petty, C. S., 1965. Normal variations with aging of the amount of hemopoietic tissue in bone marrow from the anterior iliac crest. *American Journal of Clinical Pathology, 43*, 326–331.

Hausman, G. J., 1985. The comparative anatomy of adipose tissue. In *New Perspectives in Adipose Tissue: Structure, Function and Development*, ed by A. Cryer & R. L. R. Van (Butterworths, London), pp. 1–21.

Haynes, R. M., 1988. The distribution of domestic radon concentrations and lung cancer mortality in England and Wales. *Radiation Protection Dosimetry, 25*, 93–96.

Henshaw, D. L., Hatzialekou, U. & Randle, P. H., 1988. Analysis of alpha particle autoradiographs of bone samples from adults and children in the UK at natural levels of exposure. *Radiation Protection Dosimetry, 22*, 231–242.

Henshaw, D. L., Eatough, J. P. & Richardson, R. B., 1990. Radon as a causative factor in the induction of myeloid leukaemia and childhood cancer. *Lancet, i*, 1008–1012.

Hill, C. R., 1965. Polonium-210 in man. *Nature, 208*, 423–428.

Hiragun, A., 1985. Cell and tissue culture models of adipocyte development. In *New Perspectives in Adipose Tissue: Structure, Function and Development*, ed. by A. Cryer and R. L. R. Van (Butterworths, London), pp. 333–352.

Hofmann, W., Steinhäusler, F. & Pohl, E., 1979. Dose calculations for the respiratory tract from inhaled natural radioactive nuclides as a function of age. I. Compartmental deposition, retention and resulting dose. *Health Physics, 37*, 517–532.

—— 1982. Age-, sex-, and weight-dependent dose patterns due to inhaled natural radionuclides. In *Natural Radiation Environment*, ed. by K. G. Vohra, U. C. Mishra, K. C. Pillai & S. Sadasivan (J. Wiley & Sons, New York), pp. 1116–1144.

Holtzman, R. B., 1963. Measurement of the natural contents of RaD (Pb^{210}) and RaF (Po^{210}) in human bone—estimates of whole-body burdens. *Health Physics, 9*, 385–400.

—— 1970. Sources of ^{210}Pb in uranium miners. *Health Physics, 18*, 105–112.

Howarth, J. L., 1965. Calculation of the alpha-ray absorbed dose to soft tissue cavities in bone. *British Journal of Radiology, 38*, 51–56.

Hughes, J. S., Shaw, K. B. & O'Riordan, M. C., 1988. *Radiation Exposure of the UK Population—1988 Review (NRPB-R227)* (HMSO, London).

Hunt, V. R., Radford, E. P. & Segall, A. J., 1963. Comparison of concentrations of alpha-emitting elements in teeth and bones. *International Journal of Radiation Biology, 7(3)*, 277–287.

ICRP, 1975. *Report of the Task Group on Reference Man. Publication 23* (Pergamon Press, Oxford).

—— 1979. *Limits for Intakes of Radionuclides by Workers. Publication 30, Part 1. (Annals of ICRP 2 No. 3/4)* (Pergamon Press, Oxford).

—— 1980. *Limits for Intakes of Radionuclides by Workers. Publication 30, Part 2. (Annals of ICRP 4 No. 3/4)* (Pergamon Press, Oxford).

IEHO, 1988. *Radon: Report of the IEHO Survey on Radon in Homes 1987/8* (The Institution of Environmental Health Officers, London).

Jacobi, W. & Eisfeld, K., 1980. *Dose to Tissues and Effective Dose Equivalent by Inhalation of Radon-222, Radon-220 and Their Short-lived Daughters. GSF Report S-626* (Gesellschaft für Strahlen- und Umweltforschung, Munich-Neuherberg).

—— 1982. Internal dosimetry of radon-222, radon-220 and their short-lived daughters. In *Natural Radiation Environment*, ed. by K. G. Vohra, U. C. Mishra, K. C. Pillai & S. Sadasivan (J. Wiley & Sons, New York), pp. 131–143.

James, A. C., 1988. Lung dosimetry. In *Radon and Its Decay Products in Indoor Air*, ed. by W. W. Nazaroff and A. V. Nero (Wiley Interscience, New York), pp. 259–309.

James, A. C., Stahlhofen, W., Rudolf, G., Egan, M. J., Nixon, W. & Briant, J. K., 1990. The respiratory tract deposition model proposed by the ICRP Task Group. Presented at the 3rd International Workshop on Respiratory Tract Dosimetry, July 1–3, Albuquerque, New Mexico. *Radiation Protection Dosimetry* (in press).

Ladinskaya, L. A., Parfenov, Y. D., Popov, D. K. & Fedorova, A. V., 1973. ^{210}Pb and ^{210}Po content in air, water, foodstuffs, and the human body. *Archives of Environmental Health, 27*, 254–258.

Lord, B. I. & Schofield, R., 1980. Some observations on the kinetics of haemopoietic stem cells and their relationship to the spatial cellular organisation of the tissue. In *Biological Growth and Spread, Vol. 38*, ed. by W. Jäger, H. Rost and P. Tautu (Lecture Notes in Biomathematics), pp. 9–22.

Lucie, N. P., 1989. Radon exposure and leukaemia. *Lancet, ii*, 99–100.

Lykken, G. I., Ong, H.-S. & Speaker, K. K., 1991. Correlations among radon in the bedroom, the body and body fat mass (personal communication).

Martz, D. E., Falco, R. J. & Langner, G. H., 1990. Time-averaged exposures to ^{220}Rn and ^{222}Rn progeny in Colorado homes. *Health Physics, 58*, 705–713.

Nero, A. V., 1988. Radon and its decay products in indoor air: an overview. In *Radon and Its Decay Products in Indoor Air*, ed. by W. W. Nazaroff & A. V. Nero (J. Wiley & Sons, New York), pp. 1–53.

NRPB, 1990. *Human Exposure to Radon in Homes. Documents of the NRPB, Vol. 1, No. 1* (HMSO, London).

Nussbaum, E. & Hursh, J. B., 1957. Radon solubility in rat tissues. *Science, 125*, 552.

Nussbaum, E. & Hursh, J. B., 1958. Radon solubility in fatty acids and triglycerides. *Journal of Physical Chemistry, 62*, 81–84.

OPCS, 1985. *Mortality Statistics Cause. England and Wales, 1984*. Series DH2, No. 11 (HMSO, London).

Parfenov, Y. D., 1974. Polonium-210 in the environment and in the human organism. *Atomic Energy Review, 12*, 75–143.

Peterman, B. F. & Perkins, C. J., 1988. Dynamics of radioactive chemically inert gases in the human body. *Radiation Protection Dosimetry, 22*, 5–12.

Peto, J., 1990. Radon and the risks of cancer. *Nature, 345*, 389–390.

Pohl, E., 1964. Dose distribution received on inhalation of Rn^{222} and its decay products. In *Radiological Health and Safety in Mining and Milling of Nuclear Materials, Vol. 1* (IAEA, Vienna), pp. 221–236.

Pohl, E. & Pohl-Rüling, J., 1967. The radiation dose received by inhalation of air containing Rn222, Rn220, Pb212 (ThB) and their decay products. *Anais da Academia Brasileira de Ciências, 39*, 393–404.

—— 1977. Dose calculations due to the inhalation of ^{222}Rn, ^{220}Rn and their daughters. *Health Physics, 32*, 552–555.

Pohl-Rüling, J., Steinhäusler, F. & Pohl, E., 1982. Radiation exposure and resulting risk due to residence and employment in a radon spa. In *Natural Radiation Environment*, ed. by K. G. Vohra, U. C. Mishra, K. C. Pillai & Sadasivan (J. Wiley & Sons, New York), pp. 107–113.

Raabe, O. G., 1970. Concerning the relationship of lead-210 and inhalation exposure to radon-222. *Health Physics, 18*, 733–734.

Radford, E. P., 1990. Cancer in Swedish iron miners: a nearly complete follow-up study. Abstract in "Radiation protection: sense or nonsense?" (Proceedings of the BIR). *British Journal of Radiology, 63*, 373.

Radford, E. P. & Hunt, V. R., 1964. Polonium-210: a volatile radioelement in cigarettes. *Science, 143*, 247–249.

Richardson, R. B., 1990. Past and revised risk estimates for cancer induced by irradiation and their influence on dose limits. *British Journal of Radiology, 63*, 235–245.

Richardson, R. B. & Henshaw, D. L., 1990. Fetal and post-natal dose to red bone marrow from natural and artificial radiation exposure. Presented at a *EULEP Meeting, Chilton, 6–7th November* (EULEP Newsletter in press).

Richardson, R. B., Eatough, J. P. & Henshaw, D. L., 1990a. The contribution of radon exposure to the radiation dose received by the red bone marrow and the fetus. *International Journal of Radiation Biology, 57*, 597.

Richardson, R. B., Preece, A. W. & Henshaw, D. L., 1990b. The biodistribution and placental transfer of radiobismuth. Presented at a UKCCCR meeting, London, November 15.

Robinson, R. A., 1960. Chemical analysis and electron microscopy of bone. In *Bone As a Tissue*, ed. by K. Rodahl, J. T. Nicholson and E. M. Brown (McGraw-Hill, New York), pp. 186–250.

Russ, G. A., Bigler, R. E., Tilbury, R. S., Woodard, H. Q. & Laughlin, J. S., 1975. Metabolic studies with radiobismuth: I. Retention and distribution of ^{206}Bi in the normal rat. *Radiation Research, 63*, 443–454.

Schery, S. D., 1985. Measurements of airborne ^{212}Pb and ^{220}Rn at varied indoor locations within the United States. *Health Physics, 49*, 1061–1067.

Sikov, M. J., 1987. Placental transfer of the actinides and related heavy elements. In *Age-related Factors in Radionuclide Metabolism and Dosimetry*, ed. by G. B. Gerber, H. Métivier and H. Smith (CEC, published by Martinus Nijhoff, Dordrecht), pp. 303–314.

Sjöström, L., Björntorp, P. & Vrana, J., 1971. Microscopic fat cell size and measurement on frozen-cut adipose tissue in comparison with automatic determinations of osmium-fixed cells. *Journal of Lipid Research, 12*, 521–527.

Smith-Briggs, J. L. & Bradley, E. J., 1984. Measurement of natural radionuclides in UK diet. *The Science of the Total Environment, 35*, 431–440.

Spiers, F. W., 1966. Dose to bone from strontium-90: implications for the setting of the maximum permissible body burden. *Radiation Research, 28*, 624–642.

—— 1988. Particle dosimetry in bone and the toxicity of bone-seeking radionuclides. *Physics in Medicine and Biology, 33*, 395–411.

Stather, J. W., Dionian, J., Brown, J., Fell, T. P. & Muirhead, C. R., 1986. *The Risks of Leukaemia and Other Cancers in Seascale from Radiation Exposure (NRPB-R171 addendum)* (HMSO, London).

Stover, B. J., 1959. Pb^{212} (ThB) tracer studies in adult beagle dogs. *Proceedings of the Society for Experimental Biology and Medicine, 100*, 269–272.

SZYMAŃSKA, J. A., ZELAZOWSKI, A. J. & KAWIORSKI, S., 1981. Some aspects of bismuth metabolism. *Clinical Toxicology, 18(11)*, 1291–1298.

TAVASSOLI, M., 1976. Ultrastructural development of bone marrow adipose cell. *Acta Anatomica, 94*, 65–77.

THOMAS, R. G., 1964. The binding of polonium by red cells and plasma proteins. *Radiation Research, Suppl. 5*, 29–39.

UNSCEAR, 1982. *Ionizing Radiations. Sources and Biological Effects* (United Nations, New York).

—— 1988. *Sources, Effects and Risks of Ionizing Radiation* (United Nations, New York).

VAN, R. L. R., 1985. The adipocyte precursor cell. In *New Perspectives in Adipose Tissue: Structure, Function and Development*, ed. by A. Cryer and R. L. R. Van (Butterworths, London), pp. 353–382.

WALDRON, H. A. & STÖFEN, D., 1974. *Sub-clinical Lead Poisoning* (Academic Press, London).

WALTERS, B. N. J., 1989. Calcium metabolism in pregnancy. *Fetal Medicine, 1*, 213–222.

WATANABE, G. & YANA, T., 1953. Distribution of lead in blood. *Archives of Industrial Hygiene and Occupational Medicine, 7*, 444–445.

WEISS, L., 1970. The histology of the bone marrow. In *Regulation of Hematopoiesis*, ed. by A. Gordan (Appleton-Century-Crofts, New York), pp. 79–92.

WOODARD, H. Q., 1962. The elementary composition of human cortical bone. *Health Physics, 8*, 513–517.

WRIXON, A. D., GREEN, B. M. R., LOMAS, P. R, MILES, J. C. H., CLIFF, K. D., FRANCIS, E. A., DRISCOLL, C. M. H., JAMES, A. C. & O'RIORDAN, M. C., 1988. *Natural Radiation Exposure in UK Dwellings (NRPB-R190)* (HMSO, London).

ZIEGLER, J. F., 1977. *Helium: Stopping Powers and Ranges in All Elemental Matter. (Vol. 4 of The Stopping and Ranges of Ions in Matter)* (Pergamon Press, New York).

ZUCKER-FRANKLIN, D., GRUSKY, G. & MARCUS, A., 1978. Transformation of monocytes into "fat" cells. *Laboratory Investigation, 38*, 620–628.

1991, *The British Journal of Radiology*, *64*, 625–626

Case reports

Anaphylactoid reaction associated with the use of ^{99}Tc^{m} hexamethyl propylene amine oxime as a leukocyte labelling agent

By M. H. Giaffer, MB, MRCP, *W. B. Tindale, MSc, PhD, *S. Senior and C. D. Holdsworth, MD, FRCP

(Received February 1990 and in revised form October 1990)

Keywords: Anaphylactoid reaction, ^{99}Tc^{m}-HMPAO, Labelled leukocytes, Crohn's disease

^{99}Tc^{m}-HMPAO-labelled leukocyte bowel scanning is being increasingly used in the assessment of disease extent and activity in patients with inflammatory bowel disease, particularly Crohn's disease, when clinical and laboratory indices of activity can be unreliable. Initial experience with this compound has shown that it is safe. No reported adverse reactions have been associated with its use in white cell studies. This case report describes an anaphylactoid reaction related to the use of this new granulocyte labelling tracer.

Case report

A 41-year-old woman with Crohn's disease was admitted to hospital for assessment of recurrent abdominal pain, watery diarrhoea and generalized lethargy. Crohn's disease affecting the terminal ileum and the proximal colon had been diagnosed on radiological grounds in 1969. Owing to worsening symptoms that failed to respond to medical treatment, a subtotal colectomy with ileo-sigmoid anastomosis was performed in 1973. She continued to have mild bowel symptoms after her operation and further assessment in 1987 showed radiological evidence of disease recurrence at the anastomosis site. She responded clinically to a course of steroids and was subsequently maintained on sulphasalazine. There was no previous history of any drug allergy or atopy.

On admission she was afebrile with a radial pulse of 80/min and blood pressure of 130/85 mmHg. The abdomen was soft but tender in the left iliac fossa. Basal investigations including haemoglobin, total leukocyte and platelet counts, urea, electrolytes, albumin, alkaline phosphatase, transaminases C-reactive protein and alpha-1 acid glycoprotein were normal. In view of the presence of significant symptoms but otherwise normal laboratory measurements, a ^{99}Tc^{m}-HMPAO-labelled leukocyte bowel scan was performed to assess disease activity.

The method of leukocyte labelling using ^{99}Tc^{m}-HMPAO was that described by Danpure et al (1988). Briefly, 102 ml of venous blood were taken and anti-coagulated with 18 ml of acid-citrate-dextrose. 20 ml of this mixture were centrifuged to obtain the cell-free plasma (CFP1); 10 ml of 6% hydroxyethyl starch were added to the remaining 100 ml and left at room temperature to sediment the erythrocytes. The leukocyte- and platelet-rich supernatant was then removed and centrifuged slowly to sediment the leukocytes. After removal of the platelet-rich plasma the mixed leukocytes were resuspended in the cell-free plasma (CFP1) and incubated with ^{99}Tc^{m}-HMPAO. The platelet-rich plasma was centrifuged to obtain cell-free plasma (CFP2), which was used for washing the radiolabelled leukocytes. The cells were then resuspended in cell-free plasma uncontaminated by starch (CFP1) and then administered intravenously using a 19G needle to the patient in the seated position. Immediately following the injection of the radiolabelled leukocyte suspension, the patient collapsed and became pale and hypotensive. The radial pulse was 110/min and the supine blood pressure (BP) was 100/70 mmHg. She was immediately given 100 mg of hydrocortisone intravenously and 0.5 ml of 1:1000 adrenaline intramuscularly. The BP rose to 120/70 mmHg and remained stable. Despite the normal BP, she continued to have postural fainting for about 5 h after the injection. She was nursed in a supine position but no other treatment was needed. By 24 h, her recovery was complete and she was later discharged from hospital. As a result of the patient's condition in the first few hours after administration of radiolabelled leukocytes, imaging was not carried out.

Discussion

Adverse reactions to radiopharmaceuticals are fortunately uncommon, and life-threatening reactions are exceedingly rare. The majority of adverse reactions related to the use of radiopharmaceuticals are of the hypersensitivity (idiosyncratic) type and usually follow a recognizable clinical pattern such as skin rash, urticaria, angioedema or anaphylaxis. It is not always possible to foresee the occurrence of these reactions since a previous history of atopy or drug allergy is not usually associated with a propensity to develop an adverse drug reaction.

^{99}Tc^{m}-HMPAO (Amersham International PLC) is a recently introduced agent for brain imaging (Ell et al, 1985; Nowotnik et al, 1985). Its lipophilic characteristics have, in addition, enabled its use as a leukocyte label for the localization of inflammation and infection (Peters et al, 1986). In inflammatory bowel disease the technique has been used to assess disease extent and severity with encouraging results (Scholmerich et al, 1986). From a radiation dose and image quality viewpoint, it is preferred to indium-111-labelled leukocytes, which are also widely used in the assessment of patients with inflammatory bowel disease, particularly Crohn's disease, which may affect parts of the gastrointestinal tract inaccessible to conventional diagnostic procedures. The use of ^{99}Tc^{m}-HMPAO has not previously been associated with serious adverse reactions. Vasomotor changes such as faintness, loss of consciousness and hypotension have, however, complicated the clinical use of other ^{99}Tc^{m} complexes (Keeling, 1984).

Gastroenterology Unit and *Department of Medical Physics, Royal Hallamshire Hospital, Sheffield S10 2JF, UK

The anaphylactoid reaction observed in our patient is likely to have resulted from the radiopharmaceutical moiety itself, although theoretically the small quantity of hydroxyethyl starch (molecular weight 45 000) that was added during the process of leukocyte labelling may have contributed to this reaction. The leukocytes were washed free of starch according to the Hammersmith protocol, but since the whole of the labelled leukocyte suspension was administered to the patient, none was available for analysis to assess residual starch contamination. We have used ^{99}Tc^{m}-HMPAO-labelled leukocyte bowel scanning in over 60 patients and so far this is the only adverse reaction observed. It seems unlikely therefore that this reaction was a result of systematic fault in the cell washing process. Psychomotor changes resulting from the injection itself do not seem to be relevant in our case since the symptoms were protracted and lasted for over 5 h. Venous blood was obtained from the patient using a needle of similar size to the one used to administer the labelled cell suspension 2 h earlier without any reaction. During the current hospital admission and in the past, venepuncture was performed on our patient for various blood tests. It was never associated with a vasomotor reaction.

References

DANPURE, H. J., OSMAN, S. & CARROLL, M. J., 1988. The development of a clinical protocol for the radiolabelling of mixed leucocytes with ^{99m}Tc-hexamethyl propylene amine oxime. *Nuclear Medicine Communications*, *9*, 465–475.

ELL, P. J., JARRITT, P. H., CULLUM, I., COSTA, D. C., HOCKNELL, J. M. L., LUI, D., JEWKES, R. F., STEINER, T. J., NOWOTNIK, D. P., PICKETT, R. D. & NEIRINCKX, R. D., 1985. Regular cerebral blood flow mapping with ^{99m}Tc labelled compound. *Lancet*, *ii*, 50–51.

KEELING, D. H., 1984. Adverse reactions to radiopharmaceuticals: United Kingdom 1977–1983. *British Journal of Radiology*, *57*, 1091–1096.

NOWOTNIK, D. P., CANNING, L. R., CUMMING, S. A., HARRISON, R. C., HIGLEY, B., NECHVATAL, G., PICKETT, R. D., PIPER, R. M., BAYNE, V. J., FORSTER, A. M., WEISNER, P. S. & NEIRINCKX, R. D., 1985. Development of a ^{99m}Tc labelled radiopharmaceutical for cerebral blood flow imaging. *Nuclear Medicine Communications*, *6*, 499–506.

PETERS, A. M., DANPURE, H. J., OSMAN, S., HAWKER, R. J., HENDERSON, B. L., HODGSON, H. J., KELLY, J. D., NEIRINCKX, R. D. & LAVENDER, J. P., 1986. Clinical experience with ^{99m}Tc hexamethyl propylene amine oxime (labelling leucocytes and imaging inflammation). *Lancet*, *ii*, 946–949.

SCHOLMERICH, E. J., SCHMIDT, C., SCHUMICHEN, P., BILLMAN, P., SCHMIDT, H. & GEROK, W., 1988. Scintigraphic assessment of bowel involvement and disease activity in Crohn's disease using Technetium ^{99m}-hexamethyl propylene amine oxime as leukocyte label. *Gastroenterology*, *95*, 1287–1293.

SCHUMICHEN, C., SCHOLMERCH, J. & FREIBURG, B., 1986. ^{99m}Tc HMPAO labelling of leucocytes for detection of inflammatory bowel disease. *Compact News in Nuclear Medicine*, *5*, 274–276.

Radiology of secondary amyloidosis of the stomach in a patient with rheumatoid arthritis

By S. Kawamura, MD, *A. Imai, MD, M. Kawamura, MD, M. Kataoka, MD, H. Itoh, MD, A. Komatsu, MD and K. Hamamoto, MD

Department of Radiology, Ehime University School of Medicine, Shitsukawa 454, Shigenobu-cho, Onsen-gun, Ehime, Japan and *Department of Rheumatology, Dogo Spa Hospital, Matsuyama, Ehime, Japan

(*Received July 1990 and in revised form January 1991*)

Keywords: Stomach, Ultrasonography, Barium meal radiology, Secondary amyloidosis, Rheumatoid arthritis

Ultrasonography (US) of the fasting stomach in a patient suffering from secondary amyloidosis with a confirmed diagnosis of rheumatoid arthritis revealed thickening of the wall, as well as retention of secretions and delayed emptying of contents despite no administration of an anticholinergic agent such as butylscopolamine (Buscopan, Schering Pharmaceutical Co.). The US findings in the stomach of a patient with secondary amyloidosis are as non-specific as those of barium meal radiography. Nevertheless, US is useful not only as a supplement to endoscopic examination and a barium meal, but also as a diagnostic alternative in selected patients who cannot be scanned by standard methods.

Case report

For the previous 2 months, a 68-year-old female with rheumatoid arthritis had complained of fever, persistent severe diarrhoea, and pitting oedema of the foot, as well as weight loss. Laboratory examinations showed hyponatremia and hypoalbuminemia. There was occult blood in the faeces. Secondary amyloidosis was suspected. Ultrasound of the fasting stomach (Fig. 1), with a 3.5 MHz linear transducer (Toshiba Co. Ltd.), revealed remarkable wall thickening measuring up to a maximum of 7 mm, as well as increased

---

Address reprint requests to Sachiko Kawamura, MD, Department of Radiology, Ehime University School of Medicine, Shitsukawa 454, Shigenobu-cho, Onsen-gun, Ehime, 791-02, Japan.

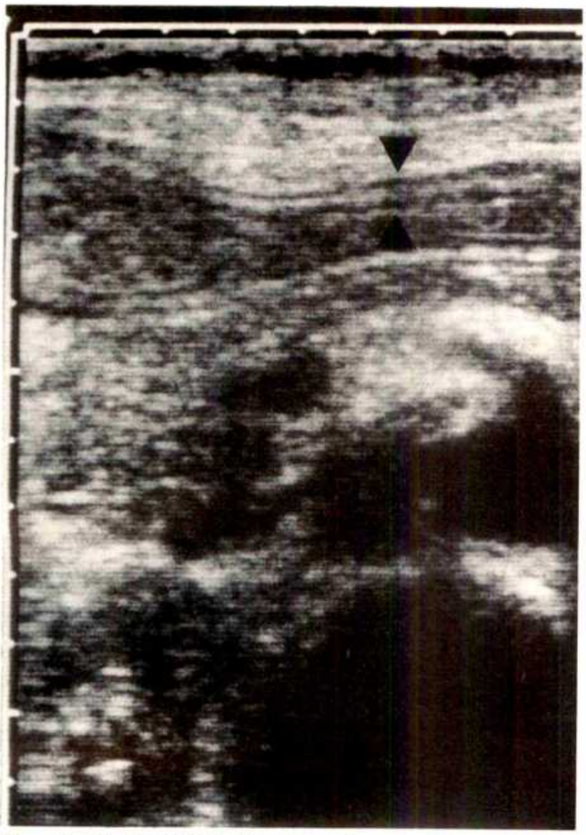

Figure 1. The initial US when the patient suffered from severe persistent diarrhoea. US of the fasting stomach (transverse section of the upper abdomen) showed wall thickening of 7 mm (arrowheads), retained secretions and delayed emptying despite no use of butylscopolamine.

echogenicity in the wall, retention of secretions and delayed emptying of gastric contents despite no administration of butylscopolamine. These US findings strongly suggested secondary amyloidosis. She then received an intensive treatment of prednisolone and intravenous hyperalimentation. After 1 month diarrhoea subsided. Follow-up US of the fasting stomach (Fig. 2a) showed wall thickening up to a maximum of 8 mm and a decrease in the gastric contents as compared with the first US scan. Following the fasting US, the patient was given 300 ml of water, and rescanning (Fig. 2b) revealed once again remarkable wall thickening, up to a maximum of 7 mm, and increased echogenicity in the wall. At that time barium meal showed retention of secretions within the normal range and no rigidity of the wall in the upright position (Fig. 3a), but rather an absence of the normal rugal pattern in the supine position (Fig. 3b). Histological examinations of the gastric wall biopsy revealed extensive amyloid deposition in the wall of the blood vessels and mild deposition in the lamina propria mucosa.

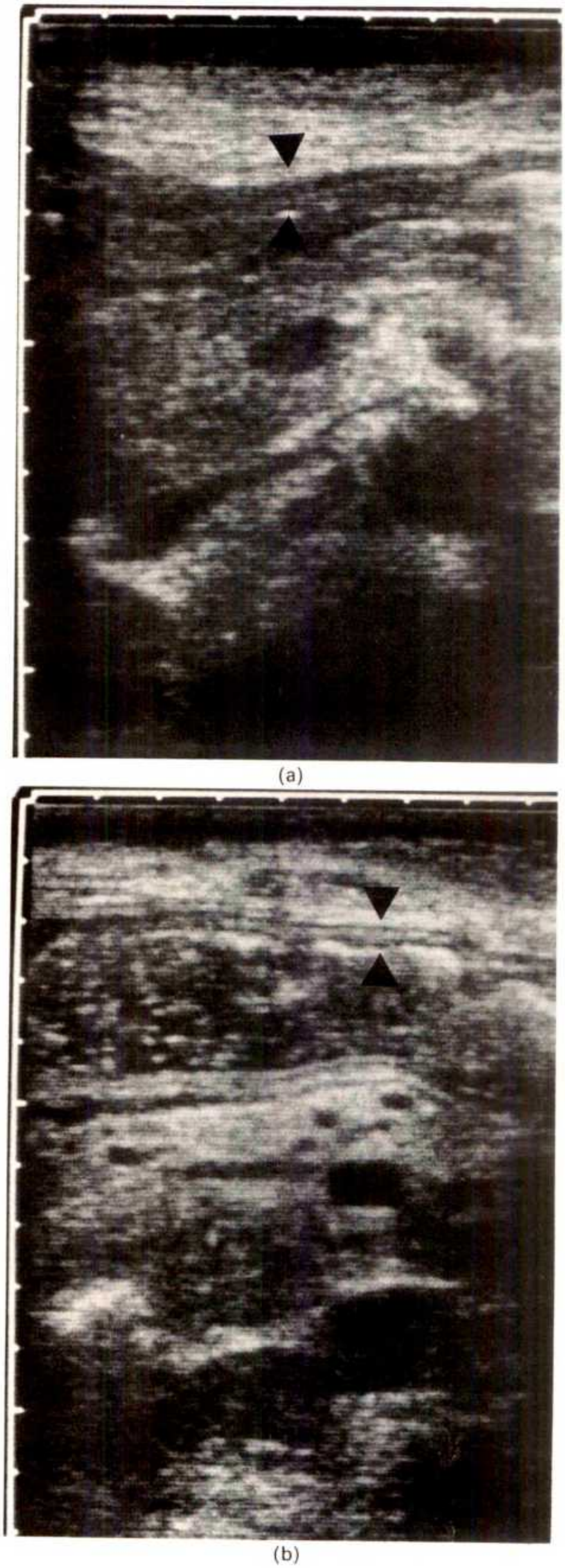

Figure 2. Follow-up US when diarrhoea stopped (the same section as shown in Fig. 1). (a) US of the fasting stomach revealed wall thickening of 8 mm (arrowhead) and gastric contents decreased as compared with the first US. (b) In the fluid-filled stomach, after 300 ml of water, wall thickening of 7 mm maximum and increased echogenicity in the wall (arrowheads) were still seen.

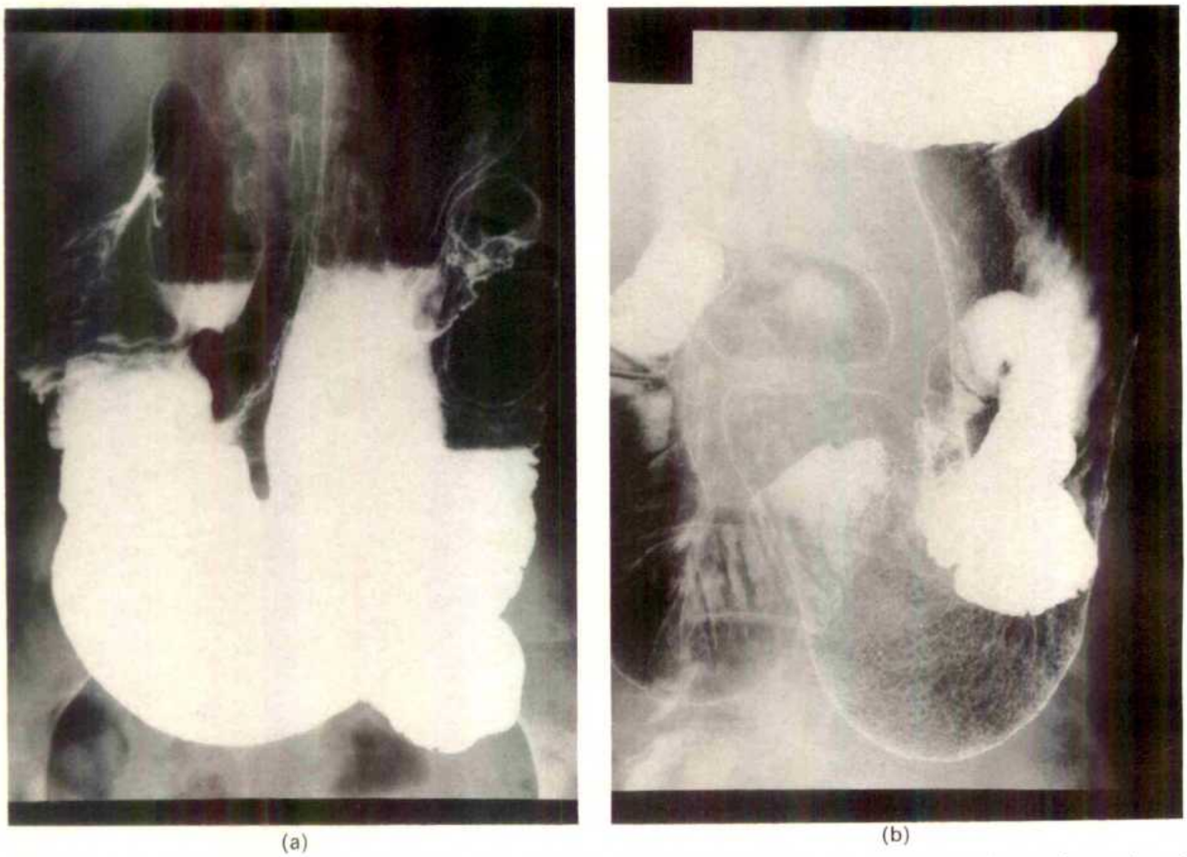

Figure 3. Barium meal at the time of follow-up US. (a) The upright barium meal radiography showed normal retention of secretions and no wall rigidity. (b) Supine view with loss of rugal folds.

Discussion

A combination of amyloidosis and malabsorption in patients suffering from gastrointestinal disturbances in association with severe rheumatoid arthritis has been reported by Cohen (1967) and Pettersson et al (1970). In gastrointestinal amyloidosis, the whole thickness of the intestinal wall may be involved, resulting in a wide spectrum of symptoms (Cohen, 1967; Pettersson et al, 1970). Legge et al (1970) described the effects of gastrointestinal amyloidosis as dysphagia, gastric retention, constipation or diarrhoea, and eventually intestinal obstruction which can prove fatal. A correct diagnosis is important in patients with gastrointestinal amyloidosis, because surgical treatment may be useless and will result in complications and a high mortality rate.

The findings on barium meal examination are: (1) gastric mucosal changes with a loss of rugal folds; (2) wall rigidity with a small stomach mimicking of scirrhous carcinoma in severe involvement; and (3) motor abnormalities such as retained gastric secretions and delayed emptying (Legge et al, 1970). The US findings included wall thickening, retained gastric secretions and delayed emptying in the fasting stomach. To assess the gastric wall thickness by US, we employed Fleischer's method (Fleischer et al, 1981), of measuring wall thickness in the distended and non-distended stomach with a range up to 6 mm in the non-distended state and up to 4 mm in the distended state.

In our present patient, persistent severe diarrhoea was a prominent symptom. US of the fasting stomach revealed remarkable wall thickening up to a maximum of 7 mm. In contrast, the barium meal revealed no suspicion of wall thickening. Moreover, comparing the first and follow-up US of the fasting stomach, the gastric residue was reduced following treatment. In severe diarrhoea, nausea and vomiting, an US may be superior to a barium meal (Worlicek et al, 1989) in assessing the stomach wall.

Acknowledgments

The authors thank Mr Patrik Mohr, Mr Jim King and Miss Catherine Betz for helping to prepare of this manuscript.

References

COHEN, A. S., 1967. Amyloidosis. *New England Journal of Medicine*, *277*, 522–530, 574–583, 628–638.

FLEISCHER, A. C., MUHLETALER, C. A. & JAMES, A. E., 1981. Sonographic assessment of the bowel wall. *American Journal of Roentgenology*, *136*, 887–891.

LEGGE, D. A., CARLSON, H. C. & WOLLAEGER, E. E., 1970. Roentgenologic appearance of systemic amyloidosis involving gastrointestinal tract. *Radiology*, *110*, 406–412.

PETTERSSON, T., WEGELIUS, O. & SKRIFVARS, B., 1970. Gastrointestinal disturbances in patients with severe rheumatoid arthritis. *Acta Medica Scandinavica*, *188*, 139–144.

WORLICEK, H., DUNZ, D. & ENGELHARD, K., 1989. Ultrasonic examination of the wall of the fluid-filled stomach. *Journal of Clinical Ultrasound*, *17*, 5–14.

Sling left pulmonary artery with congenital airway stenosis: non-invasive investigation and conservative management?

By *G. M. A. Hendry, MB, BS, DMRD, FRCR, A. T. Edmunds, MA, BM, BCh, FRCP, T. G. Marshall, MB, ChB, MRCP and N. Chalmers, MB, ChB, MRCP, FRCR

Royal Hospital for Sick Children, 9 Sciennes Road, Edinburgh EH9 1LF, UK

(*Received August 1990 and in revised form October 1990*)

Keywords: Pulmonary arteries, Abnormalities, Trachea, Stenosis

A 3-month-old boy presented with stridor and respiratory distress. Investigations showed him to have a long-segment upper airway stenosis with a sling left pulmonary artery. Investigation and management is discussed.

Case report

A 3-month-old boy presented with a short history of progressive respiratory distress and stridor. A chest radiograph showed mediastinal shift to the right. A high-kV radiograph showed apparent complete occlusion of the right main bronchus (RMB) about 1 cm from the carina.

At bronchoscopy the RMB was thought to be compressed by an extrinsic mass. Adequate ventilation was impossible. Blood gases showed respiratory acidosis. A thoracotomy failed to reveal any mass compressing the RMB. Repeat bronchoscopy confirmed a "pit-like" RMB orifice and an inflamed and narrowed left main bronchus (LMB). A brief cardiac arrest followed bronchoscopy. He was successfully resuscitated with adrenaline instilled into the endotracheal tube. Post-operatively, ventilation pressures of 60/15 were required to maintain slight chest movement and acceptable blood gases. He was treated with nebulized adrenaline, ribavirin, steroids and antibiotics. He gradually improved and was extubated after 11 days.

Bronchography (Fig. 1) showed a rudimentary RMB with an abnormally high carina. The proximal LMB took an almost vertical course through the mediastinum and bifurcated at the T6 level into a bronchus to the right lung (the "bridging bronchus" (Gonzalez-Crussi et al, 1976)) and one to the left lung. These bronchi had an almost horizontal course, forming an "inverted T" shape with the proximal LMB.

Barium swallow (Fig. 2) performed immediately after bronchography, with some residual contrast medium in the bronchial tree, showed anterior displacement of the proximal portion of the LMB from the oesophagus and an indentation on the anterior surface of the oesophagus, indicating a sling left pulmonary artery (SLPA), confirmed by echocardiography.

A computed tomographic (CT) scan with dynamic contrast enhancement (Fig. 3) showed the aberrant left pulmonary artery (LPA) arising from the right pulmonary artery (RPA) passing between the LMB anteriorly and the oesophagus and descending aorta posteriorly. The proximal portion of the LMB was only 3–4 mm in diameter over its entire length, but it was not locally compressed by the aberrant vessel. Computed tomography confirmed hypoplasia of the right lung.

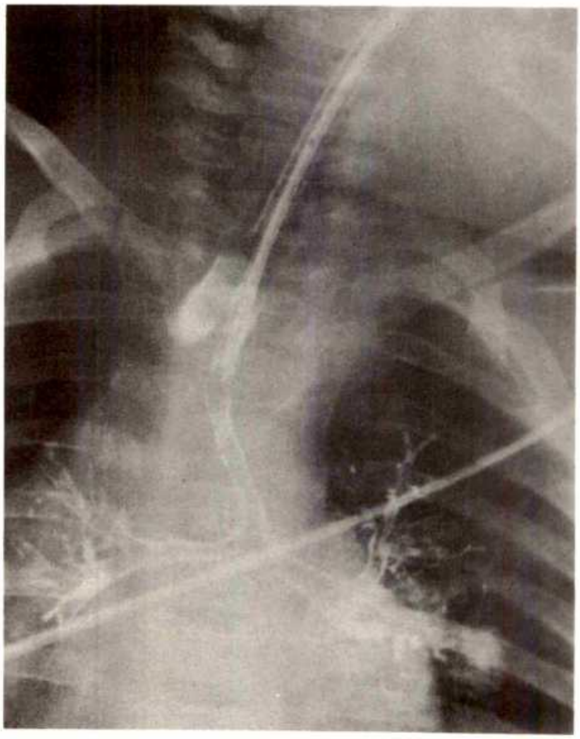

Figure 1. Bronchogram showing the high carina projected over T3, with the rudimentary RMB, the nearly vertical proximal LMB and the low "pseudocarina" at T6–7 forming an "inverted T".

---

*Author for correspondence.

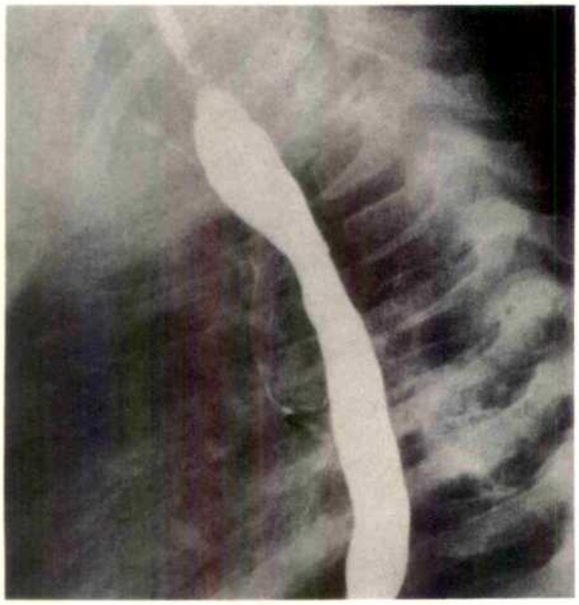

Figure 2. Barium swallow following bronchography showing anterior displacement of the airway from the oesophagus owing to interposition of SLPA.

He was discharged home 2 weeks after extubation. He has had numerous further admissions with respiratory distress during upper respiratory tract infections and has been treated conservatively with frequent inhalations of nebulized adrenaline. He is now 2½ years old and developmentally normal. He has some wheeze on exertion but is otherwise asymptomatic.

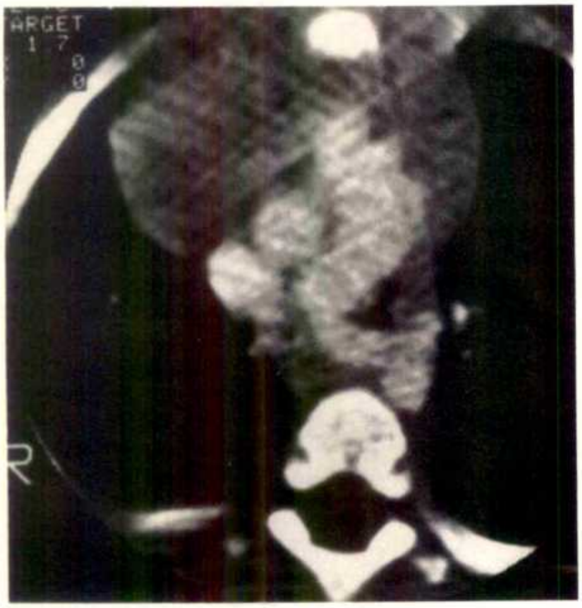

Figure 3. CT scan showing SLPA passing between the proximal LMB anteriorly and descending aorta posteriorly. The LMB measures only 3–4 mm in diameter.

Discussion

Sling left pulmonary artery may occur as an isolated anomaly with a relatively good prognosis or in association with airway stenosis, as in this case, with a much less favourable outlook. Until recently, SLPA was recognized as being associated in some cases with tracheo-bronchial anomalies consisting of long-segment tracheal stenosis, complete "napkin-ring" tracheal cartilage rings and a low "inverted-T" shaped tracheal bifurcation (Berdon et al, 1984).

Wells et al (1988) have recently re-classified SLPA into four types, depending on the tracheo-bronchial anatomy. In Type 1A the tracheo-bronchial anatomy is normal, with the aberrant LPA arising from the RPA and passing over the RMB and behind the trachea, which may be locally compressed. Type 1B is the same except that the right upper lobe is supplied by a bronchus arising directly from the trachea (a pre-eparterial bronchus). In Type 2A the RMB supplies only the right upper lobe. The LMB takes a steep course through the mediastinum and divides at a low "pseudocarina" into a bronchus supplying the left lung and one (the "bridging bronchus") supplying the right middle and lower lobes. The aberrant LPA passes over the bridging bronchus and posterior to the mediastinal segment of the LMB. Type 2B is similar except that the RMB is rudimentary or absent and the entire right lung is supplied by the bridging bronchus. Our case is an example of Type 2B, which is the commonest form (51% of cases). Type 2 is associated with long-segment tracheo-bronchial narrowing and variable absence of the pars membranacea of the trachea. The length of the tracheo-bronchial stenosis in Type 2 accounts for the poorer prognosis compared with Type 1.

Whereas previous accounts of SLPA described increased numbers of tracheal cartilage rings, a low carina and a tracheal diverticulum, this new classification re-interprets the "tracheal diverticulum" as the rudimentary RMB. The evidence supporting this comes from the number of cartilage rings. A dissection specimen of SLPA Type 2B reported by Wells et al (1988) shows a normal number of tracheal cartilage rings down to the level of the rudimentary right main bronchus. The previous reports of increased numbers of tracheal cartilage rings are presumably due to misinterpretation of the proximal portion of the left main bronchus as a narrowed trachea and the origin of the bridging bronchus as the tracheal bifurcation.

The majority of cases of SLPA Type 2 are associated with hypoplasia of the right lung. However, SLPA is a rare anomaly, hence unilateral pulmonary hypoplasia is much more commonly encountered in other situations, notably pulmonary artery aplasia (or hypoplasia), MacLeod's (Swyer–James) syndrome and Scimitar syndrome (Kuhn, 1985). The plain radiograph may suggest the correct diagnosis. In pulmonary artery aplasia (or hypoplasia) the hilum is small and the lung parenchyma may show the reticulo-nodular pattern of enlarged bronchial arteries. The perfusion lung scan shows absent (or diminished) accumulation of tracer in

1991, *The British Journal of Radiology*, *64*, 631–633

the affected lung and contrast-enhanced CT demonstrates the pulmonary artery anatomy. In MacLeod's syndrome the pulmonary artery is small and the affected lung is relatively radiolucent. Because of air-trapping, the mediastinum moves away from the affected side on an expiratory radiograph, and there is prolonged retention of tracer during the washout phase of a ventilation scan. In Scimitar syndrome, there is hypoplasia of the right lung associated with partial anomalous pulmonary venous drainage. The abnormal vein drains into the inferior vena cava, hepatic or portal veins and produces a characteristic curvilinear shadow, which gets broader as it descends through the right lung towards the diaphragm. In SLPA Type 2, a high-kV radiograph of the mediastinum may enable the diagnosis to be made. This may show the high carina with the rudimentary RMB and/or the abnormally low "pseudocarina" (Fig. 1).

We feel this case illustrates several important points. Firstly, infants with severe airway stenosis may be relatively asymptomatic for some months before presentation. Secondly, bronchoscopy and bronchography are likely to be hazardous and the diagnosis can be made without these invasive techniques. A CT scan with dynamic contrast enhancement gives a satisfactory demonstration of the anatomy. Finally, whereas the short focal airway stenoses of SLPA Type 1 are amenable to surgical correction, results of surgical intervention in the long stenoses of Type 2 are poor (Wells et al, 1988). As this case shows, a good result may be obtained in some cases of SLPA Type 2 with aggressive conservative treatment without resorting to high-risk tracheal reconstructive surgery.

References

BERDON, W. E., BAKER, D. H., WUNG, J. T., CHRISPIN, A., KOSLOWSKI, K., DE SILVA, M., BALES, P. & ALFORD, B., 1984. Complete cartilage ring tracheal stenosis associated with anomalous left pulmonary artery: the ring-sling complex. *Radiology*, *152*, 57–64.

GONZALEZ-CRUSSI, F., PADILLA, L.-M., MILLER, J. K. & GROSFELD, J. L., 1976. "Bridging bronchus". A previously undescribed airway anomaly. *American Journal of Diseases of Childhood*, *130*, 1015–1018.

KUHN, J. P., 1985. The lungs and bronchi. In *Caffey's Pediatric X-Ray Diagnosis. An Integrated Imaging Approach*. Ed. by F. N. Silverman (Year Book Medical Publishers, Chicago), pp. 1130–1284.

WELLS, T. R., GWINN, J. L., LANDING, B. H. & STANLEY, P., 1988. Reconsideration of the anatomy of sling left pulmonary artery: the association of one form with bridging bronchus and imperforate anus. Anatomic and diagnostic aspects. *Journal of Pediatric Surgery*, *23*, 892–898.

Laurence–Moon–Biedl syndrome: renal ultrasound appearances in the neonate

By S. J. Garber, MRCP and R. de Bruyn, FRCR

Hospitals For Sick Children, Great Ormond St, London WC1, UK

(*Received September 1990 and in revised form December 1990*)

Keywords: Laurence–Moon–Biedl, Renal, Ultrasound, Neonate

Renal disease is now considered one of the cardinal features of the Laurence–Moon–Biedl syndrome (LMBS). The most commonly described radiographic changes are calyceal distortion with cortical and medullary cysts on intravenous urography (IVU). We present two cases of LMBS who, on ultrasound (US) imaging in the neonatal period, had enlarged hyperechoic kidneys indistinguishable from autosomal recessive polycystic kidneys (ARPK). To our knowledge only one such case has previously been reported in the literature (Ritchie et al, 1988).

Case reports

Case 1

A 35-year-old woman, gravida 2 para 1, had a normal US examination at 16 weeks of pregnancy. A repeat examination at 36 weeks showed bilaterally enlarged hyperechoic kidneys with oligohydramnios. At birth the male infant was found to have polydactyly and dysmorphic facial features. Postnatal US confirmed the presence of large, hyperechoic kidneys with loss of corticomedullary differentiation (Fig. 1).

The kidneys could not be adequately defined with IVU and a dynamic computed tomography (CT) scan was performed. Diffuse, homogeneous opacification was seen with contrast medium in the parenchyma and collecting system (Fig. 2). Appearances were thought to be not those of ARPK where a streaky, radiating pattern of enhancement occurs, but renal dysplastic change.

The child subsequently developed renal impairment and showed developmental delay, with weight on the 90th centile and height on the 10th. A clinical diagnosis of LMBS was made.

Case 2

Routine post-natal examination of a male infant born to a 24-year-old woman with a normal 2-year-old son revealed polydactyly and a left-sided abdominal mass. Ultrasound

---

Address correspondence to Dr S. J. Garber, Department of Radiology, The Middlesex Hospital, Mortimer Street, London W1, UK.

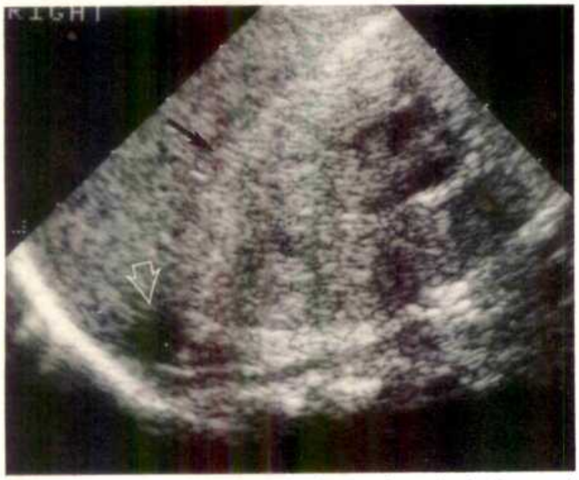

Figure 1. Longitudinal ultrasound scan through the liver and right kidney. The kidney (arrow) is enlarged and highly reflective with loss of cortico-medullary differentiation. The hypoechoic adrenal gland (open arrow) is seen above the kidney.

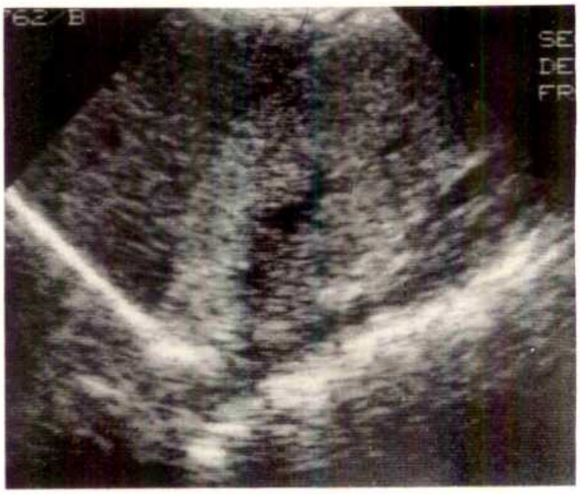

Figure 3. Longitudinal ultrasound scan through the liver and right kidney. The kidney is enlarged with an increase in parenchymal echogenicity and a loss of cortico-medullary differentiation.

examination at 5 days showed two large echogenic kidneys with a loss of corticomedullary differentiation (Fig. 3). Follow-up US examinations remained unchanged. An IVU at 4 months showed mild calyceal distortion with asymmetrical loss of cortical thickness (Fig. 4). The child subsequently developed impaired renal function and showed developmental delay. A diagnosis of LMBS was made.

Discussion

Laurence–Moon–Biedl syndrome, termed the Bardet–Biedl syndrome, is an autosomal recessive disorder characterized by obesity, polydactyly, mental retardation, hypogonadism and pigmented retinal dystrophy (Smith, 1988). More recently it has been recognized that renal disease occurs at least as commonly as the other cardinal features (Churchill et al, 1981; Williams et al, 1988). The incidence of severe renal impairment varies from 15% in one study of 20 patients (Harnett et al, 1988) to 55% of patients developing uraemia before the age of 15 years (Hurley et al, 1975). This variation may reflect a small sub-group of patients with LMBS with more severe renal disease. Both our patients had evidence of renal impairment within the first few years of life and perhaps they will fall into this group.

The IVU appearance of LMBS has been well described, with a reduction in renal size, asymmetrical parenchymal loss, calyceal blunting and distortion, and cortical and medullary cyst formation (Linne et al, 1986; Teider et al, 1982). The US findings of enlarged, echogenic kidneys, detected ante-natally in one of our cases and in the immediate post-natal period in the

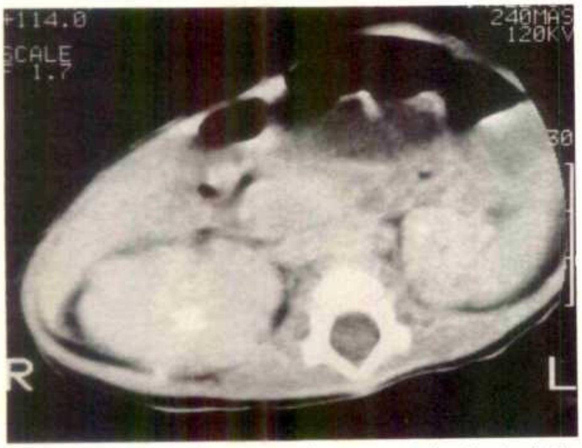

Figure 2. Computed tomography scan at the level of the kidneys. There is diffuse enhancement of the renal parenchyma with some contrast medium seen in the renal pelvis.

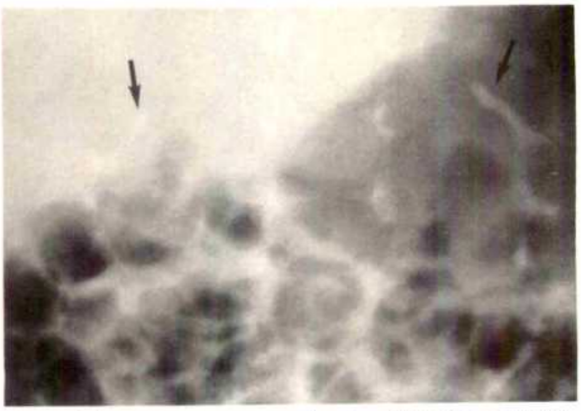

Figure 4. Intravenous urogram showing distortion and clubbing of the calyces bilaterally (arrows).

other, may reflect predominance of medullary cystic changes early in the disease. This might explain the similarity with ARPK where the cystic change is also predominantly intramedullary. Although the incidence of neonatal renal ultrasound changes is not known, LMBS should be included in the differential diagnosis of bilateral hyperechoic large kidneys in early infancy.

Acknowledgments

We would like to thank Dr I. Gordon for reading the manuscript. We are also grateful to Professor T. M. Barratt for allowing us to report his patients.

References

Churchill, D. N., McManamon, P. & Hurley, R. M., 1981. Renal disease: a sixth cardinal feature of the Laurence–Moon–Biedl syndrome. *Clinical Nephrology*, *16*, 151–154.

Harnett, J. D., Green, J. S., Cramer, B. C., Johnson, G., Chafe, L., McManamon, P., Farid, N. R., Pryse-Philips, W. & Parfrey, P. S., 1988. The spectrum of renal disease in Laurence–Moon–Biedl syndrome. *New England Journal of Medicine*, *319*, 615–618.

Hurley, R. M., Dery, P., Nogrady, M. B. & Drummond, K. N., 1975. The renal lesions of the Laurence–Moon–Biedl syndrome. *Journal of Pediatrics*, *87*, 206–209.

Linne, T., Wikstad, I. & Zetterstrom, R., 1986. Renal involvement in the Laurence–Moon–Biedl syndrome. *Acta Paediatrica Scandinavica*, *75*, 240–244.

Ritchie, G., Jequier, S. & Lussier-Lazaroff, J., 1988. Prenatal renal ultrasound of Laurence–Moon–Biedl syndrome. *Pediatric Radiology*, *19*, 65–66.

Smith, D. W., 1988. *Recognizable Patterns of Human Malformation*, 4th edn (W. B. Saunders, Philadelphia), pp. 530–531.

Teider, M., Levy, M., Gubler, M. C., Gagnadoux, J. R. & Broyter, M., 1982. Renal abnormalities in the Bardet–Biedl syndrome. *International Journal of Pediatric Nephrology*, *3*, 199–203.

Williams, B., Jenkins, D. & Walls, J., 1988. Chronic renal failure: an important feature of the Laurence–Moon–Biedl syndrome. *Postgraduate Medical Journal*, *64*, 462–464.

Intracranial chondrosarcoma in a patient with Ollier's disease

By A. G. Clifton, MA, MRCP, FRCR, B. E. Kendall, FRCP, FRCR, H. A. Crockard, FRCS and T. Hughes, FRCS

The National Hospitals for Nervous Diseases, Maida Vale, London W9 1TL and University College Hospital, London WC1E 6JJ, UK

(*Received May 1990*)

Keywords: Intracranial chondrosarcoma, Ollier's disease, Computed tomography

Cartilaginous intracranial tumours are rare. A case of intracranial chondrosarcoma is described in a patient with Ollier's disease. The patient also had evidence on computed tomography of enchondromata involving the ethmoid sinuses.

Case report

A 36-year-old woman with Ollier's disease diagnosed at the age of 13 months, involving mainly her right side and affecting hand, rib cage, right femur, and right toes, presented with a 10-month history of intermittent diplopia on right gaze. Examination showed a mild right proptosis (2 mm) with restriction of right eye movements, particularly in abduction and elevation. The visual acuities, fields and the optic discs were normal. There was no demonstrable trigeminal nerve dysfunction.

A chest radiograph revealed multiple enchondromata involving the anterior ends of the left 2nd and right 4th, 5th and 7th ribs, as well as the medial borders of both scapulae (Fig. 1).

Computed tomography (CT) showed a large mass, isodense with brain and strongly enhancing in the medial half of the right middle fossa. It eroded the right side of the clivus, sella turcica and the greater wing of the sphenoid. Its anterior margin impinged on the superior orbital fissure and its outer margin was clearly defined against the temporal lobe. Multiple mixed density lesions with regions of bone density consistent with enchondromata were seen expanding the ethmoid labyrinths (Fig. 2).

Selective right internal and external carotid angiography showed the large mass to be displacing the precavernous segment of the right internal carotid artery medially and anteriorly and the proximal part of the cavernous segment antero-inferiorly. There was a hypovascular region between the displaced segment and the vessels on the inferior surface of the temporal lobe (Fig. 3).

A right pterional craniotomy and excision of the tumour was performed. Cytology was consistent with a chondroid tumour, its benign or malignant nature being indeterminate. Formal histology showed a low-grade chondrosarcoma.

Discussion

Intracranial cartilaginous tumours (chondromas, chondrosarcomas, osteochondromas) are uncommon. In Cushing's series of 2023 tumours, only three were of cartilaginous origin (Cushing, 1932). They usually arise at the base of the skull, the most frequent site being the

---

Address correspondence to: Dr A. G. Clifton, Department of Radiology, Atkinson Morley's Hospital, Wimbledon, London SW20 0NE.

parasellar region (Reuter & Weber, 1981), other sites such as the dura, choroid plexus, leptomeninges or within the brain parenchyma being even more rare (Ozgen et al, 1984). They may be solitary or a component of multiple enchondromatosis (Ollier's disease) and probably arise from cartilaginous rests in the area of the basal synchondroses (Imagawa et al, 1977).

Ollier's disease is a rare non-hereditary disorder characterized by masses of cartilage persisting in the metaphysis and diaphysis, subperiosteal deposition of cartilage, and asymmetric involvement of the limbs,

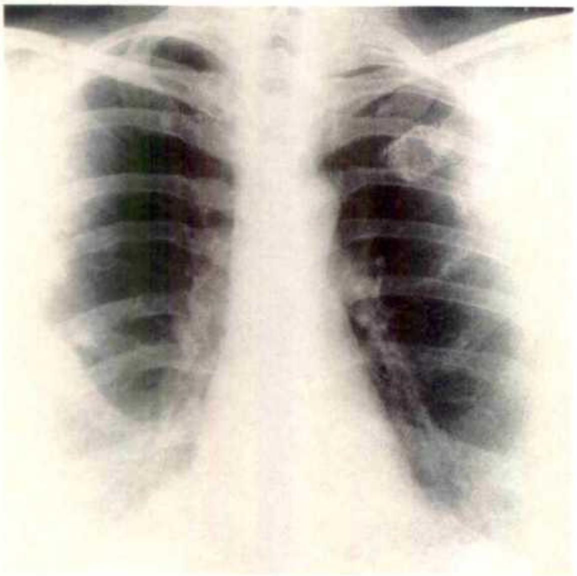

Figure 1. Postero-anterior chest radiograph showing multiple enchondromata involving the ribs and scapulae.

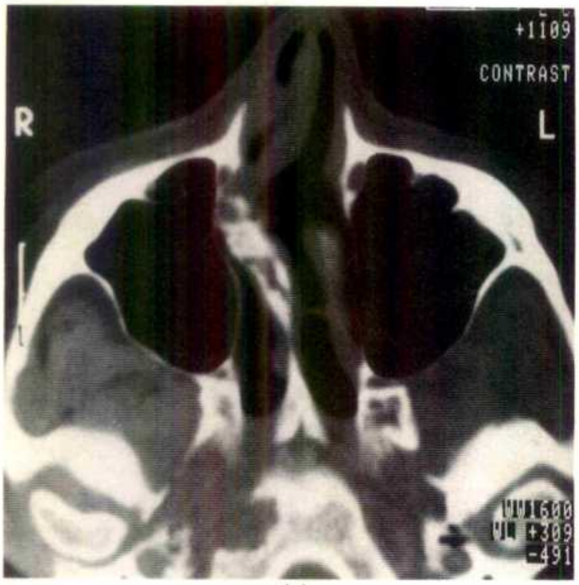

(a)

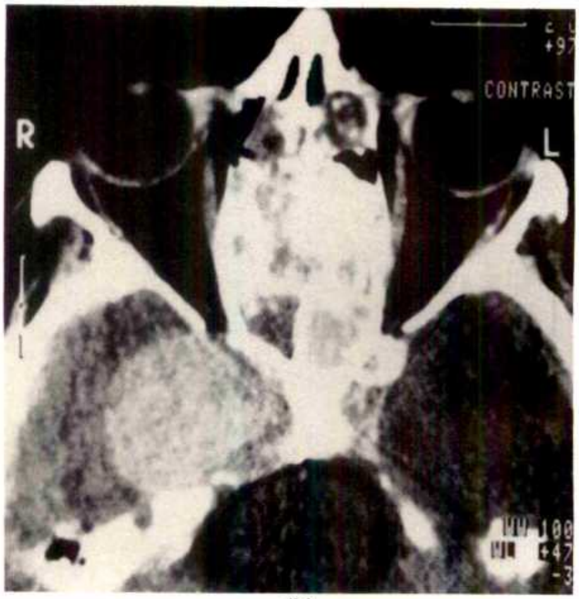

(b)

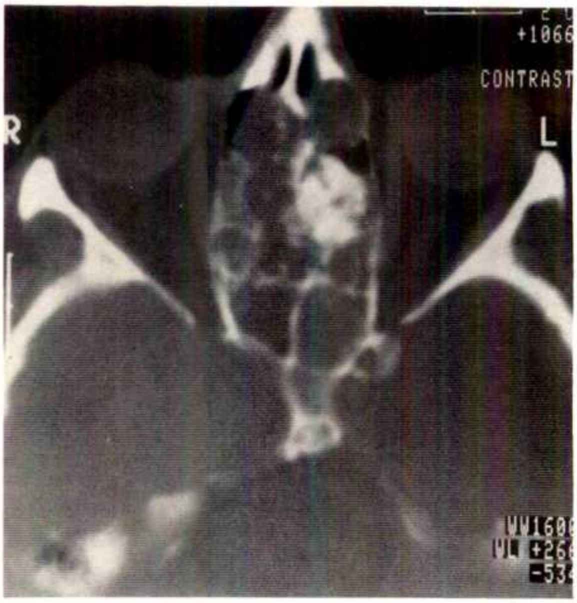

(c)

Figure 2. (a) CT scan (bone window: WW 1600, WL 309) showing erosion of the right side of the clivus and skull base. (b) CT scan after intravenous contrast medium (soft-tissue window: WW 100, WL 47). A strongly enhancing mass is seen in the medial half of the right middle fossa eroding the sella. Its lateral margin is well defined against the brain's substance, and its anterior margin impinges on the superior orbital fissure. (c) CT scan (bone window: WW 1600, WL 266) There is a mixed density mass in the left anterior ethmoids with regions of dense calcification consistent with an enchondroma.

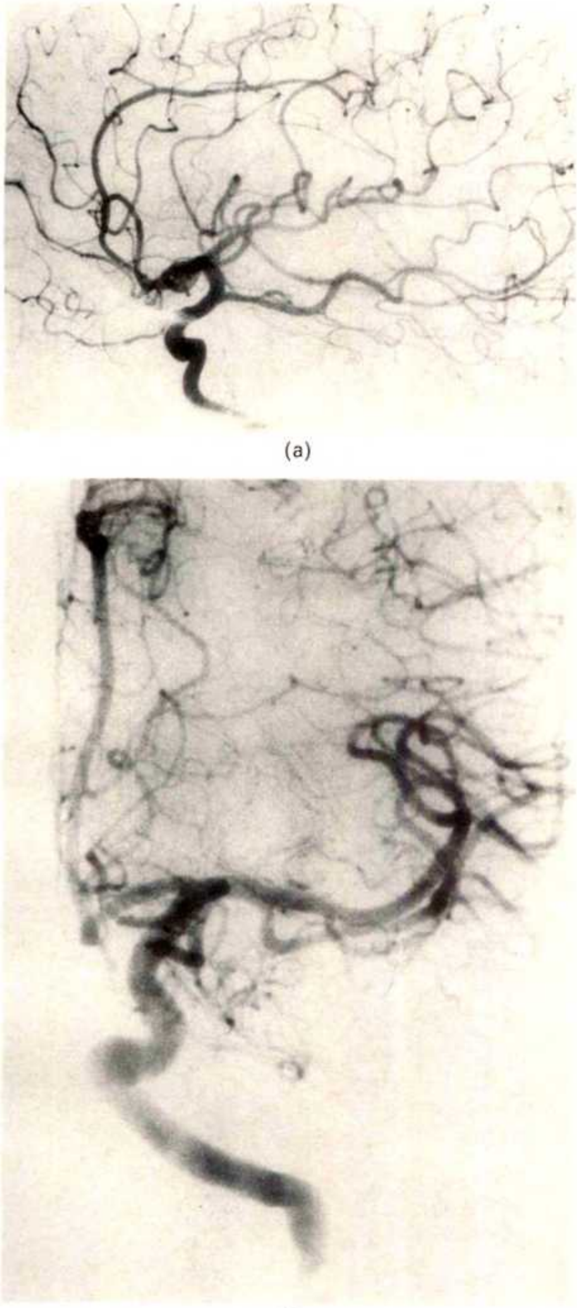

(a)

(b)

Figure 3. (a, b) Subtraction angiograms after selective injection of the right internal carotid artery (see text).

with one side being exclusively or predominantly involved. In a patient with Ollier's disease a chondroid tumour should be considered the most likely diagnosis for a mass at the base of the skull. Chondrosarcoma can result from malignant degeneration of a chondromatous lesion and up to 30% of patients with Ollier's disease develop a malignant lesion, most likely a chondrosarcoma (Ollier, 1900; Liu et al, 1987).

In up to 60% of intracranial chondromas and chondrosarcomas, calcification is seen (Sarwar et al, 1976). Angiography in cranial chondromas and chondrosarcomas shows displacement of vessels around an avascular mass (as in our case) (Sarwar et al, 1976; Bahr & Gagler, 1977). Computed tomography is usually performed as the primary investigation and clearly shows the extradural location and extent of the lesion, presence of calcification and any bone destruction. Bone destruction suggests malignant change. Reports of enhancement after intravenous contrast medium at CT vary. Bahr et al (1977) report very slight enhancement of a single chondrosarcoma with contrast medium but marked enhancement was shown in a case reported by Reuter and Weber (1981). Grossman and Davis (1981) reviewed the CT findings of five chondrosarcomas of the skull base; high density on plain CT, contrast enhancement and osteolytic changes of the contiguous bone were highly suggestive of the diagnosis.

The differential diagnosis for masses at the skull base include chordoma and meningioma. If the lesion is calcified a carotid aneurysm (Sarwar et al, 1976) may need to be excluded in parasellar lesions.

It can be difficult to differentiate meningioma, chordoma and chondrosarcoma. Meningiomas tend to extend along the meninges; the other tumours are extradural in origin and tend to displace the meninges, which tend to give the mass a well defined edge. Meningiomas usually show marked enhancement on CT, but, as in this case, chondrosarcoma may show marked enhancement; chordoma also may show variable enhancement. Meningiomas usually cause hyperostosis; chondrosarcomas and chordomas are destructive. Chordomas usually involve the midline but may be very asymmetrical; chondrosarcomas are generally parasellar in location. At angiography, meningiomas are usually highly vascular and chondrosarcomas hypovascular.

Enchondromata are very rare in the paranasal sinuses and nose. Those in the nose usually arise from the nasal septum and are found incidentally. The most common sinus to be involved is the ethmoid (Lloyd, 1988). Kilby and Ambegoakar (1977) on reviewing the literature found that 50% of reported tumours arose from the ethmoids and 17% from the septum. These tumours are also thought to arise from cell rests. When the ethmoid tumour is large, symptoms are of nasal obstruction or pressure effects and deformities. They may recur following excision and late sarcomatous change occurs.

References

BAHR, A. L. & GAGLER, B. W., 1977. Cranial chondrosarcomas. *Radiology*, *124*, 151–156.

CUSHING, H., 1932. Notes on a series of two thousand verified cases with surgical-mortality percentages pertaining thereto. In *Intracranial Tumours*. Ed. by H. Cushing (Thomas Springfield, Illinois), ch. 8, p. 133.

GROSSMAN, R. I. & DAVIS, K. R., 1981. Cranial computed tomographic appearance of chondrosarcoma of the base of the skull. *Radiology*, *141*, 403–408.

IMAGAWA, K., TODA, I. & HAYASHI, M., 1977. A case of enchondroma of the skull base—a manifestation of generalized chondromatosis. *No Shinkei Geka, 5,* 457–463.

KILBY, D. & AMBEGOAKAR, A. G., 1977. The nasal chondroma. Two case reports and a survey of the literature. *Journal of Laryngology and Otology, 91,* 415–426.

LIU, J., HUDKINS, P., SWEE, R. G. & UNWI, K., 1987. Bone sarcomas associated with Ollier's disease. *Cancer, 59,* 1376–1385.

LLOYD, G. A. S., 1988. *Diagnostic Imaging of the Nose and Paranasal Sinuses.* (Springer Verlag, Berlin), pp. 163–166.

OLLIER, L. L. X. E., 1900. Dyschondroplasie. *Lyon Medicale, 93,* 23–24.

OZGEN, T., PAMIR, M., AKALAN, N., BERTAN, V. & BEHSAN, O., 1984. Intracranial solitary chondroma. *Journal of Neurosurgery, 61,* 399–401.

REUTER, K. & WEBER, A. L., 1981. Parasellar chondrosarcoma in a patient with Ollier's disease. *Neuroradiology, 22,* 151–154.

SARWAR, M., SWISCHUK, L. & SCHECHTER, M. M., 1976. Intracranial chondromas. *American Journal of Roentgenology, 127,* 973–977.

1991, *The British Journal of Radiology*, *64*, 637–638

Case of the month

A clinical red herring

By *C. R. Murch, MRCP, FRCR and A. J. Newman Taylor, FRCP

Royal Brompton National Heart and Lung Hospital, Sydney Street, London SW3 6NP

(*Received October 1989 and in final form January 1991*)

A previously healthy 16-year-old school boy was admitted to hospital with a 4-month history of increasing shortness of breath, which had followed a sore throat. Two months later, he was short of breath after climbing stairs and hills, and was unable to participate in sports. He had no previous medical history other than migrainous headaches. Both of his parents had had sarcoidosis, although neither had received treatment. At the time of his hospital admission he seemed a fit young man without abnormal physical signs. His chest radiograph showed prominent hila but a computed tomography (CT) scan identified no enlarged hila or mediastinal lymph nodes. He was discharged from hospital and remained stable for 2 months after which he became increasingly short of breath over a period of 2 days. He was referred and admitted to this hospital.

On examination at this time, he was cyanosed both centrally and peripherally; he had a pulse rate of 120/min and a blood pressure of 120/60 with a fourth heart sound and a raised jugular venous pressure. He had end inspiratory crackles audible over the bases of both lungs.

Investigations showed him to be hypoxic with a respiratory alkalosis ($p\text{O}_2$ 7.20 kPa (54 mmHg), $p\text{CO}_2$ 1.93 kPa (14 mmHg), pH 7.55, HCO_3 −12.6 mmol/l) breathing 28% oxygen. Lung function tests showed a mixed mild obstructive and restrictive defect without response to inhaled broncho dilator with reduced carbon monoxide transfer. The serum angiotensin converting enzyme was normal. He had a bronchoscopy which was normal and broncho-alveolar lavage which had a normal cell count. His ECG showed "p" pulmonale, right axis deviation with tall *R* waves and ST depression between V1 and V4, changes consistent with right ventricular hypertrophy.

His chest radiograph at the time of this admission with enlargement of the right base are shown in Figs 1 and 2. What radiological abnormalities are present and what is the most probable diagnosis?

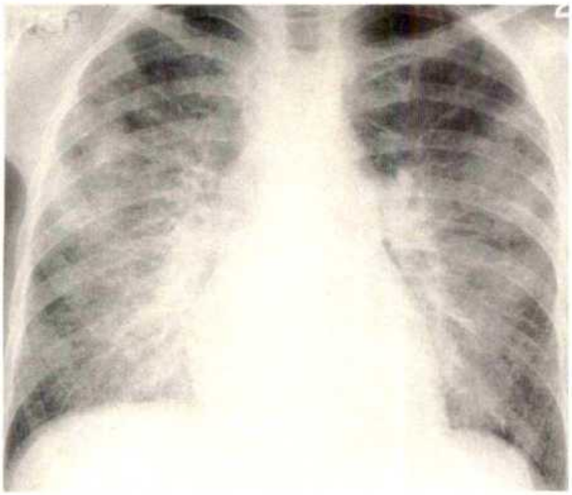

Figure 1. PA chest radiograph.

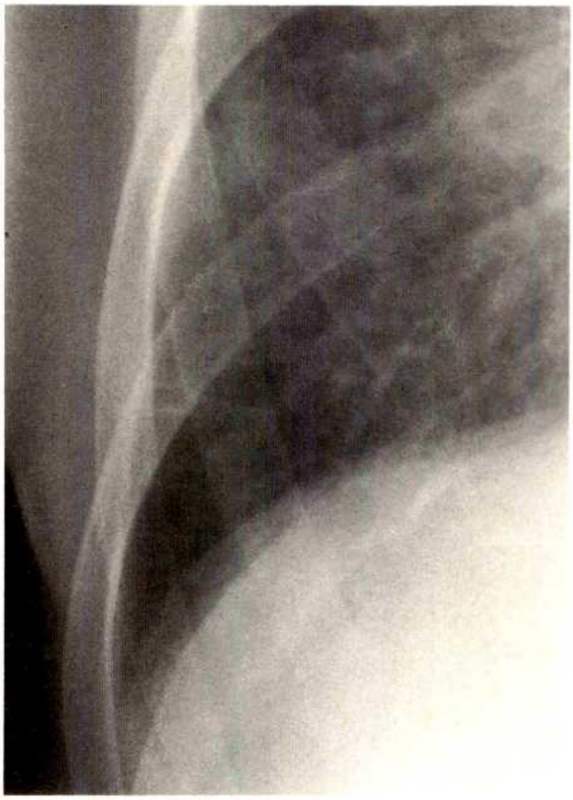

Figure 2. Enlargement of the right base.

---

*Current address: Department of Radiology, Ayr County Hospital, Ayrshire.

Keywords: Pulmonary hypertension, Pulmonary oedema.

His hypoxia became more severe despite increasing concentrations of inspired oxygen. On the third day of his admission the patient arrested and died.

At post-mortem there was patchy congestion of the lungs with septal oedema and dilated lymphatics. Haemosiderin was present within the alveolar septa, macrophages and in elastic tissue. Medium sized pulmonary arteries were hypertrophied. Almost all pulmonary veins showed partial or complete occlusion by intimal fibro-elastic tissue. Multiple lumina within veins suggested recanalization of organizing thrombus. There was marked right ventricular hypertrophy. The findings were those of pulmonary veno-occlusive disease (PVOD).

The chest radiograph shows enlargement of the proximal pulmonary arteries with fine hazy shadowing throughout both mid and lower zones, mainly centrally within the lungs, sparing the periphery, best seen in the left lung. Interstitial (Kerley "B") lines are present at the bases (Fig. 2).

The diagnosis of PVOD is suggested by the combination of pulmonary oedema and pulmonary arterial hypertension in the absence of mitral valve disease. PVOD was first described in 1934 and some 40 cases have since been reported. It predominantly occurs in children and young adults, the youngest recorded case being an infant of 8 weeks and the oldest a woman of 67 years. More than one half of reported cases have been aged below 20 years.

This case demonstrates the features of PVOD very well. Progressive exertional dyspnoea is a constant symptom variably accompanied by cyanosis, orthopnoea, syncope, dizziness, clubbing and haemoptysis. On examination, crackles in the lungs owing to pulmonary oedema and signs of pulmonary arterial hypertension may be found. Hypoxia, hypocapnia and respiratory alkalosis are also typical. The chest radiograph showing pulmonary arterial hypertension, pulmonary oedema and septal lines, without evidence of raised left atrial pressure associated with ECG changes of right ventricular hypertrophy and "strain", are characteristic. The diagnosis may be confirmed by cardiac catheterization and lung biopsy.

The cardiac catheter findings of marked pulmonary arterial hypertension with a normal capillary wedge pressure and pulmonary oedema on the plain chest radiography are reported to be diagnostic of PVOD (Rambihar et al, 1979). This paper advocates measuring the wedge pressure using a balloon floatation catheter, as measurements taken using an end hole catheter are unreliable in pulmonary arterial hypertension owing to peripheral arterial occlusion. The patchy involvement of the lungs, present in this case, is a frequent finding (Thadani et al, 1975) and can be offset by taking repeated readings in different segments of lung.

Histological examination of the lungs shows narrowing or occlusion of pulmonary veins and venules by intimal fibrosis. Recent thrombus in various stages of organization occurs occasionally but recanalization is frequently seen, causing eccentricity of the lumen and the presence of intraluminal fibrous septa. Larger pulmonary veins may be involved and venous arterialization may occur. Patches of oedema, haemorrhage (where haemosiderin is often present) and interstitial fibrosis may also occur in the lungs (Hasleton et al, 1986). Interstitial pneumonitis and hypertrophy of mucous glands and goblet cells has also been reported (Wagenvoort, 1976).

The aetiology of PVOD is unknown and may result from a variety of causes. Pulmonary venous endothelium contains less plasminogen activator than endothelium elsewhere in the circulation. It is postulated that any inhibition of this may result in a greater tendency to thrombosis. An infective agent, such as a virus, is believed by many to be the cause, although none has yet been isolated. Many of the patients describe a flu-like illness prior to the onset of symptoms. In addition, some of the histological changes, interstitial pneumonitis and mucous cell hypertrophy are also found during infections (Wagenvoort, 1976). Several cases of PVOD occurring in siblings have been described and this would suggest a genetically determined predisposition (Hasleton et al, 1986). At least three cases have been associated with Raynaud's disease. All were women, aged between 46 years and 67 years, the oldest group of patients with this disease. In one of these patients immune complexes were identified in the alveolar wall, possibly activating clotting factors or platelets (Sanderson et al, 1977). This patient was treated with azothioprine with improvement in her disease. With the exception of this one patient, treatment with corticosteroids, anticoagulants, antibiotics and vasodilator drugs have all failed to alter the invariably fatal outcome of this disease.

The patient presented here, on initial assessment, was diagnosed as suffering from sarcoidosis, owing largely to his strong family history and absence of physical signs to suggest otherwise. Subsequently, this diagnosis became untenable; however, correct diagnosis at an earlier stage of the disease is unlikely to have altered the final outcome.

Acknowledgments

The authors wish to thank the histopathology department, Royal Brompton National Heart and Lung Hospital, and in particular Dr E. Sheffield, for their assistance.

References

HASLETON, P. S., IRONSIDE, J. W., WHITTAKER, J. S., KELLY, W., WARD, C. & THOMPSON, G. S., 1986. Pulmonary veno-occlusive disease. A report of four cases. *Histopathology, 10,* 933–944.

RAMBIHAR, V. S., FALLEN, E. L. & CAIRNS, J. A., 1979. Pulmonary veno-occlusive disease: antemortem diagnosis from roentgenographic and hemodynamic findings. *Canadian Medical Association Journal, 120,* 1519–1522.

SANDERSON, J. E., SPIRO, S. G., HENDRY, A. T. & TURNER-WARWICK, M., 1977. A case of pulmonary veno-occlusive disease responding to treatment with azothioprine. *Thorax, 32,* 140–148.

THADANI, U., BURROW, C., WHITAKER, W. & HEATH, D., 1975. Pulmonary veno-occlusive disease. *Quarterly Journal of Medicine, New Series, XLIV, 173,* 133–159.

WAGENVOORT, C. A., 1976. Pulmonary veno-occlusive disease. Entity or syndrome? *Chest, 69(1)* 82–86.

1991, *The British Journal of Radiology*, 64, 639–642

Correspondence

(The Editors do not hold themselves responsible for opinions expressed by correspondents)

A new phantom for mammography

THE EDITOR—SIR,

I wish to comment on the paper entitled "A new phantom for mammography" by J. Law (1991). In this paper the author compares the performance of a mammographic test phantom from Du Pont with the Bart's phantom (White & Tucker, 1980) by measuring the numbers of image details visible in images of each phantom for different radiographic factors; kV, focal-spot size, screen/film combination and processing. Unfortunately the comparison as presented is quite inconsistent and highlights the need for great care when attempting to compare the performance of test phantoms.

In the case of the Bart's phantom six images were produced for each set of radiographic conditions. A "global" image-detail score was then measured for each image and the average of the six images formed. Thus, for this phantom the average global score per single image was the measure of performance for a particular set of radiographic conditions.

For the Du Pont phantom the author produced three images for each set of radiographic conditions and then added the contrast-detail scores averaged for two observers and formed a separate assessment of the resolution scores. Thus, for this phantom the summed score of contrast detail for three images was the measure of performance for a particular set of radiographic conditions. In Figures 3 and 4 of the paper this three image Du Pont score was plotted against the average global single image score for the Bart's phantom for different radiographic factors. The author then concludes that the gradient of the resulting linear plot favours the Du Pont phantom.

There are a number of fundamental weaknesses in this approach, not least of which is the fact that the author has not plotted like against like. First of all by taking 3 x the single image score for a Du Pont phantom the gradient of any linear plot will be so multiplied relative to the single image score. Presumably the author has done this in order to produce a numerical score for the Du Pont phantom which is similar in magnitude to that of the Bart's phantom, since the latter contains more detail. However, the only meaningful way of comparing any phantoms must be in terms of single image performance and not 3 x for one and single for another.

The problem of comparison is further complicated in this paper by the author forming a global image score for the Bart's phantom whilst separating the contrast detail score from the resolution measurement (line pairs per mm) in the Du Pont phantom. All test phantoms contain a range of image detail some of which is more sensitive to resolution related factors; focal spot size, screen/film combination etc., and some to contrast related factors; kV, screen speed, film characteristics etc., and some a combination of both. Consequently, image detail at threshold contrast is resolution limited, contrast or noise limited or a variable combination of both.

When evaluating the performance of test phantoms over a range of radiographic factors which affect resolution, contrast, noise etc., it is vital to keep the scores for individual image detail separate. For instance, for the Bart's phantom changing the kV from 25 to 28 kV might only change the global image score from 54 to 55, approximately a 2% variation. However, if this change always affects the score of one particular detail, say from a score of 4 details to 5 being visible, then the sensitivity is in fact 20% which is excellent.

The disadvantage of only forming a global score is demonstrated quite clearly by reference to Table II of the paper by Law. Employing the Du Pont phantom with X-ray set number 2 which possesses a focal spot size of 0.96 x 0.84 mm and 28 kV setting gave a single image score of 11.5 for the contrast detail and 8.5 lp/mm for resolution. These two scores added together form a global score of 20. In the same Table X-ray set number 3 with broad focus 0.37 x 0.47 mm and 35 kV also gives a global score of 20 (nine contrast, 11 lp/mm resolution). Consequently, if the same data analysis global score regime had been employed for the Du Pont phantom as it was for the Bart's phantom, the former would clearly have been less sensitive to radiographic changes.

This paper clearly highlights the considerable care which is needed to avoid bias and confusion when attempting to assess the relative performance of test phantoms. The results presented in this paper, which are based upon an inconsistent framework for evaluation, cannot be used to draw any meaningful conclusions regarding the relative performance of the two test phantoms.

The Radiation Protection Research Programme of the Commission of European Communities is already aware of the extremely wide variety of test phantom designs which presently exist throughout Europe. In order to address this problem the Commission is organising a meeting on test phantoms, in conjunction with ICRU and GSF Munich, scheduled for June, 1992. Hopefully this meeting will provide the necessary scientific forum for discussions on standardization of test phantom design as well as test procedures for their evaluation.

Yours etc.,
B. M. MOORES

R. P. S. Centre,
42 Rodney Street,
Liverpool L1 9AA

(*Received February 1991*)

References

LAW, J., 1990. A new phantom for mammography. *British Journal of Radiology*, *64*, 116–120.

WHITE, D. R. & TUCKER, A. K., 1980. A test object for assessing image quality in mammography. *British Journal of Radiology*, *53*, 331–335.

Author's reply

THE EDITOR—SIR,

In reply to Dr Moores, the account he gives of my paper in paragraphs 1–6 of his letter in broadly correct, but I do not think it affects the conclusions reached. The Du Pont scores may be divided by three (or the relevant vertical axes of the graphs relabelled) to obtain a mean single-film result if desired. For the Du Pont phantom films, scores for contrast details and for resolution have been separated in Tables and Figures exactly as Dr Moores advocates in his seventh paragraph but appears to criticize in paragraph six. The contrast details in the Du Pont phantom were so-called only to distinguish them from the resolution details (bar patterns). Some of these contrast details are very fine and their visibility depends, to some degree, on both contrast and resolution; this is also true of many features of the Bart's phantom (which does not contain bar patterns), and in counting visible details in each phantom, I was comparing like with like, contrary to Dr Moores' fifth paragraph.

It might be thought an advantage of the Du Pont phantom that resolution can be treated separately from the other details, as in Table II, which is criticized by Dr Moores in his eighth paragraph. In that Table, contrast detail visibility broadly decreases as kV rises, while resolution is influenced by focus size rather than kV, as might be expected. I have nowhere added the two together, I wonder why Dr Moores, in paragraph eight, writes as though I did.

A phantom of this kind must give results consistent for each user. If results are also numerically comparable between different users, it is an advantage but not essential. Different users may find they reach the same conclusions (*e.g.* about a type of film) even though their scores are different and possibly without an underlying theory in support. On this point I would refer readers to the penultimate paragraph of my paper.

Regarding avoidance of bias, work by Dr A. Underwood and Mr A. Robinson in Sheffield (independent of my own and acknowledged in my paper) led them to similar conclusions on the Du Pont phantom. Their work remains unpublished in a journal but our combined results have been displayed at two meetings (IPSM and RCR). Later (with Dr H. C. Starritt in Bath and Ms A. Burch in Cardiff), we made good progress on a common scoring system, suspending this only when doubts arose over future availability of the phantom.

The outcome of the CEC meeting referred to by Dr Moores will be greeted with interest by many of us, but predictions based on theory will still need to be confirmed by experience in the field, and by several users. Meanwhile we can only make the best of what we have.

Yours etc.,
J. LAW

Department of Medical Physics and Medical Engineering,
Western General Hospital,
Edinburgh EH4 2XU
(Received March 1991)

Scoring of image quality phantom films in mammography.

THE EDITOR—SIR,

We were very interested to read the paper by J. Law "A new phantom for mammography" (1991). We have been advocates of this particular phantom for some time and have used it regularly on a total of 29 mammography units (nine different makes/types in all) over the past 2 years.

One could of course use different methods of scoring the image quality perceived on test films and the degree of sensitivity to changes of kilovoltage, film processing etc. will clearly depend on the scoring system chosen.

The scoring system we adopted initially was simply to count the number of perceptible plastic wires and carbohydrate spheres within each circle (as in Law's description of the phantom) whilst allocating a score of 0, 0.5 and 1 for the Al_2O_3 specks and discs with 'number' holes. This gives a maximum score of 71, whilst the score for test films usually lies between 56 and 68.

In retrospect this system gives undue weight to the large numbers of wires and spheres which are always seen and does not give sufficient emphasis to how well they are visualized. We now consider that a simple 0–3 (or possibly 0–5) scale of visibility of all the ringed features gives a 'better' assessment of image quality and differentiates more clearly between images influenced by the various crucial parameters. We have not attempted to score the 'clinical' features.

In practice, however, we have found that even our 'non-ideal' scoring system gives very good differentiation between films from different mammography units and enables reproducible assessments of image quality which correlate well with assessments by radiologists of clinical films. Generally, we also find very good agreement between two film readers, with all our image quality films being double-read — though only one film is normally obtained from each centre for a given set of conditions.

Similarly to Dr Law, we have also shown that the Du Pont phantom gives a decreasing image score with increasing kVp, as expected, and that results with the phantom are sensitive to changes in optical density, film-screen combination and tube filter material. The phantom can therefore be used to indicate faults in equipment and techniques, *e.g.* poor processing, film-screen contact, non-optical choice of mean film density, etc.

In particular we find that low scores are usually associated with too low a mean density (sometimes over-enthusiastic attempts to minimize the average glandular dose), poor film processing (*e.g.* giving artefacts from rollers), excessive processing speed which accentuates film mottle or grid artefacts. Conversely, high scores are obtained with good systems, but may also be associated with 'slow' processing with resulting high doses. These effects are very similar to those produced with clinical radiographs.

We have also compared the image quality results obtained with the Du Pont phantom with results obtained with the Faxil TOR (mAs) phantom, specifically developed for the Breast Screening Programme and exposed under identical conditions. The results for the line pairs resolution test patterns were highly significantly correlated ($p < 0.001$) for the two phantoms. Scores for the contrast and resolution details were also significantly correlated ($p < 0.01$) but the Du Pont phantom appears to give a larger spread of numerical scores with easier identification of very good and, more importantly, very poor X-ray unit/processing systems.

Image quality assessment using the RMI Type 152D and CIRS Model XI has also recently been made on 12 units (nine with magnification facility on fine focus). These films were exposed under identical conditions using all four phantoms at each centre and using local films, cassettes and processing — the same cassette for each of the four films at each centre. Scoring of films from the Faxil TOR (mAs), RMI and CIRS phantoms was carried out by simply adding the number of details visible (*e.g.* 'masses', 'fibres' and 'specks') as outlined for the Du Pont phantom in the third paragraph. In the case of the Faxil TOR (mAs) the number of 6, 0.5 and 0.25 mm discs visible was added to the number of groups of low contrast line-pair details perceptible (since this latter is analagous to the 'fibres' of the Du Pont and RMI phantoms).

Initial analysis of these results seems to indicate that the latter two phantoms give a roughly similar ranking to image quality of mammographic films. However, the lower global scores give a greater random error in assessment so that the RMI and CIRS phantoms appear to give a less precise estimate of image quality, with a greater element of variation between observers.

We understand that a new mammography phantom has now been developed by Faxil (Leeds) which is reported to have greater sensitivity, but as yet we have made no comparisons of this new phantom with the Du Pont phantom.

In the meantime we shall continue to base most of our image quality assessment on the results of the Du Pont phantom, using the revised "0–3" scoring system described in the fourth paragraph. It is hoped that this phantom will become more readily available so that wider use and experience will accrue and interchange of information on image quality will be facilitated.

Yours etc.,
A. Robinson
A. C. Underwood

Department of Medical Physics & Clinical Engineering,
Sheffield University and Health Authority,
Weston Park Hospital,
Whitham Road,
Sheffield S10 2SJ
(Received March 1991)

Author's reply

The Editor—Sir,
I would like to comment briefly on the interesting letter from Mr A. Robinson and Dr A. C. Underwood.

The "0–3 scale of visiblity" referred to in the fourth paragraph of the letter from Robinson and Underwood was the basis of the "common scoring system" referred to in my reply to Dr Moores. Since learning of it from them, I have made some use of it with the Du Pont phantom and elsewhere, and found it helpful. I understand it is used by colleagues in the FAXIL laboratory in Leeds with their new TOR (MAM) phantom and it may prove to be of value for phantom film scoring in general.

The Leeds TOR (MAM) phantom is referred to by Robinson and Underwood in their penultimate paragraph. Preliminary results from a few film-screen combinations for this phantom, the Du Pont and the Bart's phantom are well correlated.

Yours etc.,
J. Law

(Received May 1991)

Body aprons in radiation protection

The Editor—Sir,
The Guidance Notes associated with the Ionising Radiation Regulations (1985) state that protective aprons for the body shall comply with British Standard 3783 and that they should be examined visually at frequent intervals.

This latter clause further states that thorough examination should be carried out at least once a year to ensure that no cracks have developed, and that radiographic examinations are only likely to be justified when the protective material is covered. Uncovered body aprons would seem rarely to be used and it is therefore required of those involved to carry out radiographic, or possibly fluorographic examinations of body aprons at least once a year. It is the carrying out and assessment of such tests which is the subject of this communication.

Firstly, British Standard 3783 states that aprons "shall be free from defects such as patches, blisters, porosity, embedded foreign matter or other defects in the material". Even a cursory examination of available aprons shows that this is far from the actual case. Most aprons would seem to suffer from these defects although the relevant British Standrad was published 26 years ago. It is probably correct to say, however, that many of these defects are quite minor and do not represent any significant increased hazard to the wearer. Indeed one manufacturer states that in fact the overall thickness of the material may be slightly increased from the nominal value in order to compensate for any such deficiencies.

Consideration of how to assess the significance of these defects naturally leads on to assessment of the significance of cracks developing in the protective material. The Guidance Notes state that "any defects .... should be reported immediately and the defective items replaced as soon as possible". But what constitutes a defect? The extreme cases are of course obvious — where the material is cracked through the entire thickness — but what of fine and superficial cracking where the increase in density on a radiograph may be no greater than that of some of the manufacturing defects already mentioned?

Turning to the British Standard again we can use the test specified by which the lead equivalent of an apron is determined. In the foreward to the Standard it is recommended that we measure the lead equivalent of a crack or defect to discover whether the required nominal standard of protection is being achieved. Some simple practical tests were carried out to this end.

The prescribed procedure is to compare the density of the radiograph exposed through the apron with that of a lead step-wedge exposed simultaneously to a primary beam at 150 kVp. Two problems immediately arise. Firstly, any cracks visible on the film are often too narrow to read the density satisfactorily with the ordinary type of densitometer and, secondly, cracks may be present which are not visible on the radiograph. There are two reasons why the cracks may not be seen. The cracks may close up tightly (or open up) when the apron is laid on a flat surface and associated with this the angle of the crack may be acute with respect to the surface of the apron. However, it should be noted that this test is rather unrealistic from another point of view — aprons are never to be used as protection against an unattenuated primary beam. The occasions when aprons are worn to protect the wearer from the primary beam after attenuation by the patient are few and, in the large majority of cases, aprons are worn for protection against scattered radiation only.

Some further simple experiments were then performed using water as the scattering medium — thus testing the apron by exposing it to scattered radiation only. As might be expected frank cracks in the material were no longer sharply defined but the increased density that represented them was diffused over a wider area. This made possible not only the accurate reading of the photographic density with an ordinary densitometer but also represents, far more realistically, the actual leakage of radiation through the garment under typical conditions of use.

As in all areas of radiation protection it is usual to take the most cautionary approach so it may be presumed that staff are not at any particular or significant risk from this uncertainty. However, it is reasonable to conclude that in this matter some highly subjective judgements are continually being made.

Is there not a case for a review of this entire subject?

Yours etc.,
L. J. Ramsey

45 Harvest House,
Cobbold Road,
Felixstowe IP11 7SP
(Received January 1991)

The role of the single photon emission computed tomography (SPECT) in detection of ossific mediastinal and pulmonary metastases

The Editor—Sir,

We have read with considerable interest the case report on the scintigraphic detection of ossific mediastinal and pulmonary metastases in osteosarcoma (Brady & Ennis, 1990).

Our recently reported experience of two cases of osteosarcoma (Goddard et al, 1990) has been similar. In one case the pulmonary uptake of $^{99}\text{Tc}^{\text{m}}$ MDP demonstrated a metastatic deposit from osteosarcoma that had previously been missed by computed tomography (CT). In the other case, however, CT demonstrated more metastases than scintigraphy.

In both cases pulmonary lesions were seen on the planar bone scans but the exact intrapulmonary location was more clearly demonstrated by single photon emission computed tomography (SPECT). This technique is an addition to the bone scan that requires no extra irradiation. If the gamma camera has a SPECT facility it can be used to provide greater anatomical localization and comparison with transmission CT is facilitated. Transmission CT provides a fine display of anatomical detail and comparison of SPECT images with those of transmission CT enables areas of increased activity to be identified with anatomical structures or pathological lesions (McMillan et al, 1983). This assists in determining the exact nature of the lesion, which is of prime importance for clinical management. The combination of the two techniques is recommended in the evaluation of equivocal thoracic bone scan images.

Yours etc.,

P. R. Goddard

E. Rhys Davies

Department of Radiodiagnosis,
Bristol Royal Infirmary,
Bristol BS2 8HW

(Received January 1991)

References

Brady, A. P. & Ennis, J. T., 1990. The Scintigraphic Detection of Ossific Mediastinal and Pulmonary Metastases in Osteosarcoma. *British Journal of Radiology, 63*, 978–980.

Goddard, P. R., Bell, J., Jackson, P., Pitcher, E., Bullimore, J. A. & Davies, E. R., 1990. Pulmonary Uptake of MDP: Demonstration of Site by Correlation of Emission and Transmission Computed Tomography. *West of England Medical Journal, 105* (ii), 43–46.

McMillan, P., Jackson, P., Davies, E. R. & Goddard, P., 1983. Emission and Transmission Pulmonary Computed Tomography. *British Journal of Radiology, 56*, 991–992.

1991, *The British Journal of Radiology*, *64*, 643–670

Proceedings of the British Medical Ultrasound Society

Twenty-second Annual Meeting, held at the Harrogate International Centre, Harrogate, December 4–6, 1990

List of sections

	Page
Abdominal interventional ultrasound	643
Paediatric ultrasound	647
Orthopaedic ultrasound	648
Clinical audit of diagnostic ultrasound	649
New instrumentation and techniques	650
Veterinary ultrasound	652
Vascular ultrasound	655
Gynaecology	657
Echocardiography	659
Obstetrics	661
Posters	664

Abdominal interventional ultrasound

Chairmen: R. Fowler and G. Plant

Does gall bladder volume alter during cooking of food?, by B. Banerjee and I. Brett
Masses in the gallbladder: from the banal to the bizarre, by B. D. Daly, M. Arnold and C. Metreweli
The role of duplex Doppler in the staging and characterization of pancreatic and biliary tumours, by S. J. Garber and W. R. Lees
Staghorn calculi treated primarily by percutaneous surgery using a Storz ultrasound lithotripter: summary of early results, by W. Hately and D. Badenoch
Can ultrasound replace barium for the detection of small intestinal Crohn's disease?, by D. A. Nicholson, M. B. Sheridan and D. F. Martin
Intra-operative liver ultrasound in the detection and evaluation of liver secondaries in colorectal carcinoma, by A. H. Davies, C. P. De Angelis, R. Cobb, D. Lindsell and N. J. M. Mortensen
Ultrasound in polycystic disease, by D. Ll. Cochlin and G. R. J. Sissons
Ultrasonography of renal allografts: collecting system dilatation and its clinical significance, by S. H. Kashi, G. R. Giles and H. C. Irving
Assessment of vasculogenic male impotence using colour duplex ultrasound, by C. P. Oates, R. S. Pickard, T. A. Whittingham and P. H. Powell
Spectral Doppler and colour flow imaging in impotence, by W. R. Lees, S. J. Garber, A. E. Kulatilake and S. Hamson
Lymphoedema following breast cancer treatment: venous and arterial causes shown by colour and spectral Doppler, by W. E. Svensson, P. Mortimer, C. Badger, D. O. Cosgrove, E. Tohno and B. Al Murrani
Acute inflammation of the breast: the role of breast ultrasound in diagnosis and management, by R. Hayes, M. Michell and N. Nunnerley

Does gallbladder volume alter during cooking of food?

B. Banerjee and I. Brett
Department of Radiodiagnosis and Imaging, Tameside General Hospital, Fountain Street, Ashton-under-Lyne, Lancashire

Over a period of several years it has been noticed that in a number of patients undergoing cholecystosonography, as in outpatient procedures, the gallbladder was found to be contracted although otherwise appeared normal. On questioning, these patients denied any intake of food for at least 8 hours prior to the examination, but it was revealed that a large proportion of these patients had been preparing food for the family prior to their visit to the hospital. The principal mechanism of gallbladder emptying has long been considered to be the release of hormone cholecystokinin (CCK) from duodenal mucosa, stimulated by the passage of food. Although neural control of gallbladder emptying has been generally regarded as fairly unimportant, recent experimental studies suggest that the control mechanism involves much more than release of CCK. A prospective study was undertaken to establish whether there is any change in the gallbladder volume during cooking of food so that the instructions for patient preparation may be revised to include avoidance of food preparation prior to cholecystosonography. Thirty volunteers were included in the study. A strict regime of starvation was adhered to and the volunteers refrained from the sight or smell of food prior to the initial sonography for determining fasting gallbladder volumes. The volunteers then participated in preparing a cooked breakfast. Following this, a second scan for estimation of gallbladder volume was undertaken and recorded. A statistically significant reduction in the gallbladder volume was found using a paired sample '*t*' test at a confidence level of 95%. In a total of 63% ($n = 19$) there was reduction of gallbladder volume. In 7% ($n = 2$) reduction of more than 50% and in 20% ($n = 6$) reduction of volume more than 25% were noted. Therefore, in conclusion, it is probably not unreasonable to include the advice of refraining from the cooking of food for optimal gallbladder distension prior to cholecystosonography.

Masses in the gallbladder: from the banal to the bizarre

B. D. Daly, *M. Arnold and C. Metreweli
Department of Radiology and Organ Imaging and
**Department of Anatomical and Cellular Pathology, Chinese University of Hong Kong, Prince of Wales Hospital, Shatin, Hong Kong*

We presented a series of cases of unusual tumour and tumour-like masses of the gallbladder that were documented at our hospital over a 5-year period. These cases included cholesterol polyps, adenomyomatosis, benign and malignant primary epithelial tumours, sarcoma, haematomas and metastases. Histological confirmation was available in 39 cases. We discussed the sonographic features that may allow differentiation between the various causes for a mass in the gallbladder and emphasized some of the practical problems that allow such lesions to be misdiagnosed or overlooked.

The role of duplex Doppler in the staging and characterization of pancreatic and biliary tumours

S. J. Garber and W. R. Lees
Department of Ultrasound, The Middlesex Hospital, London

The advent of duplex Doppler has permitted accurate definition of the vascular changes associated with abdominal tumours. Pancreatic and bile duct tumours may alter the surrounding vessels in several ways. Easiest to detect is involvement of contiguous vessels, with the portal vein most commonly affected. Constriction produces a high-velocity jet through the narrowed area with turbulent flow distal to the occlusion. Wall invasion produces a chaotic flow signal. In total occlusion a complete loss of flow is seen. Characteristic Doppler flow signals are detectable in the tumour itself. High-frequency signals and a low-frequency non-pulsatile signal are seen, the latter representing flow within the low-impedance vessels produced in neovascularization. This study describes our experience of Doppler assessment in 70 cases of pancreatic and biliary tumours. Patients were scanned on an Acuson 128 machine with a 3.5 MHz phased array probe. High-velocity portal vein flow was detected in 35% (14) of pancreatic and 20% (6) of biliary tumours. A chaotic Doppler flow signal was seen in 35% (14) of pancreatic and 20% (11) of bile duct tumours and complete portal vein occlusion in 28% (11) of the former and 10% (3) of the latter. Twenty-eight percent (11) of pancreatic and 7% (2) of bile duct tumours had high-frequency shift Doppler signals and 22% (9) of pancreatic tumours had a signal indicating low-impedence flow. Pulsed Doppler imaging has a potentially important place in the ultrasound assessment of portal vein wall invasion, an important criterion for pancreatic and biliary tumours and may assist in differentiating benign from malignant lesions. Colour Doppler imaging has a complementary role. It speeds up the Doppler examination and in yielding directional information allows more accurate measurement of flow velocity in the duplex mode.

Staghorn calculi treated primarily by percutaneous surgery using a Storz ultrasound lithotripter: summary of early results

W. Hately and D. Badenoch
The Royal London Hospital, Whitechapel, London E1 1BB

Recent years have seen major changes in the management of renal calculi in which ultrasound has played an important therapeutic role. External lithotripsy, sometimes using ultrasound, has proved to be a satisfactory form of treatment for the great majority of renal calculi measuring 2 cm or less in diameter and has largely replaced percutaneous nethrolithotomy in these cases. However, the management of staghorn calculi, both full and partial, has continued to require a percutaneous approach with ultrasonic disintegration of the stone supplemented by external lithotripsy as necessary. This paper related the Royal London Hospital experience of the treatment of staghorn calculi in all of which ultrasound was used to achieve at least partial clearance. The technique and apparatus were described. Forty-five staghorn stones in 39 patients were treated primarily by percutaneous surgery, with lithotripsy reserved for residual fragments. The series comprised 23 complete staghorns and 22 partial staghorns. In all 83% obtained a satisfactory result (stone-free or fragments of less than 3 mm) at 3 months from surgery; 92% of partial staghorn stones were either clear or fragments less than 3 mm at 3 months as opposed to 69% of the complete staghorn stones. At 6 months follow-up these figures remained unchanged. Only 18% of the partial staghorns required external lithotripsy. Seventy-two per cent of the complete staghorns went on to have external lithotripsy. Sepsis was found to be the most insignificant complication.

Can ultrasound replace barium for the detection of small intestinal Crohn's disease?

D. A. Nicholson, M. B. Sheridan and D. F. Martin
Department of Radiology, University Hospital of South Manchester, Withington, Manchester M20 8LR

When there is clinical suspicion of small bowel Crohn's disease (CD) then barium examination is the usual initial investigation. Despite attempts to select patients for radiology, the majority turn out not to have disease. Thus a significant radiation burden may be incurred by patients without disease, many of whom are young. In order to assess whether ultrasound examination of the small bowel can detect features of CD, allowing more selective use of small bowel barium examination, we have undertaken preliminary ultrasound in all patients referred for barium radiology with the clinical suspicion of small bowel CD. All patients underwent ultrasound using a variety of 5 MHz transducers after preparation for barium examination. Assessments made included small bowel wall thickness, presence of peristalsis and intra-abdominal collections. Results were recorded at the time of examination. Barium examination was undertaken by a different radiologist who was unaware of the ultrasound findings. To date 67 patients have been examined, age range 18–84 years (mean 43 years), 43 female and 24 male. Fifteen were known to have had CD. In these 15 patients, active CD was correctly diagnosed by ultrasound in six of seven patients and absence of CD was correctly diagnosed in four. There were four false positive ultrasound diagnoses. In the 52 patients with no history, CD was correctly diagnosed in nine of 11 with disease and a normal bowel was accurately demonstrated in 40. There was one false positive. Overall sensitivity of small bowel ultrasound was 83% with a specificity of 90%. Most false negative examinations were encountered early in our experience. It seems likely that with experience and adequate equipment, small bowel CD can be reliably detected or excluded using ultrasound alone and that small bowel barium radiology can be reserved for assessment of patients demonstrated to have disease or those few in whom clinical suspicion remains high despite negative ultrasound.

Intraoperative liver ultrasound in the detection and evaluation of liver secondaries in colorectal carcinoma

A. H. Davies, C. P. De Angelis, R. Cobb, D. Lindsell and N. J. M. Mortensen
Department of Surgery, John Radcliffe Hospital, Oxford

Pre-operative ultrasound is often used to detect secondaries in the liver. Early detection of secondaries is more important as adjuvant medical and surgical techniques are becoming available. This study was designed to see if intraoperative ultrasound would optimize the detection and evaluation of the liver. One hundred and forty patients (79 females, 51 males) with a median age of 66 years (range 32–90 years) were studied prospectively. Pre-operative ultrasound was performed by a radiologist using either an ATL Mark 8 or Acuson 128 ultrasound scanner. Intraoperative ultrasound was performed by the surgeon with a Bruel & Kjaer type 1846 machine with a 7 MHz transducer. Twenty-two patients (16%) had liver secondaries diagnosed. The sensitivity, specificity and accuracy of the diagnosis was 95%, 85% and 99% for intraoperative ultraound and 41%, 92% and 90% for pre-operative ultrasound, respectively. However, palpation at the time of operation only missed secondary deposits in four livers (18%). In this preliminary study, palpation of the liver at the time of operation was more sensitive than pre-operative ultrasound; this raises the question as to the role of pre-operative ultrasound. Intraoperative ultrasound was the most sensitive technique in detecting metastatic disease in the liver and its widespread use may allow the earlier use of adjuvant medical or surgical treatment of colorectal secondaries in the liver.

Ultrasound in polycystic disease

D. Ll. Cochlin and G. R. J. Sissons
Department of Radiology, Cardiff Royal Infirmary, Newport Road, Cardiff CF2 1SZ

The classical ultrasound appearances of polycystic disease—multiple cysts in enlarged kidneys with or without cysts in other organs—is well described. Early in the course of the disease, however, the differentiation between simple cortical cysts and polycystic disease may be difficult; the older the patient the greater the difficulty. As part of an ongoing study into polycystic disease we have examined 130 affected patients and their families. This has given us insight into the spectrum of changes that are seen in early disease and their progress. In late disease the difficulty in excluding co-existing obstruction and the symptomatic treatment of pain and pressure symptoms are also addressed. Early cases have normal-sized kidneys with few cysts demonstrable on ultrasound. Very small cysts are represented by hyperechoic foci. Many more small cysts may be seen by computed tomography. A high probability of polycystic disease exists when a combination of renal cysts and cysts in other organs is present, regardless of number. Even a single renal cyst in a patient below the age of 30 years, and three or more cysts in each kidney in a patient between the ages of 30 and 50 years, suggests the diagnosis. Above the age of 50 years, cysts in other organs, enlargement of the kidneys or an unusual pattern of cysts is required to make the diagnosis. Initial progress in early cases is by slow enlargement of the cysts and by more rapid appearance of more cysts. Change is always seen within a year. Co-existing obstruction in advanced cases may sometimes be excluded if the calyceal system is well visualized, but often requires retrograde pyelography. The complication of acute pain may be due to rapid expansion of one or more cysts due to haemorrhage or infection. Increased echodensity of the cyst contents indicates which are affected. These should be drained percutaneously.

Ultrasonography of renal allografts: collecting system dilatation and its clinical significance

S. H. Kashi, G. R. Giles and H. C. Irving
Departments of Surgery and Radiology, St James's University Hospital, Leeds

The reports and ultrasound scans (658 studies) of 135 renal allografts, transplanted in the years 1987 and 1988, have been reviewed. The records of the recipients were also studied in order to determine the clinical status of the kidney at the time of each ultrasound examination and to obtain long-term follow-up of allograft function. Seventy-seven allografts (57%) never showed pelvicalyceal dilatation on 342 serial examinations. Forty-two kidneys (31%) had mild dilatation reported on at least one scan, which did not progress. However, 11 mildly dilated allografts developed moderate to severe dilatation on later examinations, and these, together with five allografts that were reported as exhibiting moderate to severe hydronephrosis on their first dilated scan, were classed as moderate to severe ($n = 16$, 12%). Thirty-eight patients (90%) with mild dilatation of the collecting system had no evidence of obstruction. However, in allografts with moderate to severe dilatation and poor or deteriorating function, 10 patients (70%) were found to have ureteric obstruction. There was no significant difference in 1-year graft survival (87% *vs* 81.8%) and the median serum creatinine at 3 and 12 months post-transplantation between non-obstructed "dilated" and non-dilated allografts (140 μmol/l *vs* 153.7 μmol/l; 139 μmol/l *vs* 143.3 μmol/l). All 14 obstructed allografts were salvaged with a graft survival of 85.7% at 1 year. Median serum creatinine in these patients was significantly elevated at 200 μmol/l and 189 μmol/l at 3 and 12 months; $p = 0.05$ and 0.01 compared with dilated non-obstructed allografts. Our results indicated that grafts with moderate to severe dilatation should be urgently investigated to minimize further allograft damage.

Assessment of vasculogenic male impotence using colour duplex ultrasound

C. P. Oates, *R. S. Pickard, T. A. Whittingham and *P. H. Powell
*Department of Medical Physics, Newcastle General Hospital, Newcastle Upon Tyne and *Department of Urology, Freeman Road Hospital, Newcastle Upon Tyne*

A large percentage of erectile dysfunction is due to vasculogenic causes. This may result from inadequate inflow, sinusoidal pathology or venous leakage. The differential diagnosis of these factors may be assisted by examining the Doppler waveforms in the cavernosal arteries on intracorporeal injection of a vasodilator. Locating the cavernosal arteries is greatly facilitated by the use of colour flow mapping. We described a novel approach to visualizing and obtaining Doppler waveforms from the cavernosal arteries. The view obtained eliminates angle uncertainty in the Doppler equation and maximizes sensitivity to changes in blood flow. An appraisal of the usefulness of a number of Doppler waveform indices and a selection procedure for further management were given.

Spectral Doppler and colour flow imaging in impotence

W. R. Lees, S. J. Garber, *A. E. Kulatilake and *S. Hamson
*Departments of Radiology and *Urology, The Middlesex Hospital, London W1 8AA*

We studied 50 patients with male impotence. Colour Doppler imaging was used to map penile vascular anatomy combined with spectral Doppler measurements of systolic maximum velocity ($V_{\max}$), end diastolic velocity ($V_{\min}$) and pulsatility index (PI). All readings were taken before, and at regular intervals after, administration of 40–70 mg of intracorporal papaverine sulphate. The erectile responses were graded 0–3. Thirteen patients had normal erectile responses. All had a $V_{\max}$ greater than 30 cm/s and a $V_{\min}$ less than 5 cm/s. Sixteen patients had known generalized arterial disease. Only three had a $V_{\max}$ greater than 30 cm/s and only two a $V_{\min}$ greater than 5 cm/s. Ten patients had a normal arterial response but had venous leaks confirmed by pharmacocavernosography. Only one had a $V_{\max}$ of less than 30 cm/s and none had a $V_{\min}$ of less than 7 cm/s. There were 11 elderly patients with non-specific clinical histories. Their response pattern was typically a moderately poor arterial response coupled with a $V_{\min}$ of greater than 5 cm/s. Doppler papaverine stimulation studies of the penile circulation can separate out the three main causes of male impotence: psychogenic, arteriopathic and venous leak. Monitoring of the three parameters in the same segment of cavernosal artery at 2-minute intervals is necessary for reliable results. In this presentation we discussed the significance of $V_{\max}$ and $V_{\min}$ in assessing impotence and demonstrated the value of the PI, which correlated well with the erectile response and adds further information.

Lymphoedema following breast cancer treatment: venous and arterial causes shown by colour and spectral Doppler

W. E. Svensson, P. Mortimer, C. Badger, D. O. Cosgrove, E. Tohno and A. Al Murrani
Departments of Nuclear Medicine & Ultrasound and Dermatology, Royal Marsden Hospital, London

Fifty-six patients with post-surgery/radiotherapy swollen arm were examined with colour Doppler. Fifty-three had breast carcinoma treated surgically (mastectomy or wide local excision) followed by radiotherapy in 50, while three had axillary dissection and radiotherapy for melanoma metastases. In 50%, obstructed or narrowed subclavian or axillary veins were demonstrated and colour Doppler clearly showed collaterals that were not apparent on grey-scale imaging using state-of-the-art equipment. A further 25% had normal venous anatomy but abnormal venous flow patterns with loss or smoothing of the normal respiratory and cardiac phasic variation. Two cases presented with acute swelling of the arm, initially thought to be due to cellulitis. Colour Doppler demonstrated subclavian vein thrombosis in both. Axillary artery flow was estimated in 24 patients. Angle-corrected time-averaged mean flow, measured with Doppler, was multiplied by the cross-sectional area of the artery to derive mean inflow of the swollen and contralateral normal arms. Ten patients had differences of flow greater than 1 : 1.7 between the two arms. In eight the increased flow was in the swollen arm. Post-mastectomy/radiotherapy swollen arm probably has more than one aetiology. Lymphatic damage secondary to surgery and radiotherapy is well documented. This study showed a high incidence of venous obstruction with collaterals. Our initial studies also demonstrated an increased arterial inflow in some patients. This could be caused by inflammation of the arm or by damage to the sympathetic nerves supplying the arm. This study suggested a multiple aetiology in many cases of secondary lymphoedema following treatment for breast cancer. The wide range of causes that have been proposed by previous workers and the great difficulty of producing an animal model of lymphoedema supports our hypothesis of a varied multiple aetiology.

Acute inflammation of the breast: the role of breast ultrasound in diagnosis and management

R. Hayes, M. Michell and H. Nunnerley
Department of Radiology, King's College Hospital, Denmark Hill, London SE5 9RS

The diagnosis of breast abscess from clinical signs alone may be difficult in patients with acute inflammation of the breast. Ultrasound examination is helpful in demonstrating the presence or absence of an abscess collection. Twenty female patients, aged between 24 and 69 years, were referred for breast ultrasound examination between June 1989 and June 1990, with a clinical diagnosis of breast abscess. Six were currently lactating. Ultrasound examination was performed using a real-time 7.5 MHz linear array transducer (Siemens Sonoline SL1). Ultrasound examination confirmed the presence of an abscess collection in nine out of 20 patients. Seven of these patients subsequently had surgical incision and drainage, with satisfactory results. Two settled on medical treatment. Eleven out of 20 patients had no detectable abscess on initial ultrasound examination, and were treated conservatively with antibiotics. Ten made a full recovery. One patient, who had markedly dilated ducts on initial ultrasound examination, remained symptomatic. Follow-up ultrasound demonstrated a small fluid collection, which within 12 days developed into a large multiloculated abscess, requiring surgical management. Ultrasound examination accurately demonstrates the presence or absence of an abscess in breasts that are acutely inflamed, and thereby allows appropriate selection of patients for surgical management. In this series 10 out of 20 patients had negative serial ultrasound examinations, and therefore avoided surgical intervention.

Paediatric ultrasound

Chairmen: R. Arthur and A. Coral

Scrotal ultrasound in children: grey scale and colour, by A. S. Hollman and S. Ingram
Renal candidiasis in the neonate: ultrasound appearance and treatment, by S. J. Garber and R. De Bruyn
Renal sonography in long-standing Lesch–Nyhan syndrome, by I. J. Kenney
Renal ultrasound compared with DMSA scintigraphy in the detection of focal nephronia and scarring following childhood urinary tract infection, by S. T. Meller, D. O. Cosgrove, B. Al. Murrani and W. E. Svensson

Scrotal ultrasound in children: grey scale and colour

A. S. Hollman and S. Ingram
Department of Radiology, Royal Hospital for Sick Children, Yorkhill, Glasgow G3 8SJ

Ultrasound is widely accepted as the imaging modality of choice in the initial evaluation of suspected scrotal pathology in infants and children. The examinations were performed by direct contact scanning with a 10 MHz sector probe (ATL Ultramark 4) or more recently with a 7 MHz linear array transducer (Acuson 128). A *thin* stand-off material may be helpful, but in the younger child who is apprehensive, or who has a red, hot scrotum, then a water bath technique is invaluable, in which the child is examined sitting in a warm baby bath. Present uses in infants and children include evaluation of scrotal masses, scrotal pain, scrotal trauma and search for undescended testes. A wide range of scrotal pathology has been observed over a 2-year period, the most common conditions diagnosed being hydrocele and epidymo-orchitis; testicular tumours are rare in children. The introduction of colour Doppler ultrasound 6 months ago has resulted in a higher referral rate for assessment to exclude or confirm testicular torsion. Using colour, a much more confident diagnosis can be issued of torsion versus infection. This paper discussed techniques for examining the paediatric scrotum, outlined the ultrasound features of scrotal pathology and indicated where colour Doppler ultrasound has been useful in this age group.

Renal candidiasis in the neonate: ultrasound appearance and treatment

D. J. Garber and R. De Bruyn
Department of Radiology, The Hospital for Sick Children, Great Ormond Street, London

Candida albicans is a common commensal organism. However, in the premature neonate it may produce acute renal infection and septicaemia. It is associated with a poor prognosis. We presented three cases of neonatal renal candidiasis. Case 1 was a 24-week premature infant who developed septicaemia and anuria. Renal ultrasound demonstrated bilateral hyperechoic kidneys with dilated pelvicalyceal (PC) systems containing fungal balls. Candida was isolated from urine and blood samples. Case 2 was a 30-week premature infant who developed candida septicaemia after recovering from necrotizing enterocolitis. Renal ultrasound showed an echogenic left kidney with PC dilatation and the presence of fungal balls. Case 3 was a 26-week premature infant who, following intermittent, intravenous antifungal therapy for candida septicaemia, suddenly developed acute renal failure. Ultrasound showed bilateral PC dilatation and the presence of fungal balls. In all three cases the mainstays of treatment were draining the obstructed renal systems and direct instillation of an antifungal agent. In this paper we described the ultrasound features of renal candidiasis and discussed the role for ultrasound in the diagnosis, treatment and long-term follow-up of this difficult condition. Current literature on the subject was reviewed.

Renal sonography in long-standing Lesch–Nyhan syndrome

Ian J. Kenney
Royal Alexandra Hospital, Dyke Road, Brighton BN1 3JN

Lesch–Nyhan Syndrome (LNS) is an X-linked disorder of purine metabolism characterized by the distinctive but variable clinical picture of mental retardation, athetoid cerebral palsy, self-mutilation and hyperuricaemia. Deficiency of the enzyme hypoxanthine guanine phosphoribosyl transferase (HGPRT), which converts the purine bases hypoxanthine and guanine to their respective nucleotides, is the basic defect. The renal complications of uric acid crystal nephropathy and calculus disease are a common feature of this rare disease. The renal ultrasound appearances of four children with long-standing LNS were presented. All showed multiple renal calculi of varying size. Three showed increased echogenicity of the renal pyramids, also of varying degree. The combination of multiple calculi and increased pyramidal echogenicity results in a striking "spotty" appearance which in our experience is quite characteristic. One case had diffuse renal scarring. Where possible, analysis of calculi showed, in addition to uric acid, xanthine and oxypurines. Elevated urinary xanthine and oxypurines are the result of treatment with allopurinol, which all our patients had been taking over many years. This drug is used together with alkalinization of the urine to reduce uric acid excretion and allow the resolution of uric acid calculi. The relevant biochemistry was briefly reviewed. We believe that our cases in reality represent the ultrasound appearances of long-standing allopurinol-induced crystal nephropathy and calculus disease rather than uric acid nephropathy.

Renal ultrasound compared with DMSA scintigraphy in the detection of focal nephronia and scarring following childhood urinary tract infection

S. T. Meller, D. O. Cosgrove, B. Al Murrani and W. E. Svensson
Royal Marsden Hospital, Sutton, Surrey

A semi-blind prospective study was performed on 42 children (aged 3 months to 17 years: 24 children under 5 years) referred consecutively to the department following urinary tract infection. Six children were scanned on two separate occasions and 96 kidneys were evaluated by DMSA scintigraphy and high-resolution real-time ultrasound by experienced sonologists under ideal conditions. In 76 kidneys (50 normal, 26 abnormal) there was agreement between the DMSA and ultrasound findings. In 15 kidneys the DMSA showed a focal abnormality that was not detected by ultrasound. One kidney showed caliectasis on ultrasound but was normal on the DMSA scan. Four left kidneys showed splenic impressions suspected on the DMSA scan and confirmed on ultrasound. In this series, renal ultrasound underestimated focal renal involvement by 15% following urinary tract infection. Although the techniques are complementary, the DMSA scan should be regarded as the gold standard for the detection of focal nephronia and renal scarring in children. The possible reasons for false negative renal ultrasound scans in this situation were discussed.

Orthopaedic ultrasound

Chairmen: R. Arthur and A. Coral

Ultrasound in the acute clinical management and follow-up of achilles tendon disorders, by M. R. Gandhi and D. R. Naik
Percutaneous ultrasound-guided removal of soft-tissue foreign bodies, by M. J. Bradley, E. Kadzombe, P. Sims and B. Eyes

Ultrasound in the acute clinical management and follow-up of Achilles tendon disorders

M. R. Gandhi and D. R. Naik
Department of Radiology, Northern General Hospital, Sheffield 5

The ultrasound appearances of ankle disorders have been well described in several papers since the late 1970s. Ultrasound would seem to have a useful role to play in diagnosing Achilles tendon tears, bursitis, tenosynovitis and enthesopathies around the ankle joint. There are conflicting views about its role in diagnosing tendonitis. We have attempted to determine whether ultrasound has a useful role in the acute clinical management and follow-up of Achilles tendon disorders. Ultrasound of the ankle was performed in patients presenting with acute symptoms related to the Achilles tendon. Patients attending the A & E department with acute symptoms related to the Achilles tendon were referred for ultrasound examination. All scans were performed in a standard manner using a real-time linear array scanner with a 7.5 MHz probe. Both ankles were scanned in longitudinal and transverse planes with static and dynamic scans being performed. The clinical assessment of Achilles tendon disorders, and in particular tears, is difficult. We hope to evaluate the role of ultrasound in influencing the clinical management of Achilles tendon disorders. Preliminary results show that orthopaedic surgeons tend to manage patients with suspected tears on the basis of their scan results, even if the latter disagree with the initial clinical diagnoses. This confirms our view that ultrasound is a valuable adjunct to the clinical management of Achilles tendon disorders. We are also performing follow-up scans of patients with positive tears on scanning to assess healing. This will be the first study assessing healing of Achilles tendon tears with conservative treatment (following immobilization in a plaster of Paris).

Percutaneous ultrasound-guided removal of soft-tissue foreign bodies

M. J. Bradley, E. Kadzombe, P. Simms and B. Eyes
University Department of Radiodiagnosis, Royal Liverpool Hospital, Prescot Street, Liverpool

Low-kV radiography, and more recently ultrasound, have been widely used in the diagnosis and localization of the soft-tissue foreign body (FB). We described our preliminary experience using ultrasound as the guiding tool for percutaneous extraction. The FBs chosen for this technique were impalpable and would thus require "blind" surgical exploration. Five patients were referred from the Accident and Emergency Department at acute presentation or as a result of referral from a local psychiatric unit where various FBs had been placed intentionally. Our aim was to diagnose and localize the FB in each case using ultrasound, and to assess the feasibility of percutaneous extraction with local anaesthesia to prevent more invasive surgery. Ultrasound correctly localized 11 FBs (eight radio-opaque, three non-radio-opaque) ranging 3 mm–8 cm in length. All were strongly echogenic causing "comet" tails or acoustic shadowing. Seven were in the forearm, three in the thigh and one adjacent to the lateral malleolus, lying 1–6 cm deep to the skin surface. Ultrasound localization was performed, a small incision made and the FB grabbed by forceps using continuous ultrasound visualization. Of the 11 FBs, five were removed successfully by this technique, the remainder being found at surgery. The early failures were blamed on making too large an incision, which caused artefacts from blood and air in the wound masking the FB. We believe that this is a useful technique for removal of the clinically "difficult FB" and intend to develop the technique further.

Clinical audit of diagnostic ultrasound

Chairmen: A. Coral and J. Wilson

Accuracy and reproducibility of screening in the community for aortic aneurysm in the elderly male using a portable ultrasound scanner, by G. M. Grimshaw, J. D. Hamer and M. X. Gannon
Emergency ultrasound in the acute abdomen, by A. H. Davies, I. Mostarakou, R. Cobb, D. L. Lindsell and N. J. Mc. C. Mortensen
Quality assurance of obstetric ultrasound screening scans, by N. J. Dudley and R. Potter

Accuracy and reproducibility of screening in the community for aortic aneurysm in the elderly male using a portable ultrasound scanner

G. M. Grimshaw, J. D. Hamer and M. X. Gannon
Department of Vascular Surgery, Queen Elizabeth Hospital, Edgbaston, Birmingham

A community-based aortic screening programme has been established to assess the prevalence of abdominal aortic aneurysms in men between the ages of 65 and 75 years and to assess the feasibility, accuracy and reproducibility of this type of screening. It is documented that in terms of QALY factors (Quality Adjusted Life Years), aortic screening has been demonstrated to have a factor of £830 compared with the use of low-absorption cassettes (£920) and cervical screening (£4688). To place the screening at the patients own GP, if practical, can make this one of the most successful screening services available. One thousand five-hundred and thirty-nine patients from 15 group practices—29 general practitioners—have been studied so far. Compliance varies from practice to practice but has a mean of approximately 60% within the range 42–84%. Satisfactory scans have been obtained, using the pie data 150S sector scanner on 1501 patients (98%); 1354 (90.3%) of these patients were within the normal ranges (12–28 mm). One hundred and forty-six patients had abnormal aortas, 6.6% showing a slight dilatation up to 39 mm, 1.9% having moderate operable dilatations of up to 50 mm and 1.2% (17) with acute aneurysms. Twenty-four patients with dilatations greater than 39 mm had CT and in some cases hospital ultrasound scans were performed to verify the community ultrasound scan result. The mean difference between CT and ultrasound scanners was 0.1 mm, showing no bias between the methods. The standard deviation of the differences between the two measurements was calculated to be 1.78 mm with a standard error on the distribution of differences of only 0.37 mm. The excellent agreement between CT and community-based ultrasound scanning demonstrated the feasiblity of examining the abdominal aorta for the "at risk" cohort. It is cheap, easy and an effective means of diagnosis, and is proving popular with patients and their GPs.

Emergency ultrasound in the acute abdomen

A. H. Davies, I. Mostarakou, R. Cobb, D. Lindsell and N. J. Mc. C. Mortensen
Departments of Surgery and Radiology, John Radcliffe Hospital, Oxford

A misdiagnosis in the acute abdomen can be associated with morbidity and mortality. The role of emergency ultrasound in the management of the acute abdomen and its possible use by surgical trainees are controversial. One hundred and thirty consecutive patients (72 males, 58 females) of mean age 52 years (range 1–94 years) presenting with an acute abdomen were studied. All patients were clinically assessed by a middle-grade surgeon and a management plan formulated. An ultrasound examination was then performed by a radiologist, the surgeon was informed of the result and any influence on management noted. Twelve patients (9%) would have had an emergency ultrasound scan requested, 55 patients (42%) would have had a request for a routine ultrasound scan and 63 patients (48%) would not have had one. Ultrasound altered the diagnosis in one patient from probable appendicitis to cholecystitis. Ultrasound missed one abdominal aortic aneurysm, one appendicitis and one empyema of gallbladder. In 22 patients who underwent appendicetomy, 20 had appendicitis. In this group ultrasound had a sensitivity of 95%, a positive predictive value of 95% and an accuracy of 91% in detecting appendicitis. In most cases of the acute abdomen, immediate ultrasound was required to rule out life-threatening surgical pathology. In the other cases it was rarely helpful, with the exception of appendicitis where we found a surprisingly high accuracy. Where an urgent ultrasound scan is necessary on clinical grounds, the skills of a radiologist are probably required, whereas in specific areas, for example the diagnosis of appendicitis, there may be a place for training surgical staff.

Quality assurance of obstetric ultrasound screening scans

N. J. Dudley and R. Potter
Department of Medical Physics and Computing, County Hospital, Sewell Road, Lincoln LN2 5QY

Much attention has been given to the quality assurance (QA) and safety of ultrasound equipment. However, there has been no reported QA of ultrasound scans. Following the Government's White Paper on the NHS there is increasing interest in establishing measurable standards of service. The aim of this study was to develop and test the efficacy of a simple QA technique for obstetric ultrasound screening scans. Careful examination of the fetal head is now a major part of screening for fetal anomalies. Experienced sonographers may do this in conjunction with obtaining a biparietal diameter (BPD) section for measurement. This section was therefore selected for QA. In this study sonographers were asked to photograph the section used for BPD measurement, including calipers. Images were then inspected for eight quality factors and any signs of abnormality and scored accordingly. In addition, gestational ages predicted from BPD and femur length were compared to identify any systematic measurement errors. The study was performed in three phases. In order to establish a baseline of performance, sonographers were not made aware of the quality factors during the first phase, although these had been part of initial training. At the end of this phase, scores were bar-charted and explained to the staff as a group, with some general instruction on how problems could be overcome. During the second phase, therefore, sonographers were aware of the quality factors. Where problems persisted during the second phase, sonographers were coached individually prior to the third phase. Results showed significant improvement in quality over the latter two phases of the study suggesting that the factors identified were effective in monitoring the quality of obsetric ultrasound screening scans. Standards will be maintained by continuing the QA programme.

New instrumentation and techniques

Chairmen: A. Hall and T. A. Whittingham

Techniques for ultrasound 3-D imaging, by J. E. Gardener and W. R. Lees
Prototype systems for 180° and 360° ultrasound tomography, by J. R. Jago and T. A. Whittingham
Imaging flow and shear by speckle tracking with a neural network, by J. C. Bamber, C. Dance, D. Bell and N. L. Bush
New advances in colour flow mapping: quantitative velocity measurement beyond the Nyquist limit, by R. Fehr, B. Dousse and B. Grossniklaus
A new acoustic probe for quality assurance and treatment planning in extracorporeal lithotripsy, by S. D. Pye, N. J. Parr, T. Anderson, A. W. S. Ritchie, D. Tolley and W. N. McDicken
Image recording and archiving: today and tomorrow, by A. Hall

Techniques for ultrasound 3-D imaging

J. E. Gardener and *W. R. Lees
*Departments of Medical Physics and *Radiology, University College Hospital and the Middlesex Hospital, London*

The imaging of complete solid regions of tissue is becoming increasingly important in a number of clinical areas and most CT and MRI scanners and at least one ultrasound machine now have 3D facilities in some form. There are special problems for imaging ultrasound in 3D: the data acquisition and display rate is extremely high; few machines store or provide access to digital data; and the character of the images makes 3D rendition difficult. In order to tackle these problems and to demonstrate that 3D reconstruction of ultrasound can be clinically useful, we have developed a low-cost 3D workstation that will operate as an add-on to most types of scanner. Data are acquired as sets of video frames at real-time rates, controlled by probe position. Data may then be rapidly redisplayed in several formats, including interactively selected cut-planes and synthetic surface-shaded views. The hardware employs an array of transputers that economically provide high-speed processing and display. Since the complete volume is imaged and stored, the data may be archived and subsequently reconstructed for review, for surgical planning or as a teaching aid. The reconstruction methods offer previously inaccessible views to resolve questions about complex structures. Quantitative measurements of dimensions or echo statistics may be made on volumes of tissue. We have applied the technique to a range of investigations which so far includes intravascular imaging; endoscopic studies of the oesophagus and rectum; abdominal and fetal imaging. Used with intravascular studies, the method can show the intimal surface of the vessel shaded to reveal irregularities, from which size and shape of plaque deposits can be measured. Sectional views show detail of the layered structure of vessel walls in any chosen cut plane. Videotape recordings can be made from the output during reconstruction and examples of these were shown to illustrate the speed of the system.

Prototype systems for 180° and 360° ultrasound tomography

J. R. Jago and T. A. Whittingham
Regional Medical Physics Department, Newcastle General Hospital, Newcastle upon Tyne

Two ultrasound tomography systems have been built and evaluated. In both systems, linear array images from a range of directions within a common scan plane are combined and processed to produce a high-resolution image. In the 180° system the scan plane is vertical and a single 3.5 MHz linear array probe is rotated through 180° in a water bath beneath the target section. Potential applications for this system include investigation of limbs, the neck, the breast, the scrotum, and the abdomen and head of horizontal neonates. In the 360° system a pair of diametrically opposed linear array probes are rotated through 360° in a water bath, in a horizontal scan plane. Applications of this arrangement might include coronal sections of the breast, vertically disposed limbs and neonates supported in an erect posture. In both systems a SUN 386i microcomputer controls the movements of the probe as well as storing and processing the images. Scan times with the prototype systems are typically 30 seconds, but these could be reduced in a clinical system to a few seconds. Processing techniques include simple back-projections and inverse Wiener filtering. In addition, as the 360° system allows simultaneous mapping of the speed of sound distribution within the target section, it has been possible to correct the reflection-mode images for registration errors caused by speed of sound variations between tissues. This development may be of particular value in breast imaging. Examples of images of simple phantoms and human subjects were presented and discussed.

Imaging flow and shear by speckle tracking with a neural network

J. C. Bamber, C. Dance, D. Bell and N. L. Bush
Physics Department, Institute of Cancer Research, Royal Marsden Hospital, Downs Road, Sutton, Surrey SM2 5PT

Time domain methods for the measurement and imaging of blood flow or solid tissue movement offer a number of interesting potential advantages over methods based on the Doppler effect. These include overcoming the aliasing problems for high flow rates, high sensitivity to low velocities and the provision of quantitative (angle independent) velocity information. We have previously described a method for movement imaging based on observing speckle decorrelation rate in B-scans. A more advanced approach, which provides information on direction as well as magnitude of velocity, works by using correlation techniques to recognize and track the motions of sections of the echo speckle pattern. Previous use of neural networks for pattern or object recognition suggests that they might, in principle, be used advantageously to track speckle, particularly if the speckle pattern changes as it moves. We have begun to investigate this possibility using a new hardware "Fussy Set Comparator" (Micro Devices MD1210). Experiments on speckle phantoms demonstrated that the pattern "match coefficient" produced by the MD1210 represents a good alternative to the correlation coefficient. A speckle tracking algorithm was constructed in which the MD1210 was used repeatedly to simultaneously compare eight two-dimensional speckle patterns with a reference pattern and choose the closest match. The final result is a two-dimensional image showing both magnitude and direction of velocity. Comparisons between this, conventional colour Doppler and the correlation method were made using a rotating speckle phantom, which was also used to study the anomalous speckle motion seen out of the focal plane.

New advances in colour flow mapping: quantitative velocity measurement beyond the Nyquist limit

R. Fehr, B. Dousse and B. Grossniklaus
Ultrasound Research Group Roche, Hoffmann-La Roche, Basle, Switzerland

One of the major limitations in colour flow mapping (CFM) is the limited velocity range, defined by the pulse repetition frequency (Nyquist limit). A new method (patent pending) allows the extension of the Nyquist limit by a factor up to 5. This method uses two colour flow units working at different transmit/receive frequencies. Owing to the Doppler formula, the resulting frequency shifts will be different. The comparison of both shifts allows measurement up to 3 m/s instead of 0.6 m/s at a PRF of 4 kHz. The new Nyquist limit is defined by the difference between the transmit frequencies of the two channels. Measuring by this technique makes it possible to analyse colour flow images quantitatively up to unambiguous velocity of 3 m/s. This method is used in the Kontron Instruments Sigma 44 HVCD colour flow system based on mechanical transducers, and results were obtained on Doppler phantoms as well as in clinical trials. New filter methods and special biometry software used with the anti-aliasing system described will give a substantial amount of new information, which will considerably enhance the value of colour flow mapping in cardiology.

A new acoustic probe for quality assurance and treatment planning in extracorporeal lithotripsy

S. D. Pye, *N. J. Parr, T. Anderson, *A. W. S. Ritchie, *D. Tolley and W. N. McDicken
*Department of Medical Physics and Medical Engineering, Western General Hospital, Edinburgh and *Scottish Lithotriptor Centre, Edinburgh*

Extracorporeal shockwave lithotripsy has become an established method of treatment for kidney stones. A Wolf 2300 piezoelectric lithotriptor was installed at the Scottish Lithotriptor Centre in Edinburgh in 1988. Treatment is expensive because of the high capital and maintenance costs of the equipment. The acoustic output (the size of the shockwave) produced by the lithotriptor changes with time as the piezoelectric bowl deteriorates and as some of the electronic circuits for generating the shockwave wear out. When delivering any form of energy at therapeutic levels, accurate monitoring is desirable to ensure safe clinical practice. The manufacturer provides no method of regularly checking the output. Such information is clearly necessary to optimize treatment regimes. There is currently no instrument available that is easy to use and suitable for making regular measurements of lithotriptor pulses. Manufacturers and research workers use PVDF needle hydrophones and thin membrane hydrophones to detect the pressure waveform. However, these are expensive, need to be used very carefully, and are also ultimately destroyed by the lithotriptor. A new type of acoustic probe designed in the Medical Physics Department in Edinburgh has been used to monitor the output of a Wolf 2300 lithotriptor over a 10-month period. The probe design involves coupling the energy of the shockwave into an electromagnetic transducer via a steel ball. The probe is robust and has withstood several thousand lithotriptor pulses. It is also easy to use and inexpensive and would be much cheaper to produce than present needle or membrane hydrophones. The probe has been calibrated against a PVDF membrane hydrophone. The results of monitoring the Wolf 2300 output over the past 10 months show that large changes in output have occurred, with pulse energies varying by up to 350%. Some of these changes have taken place over a period of months as the piezoelectric bowl has deteriorated, and some have happened suddenly as electronic components have failed, or following visits by the service engineers.

Image recording and archiving: today and tomorrow

A. J. Hall
Sony Scientific & Medical, Sony (UK) Ltd, Basingstoke

The recording and long-term storage of ultrasound images is becoming increasingly important as ultrasound scanning applications proliferate. The rapidly changing technology as applied to ultrasound recording was reviewed, including conventional photographic methods, the multi-format camera, dry silver printing and the more recent video printing. The printing methods were related to the various ultrasound techniques including monochrome and colour flow Doppler. To conclude the section on printing the latest products were examined with a preview of likely future developments. The various media available for archival or long-term storage of ultrasound images were discussed. These included conventional X-ray film, video storage of dynamic images and the opportunities opened up by electronic storage. The differences between analogue and digital storage were compared in terms of quality, cost, speed of access, ease of retrieval, storage capacity and integrity of image. Examples of the printing and storage technologies were shown in the Exhibition.

Veterinary ultrasound

Chairman J. S. Boyd

Pulsed- and continuous-wave Doppler echocardiography in the dog: technique and interpretation, by J. M. N'dungu, C. Paterson and J. S. Boyd
Mitral value echocardiography in the dog and cat, by J. Dukes
Case studies in canine congenital heart disease by colour flow Doppler, by P. G. Darke, V. Luis Fuentes and M. W. Martin
Ocular ultrasonography in the domestic species, by J. S. Boyd
Ultrasonic ocular examination in the dog, by P. Boydell
Ultrasonography of the reproductive tract of the dog, by G. C. W. England
The use of ultrasound in llama reproduction, by D. A. Bourke and C. L. Adam
Ultrasound imaging of the reproductive tract of the male bottlenose dolphin and its significance in clinical and breeding management, by F. Brook, D. Chow, Y. T. Lam and P. Schroeder
Relative echogenicity of the renal cortex and liver in normal dogs, by L. E. Hartzband, A. S. Tidwell and C. R. Lamb

Pulsed- and continuous-wave Doppler echocardiography in the dog: technique and interpretation

J. M. Ndung'U, *C. Paterson and J. S. Boyd
*Departments of *Veterinary Medicine and Anatomy, University of Glasgow Veterinary School, Bearsden, Glasgow G61 1QH*

Application of Doppler echocardiography in diagnostic veterinary cardiology is increasing. As such it is necessary that the technique be properly understood and normal reference values be obtained for different animal species. The present work was therefore designed to establish optimal sites for studying blood flow dynamics across cardiac valves, and to determine normal blood flow indices by pulsed-wave (PW) and continuous-wave (CW) Doppler in dogs. Fifteen 7-month-old normal beagles (9.6 ± 1.67 kg) were used. The dogs were placed in right lateral recumbency and determination of valvular incompetence carried out by PW Doppler on all cardiac valves from the right thoracic wall. Mitral and aortic incompetence was further investigated from the subcostal window by PW Doppler, with the dog in a semi-dorsal recumbency position. Mitral and aortic blood flow velocity was determined from the subcostal window by both PW and CW Doppler. From the thoracic inlet, the velocity of blood flow in the ascending aorta was estimated by CW Doppler with the dog in a sitting position. Studies on each dog were carried out on 2 days and average values determined. By CW Doppler, mitral E peak blood flow velocity was 0.755 ± 0.106 m/s and 0.531 ± 0.076 m/s for the A peak, and was higher than velocities obtained by PW Doppler (E: 0.691 ± 0.075 m/s; A: 0.464 ± 0.064 m/s). Aortic flow velocity, estimated by CW Doppler from the subcostal window (1.577 ± 0.170 m/s), was significantly ($p < 0.05$) higher than that obtained by PW Doppler (1.39 ± 0.129 m/s), and similar to values obtained by CW Doppler from the suprasternal window (1.56 ± 0.201 m/s). It was possible to calculate indices of diastolic function from mitral flow velocity, and cardiac output by combining aortic blood flow velocity with aortic root measurements. The present work demonstrated further the diagnostic potential of Doppler echocardiography in veterinary cardiology.

Acknowledgements: This work was funded by the UNDP/World Bank/WHO Special Programme for Research and Training in Tropical Diseases. J. M. N., from Kenya Trypanosomiasis Research Institute, was sponsored by The British Council.

Mitral valve echoradiography in the dog and cat

J. Dukes
Department of Veterinary Medicine, University of Glasgow Veterinary School, Bearsden, Glasgow G61 1QH

Two-dimensional echocardiography can be used to image the mitral valve in short-axis (fish mouth) and long-axis views. Degenerative changes associated with valvular endocardiosis or vegetations due to endocarditis can be visually appreciated. Normal mitral M-mode demonstrates anterior leaflet motion to have two opening phases, the E peak corresponding to early diastolic filing and the A peak subsequent to atrial contraction. Increased E point to septal separation, often associated with poor left ventricular function, is pathognomonic of dilated cardiomyopathy. Atrial fibrillation results in abnormal anterior leaflet motion with no A peaks. In the normal animal, the excursion of the E peak should be greater than the A. In situations of diastolic failure, ventricular filling becomes more dependent on atrial contraction, the excursion of A becoming dominant. In addition, the closure descent after the A peak (A–C slope) may be ragged, with B bumps, indicating elevated diastolic pressures. Murmurs of mitral regurgitation are probably the most commonly auscultated in small animal practice, usually due to valvular endocardiosis. This can be readily documented and a systolic regurgitant jet demonstrated by pulsed Doppler echocardiography. Normal diastolic mitral flow has two phases, labelled E and A as indicated earlier. Again, normal diastolic mitral flow should have a greater proportion occurring passively, the E peak dominating. Evidence of diastolic failure can be gained if the A peak is consistently dominant. A cat with restrictive cardiomyopathy was presented for illustrative purposes. Finally, a case was presented of a Bull Terrier with mitral dysplasia. As well as mitral incompetence, the dog had high mitral inflow velocity and prolonged pressure half-time, consistent with mitral stenosis. This abnormality has never been reported in veterinary literature to the author's knowledge.

Case studies in canine congenital heart disease by colour flow Doppler

P. G. G. Darke, V. Luis Fuentes and M. W. Martin
Small Animal Clinic, Royal (Dick) School of Veterinary Studies, Summerhal, Edinburgh

Colour flow Doppler (CFD) provides a non-invasive angiographic portrayal of blood flow superimposed on a two-dimensional echocardiographic image. This is of particular value in the investigation of congenital heart disease. Colour flow readily demonstrates the presence of abnormal cardiac blood flow. For example, the abnormal jet of blood through a ventricular septal defect (VSD) is easily identified in dogs, as is the disturbed (turbulent) flow through a patent ductus arteriosus at the heart base. Disturbed flow is also seen with pulmonic or aortic stenosis and it is portrayed by most CFD systems as a contrasting colour (usually green). Occasionally, careful observation of colour flow will reveal high-velocity flow in the absence of turbulence. For example, in congenital mitral stenosis in dogs an aliased core of high-velocity flow can be observed. Furthermore, CFD is sufficiently sensitive to show abnormal flow through a restrictive ductus even in the absence of an audible murmur. Care must be taken to identify the precise source of a turbulent jet, which can project far beyond its origin: for example, from a VSD through the pulmonic valve into the pulmonary artery. CFD is particularly valuable both in catching the eye of the observer and helping in the placement of the range gate accurate for spectral pulsed-wave Doppler recordings.

The generous support of the British Small Animal Veterinary Association Clinical Studies Trust Fund and the Home of Rest for Horses in this work is gratefully acknowledged.

Ocular ultrasonography in the domestic species

J. S. Boyd
University of Glasgow Veterinary School, Bearsden, Glasgow G61 1QH

The eyes of a number of various domestic species were examined ultrasonographically to demonstrate the anatomy of the healthy eye and also a variety of pathological conditions. The animals were examined in a conscious state using minimal restraint and, in some cases, mild sedation. The bulbar conjunctiva was anaesthetized using local anaesthetic drops and non-irritant lubricating jelly was applied around the palpebral orifice and on to the transducer's contact surface. A 7.5 MHz sector transducer with a built in stand-off and a 10 MHz focus sector transducer, making direct contact with the bulbar surface, were used in the scanning process. The ultrasonographic images obtained in both longitudinal and transverse planes were described and further illustrated by comparison with frozen sectioned anatomical specimens. In the pathological cases where the eye required to be sacrificed the gross pathology was compared with the ultrasonographs. The application of the technique of ocular ultrasonography proved to be most useful in cases of corneal opacity and cataract as well as providing useful information in identifying space-occupying retrobulbar lesions.

Ultrasonographic ocular examination in the dog

P. Boydell
Department of Small Animal Studies, The Royal Veterinary College, Hawkshead House, North Mymms, Hatfield, Herts AL9 7TA

On dogs with anterior ocular opacities, ultrasonographic examination was performed as part of the routine diagnostic protocol. Opacities included corneal pigmentation, corneal oedema, pupillary membrane, cataract and anterior and posterior haemorrhage. All the opacities prevented adequate ophthalmoscopic inspection of posterior structures. None of the eyes had been examined before development of the opacity. The commonest presenting ocular opacity occurring in the dog was cataract. Visual function was determined by assessment of the pupillary light reflex; electrophysiological tests were not available. Over a 2-year period, over 10% of the eyes examined were shown to have an anatomical abnormality behind the cataract, which would not have been evident without ultrasonography. The most common abnormalities were vitreous membranes and retinal detachment. In most cases where follow-up was available, the pupillary light reflex became sluggish and was extinguished within a year of the initial presentation. One breed that figured prominently in the data was the Old English Sheepdog, in which, in cases of cataract, there was a 100% incidence of retinal detachment. Examples of cataract and neoplasia behind corneal opacities, and retinal detachment concealed by haemorrhage, were also illustrated. These findings demonstrated the value of a pre-surgical ocular ultrasonographic evaluation and showed that the technique of B-scan ultrasonography has a place in the diagnostic armoury of the veterinary ophthalmologist.

Ultrasonography of the reproductive tract of the dog

G. C. W. England
Royal Veterinary College, University of London, Hatfield, Herts

High-resolution ultrasound transducers allow imaging of both the external and the internal genitalia when used in a transabdominal and transrectal manner. Whilst ultrasound imaging of the reproductive tract of the male is widely practised in several species, there have been few studies using the technique in the male dog, with the exception of imaging the prostate gland. Scrotal ultrasonography of the dog provides images similar to those seen in other species and transrectal ultrasonography provides detailed images of the prostate gland and urethra. The indications and techniques for examination of the canine male reproductive tract were discussed. The normal ultrasonographic anatomy of the canine male reproductive tract was demonstrated using standardized images and some pathological conditions were illustrated.

The use of ultrasound in llama reproduction

D. A. Bourke and C. L. Adam
Rowett Research Institute, Bucksburn, Aberdeen AB2 9SB

Llamas and other camelids do not have regular oestrous cycles like other domestic species. Rather they show prolonged periods of sexual receptivity and ovulation being induced by copulation. As a consequence, accurate assessment of ovarian status and early pregnancy diagnosis are essential for successful pharmacological control of reproduction. A B-mode linear array scanner with a 5 MHz transrectal transducer has been used at regular intervals to visualize the ovaries and reproductive tract of adult female llamas. Normal patterns of ovarian activity as well as ovarian response to treatment with human chorionic gonadotrophin (HCG), pregnant mare serum gonadotrophin (PMSG) and prostaglandin $F2\alpha$ ($PGF2\alpha$) and the uterine changes in early pregnancy have been observed. The ultrasound images of follicles (non-echogenic) and corpora lutea (echogenic) were readily distinguishable. In each llama there was follicular activity in one or other ovary at all times, with waves of follicular development and regression. Follicles were visually detectable from 0.3 cm developed to maximum size (0.9–1.3 cm), deemed to be ovulatory, within 9 days. If not induced to ovulate, the follicles remained at maximum size for an average of 8 days before undergoing rapid atresia. There appeared to be an interesting temporal arrangement of follicular waves; generally in each wave only one follicle reached mature size and as this follicle regressed there was coincident development of another follicle in the same or opposite ovary. Ovulation, induced by mating or administration of HCG (Day 0), was detected by disappearance of the large follicle and subsequent identification of the corpus luteum 4–6 days later. The corpus luteum reached maximum size (0.9–1.4 cm) by Day 7, and, in the absence of pregnancy, regressed fully by Day 11. Where conception had occurred, small fluid-filled (non-echogenic) structures, indicative of pregnancy, were recognizable by Day 19 post-mating and the embryo was detectable by Day 21. Administration of PGF2α induced luteolysis and the corpus luteum was indefineable within 4 days of treatment. Administration of PMSG resulted in superstimulation of follicles with up to nine reaching ovulatory size. Ultrasonography allows accurate non-invasive assessment of ovarian and uterine changes in the llama.

Ultrasound imaging of the reproductive tract of the male bottlenose dolphin and its significance in clinical and breeding management

F. Brook, D. Chow, Y. T. Lam and P. Schroeder
Veterinary Hospital, Ocean Park Corporation, Hong Kong

In recent years, owing to a general increase in ecological and conservational awareness, as well as in the stringency of legislative control over marine mammal protection, many oceanaria and marine mammal research organizations holding captive animals are becoming more determined in their efforts to further advance and improve the clinical management of these animals and to instigate effective breeding programmes. Continued development of non-invasive techniques for the investigation and evaluation of reproductive performances in cetaceans is required and at Ocean Park we are conducting studies to determine the use and efficacy of diagnostic ultrasound in this area, amongst others. A 3.5 MHz linear array transducer was used, in conjunction with an Aloka 630 ultrasound unit, to identify the reproductive tract in several male bottlenose dolphins of varying maturity. The testes in this species are large and easily identifiable and it is also possible to examine the epididymides, the vasa deferentia, prostate, penis and adjacent structures with ultrasound. The parenchymal echopattern and echogenicity of the testes were studied and various measurements taken to determine size and volume. Blood samples for serum testosterone levels were collected at the same time to correlate morphometric indices with physiological function. Comparative techniques, ultrasound appearances and findings were presented.

Relative echogenicity of the renal cortex and liver in normal dogs

L. E. Hartzband, A. S. Tidwell and *C. R. Lamb
Department of Surgery, Tufts University School of Veterinary Medicine, 200 Westboro Road, North Grafton, MA 01536, USA
**Present address: Goddard Veterinary Group, 84 New Wanstead, London E11 2SY*

Recognition of diffuse changes in renal echogenicity relies partly on comparison of the kidney with an adjacent organ, which is assumed to be normal. The right kidney may be conveniently compared with the adjacent caudate lobe of the liver. It has been assumed that the echogenicity of the renal cortex in dogs and cats is normally hypo- or isoechoic compared with the liver, as is the case in most humans. We examined 34 healthy, 6–8-month-old female dogs using a real-time sector scanner. The right kidney and liver were imaged in a dorsal plane so that both were seen in a single sector image. The renal cortex was graded as hypo-, iso- or hyperechoic compared with adjacent liver by three observers reaching a consensus. Subjects were examined with both 5 MHz and 7.5 MHz transducers to note any effects frequency might have on relative echogenicity. Wedge and core biopsies obtained 2 days later confirmed that the tissues were normal. At 5 MHz 33 out of 34 dogs had a renal cortex hypo- or isoechoic compared with the liver. One dog had a hyperechoic renal cortex although it was histologically normal. When imaged at 7.5 MHz 26 out of 34 renal cortices were more echogenic than at 5 MHz, and 14 out of 34 were hyperechoic compared with the liver. Therefore, renal echogenicity met the previously accepted criterion for normal in 33 out of 34 cases (97%) when imaged at 5 MHz, but in only 20 out of 34 cases (59%) at 7.5 MHz. At both frequencies, hyperechoic normal kidneys were found. Although there does appear to be a relationship between renal echogenicity and certain kidney diseases, comparing the echogenicity of the kidney cortex with that of the liver is not likley to be a reliable method of diagnosing renal disease in dogs.

Proceedings of the BMUS meeting

Vascular ultrasound

Chairmen: D. H. Evans and H. B. Meire

Intravascular ultrasound with 3-D reconstruction: a new way to image vascular disease, by W. R. Lees, W. K. Chong, R. Lawrence and J. R. Gardener

Use of an intra-arterial Doppler ultrasound catheter in peripheral vessels: restrictions and results, by E. Berry, G. Hartnell and M. Halliwell

Intravascular ultrasound, by A. R. Essop, P. J. Scott, G. J. Williams and W. Ashab

Can colour flow Doppler be used to identify fetal renal obstruction?, by J. A. Bates and H. C. Irving

Intra-renal arterial Doppler flows in normal and obstructed native kidneys, by P. M. Rogers, J. Bates and H. C. Irving

Early detection of acute renal failure with duplex Doppler ultrasound in at-risk patients, by I. Mastorakou, D. Lindsell, R. Sheriff and J. Ledingham

Intravascular ultrasound with 3D reconstruction: a new way to image vascular disease

W. R. Lees, W. K. Chong, *R. Lawrence and †J. Gardener
*Departments of Radiology, *Surgery and †Medical Physics, The Middlesex Hospital and University College Hospital, London*

In recent years there have been major advances in the development of catheter-based ultrasound transducers. We have used a newly developed intravascular ultrasound system (IVUS) to evaluate plaque morphology and vascular cross-sectional area *in vitro* and *in vivo*. The device consists of a 20 MHz transducer mounted on the end of a mechanically rotated core, lying within a fluid filled 6.6 F polyethylene sheath (Diasonics/Boston Scientific Corporation). This generates a cross-sectional real-time image of the vessel wall and lumen. We have developed a workstation for multiplanar reformatting (MPR) and limited three-dimensional (3D) reconstruction. Studies were performed of normal and atheromatous cadaver iliac, carotid and superficial femoral arteries. Histological correlation was obtained. Images were obtained pre- and post-balloon and laser angioplasty. Angiographic and IVUS measurements of luminal cross-sectional area were compared. Ten *in vivo* studies were performed, two pre- and post-angioplasty. The device was inserted through a percutaneous sheath by the femoral route. IVUS identified the intima, media and adventitia and could differentiate muscular and elastic arteries. Fibrosis and calcification within a plaque were recognized and plaque thickness measured. Thrombus could be differentiated from plaque. Luminal size and shape could be measured accurately. IVUS and radiographic measurements of cross-sectional area correlated closely when the lumen was circular but differed when the lumen was eccentric. Plaque fissuring and dissection were detected following angioplasty *in vivo*. Unique 3D images of plaque morphology generated by MPR were shown. IVUS can characterize plaque, measure luminal size and shape accurately and identify complications of angioplasty. It has considerable promise as a complement to angiography and angioplasty. MPR techniques allow a much better assessment of plaque morphology than simple axial scans. Its potential was discussed.

Use of an intra-arterial Doppler ultrasound catheter in peripheral vessels: restrictions and results

E. Berry, *G. Hartnell and M. Halliwell
*Department of Medical Physics, Bristol General Hospital, Guinea Street, Bristol BS1 6SY and *Department of Radiodiagnosis, University of Bristol, Bristol Royal Infirmary, Bristol BS2 8HW*

Intra-arterial Doppler ultrasound has been used to study coronary artery flow patterns but there are no reports of its use in peripheral arteries. We have undertaken a study to determine whether intravascular Doppler ultrasound is a useful method for assessing the functional significance of arterial stenoses using flow indices, and for assessing the results of treatment by angioplasty or surgery. A 20 MHz transducer with pulse repetition frequency 62.5 KHz was mounted on a 4F catheter tapering to 3F at the tip (Millar Instruments Inc). The Doppler flow signal was analysed using a dedicated spectrum analyser (Dopstation, Scimed Ltd). Laboratory studies were performed using non-pulsatile flow in a phantom of circular cross-section, diameter 5 mm. Measurements were made with flow towards and away from (the more usual clinical situation) the transducer. With the catheter positioned centrally in the phantom, reduction in velocity around the tip of the catheter was apparent. At volume flow rates of approximately 400 ml/minute (equivalent to a peak velocity of 68 cm/second assuming a parabolic flow profile) towards the catheter, disturbance was noted up to 4 mm from the tip; the effect was greater with flow away from the catheter, with reduction up to 8 mm from the tip. Without a coaxial guidewire the catheter will position its tip against the vessel wall. In this location similar velocity reductions were noted around the tip as when centred, together with a loss of signal beyond 7 mm. Including consideration of the beam profile it was concluded that *in vivo* measurements were valid if made at the greatest range from which a reproducible signal was obtainable. Measurements taken before and after angioplasty from different groups of patients were presented.

Intravascular ultrasound

A. R. Essop, P. J. Scott, G. J. Williams and W. Ashab
Non-Invasive Cardiac Unit, Killingbeck Hospital, York Road, Leeds LS14 6UQ

Whilst angiography remains the "gold" standard in assessing vascular disease, recent advances in interventional techniques have overwhelmed conventional imaging methods. Intravascular ultrasound (IVUS) promises to be a powerful new tool to supply not only the requisite diagnostic data and operational feedback but also to provide invaluable data on the pathophysiology of cardiovascular disease and the impact of treatment upon it. Following *in vitro* studies of human and porcine material, we studied 17 patients undergoing varying combinations of coronary (2) or peripheral artery (15) procedures. This included: percutaneous laser/balloon angioplasty (TPA) (13), atherectomy (4), and endovascular stent implants (8). IVUS was performed with a rotating 20 MHz mechanical probe (Boston Scientific). IVUS gave excellent definition of endoprostheses and diseased *vs.* normal vessels in all cases. It distinguished between hard/calcific atheroma, soft/lipid atheroma, myointimal proliferation and fibrous hyperplasia in 15 out of 17 cases. On-line measurements allowed luminal cross-sectional area, diameter, circumference and percentage stenosis calculations. It also elucidated the immediate effect of various endovascular manipulations. TPA caused plaque rupture, splitting of intima and media and intimal flaps in nine out of 11 cases; wall disruption was greater compared with the four atherectomies. "On-line" data were invaluable in choosing the most appropriate mode of treatment, selecting balloon and stent size, and in assessing the therapeutic outcome, complications and extent of residual disease after intervention, which was not apparent on angiography or angioscopy. Limitations of the technique are that there is a longer learning curve with IVUS, in great measure due to the significantly larger amount of data provided. Other imaging techniques have some advantages such as colour, stereoscopic views and forward viewing with angioscopy, and familiarity and simplicity with angiography. On the converse, IVUS is a unique imaging tool which provides information not available with present imaging techniques. Current IVUS development in forward-viewing transducers, wire-guided probes and more flexible catheters should revolutionize its clinical applications.

Can colour flow Doppler be used to identify fetal renal obstruction?

J. A. Bates and H. C. Irving
Ultrasound Department, St James' University Hospital, Leeds

Dilatation of the renal collecting system is a common finding during routine ante-natal ultrasound examination and may indicate urinary obstruction, other urinary tract pathology, or may be a variant of normal developmental anatomy. Measurement of the degree of dilatation has been used to differentiate physiological renal dilatation from obstruction and to predict post-natal renal function. However, the generally accepted upper limit of 5 mm for the antero-posterior (AP) diameter of the renal pelvis has an unacceptably low specificity for the diagnosis of obstruction, and it is also apparent that the degree of dilatation correlates poorly with post-natal renal function. It has been reported that in both adults and children an elevation of intra-pelvicalyceal pressure due to an obstructive uropathy results in increased peripheral resistance within the renal vasculature. We have, therefore, investigated whether analysis of the fetal renal artery flow velocity waveform would aid in predicting the underlying nature and effect of fetal renal dilatation. Colour flow Doppler imaging was used to obtain fetal renal artery flow velocity waveforms in more than 100 normal fetuses and various gestational ages in order to build a database for the establishment of normal ranges for pulsatility index in the fetal renal artery throughout pregnancy. Twenty cases of fetal renal tract dilatation (greater than 5 mm AP diameter of the renal pelvis) have been assessed and although isolated measurements of pulsatility index do no appear to be significantly altered from the normal range, the investigation is continuing to determine whether serial measurements are of value.

Intra-renal arterial Doppler flows in normal and obstructed native kidneys

P. M. Rodgers, J. Bates and H. C. Irving
Ultrasound Department, St James' University Hospital, Leeds

A recent study in the American literature showed a correlation between renal obstruction and altered renal arterial Doppler flows with a suggestion that resistive indices (RI) greater than 70% may indicate obstruction. This study aimed to establish a normal range of resistive indices for renal arterial Doppler flows and to examine further the changes in acute renal obstruction. The authors recorded 270 individual arterial Doppler flows from both kidneys of 55 patients. These were in two groups. The first consisted of 35 patients attending for an abdominal ultrasound scan for non-renal indications. The second group were patients presenting with acute renal colic with evidence of obstruction on intravenous urography. Thirty-three patients had three or more recordings taken from each kidney to examine the reliability of individual recordings and differences between kidneys in the same patient. The normal group showed a wide range of RI values, suggesting that an individual threshold value distinguishing obstructed and non-obstructed kidneys may not be valid. A close correlation was, however, noted between the RI values obtained from each kidney in any individual patient in the normal group. But, in patients with developing renal obstruction, there is a marked difference in the RIs between the affected and the normal kidney and this difference appears to increase with the severity of that obstruction.

Early detection of acute renal failure with duplex Doppler ultrasound in at-risk patients

I. Mastorakou, D. Lindsell, *R. Sheriff and *J. Ledingham
*Radiology Department and *Nuffield Department of Clinical Medicine, John Radcliffe Hospital, Oxford*

Duplex Doppler ultrasound is widely used for the measurement of blood flow within various vessels. Direct measurement of renal blood flow has, however, proved difficult, especially when applied in everyday clinical practice. On the other hand, when indices such as pulsatility index (PuI) and Pourcelot index (PoI) are used, alterations in renal blood flow can be demonstrated. In order to assess changes in renal blood flow (RBF) in patients at risk of acute renal failure (ARF), two groups of patients were studied. These were patients undergoing cardiovascular surgery (Group I) and patients undergoing surgery for abdominal aortic aneurysm repair (Group II). The peak systolic, end diastolic and mean velocities were measured from the waveform of an interlobar artery and PoI and PuI were then calculated. At least three examinations were carried out in each patient: one pre-operatively, one immediately post-operatively and one 24 hours after the operation. In Group I, 16 patients with a mean age of 56.4 years were studied. None of these developed ARF. A significant reduction in both indices during the immediate post-operative period was demonstrated, with the mean values being PoI1 = 0.719, PoI2 = 0.658, PoI3 = 0.667 and PuI1 = 1.54, PuI2 = 1.39, PuI3 = 1.42. In Group II, 13 patients with a mean age of 70.3 years were studied. Four of them developed ARF. In those nine who did not develop ARF, the mean values were PoI1 = 0.66, PoI2 = 0.62, PoI3 = 0.68 and PuI1 = 1.38, PuI2 = 1.28, PuI3 = 1.47. In the four patients with ARF, the mean values were PoI1 = 0.74, PoI2 = 0.68, PoI3 = 0.83 and PuI1 = 1.86, PuI2 = 1.48, PuI3 = 2.30, being well above the mean values of those who did not develop ARF. This was an indication of increased vascular resistance, predicting the onset of ARF well before any other clinical indices. The reduction in indices, which indicates a lowering of resistance in the renal vessels, is thought to be due to treatment given during and immediately after the operation in order to prevent ARF. The method proved to be sensitive in detecting these changes and also in predicting the onset of ARF before any other indices become abnormal. Early prediction of ARF may allow post-operative intervention to modify the severity of subsequent renal dysfunction.

Gynaecology

Chairmen: J. K. Watters and J. O. Drife

Transvaginal colour Doppler assessment of pelvic vessels in normal menstrual cycles, by S. Krishnamurthy, A. D. Cameron, F. Fairlie, J. R. MacKenzie, R. Yates and J. J. Walker
The use of transvaginal colour flow imaging to assess blood flow within the human pre-ovulatory follicle and corpus luteum, by T. H. Bourne, D. Jurkovic, J. Waterstone, S. Campbell and W. P. Collins
Transvaginal ultrasonography with colour flow imaging to monitor hormone replacement therapy in post-menopausal women, by T. H. Bourne, T. Hillard, M. Whitehead, S. Campbell and W. P. Collins
Monitoring of ovulation induction by ultrasound alone in women with polycystic ovary syndrome on low-dose gonadotrophin therapy, by D. S. Kiddy, D. Hamilton-Fairley, H. Watson, T. Rae and S. Franks
Transvaginal-ultrasound-directed follicle aspiration: how universally applicable is the technique? A review of 550 patients, by J. J. Waterstone and J. H. Parsons
Transvaginal-ultrasound-directed follicle aspiration: its acceptability and complication rate. A review of 2500 procedures, by S. J. Bennet, J. J. Waterstone, D. Abayomi, W. C. Cheng, and J. H. Parsons

Transvaginal colour Doppler assessmment of pelvic vessels in normal menstrual cycles

S. Krishnamurthy, A. D. Cameron, F. Fairlie, J. R. MacKenzie, R. Yates and J. J. Walker
Department of Obstetrics and Gynaecology, Glasgow Royal Maternity Hospital, Glasgow

Haemodynamic changes of the uterine and ovarian arteries were serially assessed in seven women with normal menstrual cycles using a high-frequency transvaginal colour Doppler system. A 7.5 MHz transvaginal phased-array transducer with Doppler (Acuson 128) was used to visualize both uterine arteries and the ovarian arterial tree within the ovarian substance. Patients were examined on every second or third day from the third post-menstrual day until they commenced their subsequent menstrual period. The pulsatility and resistance indices (PI, RI) were measured in both vessels. The changes in haemodynamics of the ovulating ovary and the quiescent ovary were compared by analysing the differences in PI and RI of the ovarian artery. Also, the PI and RI of the uterine artery on the ovulatory side and on the opposite side were compared. The PI and RI of the ovulating ovary were 0.8 and 0.52, respectively. In comparison, the non-ovulating ovary showed statistically significant different indices. These results were suggestive of a high impedance to blood flow ($PI = 1.7$, $RI = 0.73$). These results form a baseline providing normal data which will be useful when investigating abnormal pelvic blood flow. Similar studies are currently being performed in cases of recurrent miscarriage, unexplained infertility and ovulation induction procedures.

The use of transvaginal colour flow imaging to assess blood flow within the human pre-ovulatory follicle and corpus luteum

T. Bourne, D. Jurkovic, J. Waterstone, S. Campbell and W. P. Collins
Department of Obstetrics and Gynaecology, King's College School of Medicine and Dentistry, London SE5 8RX

Transvaginal ultrasonography with colour flow imaging is being used to study changes in the morphology and blood flow of the pre-ovulatory follicle and corpus luteum. Associated aspects of uterine morphology and blood flow are also being recorded. To date four subjects have been studied in detail. At least 12 scans were performed over 96 hours and peripheral blood was taken immediately after each examination for the analyses of reproductive hormones. Blood flow velocity waveforms were clearly recorded within the follicle around the time of the oestradiol peak and LH surge in peripheral plasma. Blood vessels became visible (*i.e.* the velocity was > 7 cm/s) around the time of the LH and FSH peaks and the first rise in plasma progesterone. Values for the pulsatility index and resistance index did not change significantly over the peri-ovulatory period. The peak shift velocity, however, increased during the ovarian cycle to reach a maximum value around the time of ovulation. Blood flow impedance in the uterine arteries suggested the presence of a circadian rhythm, but no pronounced changes were observed over the peri-ovulatory period. In contrast, flow velocity waveforms were clearly visible in the endometrium around the time of ovulation. These preliminary data suggest that intra-follicular and endometrial angiogenesis and blood flow may be critical processes that might be used to predict ovulation, and could possibly be modified to help achieve or avoid a pregnancy.

Transvaginal ultrasonography with colour flow imaging to monitor hormone replacement therapy in post-menopausal women

T. Bourne, T. Hillard, M. Whitehead, S. Campbell and W. P. Collins
Department of Obstetrics and Gynaecology, King's College School of Medicine and Dentistry, London SE5 8RX

There is good evidence to suggest that oral oestrogens reduce the risk of arterial disease in post-menopausal women. The mechanism of this action, however, has not been elucidated. The extent to which progestagens may reverse the protective effect is also unknown. We have used transvaginal colour flow imaging to assess aspects of blood flow in the uterine arteries of post-menopausal women receiving hormone replacement therapy (HRT). The aim of the study was to assess whether defined changes in blood flow could be used as indices of the vascular response to HRT. Blood flow impedance and peak shift velocity were determined in 12 previously untreated post-menopausal women receiving transdermal oestradiol and sequential doses of norethisterone acetate or medroxyprogesterone acetate. Measurements were taken pre-treatment and subsequently in the estrogen and progestogen phases of the 1st, 2nd, 6th, 7th and 10th treatment cycles. An increment dose of oestradiol was given during the 11th treatment cycle. Peripheral blood was taken at all visits for the measurement of plasma oestradiol, oestrone, progesterone, FSH and sex hormone binding globulin. Oestradiol reduced the mean value for the pulsatility index by about 50% and the effect was partially reversed by the addition of a progestagen. The time course of these changes and their relationship to the concentration of circulating hormones were presented and discussed. These data provide direct evidence for a non-lipid mediated mechanism whereby estrogens affect arterial status in postmenopausal women.

Monitoring of ovulation induction by ultrasound alone in women with polycystic ovary syndrome on low-dose gonadotrophin therapy

D. S. Kiddy, D. Hamilton-Fairley, H. Watson, T. Rae and S. Franks
Department of Obstetrics and Gynaecology, St Mary's Hospital Medical School, London W2 1PG

Ultrasound has been used for several years to monitor follicular development in women undergoing ovulation induction with gonadotrophins. Management of the patients has, however, usually been based on serial serum oestradiol levels. Gonadotrophin therapy is associated with a high incidence of multiple follicular cycles with a consequent risk of multiple pregnancy and ovarian hyperstimulation syndrome. We therefore adopted a low-dose gonadotrophin regimen starting each cycle at a daily dose of between 0.5 and 1 ampoule. One hundred women with clomiphene resistant polycystic ovary syndrome (PCOS) have received 401 cycles. Monitoring was by ultrasound alone. The women were scanned twice a week on average during the follicular phase and once during the luteal phase. On each occasion the uterine cross-sectional area, endometrial thickness and diameter of any follicle(s) in three dimensions were measured. HCG (5000U) was given to release the dominant follicle(s) when the follicular diameter was 18 mm. A serum progesterone level of 30 nmol/l taken 7 days after HCG was considered ovulatory. Ninety-five women ovulated at least once; 74% of the cycles were ovulatory and in the majority of these (74%) a single dominant follicle developed. The cumulative conception rate was 54% at 6 months with only two multiple pregnancies. The complication rate was low with 5% of cycles abandoned because of the presence of three or more follicles and no cases of severe hyperstimulation. In summary, low-dose gonadotrophin therapy is safe and effective and can be successfully monitored by ultrasound alone.

Transvaginal-ultrasound-directed follicle aspiration: how universally applicable is the technique? A review of 550 patients

J. J. Waterstone and J. H. Parsons
Assisted Conception Unit, King's College Hospital, Denmark Hill, London SE5 8RX

Eggs for *in vitro* fertilization were initially collected laparoscopically. "Inaccessible ovaries" then referred to ovaries buried beneath pelvic adhesions and ovariolysis operations were actually performed to render such ovaries accessible for laparoscopic egg collection. The advent of ultrasound-directed follicle aspiration, particularly by the transvaginal route, has changed all this. Pelvic adhesions have become irrelevant and may actually make the procedure easier by immobilizing the ovaries. In units where transvaginal-ultrasound-directed follicle aspiration (TV UDFA) is performed whenever possible, "inaccessible" now refers to ovaries either hidden behind the uterus or situated high up in the pelvis. Such ovaries may have to be aspirated by a route other than the transvaginal one. How common are vaginally inaccessible ovaries? Since January 1988, all egg collection procedures at King's College Hospital have been performed by TV UDFA wherever possible. Transabdominal and perurethral UDFA have been reserved for inaccessible ovaries. Laparoscopic egg collection has been avoided if at all possible. The records of 550 patients having their first egg collection procedure on or after 1 January 1989 were reviewed. Seven out of 550 patients (1.3%) had follicle aspiration performed by a route other than transvaginal. The characteristics of these patients and the results achieved were presented.

Transvaginal-ultrasound-directed follicle aspiration: its acceptability and complication rate. A review of 2500 procedures

S. J. Bennett, J. J. Waterstone, D. Abayomi, W. C. Cheng and J. H. Parsons
Assisted Conception Unit, King's College Hospital, Denmark Hill, London SE5 8RX and Thomson Fertility Clinic, Thomson Road, Singapore

The introduction of transvaginal egg collection using a vaginal ultrasound probe and needle guide has greatly simplified assisted conception treatment protocols. The technique is easy to learn and can be performed without general anaesthesia on an outpatient basis. On theoretical grounds, a significant incidence of bleeding and infection might be expected to complicate the technique. The first 2500 transvaginal-ultrasound-directed follicle aspiration (TV UDFA) procedures performed at King's College Hospital Assisted Conception Unit and at Thomson Fertility Clinic, Singapore, were reviewed. Although the incidence of minor vaginal haemorrhage is considerable (5–10%), it invariably ceases on application of local pressure. The incidence of major haemorrhage is very low: there were no pelvic haematomata and only one major haemoperitoneum. Severe pelvic infection is rare (< 3 per thousand) and appears related to previous pelvic sepsis.

Echocardiography

Chairmen: J. Gibbs and G. J. Williams

Atrial thrombus and prosthetic mitral valves: what are we missing?, by P. J. Scott, A. R. Essop, G. A. Wharton and G. J. Williams
Clinical and technical evaluation of six cardiac ultrasound machines and consideration of the parameters and methods used, by A. Houston, P. D. Clark, M. Davison, I. Ford, J. Gnanapragasam, D. Northridge, S. Pringle, J. Rodger and I. Simpson
Intraluminal real-time cross-sectional ultrasound imaging of normal and diseased pulmonary arteries in humans, by P. J. Scott, A. R. Essop, W. Ashab, G. J. Williams and N. Wilson
Is colour Doppler really necessary for the assessment of congenital heart disease?, by J. Gnanapragasam, A. Houston, R. Fraser, S. Lilley, E. Murtagh and G. Olaffson
Cardiac output in the premature neonate: the influence of ductus arteriosus, by J. R. Skinner, S. Hunter and E. N. Hey
Screening for congenital heart disease prenatally, by G. K. Sharland and L. D. Allan

Atrial thrombus and prosthetic mitral valves: what are we missing?

P. J. Scott, A. R. Essop, G. A. Wharton and G. J. Williams
Non-Invasive Cardiac Unit, Killingbeck Hospital, York Road, Leeds LS14 6UQ

Sixty-eight consecutive patients with mitral valve replacements referred for cardiac ultrasound underwent both transthoracic and transoesophageal echocardiography (TTE and TOE, respectively). Forty-three patients were female and 25 male, age range 11–78 (mean 56) years. Thirty-five patients had biological valve replacements and 33 mechanical prostheses. Fourteen of the subjects were specifically studied following a recent (within the previous 30 days) suspected embolic event (stroke = seven patients, transient ischaemic attack = six patients and peripheral arterial occlusion = one patient). TTE was performed with a 2.25 MHz transducer and images were recorded onto videotape for later analysis. All TOE studies were performed immediately after the TTE by an experienced clinician, using a 5 MHz transducer mounted on a modified gastroscope. The TOE operator had no knowledge of the prior TTE examination. All patients gave written consent to the procedure, which was carried out under light intravenous sedation and no complications occurred. TTE failed to demonstrate left atrial clot in any of the 68 patients. In contrast, TOE detected thrombus in 10 (15%) of the 68 and was most commonly seen in patients who had suffered a recent suspected embolic event; seven out of 14 (50%) had atrial clot compared with three out of 54 (6%) of those patients studied for other clinical reasons. Thrombus was extensive within the left atrium in three cases, located on the valve apparatus in two, in the left atrial appendage region in four and in the roof of the atrium in one. Clot was more common in patients with biological valves (eight out of 35) than mechanical (two out of 33). All patients with mechanical valves were anticoagulated compared with 15 out of 35 of those with biological valves. Of the patients with biological valves and atrial thrombus, three out of eight were anticoagulated. TOE provides unique views of the left atrium and is far superior to TTE for the detection of left atrial thrombus in patients with mitral valve replacements. TOE is therefore recommended for patients with mitral prostheses who suffer a suspected systemic embolus, as a significant number (50% in our series) will have clot.

Clinical and technical evaluation of six cardiac ultrasound machines and consideration of the parameters and methods used

A. Houston, P. Clark, M. Davison, I. Ford, J. Gnanapragasam, D. Northridge, S. Pringle, J. Rodger and I. Simpson

Summary of Report for the Ultrasound Equipment Evaluation Project of the Scottish Home and Health Department

The clinical and technical performance for imaging spectral and colour Doppler for adult cardiology have been compared in the following: Acuson 128, Aloka SSD 870, ATL Ultramark 9, Hewlett Packard Sonos 1000, Toshiba SSH 160 and Vingmed CFM 750. Nine patients were studied and the videotape images were subsequently evaluated and scored by a panel of six clinicians. There were seven sources of effects on the clinical scores: observer, equipment, patient, observer/equipment interaction, observer/patient interaction, equipment/patient interaction and random error. The size and significance of these effects varied for imaging, spectral and colour Doppler. The perceived differences between machines were as follows: barely detectable but small for M-mode and spectral diastolic inflow; detectable but relatively small for two-dimensional imaging and colour inflow; detectable and of possible clinical significance for spectral and colour regurgitation. A comparison of technical and clinical assessments showed that physical indicators could be predictive of clinical value. We conclude that it is possible to distinguish the clinical and technical capabilities of individual machines and thus provide a quantitative assessment of their individual capabilities.

Intraluminal, real-time, cross-sectional ultrasound imaging of normal and diseased pulmonary arteries in humans

P. J. Scott, A. R. Essop, W. Ashab, G. J. Williams and N. W. Wilson
Non-Invasive Heart Unit, Killingbeck Hospital, York Road, Leeds LS14 6UQ

Intravascular ultrasound is the latest of imaging techniques and allows direct and accurate visualization of vessel wall morphology. Real-time, cross-sectional images of the main pulmonary artery and its branches were obtained using a 20 MHz transducer mounted on a 100 cm long, 2 mm diameter guiding catheter in five patients undergoing routine, diagnostic right and left heart catheterization. Two patients, aged 47 and 52 years, had normal pulmonary artery pressures and their ultrasound examination revealed normal pulmonary arterial cross-sectional morphology. Normal morphological appearances were also observed in a patient, aged 8 years, with moderate pulmonary hypertension (mean PA pressure 60% of systemic) due to an atrial septal defect. Thickening of the medial layer and areas of intravascular, mural thrombus were seen in a patient, aged 7 years, with more severe pulmonary hypertension (mean pressure 80% systemic), secondary to multiple pulmonary emboli. In the final patient, aged 32 years, with systemic level pulmonary hypertension due to ventricular septal defect, medial thickening and early intimal proliferation were demonstrated. Intraluminal, two-dimensional cross-sectional ultrasound imaging of the pulmonary arteries revealed unique information about arterial ultrastructure which is unavailable by any other means. It can differentiate normal from abnormal vessel wall morphology in patients with pulmonary hypertension and may thus become an important investigation in the assessment of patients with pulmonary vascular disease.

Is colour Doppler really necessary for the assessment of congenital heart disease?

J. Gnanapragasam, A. Houston, R. Fraser, S. Lilley, E. Murtagh and G. Olaffson
Royal Hospital for Sick Children, Yorkhill, Glasgow G3 8SJ

We evaluated the additional information provided by colour Doppler in the ultrasound assessment of congenital heart disease by a prospective study of 190 children (age range 1 day–15 years) with clinical signs of heart disease. The cardiac ultrasound study was performed in three stages: first by cross-sectional echocardiography and basic stand alone Doppler, then by duplex Doppler and finally by colour Doppler. Seventy-three patients had ventricular septal defect (VSD) (excluding those with complex heart disease). The site of the defects could be identified only by using colour Doppler in five out of 48 patients with a single isolated VSD, in five out of 21 patients with a VSD associated with other abormalities and in three out of four patients with multiple VSDs. Colour Doppler was essential to make the diagnosis of anomalous origin of the left coronary artery from the pulmonary trunk (1), partial anomalous venous drainage (1) and mitral regurgitation misdiagnosed as VSD (1). Colour Doppler provided additional information in the following situations: assessment of valve regurgitation in atrioventricular septal defects (12); assessment of mixing through a patent foramen ovale in transposition (10); confirmation of the diagnosis of pulmonary valve atresia (7) and differentiating it from critical pulmonary stenosis (1); confirmation of unrestrictive VSD flow to outlet chamber (2); establishment of the site of coarctation of the aorta (4/14); and confirmation of unobstructed flow across a right atrial membrane (1). We concluded that although a diagnosis can be made by imaging and spectral Doppler in most cases of congenital heart disease, colour Doppler should be routinely used if an important diagnosis is not to be missed.

Cardiac output in the premature neonate: the influence of the ductus arteriosus

J. R. Skinner, S. Hunter and E. N. Hey
Department of Child Health, University of Newcastle Upon Tyne

Serial echocardiograms with Doppler were obtained from 30 premature neonates with hyaline membrane disease (HMD) before, during and after ductal closure. Closure was spontaneous in 20 (Group 1), and induced by indomethacin for symptomatic left to right (L–R) shunt in 10 (Group 2). Ductal size was assessed using cross-sectional echocardiography with pulsed-wave Doppler. Left atrial to aortic root (LA : AO) ratio, measured on M-mode, was taken as a measure of L–R shunt. In assessing cardiac output, aortic stroke distance (SD), analogous to stroke volume, was measured by continuous-wave Doppler from the suprasternal notch. Systolic upper limb blood pressure (BP) was recorded by arterial line or Doppler sphygmomanometry.

	Group 1 (spontaneous)		Group 2 (induced)	
	Patent	Closed	Patent	Closed
Stroke distance (m)	13.3 ± 3.0	9.8 ± 1.7**	14.8 ± 2.3	9.5 ± 1.8**
Heart rate	148 ± 11	149 ± 10 (NS)	161 ± 13	154 ± 14 (NS)
LA : AO ratio	1.32 ± 0.27	1.03 ± 0.19*	1.70 ± 0.26	1.11 ± 0.19**
BP (mmHg)	51 ± 6	62 ± 10*	51 ± 7	65 ± 11*

(*$p < 0.01$, **$p < 0.001$, paired-t tests; NS = not significant).

The fall in SD correlated with a fall in LA : AO ratio ($r = 0.61$). In two babies indomethacin failed, and SD, heart rate, BP and LA : AO ratio did not change. It was concluded that cardiac output rises in association with L–R ductal shunting in the premature neonate with HMD. This is achieved primarily by an increase in stroke volume and *not* heart rate. Ductal closure, whether spontaneous or induced, and accompanying cessation of L–R shunting, is associated with a fall in stroke volume and a rise in systemic BP.

Screening for congenital heart disease prenatally

G. K. Sharland and L. D. Allan
Department of Perinatal Cardiology, Guy's Hospital, London

Pregnancies at increased risk for congenital heart disease in the fetus are frequently referred for fetal echocardiography. However, the majority of cases of fetal structural cardiac malformation do not occur in "high-risk" pregnancies and may therefore not be referred for a specialized scan. Many of these, however, could be detected by examining the four-chamber view of the fetal heart during the routine obstetric scan. Approximately five cases of severe heart disease should be detected per 1000 pregnancies using this view only. In 1988 and 1989, 225 cases of structural cardiac malformation were diagnosed in our unit. Of these 185 (82%) were referred as an abnormality of the four-chamber view of the fetal heart had been detected on routine scanning. Over the past 2 years a four-chamber view screening study has been started in 10 selected units in the South East Thames Region. It was predicted that 63 abnormalities should have been detected during the study period. Forty-three cases of congenital heart disease were actually detected by screening plus a further six referred for other reasons. There were 12 abnormalities known to be missed that were thought to be detectable on a four-chamber view. Most of the abnormalities that were missed were in the earlier part of the study for each unit. Common reasons for not achieving an adequate four-chamber view included maternal obesity, fetal lie and a gestational age of less than 18 weeks. The other important factor was the quality of equipment used. Our results showed that the four-chamber view could be an effective screening method for detecting major cardiac defects prenatally, although there are important limiting factors that have to be taken into account.

Obstetrics

Chairmen: H. C. Irving and M. B. McNay

Vaginal ultrasound and early confirmation of fetal anatomy: the way forward?, by P. Johnson, G. K. Sharland, S. Chita, L. Allan and D. Maxwell
Is a short femur length a useful marker for Down's syndrome?, by P. Twining, D. R. Whalley, E. Lewin and K. Fowkes
Clinical practices in fetal biometry, by V. Aitken and A. Lando
Prognosis in diaphragmatic hernia, by S. Lockhart, L. D. Allan, G. K. Sharland and A. Heward
Ultrasonic measurement of fetal chest circumference to predict pulmonary hypoplasia in at-risk pregnancies, by A. D. Cameron, S. Krishnamurthy and J. J. Walker
Second-trimester oligohydramnios, the combined approach: transvaginal and transabdominal colour flow Doppler, by P. Twining
Continuous Doppler ultrasound of the umbilical artery used to assess the fetoplacental circulatory effects of two intravenous anaesthetic agents: a preliminary study, by M. Iftikhar, D. A. Orr, R. B. Beattie, K. M. Bill, J. Dornan, W. Thompson and J. Moore
Asymptomatic placenta praevia diagnosed by ultrasound: a prospective view of obstetric management, by K. Neales, N. Morgan and M. Downes
A quantitative and qualitative comparison of transabdominal and transvaginal ultrasound images of low placentae, by W. G. Taylor

Vaginal ultrasound and early confirmation of fetal anatomy: the way forward?

P. Johnson, G. K. Sharland, S. Chita, L. Allan and D. Maxwell
Departments of Fetal Medicine and Perinatal Cardiology, Guy's Hospital, London SE1 9RT

The advent of vaginal ultrasound transducers has enabled us to inspect the anatomy of the first trimester fetus in greater detail. Interest so far has concentrated on the early detection of structural abnormality. We have started a screening programme in a low-risk population to assess what fetal anatomy, including cardiac anatomy, can be reliably examined using the vaginal probe between 8 and 15 weeks gestation. Patients are recruited at their booking visit to the ante-natal clinic and the nature of the examination explained. Patients scanned before 10 weeks have a repeat scan 3 or 4 weeks later. A 5 MHz vaginal probe is used with an Acuson 128 ultrasound system. Anatomy seen is recorded and all scans are videotaped and reviewed by a second examiner independently. Only anatomy seen by both examiners is recorded. In our first 150 patients, gestation varied between 7+6 and 15+3 weeks, with six non-viable pregnancies being detected. All patients had a routine scan at 18 weeks and the vaginal findings are correlated with this result.

Gestation (weeks)	10	10–12	12–14	14
Patients	19	34	65	26
Four-chamber	—	13 (37)	44 (68)	21 (81)
Head	—	13 (37)	43 (66)	16 (62)
Spine	—	5 (15)	28 (43)	8 (31)
Stomach	2 (10)	19 (56)	62 (95)	24 (92)
Kidneys	—	5 (15)	38 (58)	14 (54)
Bladder	3 (16)	14 (42)	52 (80)	23 (88)

(Percentages in parentheses.)

Between 8 and 15 weeks, vaginal scanning does not reliably detect fetal anatomy in all cases. However, between 12 and 15 weeks clear views are obtained in the majority of patients. While this method does not, at present, replace anomaly scanning at 18–20 weeks, it may be of value in the early detection of anomaly in high-risk pregnancies.

Is a short femur length a useful marker for Down's syndrome?

P. Twining, D. R. Whalley, E. Lewin and K. Fowkes
Departments of Radiology and Medical Physics, Queen's Medical Centre, University Hospital, Nottingham NG7 2UH

In order to assess the significance of a short femur length measurement in the ante-natal diagnosis of Down's syndrome, a retrospective analysis was made of all Down's syndrome fetuses diagnosed either by amniocentesis or post-natal karyotyping. Over a three-year period 21 fetuses were identified. The ante-natal scans were reviewed and eight fetuses were found to have had biparietal diameter and femur length measurements taken between 17 and 22 weeks gestation. Normal graphs were plotted for femur length to gestational age, femur length to biparietal diameter and biparietal diameter/femur length to gestational age. The normal range was calculated as mean, plus or minus two standard deviations. One fetus had a femur length measurement outside the normal range on the femur length to gestational age and femur length to biparietal diameter graphs. Two fetuses had a significantly raised biparietal diameter/femur length ratio. These four abnormal measurements, however, represented two fetuses both of which had other abnormalities on the antenatal scan: one cystic hygroma and one duodenal atresia. We do not feel, therefore, that the femur length measurement is useful in the antenatal diagnosis of Down's syndrome.

Clinical practices in fetal biometry

V. Aitken and A. Lando
Islington and Hampstead School of Radiography, 61 Belsize Avenue, London NW3 4BN

This paper described the preliminary findings of a study being undertaken to look at work practices in fetal biometry. Earlier this year, the examiners in the Practical Applications paper of the Diploma in Medical Ultrasound reported that many candidates had difficulty plotting correctly fetal ultrasound measurements. The examiners queried where the fault for this problem lay. As a result, a study is being carried out to see where the problems are and why they are occurring. It is posed that there are three main possible problem areas: the graphs used, the plotting of the measurements on to the graphs, and the interpretation of the graphically represented data. The study began by asking 23 centres to submit their departmental graphs, and a comparison was made between them. This small sample of departments produced a wide variety of graphs differing both in format and data on which they were based: 11 for head circumference, 12 for biparietal diameter, and 14 for abdominal circumference (AC). Mean numerical values were plotted for a selection of different gestational ages for each of the variables. There was found to be a diversity of readings of such magnitude that they would be of major clinical significance, *e.g.* from a minimum of 3.5 mm for the BPD at 30 weeks to a maximum of 80 mm for AC at 34 weeks. Although the excellent work carried out by BMUS produced a "British Gold Standard" for fetal biometry, it is disappointing to find that this work is not being used. Furthermore, the implications from these preliminary findings are of major concern and it is felt that an effort must be made by all working in ultrasound to address this problem.

Prognosis in diaphragmatic hernia

A. Lockhart, L. D. Allan, G. K. Sharland and A. Heward
Department of Perinatal Cardiology, Guy's Hospital, London SE1 9RT

In a recent report of prenatally diagnosed diaphragmatic hernia, there were no survivors, despite the availability of ECMO, in 14 cases seen before 25 weeks gestation, suggesting that early diagnosis is an important factor influencing the outcome. This experience of the natural history has been used to justify prenatal operative techniques involving hysterotomy. As the resource implications of either ECMO or prenatal operation is very great, it is important to reassess the outcome in this condition. Of 40 cases seen in our department over the last 10 years, there was an overall mortality of 78%, or 72% if the eight cases where termination of pregnancy took place are excluded. There was a mortality of 91% in the cases presenting prior to 25 weeks compared with a mortality of 60% in those seen after this gestation, or 56% if those fetuses with other defects are excluded. We confirmed the previously reported usefulness of left heart compression as an indicator of a poor outcome. In our series, there were no fetuses with a chromosomal anomaly compared with 16% in the series of Adzick. There were four fetuses out of 40 with major congenital heart disease and one with other defects. We were unable to confirm the predictive nature of hydramnios suggested by Adzick et al. In summary, although diagnosis before 25 weeks gestation in this condition is associated with a poorer survival rate than those detected later, it is not universally fatal. If congenital heart disease and chromosomal anomalies are excluded in an individual case, and there is little or no evidence of left heart hypoplasia, the odds will improve and a 50/50 chance of survival would be reasonable to offer. Further observation of this condition and closer attention to the postnatal perioperative management and the influence of this on outcome should take place before comtemplating prenatal therapy.

Ultrasonic measurement of fetal chest circumference to predict pulmonary hypoplasia in at-risk pregnancies

A. D. Cameron, S. Krishnamurthy and J. J. Walker
Department of Obstetrics and Gynaecology, Glasgow Royal Maternity Hospital, Glasgow

Adequate fetal lung growth depends on various factors: adequate intrathoracic space, adequate liquor volume and fetal breathing movements. Fetal pulmonary hypoplasia (PH) is commonly associated with chronic amniotic fluid leakage and fetal renal disease. The extent of the condition depends on the severity of oligohydramnios, its duration and perhaps most importantly, the gestational age and stage of lung development when oligohydramnios occurred. The condition is almost uniformly fatal and therefore if it could be predicted antenatally, adequate counselling of the mother and appropriate management can take place. Methods of predicting PH have included chest circumference (CC) measurements, chest/abdomen ratios, fetal breathing and intrauterine manometry. The aim of this study was to investigate the application of ultrasound CC measurements in the prediction of PH. The fetal CC was measured at the level of the four-chamber view and plotted on a normogram. The last CC prior to delivery was used and the clinical outcome was noted. Fifteen patients who were felt to be at risk of developing fetal pulmonary hypoplasia had CC measured. The clinical problems were those of premature rupture of membranes (PROM) ($n = 10$), oligohydramnios ($n = 3$) and renal abnormalities ($n = 2$). Four infants had pulmonary hypoplasia, with three of these having CC < 5th centile. There was one false positive but the infant did have significant respiratory pathology. In this preliminary report, it was concluded that ultrasound CC measurement to predict fetal pulmonary hypoplasia is a worthwhile procedure. Further studies and a larger series are required before it is introduced into clinical practice.

Second-trimester oligohydramnios, the combined approach: transvaginal and transabdominal colour flow Doppler

P. Twining
Department of Radiology, University Hospital, Queen's Medical Centre, Nottingham NG7 2UH

The main problem in second-trimester oligohydramnios is to differentiate Potters syndrome from premature rupture of membranes and early growth retardation. In order to improve the diagnostic accuracy, patients with severe oligohydramnios were assessed using colour flow Doppler via the transabdominal and transvaginal route. Over a 9-month period six fetuses with severe oligohydramnios were scanned between 16 and 19 weeks gestation. All fetuses were followed-up and, where appropriate, pathological specimens examined to obtain a definitive diagnosis. In two patients transvaginal scanning revealed renal pathology which was equivocal using the transabdominal technique. One fetus showed bilateral cystic dysplastic kidneys, and the second a solitary multicystic kidney. One other patient showed normal kidneys. In three patients colour flow Doppler revealed absent renal artery flow; this was confirmed pathologically in two cases, the third showing normal kidneys. All fetuses demonstrated normal umbilical artery Doppler. The improvement in resolution using the transvaginal probe makes the demonstration of renal pathology considerably more accurate. The addition of colour flow demonstrates absence of renal artery flow in cases of renal agenesis, and aids in the localization of the umbilical artery for

Doppler measurements. In second-trimester oligohydramnios the combination of transabdominal and transvaginal scanning with colour flow mapping establishes renal pathology with greater certainty than transabdominal scanning alone.

Continuous Doppler ultrasound of the umbilical artery used to assess the fetoplacental circulatory effects of two intravenous anaesthetic agents: a preliminary study

M. Iftikhar, D. A. Orr, R. B. Beattie, K. M. Bill, J. Dornan, W. Thompson and J. Moore
Department of Obstetrics & Anaesthetics, Jubilee Maternity Hospital, Belfast BT9 7AB and Queen's University of Belfast

Thiopentone has long been the agent of choice for the induction of anaesthesia for Caesarean section. Propofol would appear to have theoretical benefits (such as rapid clean-headed awakening and reduced incidence of nausea or vomiting) although experience in obstetrics is limited. Propofol is thought to have a greater hypotensive effect than thiopentone. In this study the effects of these two induction agents on umbilical artery waveform were studied. After random allocation, five patients received thiopentone ($4\,\mathrm{mg\,kg^{-1}}$) and another five propofol ($2\,\mathrm{mg\,kg^{-1}}$). Umbilical artery velocity waveform as produced by a Doptek 9000 was recorded continuously onto the sound channels of a stereo VHS videorecorder. A Sony video 8 camera filmed maternal haemodynamic parameters from anaesthetic monitors and this information was recorded on the picture channel of a videorecorder. After recording baseline values for at least 5 minutes, the selected induction agent was given followed by a 2-minute period when no other drugs were given, *i.e.* any changes observed during this period must be due to the induction agent. Intubation was facilitated with suxamethonium and anaesthesia maintained with isoflurane and nitrous oxide. Doppler recordings were stopped after intubation when the surgeon started to prepare the abdomen. At delivery, cord blood gases, pH and apgar scores were checked. Maternal blood sampling for catecholamines was performed at five comparable times in all patients. Off-line spectral analysis of umbilical artery velocity waveform included determination of fetal heart rate, pulsatility index, resistance index and S/D ratio. There was no change in any of these parameters, either with respect to time or between groups. At induction there was a small rise in systolic BP after thiopentone and a small fall after propofol; diastolic pressure fell slightly in both groups, but there was no statistically significant difference between the groups, although post-intubation hypertension and tachycardia was more common in the thiopentone group. Babies exposed to propofol scored as highly on post-delivery testing as did babies exposed to thiopentone. We did not demonstrate any deleterious effects on umbilical artery velocity waveform as a result of using propofol. We can recommend this method of stimultaneous recording of Doppler signal and maternal variables for use in future studies.

Asymptomatic placenta praevia diagnosed by ultrasound: a prospective view of obstetric management

K. Neales, N. Morgan and M. Downes
Kent and Canterbury Hospital, Ethelbert Rd, Canterbury, Kent

Routine obstetric ultrasound is increasingly used in the third trimester to assess fetal growth. This has led to a rise in the number of cases of placenta praevia diagnosed ante-natally. These would otherwise have been undetected unless symptoms arose. The management of these patients and specific advice that should be given remains controversial. The traditional teaching of observation in hospital until delivery was based on patients who were symptomatic and would appear to be unduly conservative. Fifty consecutive patients with a low-lying placenta at 32 weeks were enrolled in this prospective study, which was instituted following a well publicized case at the hospital, and carried out over a 10-month period. The total number of eligible patients was 1786, of which 108 (6.1%) had low-lying placenta at 18 weeks. The placenta was within 5 cm of os at 32 weeks in 50 (2.8%) patients. The patients were admitted and followed with fortnightly ultrasound examinations throughout the remainder of pregnancy, or until the placenta was greater than 5 cm from the os. The results were analysed in three groups. Group 1: covering the os (11 patients); Group 2: 0–2 cm from os (18 patients); and Group 3: 2–5 cm from os (21 patients). The incidence of bleeding, results of serial ultrasound examinations, mode and timing of delivery and pregnancy outcome for each group were presented and natural history of placenta praevia was discussed. The scanning techniques, difficulties of diagnosis and placental localization were addressed and a review of recent literature presented. Our current management, in the light of the study findings, is to allow all patients with an asymptomatic placenta praevia, including Grade IV, to remain at home until 36 weeks or until bleeding occurs. For the past 12 months we have implemented such a policy and the outcomes of pregnancies treated in this manner was presented.

A quantitative and qualitative comparison of transabdominal and transvaginal ultrasound images of low placentae

W. G. Taylor
Liverpool Maternity Hospital, Oxford Street, Liverpool L7 7BN

Vaginal ultrasound has a role to play in the assessment of ante-partum haemorrhage, but its advantage over abdominal ultrasound in many cases is yet to be fully assessed. This study compares transvaginal with transabdominal ultrasound images of placental site. The aim of the study was to compare the two methods quantitatively. Women scanned at 18 weeks onwards who subjectively had a low placenta were recruited, and serial assessment made at 18, 24 and 32 weeks when possible. The main placental site was noted and paired measurements of the distance from the lower most placental edge to the internal os measured (in mm) using transabdominal (partly filled bladder) and transvaginal scanning (empty bladder) were calculated. Sixty-one paired measurements were possible on 74 examinations. A Toshiba Sonolayer SAL 77B machine with convex array at 3.75 MHz (transabdominal imaging) and a 5 MHz curvilinear transvaginal probe (model No. PVE 582V) were used. For paired measurements, application of a 95% confidence interval to the differences between them, by the two different examination modes, showed the differences to be no greater than 2 mm. A subjective assessment of image quality of the internal os and lower placental edge showed good visualization of the former in all transvaginal examinations and in 68% of transabdominal images there was a significant difference in the image quality of the lower placental edge between the two methods. This study supports the view that where lower placental edge and internal os can be clearly seen, a reliable measurement can be made by either method, but image quality by transvaginal scanning is superior.

Posters

The DMU, by R. Conlon
The BMUS Historical Collection, by J. E. E. Fleming
Fitz-Hugh-Curtis syndrome: another cause of pelvic mass and focal hepatic lesion masquerading malignancy, by B. Banerjee, A. Renniuson and B. E. Boyes
Transrectal ultrasound in the investigation of haemospermia, by D. J. Chadwick, K. Ganabathi, D. A. Gillatt and J. C. Gingell
Ultrasound in the diagnosis of gallbladder carcinoma, by B. D. Daly, H. Cheung, M. Arnold and C. Metreweli
Rigler's triad demonstrated by ultrasound, by R. J. Davies and A. E. A. Joseph
Diaphragmatic muscular bundles (slips): ultrasound evaluation of incidence and appearance, by S. P. Hawkins and A. L. Hine
The mobile pancreas and kidney, by R. A. Morgan and P. A. Dubbins
The role of ultrasound in the assessment of renal parenchymal disease in patients referred for renal biopsy, by J. E. Page, S. H. Morgan, D. Webb, S. Dilly, J. B. Eastwood and A. E. Joseph
Normal sonographic appearances of the profunda femoris vein: the role of colour flow Doppler, by G. R. J. Sissons and N. D. Pugh
Cerebral blood flow velocity changes pre and post successful ventricular peritoneal shunting in children, by D. Goh, S. D. Pye, J. Steers and R. A. Minns
A further ultrasound sign of ureteric reflux, by N. Joshi, P. Woodhead and S. Pablot
Ultrasound in the detection of Achilles tendon xanthomata, by A. J. Jones, S. Freeman, M. Hartog and A. E. Mitchelmore
Ultimate limits in ultrasonic imaging resolution, by R. A. Harris, D. H. Follett, M. Halliwell and P. N. T. Wells
The measurement of the dynamic range of ultrasound imaging systems: potential pitfalls, by J. M. Pelmore and A. C. Lamont
Serial Doppler ultrasound of the umbilical artery and fetal aorta in ovine pregnancy, by A. D. Cameron, J. Boyd and C. Paterson
The normal canine heart: anatomical criteria for the study of real-time ultrasonography and Doppler echocardiography, by C. Paterson and J. S. Boyd
The Doppler ultrasound appearance of pelvic varices, by T. J. Hodgson, M. W. Reed and R. J. Peck
Improved assessment of malignant involvement of the heart by transoesophageal echocardiography, by P. J. Scott, A. R. Essop, G. A. Wharton, G. J. Williams and J. L. Gibbs
The sonographic appearance of asymptomatic uterine dehiscence in the third trimester, by S. K. Dhanjil, L. Worswick, M. Sampson and A. H. Hassan
Colour Doppler ultrasound: a reliable way to diagnose nuchal cord in late pregnancy, by K. Neales, J. Wilson and D. Maxwell
The fetal profile: an aid in the diagnosis of fetal anomalies, by P. Twining
Fetal choledochal cyst: ultrasound demonstration at the routine 18-week scan, by L. Worswick and M. Sampson

The DMU

R. Conlon
56 Sherbrooke Avenue, Halton, Leeds LS15 0LS (currently a DMU student at East Leeds School of Radiography)

This poster expressed humorously the trials and tribulations of a DMU student (18 months as a DMU student expressed in a Doppler waveform). A qualification with such well deserved recognition is not attained easily but the hard work has to be worthwhile. The right-hand side of the poster was formed by interesting points, *e.g.* cost of DMU, subject with lowest pass rate, number of hours involved in log book. D is the Dedication, Devotion, Determination; M is for Mental agility; U is for Unbelievably worthwhile.

The BMUS Historical Collection

John E. E. Fleming
Department of Midwifery, University of Glasgow, Queen Mother's Hospital, Glasgow G3 8SH

The BMUS Historical Collection was started in 1984 as part of the Societies' educational programme. The aims are:

(1) to provide a source of material for future study and exhibition;
(2) to maintain a record of advances and also the setbacks in the development of present instruments and techniques;
(3) to retain a pool of ideas for rediscovery or exploitation using modern technology; and
(4) to record the work of the many individuals who have contributed to the development of medical ultrasound.

The Collection contains: ultrasound instruments, transducers, images and recordings, photos of instruments and people involved in ultrasound, films, video and audio tapes, manufacturers manuals/pamphlets/specifications, commercial documents, personal accounts, letters, manuscripts, and original copies of papers. Pictures of a selection of these were displayed on this poster. The present work is mainly the collection of representative material and the establishment of a system of accession. To keep this project going we need a continual flow of material—not only old items but also those which have recently gone out of use. Please look in your cupboards—think of the Collection before scrapping your old machine or putting a photo or manual in the bin. Plans for the long-term care of the collection are being discussed with the Director of the Hunterian Museum, University of Glasgow. Although the Collection is not on permanent display it is available for inspection or exhibition. If you wish to make use of the Collection or contribute to it in any way, or if you need any information on the history of medical ultrasound, please contact John Fleming.

Fitz-Hugh-Curtis syndrome: another cause of pelvic mass and focal hepatic lesion masquerading malignancy

B. Bannerjee, A. Renniuson and B. E. Boyes
Department of Radiology and Medicine, Tameside General Hospital, Ashton-under-Lyne, Lancashire OL6 9RW

Chlamydia trachomatis is now recognized as a common cause of pelvic inflammatory disease. Occasionally, pelvic inflammatory disease, due to *Chlamydia trachomatis* may be associated with perihepatitis, known as Fitz–Hugh–Curtis syndrome. In the past, it had been postulated that the perihepatitis is due to associated gonococcal infection but recent publications tend to support *Chlamydia trachomatis* as the causative factor. The authors presented a case report of a 42-year-old woman suffering from Fitz–Hugh–Curtis syndrome. The patient presented with vague abdominal pain, anorexia and loss of weight over a period of 2 months prior to seeking medical advice. On examination, the liver was found to be slightly enlarged and tender. Liver function tests were abnormal. An ultrasound scan of the abdomen and pelvis revealed pelvic mass lesion involving both adnexae with enlargement of pelvic lymph nodes suggestive of invasive malignancy. There were also multiple target lesions in both lobes of the liver and some irregularity of the surface of the liver. A diagnosis of pelvic malignancy with hepatic metastases was suggested. Laparoscopic findings were, however, more in keeping with pelvic inflammatory disease than malignancy. A tentative diagnosis of Fitz–Hugh–Curtis syndrome was made and confirmed by serological tests for Chlamydia antibody. The patient responded well to tetracycline therapy. Serial ultrasound scans of the liver and the pelvis showed gradual regression of the hepatic lesions, but the pelvic changes, although improved considerably, did not return to normal. To the authors' knowledge, the ultrasound appearance of Fitz–Hugh–Curtis syndrome has not been previously reported. When focal lesions of the liver and pelvic mass co-exist in a relatively young person, diagnosis of Fitz–Hugh–Curtis syndrome should be considered.

Transrectal ultrasound in the investigation of haemospermia

D. J. Chadwick, K. Ganabathi, D. A. Gillat and J. C. Gingell
Department of Urology, Southmead Hospital, Bristol BS10 5NB

Haemospermia is a common symptom in urological practice. It is often regarded as being of little significance but to the patient haemospermia frequently causes concern, particularly because of the fear of cancer. Investigations, when they are performed, include urine culture, intravenous urography, seminal analysis, urethrocystoscopy, prostatic biopsy and vasography. In an ongoing study, 20 consecutive patients presenting with haemospermia have undergone transrectal ultrasound. Each examination was performed by one clinician (D.J.C.) using a Bruel and Kjaer 8551 multiplanar probe with a 7 MHz transducer. The mean age of the patients was 53.3 years (range 25–70 years). Associated urological symptoms were present in six patients. Seven patients had normal scans. In five patients there were ultrasonic changes of benign prostatic hyperplasia. In one of these there was marked calcification peripherally within the gland. Five patients had abnormalities of the seminal vesicles. This consisted of dilatation, atrophy, cyst formation and asymmetry. No cases of seminal vesicle calculi were seen. One patient had a cyst of the ejaculatory duct. In three cases a hypoechoic lesion was seen within the prostate, which was biopsied under ultrasound control. One biopsy demonstrated benign prostatic hyperplasia and two revealed adenocarcinoma of the prostate. This study demonstrated two points. Firstly, transrectal ultrasound can suggest a cause of haemospermia in the majority of patients without recourse to more invasive and expensive investigations. This, in many cases, will provide adequate reassurance to patients and clinicians alike. Secondly, this series illustrated that haemospermia is not a totally benign condition. In addition to the two patients with prostate cancer, one of the patients with a normal transrectal ultrasound scan was found at cystoscopy to have carcinoma of the bladder.

Ultrasound in the diagnosis of gallbladder carcinoma

B. D. Daly, H. Cheung, *M. Arnold and C. Metreweli
Departments of Radiology and Organ Imaging and
**Anatomical and Cellular Pathology, Chinese University of Hong Kong, Prince of Wales Hospital, Shatin, Hong Kong*

We reviewed the clinical records, sonographic appearances and surgical findings in 21 histopathologically proven cases of gallbladder carcinoma. The sonographic appearances included undetectable tumour in a uniformly thickened gallbladder wall, irregular polypoid nodules, sessile lesions, often with evidence of disseminated tumour and complete replacement of the gallbladder by tumour, which on occasion mimicked acute empyema of the gallbladder. Evidence of metastic tumour was present in more than 50% of cases on initial sonographic evaluation, often with features of obstructive jaundice secondary to nodal spread. The presence of coexisting gallbladder calculi, wall calcification and the infiltrating nature of some tumours led to an initial misdiagnosis in over 30% of the cases in our series. The current trend towards treatment of gallstone disease without cholecystectomy suggests that the incidence of gallbladder carcinoma is likely to increase and features that may aid earlier diagnosis were discussed.

Rigler's triad demonstrated by ultrasound

R. J. Davies and A. E. A. Joseph
Department of Diagnostic Radiology, St George's Hospital, London SW17

In 1941 Rigler described the classic plain radiographic appearances of gallstone ileus consisting of the triad of small bowel obstruction, pneumobilia and an ectopic calcified gallstone. Mortality and morbidity in this condition remains high, however, and this can partly be accounted for by difficulties and delay in diagnosis. At least 50% of patients have no clinical features of biliary disease and plain radiographs show Rigler's triad in only one-third of cases. This is because plain radiographs are insensitive for faintly calcified gallstones and small quantities of biliary air, and dilated bowel loops may not be correctly identified if they are fluid-filled. Case reports have recently appeared in the literature showing that ultrasound may detect gallstone ileus when it is not suspected. To illustrate this a case was presented where plain radiographs showed small bowel obstruction but no other abnormality. Ultrasound, however, was able to detect not only the dilated bowel loops, but also air in the gallbladder and an ectopic gallstone permitting a confident diagnosis of gallstone ileus. We suggest that ultrasound complements plain radiographs in the investigation of patients with small bowel obstruction as unsuspected gallstone ileus may be detected.

Diaphragmatic muscular bundles (slips): ultrasound evaluation of incidence and appearance

S. P. Hawkins and A. L. Hine
Radiology Department, Central Middlesex Hospital, Acton Lane, London NW10 7NS

Diaphragmatic muscular bundles (slips) connect the central tendon of the diaphragm to the inner aspect of the lower thoracic cage. They cause hepatic invaginations which may be visualized on ultrasound or computed tomography. Two hundred patients underwent prospective ultrasound of the diaphragm and liver to determine the incidence and characteristics of slips. The incidence was 15%, rising to 30% in those aged 80 years and over. Slips average 1.2 cm in depth (range 0.1–3.6 cm) and their occurrence has no racial or sexual bias. Multiple slips were seen in 4% of patients, all females. Slips are echogenic and has a variety of appearances, typically nodular on transverse section and strand-like longitudinally. Knowledge of these structures will avoid confusion with liver peridiaphragmatic pathology.

The mobile pancreas and kidney

R. A. Morgan and P. A. Dubbins
Derriford Hospital, Plymouth

It has became apparent with the use of real-time ultrasound that the position of the pancreas can be variable in the retroperitoneal space depending on the phase of respiration and patient position. One hundred and forty-five patients undergoing ultrasound examination for unrelated symptomatology were examined with respect to pancreatic position. Patients likely to have distorted upper abdominal anatomy were excluded. All were examined in the supine and left posterior oblique positions in the sagittal and transverse planes. Criteria for pancreatic position were pre-caval, pre-aortic and to the left of the aorta. The pancreas was not visualized in 25 patients, and these were excluded from the study. Of the remaining 120 patients the pancreas changed position with patient movement in 45 (42 of 86 females, three of 34 males). In eight females a change in position of the right kidney was also noted. There was no correlation of extent of movement of the pancreas with patient age nor was there any apparent association of pancreatic and renal mobility. This study demonstrates that pancreatic, and to a lesser extent renal, mobility is common, particularly in women. Operators in ultrasound should be aware of this phenomenon causing distorted biliary and pancreatic anatomy because the altered landmarks usually used for accurate anatomical localization may cause confusion in the correct interpretation of normal and abnormal structures.

The role of ultrasound in the assessment of renal parenchymal disease in patients referred for renal biopsy

J. E. Page, S. H. Morgan, D. Webb, S. Dilly, J. B. Eastwood and A. E. Joseph
Departments of Radiology and Nephrology, St George's Hospital, London SW17 0QT

Ultrasound examination of the kidneys was carried out in 44 patients referred for renal biopsy over an 18-month period. The indications for renal biopsy were acute renal failure or impaired renal function (22 patients), nephrotic syndrome (eight patients), proteinuria (five patients) and haematuria (nine patients). Biopsy was unsuccessful in one patient. The sonographic features recorded were renal size or outline, parenchymal echogenicity and papillary prominence. Initial results suggested that there was no correlation between renal size or outline and histological findings. Renal papillae were prominent in 14 kidneys, all of which were histologically abnormal. In all cases, parenchymal echogenicity was also abnormal. Renal biopsy confirmed parenchymal disease in all 20 patients with abnormally echogenic kidneys on ultrasound. However, of the seven cases reported to show minimally increased echogenicity, two were histologically normal. Six other patients with a normal ultrasound had parenchymal disease on biopsy. In all six patients there were overriding clinical indications to proceed to biopsy. The role of ultrasound in renal parenchymal disease is twofold. It has an undisputed place in guidance of the needle during renal biopsy. Patients in whom ultrasound shows an increase in renal parenchymal echogenicity, particularly where this is associated with prominent papillae, should be referred for renal biopsy. In those patients with sonographically normal kidneys, the decision to biopsy depends on clinical criteria, *i.e.* biopsy should be performed in all patients with impaired renal function ± macroscopic haematuria, but may be deferred in patients with non-nephrotic proteinuria ± microscopic haematuria.

Normal sonographic appearances of the profunda femoris vein: the role of colour flow Doppler

G. R. J. Sissons and N. D. Pugh
Department of Radiology, Cardiff Royal Infirmary, Cardiff CF2 1SZ

Real-time sonography is a useful technique in the diagnosis of femoro-popliteal deep vein thrombosis. Comparative studies with contrast venography show impressive sensitivity and specificity. Compressibility studies are the mainstay of diagnosis; the role of duplex and colour flow Doppler remain to be established. The profunda femoris vein is not reliably visualized at contrast venography yet is a recognized site of thrombosis within the deep venous system. Colour flow Doppler analysis was performed in 32 healthy volunteers with no history and few risk factors for venous thrombosis. The profunda femoris vein was imaged in both longitudinal and transverse planes in all cases. In all subjects no more than 12.5 cm of the main vessel or its branches could be imaged. Complete compressibility was achieved in 26 out of 32 cases. Where compression was incomplete, "fill-in" of the vessel lumen by the colour flow signal was always seen. It is concluded that the profunda femoris vein is a constant landmark in lower extremity venous ultrasound. Only a short segment is usually imaged. Incomplete compressibility is seen as a normal variant. Colour flow Doppler, by showing normal flow within the lumen, provides additional information that cannot be obtained by real-time B mode or duplex sonography.

Cerebral blood flow velocity changes pre and post successful ventricular peritoneal shunting in children

D. Goh, S. D. Pye, J. Steers and R. A. Minns
Department of Paediatric Neurology, Royal Hospital for Sick Children and Department of Medical Physics & Medical Engineering, Western General Hospital, Edinburgh

In children, hydrocephalus of varying aetiology can result in increased ventricular dilatation and raised intracranial pressure (ICP). Secondary ischaemic damage can result from impaired cerebral perfusion due to raised ICP. The aim of intervention is to prevent further ischaemic damage. We have been assessing the use of transcranial Doppler ultrasound as a non-invasive method of monitoring cerebral haemodynamics. Eleven patients (five neonates, six infants and children) underwent ventricular peritoneal shunting operations for hydrocephalus. Four were shunt revisions, for broken or poorly functioning pre-existing shunts. All 11 had raised ICP or ventricular dilation prior to surgery. ICP was measured directly from the ventricles via a Richam reservoir or by direct ventricular taps. Cerebral blood flow velocity (CBFV) measurements were carried out using transcranial Doppler ultrasound with 2 MHz or 4 MHz probes. Measurements were made on several occasions both before and after shunting. In all but one patient, CBFV measurements were made on the middle cerebral arteries. The resistance index (RI) was calculated using S–D/S and also the time averaged mean velocity (TAMV) was obtained. In all patients the RI decreased and in nine patients TAMV increased after successful shunting. In the neonatal group, the mean pre-operative RI was 0.77 ± 0.04 (1 standard deviation) and the mean post-operative RI was 0.68 ± 0.04. The pre-operative TAMV was $41 \pm 10\ \mathrm{cm\ s^{-1}}$ and the post-operative TMAV was $54 \pm 11\ \mathrm{cm\ s^{-1}}$. In the older infants and children, the mean pre-operative RI was 0.66 ± 0.05 and the mean post-operative RI was 0.53 ± 0.04. The mean pre-operative TAMV was $54 \pm 15\ \mathrm{cm\ s^{-1}}$ and the mean post-operative TAMV was $66 \pm 17\ \mathrm{cm\ s^{-1}}$. Our results suggested that after successful shunting a reduction in cerebral resistance gives improved cerebral blood flow.

A further ultrasound sign of ureteric reflux

Nutan Joshi, Patricia Woodhead and Suzanne Pablot
Queen Mary's Hospital for Children, Carshalton, Surrey

Ureteric reflux is a common urological problem in children. The diagnosis requires co-ordinated investigations including ultrasound, nuclear medicine and micturating cystography. Ultrasound should be the first radiological investigation from which the renal size, cortical thickness, presence of large scars and dilatation of collecting system are all indicators of reflux nephropathy. During routine ultrasound examination of the urinary tract in children with urinary infection at Queen Mary's Hospital for Children, we have observed occasional urothelial thickening of the renal pelvis, pelvi–ureteric junction and occasionally of proximal and distal ureters, and have looked at the relationship to proven ureteric reflux. Between July 1989 and August 1990, 150 micturating cystograms have been performed on children between the ages of 3 weeks and 7 years. Ninety-five of these were positive for reflux (either unilateral or bilateral). Twenty-four patients showed urothelial thickening in the absence of frank hydronephrosis or other signs of reflux nephropathy. Three patients had unilateral scarring. Most of the 24 cases demonstrated Grade II/III reflux. We feel that even in the absence of dilatation or renal cortical loss, the presence of urothelial thickening on ultrasound warrants further investigation. Urothelial thickening was present in 25% of our patients with proven reflux.

Ultrasound in the detection of Achilles tendon xanthomata

A. J. Jones, S. Freeman, M. Hartog and A. E. Mitchelmore
Department of Radiology and Medicine, Southmead Hospital, Bristol BS10 5NB

The normal appearance of the Achilles tendon on ultrasound is well described and ultrasonography of the Achilles tendon is well established as a useful technique in trauma, particularly in the assessment of partial rupture and post-operative changes, which may be difficult to confirm clinically. When used in the transverse plane, ultrasound is an accurate method of measuring the thickness of the tendon. The oval cross-sectional shape of the tendon may lead to inaccurate measurement on longitudinal ultrasound, or on plain lateral radiographs. Lipid accumulation in tendons in hypercholesterolaemia causes tendon xanthomata to be among the most frequent overt stigmata of familiam and acquired hypercholesterolaemias. The Achilles tendon is one of the most accessible for radiographic or, more accurately, ultrasound assessment and measurement. Ultrasound may also show alteration in internal structure due to xanthomata. The severity of the disease, and in particular the likelihood of associated ischaemic heart disease increases with increasing Achilles tendon thickness, particularly in the familial hypercholesterolaemias. The response to treatment may also be monitored by serial examinations. We described the technique of ultrasound examination and measurement of the Achilles tendon. Images of a group of patients and controls were shown. We believe this is a simple, cheap and non-hazardous method for follow-up of patients and for scanning families.

Ultimate limits in ultrasonic imaging resolution

R. A. Harris, D. H. Follett, M. Halliwell and P. N. T. Wells
Department of Medical Physics and University Departments of Electrical Engineering and Radiodiagnosis, Bristol General Hospital, Bristol BS1 6SY, UK

The resolution of an ultrasound imaging system increases with the ultrasonic frequency, which is limited by frequency-dependent attenuation. For imaging at a required depth, resolution improvements beyond the limits imposed by ultrasonic frequency can be obtained by increasing the ultrasonic intensity. This is itself, however, dependent on safety considerations and the effects of non-linearity. In homogeneous media, resolution increases with decreasing *f*-number. Particularly at low *f*-numbers, however, tissue inhomogeneity leads to a deterioration in image quality. Inhomogeneity may be considered in terms of phase aberration. It has been found that for a given aperture, image degradation due to phase aberration is worse at higher frequencies. Schemes have been proposed for correction of this problem, but so far model systems do not lend themselves to clinical application. Deconvolution is unsatisfactory, speed correction is impracticable, and synthetic aperture scanning and holography are virtually useless in biological tissues. Ultrasound computed tomography has had only limited success. Speckle reduction can improve target detectability, but at the expense of resolution. Time–frequency control provides a useful partial solution to the problem of resolution reduction resulting from attenuation. It is clear that improved resolution would result in significant clinical benefits. An optimization system for aperture size and ultrasonic frequency is proposed. This would have a compact ultrasonic beam and would allow frame rate to be traded for resolution, by means of signal averaging.

The measurement of the dynamic range of ultrasound imaging systems: potential pitfalls

J. M. Pelmore and *A. C. Lamont
*Departments of Medical Physics and *Radiology, Leicester Royal Infirmary, Leicester LE1 5WW*

The measured dynamic range of two ultrasound systems has been studied in detail. A larger, less detailed survey has been made of 15 systems. The two methods used have been the Cardiff Greyscale Test Object and the Acoustic Signal Injection technique (ASIST). Both of these devices produce a greywedge on the system display. Currently available imaging systems can give a dynamic range of 50 dB or more. The ASIST gives a greywedge of 40 dB and the Cardiff system can give a greywedge of 60 dB or more. A difficulty common to both methods is delineating the appropriate end-points of the wedge and there can be interobserver errors. With the Cardiff system, relatively large errors can result from lack of knowledge of the frequency. The problem with the ASIST is to ensure that receiver gain is truly independent of range. Both methods are capable of monitoring changes in dynamic range of a given system but the ASIST has been found to give more accurate absolute measurements if used with caution. A modified ASIST to produce a 60 dB wedge display was briefly described.

Serial Doppler ultrasound of the umbilical artery and fetal aorta in ovine pregnancy

A. D. Cameron, *J. Boyd and *C. Paterson
*Departments of Obstetrics and Gynaecology and *Department of Veterinary Anatomy, Glasgow University*

In order to study any complications of pregnancy it is necessary to acquire normal physiological data. Doppler studies of ovine pregnancy have been carried out previously. Continuous-wave ultrasound has been used by one group to study the umbilical flow in the normal sheep pregnancy from 66 to 140 days gestation. A decline in the peak systolic to diastolic flow in the umbilical artery from 66 to 115 days, with no significant variation thereafter, was found. It was concluded that this was consistent with previous work using electromagnetic flow meters which showed a lack of a further decrease in umbilical impedance in late gestation. In this present study, pulsed Doppler assessment of the umbilical artery and fetal aorta was carried out in the last 4 weeks of ovine pregnancy in six animals. The sheep were of grey face or Suffolk breeds and had synchronized pregnancies. The ultrasound equipment was an Interspec XL with either 3.5 MHz or 5 MHz transducers. The umbilical artery SD ratios were stable and varied between 2.0 ± 0.4 at the first study to 2.1 ± 0.6 at the final study period. The aortic SD ratio ranged from 3.2 ± 0.1 at the first study to 4.2 ± 2.0 at the final study period. The results of this study revealed a stable resistance in both vessels through the last 4 weeks of ovine gestation. This is in keeping with previous work and is thought to reflect the portion of gestation when the placental and fetal vasculature are stable. The results will prove useful when studying animal models of pathological pregnancy.

The normal canine heart: anatomical criteria for the study of real-time ultrasonography and Doppler echocardiography

C. Paterson and J. S. Boyd
Department of Veterinary Anatomy, University of Glasgow Veterinary School, Bearsden, Glasgow G61 1QH

The last decade has witnessed the increasing popularity of both real-time and pulsed-wave (PW) Doppler echocardiography in veterinary medicine. The present work has two objectives: to examine the optimal scanning sites which allow the identification of anatomical structures of the dog heart, and the recording of blood flow velocities through the cardiac valves. Twelve beagles aged between 7 months and 3 years along with three greyhounds aged 4, 5 and 7 years were examined in the right parasternal recumbency with the probe placed between the third and fifth intercostal space. The heart was scanned in short and long axial planes using M-mode and PW. The anatomical structures of the left heart were identified and blood flow velocities through the mitral, aortic and tricuspid valves were recorded with PW. The procedure was repeated in the parasternal recumbency where visualization of the right heart anatomy along the blood flow velocities of the aortic, mitral, tricuspid and pulmonary valves were recorded. The subcostal window was achieved with the dog in a semi-dorsal recumbency and scanned with a 3.5 MHz transducer. Blood flow velocities through the mitral and aortic valves were recorded with PW and a 2 MHz continuous-wave (CW) transducer. The suprasternal view through the thoracic inlet with the dog in a sitting position was used to measure blood flow velocity of the ascending aorta with CW. Colour flow Doppler was also employed enabling a clearer understanding of the direction of blood flow. Our study underlined the potential of pulsed- and continuous-wave Doppler echocardiography as a non-invasive tool.

Acknowledgements: The authors gratefully acknowledge the help of Toshiba, Vingmed (BMS (Scotland) Ltd) and Hewlett Packard for the use of the colour flow Doppler scanners.

The Doppler ultrasound appearances of pelvic varices

T. J. Hodgson, M. W. Reed and R. J. Peck
Department of Radiology, Royal Hallamshire Hospital, Sheffield

Pelvic pain in women is a common complaint with many causes. A described but often overlooked cause of pain is dilatation of the veins of the broad ligament and ovarian plexi. The Doppler ultrasound appearances of this condition have not been previously described in detail. Symptoms secondary to dilatation of the pelvic, ovarian and broad ligament veins is a well recognized condition, variously called the pelvic pain or pelvic congestion syndrome. The syndrome is associated with specific clinical features. It only occurs in multiparous women, with throbbing pelvic pain worsened by fatigue, standing and exercise. The pain is relieved by lying down. The appearances of transabdominal Doppler ultrasound of this condition are unique and represent a quick non-invasive method of diagnosis. The findings at ultrasound are of multiple dilated vessels lying within the broad ligament and around the ovaries. Doppler sampling of these vessels confirms them to be venous in origin with a signal of varying amplitude. To assist the observer the patient should be upright, performing a Vasalva manoeuvre. These two methods increase reflux and thereby distend the varices. Whilst transfemoral venography will provide the definitive diagnosis and probable future treatment via embolization, pelvic Doppler ultrasound is a valuable, non-invasive procedure which will prove useful in screening patients for this often disabling, but easily treated condition. The Doppler ultrasound findings are unique to this condition and should be recognized easily by both radiographers and radiologists.

Improved assessment of malignant involvement of the heart by transoesophageal echocardiography

P. J. Scott, A. R. Essop, G. A. Wharton, G. J. Williams and J. L. Gibbs
Non-Invasive Heart Unit, Killingbeck Hospital, Leeds LS14 6UQ

Pericardial effusion is not infrequently detected by echocardiography in patients with advanced malignant disease. Direct spread of tumour to the cardiac chambers is, however, rarely diagnosed in life. Nine patients (age range 4–69 years) were referred for transoesophageal echocardiography (TOE) to assess cardiac involvement by their malignant disease (lymphoma 2, ovarian carcinoma 2, renal carcinoma 1, hepatocellular carcinoma 1, malignant melanoma 1, sarcoma 1 and bronchogenic carcinoma 1). All patients had concomitant transthoracic echocardiography (TTE) for comparison. Pericardial effusion was present in six patients. TTE revealed intracardiac tumour in six cases, involving the left atrium on two occasions, the right atrium on three and both atria on one occasion. A large retrocardiac mass was also seen in one of the patients with a left atrial mass, but in two subjects, both with pericardial effusion, no direct cardiovascular spread was detected. TOE confirmed all the TTE findings and, in addition, revealed biatrial tumour in the patients with malignant melanoma, a large retrocardiac mass in one patient with ovarium carcinoma and external compression of the left atrium, and invasion of the wall of the descending thoracic aorta by a large lymph node mass in the patient with bronchogenic carcinoma, all unsuspected after TTE. TOE also showed the route of tumour spread to the heart in six patients: via the inferior vena cava in two, the pulmonary veins in two and by direct infiltration of the cardiac wall in two. In one instance compression of the right pulmonary artery was also shown, which again was undetected by TTE. In two cases TOE was used to guide percutaneous, transvenous biopsy of intracardiac tumour in order to establish a primary diagnosis. Intracardiac spread by malignant disease may not always be detected by TTE. If this is suspected, TOE will provide additional information unavailable from TTE, including the route by which spread has occurred. When a primary diagnosis has not been reached, TOE can be used to guide safe biopsy of intracardiac tumour.

The sonographic appearance of asymptomatic uterine dehiscence in the third trimester

S. K. Dhanjil, L. Worswick, M. Sampson and A. H. Hassan
Radiology Department, Northwick Park Hospital, Harrow, Middx HA1 3UJ

We described a case of a 32-year-old woman presenting in labour at 38 weeks gestation with a mobile upper abdominal wall mass, which changed in size and position with fetal movements. The pregnancy had been otherwise uncomplicated. The past obstetric history involved a manual removal of placenta following delivery of her first child 20 months earlier, followed by a laparotomy for uterine perforation and adhesions 5 months later. An urgent ultrasound scan confirmed a normal live fetus and demonstrated a rupture of the uterine fundus with a hole through which protruded the amniotic sac forming the palpable mass. Emergency surgery was performed, a live baby delivered and the dehiscence repaired. Ultrasound and peri-operative correlations were presented. To the knowledge of the authors, only one previous sonographic demonstration of uterine *dehiscence* in pregnancy has been reported in the world literature.

Colour Doppler ultrasound: a reliable way to diagnose nuchal cord in late pregnancy

K. Neales, J. Wilson and D. Maxwell
Department of Obstetrics and Gynaecology, Guy's Hospital, London SE1 9RT

Two hundred unselected antenatal patients underwent a colour Doppler ultrasound at term, and the presence or absence of a nuchal cord was determined and recorded. These findings were compared with a labour ward record of cord position at the time of delivery and results are summarized below.

	Cord present at delivery	Cord absent at delivery	Total
Cord present on ultrasound	49 (true positive)	7 (false positive)	56
Cord absent on ultrasound	2 (false negative)	142 (true negative)	144
Total	51	149	200

Cord position prior to the onset of labour can therefore be determined with a high degree of accuracy using colour Doppler ultrasound, particularly when excluding a nuchal cord, which gave a negative predictive value of 98%. The standardized scanning technique used to identify a nuchal cord was described, and situations where knowledge of cord position could be beneficial were discussed. Potential applications could include the patient with variable decelerations on antenatal cardiotocography, or a fetus with intrauterine growth retardation on a breech presentation. In these instances, accurate knowledge of cord position could alter timing or mode of delivery. Approximately 25% of our patients did have a nuchal cord at delivery, a figure that agrees with other studies. The umbilical artery Doppler pulsatility index (PI) was not elevated in patients with a nuchal cord, and there was no significant alteration in the PI along the length of the cord. We found no correlation between Type I and Type II decelerations in labour and the presence or absence of nuchal cord, and the umbilical artery Doppler scans did not provide an indicator for fetal distress in labour in our relatively small series. The presence of a nuchal cord can therefore be determined wth a high degree of accuracy ante-natally. Whether this information is of value clinically would require a large prospective study to show any improvement in perinatal outcome.

The fetal profile: an aid in the diagnosis of fetal anomalies

P. Twining
Department of Radiology, Queen's Medical Centre, University Hospital, Nottingham NG7 2UH

In order to assess the significance of the facial abnormalities associated with congenital anomalies, a 3-year review was made of all fetuses referred for a detailed scan at Queen's Medical Centre, Nottingham. Detailed scans are usually carried out on fetuses at 18–20 weeks gestation. A full anatomical assessment is made and, in addition, where possible, transverse coronal and profile views of the fetal face are obtained. All ante-natal scans were reviewed, as were pathological specimens and post-morten reports. Facial abnormalities were seen in 20 fetuses. The most common finding was six cases of micrognathia and this was present in four out of nine fetuses with trisomy 18, one case of camptomelic dysplasia and one case of short rib polydactyly syndrome. The most striking appearances were seen in the six cases of alobar holoprosencephaly. Five cases showed facial abnormalities ranging in severity from cyclopia with proboscis, cebocephaly, to hypotelorism, midline clefting and nasal hypoplasia. One case, however, demonstrated normal facial structures. Facial clefting was present in two cases of trisomy 13 and one case of Roberts syndrome. Depression of the nasal bridge was seen in one case of thanatophoric dwarfism and typical facial appearances were seen in the five cases of ancephaly. We feel the visualization of the fetal face is essential in the assessment of intracranial abnormalities and in any situation where a chromosomal abnormality is suspected. It also provides additional information in the assessment of skeletal dysplasias. This poster was presented in the form of the front page of that well known newspaper, *The Daily Scannner*. The headline read: "The fetal profile, have you seen these faces?"

Fetal choledochal cyst: ultrasound demonstration at the routine 18-week scan

L. Worswick and M. Sampson
Department of Radiology, Northwick Park Hospital, Harrow, Middx HA1 3UJ

We describe a finding of a transonic structure in the fetal upper abdomen seen during the routine 18-week scan. The pregnancy was otherwise uncomplicated and the scan otherwise normal. The differential diagnosis is discussed and includes duodenal atresia, duplication cysts, mesenteric cyst and choledochal cyst. The case was followed with ultrasound scans later in pregnancy and at 24 hours after delivery. The structure enlarged slightly to a maximum of 2.3 cm, and was shown to be immediately anterior to the portal vein, tapering down towards the pancreas and separate from the stomach. There was no polyhydramnios. A diagnosis of choledochal cyst was made and surgery was performed. To the knowledge of the authors this is only the *second* case in the world literature observed before 24 weeks gestation.

1991, *The British Journal of Radiology*, *64*, 671–672

Book reviews

Differential Diagnosis in Abdominal Ultrasound. By R. A. L. Bisset and A. N. Khan, pp. xii + 361, 1989 (Bailliere Tindall, Eastbourne), £9.95.
ISBN 0–7020–1483–4

The authors correctly state that "the gamut approach to differential diagnosis is very useful in ultrasound" because of the lack of specificity of ultrasound. This short book costing £10 contains seven chapters on organ systems.

The text is easy to read but there are some spelling and grammatical errors. While there is a considerable amount of useful information in the book, the layout is somewhat confusing in places *e.g.* section 4.38 is called "Perirenal fluid collections" but section 4.38.1 to 4.38.6 do not relate to perirenal fluid collections and there are other similar examples elsewhere. I also have some doubts as to whether it is useful to include pathologies that are specific to paediatrics or adults on the same gamut or list. Despite these reservations the book is attractive because of its size and price and I am sure it will be appreciated by DMU students and trainee radiologists.

M. PHELAN

Diagnostic Ultrasound of Fetal Anomalies. By David A. Nyberg, Barry S. Mahony and Dolores H. Pretorius, pp. xiii + 757, 1990 (Wolfe Publishing, London).
ISBN 0–8151–6439–4

There has been a need for some time for a comprehensive atlas of fetal anomalies and the authors of this text are to be congratulated for producing such an excellent review of the subject. The early chapters review methods of obstetric ultrasound, in particular the criteria adopted in America for the different levels of scanning. Hazards of ultrasound are discussed. The succeeding chapters are a systematic assessment of fetal anomalies, preceded by a small section on embryology of each system with many helpful lists of conditions associated with described abnormalities. The illustrations are of the highest quality and it is hard to find even the rarest abnormality which is not discussed. The bibliographies at the end of each chapter are some of the most extensive to be found anywhere. The final chapters assess the current situation of fetal surgery and its place in antenatal management.

This book will rapidly find a place on the shelves of every obstetric ultrasound department and can be most highly recommended to all involved in the field.

D. W. PILLING

Doppler Echocardiography. An Illustrated Clinical Guide. By Peter Wilde, pp x + 153, 1989 (Churchill Livingstone, Edinburgh), £29.95.
ISBN 0–443–03431–8

Peter Wilde's book fills a useful gap in the radiological literature concerning heart disease. It is comforting to see that not all echocardiography has been delegated (intentionally or otherwise) to our cardiological colleagues. As more and more ultrasound machines have Doppler (often including colour) as standard, many more requests concerning "blood flow imaging" are being initiated by clinicians. The general radiologist needs to know this field and there is now good reason why the basics of cardiac ultrasound should be included under his or her remit. More non-invasive cardiac investigations are being required by all specialties outside the mainstream of cardiology *e.g.* anaesthetists requiring documentation and significance of murmurs prior to operation. Radiologists should be in a position to respond to such service needs and hence the timely introduction of this text.

Doppler Echocardiography contains five main chapters on qualitative and quantitative Doppler studies in both children and adults, together with explanation of underlying principles and correlation with M-mode and cross sectional imaging. Although there is a good bibliography at the end of the book, the latest references are 1987 and herein lies a problem. Changes occur so rapidly in this expanding field of imaging, particularly with reference to colour Doppler, that there is a danger of parts of this book becoming outdated. This could be easily remedied by the production of a second edition earlier than would normally be expected. I hope this does indeed occur as the author has produced an excellent clear and concise picture of the place of Doppler ultrasound in cardiac imaging. Doppler echocardiography is set for a significant development over the next few years and this basic text is required reading.

The book is good value and should be readily affordable by anyone who is interested in developing skills in non-invasive cardiac imaging.

JAMIE WEIR

Video Atlas of 2-Dimensional Colour Flow Doppler Echocardiography. By G. M. Gura, set of two videos, 1990 (Churchill Livingstone, New York), £185.50.

This is a technically well presented atlas of 50 cases in which two-dimensional colour flow Doppler echocardiography is displayed in conjunction with an atlas containing still frames from the cases. The atlas contains discussion which complements the commentary on the video tape. Additionally there are some short notes about the clinical application of colour flow Doppler, physics and instrumentation and various cardiac abnormalities.

There is no doubt that video display is the only real way to appreciate colour flow Doppler examination. The quality of the images is high, being comparable to that currently achievable with a variety of instruments. The presentation on video takes a total of two and a half hours and in this respect is rather slow, slightly repetitious and a little tiring to listen to. Anyone with little experience of colour flow work would need to devote several sessions to viewing the tape to avoid losing concentration.

The main criticism of this work is that it simply displays colour flow examination in a wide range of clinical situations but has relatively little complementary information about clinical findings, other echocardiographic findings and indeed other imaging findings. There are a few angiography correlations but these are used merely to strengthen the argument for colour flow Doppler. There is no discussion of the weaknesses of this modality and in particular little comment is made about the difficulties of grading the severity of valvular regurgitation which is a well recognized problem.

At the end of the presentation there are 10 "unknown" cases, I was looking forward to testing myself on these cases until I discovered that they were simply re-presentations of previously demonstrated cases and offered no significant new challenge. It is a pity that new cases were not used. A long series of questions at the end of the book for American CME credits is of no relevance to the British reader as the answers are not available without returning the completed sheet.

The combined atlas and pair of video tapes are expensive and it is difficult to see just where this work will prove useful in the UK. The presentation presupposes basic knowledge of echocardiography and there is no doubt that comprehensive viewing of the video tapes would allow a newcomer to colour flow Doppler "to get their eye in" before challenging the real thing. This, however, may well be much better achieved by using a machine, visiting an established department or attending a course.

If a department has a very big throughput of trainees then it might be useful to have this production to support other teaching, but I think this will be an uncommon application.

P. WILDE

Arthrosonography. By Horst Sattler and Ulrich Harland, 1990 pp. xi + 164, 1990 (Springer-Verlag, Berlin), DM148.
ISBN 3-540-19482-7

This book will tell you what joints look like on ultrasound but not which patients should be examined. In 160 pages the German authors describe the physical principles of ultrasound, methods of examination and the appearance of common pathology in each of the major joints. One chapter covers abnormalities of soft tissues. The numerous illustrations are in black and white and are mainly of good quality. The overall layout is clear but the text is at times difficult to read, perhaps as a result of the translation.

Ultrasound in congenital dislocation of the hip is dealt with solely according to the methods advocated by Graf. Whilst the explanation is marginally easier to understand than Graf's original work, I would find it difficult to copy the method of examination using this text alone. The diagrams showing normal and abnormal anatomy could easily be improved.

The choice of subjects is unbalanced. A section on popliteal cysts is informative but I am surprised that meniscal cysts are dismissed in three lines when this is one of the few disorders of the knee where ultrasound has a useful role. The appearance of an osteochondroma is illustrated but without mentioning the importance of measuring the thickness of the cartilage cap. The ultrasound signs of osteo-arthritis of the hip are described without reference to plain radiographs.

Any medical examination must be seen in its clinical context and should be directed at solving clinical problems. Although aimed at those who investigate musculoskeletal disease this book does not address this subject. Is ultrasound a valid method for detecting rotator cuff tears? Is dynamic assessment of hip instability a better technique than Graf's? How does ultrasound figure in the staging of soft tissue tumours? These are but a few of the questions that might have been discussed. The authors have missed an opportunity and I fear that their audience will be limited.

DAVID WILSON

Monoclonal Antibodies in Immunoscintigraphy. Ed. by J.-F. Chatal, pp. xi + 422, 1990 (CRC Press, Florida), £128.00.
ISBN 0-8493-4716-5

This book covers the broad panorama of clinical results in cancer and other pathologies such as acute inflammation, myocardial infarction and venous thrombosis. The book is edited by a leading expert in the field, with contributions from most of the main centres involved in developing immunoscintigraphic techniques.

The book commences with a chapter on the comparison of cross sectional imaging techniques for the detection of abdominal and pelvic metastatic disease. Although well illustrated and quite interesting, somehow this chapter of 55 pages does not really add to the subject of immunoscintigraphy. The next two chapters deal with radiolabelling and data processing. The chapter on data processing deals, in depth, with image improvement and image subtraction techniques. This chapter, in fact, highlights the problem of radio-immunoscintigraphy, in that quite sophisticated methods of processing are often required before lesions become visible and even then, in some mathematical techniques such as probability, mapping is required to decide whether or not a lesion is present.

The chapters on immunoscintigraphy in oncology cover the use in gastro-intestinal disease, ovarian, thyroid, skin, lung and liver cancer. Much of the information which appears in this section has already been seen in journals, at conferences or in conference proceedings several times and those interested in the subject will be already aware of the results. However, it is useful to have the information brought together within one volume. In general these chapters give a rather optimistic view of antibody imaging, indicating good sensitivities and specificities and yet most of them end with guarded statements on the real clinical value of radio immunoscintigraphy.

I feel that the book could have benefited from a final rather critical summary of the present situation in antibody imaging; detailing the theoretical background of immunoscintigraphy and how the techniques may improve or not improve in the future. Overall the book is a fairly up-to-date volume on the current "state of the art". Certainly at £128 it is a volume for the library rather than the individual.

RALPH MCCREADY

BIR Bulletin

Honorary Editor, BIR Bulletin: D. Rickards, LRCP, MRCS, FFR(D)SA, FRCR
Please address all correspondence to: Honorary Editor, BIR Bulletin, The British Institute of Radiology,
36 Portland Place, London W1N 4AT

The British Institute of Radiology is not responsible for opinions expressed in the BIR Bulletin

Radiology & Oncology '91

Brighton, 29 April – 1 May 1991

Preview of the 49th BIR Congress

The BIR's annual meeting has grown progressively since the launch of BIR Congresses in the form of international conferences in 1985, the year of Professor Isherwood's Presidency. Advance indications this year are that delegates to the 49th Congress will be offered the most extensive choice ever.

The 1991 meeting in Brighton is structured along similar lines to last year's highly successful Congress in Harrogate, with the Annual Conference of the College of Radiographers in parallel, and with support from the Royal College of Radiologists and the Radiology Section of the Royal Society of Medicine. This meeting again incorporates Med X Ray, the country's largest radiological exhibition. The Brighton Metropole Hotel provides a superb venue — a modern conference centre where all disciplines can meet under one roof and share state-of-the-art information throughout the entire field of the radiological sciences.

The backbone of the meeting is always the proffered scientific presentations, and this year the BIR has accepted more than 240, the largest number ever at a BIR Congress. These are set in a framework of invited reviews by speakers of renown, bringing together in sessions the different disciplines concerned with each subject, a format which proved very successful last year. Sessions range from mainstream subjects like the chest, musculoskeletal imaging, pelvic tumours and brachytherapy to management, audit and para-radiological therapeutic techniques like endoscopic and laser methods. New technology predictably plays a major role, not only in magnetic resonance but also in conventional areas and one session asks, "Are Radiotherapy Machines User-friendly?" There is a tantalizing foretaste of the 1995 Centenary Congress in the session devoted to radiological history. As usual, ultrasound is well represented — this year a whole session is given to Doppler — and new diagnostic and therapeutic uses of isotopes and biological treatments are reviewed. Again "Work in Progress" sessions are provided for preliminary communication of work believed to be important.

Another trend has been the increasing international representation at the Congress. This year, foreign speakers are drawn from fifteen countries, including Eastern Europe, the Far East and the USA.

The 1990 Congress introduced Consensus Workshops, where delegates join with invited speakers in a critical examination of matters of current interest. This year there are two: one a multidisciplinary approach to bone tumours and the other questioning whether radiology departments can be financially viable in the "new NHS" — something which might just be uppermost in people's minds in April! An overview of current practice is provided by Teach-ins, this year covering the paediatric GI tract, brain tumours, gynaecological cancer, lymphoma and brachytherapy. An important innovation of the President's has been the introduction of "Meet the Professor" lunches, a chance for delegates, particularly trainees, to quiz leading experts on any subject of their choice.

But the gemstones of the meeting are undoubtedly the Eponymous Lectures and, as usual, this year's offer the chance to hear speakers of world renown approaching issues which are fundamental to the medical use of radiation. Professor Stanley Dische of Mount Vernon Hospital asks if advances in basic science have benefited patients with cancer, and Professor David Goldenberg of

New Jersey examines advances in diagnostic and therapeutic uses of radiolabelled antibodies. Dr Roger Berry, now of British Nuclear Fuels, tackles the minefield of striking a balance between benefit and risk in exposing man to radiation. In addition, the President has set himself the challenge, as we approach the end of Radiology's first hundred years, of considering the future in relation to the BIR.

The BIR Congress offers chances to share and update, compare notes, explore new areas of interest, or simply to meet one's colleagues in a scientific meeting and in congenial surroundings. In addition, Med X Ray and a social programme which includes good eating, golf, history, music, wine tasting and fishing makes the BIR Congress the UK's festival of the radiological sciences and makes Brighton the place to be in the last week of April.

Stephen Golding
Scientific Programme Chairman

Third Somerset MRI Course

There are two sorts of courses. Those which are worth a week's holiday to attend and those from which you need a week to recover. Even managers can see which is the more cost-effective but the key difference relates to cerebral blood-flow. After two days of the second sort the grey cells are grey particularly around the gills. The first sort contains a carefully balanced mixture, with a lot of cerebral stimulation, some physical exercise and small quantities of vasodilators. The boys from the cider-country got the recipe right at Chepstow. Both the teaching and the facilities at the St Pierre Country Club were excellent.

I am not sure if MR physics is beginning to sink in or if experts' explanations are improving, but Professors Peter Wells and Mike Smith did a good job on the theory, and Jeremy Jenkins and Murray Solomons added a clinical view so that even the physics seemed to only fool some of the people some of the time. Local experts John Bradshaw, Peter Cavanagh, Paul Goddard, George Hartnell, Tim Lewis and Andrew Longstaff, together with Manchester's Jeremy Jenkins, ably covered the application of MR to the various anatomical parts. Professor Graham Bydder (cerebrovascular and degenerative brain disease) Dr Adrian Dixon (knee), Dr Donald Hadley (head trauma), Dr Janet Husband (pelvic cancer) and Dr Peter Phelps, (ENT) presented their own perspective and sometimes unique experience of specialist applications. It may seem invidious to give special mention to one star among such a distinguished group of performers, but for me Dr Murray Solomons from California is a teacher of world class. Dr Solomons has an unusual facility: he lectures very fast but key new concepts emerge from a welter of educational reinforcement at just the right intervals. Only teachers in such international demand know that twelve loaded carousels fit into a duffel-bag which fits into an airliner's luggage rack.

Nothing was bad on the course but there were a few minor imperfections: the St Pierre boasts squash courts, a swimming pool, a golf course and an in-house chapel but no bike shed; the main lecture theatre just accommodated the assembled flock and the seats were a bit hard; tutorials sometimes duplicated lectures and there was no quiz. Medieval Banquets Inc. again demonstrated their skill in not only lowering the lights at the right time to hide the absence of meat on the spare-ribs but also in proffering distracting mead just before the much-heralded medieval pudding turned out to be children's jelly. But these are minor details in an excellent three and a half days. The Somerset Course in Gwent is to MRI what the London Course in Gleneagles is to CT: geographical confusion associated with a major British radiological event. The organizers are to be congratulated.

Brian Witcombe

BIR

Conference Services

Is there a seminar, conference or evening get-together you want to organize, but you don't have the time? The BIR Conference Office may be able to help you. Please call Vanessa Whitehead, Conference Manager, to discuss possibilities.

Lecture, Conference and Meeting Facilities

Available for use at 36 Portland Place, London W1

The BIR Lecture Theatre, with raked seating and extensive audiovisual equipment, accomodates 100 people in air conditioned comfort.

The conference room accommodates a maximum of 34 people with modular furniture which can be arranged to suit the needs of individual users.

For further information please contact the House Manager, British Institute of Radiology, 36 Portland Place, London W1N 4AT. Tel: 071-580 4085.

Library News

The BIR Library is open weekdays 9 a.m.–5 p.m. (7 p.m. on Tuesdays and Thursdays).

Although journals may not be taken out of the library, there is a photocopy service, also available by post or Fax.

Current Journals Held in the Library

- Acta Oncologica
- Acta Radiologica
- Activity. Selectron Brachytherapy Journal
- American Journal of Neuroradiology
- American Journal of Roentgenology
- Annales de Radiologie (France)
- Annals of Nuclear Medicine (Japan)
- Annals of the ICRP
- Applied Health Physics, Abstracts and Notes
- Applied Radiation and Isotopes
- Astro Newsletter
- Australasian Radiology
- BMUS Bulletin
- British Journal of Radiology
- British Medical Bulletin
- British Medical Journal
- British Society of Dental and Maxillofacial Radiology Newsletter
- BSI News
- Cancer
- Cancer Research
- Cancer Research Campaign Annual Report
- Cancer Treatment Reviews
- Cardiovascular and Interventional Radiology
- Cell and Tissue Kinetics
- Chinese Journal of Nuclear Medicine
- Chinese Journal of Radiology
- Clinical Imaging
- Clinical Nuclear Medicine
- Clinical Oncology
- Clinical Physics and Physiological Measurement
- Clinical Radiology
- Computerized Medical Imaging and Graphics
- Current Contents (Life Sciences)
- Current Opinion in Radiology
- Current Problems in Diagnostic Radiology
- Diagnostic Imaging (USA)
- Diagnostica per Immagini (Italy)
- Documents of the NRPB
- European Journal of Cancer and Clinical Oncology
- European Journal of Nuclear Medicine
- European Journal of Radiology
- European Journal of Surgical Oncology
- Excerpta Medica. 14 Radiology
- Gastrointestinal Radiology
- HPA Bulletin
- Health Physics
- IAEA Newsbriefs
- ICRU News
- ISRRT Newsletter
- Indian Journal of Radiology and Imaging
- International Journal of Hyperthermia
- International Journal of Radiation Biology
- International Journal of Radiation Oncology, Biology , Physics
- Journal Belge de Radiologie
- Journal de Radiologie (France)
- Journal Européen de Radiotherapie
- Journal of Clinical Oncology
- Journal of Computer Assisted Tomography
- Journal of Interventional Radiology
- Journal of Medical Imaging
- Journal of Nuclear Medicine
- Journal of Radiological Protection
- Journal of the Canadian Association of Radiologists
- Journal of The National Cancer Institute
- Journal of The Royal Society of Medicine
- Journal of Thoracic Imaging
- Journal of Ultrasound in Medicine
- Lancet
- Magnetic Resonance in Medicine
- Medical Physics
- Medical Radiography and Photography
- Meditsinskaya Radiologiya (USSR)
- NRPB Reports
- Neuroradiology
- Nuclear Medicine and Biology
- Nuclear Medicine Communications
- Pediatric Radiology
- Physics in Medicine and Biology
- Proceedings of The American Association for Cancer Research
- Proceedings of the American Society of Clinical Oncology
- Rad
- Radiation Protection Dosimetry
- Radiation Research
- Radiatsionnaya Biologiya (USSR)
- Radiographics
- Radiography Today
- Radiologia Medica (Italy)
- Radiologic Clinics of North America
- Radiological Protection Bulletin
- Radiology
- Radiology Now
- Radiotherapy and Oncology
- RöFo (Germany)
- Seminars in Interventional Radiology
- Seminars in Nuclear Medicine
- Seminars in Roentgenology
- Seminars in Ultrasound, CT and MR
- Skeletal Radiology
- Strahlentherapie und Onkologie
- Ultrasonics
- Ultrasound in Medicine and Biology
- Urologic Radiology
- Yearbook of Diagnostic Radiology

Recent Additions to the Library

DeSchepper, A. M. A. & Degryse, H. R. M., 1989. Magnetic Resonance Imaging of Bone and Soft Tissue Tumors and Their Mimics.

Dobelbower, R. R. Jr (Ed.), 1990. Gastrointestinal Cancer. Radiation Therapy.

Fukushima, E. (Ed.), 1989. NMR in Biomedicine; the Physical Basis (key papers in physics).

HMSO, 1989. Code of Practice for the Carriage of Radioactive Materials by Road. 17th Impression.

IPSM, 1986–1990. Reports Nos 46–50; 52–55; 57–62.

IRPA, 1988. Radiation Protection Practice, Vols 1–3. Seventh International Congress, Sydney, April 1988.

Suess, M. J. & Benwell-Morison, D. A. (Eds), 1989. Nonionizing Radiation Protection, 2nd edn.

WHO, 1990. Effective Choices for Diagnostic Imaging in Clinical Practice (WHO Technical Report Series, No. 795).

BIR Calendar

Unless otherwise indicated, enquiries about the following events should be addressed to the Conference Manager, British Institute of Radiology, 36 Portland Place, London W1N 4AT (Tel. 071-580 4085).

Radiation Oncology/IPSM
April 10, 1991
All day meeting organized by IPSM

RADIOLOGY AND ONCOLOGY 91 and MED X RAY
29 April–1 May
Metropole Hotel, Brighton
Speakers:
3M Mayneord Memorial Lecture:
Prof. S. Dische
Silvanus Thompson Memorial Lecture:
Dr R. Berry
Presidential Address:
Prof. C. A. Joslin
Mackenzie Davidson Memorial Lecture:
Prof. S. Dische

Radiation Oncology and Radiobiology: Particle Therapy
June 7, 1991
Organizer: Dr R. D. Errington
Speakers: Dr D. Bewley, Dr N. McNally, Prof. G. W. Griffin, Mr J. Hungerford, Dr T. Bates, Dr S. Gore and Prof. J. M. Slater

The New Legislation — Friend or Foe (After the White Paper ... and into Europe)
June 13, 1991
All day meeting organized by the Industry Committee
Chairmen: Prof. C. A. Joslin, Dr O. Craig and Miss D. Rigg
Speakers include Dr J. Roylance, Dr I. Watt, Mr E. Sutherland, Prof. I. Isherwood and Mr P. Richardson

Conversazione
June 27, 1991
Painter's Hall, London
Lecture: " Half an Eye on the Sky", by Sir Stephen Furness.

BIR THE BRITISH INSTITUTE OF RADIOLOGY

YOUR INSTITUTE NEEDS

YOU

TO RECRUIT NEW MEMBERS TO THE BIR

- TELL YOUR COLLEAGUES ABOUT THE BENEFITS OF MEMBERSHIP
  - RECEIVE THE BJR (INCLUDING BIR BULLETIN) FREE MONTHLY
  - DISCOUNT ON BIR MEETINGS AND PUBLICATIONS
  - USE OF WELL STOCKED LIBRARY
  - COMFORTABLE MEMBERS' ROOM
  - ALL NEW MEMBERS RECEIVE A 50% DISCOUNT ON THEIR FIRST YEAR'S SUBSCRIPTION PAYING BY DIRECT DEBIT
- BRING A COLLEAGUE WHEN YOU NEXT ATTEND A BIR MEETING
- INVITE YOUR COLLEAGUES TO JOIN YOU FOR COFFEE IN THE MEMBERS' ROOM

BIR MEMBERSHIP: YOU KNOW IT MAKES SENSE

BY PROPOSING A COLLEAGUE YOU COULD HELP THE INSTITUTE TO DOUBLE ITS MEMBERSHIP

Industry News

Varian Introduce New Device to Shape Radiation Beam

A multileaf collimator (MLC) that will shape the radiation beam of the Clinac accelerator beam to conform to cancer tumours has been introduced by Varian. The device can be fitted to any Varian Clinac 2100C and Clinac 2300C/D radiotherapy accelerator.

The MLC improves dose distribution and increases productivity for busy radiotherapy departments. It has 52 independently motorized, fully retractable leaves and is capable of shaping most treatment fields. With the MLC each new treatment field can be set up in less than 10 seconds. As the tumour shrinks the radiotherapist can shrink the treatment field to match it without making new shielding blocks.

The first commercial MLC is being studied at the Hospital of the University of Pennsylvania with the Royal Marsden Hospital, London being scheduled to receive an MLC along with other leading hospitals worldwide.

For further information contact: Christine Oliver, Varian Medical Equipment, Building 5B, 3045 Hanover Square, Palo Alto CA 94303, USA. Tel. 415 4214 5033.

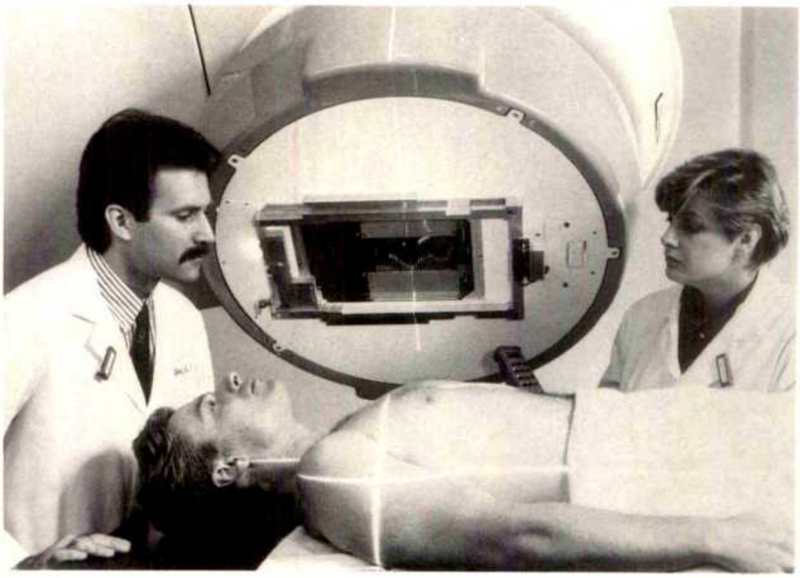

The MLC minimizes patient discomfort and setup time because each treatment field can be set up automatically in less than 10 seconds

---

Acuson Sponsorship for SET Ultrasound Users Group

Acuson are to sponsor exclusively the recently launched South East Thames Ultrasound Users Group.

The group has been formed by Superintendent Radiographers Olwen Clarke (St Thomas') Jill Freeman (King's College) and Sajarta Patel (Guy's) with the aim of promoting good relationships between departments in the region, continued updating of the latest developments in ultrasound technology, and discussion of current and controversial ultrasound issues.

Acuson were approached because their equipment is commonly used by participants and because of their well known commitment to supporting ultrasound education.

The group plans to hold quarterly meetings with regular attendances of 60–70 sonographers from within the South East Thames Health Authority.

For further information contact: Acuson Ltd, Wiltron House, Rutherford Close, Stevenage, Herts SG1 2EF. Tel. 0438 740066.

Radiation Calibration Service Launched

AEA Thermal Reactor Services' NESTOR reactor is providing a new radiation calibration service to quality assurance standards.

NESTOR is a light water cooled, graphite and light water moderated reactor, which operates at a power of up to 30 kW and is used as a source of neutrons for many applications. A particular feature of the reactor is the flexible design of the biological shield which allows it to incorporate a wide range of experimental facilities.

Already three significant contracts have been awarded to NESTOR, including a calibration service to Centronic Ltd, a major worldwide supplier of radiation detection instruments.

For further information contact: Stephen Lyons, Stephen Lyons Associates, 100 Rockingham Close, Gorse Covert, Warrington WA3 6XA.

X ray Film Processor Scanning System in the Palm of your Hand

Quality control checks can be performed in seconds with the new Miniscan X-ray film processor scanning system from Nuclear Associates. It is battery-operated for portability and can store up to 20 sets of sensitometric measurements with data analysis. Results are read on a large LCD display. Miniscan can also be used as a standard transmission densitometer. Connected to any IBM compatible computer the software program will generate comprehensive reports with control charts and corrective action forms.

For further information contact: Nuclear Associates, 100 Voice Road, Carle Place, NY 11514-1593, USA. Tel. 516 741 6360.

BIR Company Subscriber Scheme

The BIR company subscriber scheme is aimed at all companies with an interest in radiology and allied sciences.

For an annual subscription of £275 p.a. member companies are offered an attractive benefits package.

To find out why your company should join the leading edge companies listed below, please contact Mr Tony Hudson, Administration Manager, British Institute of Radiology, 36 Portland Place, London W1N 4AT. Tel: 071-580 4085.

Agfa-Gevaert Ltd
27 Great West Road, Brentford, Middlesex
TW8 9AX.
Tel. 081-560 2131. Product Areas 1. Contact Mr G. Mountford, Director.

American Medical Ltd
PO Box 971, London SW10.
Tel. 071-352 8051. Fax: 071-376 4508.
Product areas 1, 3, 4, 5, 7, 8.
Contact Betsy Riley, Managing Director.

Amersham International PLC
Lincoln Place, Green End, Aylesbury,
Bucks HP20 2TP.
Tel. 0296 395222.
Product areas 4, 5, 6.
Contact Mr James McLaughlin, Sales and Marketing Manager.

Bard Ltd
Forest Houe, Brighton Road, Crawley,
West Sussex RH 11 9BP.
Tel. 0293 27888, ext. 2204.
Product area 2.
Contact Peter Dekkers, Product Manager.

British Nuclear Fuels plc
Room 525, Hinton House, Risley, Warrington, Cheshire WA3 6AS.
Tel. 0925 835022.
Product areas 8, 11. Contact Dr R. J. Berry, Director of Health and Safety and Environmental Protection.

Bruel & Kjaer (UK) Ltd
92 Uxbridge Road, Harrow, Middlesex,
HA3 6BZ.
Tel. 081-954 2366.
Product areas 3, 6.
Contatct Mr Dennis Lewis, Sales Manager.

Calumet Coach Co.
33 Shallbourne Rise, Camberley GU1J
2EJ. Tel. 0276 64490.
Product areas: 1, 4, 5.
Contact Mr P. Supple, Managing Director of International Operations.

Cardiac Services Ltd
95A Finaghy Road, South Belfast BT10
OBY. Tel. 0232-625566.
Product areas 1, 3, 4, 5, 6.
Contact Mr R. J. Brown. Managing Director.

Cea (UK) Ltd
Nissen House, Grovesbury Road,
Leighton Buzzard, Bedfordshire
LU7 8SS.
Tel. 0525 382529. Fax: 0525 372619.
Product areas 1, 3, 4, 5, 6.
Contact John Dunster, Managing Director.

Du Pont (UK) Ltd
Wedgwood Way, Stevenage, Hertfordshire SG1 4QN. Tel. 0438 734000.
Product areas 1, 3, 4, 5, 6, 7, 9 and 10.
Contact Mr E. G. Lovat, Product Manager, Diagnostic Imaging.

E. G. & G. Limited
Vale Road, Windsor, Berkshire SL4 5JP.
Tel. 0753 855611.
Product areas 1, 6, 7, 8.
Contact Miss Susan Holgate, Sales Executive (Therapy).

Elscint (GB) Ltd
Colonial Business Park, Colonial Way,
Watford, Herts WD2 4PT.
Tel. 0923 39511.
Product areas 1, 3, 4.
Contact Faith Gorman, Marketing Manager.

E-Z-EM Ltd
1230 High Road, Whetstone, London N20.
Tel. 081-446 9714.
Product areas 1, 2, 8.
Contact Richard Bayliss, Sales and Marketing Manager.

Fuji Photo Film (UK) Ltd
125 Finchley Road, London
NW3 6JH. Tel. 071-586 9351.
Product areas 1, 3.
Contact Mr R. G. Brown, Marketing and Administration Manager.

Gammex-RMI Ltd
34 Shakespeare Street, Nottingham
NG1 4FQ. Tel. 0602 483807.
Product areas 1, 3, 4, 5, 6.
Contact Miss Eileen Parr, Commercial Manager.

IGE Medical Systems Ltd
352 Buckingham Avenue, Slough, Berks
SL1 4ER. Tel. 0753 874000.
Product areas 1, 2, 3, 4, 5, 6, 8, 9.
Contact Jill Mitchell, UK Sales Support.

Kodak Ltd
PO Box 66, Station Road, Hemel
Hempstead, Herts HP1 1JU.
Tel. 0442 61122.
Product area 1.
Contact Mr P. E. Blackwell, Manager, Health Sciences Division.

Lanmark
PO Box 317, Beaconsfield, Bucks
HP9 2LR.
Tel. 0494 791615/670586.
Product areas 1, 3, 4, 5, 9, 10, 15, 16.
Contact Liz Beckmann, Director.

3M UK PLC
3M House, Bracknell, PO Box 1,
Berks RG12 1JU.
Tel. 0344 426726.
Product area 1.
Contact Mr Alan Budge, Marketing Manager.

Mallinckrodt Diagnostica (UK) Ltd
11 North Portway Close, Round Spinney,
Northampton NN3 4RQ.
Tel. 0604-46132.
Product areas 4, 5.
Contact Mr D. G. L. Wood, Business Manager.

M. A. S. Medical Ltd
Armytage Road, Brighouse, West Yorkshire HD6 1QF. Tel. 0484 721906.
Contact Martin York, Managing Director.

Meadox (UK) Ltd
Matthew House, Matthew Street, Dunstable LU6 1SD.
Tel. 0582 605111.
Product area 2.
Contact Mrs Sheila Heap, Sales and Marketing Manager.

Medical Xray Supplies Ltd
Unit 12, Kingsbury Industrial Estate, Church Lane, Kingsbury, London NW9 8AU. Tel. 081-205 9500.
Product area 1.
Contact Mr R. J. Laird, Sales Director/Mr K. Wartnaby, Managing Director.

Mitsubishi Electric UK Ltd
Travellers Lane, Hatfield, Herts AL10 8XB.
Tel. 07072 78756.
Product area 14.
Contact T. F. McCloud, Sales and Marketing Manager.

National Power plc
14 Newgate Street, London EC1A 7AM.
Tel: 071-634 6898.
Product areas 7, 8.
Contact Mr A. J. Swanson, Assistant Company Secretary.

KEY TO PRODUCT/SERVICE AREAS

1: Diagnostic X-ray including NMR and CT
2: Interventional radiology
3: Ultrasound
4: Nuclear medicine
5: Radiopharmaceuticals
6: Radiotherapy and oncology
7: Radiobiology
8: Radiation protection
9: PACS
10: Image processing
11: Nuclear fuel cycle services
12: Quality assurance.
13. Radiology data management computer systems
14. Video printing
15. Equipment leasing
16. Hospital-shared services

Nuclear Associates
100 Voice Road, Carle Place, New York 11514-1593, USA.
Tel. 516-741 7614.
Product areas 1, 3, 4, 5, 6, 8.
Contact Mr H. Glasser, General Manager.

Nucletron Trading Ltd
Nucletron House, Tarporley Business Centre, Tarporley, Cheshire, CW6 9UY.
Tel: 0829 733611.
Product areas 6, 8.
Contact Mrs Marilyn A. Hart, Office Manager.

Nycomed (UK) Ltd
Nycomed House, 2111 Coventry Road, Sheldon, Birmingham B26 3EA. Tel. 021-742 2444.
Product areas 1, 3.
Contact Mr L. Birch Hansen, Managing Director.

Oxford Magnet Technology
Wharf Road, Eynsham, Oxford.
Tel. 0865 880880.
Product area 1.
Contact Pauline Hobday, Director of Sales and Marketing.

Philips Medical Systems
Kelvin House, 63–75 Glenthorne Road, Hammersmith, London W6 OLJ. Tel. 081-741 1666.
Product areas 1, 3–8.
Contact J. M. Woolston, Sales and Marketing Manager.

Polaroid (UK) Ltd
Ashley Road, St Albans, Herts AL1 5PR.
Tel. 0727 59191.
Product areas 1, 3.
Contact David Hollingworth, Marketing Manager.

Premise Engineering Ltd
Tibbs Hill Road, Abbots Langley, Watford, Herts WD5 ODR.
Tel. 09277-67433/63320.
Product area 8.
Contact Mr R. K. Beach, Director.

Radiological Protection Services Ltd
61 Lind Road, Sutton, Surrey SM1 4PP.
Tel. 081-643 6374.
Product area 8.
Contact B. H. Cutting, Managing Director.

Quantel Ltd
Administration Centre, Kiln Road, Newbury, Berkshire RG13 2HA.
Tel. 0444 232323.
Product areas 2, 10.
Contact Mr Christopher Trim, Publicity Officer.

Schering Health Care Ltd
The Brow, Burgess Hill, West Sussex RH15 9NE.
Tel. 0444 232323.
Product areas 1, 2, 3.
Contact Mr Simon Higginbotham or Mr S. Hearne, Product Managers.

Siemens plc
Siemens House, Windmill Road, Sunbury on Thames, Midlesex.
Tel. 0932 752334.
Product areas: 1, 2, 3, 4, 6, 8, 9, 10, 13, 14, 15.
Contact L. J. McFadyen, Marketing Assistant.

Sony (UK) Ltd
Jays Close, Viables, Basingstoke, Hants RG22 4SB.
Tel. 0256 483564.
Product area 14.
Contact Richard Holt, Marketing Manager.

Toshiba Medical Systems UK
Manor Court, Manor Royal, Crawley, West Sussex RH10 2PY.
Tel. 0293 560772.
Product areas 1, 2, 3, 4, 9, 10.
Contact Mr S. M. Weeden, Manager X-ray Products.

Toshiba Medical Systems Europe BV
Schieweg 1, 2627 An Delft, The Netherlands. Tel. 015 61 0121.
Product areas 1, 2, 3, 4, 9, 10.
Contact Mr P Blonk, Office Manager, X-ray BU.

X-rite (H. Miller Graphics Ltd)
8 Moody Street, Congleton, Cheshire CW12 4AP. Tel. 0260 279988.
Product areas 1, 12.
Contact Mrs P. Dhanani, Medical Sales.

Wardray Products Ltd
Hampton Court Estate, Summer Road, Thames Ditton, Surrey KT7 OSP. Tel. 081-398 9911.
Product area 8.
Contact Mr R. B. Wardley, Managing Director.

Meetings and Courses

As a service to our readers, notice of meetings or courses will be inserted free of charge. Please send full details to the Honorary Editor, BIR Bulletin.

HC91 — Healthcare Computing 1991
March 25–27, 1991
Harrogate
Further details: Mrs Judy Hayes, Conference Administrator, 3 Beech Avenue North, Worcester, WR3 8PX. Tel: 0905 755051. Fax: 0905 56817.

Tumor Response Monitoring and Treatment Planning
April 1–13, 1991
Munich, FRG
Further details: GSF Kongressdienst, Ingolstädter Landstrasse 1, D-8042 Neuherberg, Federal Republic of Germany. Tel: (089) 31872669. Fax: (089) 31873362.

The 1991 International Symposium on Radon and Radon Reduction Technology. "A New Decade of Progress"
April 2–5, 1991
Philadelphia, USA
Further details: Pat Heightchew, CRCPD, 205 Capital Avenue, Frankfort, KY 40601, USA. Fax: (502) 227-7862.

23rd International Diagnostic Course
April 6–13, 1991
Davos, Switzerland
Further details: Medical Congress Management, PO Box 2, CH-8029, Zürich, Switzerland. Tel: (01) 255 19 15. Fax: (01) 261 05 78.

The London/Bart's FRCR Part 1 — Revision Course
April 11–12, 1991
London
Further details: Dr P. Butler, Department of Neuroradiology, The Royal London Hospital, Whitechapel, London E1 1BB. Tel: 071-377 7164.

British Nuclear Medicine Society
April 15–17, 1991
London
Further details: Wisepress Book Exhibitions, 59 Revelstoke Road, Wimbledon Park, London SW18 5NJ. Tel: 081-947 8775. Fax: 081-879 3326.

Marie Curie Memorial Foundation Second International Cambridge Conference on Breast Cancer Screening
April 15–17, 1991
Cambridge
Further details: International Cambridge Conference on Breast Cancer Screening, Education Department, 11 Lyndhurst Gardens, London NW3 5NS. Tel: 071-435 4305.

Fundamentals of Medical Ultrasonics
April 17–19, 1991
London
Further details: Mr K. N. Humphries, Wolfson Conference Centre, Royal Postgraduate Medical School, Hammersmith Hospital, Du Cane Road, London W12 0NN.
Tel: 081-743 2030 Ext 2210.

Joint RCR/RCGP Meeting "Radiology in Practice"
April 23, 1991
London
Further details: The Conference Office, The Royal College of Radiologists, 38 Portland Place, London W1N 3DG.
Tel: 071-636 4432. Fax: 071-323 3100.

Interhospital 91
April 23–26, 1991
Dusseldorf, Germany
Further details: Monika Waraczynski, Dusseldorfer Messegesellschaft mbH, Postfach 320203, Stockumer Kirchstraße 61, D-4000 Dusseldorf 30. Tel: (0211) 4560543.

Advances in Hip and Knee Arthroplasty
April 25–27, 1991
Virginia, USA
Further details: Conference Coordinator, The Johns Hopkins Medical Institutions Office of Continuing Education, Turner 20, 720 Rutland Avenue, Baltimore, MD 21205-2195. Tel: (301) 955-2959.

8th International Workshop on Bone Dosimetry
April 28–May 2, 1991
Bad Reichenhall, Germany
Further details: Dr Deiter Felsenberg, Freie Universität Berlin, Klinikum Steglitz, Hindenburgdamm 30, D-1000 Berlin 45, Germany.

Radiology and Oncology 91
April 29–May 1, 1991
Brighton
Further details: The Conference Office, The British Institute of Radiology, 36 Portland Place, London W1N 4AT.
Tel: 071-580 4085.

Gaia European overview on Ultrasound from Diagnosis and Intervention to treatment
May 31–June 2, 1991
Vila Nova Gaia, Portugal
Further details: Ms Anabela Menezes, Dept of Imagiology and Intervention Radiology, Santos Silva Hospital, 4400 Vila Nova Gaia, Portugal. Tel: 782 0418.

The 2nd International Conference of the Kenya Association of Radiologists
August 7–9, 1991
Nairobi, Kenya
Further details: Dr J. K. Kitonyi, Conference Secretary, Department of Diagnostic Radiology, University of Nairobi, PO Box 19676, Nairobi, Kenya. Tel: 724722. Fax: 340969.

6th World Congress in Ultrasound
September 1–6, 1991
Copenhagen, Denmark
Further details: Torben Larsen, Department of Gynecology, Herlev Hospital, DK-2730 Herlev, Denmark.

European Congress of Radiology '91
September 15–20, 1991
Vienna, Austria
Further details: The Congress Secretariat ECR '91, c/o Vienna Academy of Postgraduate Medical Education and Research, Alser Straße 4, A-1090 Vienna, Austria. Tel: (1) 421383. Fax: (1) 42138323.

Dublin 91: Annual Scientific Meeting and Exhibition
September 25–28, 1991
Dublin, Ireland
Further details: The Conference Office, The Royal College of Radiologists, 38 Portland Place, London, W1N 3DG.
Tel: 071-636 4432. Fax: 071-323 3100.

How to detect and to Characterise the Microcalcifications?
October 10, 1991
France
Further details: M. J. Rodiere, Institut D'Imagerie Medicale, Miniparc - Bat 2, Rue de la Croix Verte, 34090 Montpellier, France.

International Symposium on Recent Advances in Diagnostic Imaging and Radiation Oncology
March 24–27, 1992
Kathmandu, Nepal
Further details: Dr Naresh Prasad, Department of Radiology, Baylor College of Medicine, Houston, Texas 77030, USA. Tel: (713) 798 4415.
Fax: (713) 798 5556.

BIR Bulletin

Honorary Editor, BIR Bulletin: D. Rickards, LRCP, MRCS, FFR(D)SA, FRCR
Please address all correspondence to: Honorary Editor, BIR Bulletin, The British Institute of Radiology,
36 Portland Place, London W1N 4AT
The British Institute of Radiology is not responsible for opinions expressed in the BIR Bulletin

Preliminary Report of the Rare Earth Screens Working Party

Diagnostic Methods Committee

New initiatives from the Department of Health, the requirements of the Ionising Radiations (Protection of Persons Undergoing Diagnosis or Treatment) Regulations 1988 (Statutory Instrument No. 778 of 1988), the Health Services Management Circular HC(89)18, and the working document from the CEC study group on Quality Criteria for Diagnostic Radiographic Images published in February 1989 have led to the need for a reappraisal of the extent to which rare earth screens are used in the UK and of the diagnostic quality of the images obtained with them.

The Rare Earth Screens Working Party of the BIR was accordingly asked to carry out a survey to ascertain the present position, in particular to establish what trends, if any, have taken place since the survey carried out by the Department of Health in 1979, and to assess the extent to which radiology departments in the UK are complying with the legislation mentioned above in respect of the ALARA principle, and, in cases where rare earth screens are not being used, to endeavour to find the reasons behind the decision not to adopt the new technology.

The difficulties which arose in the collection of these data had not been anticipated by the Working Party, and were largely due to the difficulty of targeting the appropriate person in each department, and determining to which departments the questionnaire should be directed. It appears that there is no central body that keeps a register, for example, of district superintendent radiographers in England and, in fact, many health authorities do not designate staff as district superintendents. Many avenues of approach were followed, including the direct approach in cases where appropriate names were known to members of the Working Party, and also through health authorities themselves. These various approaches that we used may have led both to duplications and omissions and in any such case, the Working Party expresses its sincere regrets. One lesson which may have been learned is the need for a defined communication network. It was originally agreed to target hospitals in England and it was hoped to have the results back by June 1990. Owing to communication difficulties, the returns did not materialize in the hoped-for numbers until September. From the lessons learned from the attempts made to contact the appropriate people in X-ray departments in England, a different approach was adopted in the case of Wales and all hospitals believed to have an X-ray department were approached direct, but again omissions and duplications may have occurred. In October, at a meeting of the BIR at which the preliminary results were reported, Dr R. H. Corbett of Hairmyres Hospital, East Kilbride, kindly offered to circulate the questionnaire to Scottish hospitals.

This preliminary report from the Working Party is intended to present a broad picture of the data which has been received, without any attempt to analyse the comments made by participants. Although, on the whole, the reports given of the results obtained by rare earth screens are good and the rejection rate is low, few attempts have been make to carry out any dosage surveys before and after the adoption of rare earth screens.

The survey was undertaken because of a widely held belief, particularly among some industrialists, that the take-up of rare earth screens in UK X-ray departments was disappointingly low. The results of this survey show most effectively that this is not the case; however, there is a school of thought that suggests that the non-users of rare earth screens may lurk among those who, for one reason or another, did not participate in the survey.

Nevertheless, the feeling of the Working Party is that the results indicate that the take-up of rare earth screens in X-ray departments in the UK is now excellent, and this view is further strengthened by statements made by many departments not already using rare earth screens that they were shortly going to make the change in a number of cases where departments were being re-equipped.

The Rare Earth Screens Working Party considers that future attention should be directed to other ways in which patient dose can be reduced, always remembering that occupational dose largely results from secondary radiation, so that reduction in patient dose results in reduction in staff dose. The areas to be addressed include the use of carbon fibre cassettes and table tops, and also a study of other low-attenuation materials for these purposes, together with the extent to which the recommendations made in the joint RCR/NRPB publication *Patient Dose Reduction in Diagnostic Radiology* (1990) are being adopted.

Dr N. Slark of the Department of Health suggested that an assessment of the completeness of the survey carried out by the Rare Earth Screens Working Party should be carried out by comparing the number of known X-ray rooms in health authority regions in England and Wales with the numbers of rooms in each region in respect of which returns have been made. Twelve regions in England provided the DoH with information that they have 2795 X-ray rooms in use, and Wales has 275 rooms, a total of 3070 rooms. The returns for the 12 English regions covered a total of 1379 rooms and 92 rooms for Wales, so that the percentage response was 49.3% and 33.5%, respectively.

The Rare Earth Screens Working Party of the BIR extends its grateful thanks to the Department of Health, Scientific and Technical Branch, for its generous contribution towards the postal costs involved in carrying out the above survey. It is hoped that a more complete account of the results of the survey will be published when the many and various comments have been analysed. It only remains to thank all the individuals and departments who responded to the questionnaire circulated and to express our sincere regrets to all those who would have liked to participate but who, for one reason or another, we were unable to reach. Particular thanks are due to Mrs Janet Fish and Miss Amanda Dando, who dealt with the considerable amount of secretarial work involved in a survey of this type, and to Mr David Kear who helped analyse the returns from the English regions.

The members of the Rare Earth Screens Working Party are Dr Alastair Gale, Mr Derek Gifford, Miss Phyllis Hoffman, Miss Pamela Kimber, Dr Barry Moores and Dr Iain Watt.

DEREK GIFFORD

Reference

RCR/NRPB, 1990. *Patient Dose Reduction in Diagnostic Radiology. Documents of the NRPB, Vol. 1, No. 3* (HMSO, London).

COUNTRY			ENGLAND	Percentage of totals	SCOTLAND	Percentage of totals	WALES	Percentage of totals
No. of forms sent out			232		38		35	
No. of returns			139	59.9%	34	89.5%	11	31.4%
No. of hospitals			374		99		35	
No. of X-ray rooms	Total		1589		360		92	
	No. using rare earth screens		1496	94.1%	325	90.3%	89	96.7%
	No. not using rare earth screens		93	5.9%	35	9.7%	3	3.3%
No. of Patients	Total In-patients		2888981		614304		146390	
	Total Out-patients		9027579		1529415		498142	
	Rare earth screens used	In-patients	2752582	95.3%	556906	90.6%	144255	98.5%
		Out-patients	8689371	96.3%	1397463	91.4%	479132	96.2%
	Rare earth screens not used	In-patients	136399	4.7%	57398	9.3%	2135	1.5%
		Out-patients	338208	3.7%	131952	8.6%	19010	3.8%

We regret to announce the death of BIR Non-Medical Honorary Editor Dr N. J. McNally who died on 24 March 1991. He will be sadly missed. A full obituary will be published in the next bulletin.

BIR AWARDS 1991

Barclay Prize

The Barclay Prize is awarded to Professor Isherwood and his team at the University of Manchester for their pioneering contributions to diagnostic radiology published in the BJR and through other routes, particularly in the fields of CT and MRI.

Röntgen Prize

The Röntgen Prize is awarded to Dr T. E. Wheldon, BSc, PhD, F Inst. Phys. at the Cancer Research Campaign's Beatson Laboratories, University of Glasgow, for his contribution to the BJR over many years in the fields of tumour and normal tissue radiobiology as applied to the improved effectiveness of radiotherapy.

Barclay Medal

The Barclay Medal is awarded to Professor John Mallard, PhD, DSc, F Inst. P., FIEE, FRC Path, FRSE at the University of Aberdeen for his wide-ranging contributions over many years to the BJR, and to radiological science in general, particularly in his pioneering work in radioisotope imaging and tomography and in NMR imaging and tissue characterization.

New BIR Members

Medical

Dr Kathryn J. **Aitken**, MB, ChB FRCR (London), Diagnostic Radiologist

Dr Elizabeth **O'Grady**, MB, ChB (Liverpool), Diagnostic Radiologist

Dr Joseph G. **Rajendran**, MB, BS, DMRT, MD (Barbados), Radiotherapist, Oncologist

Dr David A. **Robinson**, MB, BCh, BSc, MRCP, FRCR (Gwent), Diagnostic Radiologist

Prof. Dr Ilkka **Suramo**, Specialist Diagnostic Radiology, MD (Finland), Diagnostic Radiologist

Dr Martin J. **Warren**, BSc, MB, BS, MRCP, FRCR (Oxford), Diagnostic Radiologist

Non-Medical

Mr Michael **Byrom** (Executive), Data-Med Computer Services

Mr Peter M. **Halston**, BSc (Stoke-on-Trent), Physicist

Mr Cyril C. **Nimmon**, BSc (London), Physicist

Mr Simon R. **Pinner** (Hatfield, Herts), Mitsubishi Electric UK Ltd

Dr Michael D. **Short**, BSc, PhD, C Phys, F Inst P, FIPSM (London), Physicist

Mrs Nicola M. **Strother Smith**, DCR (T) (Colchester, Essex), Radiographer

Company Profiles

We hope that the Company profile will become a regular and useful feature in the BIR Bulletin.

Upon enrolling in the Company Subscriber Scheme member companies are asked to submit a short profile of the company, about 300–500 words long.

All existing members are invited to submit a profile for publication subject to editorial discretion.

Further details on the Company Subscriber Scheme in general and on Company Profiles in particular may be obtained from Tony Hudson at the BIR.

Tel: 071-580 4085 or Fax: 071-255 3209.

BIR Calendar

Unless otherwise indicated, enquiries about these events should be addressed to the Conference Manager, British Institute of Radiology, 36 Portland Place, London W1N 4AT (Tel. 071-580 4085).

Radiation Oncology and Radiobiology: Particle Therapy
June 7, 1991
Organizer: Dr R. D. Errington
Speakers: Dr D. Bewley, Prof. G. W. Griffin, Mr J. Hungerford, Dr T. Bates, Dr S. Gore and Prof. J. M. Slater

The New Legislation — Friend or Foe (After the White Paper ... and into Europe)
June 13, 1991
Scientific Lecture Theatre
All day meeting organized by the Industry Committee
Chairmen: Prof. C. A. Joslin, Dr O. Craig and Miss D. Rigg
Speakers include Dr J. Roylance, Dr I. Watt, Mr E. Sutherland, Prof. I. Isherwood, Mrs S. Williams and Mr P. Richardson

Conversazione
June 27, 1991
Painter's Hall, London
Lecture: "Half an Eye on the Sky", by Sir Stephen Furness

MRI Meeting
October 16, 1991
Organizer: Professor B. S. Worthington

Brachytherapy — The past, present and future
October 23 and 24, 1991
Institution of Electrical Engineers
(Meeting to be held in association with Nucletron Ltd)

Hypoxic cell sensitizers: do they have a future?
November 15, 1991
Organizer: Dr R. Camplejohn

Radiosensitivity
February 11, 1992
Joint BIR/RCR meeting

Product News

Local MP attends handover of new X-Ray room at Lewisham

Joan Ruddock, MP for Lewisham, shown at the recent handover of the Philips Integris I 2000 system at Lewisham General Hospital, the first such digital imaging system in the UK.

The system is ideally suited to both interventional vascular and non-vascular procedures.

For further information contact Anita J. Littlechild, Marketing Communications, Tel. 081-741 1666

Left to right, MIss Sue Simmons, Superintendent Radiographer, Mrs Val Martin, Unit General Manager, Mr Karl Blight, Philips Medical Systems, Mrs Joan Ruddock, MP for Lewisham and Deptford, Mr Tom Black, Philips Medical Systems, Dr Charles Bradshaw, Director of Radiology, Mrs Christine Gill, Philips Medical Systems, Southern Region Branch Manager.

Nuclear Associates launch new fluoroscopic QC test tool

This new test tool helps achieve optimum image quality by providing a precise, accurate, easy-to-use means of quickly checking the image quality of permanent and mobile systems (including video tape recorders and last-image-hold systems). It consists of light and dark low contrast test objects for monitor adjustment, copper mesh for image sharpness, and resolution pattern for system resolution.

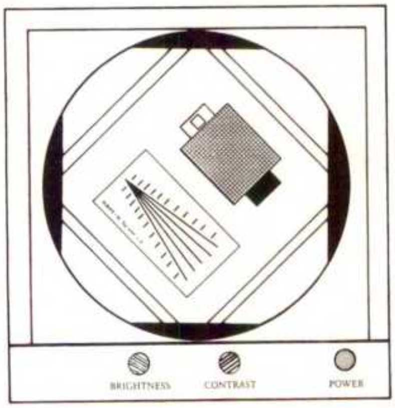

New From Wallac Ltd — CT Bone Scanner

A new high resolution CT scanner developed by Stratec Electronik GmbH is now available from Wallac Ltd. Bone sections and structures at the distal end of the radius and ulna (or tibia and fibula) can be evaluated using Quantatative CT permitting selective determination of the bone density in both the cortical and trabecular area.

Specification of bone density is made either as a unit of linear attenuation (1/cm) not requiring calibration, or as a calibrated mineral content (g/cm^3). The new technique permits higher reproducibility (VC<1% *in vivo*) with a very short measuring time of less than 2 minutes and a total examination period of around 8–12 minutes.

For more information contact Wallac Ltd, Crown House, Kings Road West, Newbury, Berks RG14 5BY.
Tel. 0635 49429

New spinal needle lowers incidence of post lumbar puncture headaches

The Sprotte Atraumatic Spin Needle is a new spinal needle, designed to lower the incidence of post lumbar puncture headaches, is now available from Rusch UK.

The new needle is the result of a 6 year test period with 34950 applications in spinal anaesthesia, diagnostic lumbar puncture, peridural anaesthesia, plexus anaesthesia, peripheral nerve blocks and lumbar sympathetic and celiac plexus blocks. Post spinal headache was observed following 0.02% of punctures (7175 patients).

The needle has a blunt tip which separates the dura fibres rather than cutting. As a result, on removal of the needle the dural tap will close the CSF. The diameter of the lateral eye is greater than the internal diameter of the needle thus allowing a more rapid backflow of CSF and easy injection of contrast media.

For more information contact: Milena Duvnjak, Rusche UK, Freepost, High Wycombe, Bucks HP12 3BR Tel. Freephone 0800 581121

3M Laser at Lister Hospital

The Queen Mother recently opened the new Medical Imaging Department at the Lister Hospital, Stevenage. Here she is shown in the CT Scanner's control room taking to Dr Peter Brooks, Consultant Radiologist (R). In the background are Dr Richard Lee (L), and Dr John Beales.

For further information contact Chris Varian, 3M . Tel. 0344 58799

New automatic injector for CT enhancement

The AS200 from Nycomed is believed to be the first automatic double-headed contrast medium injector designed specifically for CT. Two injection heads are better than one because of the flexibility offered by the pair of programmable syringes. For instance, the first syringe can be loaded with contrast, the second with saline and the two operated in sequence without the radiologist having to leave the control room. The AS 200 is a very straightforward device available at a low price.

For further information contact: Linda Stuttard, Nycomed (UK) Ltd, Nycomed House 2111 Coventry Road, Birmingham B26 3EA. Tel: 021-742 2190

The injector head of the AS200 contrast medium injector.

Medicine and Management Publications

The following reports are now available from Trent Health Authority, Commercial Department, Fulwood House, Old Fulwood Road, Sheffield S10 3TH

Imaging, mammography, MR and CT scanning, ultrasound, stereotactic radiosurgery, childhood leukaemia, osseointegrated dental implants. £5.00

Magnetic resonance spectroscopy, monoclonal antibodies, the physiology of exercises, hypertension. £10.00

Screening for colo-rectal cancer, therapeutic vascular embolism, utilisation modelling, risk limitation in anaesthesia, pain services. £10.00

CNSoftware has been appointed the European distributor of the Multidimensional Medical Imaging Software Analyze developed at the Mayo Foundation by Dr Richard Robb and co-workers.

Analyze provides a complete environment for display and analysis of medical image data as both 2-D slices and 3-D volume rendered images. Images captured from MRI, CT X-ray, SPECT, ultrasound, digital microscopy and angiography may be imported into the package which runs on standard UNIX Workstations (SUN Sparc and Silicon Graphics personal IRIS).

For more information contact CNSoftware Ltd, Stane Vue, Horsham Road, Capel, Dorking, Surrey RH5 5JH. Tel/Fax: 0306 713303.

Conference Services

Is there a seminar, conference or evening get-together you want to organise, but you don't have the time? The BIR Conference Office may be able to help you. Please call Vanessa Whitehead, Conference Manager, to discuss possibilities.

071-580 4085

BIR Company Subscriber Scheme

The BIR company subscriber scheme is aimed at all companies with an interest in radiology and allied sciences.

For an annual subscription of £275 p.a. member companies are offered an attractive benefits package.

To find out why your company should join the leading edge companies listed below, please contact Mr Tony Hudson, Administration Manager, British Institute of Radiology, 36 Portland Place, London W1N 4AT. Tel: 071-580 4085.

AEA Technology
Wigshaw Lane, Culcheth
WA3 4NE. Tel. 0925-252000 Ext. 4206
Product areas 7, 8.
Contact Mr J. G. Tyror, Director of Safety.

Agfa-Gevaert Ltd
27 Great West Road, Brentford, Middlesex
TW8 9AX. Tel. 081-560 2131.
Product Areas 1.
Contact Mr G. Mountford, Director.

American Medical Ltd
PO Box 971, London SW10.
Tel. 071-352 8051. Fax: 071-376 4508.
Product areas 1, 3, 4, 5, 7, 8.
Contact Betsy Riley, Managing Director.

Amersham International PLC
Lincoln Place, Green End, Aylesbury, Bucks HP20 2TP. Tel. 0296 395222.
Product areas 4, 5, 6.
Contact Mr C. M. T. Medley, Sales and Marketing Manager.

Bard Ltd
Forest Houe, Brighton Road, Crawley, West Sussex RH 11 9BP.
Tel. 0293 27888, ext. 2204.
Product area 2.
Contact Peter Dekkers, Product Manager.

British Nuclear Fuels plc
Room 525, Hinton House, Risley, Warrington, Cheshire WA3 6AS.
Tel. 0925 835022.
Product areas 8, 11.
Contact Dr R. J. Berry, Director of Health and Safety and Environmental Protection.

Bruel & Kjaer (UK) Ltd
92 Uxbridge Road, Harrow, Middlesex, HA3 6BZ. Tel. 081-954 2366.
Product areas 3, 6.
Contatct Mr D. Lewis, Sales Manager.

Calumet Coach Co.
33 Shallbourne Rise, Camberley GU1J 2EJ. Tel. 0276 64490.
Product areas: 1, 4, 5.
Contact Mr P. Supple, Managing Director of International Operations.

Cardiac Services Ltd
95A Finaghy Road, South Belfast
BT10 OBY. Tel. 0232-625566.
Product areas 1, 3, 4, 5, 6.
Contact Mr R. J. Brown. Managing Director.

Cea (UK) Ltd
25 Presley Way, Crownhill,
Milton Keynes MK8 0ES
Tel. 0908 263090. Fax: 0908 263546.
Product areas 1, 3, 4, 5, 6.
Contact John Dunster, Managing Director.

Clinical Press Ltd
Redland Green Farm, Redland, Bristol BS8 7HF. Tel. 0272 420526.
Product area 17.
Contact Dr Paul Goddard, Chairman.

Data-Med Computer Services Ltd
10 Faraday Building, Highfields Science Park, University Boulevard, Nottingham NG7 2QP.
Tel. 0602 431431. Fax: 0602 430782.
Product area 13.
Contact Mr C. Fields, Sales Manager.

Du Pont (UK) Ltd
Wedgwood Way, Stevenage, Hertfordshire SG1 4QN.
Tel. 0438 734000.
Product areas 1, 3, 4, 5, 6, 7, 9 and 10.
Contact Mr E. G. Lovat, Product Manager, Diagnostic Imaging.

E. G. & G. Limited
Vale Road, Windsor, Berkshire SL4 5JP.
Tel. 0753 855611.
Product areas 1, 6, 7, 8.
Contact Mr Roy Hauton, Sales Executive (Therapy).

Elscint (GB) Ltd
Colonial Business Park, Colonial Way, Watford, Herts WD2 4PT.
Tel. 0923 39511.
Product areas 1, 3, 4.
Contact Faith Gorman, Marketing Manager.

E-Z-EM Ltd
1230 High Road, Whetstone, London N20.
Tel. 081-446 9714.
Product areas 1, 2, 8.
Contact Richard Bayliss, Sales and Marketing Manager.

Fuji Photo Film (UK) Ltd
125 Finchley Road, London
NW3 6JH. Tel. 071-586 9351.
Product areas 1, 3.
Contact Mr R. G. Brown, Marketing and Administration Manager.

Gammex-RMI Ltd
34 Shakespeare Street, Nottingham
NG1 4FQ. Tel. 0602 483807.
Product areas 1, 3, 4, 5, 6.
Contact Miss Eileen Parr, Commercial Manager.

IGE Medical Systems Ltd
352 Buckingham Avenue, Slough, Berks
SL1 4ER. Tel. 0753 874000.
Product areas 1, 2, 3, 4, 5, 6, 8, 9.
Contact Jill Mitchell, UK Sales Support.

Kodak Ltd
PO Box 66, Station Road, Hemel Hempstead, Herts HP1 1JU.
Tel. 0442 61122.
Product area 1, 3, 4, 6, 8, 9, 12, 13, 14, 15
Contact Mr J. J. G. Tweed, Manager, Health Sciences Division.

Lanmark
PO Box 317, Beaconsfield, Bucks
HP9 2LR. Tel. 0494 791615/670586.
Product areas 1, 3, 4, 5, 9, 10, 15, 16.
Contact Liz Beckmann, Director.

3M UK PLC
3M House, Bracknell, PO Box 1,
Berks RG12 1JU. Tel. 0344 426726.
Product area 1.
Contact Mr Alan Budge, Marketing Manager.

Mallinckrodt Diagnostica (UK) Ltd
11 North Portway Close, Round Spinney, Northampton NN3 4RQ. Tel. 0604-46132.
Product areas 4, 5.
Contact Mr D. G. L. Wood, Business Manager.

M. A. S. Medical Ltd
Armytage Road, Brighouse, West Yorkshire HD6 1QF. Tel. 0484 721906.
Contact Martin York, Managing Director.

Meadox (UK) Ltd
Matthew House, Matthew Street, Dunstable LU6 1SD. Tel. 0582 605111.
Product area 2.
Contact Mrs Sheila Heap, Sales and Marketing Manager.

Medical Xray Supplies Ltd
Unit 12, Kingsbury Industrial Estate, Church Lane, Kingsbury, London NW9 8AU. Tel. 081-205 9500.
Product area 1.
Contact Mr R. J. Laird, Sales Director/Mr K. Wartnaby, Managing Director.

Mitsubishi Electric UK Ltd
Travellers Lane, Hatfield, Herts AL10 8XB.
Tel. 07072 78756.
Product area 14.
Contact T. F. McCloud, Sales and Marketing Manager.

National Power plc
14 Newgate Street, London EC1A 7AM.
Tel: 071-634 6898.
Product areas 7, 8.
Contact Mr A. J. Swanson, Assistant Company Secretary.

Nuclear Associates
100 Voice Road, Carle Place, New York 11514-1593, USA. Tel. 516-741 7614.
Product areas 1, 3, 4, 5, 6, 8.
Contact Mr H. Glasser, General Manager.

Nucletron Trading Ltd
Nucletron House, Tarporley Business Centre, Tarporley, Cheshire, CW6 9UY.
Tel: 0829 733611.
Product areas 6, 8.
Contact Mrs Marilyn A. Hart, Office Manager.

Nycomed (UK) Ltd
Nycomed House, 2111 Coventry Road, Sheldon, Birmingham B26 3EA.
Tel. 021-742 2444.
Product areas 1, 3.
Contact Mr L. Birch Hansen, Managing Director.

Oxford Magnet Technology
Wharf Road, Eynsham, Oxford.
Tel. 0865 880880.
Product area 1.
Contact Pauline Hobday, Director of Sales and Marketing.

Philips Medical Systems
Kelvin House, 63–75 Glenthorne Road, Hammersmith, London W6 OLJ.
Tel. 081-741 1666.
Product areas 1, 2, 3, 4, 6, 9.
Contact Mr R. Van der Ploeg, Marketing Manager.

Polaroid (UK) Ltd
Ashley Road, St Albans, Herts AL1 5PR.
Tel. 0727 59191.
Product areas 1, 3.
Contact David Hollingworth, Marketing Manager.

Premise Engineering Ltd
Tibbs Hill Road, Abbots Langley, Watford, Herts WD5 ODR.
Tel. 09277-67433/63320.
Product area 8.
Contact Mr R. K. Beach, Director.

Quantel Ltd
Administration Centre, Kiln Road, Newbury, Berkshire RG13 2HA.
Tel. 0444 232323.
Product areas 2, 10.
Contact Mr Christopher Trim, Publicity Officer.

Radiological Protection Services Ltd
61 Lind Road, Sutton, Surrey SM1 4PP. Tel. 081-643 6374.
Product area 8.
Contact B. H. Cutting, Managing Director.

Schering Health Care Ltd
The Brow, Burgess Hill, West Sussex RH15 9NE. Tel. 0444 232323.
Product areas 1, 2, 3.
Contact Mr Simon Higginbotham or Mr S. Hearne, Product Managers.

Siemens plc
Siemens House, Windmill Road, Sunbury on Thames, Midlesex. Tel. 0932 752334.
Product areas: 1, 2, 3, 4, 6, 8, 9, 10, 13, 14, 15.
Contact L. J. McFadyen, Marketing Assistant.

Sony (UK) Ltd
Jays Close, Viables, Basingstoke, Hants RG22 4SB. Tel. 0256 483564.
Product area 14.
Contact Richard Holt, Marketing Manager.

Toshiba Medical Systems UK
Manor Court, Manor Royal, Crawley, West Sussex RH10 2PY. Tel. 0293 560772.
Product areas 1, 2, 3, 4, 9, 10.
Contact Mr S. M. Weeden, Manager X-ray Products.

Toshiba Medical Systems Europe BV
Schieweg 1, 2627 An Delft, The Netherlands. Tel. 015 61 0121.
Product areas 1, 2, 3, 4, 9, 10.
Contact Mr P Blonk, Office Manager, X-ray BU.

Vertec Scientific Ltd
5 Comet House, Calleva Park Estate, Aldermaston, Reading RG7 4QW.
Contact Mr Frans Verlaan, Managing Director

Wardray Products Ltd
Hampton Court Estate, Summer Road, Thames Ditton, Surrey KT7 OSP.
Tel. 081-398 9911.
Product area 8.
Contact Mr R. B. Wardley, Managing Director.

William Cook (Eur) Ltd
6 Such Close, Letchworth, Hertfordshire SG6 1JF. Tel. 0462 482884 Fax: 0462 480944.
Product area 2.
Contact Tessa Phizacklea, Product Manager.

X-rite (H. Miller Graphics Ltd)
8 Moody Street, Congleton, Cheshire CW12 4AP. Tel. 0260 279988.
Product areas 1, 12.
Contact Mrs P. Dhanani, Medical Sales.

KEY TO PRODUCT/ SERVICE AREAS

1: Diagnostic X-ray including NMR and CT
2: Interventional radiology
3: Ultrasound
4: Nuclear medicine
5: Radiopharmaceuticals
6: Radiotherapy and oncology
7: Radiobiology
8: Radiation protection
9: PACS
10: Image processing
11: Nuclear fuel cycle services
12: Quality assurance.
13. Radiology data management computer systems
14. Video printing
15. Equipment leasing
16. Hospital-shared services
17. Medical Publishing

Meetings and Courses

As a service to our readers, notice of meetings or courses will be inserted free of charge. Please send full details to the Honorary Editor, BIR

Breast Group Summer Meeting
June 18–19, 1991
Stratford Upon Avon
Further details: The Conference Office, The Royal College of Radiologists, 38 Portland Place, London W1N 3DG.
Tel: 071-636 4432. Fax: 071-323 3100.

CAR '91 (Computer Assisted Radiology)
July 3–6, 1991
Berlin, Germany
Further details: Professor Heinz U. Lemke, c/o University Klinikum Rudolf Virchow–Wedding, Altes Rontgenhaus-Raum 1005, Augustenburger Platz 1, D-1000 Berlin 65.

IPMI '91
July 7–12, 1991
Kent
Further details: Professor Heinz U. Lemke, c/o University Klinikum Rudolf Virchow–Wedding, Altes Rontgenhaus-Raum 1005, Augustenburger Platz 1, D-1000 Berlin 65.

9th International Congress of Radiation Research
July 7–12, 1991
Toronto, Canada
Further details: 9th International Congress of Radiation Research, 1891 Preson White Drive, Reston, VA 22091, Canada. Tel: (703) 648-3780. Deadline for abstracts: January 15, 1991 and for Junior Investigators Awards: October 15, 1990. Alternatively, contact Miss B. M. de Vere, The Royal Society, 6 Carlton House Terrace, London SW1Y 5AG.

Second European Summer School on Radiological Protection
July 8–11, 1991
Cambridge
Further details: Liz Hide, IBC Technical Services Ltd, Bath House (3rd Floor), 56 Holborn Viaduct, London EC1A 2EX.
Tel: 071-236 4080. Fax: 071-489 0849.

Neuro and Musculoskeletal MRI - Summer in Aspen
July 8–12, 1991
Colorado, USA
Further details: Radiology Postgraduate Education, Room C-324, University of California School of Medicine, San Francisco, California 94143-0628, USA.
Tel: (415) 476 5731. Fax: (415) 476 9213.

Advanced Statistical Methods in Cancer Epidemiology — some current topics.
July 15–19, 1991
Lyon, France
Further details: Unit of Education and Training, International Agency for Research on Cancer, 150 Cours Albert-Thomas, 69372 Lyon, France.
Tel: (33) 72 73 8485. Fax: (33) 72 73 8575.

English for Doctors
August 12–30, 1991
Edinburgh, Scotland
Further details: Institute for Applied Language Studies, 21 Hill Place, Edinburgh, Scotland EH8 9DP.
Tel: 031 650 6183. Fax: 031 667 5927

6th World Congress in Ultrasound
September 1–6, 1991
Copenhagen, Denmark
Further details: Torben Larsen, Department of Gynecology, Herlev Hospital, DK-2730 Herlev, Denmark.

2nd International Workshop on Auger Spectroscopy and Electronic Structure.
September 4–6, 1991
Lund, Sweden
Further details: Professor C. O. Almbladh, Dept. of Theoretical Physics, Lund University, Solvegatan 14A, S-22362 Lund, Sweden.

European Congress of Radiology '91
September 15–20, 1991
Vienna, Austria
Further details: The Congress Secretariat ECR '91, c/o Vienna Academy of Postgraduate Medical Education and Research, Alser Straße 4, A-1090 Vienna, Austria.
Tel: (1) 421383. Fax: (1) 42138323.

Second International Congress on Ultrasound and the Skin
September 18–21, 1991
Modena, Italy
Further details: Stefania Seidenari, Dept. of Dermatology, Policlinico — via del Pozzo, 71 41100 Modena, Italy.
Deadline for abstracts: June 15 1991.

Second International Conference on Eicosanoids and Other Bioactive Lipids in Cancer, Inflammation and Radiation Injury
September 18–21, 1991
Berlin, West Germany
Further details: Dr Santosh Nigam, Local Organizing Secretariat, Eicosanoid Research, Dept. of Gynecological Endocrinology, Universitatsklinikum Steglitz, Free University Berlin, Hindenburgdamm 30, D-1000 Berlin 45, Federal Republic of Germany.

Practical Implications of ICRP 1991
October 1, 1991
London
Further details: Dr D. N. S. Dixon, Programme Committee Secretary, The Society for Radiological Protection, 67 Oatlands Park, Linlithgow, West Lothian, EH49 6AS.
Tel: 031 - 244 2779.

7th Symposium on Neutron Dosimetry
October 14–18, 1991
Berlin, Germany
Further details: Seventh Symposium on Neutron Dosimetry, Dr R. Jahr, Abt. 7, Physikalisch-Technische Bundesanstalt, Bundesallee 100, D-3300 Braunschweig, Germany.
Tel: (49) 531-592 7010. Fax: (49) 531-592 4006.

The Tenth Annual Scientific Meeting and Exhibitin of the Society of Magnetic Resonance in Medicine
October 16, 1991
California, USA
Further details: SMRM, 1918 University Avenue, Suite 3c, Berkeley, CA 94704, USA.
Tel: (415) 84 -1899. Fax: (415) 841-2340.

Progress in Magnetic Resonance Imaging
October 24–25, 1991
Cologne, Germany
Further details: European Magnetic Resonance Forum, PO Box 161, CH 1807 Blonay, Switzerland.
Tel: (41) 21943 3834. Fax:(41) 21943 3593.

13th Annual International Conference of the IEEE Engineering in Medicine and Biology Society
October 31–November 3, 1991
Florida, USA
Further details: Dr Joachim H. Nagel, Conference Chair, Dept. of Biomedical Engineering, University of Miami, PO Box 248294, Coral Gables, Florida 33124, USA.
Tel: (305) 284-2442. Fax: (305) 284-4792.

Please send articles for the Bulletin or any comments or suggestions you may have about the Bulletin to The Honorary Editor, BIR Bulletin, 36 Portland Place, London W1N 4AT.

BIR Bulletin

Honorary Editor, BIR Bulletin: D. Rickards, LRCP, MRCS, FFR(D)SA, FRCR
Please address all correspondence to: Honorary Editor, BIR Bulletin, The British Institute of Radiology,
36 Portland Place, London W1N 4AT

The British Institute of Radiology is not responsible for opinions expressed in the BIR Bulletin

Nicolas John McNally
4.11.39 – 24.03.91

It is a cruel twist of fate that after spending 25 years seeking improved methods of treating cancer, Nic McNally should have succumbed to a particularly aggressive and unresponsive tumour in March 1991. He died at Mount Vernon Hospital after a tragically brief illness during which his stoic and philosophical response to his condition was admirable. His cremation took place at Mortlake Crematorium, after a very moving service at which his daughter and Desmond Wilcox read two very appropriate passages. Friends and colleagues from all over Britain joined his widow Joanna and daughter Rachel in mourning his passing, but at the same time remembering his vitality, kindness and consideration and wisdom.

Nic was an unusual mix in these days of super-specialisation in science; he had a very active involvement in the arts and broad research interests in science but was nevertheless a highly regarded "expert". He was involved in projects in physics, biochemistry, biology and medicine and had a great curiosity and drive to understand ionising radiation and to find ever better ways of using it to treat patients with cancer. After training as a physicist at Bristol University, he undertook further studies in medical physics and finally in radiation physics and radiobiology. This latter subject became the main theme of his work for the next 25 years, initially with the Medical Research Council in the Cyclotron Unit at Hammersmith Hospital and since 1972 with the Cancer Research Campaign in the Gray Laboratory at Mount Vernon Hospital, Northwood. He was quick to point out that radiobiology had much to do with rays and nothing to do with broadcasting!

Since 1978, he headed the Tumour and Cellular Radiobiology Group at the Gray Lab, with a special interest in the type of damage produced in normal and tumour cells by different forms of radiation that might be considered for therapy, including both X-rays and the recently topical cyclotron neutrons. He showed that cells can handle the lesions induced by X-rays and "detoxify" them much more easily that those produced by more exotic radiations.

In the mid eighties, Nic was part of the team that developed a new technology for directly measuring the rate of cell production in tumours. This involved combining new monoclonal antibodies to detect bromine molecules incorporated in the newly synthesised DNA, and the simultaneous recognition of two different fluorescent markers in a high technology machine called a flow cytometer. After developing the techniques with experimental tumour cells, this has now become the "gold standard" method of measuring proliferation in human tumours from a simple biopsy. This important step forward led to the development of a new form of radiotherapy (CHART or continuous hyperfractionated accelerated radiotherapy) which was pioneered at Mount Vernon by Professor S. Dische and Dr A. Saunders, and which is showing great promise. If generally adopted, it will revolutionise radiotherapy departments since it could allow the tailoring of treatment according to the proliferation characteristics of each individual tumour. Fast proliferating tumours should benefit from much faster treatment, for example at 6 hour intervals over 12 days (as in CHART) compared with the more conventional daily treatments over 6 or 7 weeks. The new flow cytometry techniques Nic helped to devise allow fast proliferating tumours to be detected even if they appear slow and indolent by external appearance of conventional pathology. At present, a multicentre trial of this novel therapy, coordinated by Professor S. Dische and Dr A.'92'92'92 Saunders, is under way with all proliferation measurements being performed in Nic's group by Dr. George Wilson. These trials are being watched with great interest by the scientific and medical community and by hospital administrators. If the present promise is fulfilled new staffing arrangements will be needed in radiotherapy departments to allow treatments to extend over 12 hours each day, including weekends. The principle may also influence the design of other forms of cancer therapy, e.g. with cytotoxic drugs or combinations of surgery and radiation.

Over the past 25 years, Nic has left his indelible mark in the cancer community by dint of his presentations at conferences (often giving invited lectures), his 80 or so publications in learned journals and also as memories of his vivacious and entertaining conversations and helpful interactions with staff at all levels. As well as training junior staff and visiting workers in scientific methods, he enjoyed introducing them to English theatre, literature, music, sport and the countryside, with the Isabella plantation in Richmond Park at azalea time being a special favourite. He was even willing to explain the mysteries of cricket, and was an active member of the Lab cricket team. He maintained an excellent balance between his own scientific research, voluntary work for the national and international scientific community and time with his wife and daughter of whom he was very proud and to whom he was completely devoted. Many colleagues and visitors will remember the sparkling repartee and the generous warm hospitality at their dinner parties. Nic had served on various committees and often helped with conference organisation. He was the non-medical Honorary Editor of the British Journal of Radiology and the President Elect of the British Institute of Radiology, the oldest established society in the radiation field. He had also recently been voted vice president of the European Society of Radiation Biology, another mark of his popularity and respect in the international community of scientists.

Nic will be sorely missed by his family, friends and colleagues but we all have an ample store of memories of him regaling us with his wit and wisdom or participating with style and ease in so many social functions and sporting activities. Because of his multi-faceted personality we will each remember him in our own special way, but all with affection and appreciation of what he contributed to our world. His loss will be an added stimulus to his colleagues in their fight against cancer on all fronts.

J. Denekamp
Gray Laboratory

The History of Radiology — Radiology Centennial, Inc.

I read with interest J. M. Guy's comment in the BIR Bulletin of February this year on "Who is writing the history of radiology?" Your readers might be interested to know that in the United States an organization called Radiology Centennial, Inc. has been established to coordinate all X ray centennial activities. Approximately 40 societies, associations and colleges dealing with all aspects of radiology in the United States were involved in forming Radiology Centennial, Inc. President of this corporation os Dr John P. Tampas, of Burlington, Vermont. I chair the books committee and we are preparing several volumes for this occasion. There will be a three volume set of books covering the history in the United States of diagnostic radiology, radiation oncology and radiological physics. These volumes will be written and edited by members of the various radiological professions. A separate book, to be written by a professional science wrtier, will be for the general public and will cover not only the history of radiology but also recent developments and advances. Finally, a children's book targeted for 12–15 year olds, which will also be written by a professional writer is planned, primarily for placement in school libraries. I am being ably assisted by Dr Nancy Knight, curator of the historical collection, including books and manuscripts, of the American College of Radiology. We would be more than pleased to hear from any of your readers who might have pertinent memorabilia of recollection of the history of radiology in the United States.

Peter R. Almond

For further information please contact:
Dr Peter R. Almond,
Department of Radiation Oncology,
School of Medicine,
James Graham Brown Cancer Center,
Louisville, Kentucky 40292, USA
Tel: (502) 588-5254

Library News

The BIR Library is open weekdays 9 a.m.–5 p.m. (7 p.m. on Tuesdays and Thursdays).

The journal stock includes more than 100 titles. Though journals may not be taken out of the library, there is a photocopy service, also available by post or FAX. A list of current journals is available on request and is also published in the March and September issues of the Bulletin. Most books (excepting the historical collection) are available on loan.

Recent additions to the library

Bellon, E. M. & Reid, J. D., 1986. Arteriography and histopathology in experimentally produced athero sclerosis in rhesus and fascicularis monkeys.

Bradac, G. B., Ferszt, R. & Kendall, B. E. (Eds), 1990. Cranial meningiomas. Diagnosis. Biology. Therapy.

DHSS, 1991. DHSS evaluation documents. Nov. 1989–Feb. 1991.

ICRU Report 44, 1989. Tissue substitutes in radiation dosimetry and measurements.

Why not write for the BIR Bulletin?

The BIR Bulletin is an open forum for discussion for all those involved in the radiological sciences.

If you have an article that you would like published in the BIR Bulletin please send your material to the Honorary Editor, BIR Bulletin, The British Institute of Radiology, 36 Portland Place, London W1N 4AT.

Company Profile

Data-Med Computer Services Ltd

Data-Med Computer Services Limited is a company established and wholly owned by ex-NHS computing professionals. The company has been trading since September 1985 and continues to grow rapidly with approximately 70 health computing specialists now employed. The company is wholly-owned by its employees and has no financial investment in any other company. Our anticipated turnover for the financial year 1990–1991 will be close to £2m.

Because Data-Med work exclusively for the health service, our staff invariably have a background of NHS experience. Perhaps more importantly, the staff cover a wide range of skills covering areas like PAS, medical records, nursing and radiography. All the senior managers within Data-Med have a background working in health service computing.

Data-Med is devoted exclusively to providing computer services to the health service. In particular Data-Med specialise in three major areas of business within the Healthcare environment:

Consultancy

Undertaking district IT strategies, tender evaluations, system integration studies etc.

F.M.

Data-Med provide long-term computing services to Bassetlaw and Nottingham Health Authorities ranging from operations and system support to high -level consultancy.

Development

Data-Med are a MUMPS software house developing a number of application systems for the Health Service. In particular, both our DM-Rad Radiology Management system and our Nurse Management System DM-Nurse have proved to be extremely popular.

The company is based in Nottingham with an office in Dronfield (near Sheffield). Data-Med have worked with numerous health authorities from Cornwall to Scotland.

Data-Med Computer Services are agents for two of the leading hardware manufacturers in the world: Digital Equipment Co. (DEC) and IBM (UK) Ltd. This status as agents means that we are able to offer competitively priced 'turnkey' solutions for our range of software applications.

Part of our responsibility as agents for these manufacturers requires us to provide a technical configuration, installation, back-up and support service for the system software running on the processors we supply. This has required our senior technical and development staff to attend and obtain technical certificates of competence in the hardware and system software.

Lucien Appel Foundation for Neuroradiology

Honoring the memory of Professor Lucien Appel, the "Lucien Appel Foundation for Neuroradiology" has created a biannual prize.

The prize to the amount of 100.000 Belgian francs, will reward the neuroradiological work of young radiologists.

The first prize will be awarded in March 1992 during an academic session held in Antwerp and after this it will be awarded biannually.

All candidates interested in this prize have to send their work and curriculum vitae before 30 September 1991 to Dr B. Appel.

For further information please contact: Dr B. Appel, Department of Neuroradiology-CT-MRI, Middelheim Hospital, 1 Lindendreff, 2020 Antwerp, Belgium.

Membership Matters: A stand with a view

Visitors to the Med X Ray exhibition could not fail to be impressed by the cornucopia of products and services on display concerning all aspects of radiology and radiotherapy.

This year saw a relative newcomer to the exhibition hall. Nestling between SIMIS and Konica was the BIR stand. The object of the stand was to promote the various activities of the Institute, to recruit new members, and finally to sell BIR publications and products.

On Sunday evening the BIR stand designers put the final touches to the stand design. The number of permutations for two chairs, a bookcase and a table seemed endless! Finally, the BIR stand was ready for business.

Business on the stand was certainly brisk over the three day period. Both publications and products sold well with some items selling out. Twenty-six individuals and one company, Technical Photo Services, applied for membership.

The success of the stand was in no small part due to the professionalism and good humour of the members and staff who manned it. Whilst it was very much a team effort the hard work of the two Bobs, Messrs Corbett and Atkinson cannot go unrecorded. Every other enquirer at the stand seemed to say "Bob sent me!"

We hope that more members will help man the stand next year at Med X Ray in Birmingham. However, members need not wait until 1992 to recruit new members and promote the Institute.

Members can help recruit their colleagues by passing them the information leaflets inserted in this month's issue of the BJR. The leaflet briefly describes the activities of the Institute and lists the benefits of membership. For an appliction form prospective members need only complete and cut out the pre-paid post card.

Product News

New Bruel & Kjaer 3535 Diagnostic System for radiologists

The 3535 System from Bruel & Kjaer provides unparalleled diagnostic flexibility and uncompromised image quality. The core of the system is a new generation array unit which can be expanded in many ways with a wide range of application-optimized hardware and software modules. The system can therefore be configured to meet your exact requirements — from basic B-mode scanning to FFT and full color Doppler.

System 3535 is backed up by a comprehensive transducer program including convex, linear and wide aperture annular array probes for general abdominal and small-part scanning and a number of task-specific transducers for special applications such as endoluminal and intraoperative scanning.

For documentation purposes, the 3535 can be coupled to a video printer, VCR or multi-format camera. The 3535 also features a cine-memory for real-time image review which permits continuous and frame-by-frame replay of recorded images. The console is equipped with a built-in 3.5" floppy disk and hard disk for image storage and retrieval. Information can also be transferred to a PC over the system's computer interface.

For further information contact: Mr Dennis Lewis, Bruel &Kjaer (UK) Ltd, Harrow Weald Lodge, 92 Uxbridge Road, Middlesex HA3 6BZ
Tel. 081 954 2366

Kontron announces first KUDAIS installation

The Royal Hallamshire hospital in Sheffield has installed a Kontron Unit Data and Information System (KUDAIS) for rapid gathering and analysis of patient data. The system was first shown at the Healthcare Computing Exhibition in Harrogate where visitors were impressed by the system's blend of data acquisition, operational assistance, management statistics and reporting.

For further information contact: Melvin Reynolds, Medical Sales, Kontron Instruments Ltd, Blackmoor Lane, Croxley Centre, Watford, Herts WD1 8XQ
Tel: 0923 245991

3cx X-ray scanner works with DTP software

The 3cx OmniMedia colour/grayscale scanner is specially designed for medical, dental and bio-technology applications. Featuring an optical density of 0.01 to 3.5, the 3cx digitizes low contrast, dark transmissive images such as X-rays and gels, up to 8.5" x 14". With this system and a computer any X-ray can be viewed, diagnosed, archived, printed and transmitted electronically. The OmniMedia technology also digitizes colour or black and white artwork for desktop publishing applications. With leading optical character recognition (OCR) software, the 3cx can scan text from journals, publications and other documents directly into a word processor.

For further information please contact: David Robson, IMC, 281 St Leonard's Road, Windsor, SL4 3DR Tel. 0753 830999 Fax. 0753 831094

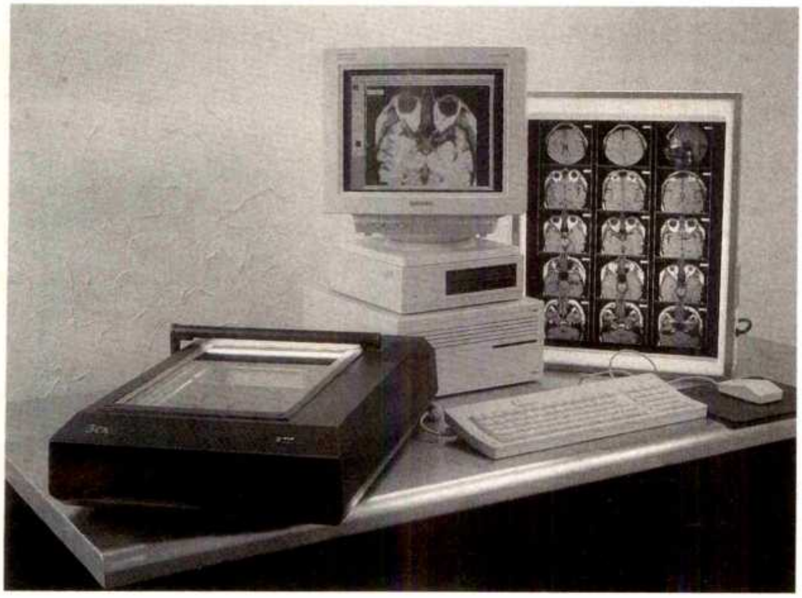

An ecological solution to X-ray waste products

Lokas Ltd has expanded its original services of bulk collection of used photographic and X-ray fixer and processing of film by incineration to include chemical stripping of film and paper, collection and treatment of developer, provision of recycling equipment and design and installation of pump/tank systems.

For more information on Lokas' services contact: Lokas Ltd, Winstanley Industrial Estate, Scot Lane, Blackrod, Bolton, Lancs BL6 5SL

ALRA radiation therapy lotion gives relief from acute radiation dermatitis

ALRA is a new radiation therapy skin care lotion that has been specially formulated to provide soothing relief from acute radiation dermatitis. It does not interfere with ongoing treatment in any way.

For a free sample contact: Nuclear Associates, 100 Voice Road, Carle Place, NY 11514 USA.
Tel: 516 741 6360 Fax: 516 741 5414

BIR Calendar

Unless otherwise indicated, enquiries about these events should be addressed to the Conference Manager, British Institute of Radiology, 36 Portland Place, London W1N 4AT (Tel. 071-580 4085).

MRI meeting
October 16, 1991
Organizer: Professor B. S. Worthington

Brachytherapy — The past, present and future
October 23 and 24, 1991
Institution of Electrical Engineers
(Meeting to be held in association with Nucletron Ltd)
Organizer: Professor C. A. Joslin

Imaging of the oesophagus
November 5, 1991
Organizer: Dr A. Freeman

Hypoxic cell sensitizers: do they have a future?
November 15, 1991
Organizer: Dr R. Camplejohn

Ischaemic heart disease — limitations of non-invasive assessment
November 22, 1991
Royal London Hospital
Organizer: Dr N. Garvie

Vascular systems imaging
January 24, 1992
Organizer: Dr J. F. Reidy

Radiosensitivity
February 11, 1992
Joint BIR/RCR meeting
Organizer: Dr A. Gregor

Quality standards in nuclear medicine
February 18, 1992
Organizer: Dr A. Smith

3–D image analysis in medical imaging
February 25, 1992
Organizer:Professor M. A. Smith

Megavoltage portal imaging
April 9, 1992
Joint meeting with IPSM
Organizer: Dr W. Jones

Radiology & Oncology '92
18–20 May 1992
International Convention Centre, Birmingham

BIR Company Subscriber Scheme

The BIR company subscriber scheme is aimed at all companies with an interest in radiology and allied sciences.

For an annual subscription of £275 p.a. member companies are offered an attractive benefits package.

To find out why your company should join the leading edge companies listed below, please contact Mr Tony Hudson, Administration Manager, British Institute of Radiology, 36 Portland Place, London W1N 4AT. Tel: 071-580 4085.

AEA Technology
Wigshaw Lane, Culcheth
WA3 4NE. Tel. 0925-252000 Ext. 4206
Product areas 7, 8.
Contact Mr J. G. Tyror, Director of Safety.

Agfa-Gevaert Ltd
27 Great West Road, Brentford, Middlesex
TW8 9AX. Tel. 081-560 2131.
Product Areas 1.
Contact Mr G. Mountford, Director.

American Medical Ltd
PO Box 971, London SW10.
Tel. 071-352 8051. Fax: 071-376 4508.
Product areas 1, 3, 4, 5, 7, 8.
Contact Betsy Riley, Managing Director.

Amersham International PLC
Lincoln Place, Green End, Aylesbury,
Bucks HP20 2TP. Tel. 0296 395222.
Product areas 4, 5, 6.
Contact Mr C. M. T. Medley, Sales and Marketing Manager.

Bard Ltd
Forest Houe, Brighton Road, Crawley,
West Sussex RH 11 9BP.
Tel. 0293 27888, ext. 2204.
Product area 2.
Contact Peter Dekkers, Product Manager.

British Nuclear Fuels plc
Room 525, Hinton House, Risley, Warrington, Cheshire WA3 6AS.
Tel. 0925 835022.
Product areas 8, 11.
Contact Dr R. J. Berry, Director of Health and Safety and Environmental Protection.

Bruel & Kjaer (UK) Ltd
92 Uxbridge Road, Harrow, Middlesex,
HA3 6BZ. Tel. 081-954 2366.
Product areas 3, 6.
Contatct Mr D. Lewis, Sales Manager.

Calumet Coach Co.
33 Shallbourne Rise, Camberley GU1J
2EJ. Tel. 0276 64490.
Product areas: 1, 4, 5.
Contact Mr P. Supple, Managing Director of International Operations.

Cardiac Services Ltd
95A Finaghy Road, South Belfast
BT10 OBY. Tel. 0232-625566.
Product areas 1, 3, 4, 5, 6.
Contact Mr R. J. Brown. Managing Director.

Cea (UK) Ltd
25 Presley Way, Crownhill,
Milton Keynes MK8 0ES
Tel. 0908 263090. Fax: 0908 263546.
Product areas 1, 3, 4, 5, 6.
Contact John Dunster, Managing Director.

Clinical Press Ltd
Redland Green Farm, Redland, Bristol BS8
7HF. Tel. 0272 420526.
Product area 17.
Contact Dr Paul Goddard, Chairman.

Data-Med Computer Services Ltd
10 Faraday Building, Highfields Science Park, University Boulevard, Nottingham
NG7 2QP.
Tel. 0602 431431. Fax: 0602 430782.
Product area 13.
Contact Mr C. Fields, Sales Manager.

Du Pont (UK) Ltd
Wedgwood Way, Stevenage, Hertfordshire SG1 4QN.
Tel. 0438 734000.
Product areas 1, 3, 4, 5, 6, 7, 9 and 10.
Contact Mr E. G. Lovat, Product Manager, Diagnostic Imaging.

E. G. & G. Limited
Vale Road, Windsor, Berkshire SL4 5JP.
Tel. 0753 855611.
Product areas 1, 6, 7, 8.
Contact Mr Roy Hauton, Sales Executive (Therapy).

Elscint (GB) Ltd
Colonial Business Park, Colonial Way,
Watford, Herts WD2 4PT.
Tel. 0923 39511.
Product areas 1, 3, 4.
Contact Faith Gorman, Marketing Manager.

E-Z-EM Ltd
1230 High Road, Whetstone, London N20.
Tel. 081-446 9714.
Product areas 1, 2, 8.
Contact Richard Bayliss, Sales and Marketing Manager.

Fuji Photo Film (UK) Ltd
125 Finchley Road, London
NW3 6JH. Tel. 071-586 9351.
Product areas 1, 3.
Contact Mr R. G. Brown, Marketing and Administration Manager.

Gammex-RMI Ltd
34 Shakespeare Street, Nottingham
NG1 4FQ. Tel. 0602 483807.
Product areas 1, 3, 4, 5, 6.
Contact Miss Eileen Parr, Commercial Manager.

IGE Medical Systems Ltd
352 Buckingham Avenue, Slough, Berks
SL1 4ER. Tel. 0753 874000.
Product areas 1, 2, 3, 4, 5, 6, 8, 9.
Contact Jill Mitchell, UK Sales Support.

Kodak Ltd
PO Box 66, Station Road, Hemel Hempstead, Herts HP1 1JU.
Tel. 0442 61122.
Product area 1, 3, 4, 6, 8, 9, 12, 13, 14, 15
Contact Mr J. J. G. Tweed, Manager, Health Sciences Division.

Lanmark
PO Box 317, Beaconsfield, Bucks
HP9 2LR. Tel. 0494 791615/670586.
Product areas 1, 3, 4, 5, 9, 10, 15, 16.
Contact Liz Beckmann, Director.

3M UK PLC
3M House, Bracknell, PO Box 1,
Berks RG12 1JU. Tel. 0344 426726.
Product area 1.
Contact Mr Alan Budge, Marketing Manager.

Mallinckrodt Diagnostica (UK) Ltd
11 North Portway Close, Round Spinney,
Northampton NN3 4RQ. Tel. 0604-46132.
Product areas 4, 5.
Contact Mr D. G. L. Wood, Business Manager.

M. A. S. Medical Ltd
Armytage Road, Brighouse, West Yorkshire HD6 1QF. Tel. 0484 721906.
Contact Martin York, Managing Director.

Meadox (UK) Ltd
Matthew House, Matthew Street, Dunstable LU6 1SD. Tel. 0582 605111.
Product area 2.
Contact Mrs Sheila Heap, Sales and Marketing Manager.

Medical Xray Supplies Ltd
Unit 12, Kingsbury Industrial Estate, Church Lane, Kingsbury, London NW9 8AU. Tel. 081-205 9500.
Product area 1.
Contact Mr R. J. Laird, Sales Director/Mr K. Wartnaby, Managing Director.

Mitsubishi Electric UK Ltd
Travellers Lane, Hatfield, Herts AL10 8XB. Tel. 07072 78756.
Product area 14.
Contact T. F. McCloud, Sales and Marketing Manager.

National Power plc
14 Newgate Street, London EC1A 7AM. Tel: 071-634 6898.
Product areas 7, 8.
Contact Mr A. J. Swanson, Assistant Company Secretary.

Nuclear Associates
100 Voice Road, Carle Place, New York 11514-1593, USA. Tel. 516-741 7614.
Product areas 1, 3, 4, 5, 6, 8.
Contact Mr H. Glasser, General Manager.

Nucletron Trading Ltd
Nucletron House, Tarporley Business Centre, Tarporley, Cheshire, CW6 9UY. Tel: 0829 733611.
Product areas 6, 8.
Contact Mrs Marilyn A. Hart, Office Manager.

Nycomed (UK) Ltd
Nycomed House, 2111 Coventry Road, Sheldon, Birmingham B26 3EA.
Tel. 021-742 2444.
Product areas 1, 3.
Contact Mr L. Birch Hansen, Managing Director.

Oxford Magnet Technology
Wharf Road, Eynsham, Oxford.
Tel. 0865 880880.
Product area 1.
Contact Pauline Hobday, Director of Sales and Marketing.

Philips Medical Systems
Kelvin House, 63–75 Glenthorne Road, Hammersmith, London W6 OLJ.
Tel. 081-741 1666.
Product areas 1, 2, 3, 4, 6, 9.
Contact Mr R. Van der Ploeg, Marketing Manager.

Polaroid (UK) Ltd
Ashley Road, St Albans, Herts AL1 5PR.
Tel. 0727 59191.
Product areas 1, 3.
Contact David Hollingworth, Marketing Manager.

Premise Engineering Ltd
Tibbs Hill Road, Abbots Langley, Watford, Herts WD5 ODR.
Tel. 09277-67433/63320.
Product area 8.
Contact Mr R. K. Beach, Director.

Quantel Ltd
Administration Centre, Kiln Road, Newbury, Berkshire RG13 2HA.
Tel. 0444 232323.
Product areas 2, 10.
Contact Mr Christopher Trim, Publicity Officer.

Radiological Protection Services Ltd
61 Lind Road, Sutton, Surrey SM1 4PP. Tel. 081-643 6374.
Product area 8.
Contact B. H. Cutting, Managing Director.

Schering Health Care Ltd
The Brow, Burgess Hill, West Sussex RH15 9NE. Tel. 0444 232323.
Product areas 1, 2, 3.
Contact Mr Simon Higginbotham or Mr S. Hearne, Product Managers.

Siemens plc
Siemens House, Windmill Road, Sunbury on Thames, Midlesex. Tel. 0932 752334.
Product areas: 1, 2, 3, 4, 6, 8, 9, 10, 13, 14, 15.
Contact L. J. McFadyen, Marketing Assistant.

Sony (UK) Ltd
Jays Close, Viables, Basingstoke, Hants RG22 4SB. Tel. 0256 483564.
Product area 14.
Contact Richard Holt, Marketing Manager.

Toshiba Medical Systems UK
Manor Court, Manor Royal, Crawley, West Sussex RH10 2PY. Tel. 0293 560772.
Product areas 1, 2, 3, 4, 9, 10.
Contact Mr S. M. Weeden, Manager X-ray Products.

Toshiba Medical Systems Europe BV
Schieweg 1, 2627 An Delft, The Netherlands. Tel. 015 61 0121.
Product areas 1, 2, 3, 4, 9, 10.
Contact Mr P Blonk, Office Manager, X-ray BU.

Vertec Scientific Ltd
5 Comet House, Calleva Park Estate, Aldermaston, Reading RG7 4QW.
Contact Mr Frans Verlaan, Managing Director

Wardray Products Ltd
Hampton Court Estate, Summer Road, Thames Ditton, Surrey KT7 OSP.
Tel. 081-398 9911.
Product area 8.
Contact Mr R. B. Wardley, Managing Director.

William Cook (Eur) Ltd
6 Such Close, Letchworth, Hertfordshire SG6 1JF. Tel. 0462 482884 Fax: 0462 480944.
Product area 2.
Contact Tessa Phizacklea, Product Manager.

X-rite (H. Miller Graphics Ltd)
8 Moody Street, Congleton, Cheshire CW12 4AP. Tel. 0260 279988.
Product areas 1, 12.
Contact Mrs P. Dhanani, Medical Sales.

KEY TO PRODUCT/ SERVICE AREAS

1: Diagnostic X-ray including NMR and CT
2: Interventional radiology
3: Ultrasound
4: Nuclear medicine
5: Radiopharmaceuticals
6: Radiotherapy and oncology
7: Radiobiology
8: Radiation protection
9: PACS
10: Image processing
11: Nuclear fuel cycle services
12: Quality assurance.
13. Radiology data management computer systems
14. Video printing
15. Equipment leasing
16. Hospital-shared services
17. Medical Publishing

Meetings and Courses

As a service to our readers, notice of meetings or courses will be inserted free of charge. Please send full details to the Honorary Editor, BIR

The 14th Annual Conference of the Australasian College of Physical Scientists in Medicine
July 22–25, 1991
Sydney, Australia
Further details: Secretariat EPSM 91 Conference,The IPACE Institute, Box 1 PO, Kensington, 2033, Australia.
Tel: 02 6973178; Fax: 02 662 6983.

"Hands On"
July 27–28, 1991
Birmingham
Further details: Miss Ann Case, Frenchay Hospital, Bristol, BS16 1LE.
Tel: 0272 701212 Ext. 2725.

MRI: Musculoskeletal/Body
July 29–August 2, 1991
Kauai, Hawaii
Further details: Radiology Postgraduate Education, Room C-324, University of California School of Medicine, San Francisco, California 94143-0628.
Tel: (415) 476 5731. Fax: (415) 476 9213.

A Practicum in Breast Imaging
By appointment only
Maryland, USA
Further details: Program Coordinator, The Johns Hopkins Medical Institutions, Office of Continuing Education, Turner Building, 720 Rutland Avenue, Baltimore, Maryland 21205, USA.
Tel: (301) 955-2959.

The 2nd International Conference of the Kenya Association of Radiologists
August 7–9, 1991
Nairobi, Kenya
Further details: Dr J K Kitonyi, Conference Secretary, Dept. of Diagnostic Radiology, University of Nairobi, PO Box 19676, Nairobi, Kenya.
Tel: 724722. Fax: 340969.'

Tenth Annual Scientific Meeting and Exhibition
August 10–16, 1991
California, USA
Futher details: SMRM Business Office, 1918 University Avenue, Suite 3C, Berkeley, CA 94704, USA.
Tel: (415) 841 1899. Fax: (415) 841 2340.

Paediatric Radiology Course
September 5–6, 1991
Sheffield
Further details: Dr G M Steiner, Consultant Radiologist, Children's Hospital, Western Bank, Sheffield S10 2TH. Tel: 0742 761111.

Dublin 91: Annual Scientific Meeting and Exhibition
September 25–28, 1991
Dublin, Ireland
Further details: The Conference Office, The Royal College of Radiologists, 38 Portland Place, London, W1N 3DG.
Tel: 071-636 4432. Fax: 071-323 3100.

XIIIth International Congress of Lymphology
September 29–October 5, 1991
Paris, France
Further details: Medical Congress Management, PO Box 2, CH-8029, Zurich, Switzerland.
Tel: (01) 255 19 15. Fax: (01) 261 05 78.

BIOBURDEN workshop
September 30–October 1, 1991
Frankfurt, Germany
Further details: Charlotte Thornton, IBC Ltd, Bath House - 3rd Floor, 56 Holborn Viaduct, London EC1A 2EX.
Tel: 071-236 4080. Fax: 071-489 0849.

XIIth International Congress of Head and Neck Radiology
October 6–9, 1991
Zurich, Switzerland
Further details: Medical Congress Management, PO Box 2, CH-8029, Zurich, Switzerland.
Tel: (01) 255 19 15. Fax: (01) 261 05 78.

XVIIth Congress of the European Society of Neuroradiology
October 8-12, 1991
Zurich, Switzerland
Further details: Medical Congress Management, PO Box 2, CH-8029, Zurich, Switzerland. Tel: (01) 255 19 15.
Fax: (01) 261 05 78.

Advances in Molecular Research
October 9–12, 1991
Garmisch-Partenkirchen, Germany
Further details: Georgina Mason, IBC Technical Services Ltd, Bath House, 56 Holborn Viaduct, London EC1A 2EX.
Tel: 071-236 4080. Fax: 071-489 0849.

How to detect and to Characterise the Microcalcifications?
October 10, 1991
France
Further details: M J Rodiere, Institut D'Imagerie Medicale, Miniparc - Bat 2, Rue de la Croix Verte, 34090 Montpellier, France.

Erasmus Course for Magnetic Resonance Imaging
October 14–18, 1991
Aachen, Germany
Further details: Klaus Bohndorf, Department of Radiology, Technical University of Aachen, Pauwelsstr. 1, D-5100 Aachen, Germany.
Fax: (241) 878 992.

United Medical and Dental Schools
October 25–26, 1991
London
Further details: Kim Latimer, Post Graduate Department, Guy's Hospital, London SE1 9RT. Tel: 071-955 4300.

The Society for Minimal Invasive Therapy Third Annual World Conference
November 10–12, 1991
Massachusetts, USA
Further details: Fay Harrison, Secretary to the Society for Minimal Invasive Therapy, 25 John Street, London WC1N 2BL.
Tel: 071-430 2858. Fax: 071-831 6745.

Thoracic Imaging Update
November 14, 1991
London
Further details: Margaret Johnson, National Heart & Lung Institute, London Chest Hospital, Bonner Road, London E2 9JX.
Tel: 081-983 2342. Fax: 081-983 2202.

New Drugs for Asthma
November 14–15, 1991
London
Further details: Georgina Mason, IBC Technical Services Ltd, Bath House, 56 Holborn Viaduct, London EC1A 2EX.
Tel: 071-236 4080. Fax: 071-489 0849.

2nd International Congress on Oral Cancer
Decermber 2–5, 1991
New Delhi, India
Further details: Organising Secretary, B4 NDSE Part II, New Delhi-110 049, India.
Tel: (91 11) 6462354.Fax: (91 11) 6444966.

Please send articles for the Bulletin or any comments or suggestions you may have about the Bulletin to The Honorary Editor, BIR Bulletin, 36 Portland Place, London W1N 4AT.

Assurance of Quality in the Diagnostic X-Ray Department

The report of the BIR Diagnostic Methods Committee

Editors

J A Garrett, Director of Medical Equipment Management Organisation, Bristol & Weston Heath Authority, UK
D Gifford, Deputy Chief Physicist, Frenchay & Southmead Health Authorities, UK
M J Harvey, Middlesex Hospital, London, UK
P Goddard, Consultant Radiologist, Bristol Royal Infirmary, UK

Producing images, whether photographically or in electronic form, is the primary purpose of the diagnostic radiology department.

As the range of imaging modalities increases and the equipment for each becomes more sophisticated, awareness is growing of the necessity to review and assess the quality of the imaging process. While there are many interdependent factors that may affect image quality, each may in many cases be assessed by quite simple tests. As well as addressing the organisational, economic and human factors, which are a vital part of the imaging process, this handbook represents a wide range of well-tried tests suitable for use in both small and large X-ray departments.

The second section of the book presents the wider systems approach to quality assurance with reference to recent standards for QA and how these may be applied to diagnostic radiology.

The final part discusses quality assurance in computer assisted imaging, computed tomography, magnetic resonance imaging, and digital subtraction angiography.

Radiologists, radiographers, physicists and technicians alike will find *Assurance of Quality in the Diagnostic X-Ray Department* both a practical handbook for day-to-day use and a stimulus in developing their understanding of the scope of quality assurance.

November 1988 108 pages 296x208mm Spiralbound
0 905 74917 0 Illustrated £20.00

ORDER FORM

British Institute of Radiology, 36 Portland Place, London W1N 4AT.
Telephone Orders: 071 580 4189. Fax: 071 255 3209

I would like to order..............(copies) of ASSURANCE OF QUALITY IN THE DIAGNOSTIC X-RAY DEPARTMENT

I enclose payment to the sum of £.................. by: ☐ cheque ☐ Access
☐ Barclaycard/Visa

My card number is ☐ Expiry date / /19

Signature ....

Please send to this address: (BLOCK CAPITALS)
Name .... Position ....
Address ....
....
Postcode ....

BIR Publications. BIR Publications. BIR Publications. BIR Publications. BIR Publications. BIR Publications. BIR Publications. BIR Publications. BIR Publications.

OPTIMIZATION OF IMAGE QUALITY AND PATIENT EXPOSURE IN DIAGNOSTIC RADIOLOGY

(BIR Report 20)

Editors:

B M Moores, B F Wall, H Eriskat and H Schibilla.

Contents: Introduction. Image Perception. Physical Assessment of Image Quality. Clinical Assessment of Image Quality. Optimization of Image Quality and Patient Dose - Paediatric Radiology - Mammography - Chest Radiography - Technical Factors. Patient Dose Measurements and Quality Assurance. CEC Image Quality and Exposure Criteria Trial. Panel Discussions. Conclusions and Perspectives for Future Research. CEC Study Group Document on Quality Criteria for Diagnostic Radiographic Images.

Key components in quality assurance in diagnostic radiology are image quality and patient exposure. Quality criteria defining optimum procedures should ensure that the most accurate and reproducible diagnostic information is obtained from radiographs, but at the same time minimize exposure of the patient to ionizing radiation. Formulation of such criteria was the aim of a workshop organized jointly by the CEC and NRPB, of which this book is the edited proceedings. A revised list of quality criteria for common diagnostic examinations was drawn up by a CEC Study Group and is appended to the proceedings.

October 1989 200 pages approx 266 x 196 mm
Softcover 0 905 74921 9 Illustrated £30.00

ns. BIR Publications. BIR Publications. BIR Publications. BIR Publications. BIR Publications. BIR Publications. BIR Publications. BIR Publications. BIR Publicatio

---

THE FINER POIN

ULTRAVIST PRESCRIBING INFORMATION Presentation: Intravascular injections of non-ionic iopromide in strengths of 150mg, 240mg, 300mg and 370mg of iodine/ml. **Uses:** Delineation of the vascular and renal systems. **Dosage and Administration:** Intravenous urography: Adult minimum doses: Ultravist 370: 0.8ml/kg body weight; Ultravist 300: 1ml/kg body weight; Ultravist 240: 1.3ml/kg body weight. Computed Tomography: Cranial CT: Ultravist 240: 1.5-2.5ml/kg body weight; Ultravist 300: 1-2ml/kg body weight; Ultravist 370: 1-1.5ml/kg body weight. Whole-body CT: Dosage depends on investigation and scanner. Angiography: Dosage (6-80ml) depends on age, weight, cardiac output, general condition, and investigation. Checking function of dialysis shunt: Ultravist 150: 100ml. **Contra-indications, warnings, etc:** Contra-indications: Possible hypersensitivity to contrast media, thyrotoxicosis, cardiac decompensation,

hysterosalpingography during pregnancy, acute pelvic inflammation. Warnings, e
Caution if there is: severe hepatic or renal impairment; cardiac or circulat
insufficiency; cerebral arteriosclerosis; cerebral spasmodic conditions; epile
juvenile-onset or long-standing diabetes; pulmonary emphysema; poor general he
hyperthyroidism, multiple myeloma; a history of allergy, especially if patient has rec
a contrast medium before. Use during pregnancy only if essential. Do not mix co
media and anti-allergic agents. Do not restrict fluid supply. Correct disturbances o
balance of water and electrolytes before administration. With phaeochromocyto
premedicate with an alpha-blocker. Do not allow Ultravist to remain in contact with bl
in a syringe. Flush intravascular catheters frequently to minimise clotting
Administer Ultravist to recumbent patients and closely observe for at least 30 min

The Scientific Basis of Modern Radiotherapy

(BIR Report 19)

Editor

N J McNally, Gray Laboratory, Mount Vernon Hospital, Middlesex

The last ten years have seen a dramatic shift of emphasis in the application of radiobiology to radiotherapy practice. This volume is the edited proceedings of an international symposium held in Jack Fowler's honour and to mark his achievement as Director of the Gray Laboratory.

There are excellent reviews on modern theories of fractionation and of the new clinical options in dose fractionation. The growing significance of vascular approaches to treating cancer is reported in papers on the vasculature of tumours, the activation of bioreductive drugs, and the manipulation of blood flow for therapeutic benefit. Chemical modifiers, both sensitisers and protection, are discussed at both the experimental and the clinical level. The important and growing subject of prognostic indicators is reviewed with papers on prediction of radiosensitivity, repopulation and the possible role of PET scanning for functional measurements. Finally, two papers review the current status of the clinical use of hyperthermia.

These proceedings will be of interest to all who are concerned with the treatment of cancer by radiation, and provide an excellent basis for anyone who wishes to undertake research in experimental radiotherapy.

May 1989 142 pages 266x196mm Softcover
0 905 74920 0 Illustrated £30.00

TS OF ULTRAVIST

iopromide

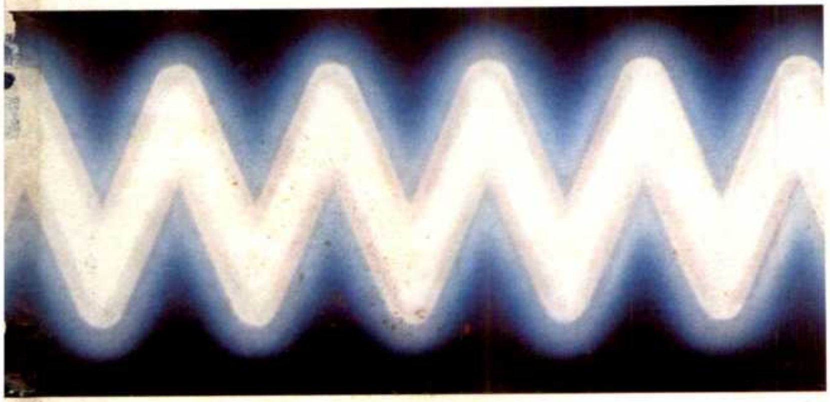

Low viscosity[1] for ease of injectio

Facilitates a fast bolus injection when spee is important; allows the use of less expensive smaller-gauge needles and minimises the problems of dealing with fin catheters.

Low osmolality[1] for patient comfor

With lower osmolality than iopamidol and iohexol[2] Ultravist is associated with a lo incidence of vascular pain and side-effects

Ultravist – it's the fine points that make i a fine product.

SCHERING
HEALTH CARE
Expertise in Action

he capacity of the thyroid to take up iodine is reduced. If marked side-effects or suspected allergic reactions ccur during injection, and do not disappear when it is interrupted, stop the investigation. Even minor side-ffects may be signs of severe reaction. Life-threatening side-effects include hypotensive collapse, circulatory ailure, ventricular fibrillation, cardiac arrest, pulmonary oedema, anaphylactic shock or other allergic nanifestations and convulsions or other cerebral symptoms. **List Price:** Ultravist 370 1x100ml £41.33. **roduct Licence No:** 0053/0209 Ultravist 150; 0053/0173 Ultravist 240; 0053/0174 Ultravist 300; 0053/0175 ltravist 370. **Product Licence Holder:** Schering Health Care Limited, The Brow, Burgess Hill, West ussex RH15 9NE.

eferences: 1. Data on file, Schering Health Care. 2. Kennedy C, et al., (1988), Brit J Radiol; 261:288-293.

urther information is available from – Schering Health Care, The Brow, Burgess Hill, West Sussex 15 9NE.

'Ultravist' is a registered trade mark.

PUBLICATIONS OF THE BRITISH INSTITUTE OF RADIOLOGY

BJR Supplements:	
23. **Treatment Simulators**, 1989, 48pp., ISBN: 0 905 74919 7	£10.00
22. **Megavoltage Radiotherapy 1937-1987**, 1988, 158 pp., ISBN: 0 905 74916 2	£28.50
21. **Radionuclides in Brachytherapy: Radium and After**, 1987, 54 pp., ISBN: 0 905 74915 4	£15.00
20. **The Safety of Diagnostic Ultrasound**, 1987, 48 pp., ISBN: 0 905 74914 6	£12.00
18. **Criteria and Methods for Quality Assurance in Medical X-ray Diagnosis**, 1985, 180 pp., ISBN: 0 905 74912 X	£27.50
17. **Central Axis Depth Dose Data for use in Radiotherapy** This standard work replaces BJR Supplement 11 (1972), 1983, 148 pp., ISBN: 0 905 74911 1	£25.00
Other Publications:	
Assurance of Quality in the Diagnostic X-ray Department, 1988, 108 pp., ISBN: 0 905 74917 0	£20.00
Basic Clinical Ultrasound Hylton B Meire and Pat Farrant, 1982 (BIR Teaching Series No 4) 170 pp., ISBN: 0 905 74910 3	£12.50
Special Report 17: High Dose Rate Afterloading in the Treatment of Cancer of the Uterus, 1980, 200 pp., ISBN : 0 905 74907 3	£18.50
Report 18: Technical and Physical Parameters for Quality Assurance in Medical Diagnostic Radiology, 1989, 166 pp., ISBN: 0 905 74918 9	£30.00
Report 19: The Scientific Basis of Modern Radiotherapy, 1989, 142 pp., ISBN: 0 905 74920 0	£30.00
Report 20: Optimization of Image Quality and Patient Exposure in Diagnostic Radiology, 1989, 288 pp., ISBN: 0 905 74921 9	£30.00
Report 21: Risks from Radium and Thorotrast, 1989, 188 pp., ISBN : 0 905 74922 7	£40.00
Current Research in Osteoporosis and Bone Mineral Measurement, 1990, 96 pp., ISBN: 0 905749 23 5	£22.00
Clinical Applications of Ultrasonic Fetal Measurements, 1991,30 pp., ISBN: 0 905749 24 3	£13.50
Guidelines for the Evaluation of Radiological Technologies, 1991, 28 pp, ISBN: 0 905 74925 1	£13.50

The British Institute of Radiology
36 Portland Place, London W1N 4AT Tel. 071-580 4189 Fax. 071-255 3209

Please send me the following publications: ________________________

I enclose payment to the sum of £..................by cheque ☐ Barclaycard/Visa ☐
My card number is ☐ Access ☐

Signature ....Please send to this address: (BLOCK CAPITALS)
Name ....Position ....
Address ....
Postcode ....Country ....

American orders to: Medical Physics Publishing Corporation, 27B, 1300 University Avenue, Madison W1 53706, USA. Fax: 608 262 2413 for dollar price.